



TÜRKİYE BİLİMLER AKADEMİSİ
TURKISH ACADEMY OF SCIENCES

TUBA World Conference
on
Energy Science and Technology
(TUBA WCEST-2021)
8-12 August 2021

 <https://wcest.tuba.gov.tr>
 wcest@tuba.gov.tr

BOOK OF PROCEEDINGS

ISBN:978-605-2249-75-8

DOI: 10.53478/TUBA.2021.017

CONTENT

Preface	2
Committees	4
Scientific Program.....	6
Plenary Speakers.....	16
Keynote Speakers.....	19
Invited Talks.....	49
Specialized Talks.....	73
General Presentations.....	78



PREFACE FROM GENERAL CHAIR



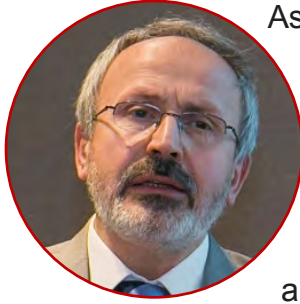
Turkish Academy of Sciences (TÜBA) continues to promote and support science and scientist with projects, research activities, scientific meetings, and reveals books and reports with working groups in an interdisciplinary manner. TÜBA Energy Working Group and other thematic working groups which consist of experienced scientists in related fields continue science-based activities in line with the needs of society and innovations in technology.

Energy has always been at the forefront throughout human history and shaped modern times. Therefore, we focus on it a holistic approach during the programs of the TÜBA Energy Working Group. In science, there is not any field or scientific discipline that does not have a relation with energy. Energy is a common value of human beings. Meanwhile, the production of useful and sustainable energy sources including increasing carbon-free consumption is a helpful and vital instrument for the health and welfare of our country, and peace in the region and international affairs.

Today, energy investments and roadmaps are planned with the common perspective of many disciplines such as economics, international politics, Social Sciences, informatics, health, and natural and applied sciences. In this context, on behalf of the Turkish Academy of Sciences, I would like to invite you to the TÜBA World Conference on Energy Science and Technology (TÜBA WCEST-2021), to be held between 8 – 12 August 2021, to discuss the energy technologies, strategies, and policies in a multidisciplinary aspect.

Prof. Dr. Muzaffer Şeker
General Chair of TUBA WCEST-2021
President of Turkish Academy of Sciences (TÜBA)

PREFACE FROM CONFERENCE CHAIR



As the chair for Energy Working Group at the Turkish Academy of Sciences (TUBA), it is my distinct pleasure to welcome you all to this unique event (so-called: TUBA World Conference on Energy Science and Technology (TUBA WCEST-2021)), which is held online virtually. This distinct conference aims to bring/connect internationally renowned researchers and scientists, leading policymakers and strategists, and society presidents and committee chairs to deliver plenary, keynote, and invited talks in various areas of energy science and technology.

The program starts on Sunday (August 8th) with two panel discussion sessions, one on “Energy, Environment and Economy” and the other one on “Energy and Education” where current challenges, potential solutions, opportunities and future directions are discussed by the leading experts. The program opens its technical sessions on Monday with the formal opening talks where the TUBA President, Minister of Industry and Technology, and Minister of Energy and Natural Resources deliver their speeches. The program continues with 29 plenary/keynote speakers, 27 invited speakers and over 121 general speakers on four days which make an exceptionally designed conference in the area of energy science and technology. It then ends on Thursday (August 12th) with a panel discussion session and closing remarks.

Furthermore, there are general sessions where many research talks are delivered by researchers, scientists, engineers, and technologists to disseminate high-quality research results and present new findings. Local and global online participations are expected from academia, government agencies, and industry to bring all players together, and the conference is then expected to lead to effective and fruitful discussions and collaborations among these attendants from different disciplines, institutes, and sectors from all over the world. Moreover, it is planned to have some special issues in various reputable international journals to publish high-quality papers out of the conference.

In closing, I warmly welcome you all to attend this unique conference and help a create a fruitful virtual platform. I wish you all a successful event.

Prof. Dr. İbrahim Dincer
Conference Chair of TUBA WCEST-2021

Conference Honorary Chairs

H.E. Mustafa Varank, Minister of Industry and Technology of Turkey
H.E. Fatih Donmez, Minister of Energy and Natural Resources of Turkey

Conference General Chair

Prof. Dr. Muzaffer Seker, President of Turkish Academy of Sciences

Conference Chair

Prof. Dr. Ibrahim Dincer, Chair of Energy Working Group at TUBA

Executive Organizing Committee (In alphabetical order)

Prof. Dr. Mehmet Hakki Alma
Prof. Dr. Erol Arcaklioglu
Prof. Dr. Yildiz Bayazitođlu
Prof. Dr. Arif Hepbasli
Prof. Dr. Sadik Kakac
Prof. Dr. Kamil Kaygusuz
Prof. Dr. Adnan Midilli
Prof. Dr. Murat Öztürk
Prof. Dr. Niyazi Serdar Sariciftci
Prof. Dr. Bahri Sahin
Prof. Dr. Rasit Turan

Track Chairs (In alphabetical order)

Prof. Dr. Mehmet Hakki Alma
Prof. Dr. Erol Arcaklioglu
Prof. Dr. Alper Baba
Prof. Dr. Yildiz Bayazitoglu
Prof. Dr. Can Ozgur Colpan
Prof. Dr. Ibrahim Dincer
Prof. Dr. Arif Hepbasli
Prof. Dr. Kamil Kaygusuz
Prof. Dr. Ali Kosar
Prof. Dr. Adnan Midilli
Assoc. Prof. Dr. Samil Sen
Prof. Dr. Rasit Turan

Technical Assistant

Fatih Akin Ozdemir

Conference Secretariat

Gökçen Oral

International Advisory Board

- Alma, M. H. / Turkey
Aloui, F. / France
Apak, M. R. / Turkey
Arcaklioglu, E. / Turkey
Bayazitoglu, Y. / USA
Bejan, A. / USA
Cengel, Y. / USA
Chen, W.H. / Taiwan
Demirel, Y. / USA
Dincer, I. / Canada
Eroglu, I. / Turkey
Hamdullahpur, F. / Canada
Hepbasli, A. / Turkey
Kakac, S. / Turkey
Kaygusuz, K. / Turkey
Klemeš, J. J. / Czechia
Li, X. / Canada
Midilli, A. / Turkey
Naterer, G. F. / Canada
Ni, M. / Hong Kong
Nižetić, S. / Croatia
Rosen, M. A. / Canada
Sariciftci, N. S. / Austria
Saghir, Z. / Canada
Sahin, B. / Turkey
Sen, Z. / Turkey
Tsatsaronis, G. / Germany
Turan, R. / Turkey
Veziroglu, T. N. / USA



Scientific Progra

Sunday - August 8, 2021 - [Zoom Link](#)

Panel Discussion Session 1: Energy, Environment & Economy

Moderator: Ilgi Karapinar, Turkey

Panel Speakers

Azize Ayol, Dokuz Eylül University, Turkey

14:00

Chris Cook, ISRS at University College London, UK

16:00

(GMT+3)

Mihri Ozkan, University of California, Riverside, USA

Seeram Ramakrishna, National University of Singapore, Singapore

Olçay Unver, Arizona State University, USA

Zafer Üre, PCM Products, UK

16:00 - 16:15 (GMT+3)

Break

Panel Discussion Session 2: Energy & Education

Moderator: Hatice Eser Okten, Turkey

Panel Speakers

Feridun Hamdullahpur, University of Waterloo, Canada

16:15

İbrahim Dinçer, Ontario Tech University, Canada & Yıldız Technical University, Turkey

18:15

(GMT+3)

Celile Eren Okten, Yıldız Technical University, Turkey

Bestami Ozkaya, Yıldız Technical University, Turkey

Marc A. Rosen, Ontario Tech University, Canada

Mehmet Yıldız, Sabanci University, Turkey

Monday - August 9, 2021 - [Zoom Link](#)

Opening Speeches

Prof. Dr. Muzaffer Seker, *President of Turkish Academy of Sciences (TUBA) & General Chair of Conference*

10:00

(GMT+3)

H.E. Fatih Dönmez, *Minister of Energy and Natural Resources, Turkey*

H.E. Mustafa Varank, *Minister of Industry and Technology, Turkey*

10:30 - 10:45 (GMT+3)

Break

Plenary Session

Session Chair: **Ibrahim Dincer**, Canada/Turkey

Christian Rakos

President of World Bioenergy Association (WBA), Austria

10:45

12:15

(GMT+3)

Transforming Bioenergy Use in the Developing World – A Key Target for Sustainable Development and Net Zero Carbon Emissions

Feridun Hamdullahpur

Past President, University of Waterloo, Canada

An Overview of the Role of Universities on Energy and Sustainability

12:15 - 13:15 (GMT+3)

Break

Monday - August 9, 2021

[Zoom Link 1](#)

Keynote Session 1

Session Chair: Adolfo Iulianelli, Italy

Keynote Talk 1

13:15 – 14:00 (GMT+3)

Benjamin K. Sovacool

University of Sussex, UK

Decarbonisation and Its Discontents: A Critical Justice Perspective on Four Low-Carbon Transitions

Keynote Talk 2

14:00 – 14:45 (GMT+3)

Richard S.J. Tol

University of Sussex, UK

The Economic Impact of Climate and Weather

13:15
14:45
(GMT+3)

[Zoom Link 2](#)

Invited Session 1

Session Chair: Ali Kosar, Turkey

Invited Talk 1

13:15 – 13:45 (GMT+3)

Umberto Desideri

University of Pisa, Italy

Power to Fuel Technologies: Is a Necessary Option for the Future?

Invited Talk 2

13:45 – 14:15 (GMT+3)

Chris Cook

The ISRS at University College London, UK

Introducing the Energy Treasury: from \$ Economics to Energy Economics

Invited Talk 3

14:15 – 14:45 (GMT+3)

James Carton

Dublin City University & Hydrogen Ireland Association, Ireland

Hydrogen; Building a Hydrogen Economy on the Island of Ireland

[Zoom Link 3](#)

General Session 1

Biofuels and Bioenergy

Session Chair: M. Hakkı Alma, Turkey

#7 "Hydrothermal Carbonization of Wet Olive Mill Waste" **G. Balmuk**, H. Cay, G. Duman Tac, I. C. Kantarli & J. Yanik

#65 "Biochar: Physical Properties and Effects on the Soil" **M.H. Alma, A. Altıkat & S. Altıkat**

#66 "Bio-Oil Separation and Upgrading Techniques" **M.H. Alma, A. Altıkat & S. Altıkat**

#89 "Utilization of Soft Drink Industry Waste as Energy Feedstock" **I.C. Kantarli**

#120 "Impact of Using Ethanol-Gasoline Compound Fuel on Performance of a Dual-Fuel Vehicle" **P. Kamarei, P. Ahmadi, N. Javani & M. Raeesi**

#126 "Sugarcane Leaves and Tops for Biogas Production by Batch Experiments" **N. Sinbuathong, B. Sillapacharoenkul, R. Khun-anake & Y. Paopun**

14:45 - 15:00 (GMT+3)

Break

Monday - August 9, 2021

[Zoom Link 1](#)

Keynote Session 2

Session Chair: İlgi Karapınar, Turkey

Keynote Talk 3

15:00 – 15:45 (GMT+3)

Neven Duić

University of Zagreb, Croatia

Decarbonisation of Energy Systems with Variable Renewables

Keynote Talk 4

15:45 – 16:30 (GMT+3)

Erol Gelenbe

Polish Academy of Sciences, Poland

Energy Consumption by ICT: Facts, Measurements, and Trends

15:00
16:30
(GMT+3)

[Zoom Link 2](#)

Invited Session 2

Session Chair: Umberto Desideri, Italy

Invited Talk 4

15:00 – 15:30 (GMT+3)

Muhammad Ali Imran

University of Glasgow, UK

5G Communication Systems and Energy Efficient Future

Invited Talk 5

15:30 – 16:00 (GMT+3)

Mehmet Sarikaya

University of Washington, USA

Energy Materials - Current & Future

Invited Talk 6

16:00 – 16:30 (GMT+3)

Alejandro H. Buschmann

Universidad de Los Lagos, Chile

Macroalgal Sea-farming and Biofuels: Desires and Facts

[Zoom Link 3](#)

General Session 2

Fuel Cell & Batteries

Session Chair: Bora Timurkutluk, Turkey

#45 "Pd-Modified Polyrhodanine for Methanol Electrooxidation Reaction" **R. Solmaz & D. Öztürk**

#52 "Selection and Synthesis of Ceramic Electrolytes for Intermediate Temperature Solid Oxide Fuel Cells" **H. Ozlu Torun**

#97 "On Energy Performance of SOFC Integrated S-CO₂ Micro-Gas Turbine" **U. Akbulut & A. Midilli**

#30 "Highly Stable Pouch Cell Scale Quasi-Solid-State Lithium-Air Batteries" **M. Çelik, A. Kizilaslan, T. Çetinkaya & H. Akbulut**

#129 "Hydrogen Fuel Cell Bus Performance Assessment with Machine Learning Degradation Prediction" **P. Ahmadi**

#116 "Investigating the Environmental Effects of a Hybrid UAV with Fuel Cell, According to Two Different Scenarios" **D. Çalısır, S. Ekici, A. Midilli & T.H. Karakoç**

16:30 - 16:45 (GMT+3)

Break

Monday - August 9, 2021

[Zoom Link 1](#)

Keynote Session 3

Session Chair: Neven Duić, Croatia

Keynote Talk 5

16:45 – 17:30 (GMT+3)

S. Ravi P. Silva CBE

University of Surrey, UK

A Net Zero Carbon World through Innovation in Energy Materials

Keynote Talk 6

17:30 – 18:15 (GMT+3)

Marc A. Rosen

Ontario Tech University, Canada

Energy Sustainability for Sustainable Development

16:45
18:15
(GMT+3)

[Zoom Link 2](#)

Invited Session 3

Session Chair: Murat Koksal, Turkey

Invited Talk 7

16:45 – 17:15 (GMT+3)

Steven Brown

Director, New Strain Development, LanzaTech, USA

Stepping on the Gas to a Circular Economy: Accelerating the Development of Carbon-Negative Chemical Production from Gas Fermentation

Invited Talk 8

17:15 – 17:45 (GMT+3)

Cengiz Sinan Ozkan

University of California, Riverside, USA

Materials Design for Sustainability and Energy Storage

Invited Talk 9

17:45 – 18:15 (GMT+3)

Tianzhen Hong

Lawrence Berkeley National Laboratory, USA

Applications of Machine Learning Techniques in Buildings: An Overview and Examples

[Zoom Link 3](#)

General Session 3

Sustainable Development - I

Session Chair: Barbaros Cetin, Turkey

#9 "Emissions and Its Driver Analysis for the United Kingdom Higher Education Institute" A. Nayak, N. Turner & E. Gobina

#32 "Evolution of Microclimate Effect of an Urban Park over Their Built Environment" M.A. Ruiz, M.F. Colli, C.F. Martinez & E.N.C. Cantaloube

#42 "Analysis of Urban Scale Energy Certification Systems for Efficient Communities" M.B. Sosa, E.N. Correa & M.A. Cantón

#71 "Bioclimate of Urban Areas at the Russian far North in the Context of Climate Change: Energy and Human Health" E.A. Grigorjeva

#92 "Production of Pan-Peg Thermal Energy Storage Nanofibers by Electrospinning Method" T. Paçacı, C. Alkan, Y. Dinç & E. Kişioğlu

#107 "A New Methodology for Distributor Selection in Refrigeration Cycles" H.A. Hacimusalar, M.H. Sökücü, M.R. Özdemir & A.S. Dalkılıç

Tuesday - August 10, 2021

[Zoom Link 1](#)

Keynote Session 4

Session Chair: Ilker Tari, Turkey

Keynote Talk 7

09:00 – 09:45 (GMT+3)

Kevin Trenberth

National Center for Atmospheric Research (UCAR), USA

The Changing Flow of Energy Through the Climate System

Keynote Talk 8

09:45 – 10:30 (GMT+3)

Jianlei Niu

The Hong Kong Polytechnic University, Hong Kong

Progresses in Thermal Energy Storage Research to Reduce the Energy Use in Buildings

09:00
10:30
(GMT+3)

[Zoom Link 2](#)

General Session 4

Renewable Energy - I

Session Chair: Arif Hepbasli, Turkey

#29 "Geothermal Energy Production from Abandoned Oil and Gas Wells: A Technical Review" A. Mukhtarov, G. Gokcen Akkurt & N. Yildirim

#69 "Working Fluid Selection and Performance Analysis of a Geothermal Binary Power Plant" Z. Ozcan & G. Gokcen Akkurt

#90 "Modeling and Performance Evaluation of the Geothermal Energy Based Combined Plant for Different Products" Y.E. Yuksel, F. Yilmaz & M. Ozturk

#34 "Determining Compensation Rate for Wind-Solar Hybrid Energy System in Istanbul Based on ANFIS Modeling" E. Gün & A.D. Şahin

#23 "Outdoor Performance of an Improved Thermoelectric Heat Pumping Solar Air Heater" J. R. Segnon & H.O. Njoku

#24 "Development of Hybrid Power Systems for North India Rural Areas" G. Muthukumaran & B. Kosoy

10:30 - 10:45

Break

Tuesday - August 10, 2021

10:45
12:15
(GMT+3)

[Zoom Link 1](#)

Specialized Session 1

New Dimensions in Fossil Fuels
Session Chair: Ismail Boz, Turkey

Specialized Talk 1
10:45 – 11:05 (GMT+3)
Emre Artun
Istanbul Technical University, Turkey
Machine-Learning Based Modeling of Hydrocarbon Reservoirs

Specialized Talk 2
11:05 – 11:25 (GMT+3)
Ozge Bozkurt
TUPRAS R&D Center, Turkey
The Clean Fuel Technology Approach of TUPRAS R&D

Specialized Talk 3
11:25 – 11:45 (GMT+3)
Salomé Larmier
Le Mans Université, France
Beef Veins: a Multi-marker for Mature Source Rock

Specialized Talk 4
11:45 – 12:05 (GMT+3)
Samil Sen
Istanbul University – Cerrahpasa, Turkey
Determination of a Deep Learning-Based Model for Shale Porosity Prediction Using World Scale Data Set

[Zoom Link 2](#)

General Session 5

Hydrogen Energy Technologies – I
Session Chair: Mert Gür, Turkey

#53 “Environmental Impact Assessment of a Novel Photoelectrochemical Reactor for Hydrogen Production” [A.E. Karaca](#) & I. Dincer

#135 “The Role of Machine Learning on Metal Hydride for Hydrogen Storage” [M.S. Karasu Asnaz](#) & A. Midilli

#64 “Activated Carbon-Decorated Spherical Titanium Oxide Nanoparticles for Enhanced Hydrogen Production” S. Sekar, D.Y. Kim & [Sejoon Lee](#)

#67 “Influence of Biohydrogen Production on the Ratio of Generated Acids and Regulation of ΔpH in *E. Coli* During Fermentation of Mixed Carbon Sources at pH 7.5” [H. Gevorgyan](#) & K. Trchounian

#80 “Design of a Future Hydrogen Supply Chain: A Multi-Objective Model for Turkey” [E. Geçici](#), A. Erdoğan & M.G. Güler

#112 “Electrospinning is a Powerful Tool for the Design of Carbon Nanofiber Towards Hydrogen Energy System” [A.K. Figen](#)

12:15 - 13:15

Break

Tuesday - August 10, 2021

13:15
14:45
(GMT+3)

[Zoom Link 1](#)

Keynote Session 5

Session Chair: Meng Ni, China

Keynote Talk 9
13:15 – 14:00 (GMT+3)
Olcay Unver
Arizona State University, USA
Pathways to Sustainability in an Increasingly Water-Scarce World

Keynote Talk 10
14:00 – 14:45 (GMT+3)
Henrik Lund
Aalborg University, Denmark
Smart Renewable Energy Systems and Decarbonisation. The Danish Target of a 70% Decrease in CO₂ Emission by 2030

[Zoom Link 2](#)

Invited Session 4

Session Chair: Can Ozgur Colpan, Turkey

Invited Talk 10
13:15 – 13:45 (GMT+3)
Umit B. Demirci
University of Montpellier, France
Boron for Carrying/Storing Hydrogen

Invited Talk 11
13:45 – 14:15 (GMT+3)
Zafer Ure
Managing Director, Phase Change Material Products Ltd., UK
Thermal Energy Storage Technologies and their Global Application Examples

Invited Talk 12
14:15 – 14:45 (GMT+3)
Erkan Oterkus
University of Strathclyde, UK
Fracture Modeling Based on Peridynamic Theory

14:45 - 15:00 (GMT+3)

Break

Tuesday - August 10, 2021

	Zoom Link 1 Keynote Session 6 Session Chair: Selda Oterkus, UK	Zoom Link 2 Invited Session 5 Session Chair: Olcay Unver, USA	Zoom Link 3 General Session 6 Renewable Energy – II Session Chair: Nader Javani, Turkey
15:00 16:30 (GMT+3)	<p>Keynote Talk 11 15:00 – 15:45 (GMT+3) Igor Pioro Ontario Tech University, Canada Current Status and Future Developments in the Nuclear-power Industry of the World</p> <p>Keynote Talk 12 15:45 – 16:30 (GMT+3) Zhu Han University of Houston, USA Distributed Deep Reinforcement Learning for Renewable Energy</p>	<p>Invited Talk 13 15:30 – 16:00 (GMT+3) Meng Ni The Hong Kong Polytechnic University, China New Developments in Zn-Air Batteries for Energy Storage</p> <p>Invited Talk 14 16:00 – 16:30 (GMT+3) Bahareh Seyedi United Nations Department of Economic and Social Affairs (UNDESA), USA Achieving Universal Energy Access and Net Zero Emissions – A Policy Perspective</p>	<p>#18 "Potential Use of Renewable Energy for Rural Electrification in Pakistan by Incorporating Blockchain Technology" <u>A. Rana</u> & G. Gróf</p> <p>#36 "Effect of Auxiliary Acceptors on Quinoline-Based Dye-Sensitized Solar Cells" <u>B. S. Arslan</u>, N. Öztürk, M. Gezgin, Y. Derin, A. Tutar, M. Nebioğlu & İ. Şişman</p> <p>#37 "A New Methodological Approach for the Techno-Economic Analysis of Hydroelectric Power Plants in Turkey" <u>S. Çelikdemir</u> & M.T. Özdemir</p> <p>#40 "Extreme Winds and Risk Analysis in Turkey for Wind Energy Applications" <u>T. Kara</u>, S.E. Yakut, O. Tek, M. Peköz, M. Aksakal & A.D. Şahin</p> <p>#77 "Techno-Economic Analysis of Onshore and Offshore Wind Power Plants" <u>S. Çelikdemir</u> & <u>M.T. Özdemir</u></p> <p>#57 "Performance Evaluation of Solar Dryer with and without Solar Photovoltaic Heat Extraction (PVHE) Duct" <u>S. Monesh</u>, A. Shankar, S. Ezhilarasan & <u>S. Tiwari</u></p>
16:30 - 16:45 (GMT+3)	Break		

Tuesday - August 10, 2021

	Zoom Link 1 Keynote Session 7 Session Chair: Alper Baba, Turkey	Zoom Link 2 Invited Session 6 Session Chair: Samil Sen, Turkey	Zoom Link 3 General Session 7 Microgrids & Smart Grids Session Chair: Sertac Bayhan, Qatar
16:45 19:00 (GMT+3)	<p>Keynote Talk 13 16:45 – 17:30 (GMT+3) Mohammad Shahidehpour Illinois Institute of Technology, USA Optimal Expansion and Operation Planning of Microgrids using a Two-Stage Data Clustering Strategy</p> <p>Keynote Talk 14 17:30 – 18:15 (GMT+3) Roland N. Horne Stanford University, USA Global Geothermal Outlook and Sustainable Development 2021</p> <p>Keynote Talk 15 18:15 – 19:00 (GMT+3) Arumugam Manthiram The University of Texas at Austin, USA Sustainable Battery Chemistries for E-Mobility and Renewable Energy Storage</p>	<p>Invited Talk 15 16:45 – 17:15 (GMT+3) Salih Saner Near East University, TRNC Geological and Geopolitical Controls on the Hydrocarbon Search in the Eastern Mediterranean Basin</p> <p>Invited Talk 16 17:15 – 17:45 (GMT+3) Ibrahim Çemen University of Alabama, USA Quantitative Natural Fracture Analysis in unconventional gas-shale reservoirs: An example from Woodford Shale in Oklahoma, USA</p> <p>Invited Talk 17 17:45 – 18:15 (GMT+3) Biröl Dindoruk University of Houston, USA Data Mining/Machine Learning in the Oil and Gas Sector: Applications in the Area of Petroleum Engineering</p>	<p>#81 "The Lightweight Deep Learning Model for Smart Grid Stability Prediction" <u>F. Ucar</u></p> <p>#48 "A Smart Monitoring and Protection System Design Using Visible Light Communication for Grid Integration of Microgrids" <u>M. Das</u>, <u>M. Sonmez</u> & <u>G. Bayrak</u></p> <p>#27 "A Supervised Learning-Based Method Using a Modified Voting Algorithm for Classification of Complex Power Quality Disturbances in a Hydrogen Energy-Based Microgrid" <u>A. Küçüker</u>, <u>A. Yılmaz</u> & <u>G. Bayrak</u></p> <p>#6 "Nature-Inspired Two-Layer Optimizations for Interconnected Heat and Power Multi-Microgrids" <u>P. Fracas</u>, <u>E. Zondervan</u>, <u>M. Franke</u> & <u>K.V. Camarda</u></p> <p>#78 "Adaptive Control Technique for Grid Integrated SPV Generating System for Power Quality Enrichment" <u>D. Prasad</u>, <u>N. Kumar</u> & <u>R. Sharma</u></p> <p>#84 "Bid Optimization in Electricity Markets" <u>E. Polat</u>, <u>M.G. Güler</u> & <u>M.Y. Ulukuş</u></p>

Wednesday - August 11, 2021

Zoom Link 1

Keynote Session 8

Session Chair: Hatice Eser Okten, Turkey

Keynote Talk 16

09:00 – 09:45 (GMT+3)

Seeram Ramakrishna

National University of Singapore, Singapore

Build Back Better Materials World to Deal with the Existential Threats to Humanity – Reimagine Materials

Keynote Talk 17

09:45 – 10:30 (GMT+3)

Andrea "Andy" Blair

President of International Geothermal Association (IGA), New Zealand

Global Geothermal Movements: What's Happening in the World of Geothermal, Current Focus, Latest Thinking, and Global Trends

09:00
10:30
(GMT+3)

Zoom Link 2

General Session 8

Green Energy

Session Chair: Azize Ayol, Turkey

#79 "State-of-Art Green Cryptocurrency Mining Models" N. Gure

#44 "Capital-Energy Substitution in Turkish Manufacturing Firms: Role of Firm Size" P. Sezer

#121 "Design and Testing of an IoT Based Carbon Monoxide Monitoring UAV: Methodology, Challenges, Opportunities" E. Ozbek, O. Aras, O. Kucukkor, S. Ekici & T.H. Karakoc

#98 "Experimental Investigation of a Vapor Compression Refrigeration System for Thermal Management" F. Coskun & M.F. Serincan

#28 "Biocomposite and Polymeric Materials in Radiation Shielding Applications: A Review" E. Demir, Z. Candan & M.N. Mirzayev

Zoom Link 3

General Session 9

Energy Conversion & Management – I

Session Chair: Pouria Ahmadi, USA

#16 "Investigation of Buildings with Optimum Insulation Thickness Depending on Different External Wall Types and Insulation Materials in Terms of Mold and Moisture Risk" O Kon & I. Caner

#59 "Energy Consumption for Silage Maize Production in Kocaeli Province of Turkey" H.H. Ozturk & H. Goker

#58 "Estimation of Crude Oil Production in Turkey Via Holt-Winters Method" E. Guler & S. Yelir Kandemir

#47 "Investigation of LSTM for Energy Demand Response Applications" M Güler & D.B. Unsal

#76 "An On-Board Energy and Environmental Analysis within the Covid-19 Effects" A. Sari, E. Sulukan, D. Özkan & T.S. Uyar

#70 "Precasted Timber-Concrete Composite as a Component of Sustainable Construction" P. Mika, S. Kuc & Ł. Wesolowski

10:30 - 10:45 (GMT+3)

Break

Wednesday - August 11, 2021

Zoom Link 1

Keynote Session 9

Session Chair: Orhan Cakir, Turkey

Keynote Talk 18

10:45 – 11:30 (GMT+3)

Qingyan (Yan) Chen

Purdue University, USA

Energy Use in Buildings: Past, Present, and Future

Keynote Talk 19

11:30 – 12:15 (GMT+3)

Onur Mutlu

ETH Zurich, Switzerland

Intelligent Architectures for Intelligent Machines

10:45
12:15
(GMT+3)

Zoom Link 2

General Session 10

Solar Energy

Session Chair: Ankica Kovač, Croatia

#72 "Performance Analysis of Double Slope Passive and Active Solar Still for Indian Climatic Condition" T.A.S.S. Krishna, S. Tiwari, R. Sharma & D.B. Singh

#75 "Comparative Analysis of Solar Energy-Based Water Purification Systems Based on Various Designs" N. Kumar, V.K. Dwivedi & D.B. Singh

#60 "Solar Energy use for Drip Irrigation of Maize Production in Harran Plain of Turkey" H.H. Ozturk & H.K. Kucukerdem

#86 "Experimental Investigation and Theoretical Model of R718/LiBr Bubble Pump Operated Absorption Refrigeration Machine" N. Ben Ezzine, R. Garma, M. Chatti & A. Bellagi

#43 "Assessment of the Floating Photovoltaic (FPV) Systems Build in Extreme Weather Locations and Comparison with Terrestrial System" M.K. Kaymak & A.D. Şahin

#74 "Effect of Water Depth on Efficiencies and Productivity of N-Alike Evacuated Tubular Solar Collectors Coupled to Solar Still of Single Slope Type by Incorporating Exergy" D. B. Singh, R.K. Yadav, Y. Chaturvedi, G.K. Sharma, S.K. Sharma & N. Kumar

Zoom Link 3

General Session 11

Hydrogen Energy Technologies – II

Session Chair: Ehsan Baniasadi, Iran

#83 "Hydrogen Energy Utilization – A Review" E. Akiskalioglu

#88 "New Enhanced Design of Hydrogen-Based Thermally Driven R717 Absorption Refrigeration System" N. Ben Ezzine, M. Chatti, R. Garma & A. Bellagi

#94 "Development of Solar-Driven and Hydrogen Integrated Charging Station for Electric Vehicles" D. Erdemir & I. Dincer

#56 "Location Selection of the Hydrogen Refueling Stations: An Istanbul Case" E. Geçici, M.G. Güler & T. Bilgiç

#119 "Teaching Fuel Cell and Hydrogen Science and Engineering Across Europe" L. Lordache

#124 "Experimental Studies to Improve the Performance, Emission and Combustion Characteristics of Sweet Almond Oil Fuelled CI Engine Using Hydrogen Injection in PCCI Mode" V.E. Geo, S. Thiyagarajan & A. Sonhalia

12:15 - 13:15 (GMT+3)

Break

Wednesday - August 11, 2021

Zoom Link 1

Keynote Session 10

Session Chair: Erkan Oterkus, UK

Keynote Talk 20

13:15 – 14:00 (GMT+3)

Bruce Rittmann

Arizona State University, USA

Moving from Treatment to Resource

Keynote Talk 21

14:00 – 14:45 (GMT+3)

Mohamed-Slim Alouini

King Abdullah University of Sciences and
Technology (KAUST), Saudi Arabia

**Towards Sustainable and Environment-Aware
Wireless Networks**

13:15
14:45
(GMT+3)

Zoom Link 2

Invited Session 7

Session Chair: Safa'a Riad, Egypt

Invited Talk 18

13:15 – 13:45 (GMT+3)

Ali Kindap

Zorlu Energy & Geothermal Energy Association, Turkey

Geothermal Energy in Turkey

Invited Talk 19

13:45 – 14:15 (GMT+3)

Alper Baba

Izmir Institute of Technology, Turkey

**Importance of the Geothermal Resources and Its
Innovative Properties: A Case Study: Turkey**

Invited Talk 20

14:15 – 14:45 (GMT+3)

Arthur Weeber

TNO and Delft University of Technology, Netherlands

**Trends and Future Aspects of PV Technology and
its Applications**

Zoom Link 3

General Session 12

Modeling & Simulation – I

Session Chair: Adnan Midilli, Turkey

#73 "A Sensitivity Study of N-Alike Partly Enclosed
with Photovoltaic Thermal Compound Parabolic
Concentrators Having Series Connection" **R.V.
Patel, R.K. Sharma, S. Tiwari, A. Raturi, D.B. Singh
& N. Kumar**

#22 "Analysis of Roof Thermal Performance with
Innovative Technology" **N. Alchapar & E. Correa**

#26 "Causal Investigation of Energy Storage
Technology Criteria by Applying a Novel Integrated
Decision-Making Methodology" **A. Karasan & I.
Kaya**

#35 "Hot Air Drying of Spherical Moist Objects in
a 3D Rectangular Channel" **S. Özcan Çoban, F.
Selimefendigil & H.F. Öztop**

#117 "Design and Modeling of a Multigeneration
System Driven by Waste Heat of a Marine Diesel
Engine" **M.E. Demir & F. Çıtakoğlu**

#131 "Exergetic Analysis of a New Hybrid Vehicle
Operating with Carbon-Free Fuels" **M. Ezzat & I.
Dincer**

14:45 - 15:00 (GMT+3)

Break

Wednesday - August 11, 2021

Zoom Link 1

Keynote Session 11

Session Chair: Arthur Weeber, Netherlands

Keynote Talk 22

15:00 – 15:45 (GMT+3)

Amar K. Mohanty

University of Guelph, Canada

**Improved Utilization of Co-Products from
Biofuel Industries in New Industrial Uses for
a Sustainable Biorefinery**

Keynote Talk 23

15:45 – 16:30 (GMT+3)

Victor C.M. Leung

The University of British Columbia, Canada

**AIoT as a Service – Framework,
Opportunities, and Challenges**

15:00
16:30
(GMT+3)

Zoom Link 2

General Session 13

Sustainable Development - II

Session Chair: Tahir A.H. Ratlamwala, Pakistan

#127 "Comparative Sustainability Investigation of
Hydrogen Production Methods" **C. Acar**

#10 "Testing Membranes for Separation of
CO₂ From Small Molecules in Landfill Gas" **P.
Ogunlode, O. Abunumah, F. Muhammad-Sukki &
E. Gobina**

#128 "Hydrogen Refuelling Stations: State of the
Art and Perspectives" **D. Marciuş, A. Kovač & M.
Paranos**

#111 "Thermodynamic Assessment of a Power
to Methane System Under Real-World Scenario"
**A.C. Ince, D. Saygan Temel, C.O. Colpan, A.
Keleş, & M.F. Serincan**

#87 "Suitability of Siderite as Oxygen Carrier in
Chemical Looping Combustion" **M. Durmaz, N.
Dilmaç & Ö.F. Dilmaç**

#125 "Improvement of Terminal Buildings'
Environmental Performance by Renewable
Energy" **A. Dalkıran, O. Ballı, M.Z. Söğüt & T.H.
Karakoç**

Zoom Link 3

General Session 14

Energy Materials,

Session Chair: Nader Javani, Turkey

#41 "Nanocellulose in Energy Applications: Current
Status and Future Prospect" **M. Yıldırım & Z. Candan**

#46 "Detection of Temperature Elevations in Encased
Smartphones Due to Multitask Processes" **C. Nubisi
& H. Njoku**

#55 "Iron Oxide-Based Photocatalysts for Hydrogen
Production and Dye Degradation Under Natural
Sunlight" **V. Preethi, S. Ananth, P.S. Chandana, M.G.
Krishna & S.L. Subramanyam**

#91 "A Structure Property Issue in Organic Solid-
Solid Phase Change Materials: 1,3-Bis(stearoyl)urea
and 1,1,3,3-Tetrastearoylurea for Potential Solar
Applications" **N. Gökşen Tosun, A. Çetin & C. Alkan**

#99 "Interfacial Thermal Resistance Between Water
and Metals Using Molecular Dynamics Simulation"
M.M. Aksoy & Y. Bayazitöglü

#100 "Thermal Conductivity of Copper-Single Walled
Carbon Nanotube Using Non-Equilibrium Molecular
Dynamics" **K. Toprak & Y. Bayazitöglü**

16:30 - 16:45 (GMT+3)

Break

Wednesday - August 11, 2021

Zoom Link 1

Keynote Session 12

Session Chair: Can Ozgur Colpan, Turkey

Keynote Talk 24

16:45 – 17:30 (GMT+3)

Li Shi

The University of Texas at Austin, USA

Atomic-Scale Phonon Band Engineering of Semiconductors

Keynote Talk 25

17:30 – 18:15 (GMT+3)

Mochammad Hadid Subki

International Atomic Energy Agency (IAEA), Austria

Advances on Small Modular Nuclear Reactor Technology Developments

16:45
18:15
(GMT+3)

Zoom Link 2

Invited Session 8

Session Chair: Nuri Azbar, Turkey

Invited Talk 21

17:15 – 17:45 (GMT+3)

Sandro Nižetić

University of Split, Croatia

Photovoltaic Thermal Collectors with Incorporated Phase Change Materials: Analysis of Design Approaches

Invited Talk 22

17:45 – 18:15 (GMT+3)

David G. Whitten

The University of New Mexico, USA

Novel, Light-Activated Antimicrobials for Elimination of Viral Pathogens

Zoom Link 3

General Session 15

Energy & Environment – II,

Session Chair: Farrukh Khalid, Turkey

#17 "Experimental Study of Red Pine Biocoal and Soma Lignite Blends in a Circulating Fluidised Bed Under Oxy-Fuel Combustion" B. Keivani, H. Olgun & A.T. Atimtay

#114 "Development of Environmental Sustainability Indicators Based on the Efficiency of Integrated Buildings" M.Z. Sogut

#106 "Thermo-Environmental Performance Assessments of a Medium-Scale Aero Turbojet Engine" H.Y. Akdeniz, O. Bali & H. Caliskan

#104 "Effects of Design Variables on Exergy and Environmental Parameters of Commercial Turbofan Engine" H. Aygun, M.B. Sheikhi & H. Caliskan

#110 "A Methodology for Thermodynamic Performance Comparison of the Crop Production" M.T. Balta

#14 "Cost Description and Characterisation of Gas Enhanced Oil Recovery Processes" O. Abunumah, P. Ogunlode & E. Gobin

Thursday - August 12, 2021

Zoom Link 1

Keynote Session 13

Session Chair: Sandro Nižetić, Croatia

Keynote Talk 26

09:00 – 09:45 (GMT+3)

Lidia Morawska

Queensland University of Technology (QUT), Australia

Air Pollution and Energy: "this discussion is closed!"

Keynote Talk 27

09:45 – 10:30 (GMT+3)

Keith Bell

UK Energy Research Centre & University of Strathclyde, UK

Powering Past Fossil Fuels: Electricity and Net-Zero Greenhouse Gas Emissions

09:00
10:30
(GMT+3)

Zoom Link 2

General Session 16

Energy Management & Strategies

Session Chair: Emrah Biyik, Turkey

#113 "Assessment of Operational Control Strategies on Energy Efficiency and Management of Production Processes" M.Z. Sogut & T.H. Karakoc

#118 "An Urban Green Energy Strategy Proposals for Local Governments" M.O. Balta

#33 "Methylene Blue Adsorption on Biochar Prepared from Pumpkin Shell" D. Bala, Ç. Özer & M. İmamoğlu

#85 "Production Scheduling of a Natural Gas Power Plant" M.G. Güler, E. Geçici & S.B. Gündüz

#115 "Experimental Air-Cooled Battery Thermal Management Approach" B. Tarhan, O. Yetik & T.H. Karakoc

#13 "The Effect of Pressure and Porous Media Structural Parameters Coupling on Gas Apparent Viscosity" O. Abunumah, P. Ogunlode & E. Gobin

Zoom Link 3

General Session 17

Modeling & Simulation – II

Session Chair: Hasan Ozcan, UK

#101 "Development and Analysis of a Novel Greenhouse Roof for Reduced Cooling Load in Hot Climates" Y. Bicer, M.U. Sajid & M. Al-Breiki

#102 "Development and Validation of a Dynamic Thermal Model for a Water Wall Integrated Indoor" N. Altunacar, I. Şener, Y. Yaman, B. Budakoğlu, E. Topkara, A. Esmer, M.A. Ezan, A. Tokuç, G. Köktürk & I. Deniz

#103 "Analysis of Optimum Flow Rate of a Photovoltaic Thermal System (PVT) Integrated with Phase Change Materials (PCM)" C. Kandilli & B. Mertoglu

#61 "Exergy Analysis of a Steam Power Plant at Full and Partial Load Conditions" U.G. Azubuike, H.O. Njoku & O.V. Ekechukwu

#130 "Technological Assessment of a Solar PV Collector for Freshwater, Cooling, and Electricity" E. Khalid

#68 "Mathematical Modelling of Adsorption Isotherms for Porous Bed with Axial Dispersion Model" M. Sidhareddy & S. Tiwari

10:30 - 10:45 (GMT+3)

Break

Thursday - August 12, 2021

10:45
12:15
(GMT+3)

Zoom Link 1 General Session 18 Energy Conversion & Management – II, Session Chair: Yusuf Bicer, Qatar	Zoom Link 2 General Session 19 Hydrogen Energy Technologies - III Session Chair: Canan Acar, Netherlands	Zoom Link 3 General Session 20 Energy & Environment – II Session Chair: Ayca Tokuc, Turkey
<p>#31 "Characterization of Hydroxyethyl Cellulose/Active Carbon Composites" <u>M. Zor</u>, F. Şen, B. Oran & Z. Candan</p> <p>Invited Talk 23 11:00 – 11:30 (GMT+3) Arif Günyar Managing Director ENERCON, Turkey The Future of Wind Energy Sector</p> <p>#133 "Modelling and Simulation of Molten Carbonate Fuel Cell and Copper-Chlorine Cycle Based Power Generation System with The Incorporation of PID Controller" H. Kamran, U. Mudassir, A.M. Ali, M.A. Raza, K. Khan, K. Kamal & <u>T.A.H. Ratlamwala</u></p> <p>#54 "Techno-Economic and Environmental Impact Assessments of Trigereneration Systems with Various Fuels" <u>E. Sorgulu</u> & I. Dincer</p> <p>#134 "Artificial Intelligence Based Prediction of Outputs of Geothermal Energy Based Multigeneration System" <u>Q.N. Haider</u>, S.M. Ali, K. Kamal & T.A.H. Ratlamwala</p>	<p>#122 "Green Hydrogen Production Potential in Turkey with Wind Power" I. Dincer, N. Javani & <u>G.K. Karayel</u></p> <p>#123 "Blue H₂ Generation by Steam Reforming of Synthetic Biogas in a Membrane Reactor Packed with a Novel Ruthenium-Nickel Catalyst" <u>A. Lulianelli</u>, C. Italiano, M. Manisco, A. Brunetti, A. Figoli, G. Drago Ferrante, L. Pino & A. Vita</p> <p>#95 "A Photoelectrochemical Reactor for Ion Separation and Hydrogen Production" <u>M.L. Aydin</u>, H. Selcuk & I. Dincer</p> <p>#50 "Solar and Sonolysis Assisted Hydrogen Recovery from Industrial Sulphide Wastewater using CNT-ZnS/Fe₂O₃" <u>P. Vijayarangan</u>, S. Maurya & S. Manoharan</p> <p>#109 "Coupled Thermal-Electrochemical Analysis of Polymer Electrolyte Membrane Electrolyser" F.M. Nafchi, E. Afshari & <u>E. Baniasadi</u></p> <p>#108 "Exergetic Optimization of a Combined Solar Power Plant and Hydrogen Production System with Nano-Fluid and Energy Storage System" <u>M. Shirazi</u>, E. Baniasadi, E. Afshari & N. Javani</p> <p>#136 "Multi-Objective Optimization of a Multistage Vapor Compression Refrigeration Cycle" A. Ustaoglu, B. Kursuncu, <u>A.M. Kaya</u> & H. Caliskan</p>	<p>#138 "0-D Parallel Circuit Modeling of Solid Oxide Fuel Cell" <u>A. Erdogan</u>, A.C. Ince & C.O. Colpan</p> <p>#139 "Performance of Solar Assisted Dual Source Heat Pump" <u>K. Kaygusuz</u>, Ö. Kaygusuz & T. Ayhan</p> <p>#140 "Capric and Myristic Acid Mixture with Gypsum Wallboard for Latent Heat Energy Storage" K. Kaygusuz & <u>A. Sari</u></p> <p>#105 "Asymmetric and Symmetric Coin Cell Supercapacitors by Deposition of Graphene for Energy Storage Applications" <u>O. Yargi</u>, M. Ozmen, S. Buyuk Pehlivan & A. Gelir</p> <p>#93 "Microencapsulation of Three-Component Thermochromic Systems (Fluoran Dye-Phenolphthalein-N-Tetradecanol) in Poly (Methyl Methacrylate)" C. Alkan, S. Ozkayalar, <u>S. Demirbağ</u>, <u>Geng</u>, M.S. Tözüm & S. Alay Aksoy</p> <p>#96 "Climate Impact of Blockchain in the View of Cryptocurrencies" <u>N. Gure</u></p> <p>#137 "A Policy on Renewable Hydrogen Ecosystem in Turkey" <u>A. Midilli</u></p>

12:15 - 13:15 (GMT+3)

Break

Thursday - August 12, 2021 - Zoom Link

13:15
15:15
(GMT+3)

Panel Discussion Session 3: Status and Perspectives of Photovoltaic Technologies: Global and Local Approaches

Moderator: Rasit Turan, Turkey

Panel Speakers

- Shravan Kumar Chunduri**, Head of Technology at TaiyangNews UG
- Dr. Firat Es**, Head of the R&D Department, Kalyon PV, Turkey
- Mr. Criss Jin**, Huasun Energy, China
- Dr. Paul Ni**, Vice President and CTO of Talesun Solar.
- Dr. Hariharsudan Sivaramakrishnan**, IMEC, Belgium
- Dr. Wang Wenjing**, Huasun Energy, China
- Mr. Tommy Xu**, Huasun Energy, China

15:15 - 15:30 (GMT+3)

Closing Ceremony

TÜBA – Energy Working Group Members

- Prof. Dr. İbrahim Dinçer / Chairman Prof. Dr. Kamil Kaygusuz
- Prof. Dr. Mehmet Hakkı Alma Prof. Dr. Adnan Midilli
- Prof. Dr. Erol Arcaklıoğlu Prof. Dr. Murat Öztürk
- Prof. Dr. Yıldız Bayazitoğlu Prof. Dr. Niyazi Serdar Sarıçiftçi
- Prof. Dr. Arif Hepbaşı Prof. Dr. Bahri Şahin
- Prof. Dr. Sadık Kakaç Prof. Dr. Raşit Turan



Plenary Speakers

DR. CHRISTIAN RAKOS

President of the World Bioenergy Association (WBA), Austria

Transforming Bioenergy Use in the Developing World – A Key Target for Sustainable Development and Net Zero Carbon Emissions



The traditional use of bioenergy for cooking and heating provides the main source of energy for 3 Billion people at a high cost. It is extremely inefficient, contributes significantly to deforestation with all its negative consequences and exposes women and children to high levels of air pollution that cause over 4 million premature deaths every year.

Transitioning away from the traditional use of firewood or charcoal to modern forms of bioenergy has been identified as a key sustainable development goal and also as a precondition to achieve Net zero emissions by 2050 in a recent report of the International Energy Agency.

Three steps are necessary for this transition: progressing from unprocessed biomass to dry homogenous densified biomass fuels by pelletization or briquetting, transitioning from wood harvested for energy as raw material to residues of agriculture and applying the most advanced technology for the combustion of biomass – the gasification process.

The presentation will show technologies that are available today for advanced biomass cooking and discuss the economics of this transition. While fossil fuels such as LPG are often regarded as the best solution for clean cooking it can be shown, that the energy costs of bottled LPG are more than twice as high as for biomass pellets.

The most important barrier for modern gasification cookstoves is the capital investment. These stoves cost between 50-100\$, which might seem a small investment. For poor households it is a lot. Growing voluntary markets for carbon emission certificates raise the hope, that these markets could provide the capital needed for a swift transition away from traditional bioenergy use.

PROF. DR. FERIDUN HAMDULLAHPUR

Past President, University of Waterloo, Canada

An Overview of the Role of Universities on Energy and Sustainability



“Climate change is the defining issue of our time and, we are at a defining moment” was the opening statement of the United Nations Secretary General Antonio Guterres at the September 2018 General Assembly. Today, we fully recognize that climate change is one of the most pressing global issues facing the world. As the scientific understanding of human influence on the climate system is continually refined and the impacts become more apparent, action is catalyzing across all scales. We also recognize the ever-growing need for more energy for the growing population of the world as well as satisfying the needs of many sectors including industry, transportation, agriculture, etc. This presentation provides a realistic analysis of the most up to date energy supply and demand picture and projections for the next decade. The current status of renewable energy capacity and potential of growth technologies will be incorporated into the possibility of carbon neutrality for many nations by 2050. To reach this goal, institutions and, more broadly, nations will need to align foundational directions that increase priority, improve transparency, provide financial support, and build capacity. These require action along several distinct carbon reduction pathways including efficiency improvement and reduction in energy consumption. Finally, the role of higher education institutions will be discussed to provide short and long term perspectives on the convergence of education, research and practice and how they align with institutional policy and systems toward the carbonneutral goal.



Keynote Speakers

PROF. DR. BENJAMIN K. SOVACOOOL

University of Sussex, UK

Decarbonisation and Its Discontents: A Critical Justice Perspective on Four Low-Carbon Transitions

What are the types of injustices associated with low-carbon transitions? Relatedly, in what ways do low-carbon transitions worsen social risks or vulnerabilities? Lastly, what policies might be deployed to make these transitions more just? The presentation answers these questions by first elaborating an “energy justice” framework consisting of four distinct dimensions—distributive justice (costs and benefits), procedural justice (due process), cosmopolitan justice (global externalities), and recognition justice (vulnerable groups). It then examines four European low-carbon transitions—nuclear power in France, smart meters in Great Britain, electric vehicles in Norway, and solar energy in Germany—through this critical justice lens.

In doing so, it draws from original data collected from 64 semi-structured interviews with expert participants as well as five public focus groups and the monitoring of twelve internet forums. It documents 120 distinct energy injustices across these four transitions. It then explores two exceedingly vulnerable groups to European low-carbon transitions, those recycling electronic waste flows in Ghana, and those mining for cobalt in the Democratic Republic of the Congo. The presentation aims to show how when low-carbon transitions unfold, deeper injustices related to equity, distribution, and fairness invariably arise.

PROF. DR. RICHARD S. J. TOL

University of Sussex, UK

The Economic Impact of Climate and Weather

I propose a new conceptual framework to disentangle the impacts of weather and climate on economic activity and growth: A stochastic frontier model with climate in the production frontier and weather shocks as a source of inefficiency. I test it on a sample of 160 countries over the period 1950-2014. Temperature and rainfall determine production possibilities in both rich and poor countries; positively in cold countries and negatively in hot ones. Weather anomalies reduce inefficiency in rich countries but increase inefficiency in poor and hot countries; and more so in countries with low weather variability. The climate effect is larger than the weather effect.

PROF. DR. SC. NEVEN DUIĆ

University of Zagreb, Croatia

Decarbonisation of Energy Systems with Variable Renewables

Transition to decarbonised energy systems is becoming more attractive with fall of investment costs of variable renewables and volatile prices and political insecurity of fossil fuels. The renewable energy resources are bountiful, especially wind and solar, while integrating them into current energy systems is proving to be a challenge. Solar has reached cost parity making it cheapest electricity source for retail customers in most of the World, creating new prosumer markets. The limit of cheap and easy integration for wind is 20% of yearly electricity generation, while a combined wind and solar may reach 30%. Going any further asks for implementation of really free energy markets (involving day ahead, intraday and various reserve and ancillary services markets), demand response, coupling of wholesale and retail energy prices, and it involves integration between electricity, heating and cooling, water and transport systems. The cheapest and simplest way of increasing further the penetration of renewables is integrating power and heating/cooling systems through the use of district heating and cooling (which may be centrally controlled and may have significant heat/cold storage capacity), since power to heat/cold technologies are excellent for demand response. Electrification of light road transport allows not only for significant increase of energy efficiency, but also, electric cars due to low daily use may be excellent for demand response and even as storage, through smart charging and vehicle to grid technology. Buildings and cities will become important with their high potential for demand response implemented through smart retail markets. That will allow reaching 80% renewable in energy system, but the remaining 20% may be more of an uphill battle without technology breakthrough. Long haul road transport may be driving on electrified roads, but long-distance aviation and maritime transport, as well as some high temperature industrial processes, cannot yet be easily electrified. Biomass, if not used for producing electricity and heat, may cover half of those needs, but the rest will have to come from some other technology. Inductive highways, innovative high energy density batteries and power to synthetic fuels, or so-called e-fuels, which may include hydrogen, are all very hot research issues.

PROF. DR. SAMI EROL GELENBE

Polish Academy of Sciences, Poland

Energy Consumption by ICT: Facts, Measurements and Trends

Contrary to our expectations, the energy consumption by ICT is a controversial subject where experts of different organizations express divergent views. Obviously, experts from the computer industry will tend to vaunt the increasing efficiency of digital equipment, while those that are concerned with sustainability will stress the projected increase of energy consumption by ICT, as well as the increasing use of rare and polluting materials for the fabrication of devices and computer chips. ICT is often put forward as the means to obtain energy consumption savings, and the reduction of CO2 emissions, while ICT has over the last decade substantially increased its overall share of electricity consumption, going from 4-5% a decade ago, to perhaps 8-10% of total electricity production in the years 2018-2019. Indeed, nowadays the manufacturing of ICT devices may represent as much electricity consumption in one year as the total annual electricity consumption to run the devices. It is also estimated that new applications such as Crypto-currencies consume as much electricity as a small but advanced country such as the Netherlands. It is also expected that 5G will cause an increase of energy consumption by communication networks in the first instance, before the means to reduce this consumption are included in later generations of these wireless mobile communication systems. One of the basic reasons for the controversies about ICT's energy consumption is the relative paucity of experimental data. Indeed it is technically possible to globally monitor the energy consumption by ICT but would require the industry that provides and operates ICT devices such as computers, laptops, mobile devices, network forwarders, routers, wireless base stations and IoT devices to take an active role. Thus in our talk we will first present an overview of different energy consumption figures by ICT, and then provide a specific example of the manner in which power and energy consumption can be measured in current digital equipment. Our presentation will then detail some trends and figures, and discuss them in the light of the manner in which technology and ICT systems themselves are evolving.

PROF. DR. RAVI P. SILVA CBE

University of Surrey, UK

A Net Zero Carbon World through Innovation in Energy Materials

Over the last century, humanity has produced cheap energy generated by burning coal/oil and gas to sustain industry, domestic heating and electricity. This has resulted in the energy mix to be still dominated by nearly 80% of fossil fuels despite a climate emergency. The world is now marching towards a net carbon zero position, with changes urgently needed to the world energy mix, all manufacture, including the electronic device industry as well as powering devices during its operational lifetime.

The need for novel green energy harvesting and storage materials, with a proven record for scaling and manufacture is real and present. In order to be able to deliver truly sustainable technology, the design of devices need to be full cradle to grave analysis of its carbon credentials. Plastic electronics are ideally suited to produce such devices with some of the lowest carbon footprints. This is further extended during the operational modes by being able to self-power and use low power operational modes. Within the talk we will examine next generation designs for sustainable nanodevices and renewable energy harvesting systems to help reduce the impact on the carbon foot-print. This will include energy harvesting systems that include plastic photovoltaics (OPV, PSC) and Triboelectric nanogenerators (TENG). Examples on the usage of polymers and bio-degradable and/or non-toxic materials to design and fabricate nano-devices to contribute towards a net-zero carbon society will be discussed. The Advanced Technology Institute (ATI) focus on net-zero carbon themes, by developing flexible, wearable, and unobtrusive energy harvesting and nano-storage devices including solar cells, TENGs, and supercapacitors, etc., which will be central to future IoT smart technologies. Such nanodevices can be utilized to embed in infrastructures for higher quality living.

PROF. DR. MARC A. ROSEN

Ontario Tech University, Canada

Energy Sustainability for Sustainable Development

Sustainable development is a critically important goal for societal and human activity. Energy sustainability is of great importance to any efforts for overall sustainable development. This is particularly important given the pervasiveness of energy use, its importance in economic development and living standards, and the significant impacts that energy processes and systems have on the environment.

Many factors that need to be considered and appropriately addressed in moving towards energy sustainability are examined in this talk. These include appropriate selection of energy resources bearing in mind sustainability criteria, facilitation of the use of sustainable energy resources, enhancement of the efficiency of energy-related processes, and a holistic adoption of environmental stewardship in energy activities.

In addition, other key sustainability measures are addressed, such as economics, equity, land use, lifestyle, sociopolitical factors and population. Conclusions are provided related both on options for energy sustainability and on means to achieve sustainable development.

PROF. DR. KEVIN TRENBERTH

National Center for Atmospheric Research (UCAR), USA

The Changing Flow of Energy Through the Climate System

Global warming really means global heating, which arises mainly from increasing greenhouse gases in the atmosphere from human activities. Carbon dioxide concentrations have increased by 48% mainly from burning fossil fuels. Some heat goes into raising temperatures, often referred to as global warming. Most energy goes elsewhere: warming the oceans, melting ice, and evaporating moisture. 93% of the excess energy ends up in the ocean as ocean heat content which means the ocean expands and sea level rises. Sea level also rises from melting land ice, including ice sheets of Greenland and Antarctica. However, excess energy means more drying, more water vapor in the atmosphere, stronger storms, and heavier rains, but where it is not raining, there are more heatwaves and drought, and more wildfires. The climate change effects intersect nonlinearly with weather (natural variability) so that effects move around in space and time, and can change from one extreme (heat) to another (flooding) very quickly. Extremes generally worsen, nonlinearly amplifying damages and costs, producing “The straw that breaks the camel’s back” syndrome.

PROF. DR. JIANLEI NIU

The Hong Kong Polytechnic University, China

Progresses in Thermal Energy Storage Research to Reduce the Energy Use in Buildings

In this talk, I will speak of the TES technology development from the building application perspective. Currently two technologies, namely hot/chilled water storage and ice storage, have been the dominant ones. In the case of chilled-water storage for-air-conditioning application, because of the small working temperature range, typically between 7 and 12oC, stratification of the storage tank is a norm for its effective operation. The general problem with water and ice storage is that the former relies on sensible energy, and thus tank is bulky while the phase change temperature of the latter is below 0 oC, which is far below the temperature needed for air-conditioning applications, and would significantly lower the COP of the chiller system in an energy wasteful manner. These two key issues form the two major factors that have driven the search for alternatives. In particular phase-change-materials(PCM) based thermal storage technology has been the focus. I will speak the recent progresses in tackling the overcooling problem- bottle neck of PCM applications. The possible application modes in terms of active versus passive applications, different PCM application forms in PCM/MPCM, MPCM/water slurry, PCM water emulsions will be discussed; and bulk PCM capsule packed-bed, shell and tube PCM designs and their optimization will also be covered.

DR. OLCAY UNVER

Arizona State University, USA

Pathways to Sustainability in an Increasingly Water-Scarce World

Water is an essential resource for all life on our planet and its sustainability is under threat due to environmental degradation, increasing demands from all sectors, unsustainable practices, and climate change. As it flows not only across geographical boundaries but also across social and economic sectors, its quality and quantity are impacted by our activities, which, in turn, can make it unavailable for our development plans. The speaker will review the state of this resource, level of achievement of the global commitments, possible pathways towards sectoral goals, and the consequences of these pathways.

PROF. DR. HENRIK LUND

Aalborg University, Denmark

Smart Renewable Energy Systems and decarbonisation.The Danish Target of a 70% decrease in CO₂ emission by 2030

This presentation focus on how societies can design and implement renewable energy and decarbonisation strategies. The presentation presents and discuss a set of methods and criteria to design Smart Energy Systems, while taking into account the context of 100% renewable energy on a national level. Countries should handle locally what concerns local demands, but acknowledge the international context when discussing resources and industrial and transport demands. To illustrate the method, it is applied to the case of Denmark within the context of a European and a global energy system.

Recently, the Danish Government supported by the Danish Parliament decided for the target of a 70% decrease in Greenhouse gasses by 2030. This presentation includes a list of theoretical and methodological considerations as well as a concrete proposal on how such targets can be implemented. It is highlighted that already now one have to think beyond 2030 in order to prepare for the next step to achieve a fully decarbonisation by 2040 or 2050. It is also highlighted that a country such as Denmark have to consider how to include its share of international shipping and aviation as well as how to design a solution with Denmark's share of sustainable biomass resources.

PROF. DR. IGOR PIORO

Ontario Tech University, Canada

Current Status and Future Developments in the Nuclear-power Industry of the World

Due to emerging climate change concerns coupled with growing global energy demand, eventually the world needs to move towards electricity generation with lower carbon emissions including increased use of nuclear power, and hydro, wind, geothermal, solar, and tidal sources. However, only nuclear power, is high reliability, and of potentially large installed capacity that can operate with high capacity factors (up to 90 – 100%). The other sources are lower capital cost, but mainly limited by Nature as to lower reliability, capacity factors, and location. It is clear that nuclear power can make a significant, indeed vital contribution to the stated political objectives, industrial positioning and social goals of becoming “Zero Carbon” or “Carbon Neutral” by dates varying from 2030 to 2050.

This paper is a logical continuation of our previous publications on the current status of nuclear-power industry of the world. Unfortunately, within last 9 years, electricity generation with nuclear power has decreased from 14% before the Fukushima Nuclear Power Plant (NPP) severe accident in March of 2011 to about 10%. However, the last couple of years were very important for the world nuclear-power industry, because long-term expected new Generation-III+ nuclear-power reactors / plants were put into operation in China, Russia, and S. Korea, and more reactors are planned to be put into operation in these and other countries such as Bangladesh, Belarus', Finland, India, Turkey, UAE, and USA within next 3 – 4 years.

CURRENT STATUS AND FUTURE DEVELOPMENTS IN THE NUCLEAR-POWER INDUSTRY OF THE WORLD

I. Piore and M. Tsai

University of Ontario Institute of Technology, Oshawa, Ontario, Canada
Corresponding author e-mail: Igor.Piore@uoit.ca

ABSTRACT

Ten years have passed after the Fukushima-Daiichi NPP severe accident, which was the second largest one in the world after the Chernobyl NPP disaster in April of 1986. The latter had very significant impact on the world nuclear-power industry, which we can see even today. However, the Fukushima-Daiichi NPP severe accident had very significant impact on nuclear-power industry in Japan and selected countries, but the world nuclear-power industry started to recover after the Chernobyl NPP severe accident somewhere from 2010. In spite of that, electricity generation at NPPs in the world has declined from ~14.4% before the Fukushima-Daiichi NPP severe accident to about 10.4% nowadays (Table 1). Therefore, it is important to evaluate current status of nuclear-power industry in the world with that before the Fukushima-Daiichi NPP severe accident and to understand future trends.

Keywords: Nuclear-power reactor, nuclear power plant, nuclear industry

INTRODUCTION

Nuclear power is the concentrated and reliable source of almost infinite energy, which is almost independent of weather conditions; has high-capacity factors, often in excess of 90% with long operating cycles, making units suitable for continuous base-load operation; has essentially negligible operating emissions of carbon dioxide and relatively small amounts of wastes generated plus relatively small amount of fuel required compared to that of fossil-fuel thermal power plants. As a result, nuclear power is considered as the most viable source for electricity generation within next 50 – 100 years. However, nuclear power must operate and compete in energy markets based on relative costs and strategic advantages of the available fuels and energy types.

Table 1. Electricity generation in the world and selected countries by source: Population is taken from <https://www.worldometers.info>; EEC and HDI from Wikipedia; and data on electricity-generating sources from <https://www.iea.org>.

No	Country	World	China	India	USA	Russia	Japan	Turkey	Germany	UK	France	S. Korea	
	-	0	1	2	3	4	5	6	7	8	9	10	
1	Population, M	7,867	1,444	1,392	333	146	126	84	84	68	65	51	
2	EEC	TW h/year	23,398	7,226	1,547	3,990	965	903	251	539	301	449	527
3		W/Capita	350	527	107	1387	763	816	344	732	513	765	1,163
4	HDI	Total	0.737	0.761	0.634	0.926	0.824	0.919	0.820	0.939	0.932	0.901	0.916
5		Rank	99	85	131	17	52	19	54	4	13	26	23
Electricity-generating sources													
1	Coal	36.7	66.4	71.0	24.2	15.8	31.6	37.3	29.3	2.4	1.1	39.6	
2	Gas	23.5	3.3	4.5	37.4	46.4	33.9	18.8	10.5	40.9	6.7	27.3	
3	Nuclear	10.4	4.1	2.9	19.3	18.7	6.4	-	13.7	17.3	70.0	24.7	
4	Oil	3.1	0.2	0.5	0.8	1.1	4.8	0.2	-	0.3	1.1	2.4	
Non-renewable in total		73.7	74.0	78.9	81.7	82	76.7	56.3	53.5	60.9	78.9	94.0	
1	Hydro	15.8	17.1	10.9	6.8	17.5	8.8	29.3	3.8	2.4	10.9	1.1	
2	Wind	5.3	5.1	4.1	6.9	-	0.8	7.2	24.5	19.8	6.1	0.5	
3	Solar	2.7	2.4	3.2	2.2	-	7.4	3.2	9.1	3.9	2.0	2.2	
4	Geothermal	2.5	-	-	0.4	-	0.3	2.9	-	-	-	-	
5	Biomass		1.3	2.8	1.3	-	1.8	1.1	8.6	10.2	1.1	1.5	
Renewable in total		26.3	25.9	21.0	17.6	17.5	19.1	43.7	46	36.3	20.1	5.3	
1	Other	-	0.2	-	0.5	0.3	4.2	-	0.5	2.8	1.0	0.7	

CURRENT STATUS OF NUCLEAR-POWER INDUSTRY OF THE WORLD

Current statistics on all world nuclear-power reactors connected to electrical grids are listed in Table 2. The largest group of reactors by type is PWRs (68% of the total number), and quite a significant number of PWRs are planned to be built (about 38 (+35?)). The 2nd largest group of reactors is BWRs (14%). The 3rd group is PHWRs (11%). Considering the number of forthcoming reactors, the number of BWRs and PHWRs will decrease globally within next 20 – 25 years. Furthermore, within next 10 – 15 years or so, all LGRs and AGRs will be shut down forever.

In summary: 33 countries have operating nuclear-power reactors; 20 countries from these 33 and 3 countries without reactors plan to build new nuclear-power reactors. In addition, 30 countries are considering, planning, or starting nuclear-power programs, and about 20 countries have expressed their interest in nuclear power (for details, see Table 3).

Table 2. Number of nuclear-power reactors by type connected to electrical grid and forthcoming units as per June 2021 and prior to Japan earthquake and tsunami disaster (based on data from Nuclear News (ANS, USA)).

No	Reactor type (% of total reactors / average installed capacity)	No. of units		Installed capacity, GW _{el}		Forthcoming units	
		As of June 2021	Before Mar. 2011	As of June 2021	Before Mar. 2011	No. of units	GW _{el}
1	PWRs (68% / 955 MW _{el})	303 ↑	268	289 ↑	248	38+35?	44+37? ¹
2	BWRs / ABWRs (14% / 1030 MW _{el})	62 ↓	92	64 ↓	84	4?	5.3?
3	PHWRs (11% / 500 MW _{el})	49 ↓	50	24	25	2+5?	1.3+3.3?
4	AGRs (CO ₂ -cooled) (3% / 550 MW _{el})	14 ↓	18	8 ↓	9	1*	0.2*
5	LGRs (3% / 700 MW _{el})	12 ↓	15	8 ↓	10	0	0
6	LMFBRs – SFRs (0.5% / 690 MW _{el})	2 ↑	1	1.4 ↑	0.6	2+1?	1.1+0.6?
In total		442 ↓	444	395 ↑	377	43+45?	47+46?

Explanations to Table 2: Arrows mean decrease or increase in a number of reactors and installed capacities. ¹ ? – Means “Commercial start date – indefinite”. Data in Table 1 include 33 reactors in Japan, 24 of which were not in service as of October 2020. *Forthcoming reactor is a helium-cooled reactor – High Temperature Reactor Pebble-bed Modular (HTR-PM) (China).

Table 3. Current activities worldwide on new nuclear-power-reactors build (Nuclear News (ANS, USA)).

No	Country / Nuclear supplier	Countries with new builds (No. of possible units)
1	Russia / Rosatom (outside Russia - ASE (AtomStroyExport) (Nuclear-power activities are supported by Russian government)	Russia (5+3?), Bangladesh (2), Belarus (1), China (4), Egypt (1+3?), Finland (1), Hungary (2?), India (2+2?), Iran (2), and Turkey (4): In total: 22+10?=32
2	China / Various vendors (Nuclear-power activities are supported by Chinese government)	China (9+14? ¹), Pakistan (3?), Romania ² (2? CANDU [®] reactors): In total: 9+19?=28
3	S. Korea / Doosan and Kepco	S. Korea (4) and UAE (3): In total: 7
4	India / Various vendors	India (3+3? PHWRs): In total: 6
5	France / Framatome	Finland (1), France (1?), and UK (2): In total: 3+1?=4
6	USA / GE and Westinghouse	USA (2) and Taiwan (2?): In total: 2+2?=4
7	Czech Rep. / Skoda	Slovakia (2), Ukraine (2?): In total: 2+2?=4
8	Japan / Toshiba + Hitachi	Japan (2?): In total: 2?
9	Canada / AECL (Candu Energy, Inc.) together with CGNPC (China)	Romania ² (2? CANDU [®] reactors): In total: 2?
10	Germany / KWU (KraftWerk Union AG)	Brazil (1?): In total: 1?
11	Argentina / CNEA	Argentina (1?): In total: 1?

REFERENCES

Piolo, I., Duffey, R.B., Kirillov, P.L., and Dort-Goltz, N., 2020. Current Status of Reactors Deployment and SMRs Development in the World, ASME J. NERS, **6** (4), 24 pages. Free download from: <https://asmedigitalcollection.asme.org/nuclearengineering/article/6/4044001/1085654/Current-Status-of-Reactors-Deployment-and-Small>.

Piolo, I., Duffey, R., Kirillov, P., et al., 2019. Current Status and Future Developments in Nuclear-Power Industry of the World, ASME J. NERS, **5** (2), 19 pages. Free download from: <https://asmedigitalcollection.asme.org/nuclearengineering/article/doi/10.1115/1.4042194/725884/Current-Status-and-Future-Developments-in-Nuclear>.

Handbook of Generation IV Nuclear Reactors, 2016. Editor: I.L. Piolo, Elsevier – Woodhead Publishing (WP), Duxford, UK, 940 pages.

PROF. DR. ZHU HAN

University of Houston, USA

Distributed Deep Reinforcement Learning for Renewable Energy

Nowadays, microgrids (MG) have attracted much attention, as a key technology of the Internet of Energy (IoE). A great deal of research have shown that the hierarchical microgrid is a more novel structure of IoE. Although the hierarchical microgrid model solves the problem of weak power scheduling capability across microgrids, it suffers from severe communications uncertainty, which can lead to communication delay and fluctuation. To obtain the accurate result of the renewable energy accommodation assessment capacity, a hierarchical microgrid model considering communication uncertainty is investigated. The solution to solve the problem of the assessment renewable energy accommodation capacity for hierarchical MG is a hybrid control based on distribution deep reinforcement learning. The temporal difference (TD) generation adversarial network (TD-GAN) is proposed as a value-based method. Compared with the policy-based method, it can better solve the distributed problem in hybrid control with a generation adversarial network (GAN). Moreover, the challenge that the method cannot handle a continuous action space is solved by using a normalized advantage function (NAF). The method similar with the TD error method is employed to train the GAN network. Simulation results using real power grid data demonstrate the effectiveness and accuracy of the proposed method.

PROF. DR. MOHAMMAD SHAHIDEHPOUR

Illinois Institute of Technology, USA

Optimal Expansion and Operation Planning of Microgrids Using a Two-Stage Data Clustering Strategy

This presentation offers a two-stage planning model for the optimal expansion capacity and operation of renewable power generation and storage devices in constrained microgrids. Considering the variable characteristics of renewable power generation, we devise a chronological clustering algorithm by combining similar-type data for representative operating periods (ROPs). In recent years, several data clustering algorithms were considered to attain the pertinent ROP data. Some scholars used k-means algorithm to extract the representative information from large sums of data. Hierarchical clustering (HC) and fuzzy C-means were also applied frequently. A modified HC method used the relatively fast k-means clustering and then applied the HC method to maintain the advantages of both methods. The above algorithms have made valuable discoveries on how to select ROPs. However, there is still a critical mandate for exploring suitable data clustering approaches that can capture more information with fewer operating points. Our proposed clustering model applies two time series with different resolutions for the ROP approximation. The reduced time series (RTS) is applied to those planning constraints which do not demonstrate any continuity in time, and the sequence-preserving time series (STS) is applied to multi-period temporal constraints. The use of time series methods preserves spatial and chronological information and correlations among data types. They also maintain the requirements for constraints which span over a longer planning horizon, as well as finer time resolutions required for a microgrid operation planning. We recognize that the operation constraints realized in the planning horizon afford more accurate planning results. The metrics and criteria of representativeness are utilized to evaluate the performance of our clustering method in terms of the computation time and the accuracy of planning results.

PROF. DR. ROLAND N. HORNE

Stanford University, USA

Global Geothermal Outlook and Sustainable Development 2021

Geothermal energy has undergone a renaissance over the past 15 years, as many new technologies and new countries have joined the industry. Climate change concerns have focused attention on renewable energy, supported by a global ambition to address greenhouse gas reduction. Geothermal developments have accelerated in many parts of the world, both in countries (such as Turkey, Indonesia, Kenya, New Zealand, and the US) that have a traditional interest in “conventional” geothermal resources, as well as countries without a historical community in geothermal energy (such as France and Germany). Some new developments have

followed well-worn paths using conventional hydrothermal resources in volcanic regions, while others have struck out in new directions in Enhanced Geothermal System (EGS) projects in nonvolcanic regions.

As an example of the development of traditional, volcanic geothermal resources, the United States is the world’s largest producer of geothermal electricity, with an installed capacity of 3700 MW (in 2020). In 2020, the state of California generated about 6% of its electricity from geothermal sources, while the state of Nevada generated 9%. As another example, Turkey increased capacity from 397 MW in 2015 to 1549 MW in 2020.

Technology has allowed for developments of conventional resources with lower temperature, restricted water access, and constrained surface utilization. EGS projects have launched in a variety of different directions and places. The use of innovative hybrid plants, lower resource temperatures and enhanced reservoir stimulation has made geothermal energy accessible in a much wider variety of places.

PROF. DR. ARUMUGAM MANTHIRAM

The University of Texas at Austin, USA

Sustainable Battery Chemistries for E-Mobility and Renewable Energy Storage

Rapid increase in global energy use and growing environmental concerns demand clean, sustainable, alternative energy technologies. Renewable energy sources like solar and wind are a promising solution, but efficient storage of electricity produced from them is critical as they are intermittent. Rechargeable batteries are the viable option for both renewable energy storage and electrification of transportation. However, their widespread adoption requires optimization of cost, cycle life, safety, energy density, power density, and environmental impact, all of which are directly linked to severe materials challenges. After providing a brief account of the current status, this presentation will focus on the development of sustainable battery chemistries and advanced materials for near-term and long-term battery technologies. Particularly, lithium- and sodium-based batteries that are free from expensive and scarcely available cobalt as well as those based on sulfur will be presented. The challenges of bulk and surface instability during charge-discharge cycling, advanced characterization methodologies to develop an in-depth understanding, and approaches to overcome the challenges will be presented.

PROF. DR. SEERAM RAMAKRISHNA

National University of Singapore (NUS), Singapore

Build Back Better Materials World to Deal with the Existential Threats to Humanity – Reimagine Materials

Inspired by the concern for humanity, authors of the 1972 book *The Limits to Growth* professed problems affecting the habitability of planet Earth for today's as well as future generations. Since then they were further refined and articulated. More recently, in the form of United Nations seventeen Sustainability Development Goals, SDGs. Sustainability is about the reduction of greenhouse gas emissions as well as circular solid waste management to reduce environmental pollution and waste accumulation in nature, to protect human health, to alleviate resources depletion and environmental deterioration, to regenerate biodiversity, and to overcome rising sea levels and extreme weathers caused by climate change for the well being of humans and preserving Earth for the future generations. The climate change articulation gained the attention of many people. And yet only a small fraction of humanity, as well as capital investors, are prepared to act on the sustainability solutions. Thus, sustainability articulations in the name of carbon-neutral economy, low-carbon economy, circular economy, and science-based sustainability targets with the promise of quality living conditions, jobs, and economic growth, are advocated by the governments and captains of industry. There are many facets and dimensions to myriad articulations.

Materials are central to humanity's sustainability efforts. According to recent papers published in the *Nature* journals, about 23% of global emissions can be attributed to materials production, and the global human-made mass now exceeds all living biomass of Earth. It is implicit to reimagine materials or build back better materials world so as to mitigate the existential threats to humanity i.e. environmental degradation and biodiversity loss.

ANDREA “ANDY” BLAIR

International Geothermal Association, President

Global Geothermal Movements: What’s Happening in the World of Geothermal, Current Focus, Latest Thinking, and Global Trends

Latest technologies, workstreams and thinking in international geothermal markets and how the International Geothermal Association intends to play a leadership role. Glean insights into activities, issues and opportunities for the geothermal sector and hear commentary on geothermals role in the global energy transition.

PROF. DR. QINGYAN (YAN) CHEN

Purdue University, USA

Energy Use in Buildings: Past, Present, and Future

China consumed 22% of the world energy produced and the United States 16% as the two top world energy consumers. Building heating and cooling in China used 18% of its total primary energy while the figure for the United States was 13%. This presentation will give an overview of the energy used in buildings in the two countries in the recent history. We will compare the trend of the energy use due to technology development for buildings and improved living standard. Then we will compare the strategies in the two countries for reducing energy use in buildings and discuss the similarities and differences. A few case studies will be used to illustrate the impact of the strategies on energy use in buildings. The presentation will also show the barriers in using the strategies and pinpoint to the future directions of energy conservations in the two countries.

PROF. DR. ONUR MUTLU

ETH Zurich, Switzerland

Intelligent Architectures for Intelligent Machines

Computing is bottlenecked by data. Large amounts of data overwhelm storage capability, communication capability, and computation capability of the modern machines we design today. As a result, many key applications' performance, efficiency and scalability are bottlenecked by data movement. We describe three major shortcomings of modern architectures in terms of 1) dealing with data, 2) taking advantage of the vast amounts of data, and 3) exploiting different semantic properties of application data. We argue that an

intelligent architecture should be designed to handle data well. We show that handling data well requires designing system architectures based on three key principles: 1) data-centric, 2) data-driven, 3) data-aware. We give several examples for how to exploit each of these principles to design a much more efficient and high-performance computing system. We will especially discuss recent research that aims to fundamentally reduce memory latency and energy, and practically enable computation close to data, with at least two promising novel directions: 1) performing computation in memory by exploiting the analog operational properties of memory, with low-cost changes, 2) exploiting the logic layer in 3D-stacked memory technology in various ways to accelerate important data-intensive applications. We discuss how to enable adoption of such fundamentally more intelligent architectures, which we believe are key to efficiency, performance, and sustainability. We conclude with some guiding principles for future computing architecture and system designs.

PROF. DR. BRUCE RITTMANN

Arizona State University, USA

Moving from Treatment to Resource

While wastewater treatment has focused on removing water pollutants, many of the pollutants are valuable resources if recovered in a useful form. This presentation focuses on novel means to capture the energy value in “used waters,” including domestic wastewater. New developments in anaerobic membrane biofilm reactors (to generate methane) and microbial electrochemical cells (to generate electrical power or hydrogen gas) now make it feasible to achieve energy-positive treatment of the BOD. After recovery of the energy from used water, most of the N and P are released as inorganic forms that can be recovered for recycle to agriculture. This talk will focus on P recovery, although many of the principle also apply for N. An important take-home lesson is that traditional techniques for “P removal” will not work for P recovery. P-recovery techniques that produce a product useful in agriculture include precipitation as struvite or hydroxyapatite and selective sorption to Fe-based sorbents. This talk will introduce the new technologies and offer insights into their pros and cons.

PROF. DR. MOHAMED-SLIM ALOUINI

King Abdullah University of Sciences and Technology (KAUST), Saudi Arabia

Towards Sustainable and Environment-Aware Wireless Networks

The role of Internet and Communication Technology (ICT) in bringing about a revolution in almost all aspects of human life needs no introduction. It is indeed a well-known fact that the transmission of the information at a rapid pace has transformed all spheres of human life such as economy, education, and health to name a few. In this context, and as the standardization of the fifth generation (5G) of wireless communication systems (WCSs) has been completed, and 5G networks are in their early stage of deployment, the research visioning and planning of the sixth generation (6G) of WCSs are being initiated. 6G is expected to be the next focus in wireless communication and networking and aim to provide new superior communication services to meet the future hyper-connectivity demands in the 2030s. In addition, keeping in mind that urbanized populations have been the major beneficiary of the advances offered by the previous generations of WCSs and motivated by the recently adopted united nation sustainability development goals intended to be achieved by the year 2030, 6G networks are anticipated to democratize the benefits of ICT and to bring global connectivity in a sustainable fashion in order to contribute to developing tomorrow's digitally inclusive and green world. In this context, this talk aims to (i) provide an envisioned picture of 6G, (ii) serve as a research guideline in the beyond 5G era, and (iii) go over some of the recently proposed green technologies to offer high-speed connectivity not only in urban environments but also in under-covered areas in order to serve and contribute to the development of far-flung regions.

PROF. DR. AMAR K. MOHANTY

University of Guelph, Canada

Improved Utilization of Co-Products from Biofuel Industries in New Industrial Uses for a Sustainable Biorefinery

The key points of my presentation are “why to care about climate change,” “what is the circular economy,” “why we are looking for a waste-free world.” This particular explanation will give a brief overview of the linear model and the closed-loop system. The presentation will also include how the bio & circularity to the economy is the best way to reuse the waste/co-product. The second-generation biofuel (2G biofuel) wave of the future requires advanced bio-refinery to have overall sustainability and economic recovery. In order to find an application to by-products of the bio-refinery industry, I will be talking about bio-based & sustainable materials/composites from agro-residues and biofuel co-products.

PROF. DR. VICTOR C.M. LEUNG

University of British Columbia, Canada

AIoT as a Service – Framework, Opportunities, and Challenges

With the increasing adoption of Internet of Things (IoT) and rapid advancements of Artificial Intelligence (AI) applications, the integration of AI and IoT, widely referred as AIoT, is gaining momentum. Realizing AIoT will require massive investments in infrastructure, and lessons learned from network deployments point to the use of shared hardware and software resources that can be virtualized to support various services on demand, resulting in AIoT-as-a-Service (AIoTaaS). In this talk, we start with a review of the idea of Anything-as-a-Service (XaaS), leading to IoTaaS and AIaaS, which form the basis of AIoTaaS. We present a framework for AIoTaaS, which incorporates edge and cloud computing platforms to support the AI functionalities required for different services. Enabled by cloud and edge computing, AIoTaaS can effectively implement machine learning (ML) training and inference functions on cloud and edge devices with much less complexity to enable efficient and effective AI decision making in IoT and data analytics, especially in the area of streaming data and real-time analytics associated with edge computing networks. To implement AIoTaaS, interoperability between components at the device level, software level and platform level should be extended while optimizing system and network operations as well as extracting value from data. In the future, AIoTaaS integrated with 5G and blockchain will be leveraged to achieve more efficient IoT operations, improve human-machine interactions, and enhance data management and analytics, creating a foundation for pervasive AI services and applications.

PROF. DR. LI SHI

The University of Texas at Austin, USA

Atomic Scale Phonon Band Engineering of Semiconductors

As the energy quanta of lattice vibration, phonons control the transport of heat, charge, and spin in functional materials and devices. Recent progress in first principles theoretical computation has motivated experimental manipulation of the atomic basis of the lattice structure to engineer the phonon bands and transport properties of semiconductors. In boron arsenic (BAs) with a heavy arsenic atom and a light boron atom in the basis of the cubic lattice structure, a large gap between the acoustic and optical polarizations suppresses three-phonon scattering and makes BAs the first known semiconductor with an unusual high lattice thermal conductivity. When the number of atoms in the basis is increased to the order of 100 in higher manganese silicide (HMS) with an incommensurate chimney ladder structure, the acoustic phonons are scattered strongly by numerous optical modes including an unusually low-frequency twisting polarization. Consequently, bulk HMS single crystals exhibit a similarly low lattice thermal conductivity as silicon germanium (SiGe) alloy nanowires, where high-frequency and low-frequency modes are scattered by lattice and surface disorders. As such, BAs is emerging as a next-generation electronic material, whereas HMS is being explored actively for solid-state thermoelectric power generation.

PROF. DR. MOCHAMMAD HADID SUBKI

International Atomic Energy Agency (IAEA), Austria

Advances on Small Modular Nuclear Reactor Technology Developments

The IAEA Department of Nuclear Energy continues to facilitate efforts of Member States in the development and deployment of small modular reactors (SMRs) as an option of nuclear power technology, recognizing their potential as a viable solution to meet energy supply security, both in developing and developed economies. SMRs are advanced reactors designed to generate typically up to 300 MWe that may be deployed as modules for installation as demand arises. The key driving forces of development are fulfilling the need for flexible power generation, replacing fossil-fired units, enhancing safety performance, and offering better economic affordability. There are more than seventy (70) SMR designs under development for different application. The Akademik Lomonosov floating power unit in the Russian Federation with two-module KLT40S has been connected to the grid and started commercial operation in May 2020. Two industrial demonstration SMRs are in advanced stage of construction: CAREM in Argentina and HTR-PM in China. They are scheduled to start operation between 2021 and 2023. This presentation provides a brief introductory information and technical description of the key SMR designs and technologies under different stages of development and deployment. Prospects and challenges for their deployment will also be discusses.

PROF. DR. KEITH BELL

University of Strathclyde, UK

Powering Past Fossil Fuels: Electricity and Net-Zero Greenhouse Gas Emissions

For over a hundred years, electricity production has depended primarily on the burning of fossil fuels. Prevention of excessive global temperature rise and commitments by a growing number of countries to “net-zero” greenhouse gas emissions forbid this if the emitted carbon dioxide isn’t captured and stored. Massive strides have been made in the use of wind and solar energy to produce electricity, reducing reliance on fossil fuels. Further reduction in the emissions intensity of electricity production is required at the same time as meeting an increasing demand as energy use for heat and transport is electrified and cooling demand grows. This talk addresses the successes and remaining challenges of decarbonisation of the electricity system while maintaining accustomed levels of reliability of supply.

PROF. DR. LIDIA MORAWSKA

Queensland University of Technology (QUT), Australia

Air Pollution and Energy: “This discussion is closed”!

There is overwhelming scientific evidence about the sources of air pollution, the atmospheric processes, in which pollutants are involved, and the broad impacts of pollutants. The ‘Global Burden of Disease’ analysis ranked ambient air pollution among the top ten risks faced by humans. Most of the anthropogenic air pollution is due to our energy needs: for the generation of electricity, for heating or cooling buildings, or for urban transport and transport in general. The energy transition from current dirty fuels to future clean fuels will play a vital role in eliminating the health impacts of air pollution. The arrival of new technologies makes the transition possible.

However, whether and how new technologies are used is highly dependent on political drivers, whether they allow or block the adoption of the technologies. The presentation will explore these aspects, emphasising areas that need more interdisciplinary and applied research, greater awareness and education, and international collaboration.



Invited Speakers

PROF. DR. UMBERTO DESIDERI

University of Pisa, Italy

Power to Fuel Technologies: Is a Necessary Option for the Future?

Power-to-fuel technologies are fundamental for storing energy from renewable sources in order to manage the intermittency and variability of renewable energy. Storing renewable energy in renewable fuels or chemicals is strategic for covering the needs of long term and seasonal storage, which cannot be satisfied by most of other currently available energy storage systems, and for transferring energy from the power generation sector to other sectors such as transport, heavy industry, and green chemicals production. However, the topic needs a clear approach, which requires a sound and clear, integrated approach with other short- and medium-term storage options.

In such a changing world, it is necessary to take decisions that may help the transition to a decarbonized economy which should be openly and widely discussed to agree on the fundamental steps in different directions and with different time span.

For this aim, a number of parameters should be considered, such as energy efficiency, environmental impact, and LCA, thermoeconomics, environomics.

This speech intends to open the discussion on the above points and stimulate new approaches to energy storage.

CHRIS COOK

The Institute for Strategy, Resilience & Security (ISRS) at University College London, UK

Introducing the Energy Treasury - from Dollar Economy to Energy Economy



Fifty years ago next week President Nixon detached the US dollar from the Gold Standard and began a process of market intermediation, financialisation, & digitisation leading to unsustainable concentration of wealth and in October 2008 to a global bank solvency shock marking an inflection point of Peak Debt.

Meanwhile the secular increase in energy intensity of fossil fuel extraction and secular decline in Energy Return on Energy Invested (EROEI) when combined with financialisation of oil led to an unprecedented market discontinuity in April 2020 as the Covid demand and liquidity shock marked an inflection point of Peak Rent.

This presentation outlines the evolution of the legal design of market institutions and instruments over 50 years and identifies an ongoing transition from capital and resource intensive transactional commodity markets to smart markets in services where law, accounting and ICT converge in “Financial Technology”.

The presentation concludes by proposing a new generation of distributed and networked smart market Energy Treasury institutions and instruments enabling the implementation of an Energy Standard unit of account.

DR. JAMES CARTON

Dublin City University & Hydrogen Ireland Association, Ireland

Hydrogen; Building a Hydrogen Economy on the Island of Ireland

In Ireland, today, the production and use of hydrogen is relatively modest when compared to most other developed European countries, especially as a decarbonising agent, mainly used in the semiconductor industry as well as an industry feedstock. However, hydrogen activities and projects are taking shape across the island of Ireland, with some academic studies suggesting the use of electrolyser technologies for the conversion of the growing amounts of excess wind energy on the island of Ireland into green hydrogen. A growing interest in hydrogen technologies is evident with a number of private and semi-state companies developing plans for hydrogen hubs as well as the conversion of the gas grid to hydrogen. Even though there are currently no hydrogen refuelling stations in the Republic of Ireland, BOC already provides a simple refuelling process in west Dublin to support hydrogen bus trials and a 3 hydrogen bus deployment; while Logan Energy has just commissioned the first hydrogen refuelling station near Belfast, in Northern Ireland, to support the operation of 20 hydrogen-powered buses there in the near future. This presentation will present an overview and experience of where the island of Ireland is on its journey to a decarbonised society and the role of hydrogen.

PROF. DR. MUHAMMAD ALI IMRAN

University of Glasgow, UK

5G Communication Systems and Energy Efficient Future

5G is the next generation of wireless and mobile communication systems and it is being designed to ensure energy-efficient operation. In addition to its own energy-efficient design, 5G has the potential to achieve net-zero ambition by ensuring digital connectivity for the management of many other resources. It's future version, i.e. 6G is expected to open further opportunities to reduce pressures on greenhouse emissions by enabling telepresence. This talk will provide a quick overview of technologies and potential research areas in these emerging directions.

PROF. DR. MEHMET SARIKAYA

University of Washington, USA

Energy Materials - Current & Future

All engineering systems are made up of materials where controlled hierarchical structures at different dimensional levels determine their functionalities. The three key issues in energy systems for long-term sustainability include the chemical makeup of the materials, where doping and alloying plays an important role, in particular, the significance of rare earth metals; controlling the microstructures of the materials towards achieving the desired engineering properties, and finally processing of the materials under energy-efficient and environmentally friendly conditions. The presentation will discuss the current state of the energy materials with key problems and limitations, with proposed more sustainable approaches, e.g., ocean biomining, efficient energy harvesting approaches, and biomimetic processing, for the future.

PROF. DR. ALEJANDRO H. BUSCHMANN

Universidad de Los Lagos, Chile

Macroalgal Sea-farming and Biofuels: Desires and Facts

Macroalgal production is globally one of the major aquaculture groups produced, reaching over metric 31 million tons several species are known to be exploited, however, the majority of algal biomass comes from few species: *Saccharina*, *Kappaphycus/Eucheuma*, *Undaria*, and *Gracilaria* and *Porphyra/Pyropia*. Today there is a high interest to cultivate macroalgae beyond the production in South-East Asia, North China, Korea, and Japan. As new potentially markets are under development that may increase the demand, there is a need for commercial cultivation systems. This contribution presents the recent development of the sea-farming of the brown macroalgae *Macrocystis pyrifera*, focusing on the fundamental determinants of productivity in cultivated systems, identifying the main environmental constraints and the relevance of a breeding program. Our findings demonstrate the feasibility of the *Macrocystis* sea-farming but also identify important yield differences between farming sites and strains. In our best farming locations, kelp biomass production reached 38.8 DMT/Ha. In addition, our efforts have also been devoted to transform and valuing the *M. pyrifera* biomass to achieve an economic interest in developing this industry. We have used kelp for developing human food products and as feed for abalones, however, more recently, we developed a process that includes the use of genetically modified bacteria able to transform the kelp biomass into bioethanol. Using a fermentation process, we obtained 0.213 kg ethanol kg⁻¹ dry seaweed, equivalent to 7 to 9.6 m³ of ethanol hectare⁻¹. Furthermore, we were able to extract co-products such as antioxidants. The concentration of phlorotannins achieved in the extract was 200.5±5.6 mg gallic acid equivalent (GAE)/100 g (DS) and a total antioxidant activity of the extract of 38.4±2.9 mg trolox equivalent (TE)/100 g DS. Further, it was possible to identify two phlorotannins through HPLC-ESI-MS analyses: phloroeckol and a tetrameric phloroglucinol. These results show how we have move into a more integrated use of the kelp biomass by using a biorefinery approach. Financial support: ANID(Chile): FB-0001

DR. STEVEN BROWN

Director, New Strain Development, LanzaTech, USA

Stepping on the Gas to a Circular Economy: Accelerating the Development of Carbon-Negative Chemical Production from Gas Fermentation

Climate crisis and rapid population growth are posing some of the most urgent challenges to mankind and have intensified the need for the deployment of carbon recycling technologies. Gas fermentation using carbon-fixing microorganisms offers a solution for transforming waste carbon into sustainable fuels, chemicals and polymers at a scale that can be truly impactful in mitigating the climate crisis. LanzaTech is a pioneer and world leader in gas fermentation, having successfully scaled up the process from the laboratory bench to full commercial scale, with two commercial plants in operation and several additional units in construction.

Compared to other gas-to-liquid processes, gas fermentation offers unique feedstock and product flexibility. The process can handle a diverse range of high volume, low-cost feedstocks. These include industrial emissions (e.g., steel mills, processing plants, refineries) or syngas generated from any biomass resource (e.g., municipal solid waste, agricultural waste, organic industrial waste), as well as CO₂ with green hydrogen. Synthetic biology and metabolic engineering enable the conversion of these feedstocks into an array of fuels, chemicals, or polymers to displace fossil-derived chemicals.

PROF. DR. CENGİZ SINAN OZKAN

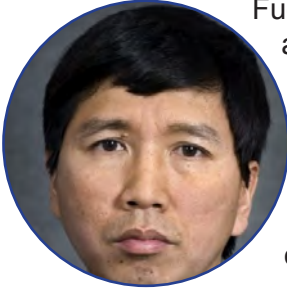
University of California, Riverside, USA

Materials Design for Sustainability and Energy Storage

One of the most important challenges of the 21st century that the nations worldwide are facing is environmental sustainability due to climate change and carbon pollution. A wide spectrum of IoT applications, mobile computing, and sophisticated handling of big data and computation leads to consuming 200 TWh+ each year which exceeds the total energy consumption of some entire countries, which directly impacts sustainability. More, the energy storage market ranging from electrified transportation to grid storage at different scales and mobile computing demand the design of new classes of materials for manufacturing high performance batteries and supercapacitors. I will describe innovations in the design of nanostructured materials for enhanced capacity; superior rate performance, cycling stability, superior gravimetric capacitance; enhanced energy density and power density.

PROF. DR. TIANZHEN HONG

Lawrence Berkeley National Laboratory, USA

Applications of Machine Learning Techniques in Buildings: An Overview and Examples

Fueled by big data, powerful and affordable computing resources, and advanced algorithms, machine learning has been explored and applied to buildings research for the past decades and has demonstrated its potential to enhance building performance. This talk presents an overview of how machine learning has been applied across different stages of the building life cycle with a focus on building design, operation, and control. A few real applications using machine learning will be presented. Challenges of applying machine learning to buildings research will also be discussed.

PROF. DR. UMIT B. DEMIRCI

University of Montpellier, France

Boron for Carrying/Storing Hydrogen

The words “new interest for old compounds” well summarize the context of the research dedicated to boron-based hydrogen carrying/storing materials over the past 2 decades. In the late 1990s, sodium borohydride that was discovered in the 1940s, emerged; it was presented as having a high potential for on-board H₂ production. In the mid-2000s, ammonia borane that was discovered in the 1950s, emerged; its gravimetric hydrogen density of 19.5 wt% attracted a lot of attention. In the early 2000s, boron nitride that was discovered in the early 19th century, emerged; it was presented as being able to adsorb up to 5-6 wt% H₂ at rooms conditions. Like many other groups, we have devoted effort to developing these compounds.

After 15-20 of (mainly academic) research, there is one question that is often raised. How mature are these compounds? I will try to answer the question during the TUBA WCEST-2021. A first step in answer is: we have to admit that if we do not change course, we will go around in circles.

ZAFER URE

Managing Director, Phase Change Material Products Ltd., UK

Thermal Energy Storage Technologies and their Global Application Examples



Thermal Energy Storage (TES) is the temporary storage of high or low-temperature energy for later use. It bridges the time gap between energy requirement and energy use. For HVAC and refrigeration application purposes, water and water ice constitute the principal storage media.

Water has the advantage of universal availability, low cost, and transport ability through other system components. However, water ice as latent heat energy storage can only be produced using inefficient low-temperature chillers for cooling applications and if it is applied for heating using purely sensible heat storage capacity designers' have to use large storage tanks.

However, Phase Change Materials (PCM) between +4°C and +90°C range offer us new horizons and practical application options.

One can provide a latent heat Coolth energy storage utilising conventional water chillers for new and retrofit applications without the need for any modifications as well as having the possibility of free cooling.

By storing day-time warm energy for evening periods and night-time cool energy for day-time cooling requirements, a PCM system can simply bridge the gap between energy availability and energy use and therefore has the potential to achieve considerable environmental as well as economical benefits for many heating and cooling applications.

A practical application guide, together with the real application examples around the World, will be presented in a format that will aid practising engineers or consultants to develop an effective and low energy design based on PCM-based thermal energy storage cooling / heating and heat recovery systems.

PROF. DR. ERKAN OTERKUS

University of Strathclyde, UK

Fracture Modeling Based on Peridynamic Theory

Structures are usually subjected to various loading and environmental conditions, which can cause various damage types, including fatigue and corrosion. Prediction of fracture and failure is a challenging research area. There are various methods available for this purpose, including the well-known finite element (FE) method. FE method is a powerful technique for deformation and stress analysis of structures. However, it has various disadvantages in predicting failure due to its mathematical structure. In order to overcome this problem, a new computational technique peridynamics was introduced. Peridynamics is a meshless approach, and it is very suitable for predicting crack initiation and propagation in structures subjected to different types of loading and environmental conditions. In this presentation, various applications of peridynamics will be demonstrated, including hydraulic fracturing, corrosion damage, underwater shock response of composite structures, fatigue damage prediction in metals, and fracture in lithium-ion batteries.

PROF. DR. MENG NI

The Hong Kong Polytechnic University, China

New Developments in Zn-Air Batteries for Energy Storage

Zn-air batteries are promising power sources for various applications due to their low-cost, intrinsic safety, and high capacity. However, the performance and durability of Zn-air batteries are still unsatisfactory due to the low discharge voltage, high charge voltage, Zn dendrite formation, and Zn electrode passivation. In order to improve the battery performance, novel hybrid Zn-metal/air batteries are developed to achieve both high discharge voltage and high capacity. In addition, the Zn-air battery performance can be further enhanced by controlling the hydrophobic level and microstructure of the air electrode. Flexible Zn-air batteries are developed for flexible electronics, such as flexible mobile phones and flexible sensors. For grid-scale electrical energy storage, Zn-air flow batteries are developed with improved performance and durability. The talk will cover the above recent developments in Zn-air batteries.

BAHAREH SEYEDI

United Nations Department of Economic and Social Affairs (UNDESA), USA

Achieving Universal Energy Access and Net Zero Emissions – A Policy Perspective

Energy lies at the heart of both the 2030 Agenda for Sustainable Development and the Paris Agreement. Sustainable energy is inextricably linked to many socio-economic outcomes, including poverty eradication, food security, health, education, prosperity, gender equality, jobs, transport, ocean, water and sanitation, and the empowerment of women and youth. Despite the progress made over the last decade, urgent action is needed to achieve clean, affordable energy for all by 2030 and net-zero emissions by 2050. Nearly 760 million people still lack access to electricity, and nearly 2.6 billion lack clean cooking fuels, causing several million deaths each year from household air pollution. Energy is also critical to addressing climate change, and it accounts for three-quarters of global emissions. Global temperatures are already 1.2 degrees higher than in the late 1800s, with climate-related disasters displacing millions of people. This presentation focuses on concrete actions and ambitious commitments that are required to improve the lives of billions who lack access to energy while accelerating energy transition to address the climate crisis.

PROF. DR. SALIH SANER

Near East University, TRNC

Geological and Geopolitical Controls on the Hydrocarbon Search in the Eastern Mediterranean Basin

Eastern Mediterranean region is located on a hydrocarbon belt which corresponds to the southern continental shelf of the Tethys Sea, where Mediterranean Sea of today is the geological remnant of it. This belt extends from Oman to Syria and then passing through the East Mediterranean towards westward along the northern edge of Africa Continent. Although total of discoveries has not reached the USGS's resource estimates published in 2011, the presence of hydrocarbons has been proven by discoveries in the region.

The exploration activities before the sharing of maritime jurisdictions in the region created an unsafe and politically unstable environment. After procurement of deep sea drilling facilities in 2019, the Turkish Republic of Northern Cyprus (TRNC) and the Republic of Turkey (TR) have begun drilling in overlapping licenses with those claimed by Southern Cyprus Greek Administration (SCGA) and Greece. Upon blockage of the possibility of a federal Cyprus solution by Greeks, in 2021 the Turkish side started implementing an independence policy for TRNC. This requires the sharing of hydrocarbon rights and defining their exclusive economic zones (EEZ) with SCGA. Until a solution in Cyprus TRNC will continue exploring in the seas around the entire island of Cyprus. Maritime jurisdictions acceptable to all littoral countries in the Eastern Mediterranean are essential for safe operations.

PROF. DR. İBRAHİM ÇEMEN

University of Alabama, USA

Quantitative Natural Fracture Analysis in Unconventional Gas-Shale Reservoirs: An example from Woodford Shale in Oklahoma, USA

Since the late 1990s horizontal drilling and hydraulic fracturing in the unconventional gas reservoirs has revolutionized gas exploration in North America. These two methods are reliant on robust predictive reservoir models, particularly addressing the geometry, spacing, and density of complex natural fracture networks within the otherwise tight unconventional gas-shale reservoirs.

One of the most important unconventional gas-shale reservoirs in the United States is the Devonian Woodford Shale of the midcontinent region.

However, the natural fractures within the Woodford Shale have not been rigorously studied despite their importance to fluid flow and ultimate recovery of hydrocarbons. Most of the subsurface fracture mapping of the Woodford has been done using 3D seismic data and seismic attribute analysis. Our group applied terrestrial Light Detection and Ranging (LiDAR) to study natural fracture patterns of Woodford outcrops located in the Arkoma Basin, southeastern Oklahoma.

The high-resolution images obtained from terrestrial LiDAR reveal fracture spacing and fracture density allowing the quantitative assessment of how these fractures vary in different sections of the Woodford Shale where bedding thickness, mineralogy, and degree of deformation (folding) differ significantly. Our group at the University of Alabama evaluated whether a statistical relationship exists between bedding thickness and the mineralogy (i.e., silica content vs organic content), fracture spacing, and fracture density of shale beds.

PROF. DR. BIROL DINDORUK

University of Houston, USA

Data Mining/Machine Learning in the Oil and Gas Sector: Applications in the Area of Petroleum Engineering

According to a newly published white paper from industry analysts IDC, 49% of upstream energy organizations are prioritizing data capitalization and monetization as preexisting challenges and 2020 turbulence has elevated digital transformation from priority to imperative status. Even about five years earlier, expectations from the digital transformation was already high, especially in the context of bottomline impact. However, with respect to these expectations the progress has been quite slow in the oil and gas industry. For most early adopters, this journey began with real-time monitoring and remote operation of equipment. In this talk, we will highlight the current environment in terms of “Disruptive”/Fast Changes where Data- Process-Software Integration and how it is almost becoming a must. In the second part of the the talk, we will have specific machine learning techniques that we have applied successfully to a certain class of problem in recent years. One of the learnings from these studies is that data quality check coupled the content knowledge was proven to be instrumental for the successful application of the machine learning and/or correlative techniques.

ALI KINDAP

Zorlu Energy & Geothermal Energy Association, Turkey

Geothermal Energy in Turkey



Turkey is the fourth-ranked country worldwide with the largest installed geothermal power capacity. While Turkey's installed power in geothermal energy was at the level of 15 MWe, this rate increased more than 100 times in the last 10 years and reached 1,650 MWe with the support of the public and private sectors. 78% of geothermal areas are located in Western Anatolia, 9% in Central Anatolia, 7 % in the Marmara Region, 5% in Eastern Anatolia, and %1 in the other regions. Considering the current 1.650 MW of installed capacity, approximately 2.000 MW additional geothermal investment opportunity exists in Turkey. As of the end of December 2020, the installed power of geothermal energy worldwide is 14.049 MW. According to the current records of the General Directorate of Mineral Exploration and Research in Turkey, geothermal power, which is stated as 35,500 MWt, has reached the estimated potential of 62,000 MWt thanks to the latest discoveries made by our sector. With a sample calculation, it is seen that geothermal power plants with a capacity of approximately 3.500 MW can be established, 3.200 hectares of greenhouse area can be heated, and approximately 5 million houses can be heated with this proven natural conventional geothermal system.

PROF. DR. ALPER BABA

Izmir Institute of Technology, Turkey

Importance of the Geothermal Resources and Its Innovative Properties: A Case Study: Turkey

Domestic green resources have become one of the primary discussion topics from a climate action point of view and promote economic stability and sustainability. In addition, the use of geothermal energy can support the United Nations (UN) sustainability development goals for zero hunger, gender equality, affordable and clean energy, decent work and economic growth, and industry, innovation, and infrastructure.

Turkey is located in a tectonically active zone and has approximately 1,000 geothermal hot springs and mineral water sources with a wide range of temperatures located all over the country. Temperatures can reach more than 295°C and are thus suitable for different utilization technologies. The total estimated geothermal potential of the country is more than 60,000 MWt. During the last decade, the geothermal power sector in Turkey has been the fastest-growing geothermal market in the world. Starting with 15 MWe in 1984, the sector has grown to 1663 MWe in 2021. In addition, the current installed direct use capacity in Turkey is about 3,589 MWt. About 41% is used for residential and commercial space heating, 35% goes to thermal spas and resorts, and 24% is used to heat greenhouses. Only 0.1% is currently used for food drying. All these practices have contributed significantly to the country's economy and affected the sustainability of rural development.

Generally, geothermal energy is an environmentally friendly energy resource. However, undesirable effects on the environment have begun to be observed due to incorrect applications of geothermal resources. The environmental impact of geothermal power plants are generally in the form of discharge of the geothermal fluid to the surrounding receiving environments without re-injection, leakages, and leaks due to deformations caused by corrosion and scaling in the power plant components, gas emission, visual pollution, microseismicity, collapses, thermal and chemical pollution. Such environmental problems can be minimized with innovative methods such as mineral extraction from fluid, use of CO₂ in industry, use integrated systems.

PROF. DR. ARTHUR WEEBER

TNO and Delft University of Technology, Netherlands

Trends and Future Aspects of PV Technology and its Applications

Huge steps have been made in reducing the cost of PV technologies. Important aspects are for example increasing the efficiency, economy of scale and standardization. However, current manufacturing technology for mainstream crystalline silicon PV based on so-called PERC technology is approaching its efficiency limits. Recent developments in making next steps for efficiency enhancement by the application of passivating contacts, but also hybrid perovskite-silicon tandems will be discussed. Furthermore, examples of technologies enabling novel applications and simultaneously improving aesthetics will be presented.

PROF. DR. SANDRO NIŽETIĆ

University of Split, Croatia

**Photovoltaic Thermal Collectors with Incorporated Phase Change Materials:
Analysis of Design Approaches**

PVT-PCM collectors can produce both electrical and thermal output on the limited surface, however specific design strongly determines electrical and thermal performance of the specific PVT-PCM collector design. The main characteristics of the usually implemented PCMs in the PVT-PCM collectors were also discussed in detail and that were focused on the experimentally tested solar collector designs in various climates. The conducted review indicated the importance of the PVT-PCM designs with respect to the overall PVT-PCM solar collector efficiency (electric and thermal), and in general it directed necessity for optimization of the main collector design parameters (such as tube geometry and layout, absorbers, PCM layer, etc.). The economic and environmental evaluation of the PVT-PCM collector designs is not properly discussed in the existing research literature and more detail research work should be conducted in that direction to determine techno-economic and environmentally suitable PVT-PCM collector designs.

PROF. DR. DAVID WHITTEN

The University of New Mexico, Mexico

Novel, Light-Activated Antimicrobials for Elimination of Viral Pathogens

This presentation will discuss recent work on our development of conjugated phenylene ethynylene and polythiophene polyelectrolytes and oligomers. The focal point of our presentation will be our development of these materials as antiviral agents vs enveloped and non-enveloped viral pathogens. We first investigated these totally synthetic organic polyelectrolytes as antimicrobials in 2005. Our initial studies indicated that the cationic phenylene ethynylene polymers (CPE) were potent antimicrobials against the biological pathogens *E. coli* and *B. anthracis* (Sterne) spores. Subsequent investigations showed that the polymers could be simplified into their subunit oligomers (OPE) and still possess potent antimicrobial activity both with light activation but also in the dark by different mechanisms. The structures of the biocidal CPE are shown below. In 2009 we made our first investigations into the antiviral activity of these compounds and materials. We found that these materials showed excellent dark and light induced inactivation of the bacteriophages, non-enveloped viruses which kill *E. coli*, but are harmless against humans. During the emergence of the current Pandemic we decided that our cationic oligomeric and polymeric materials might be able to inactivate the enveloped SARS-Cov-2 virus by a similar mechanism. Our initial study gave us an initial surprising result: all materials and compounds tested show light-activated antiviral activity against SARS-Cov-2, but no dark activity. In recent and on-going studies we are investigating several applications of our compounds and materials in the struggle to control the SARS-Cov-2 and its variants.

ARIF GUNYAR

Managing Director ENERCON, Turkey

The Future of Wind Energy Sector



This presentation covers the current situation of wind energy in Turkey, Europe, and Global within the scope of renewable energy perspectives and expected developments in Turkey, Europe, Global.

After this introductory information, the current wind energy situation and market outlook will be presented from a manufacturer's perspective.

The presentation will also include the R&D , innovations and expected developments in wind technology.

Lastly, ENERCON specified information will also be shared regarding the current situation, new technologies and trends.



Specialized Speakers

PROF. DR. EMRE ARTUN

Istanbul Technical University, Turkey

Machine-Learning Based Modeling of Hydrocarbon Reservoirs

Recent years witnessed a rapid increase in the volume of data collected in oilfield operations, with the help of enabling technological developments. Challenges in the description of static and dynamic characteristics of unconventional resources, the downturn of the oil industry, followed by a global pandemic altogether solidified the necessity of using collected data more effectively for better modeling, analysis, uncertainty quantification, and decision making. Proper management and analysis of collected data to understand reservoir behavior for both diagnostic and performance-forecasting purposes have become critical components of modern reservoir engineering practice. These developments have marked the beginning of a new scientific era in hydrocarbon reservoir engineering that is powered by data-driven analytics and modeling. Even though its full potential has not been fully realized yet, the key driving force of this era will probably be machine learning algorithms that combine traditional and modern statistical modeling tools with computational science. In this talk, some recent successful machine learning applications in the reservoir modeling domain will be presented. After exploring these applications, the current state of the industry and future challenges related to these technologies from both theoretical and practical perspectives will be briefly discussed.

DR. OZGE BOZKURT

TUPRAS R&D Center, Turkey

The Clean Fuel Technology Approach of TUPRAS R&D

With 30 million tons of annual crude oil processing capacity and four refineries, TUPRAS meets 51% of Turkey's gasoline, diesel, jet fuel and fuel oil needs. TUPRAS is currently recognizing several sustainability practices including research on alternative energy sources, collaborating with start-up companies, increasing the digitalization applications, realizing projects on energy efficiency, meeting the energy needs of TUPRAS refineries, improving the logistic infrastructure with enhanced social and environmental effects and reducing the water and carbon footprint of its operations. TUPRAS evaluates the short and long terms risks emanating from resource shortage (energy, water, etc.), sensitivity on fossil fuels (ESG, Green Deal, Paris Agreement), legislations (greenhouse gas emission limitation, carbon tax, diesel vehicle restrictions), increasing utilization of renewable fuels (biodiesel, green diesel, green jet fuel), improvement in alternative fuel Technologies (electricity, hydrogen) and electrification of vehicles. R&D is an important pillar for the future of TUPRAS in clean fuel technologies.

The eleven year-old TUPRAS R&D Center builds its project portfolio in correspondence with TUPRAS strategy and by considering the future of the oil&gas sector. There are 52 researchers comprising of 12 PhD and 23 MSc graduates, and 15 technicians. The laboratory and pilot plant buildings contain more than 150 equipment and several dedicated areas for fuel analysis, material analysis, reactor operation, distillation and fuel blending. TUPRAS R&D sets strong collaborations with national and international universities, research centers, SMEs and large enterprises. TUPRAS R&D has profitability and sustainability targets. Profitability is to support the refineries with hydrocarbon characterization, material and catalyst technology development, digital-sensor-robotic solution development and data analysis. Sustainability is related to the research and development of new technologies in to be utilized in TUPRAS in the future. Those include projects for reduction of carbon dioxide emission, production of green hydrogen from alternative sources, renewable fuel Technologies including biofuels and water and waste management technologies. Projects under the mentioned topics are funded by national and international funding mechanisms, mainly Tubitak and European Commission. TUPRAS works in collaboration with the Horizon 2020 and Horizon Europe EU Framework Programmes for Research and Innovation. With sixteen accepted Horizon 2020 projects and 7.4 million Euro funding, TUPRAS has become the most successful Turkish industrial company for the 2014-2020 period. There are currently ten active EU projects at the TUPRAS R&D Center.

DR. SALOMÉ LARMIER

Le Mans Université, France

Beef Veins: A Multi-Marker For Mature Source Rock



The natural fractures present in source rocks have a considerable impact during the process of unconventional natural oil and gas production of mature shales. They can act as a geological barrier or, on the contrary, help the hydraulic fractures propagation. The understanding of their spatial distribution as an input in DFN numerical models is therefore a key factor for oil companies. Moreover, the study of these natural fractures through different geological tools may provide information on the thermal and geodynamic history of the basin.

A certain type of fractures recurrent within source rocks are calcite-filled fibrous veins also called 'beef veins'. In order to understand the distribution of these fractures and the thermal information they contain, we conducted a three-year study with multiscale and multiproxy analysis of beef veins for one case study: the Vaca Muerta formation, which is a world-class source rock exploited by several oil majors. Several parameters controlling their distribution have been identified, the sedimentary interfaces, the TOC and the maturity of the rock being the first order controlling factors of the beef occurrences. Moreover, through geochemical studies, fractures enable to report the thermal history of the source rock, from its burial to its exhumation as well as the timing of fluids overpressure induced by the source rock maturation.

Beef veins are thus prime indicators for understanding the history of hydrocarbon generation and migration in source rocks and their distribution can be anticipated in order to improve the exploitation of unconventional resources.

PROF. DR. SAMIL SEN

Istanbul University-Cerrahpaşa, Turkey

Determination of a Deep Learning-Based Model for Shale Porosity Prediction Using World Scale Data Set

Shales are unconventional oil and gas reservoirs, top seals to conventional hydrocarbon reservoirs, and critical barriers to the leakage of CO₂ storage sites. Risking and predicting flow and leakage through these rocks requires a quantitative understanding of porosity. This is challenging since many pores in shales are only a few nanometers in size. The current industry standard protocol for porosity measurement for shales is helium porosimetry (He) technique. However, it is time consuming and not practical to obtain samples from all intervals of all wells in any shale play. Shale contains matrix porosity, organic porosity and natural fracture porosity that were formed during burial driven mechanical compaction, chemical compaction, diagenetic reactions, cementation and by maturity driven oil, condensate and gas formation processes. During this study, a data set of 287 samples from 19 wells of various locations of the organic-rich shales been used to deploy deep learning algorithm for porosity prediction. The “Neural Designer” software has been used to perform the training, testing and selection. The linear regression analysis suggests that porosity of organic-rich shales can be predicted as high as $R^2 = 0,936$ from the standard petroleum E&P activities.



General Presentations

Submission ID: 6

NATURE-INSPIRED TWO-LAYER OPTIMIZATIONS FOR INTERCONNECTED HEAT AND POWER MULTI-MICROGRIDS

Paolo Fracas^{1,2}, Edwin Zondervan², Meik Franke², Kyle V. Camarda³

¹Genport srl – Spinoff del Politecnico di Milano, Via Lecco 61, Vimercate, 20871, Italy

²University of Twente, Drienerlolaan 5, 7522 NB Enschede, The Netherlands

³University of Kansas, 1530 West 15th Street, Lawrence, KS

*paolo.fracas@genport.it

ABSTRACT

The world is currently facing massive energy- and dramatic environment challenges caused by global warming and an increase in energy demand. Through a tight integration of highly intermittent renewable distributed energy resources, the microgrid is the technology of choice to deliver the expected impacts, making clean energy affordable. The focus of this work lies on techno-economic analysis of combined heat and power multi-microgrids (CHP-MMG), a novel distribution system architecture comprising two interconnected microgrids. High computational resources are needed to investigate CHP-MMG. To this aim, a novel two-layer optimization algorithm is proposed to execute techno-economic analysis and find the settings returning the optimal financial performance, while the energy balance is achieved at minimal operational costs and highest revenues. The optimization tool is used for a sensitive analysis of hydrogen costs in off-grid and on-grid contests. With CHP-MMG, energy production surplus is converted from electricity to heat, and thus, the energy swarm keeps the LCOE lower than 15c€/kWh. The results show that at a hydrogen cost of 3€/kg, the optimal design returns an IRR of over 55%. The simulations considering both on-site hydrogen production via plasma decomposition of methane and green hydrogen let to similar high financial outcomes.

Keywords: Microgrid, Techno-economic analysis, Optimization, Evolutionary Algorithm, SLSQP.

INTRODUCTION

A microgrid (MG) is a controllable, independent small energy system comprising distributed generators (DG), loads, energy storage systems (ES), and control devices. CHP-MG systems have the ability to improve the quality of energy generated from renewable power sources, such as photovoltaic panels (PV) and wind turbines (WT). Compared with conventional CHP systems, CHP-MG have greater functionality, because they do not only satisfy cooling-, heating- and power demands (e.g., for residential, commercial, industrial buildings), but they also interact with the main grid to provide energy demand response services (i.e., reserve, peak-shaving, load shifting, load shedding) and improved capability for the integration of non-dispatchable sources (i.e., RES). When two or more CHP-MG systems are interconnected into a CHP-MMG, they become more flexible and counterbalance the variations required to match supply and demand at any time. Energy production surplus (i.e., exceeding the load demands and energy services) can be converted from electricity to heat and transferred to the nearby CHP-MG. As a consequence, the total cost of ownership (TCO) for the installations is minimized, a better LCOE is achieved, and the IRR is higher than stand-alone MG. The techno-economic viability of CHP-MMG requires optimization algorithms that, among different design, sizing, siting, select the best setting to maximize the financial performance. Several works deal with the optimization of MG operations using different metaheuristics. Notably, multi-microgrid optimization problems are rarely investigated. Typical optimal techno-economic analysis of MG deals usually with minimizations of the costs; balance equations are approximated with linear models that are solved with MILP. In this work, we propose a novel two-layer optimization architecture to simultaneously find the optimal setting of CHP-MMG under realistic operating conditions. The latter is a complex stochastic multi-objective optimization problem that requires high computing resources. For each trial setting, the simulation of energy balance among unpredictable-intermittent production with RES, not programmable grid availability and flexible energy demand, uncertain load profile, is hourly achieved with minimal operational costs and highest revenues. The trial setting is given by a novel evolutionary computing method that at the upper level select the best type (design optimization), size (sizing optimization) of DERs, the best geo-location (siting optimization) to minimize LCOE and maximize IRR.

THE TWO-LAYER OPTIMIZATION METHOD

The two-layer algorithm simultaneously (AIE) finds the optimal design, site, sizing, and operation of CHP-MMG. The inner layer is a convex piecewise-linear problem and is solved with the sequential least squares programming (SLSQP) method. The outer layer simultaneously solves a non-linear, non-convex problem, with novel evolutionary methods. The fitness values are generated by an analytical techno-economic model (ATE). A detailed description of ATE is reported in the publication of the authors (1). ATE incorporates the techno-economic models of the distributed energy resources (DER) models, the sequential least squares programming (SLSQP) algorithm, the objective

function, the electric, thermal energy balance equations of each MG and of the energy exchanged among the interconnected MG. The boundaries are dictated by outer AIE method and DER's state of health. The SLSQP method ensures that at each time-step minimize LCOE (i.e., the ratio between the TCO and the energy generated along the DER's lifetime) is minimized and LSOE (i.e., selling price deducted from the LCOE of the microgrid's products) is maximized, while the electric, the thermal generation of each microgrid and interconnections balance the demands surplus and networks losses. The DER's models dynamically adapt the boundaries and compute the states of DER after the elaboration of SLSQP. At the end of the iterations (i.e., 8760 time-steps, which are equivalent to one year), ATE exits the SLSQP loop, and the actual financial terms (LCOE, IRR) over the lifetime of the installation are computed. At the top, a novel self-adaptive evolutionary algorithm enables an efficient search of optimal CHP-MMG settings. The candidates of the DER configuration and the geo-coordinates of the evolutionary algorithms are represented by an individual having two properties: genotype (two chromosomes; the first composed of 36 genes, i.e., the size of DER and the second 2 genes, i.e., the latitude and longitude) and its quality (fitness value). Twelve individuals of a population undergo a number of variation operations to mimic genetic gene changes and search the solution space. In the early generations, the self-adaptive evolutionary algorithm (AIE) generates the mutant with a normal random distribution whose standard deviation and mean are driven by the diversity of population and fitness convergence. In the latest generations, the mutant is obtained by perturbing a base individually with the difference of a random set of other two individuals. In order to improve the search radius and converge faster, the values of the mutant- and crossover factors are adapted following the gradient of the fitness value. The crossover is obtained by randomly recombining the mutant to 1) segments of an external genotype via horizontal gene transfer; 2) the target individual via vertical gene transfer technique. The stochastic multi-objective function delivering the fitness value is formulated to obtain the highest IRR to investors. Due to the stochastic nature of this problem, clusters of probabilistic best solutions (PBS), of similar solution quality are obtained. To find the best configuration, the optimization must be repeated until the standard deviation of the PBS's genotypes reaches the desired value. Then, the PBS having the lowest fitness value can be assumed as the candidate of being a best probabilistic solution. The final task is to verify with the sample average approximation method (2) if the latter solution returns the best-expected performance over all the uncertain scenarios. The results show that AIE performs over 70% better than the original version of Differential Evolution (3) and it is well suited to compute complex CHP-MMG optimizations.

CONCLUSIONS

The simulation-optimization tool proposed in this work leads to recommendations regarding the best configurations of CHP-MMG in Southern Europe (Catania, IT) and Northern Europe (Bremen, GE). The outcomes are subsequently used to examine the impact of the location of the sites, the costs of the fuels, the price policies and their financial implication. In grid-tie scenarios, with cost of the hydrogen fixed at 3 €/kg, fuel cells are selected to be a main source of electricity and heat, followed by RES while the role of the main grid is relegated to deliver demand response services. Whenever the hydrogen costs increase to 13 €/kg, the main grid turns into the principal supplier of the loads within the CHP-MMG. The high fuel cost causes a substantial increment of PV and WT. LCOE values are similar in almost all scenarios (~15 c€/kWh), while in Catania is obtained the highest IRR (~55%). By setting the boundaries of geo-locations covering for Northern Europe a region with its center in Bremen and Catania for Southern Europe +/- 7 decimal degree both for latitude and longitude, the best siting and design of CHP-MMG in two regions of Europe with different climate conditions could be found. Within the cluster of best probabilistic solutions, AIE selects in Denmark the best siting of Northern Europe for CHP-MMG. This region has favorable wind conditions, and thus, WT is the best choice for RES coupled with fuel cells (FC) and the main grid. Thermal energy is generated with heat pumps and exchanged between the microgrids (LCOE ~12 c€/kWh; IRR~5%). Similarly, in Southern Europe, solar radiation, wind speed, and cloudiness conditions are favorable to find the optimal combination of PV combined with WT, FC, and the main grid in the East part of the Mediterranean Area (i.e., Greece, LCOE ~7 c€/kWh; IRR~29%). A further set of optimizations dealing with off-grid scenarios, has demonstrated that LCOE can remain aligned to grid-tie scenarios (~15 c€/kWh). Revenues streams deprived from incomes delivered with energy demand response services do not consistently affect IRR that still remain attractive (~13%). The optimal DER configurations, even with unfavorable initial conditions, craft a full balance of both thermal and electric energies. Further optimization with the blue-hydrogen on-site generation with thermal plasma (TP) methane decomposition technology leads to a substantial increment of the revenue stream as compared to green hydrogen if carbon black as a by-product is taken into account. These results exhibit how blue hydrogen can be a convenient bridging technology to make CHP-MMG profitable. From the operational point of view, the simulations have brought out an optimal scheme of collaboration between the two microgrids (i.e., 'swarm effect'), fostering the overall efficiency, energy resilience to uncertainty, and optimal financial performance. Interconnections are used to permit crossflows of thermal and electrical energies. Notably, a fraction of the exceeding electrical energy (i.e., not used to feed the loads or charge batteries), flows via the interconnections back, and it is converted into thermal energy. Thus, a portion of the heat swarms to the other microgrid. The whole study demonstrates the versatility of CHP-MMG technology. With different inputs, AIE always finds optimal configurations, sizing, and siting CHP-MMG deliver a good quality of energy, attractive financial performance, and out-competing costs' drawbacks.

REFERENCES

- [1] Fracas P, Camarda K v, Zondervan E. Shaping the future energy markets with hybrid multimicrogrids by sequential least squares programming. *Physical Sciences Reviews* [Internet]. 2021 Jan;0(0). Available from: <https://doi.org/10.1515%2Fpsr-2020-0050>
- [2] Kleywegt AJ, Shapiro A, Homem-de-Mello T. The Sample Average Approximation Method for Stochastic Discrete Optimization. *SIAM Journal on Optimization* [Internet]. 2002 Jan;12(2):479–502. Available from: <https://doi.org/10.1137%2Fs1052623499363220>
- [3] Storn R. Differential Evolution Research – Trends and Open Questions. In: *Advances in Differential Evolution* [Internet]. Berlin, Heidelberg: Springer Berlin Heidelberg; p. 1–31. Available from: http://link.springer.com/10.1007/978-3-540-68830-3_1

HYDROTHERMAL CARBONIZATION OF WET OLIVE MILL WASTE

¹Gizem Balmuk, ¹Hakan Cay, ¹Gozde Duman Tac, ^{2*}Ismail Cem Kantarli, ¹Jale Yanik
¹Ege University, Faculty of Science, Chemistry Department, Izmir, Turkey
²Ege University, Ataturk Medical Technology Vocational Training School, Izmir, Turkey

*Corresponding author e-mail: ismail.cem.kantarli@ege.edu.tr

ABSTRACT

In this study, hydrothermal carbonization (HTC) of olive mill waste was studied at different reaction temperatures and duration time for the production of energy-densified solid fuel (hydrochar). The effect of process conditions on the fuel and combustion characteristics of resultant hydrochars were investigated. Hydrothermal carbonization resulted in the formation of lignite coal-like solid fuels having high calorific value, whereas it did not significantly improve the combustion characteristics of raw biomass. The results obtained in this study showed that HTC appears to be a promising process for the production of solid fuel from olive mill waste having high moisture content.

Keywords: hydrothermal carbonization, two-phase olive mill waste, hydrochar, combustion

INTRODUCTION

The process of oil extraction from olives generates large amounts of by-products and waste. Olive oil is mainly extracted by continuous two-phase centrifuge systems, and a large part of olive oil industry has been using this technology due to their advantages over previously used three-phase systems, which are energy and water savings, since the 1990s. In the two-phase system, no water is added to the decanter. The system generates oil and a semi-solid waste, usually called two-phase olive mill waste (TPOMW), separately [1]. TPOMW consists of olive extract, olive seed, and plant juice and represents 80% of the total weight of the fruit processed [2]. Up to 80% of the total weight of TPOMW is water. The management of TPOMW is generally viewed as a disposal problem but converting it to energy densified hydrochar via hydrothermal carbonization (HTC) can be a good opportunity. HTC method is very applicable to wet biomass like TPOMW. It does not require the drying of biomass and is carried out in the temperature range of 180–260 °C for a duration in the range of 5 min to 8h under autogenic pressure in subcritical water [3]. As a result of the process, a carbonaceous solid (hydrochar), aqueous chemicals, and gases are obtained.

MATERIALS AND METHODS

TPOMW was supplied by a local firm. TPOMW has a solid content of 33.6% as received. It has a potassium content of 3.3% on dry basis. HTC system and characterization of resultant hydrochars were explained in our previous study [3]. Hydrochars were defined as following the “HC-temperature-duration” sequence (HC-220-60 stands for biochar obtained from HTC of TPOMW conducted at 220 °C for 60 min). Combustion behavior of raw biomass and hydrochar samples were investigated using a thermogravimetric analyzer under air with a flow rate of 200 mL/min. The combustion parameters including the ignition temperature (T_i), burnout temperature (T_b), and average combustion reactivity (R_m), were calculated from the thermogravimetry (TG)/derivative thermogravimetry (DTG) curve based on the literature [4].

RESULTS AND CONCLUSIONS

The effect of HTC temperature and duration on the properties of the resultant hydrochars is given in Table 1. At low temperatures, hydrochar yield decreased sharply with the change of duration time from 0 min. to 30 min. and did not change much for a duration longer than 30 min. This showed that duration of 30 min. was sufficient to enhance degradation of TPOMW. At high temperatures, hydrochar yield decreased for longer duration (>60 min.) due to secondary decomposition. Ash contents of hydrochars were lower than that of TPOMW, since the inorganics, mainly potassium salts, of TPOMW dissolved in subcritical water during HTC. The volatile content (VC) of hydrochar decreased and its fixed carbon (FC) content increased both with increasing temperature and duration. The higher heating values (HHV) of hydrochars increased due to the increase of C content and decrease of O content with increasing temperature and duration. The effect of duration on energy yield (EY) varied with temperature. At 200 °C, EY decreased significantly due to the decrease in mass yield. Although the HHVs of biochars increased by time at 220 °C, EY did not change significantly due to the decrease in mass yield. At 240 °C, EY increased due to the increase of the HHV between 0-60 min and then decreased due to the decrease in mass yield. At 260 °C, EY decreased mainly due to the decrease in mass yield for longer durations. The Van Kreevelen diagram given in Fig. 1 shows that HTC yielded lignite coal-like hydrochars at low temperatures for long duration and at high temperatures for a short duration, while it yielded hydrochar like bituminous coal at high temperatures for a long duration.

T_i of hydrochars obtained at 200°C did not change much with duration (except HC-200-0) and were found to be higher than that of TPOMW. On the other hand, T_i of hydrochars obtained at higher temperatures decreased to values significantly lower than that of TPOMW with the increase of duration. This decrease was due to the inclusion of the tar-like volatile structures in hydrochar that formed by repolymerization of water-soluble compounds [3]. In comparison with lignite, all hydrochars had T_i lower than lignite given in literature which depicts the risk for self-ignition [5]. T_b of all hydrochars were found to be higher than that of TPOMW and lower than that of lignite. Hydrochars obtained at low

temperatures had higher R_m than those produced at high temperatures. R_m of all hydrochars were found to be higher than lignite. In conclusion, HTC eliminated some of the disadvantages of TPOMW as fuel by converting it to hydrochar with lower ash content and higher heating value, but it was not sufficient for enhancing the combustion properties of TPOMW

Table 1. Proximate analysis, elemental analysis, fuel properties and combustion parameters of hydrochars

	Proximate analysis, %wt., dry basis			Elemental analysis, %wt., dry basis					Yield	HHV (MJ/kg)	EY	Combustion analysis		
	Ash	VM	FC	C	H	N	S	O*				T_i	T_b	R_m
TPOMW	3.78	68.5	27.7	51.47	7.02	1.09	0.13	36.51	-	26.1	-	225	487	1.32
HC-200-0	0.71	71.86	27.43	52.51	7.45	1.04	0.12	38.17	79.2	27.0	82.1	266	500	1.26
HC-200-30	0.68	66.56	32.76	58.22	6.11	0.95	0.08	33.96	61.8	27.4	65.0	285	531	1.16
HC-200-60	0.72	64.17	35.11	60.74	6.54	1.06	0.06	30.88	62.7	28.8	69.2	295	527	1.28
HC-200-120	0.65	64.70	34.65	60.84	6.35	0.72	0.01	31.43	63.2	28.6	69.4	291	513	1.48
HC-200-240	0.90	56.66	42.44	62.92	6.46	0.89	0.02	28.81	60.2	29.5	68.0	280	493	1.77
HC-220-0	0.62	66.72	32.66	54.78	6.28	0.68	0.01	37.63	68.4	26.4	69.4	286	531	1.01
HC-220-30	0.67	62.95	36.38	60.07	6.68	0.81	0.02	31.75	62.6	28.8	69.1	285	512	1.33
HC-220-60	0.67	59.56	39.77	61.98	5.81	0.69	0.01	30.84	61.4	28.4	66.9	281	515	1.36
HC-220-120	0.80	55.85	43.35	63.17	6.23	0.89	0.01	28.90	59.2	29.3	66.5	207	512	1.16
HC-220-240	0.88	51.36	48.76	63.97	5.92	0.93	0.02	28.28	58.6	29.2	65.6	204	508	1.31
HC-240-0	0.45	64.75	34.80	62.42	6.71	0.88	0.22	29.32	57.5	29.6	65.4	287	537	0.95
HC-240-30	0.83	58.26	40.91	65.54	7.04	1.03	0.16	25.40	58.5	31.1	69.7	218	524	0.90
HC-240-60	0.82	54.14	45.04	67.06	6.69	1.09	0.17	24.17	57.5	31.2	68.9	203	530	0.85
HC-240-120	0.85	49.83	49.32	69.75	6.76	1.17	0.16	21.31	54.6	32.2	67.5	202	522	0.84
HC-240-240	0.85	47.87	51.28	73.39	6.49	1.29	0.19	17.79	47.8	33.1	60.8	-	-	-
HC-260-0	0.58	56.74	42.68	63.22	6.79	0.95	0.23	28.23	57.8	30.0	66.5	224	530	1.01
HC-260-30	0.85	49.16	49.99	71.40	6.39	1.27	0.20	19.89	47.5	32.3	58.9	212	507	0.94
HC-260-60	0.90	46.73	52.37	72.60	6.71	1.29	0.16	18.34	47.1	33.1	59.9	208	555	0.97
HC-260-120	0.88	47.36	51.76	74.33	6.84	1.35	0.18	16.42	43.3	33.9	56.3	201	594	0.77
HC-260-240	1.26	36.81	61.93	74.52	6.68	1.32	0.15	16.07	40.0	33.7	51.8	194	571	1.17
Lignite**	8.9	42.1	49.0	71.0	4.4	1.5	1.4	13.0	-	26.2	-	382	546	0.76

*by difference, O% = 100-(C%+H%+N%+S%+Ash%)

**from literature [5]

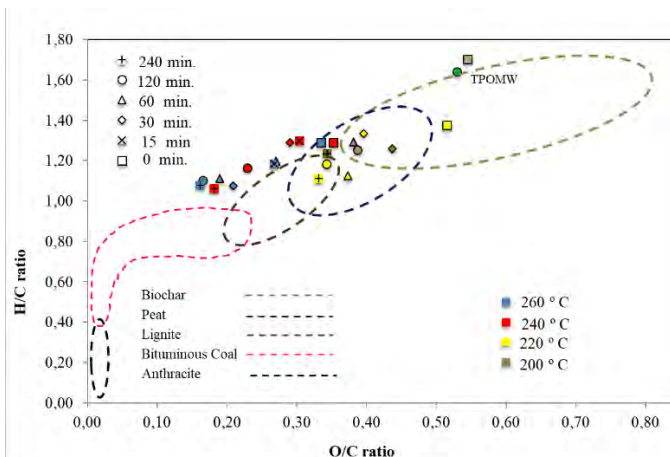


Figure 1. Van Krevelen diagram

ACKNOWLEDGEMENT

The financial support from TUBITAK (Project Contract No.117M570) under the ERANET-MED2 program of the European Union (Project Acronym, MEDWASTE) is acknowledged.

REFERENCES

- [1] Rincon B, Rodríguez-Gutierrez G, Bujalance L, Fernandez-Bolanos J, Borja R, 2016. Influence of a steam-explosion pre-treatment on the methane yield and kinetics of anaerobic digestion of two-phase olive mill solid waste or alperujo. *Process Saf. Environ. Protect.*, 102, 361-369.
- [2] Alburquerque JA, Gonzalez J, Garcia D, Cegarra J, 2004. Agrochemical characterization of "alperujo", a solid by-product of the two-phase centrifugation method for olive oil extraction. *Bioresour. Technol.*, 91, 195-200.
- [3] Duman G, Balmuk G, Cay H, Kantarli IC, Yanik J, 2020. Comparative evaluation of torrefaction and hydrothermal carbonization: effect on fuel properties and combustion behavior of agricultural wastes. *Energy Fuels*, 34, 9, 11175-11185.
- [4] Toptas A, Yildirim Y, Duman G, Yanik J, 2015. Combustion behavior of different kinds of torrefied biomass and their blends with lignite. *Bioresour. Technol.*, 177, 328-336.
- [5] Cabuk B, Duman G, Yanik J, Olgun H, 2020. Effect of fuel blend composition on hydrogen yield in co-gasification of coal and non-woody biomass. *Int. J. Hydrog. Energy* 45 (5), 3435-3443.

EMISSIONS AND ITS DRIVER ANALYSIS FOR THE UNITED KINGDOM HIGHER EDUCATION INSTITUTE

Amar Nayak, Naomi Turner, Edward Gobina^{1}
Center of Excellence for Process Integration and Membrane Technology, Robert Gordon University,
School of Engineering Aberdeen, United Kingdom, AB10 7GJ*

**Corresponding Author (Email: e.gobina@rgu.ac.uk)*

ABSTRACT

UK emissions of carbon dioxide declined from around 600 million tonnes of CO₂ (MtCO₂) in 1990 to 367 MtCO₂ in 2017, and in June 2019, the UK Government legislated an update of its greenhouse gas (GHG) emissions reduction target to attain 'net zero' by 2050. Meeting this ambitious target will require a drastic reduction in UK carbon emissions, with any remaining emissions being offset by extracting an equivalent amount from the atmosphere [1]. As a large sector of the UK economy, higher education (HEI) must contribute to the reduction in its carbon emissions if the Government's 'net zero' by 2050 target is to be met. The aim of the study is to analyze the factors driving the emissions in the UK HEI from 2014 to 2019. The study investigates the key drivers for emissions using correlation analysis, ratio analysis, and factor analysis. It also aims at determining whether the UK HEI can meet the 2020 milestone of a 43% reduction in emission with 2005 as the base year (Figure 1).

Keywords: Carbon dioxide, Emissions, Factor analysis, carbon emissions, HEI

INTRODUCTION

In the last ten years, UK Higher Education Institutions (HEIs) have increased their total income from 26 billion pounds to 80 billion pounds [2]. As one of the large sectors of the UK economy, HEIs must contribute to the reduction in its carbon emissions if the Government's 'net zero' by 2050 target is to be met. Apart from this, UK HEI's have their own milestone of reducing the CO₂e emissions by 43% by 2020 from the 2005 baseline emissions [2]. For doing so, it is essential to understand what the past data indicates regarding the drivers, progress, and benchmarking. In this study, the emission data is analyzed for the UK HEI from the year 2014-15 to 2019-2020 (5 years of data). This is an aggregate study where the analysis is carried out for the overall emissions of the HEI's. The study on individual HEI is beyond the scope of this study. The data is available from the estate's management of the HEFCE [2].

METHODOLOGY

The HEI-related data was obtained from the HESA estate management web page. Correlation and regression analysis was carried out to understand the relationship between the drivers and carbon emissions. Ratio analysis was carried out on a year-on-year basis to check how it has improved or decreased and which ratio has the highest or the lowest improvement rate.

RESULTS AND DISCUSSION

The target for the individual UK HEI's is set at a 43% reduction by 2020 from the 2005 baseline year. The data analysis indicates that the aggregate emissions for the HEI have increased by 10% from 2005 to 2014-15, thereon it reduced by 39.4% in the last five years.

Figure 1 shows the distribution of the percentage change in emissions between the year 2005 (baseline) and 2018-19. The positive percentage shows the HEI has managed to reduce the emissions, whereas the negative percentage indicates that the HEI's increased the emissions. The factors which have shown consistent high correlation are total gross internal area, total staff FTE, water consumption, energy consumption. Similarly, the maximum improvement in the ratio of the emission was observed in other non-residential income (£), a total number of cycle spaces, total grounds area (hectares), teaching income (£), total site area (hectares), teaching student FTE, total staff FTE. Car and cycle space stats for the last five years shows (figure 2 & 3) that the aggregate car parking space has decreased by 5%, the aggregate cycle space increased by 15%, the aggregate emissions reduced by 39%, emission per car parking space has reduced by 28%, emissions per cycle space has reduced by 43%.

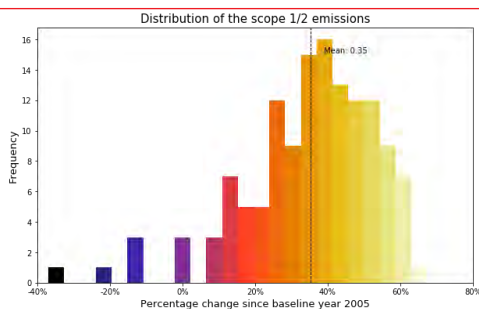


Figure 1

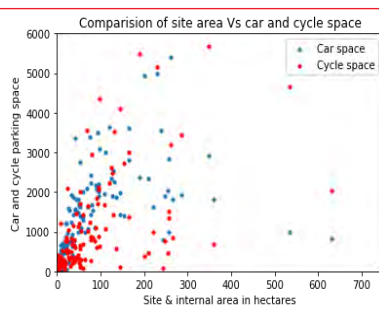


Figure 2

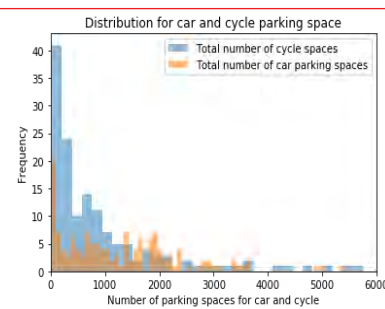


Figure 3

CONCLUSION

Among the above factors, focusing on emissions per staff FTE is more result-oriented because it also has a high correlation with the Scope 1 emissions. It appears that all the HEI's has made efforts to reduce the emissions, but they are very far away from the set benchmark. As per the present status, the HEI's have reduced 35% emissions at the aggregate level, whereas the Bright report estimated that the HEI's might achieve a 23% reduction. Only 48 HEI's have achieved the target for 43% reduction by 2020. Since 2020 is not operational for the HEI's (due to pandemic), the data till 2018-19 is considered the target year. The data indicates that the HEI's were slow to adapt to the climate change initiatives when the first awareness and regulations started in 2006-2008 [3]. It was also observed that the Scope 3 emissions reported by the HEI are the subset of the entire Scope 3 emissions which are mentioned in [4]. This is the reason why the Scope 3 emissions were found to be 0.5% of Scope 1 & 2 emissions. Few HEI's invested efforts to calculate the full Scope 3 emissions like Nottingham Trent University and Cambridge University. The result shows that the Scope 3 emission is two-third of the total emissions (Scope 1, 2, and 3 combined) [5]. HEFCE must find a way to gradually increase the Scope 3 emissions reporting from the HEI's to understand the full implications.

REFERENCES

- [1] Gov.UK. (2020). UK sets ambitious new climate target ahead of UN Summit. [online]. Available from <https://www.gov.uk/government/news/uk-sets-ambitious-new-climate-target-ahead-of-un-summit> [Accessed 20 March 2021]
- [2] HESA. (2021). Higher education providers. [online]. Available from <https://www.hesa.ac.uk/support/providers> [Accessed 20 March 2021]
- [3] Altan, H. (2010). Energy efficiency interventions in UK higher education institutions. *Energy Policy*, 38(12), 7722-7731.
- [4] Bhatia, P., Cummis, C., Rich, D., Draucker, L., Lahd, H., & Brown, A. (2011). Greenhouse gas protocol corporate value chain (scope 3) accounting and reporting standard.
- [5] Huang, Y. A., Weber, C. L., & Matthews, H. S. (2009). Categorization of scope 3 emissions for streamlined enterprise carbon footprinting.

TESTING MEMBRANES FOR SEPARATION OF CO₂ FROM SMALL MOLECULES IN LANDFILL GAS

¹Priscilla Ogunlode, ¹Ofasa Abunumah, ¹Firdaus Muhammad-Sukki, ¹Edward Gobina ^{1*}

¹Robert Gordon University, Centre for Process Integration & Membrane Technology, School of Engineering, Garthdee Road, Aberdeen AB10 7GJ

*Corresponding author e-mail: e.gobina@rgu.ac.uk

ABSTRACT

The present work is focusing on the utilization of previously fabricated membrane (synthesized in 3 days as reported in our previous work) to study the effect of hydrocarbons and its durability at the previously optimized conditions. Subsequently, gas permeation study was conducted on ceramic membranes in CO₂ separation from small gas molecules present in biogas and it was found that the permeance of CO₂, N₂, and CH₄ decreased in the order of 15 nm > 200 nm > 6,000 nm, according to the decrease in porosity of the membranes.

Keywords: Membrane, Pore size, Porosity, Permeance, Biogas

INTRODUCTION

Over the last few decades, much research has been done on the CO₂ separation especially in biogas upgrading to biomethane [1]. The presence of CO₂ in the biogas reduces the calorific value of the raw gas methane recovery during the combustion and other downstream processes [2]. Similarly, the presence of CO₂ decreases the heating value of natural gas and causes equipment corrosion in the existence of water [3]. Meanwhile, membrane separation technology has received much attention in CO₂ separation mainly due to its advantages compared to the conventional separation technologies [4]. Inorganic membranes are generally favored in the CO₂ separation among the membrane materials over polymeric membranes due to their specific unique characteristics, including well-specified pores, the molecular filtering property, ability to sustain longevity and wide pore size availability [5, 6].

MATERIALS AND METHODS

The ceramic membrane has been used as received without any modifications and typically made of aluminum oxide, titanium oxide, and zirconium oxide which all belong to the group of inorganic materials and are stable under CO₂ and water vapours conditions of biogas. They consisted of three mean pore sizes each namely: 15 nm, 200 nm and 6,000 nm (Outside Diameter 25 mm 7 cnx, pore diameter = 6 000nm, length: 368 mm, glazed section on either end: 25 mm, chemical composition: TiO₂, thickness - 1st layer TiO₂ (0.1-0.2µm), 2nd layer Al₂O₃ (15nm) respectively. The crystallinity and morphology of the membrane were characterized using an X-ray diffractometer (Bruker D8 Advance) and field emission scanning electron microscopy (Zeiss Supra 55 VP). Permeation experiments and stability tests were conducted for CH₄ and CO₂ using the flow rig shown in Figure 1. These membranes are to be scaled up for the prototype-module for use as the reference base materials. The membrane components were sealed in the proof-of-concept (PoC)-module and tested under realistic operating conditions of 50 – 100 C and pressure drops of 1 – 5 bars. Initially, the membrane sample was degassed for at least 16 hours by holding both upstream and downstream under vacuum with a series of valves closed and to select a small downstream volume or opened to select a large volume. The system leak rate was determined by manipulating a particular valve for at least 1 hour and measuring the rate of downstream pressure rise. Next, the upstream was pressurized by enabling the MFCs, opening and/or closing specific valves/valve, and placing other desired valves/valve into feedback mode. To ensure steady-state conditions, flux measurements were made after waiting a period of at least 60 mins.

RESULTS AND CONCLUSIONS

Highly permeable membrane materials show chemical instability against CO₂ and other landfill gas components. This project addresses this challenge by developing highly stable eco-friendly ceramic microporous membranes and a proof-of-concept (PoC) module for integrated CO₂ capture in landfill will be carried out using the setup shown in Figure 1. Results have shown that there is a link between porosity and pores size on membrane permeance (Figure 2). This important result will enable the investigation of four possible loadings of affinity material on the membrane and up to two flow designs using computational fluid dynamics (CFD), finite element method stress analysis (FESA) and incorporating various transport mechanisms. After evaluating the advantages and disadvantages of each pore size and porosity, we have selected the 200 nm as the most promising one. The new designs will comprise up to two asymmetric membranes on opposite side of an interlayer that provide both mechanical stability and flow channels for the biogas. The components will be configured in a tubular metal housing forming the permeator. In collaboration with our Project collaborators, we will also identify and produce a wide range of materials at the lab scale for high throughput and stability. The applications of these type of membranes are wide in range and the team will in the future focus the membrane technology demonstration on a microporous CO₂ transport mechanisms including surface flow that has superior performance regarding high CO₂ permeability, infinite methane selectivity, and high thermal,

chemical and mechanical stability. Furthermore, our intention is in the development of additional optimised membranes using both standard Al_2O_3 and multiple phase membranes. Highly stable materials that will be identified by project partners will also be considered for use with technologies like integrated catalytic membrane reactors for producing chemical energy carriers such as ammonia, hydrogen and other aspects of the developing energy transition leading to net-zero. In addition to CO_2 -capture and methane upgrading, this technology can be applied to the field of CO_2 -utilisation, waste destruction or pure gas separation. The deliverables of this project will benefit members of the scientific community working on gas separation membranes and other industries in the circular economy where carbon capture is important such as fossil power exhaust gas, fossil fuel upgrading in refinery flue gas and in iron and steel plants. It will also benefit the wider public through climate change mitigation.

REFERENCES

- [1] I. Angelidaki, et al., Biogas upgrading and utilization: current status and perspectives, *Biotechnol. Adv.* 36(2) (2018), pp. 452-466.
- [1] I.U. Khan, et al., Biogas as a renewable energy fuel – a review of biogas upgrading, utilisation and storage, Volume 150, 15 October 2017, Pages 277-294.
- [2] M. RAL MAMUN AND S. TORII (2019) *Sustainable energy & fuels* 3 (1), 166-172.
- [3] S.Z.A. Seman et al. (2018) Optimizing purity and recovery of biogas methane enrichment process in a closed landfill, Volume 131, February 2019, Pages 1117-1127.
- [4] A.G. Chmielewski, A. Urbaniak, K. Wawryniuk, Membrane enrichment of biogas from two-stage pilot plant using agricultural waste as a substrate, *Biomass Bioenergy*, 58 (2013), pp. 219-228.
- [5] S.O. Masebinu, A.O. Aboyade, E. Muzenda, Parametric study of single and double stage membrane configuration in methane enrichment process, *World Congr. Eng. Comput. Sci.*, 2 (2014), pp. 1-9.
- [6] S.Z.A.SemanI.IdrisA.AbdullahI.K.ShamsudinM.R.Othman,(2019) Optimizing purity and recovery of biogas methane enrichment process in a closed landfill *Renewable Energy*, Volume 131, Pages 1117-1127.

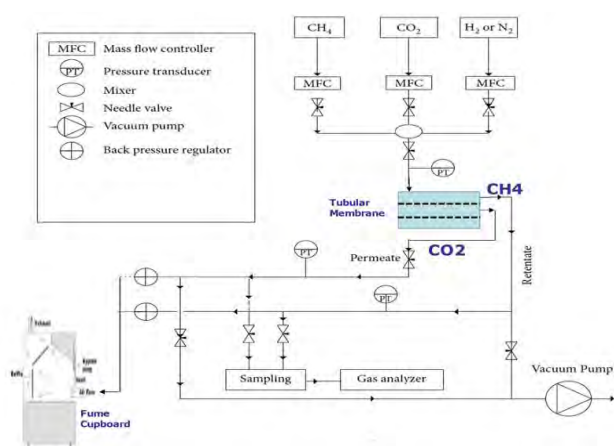


Figure 1. Schematic of the laboratory gas permeation set up

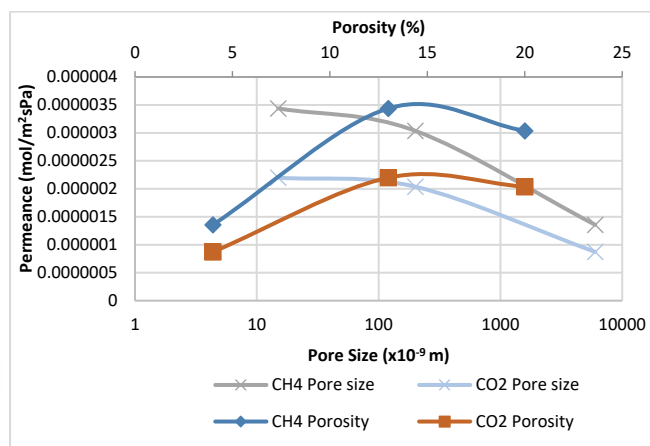


Figure 2. Permeance vs membrane pore size and porosity at 3 bar at 100 degrees Celsius

THE EFFECT OF PRESSURE AND POROUS MEDIA STRUCTURAL PARAMETERS COUPLING ON GAS APPARENT VISCOSITY

¹Ofasa Abunumah, ¹Priscilla Ogunlode, ¹Edward Gobina

¹Robert Gordon University, Centre for Process Integration & Membrane Technology, School of Engineering, Garthdee Road, Aberdeen AB10 7GJ

*Corresponding author e-mail: e.gobina@rgu.ac.uk

ABSTRACT

Crude oil production is still considered a significant contributor to global energy security. To improve oil production, gases such as CH₄, N₂, Air and CO₂ are injected into oil reservoirs in a process called gas Enhanced Oil Recovery (EOR). Authors have used several engineering, geological and geometrical quantities to characterise oil reservoirs and evaluate immiscible gas EOR processes. Viscosity is one of such critical engineering quantities. However, the relationships between viscosity and structural parameters, such as porosity, pore size, and aspect ratio, have not been directly investigated in the literature. This paper investigated the coupling effect of pressure and structural parameters on the apparent viscosity of EOR gases in reservoir pore matrix through rigorous data mining and experimental approaches. The data mining analyses demonstrated that EOR reservoirs are characterised by viscosity and porosity. The experimental investigation indicated that the viscosity of injected EOR gases increases with pressure and pore size, decreases with porosity, and initially decreases before increasing with aspect ratio. The study concluded that CO₂ is the most influenced by porosity, and CH₄ is the least. Furthermore, N₂ is the most responsive to pore size and aspect ratio, while CH₄ is the least responsive.

Keywords: Viscosity, reservoir characterisation, porosity, pore size, EOR gases

INTRODUCTION

In Enhanced Oil Recovery (EOR), viscosity is considered the single most important fluid property that lends itself to the estimation of other engineering quantities such as pressure drop, displacement velocity, momentum, diffusibility, kinetic energy, interfacial tension, capillary number, flowrate, mobility and viscous ratios, [1]. Furthermore, viscosity is featured as a critical quantity in all EOR screening models found in the literature [2].

The displacement of oil by another fluid involves the interactions between the displacing fluid and oil's viscosities, and the interactions with other reservoir properties such as pressure and structural parameters. Gases such as CO₂, N₂, CH₄ and Air are some of the fluids injected into oil reservoirs pore to displace trapped oil. Unfortunately, oil is about 100 times more viscous than these gases [3], and reservoirs are usually structurally heterogeneous. Therefore, a need to understand the interactions.

Previous authors have sparsely studied the effect of pressure and temperature on fluid's viscosity in the context of EOR gases in reservoir pore matrix. Furthermore, the impact of reservoir structural parameters such as porosity, pore size, and aspect ratio on EOR gas viscosity and the consequential effect on gas-oil displacement performance is lacking. Consequently, the study aims to characterise the apparent viscosity of reservoirs and subsequently investigate the coupling effect of pressure and reservoir structural parameters on the competitiveness of EOR gases.

MATERIALS AND METHODS

The methodology applied two rigorous empirical approaches: (1) the data mining of field data from 484 EOR projects and (2) the analyses of data from gas experiments, comprising five reservoir analogue core samples, four gases, and eight isobars. The viscosity, μ , was acquired using gas and radially modified Hagen-Poiseuille equation in Eq. (1). The porosities of the respective cores were acquired using Eq. (2). Pore sizes are as stated by the sample's manufacturer.

$$\mu = -\frac{\pi h}{4QP_2} \left((P_1^2 - P_2^2) / \left(\frac{1}{r_1} - \frac{1}{r_2} \right) \right) \quad (1)$$

$$\text{Porosity} = 1 - \left(\frac{\text{Specific Particle Density}}{\text{Specific Bulk Density}} \right) \quad (2)$$

Where Q is the gas flowrate; P_1 and P_2 are the inlet and outlet pressures; and h , r_1 and r_2 are the height, inner and outer radii of the core sample respectively.

CONCLUSIONS

The study has contributed to engineering knowledge and reservoir practices as follows: It has been demonstrated that EOR technologies and Gas processes are markedly characterised by viscosity (**Figure 1a**) and slightly characterised by porosity (**Figure 1b**). It is established in **Error! Reference source not found.a** that CH₄ and N₂ EOR processes favour relatively low viscosity reservoirs than Air and CO₂ processes. The Coefficient of Variation (CV) indicates that N₂ has the tightest clusters, suggesting that viscosity may be critical to the applicability and performance of N₂ EOR processes in a reservoir.

The study presented a strong relationship between viscosity and porosity for gas EOR technology, as shown by the grey cluster in **Figure 1c**. This relationship reveals that gas EOR is commonly applied to tight reservoirs. Furthermore, the findings from the data mining phase (**Figure 1a, b, and c**) provided an impetus for designing a gas experiment to examine and validate the field application of immiscible gas EOR.

In the experimental phase, it has been identified that porosity inversely affects apparent viscosity under certain conditions of porosity $< 20\%$ and pressure $> 1.4\text{bar}$ (Figure 2a). Beyond this threshold, the viscosity becomes self-sufficient of pressure. Hence any change in porosity and pressure have insignificant or no effect on the apparent viscosities of the EOR gases. As porosity approach unity, the gas viscosity for N_2 , Air, and CO_2 approach equality except for CH_4 . By the nature of the respective gas plots in Figure 2a, it can be concluded that CH_4 is the least competitive in attaining the desirable condition of mobility (< 1) mentioned in [4] and favorable apparent viscosity ratio (< 1) for any coupled pressure and porosity.

Figure 2b shows that N_2 is consistently the most responsive to pore size variation in reservoirs. In contrast, CH_4 is the least. Their respective thermodynamic properties cannot explain the order of the magnitude of the slopes.

Figure 2c shows a quadratic relation exists for the apparent viscosity-aspect ratio. Before attaining the aspect ratio of 5.00×10^4 , the relationship is inverse but becomes positive after that point. For all isobars, N_2 is consistently more responsive to aspect ratio than the other gases. In contrast, CH_4 is the least responsive.

Summatively, it is concluded that N_2 viscosity responds to reservoir structural parameters than the other EOR gases. This information is useful for managing the injection of gases and the displacement of trapped oil in a reservoir with structural variation (heterogeneity).

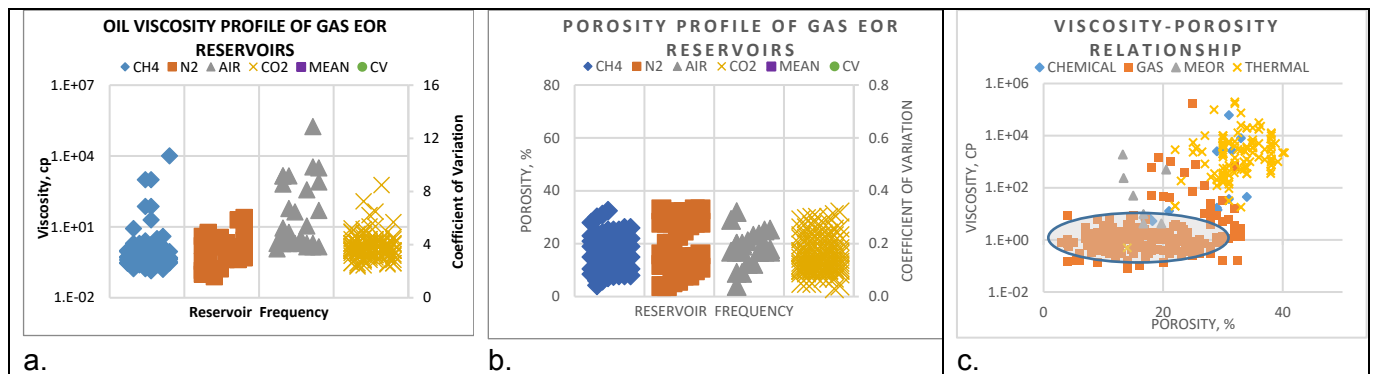


Figure 1. Showing the viscosity (a) and Porosity (b) characterisation, and the viscosity-porosity relationship (c) of EOR reservoirs

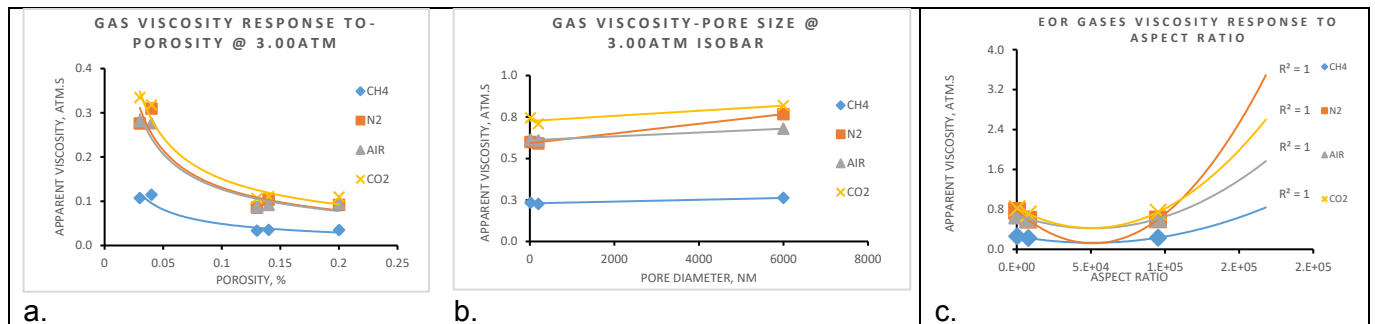


Figure 2. Showing the viscosity-porosity (a) viscosity-pore size (b) viscosity-aspect ratio (c) relationships of EOR gases.

REFERENCES

- [1] Wang X, Chen J, Ren D, Shi Z. Role of Gas Viscosity for Shale Gas Percolation. *Geofluids*. 2020 Sep 30;2020.
- [2] Nageh M, El Ela MA, El Tayeb ES, Sayyoub H. Application of using fuzzy logic as an artificial intelligence technique in the screening criteria of the EOR technologies. In *SPE North Africa Technical Conference and Exhibition 2015 Sep 14*. Society of Petroleum Engineers.
- [3] Mason, E. A., 2020. "Gas". *Encyclopedia Britannica*, <https://www.britannica.com/science/gas-state-of-matter>. Accessed 1/02/2021.
- [4] Abunumah O, Ogunlode P, Gobina E. Experimental Evaluation of the Mobility Profile of Enhanced Oil Recovery Gases. *Advances in Chemical Engineering and Science*. 2021 Apr 12;11(02):154.

COST DESCRIPTION AND CHARACTERISATION OF GAS ENHANCED OIL RECOVERY PROCESSES

¹Ofasa Abunumah, ¹Priscilla Ogunlode, ^{1*}Edward Gobina)

¹Robert Gordon University, Centre for Process Integration & Membrane Technology, School of Engineering, Garthdee Road, Aberdeen AB10 7GJ

*Corresponding author e-mail: e.gobina@rgu.ac.uk

ABSTRACT

Cost optimisation is a critical subject in energy security, such as in oil recovery and production. The cost characterisation of Gas Enhanced Oil Recovery (EOR) has been evaluated using data mining and experimental methods. The underlying engineering and economic premise are that the respective gas EOR processes would experience discrimination in certain CAPEX and OPEX cost centres, such as injectant fluid, drilling infill wells, and power costs. Several authors have examined the cost burden of implementing a gas or have compared two gas performances. However, no literature has simultaneously investigated the cost competitiveness of the four (CH₄, N₂, Air, and CO₂) gases commonly used in Gas EOR technology. This study has been able to fill this gap with a focus on injectant cost. Field data mining reveals that cost and oil price are significant drivers for EOR project initiation. It further shows that EOR reservoirs are characterisable by the injected fluid cost. This was corroborated by the experimental outcome. Therefore, it can be stated that the experimental results sufficiently validate the data mining results. The coupling of the two sets of results reveals the competitiveness of the EOR gases to be stated as: CO₂ > N₂ > Air > CH₄. The competitiveness of CO₂ also favours Carbon Capture and Storage (CCS).

Keywords: EOR cost, reservoir characterisation, Injectants, Gas EOR, Gas cost

INTRODUCTION

Cost is a major consideration in all kinds of energy production. However, crude oil has peculiar CAPEX and OPEX cost centres such as injectant, infill well, power, and compressor cost [1]. The common injectants are CH₄, N₂, Air, and CO₂ gases, and their abilities to enhanced oil recovery are expectedly different [2]. The engineering and economic premise proposes that injectant's coupling of effectiveness and efficiency would lead to a recovery and cost discrimination amongst the EOR gases. The utility of this analysis is both technical and economical. It would allow decision-makers to compare, in advance, their asset capacity to withstand the facility requirements of a proposed gas EOR process and the economic feasibility of the cumulative injectant that would be required through the life of the EOR project.

Economic optimization is the definitive aim of EOR engineering management. An example of this is observed in *Figure 3a* where EOR projects are sensitive to oil price. It has also been stated to be sensitive to injectant cost, fiscal incentives, and complex oil recovery costs [3]. The injectant cost is often treated as a major cost element separate from the OPEX by some authors [3,4,5].

Other investigators have established that the oil produced in an EOR process is quantitatively proportional to the volume of displacing fluid injected [6]. Therefore, it is expected that the oil recovered and revenue from recovered oil will be proportional to the cumulative gas injected and the cost, respectively. Previous authors have studied this topic from a limited perspective and a limited number of gases [4]. Few have compared the cost of two EOR processes [5]. However, no study has simultaneously compared the cost implication of the four EOR gases commonly encountered in EOR processes.

MATERIALS AND METHODS

The data mining phase analysed 484 EOR projects. The reservoirs were grouped into CH₄, N₂, Air, and CO₂ ga EOR processes. The potential cumulative recoverable oil was estimated using a modified Darcy equation for radial flow and the petrophysical parameters and properties of the reservoirs in the respective EOR groups. Then a statistical technique was applied to the data in each group to develop a cluster graph.

Core experiments were carried out for CH₄, N₂, Air, and CO₂, using five core samples, varying pressure (20 to 300KPa), and temperature (293 to 673K) to examine the cumulative gas production profile of the respective gases. The results were then applied to the gas-oil production proportionality principle mentioned in [6]. The optimisation objective is to minimise cumulative injectant cost.

The research used BOC gas pricing quotation for CH₄ (\$4.5E-05/cm³), N₂ (\$5.7E-06/cm³), Air (\$6.1E-06/cm³), CO₂ (\$3.4E-06/cm³) as an industry benchmark for making the analysis. The gas price was normalised to the United States

Dollars of January 1st, 2021. The competitiveness of the benchmarked unit cost of the EOR gases is, therefore: $\text{CO}_2 > \text{N}_2 > \text{Air} > \text{CH}_4$.

CONCLUSIONS

This study contributes to engineering knowledge and reservoir practices such that it has been identified, through data mining and clustering (Figure 3b), that the cumulative injectant cost can characterise gas EOR processes. Air was found to be most sensitive to the cumulative injectant cost. The length of the clusters in Figure 3b and the intersects of the clusters demonstrate that there may be other factors influencing the cumulative cost of gases. Nevertheless, the mean cumulative injectant cost in Figure 3b indicates that CO_2 EOR offers the least cost, while N_2 EOR offers the most cost. The order of cost competitiveness is, therefore: $\text{CO}_2 > \text{Air} > \text{CH}_4 > \text{N}_2$.

Furthermore, the clusters from the experimental analyses (Figure 3c) indicate that CO_2 offers the least cost, while CH_4 offers the most cost. Surprisingly, the cumulative cost of injecting N_2 and Air is higher than that of CO_2 in both reservoir and experimental data. Considering the free availability of Air has been previously mentioned to be a cost opportunity for Air EOR projects, it was expected that Air EOR would translate to a comparatively lower injectant cost. However, this was not the case with the findings of this study. The study, therefore, speculates that the practical cost of processing Air for injection in an oil field may not be as expensive as the BOC quotation. Nevertheless, for theoretical purposes, the experimental ranking of the cost competitiveness of EOR gases is, therefore: $\text{CO}_2 > \text{N}_2 > \text{Air} > \text{CH}_4$.

The coupling of the data mining and experimental results shows some similarities and differences. In both phases, CO_2 is ultimately established to offer the least expensive cumulative injectant.

Consequently, without loss of generalisation, it can now be concluded that for a given reservoir suitable for all gas EOR, CO_2 is the most cost-effective gas to inject. In conclusion, selecting CO_2 makes both economic and environmental sustainability sense as it supports Carbon Capture and Sequestration/Storage (CCS) in reservoir pores.

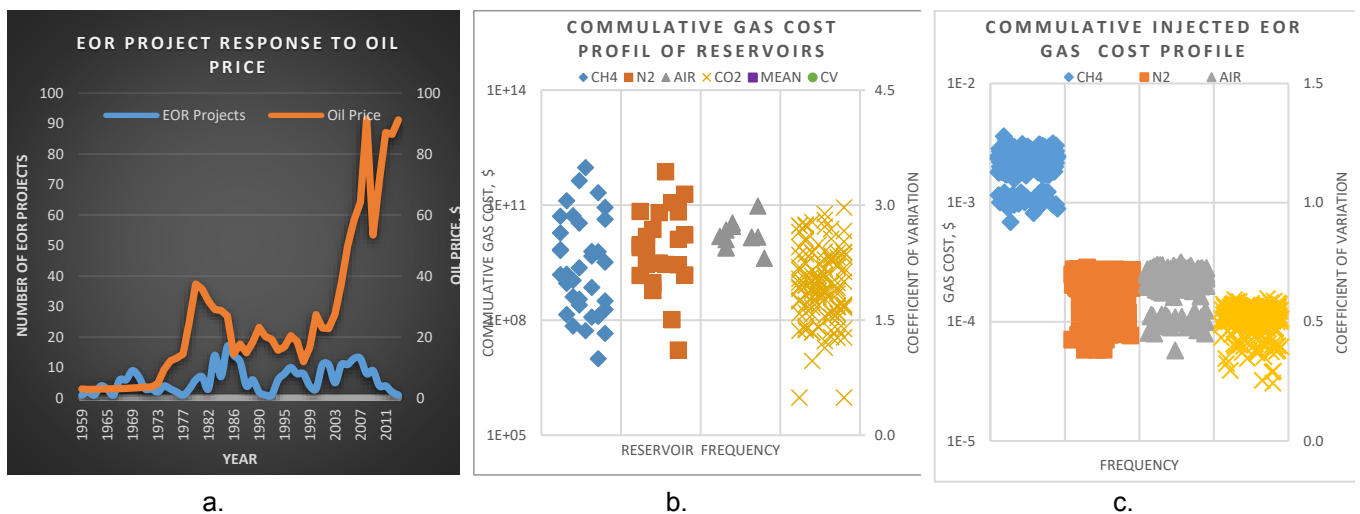


Figure 3. Showing the historical response of EOR projects initiation to oil price, and invariably to oil revenue (a) cumulative gas cost description and characterisation of global EOR reservoirs (b) and experimented EOR gases (c).

REFERENCES

- [1] Putnam JM. Enhanced Oil Recovery Field Case Studies: Chapter 14. Facility Requirements for Implementing a Chemical EOR Project. Elsevier Inc. Chapters; 2013 Apr 10.
- [2] Abunumah O, Ogunlode P, Gobina E. Experimental Evaluation of the Mobility Profile of Enhanced Oil Recovery Gases. *Advances in Chemical Engineering and Science*. 2021 Apr 12;11(02):154.
- [3] Babadagli T. Philosophy of EOR. *Journal of Petroleum Science and Engineering*. 2020 May 1; 188:106930.
- [4] Pershad, H., Durusut, E., Alan, C., Black, D., Mackay, E.J. and Olden, P., 2012. Economic impacts of CO_2 -enhanced oil recovery for Scotland.
- [5] Zekri A, Jerbi KK. Economic evaluation of enhanced oil recovery. *Oil & Gas Science and Technology*. 2002 May 1;57(3):259-67.
- [6] Warner, H.R., and Holstein, E.D., 2007. Chapter 12 – Immiscible Gas Injection in Oil Reservoirs. In Lake, L.W., Fanchi, J.R., Arnold, K., Clegg, J.D., Holstein, E.D. and Warner, H.R. eds., 2007. *Petroleum engineering handbook: reservoir engineering and petrophysics* (Vol. 5). Society of Petroleum Engineers. Pgs. 1103-1147

INVESTIGATION OF BUILDINGS WITH OPTIMUM INSULATION THICKNESS DEPENDING ON DIFFERENT EXTERNAL WALL TYPES AND INSULATION MATERIALS IN TERMS OF MOLD AND MOISTURE RISK

¹ Okan Kon, ^{2*} İsmail Caner

^{1,2} Balıkesir University, Faculty of Engineering, Department of Mechanical Engineering, Çağış Campus, Balıkesir, Turkey

*Corresponding author e-mail: ismail@balikesir.edu.tr

ABSTRACT

In this study, the risk of mold and moisture was investigated for buildings external walls depending on six different wall types (block bims 1, block bims 2, block bims 3, block bims 4, hollow brick and aerated concrete) and two different insulation materials (hemp and aerogel). As insulation thickness, optimum insulation thickness based on life cycle total cost analysis and degree-day method was chosen. While calculating the optimum insulation thickness, it has been assumed that natural gas, coal and electricity are used in the heating period and electricity is used in the cooling period as energy sources. For the reference city Balıkesir, the outdoor temperatures are taken as -3°C and -10.5°C . Hemp, which is chosen as an insulation material, is a natural insulation material with a partially low cost and partially high heat conduction coefficient. Aerogel, on the other hand, is a newly developed technological insulation material with a very high cost and a very low heat conduction coefficient. In addition, the temperature difference between the indoor environment and the inner wall surface was examined in terms of thermal comfort.

Keywords: Optimum insulation thickness, moisture and mold risk, hemp insulation, aerogel insulation

INTRODUCTION

There are numerous studies in the literature on the risk of mold growth, especially for the exterior walls of buildings. Although many studies have been carried out on the optimum insulation thickness, it has been observed that there are no studies on the risk of mold and moisture formation of the optimum insulation thickness. Mold and moisture risk in the building envelope, such as the external wall, causes deterioration of the properties of the building envelope, such as thermal resistance and storage. For mold and moisture risk, the relative humidity of the indoor environment should be above 80% and the temperature difference between the indoor environment and the inner wall surface should be higher than 3°C . The aim of the study is to examine the risk of mold and moisture and thermal comfort for block bims 1, block bims 2, block bims 3, block bims 4, hollow brick and aerated concrete and external walls with hemp and aerogel. Hemp and aerogel insulation materials, which are newly used in the literature, were used as insulation materials. It has been assumed that natural gas, coal, and electricity are used in the heating period and electricity is used in the cooling period as energy sources. The cost of these two insulation materials (hemp is $100 \text{ \$/m}^3$ and aerogel is $730 \text{ \$/m}^3$) and heat conduction coefficient (hemp 0.04 W/m.K and aerogel 0.014 W/m.K) are very different from each other. In the study, calculations were made for the province of Balıkesir, which is located in the second climate zone, according to the TS 825 Turkish insulation standard. According to the TS 2164 heating system standard, it is recommended to design a heating system by accepting the outdoor temperature as -3°C for the heating period of Balıkesir province. In addition, from the long-term data of the General Directorate of Meteorology the lowest average outdoor temperature value of Balıkesir province is given as -10.5°C . For these two temperatures, the risk of external wall moisture and mold growth was investigated. A new study has been carried out on the risk of moisture and mold growth for the optimum insulation thickness calculated based on two different insulation materials in terms of many properties. The risk of mold and moisture is a situation investigated as a result of high partial pressure, saturation pressure between the wall layers. In the study, examinations were made about whether the optimum insulation thickness, which has not been examined in the literature, is sufficient in terms of preventing mold and moisture growth [1-6].

MATERIALS AND METHODS

For hemp insulation material, the optimum insulation thickness is 0.131 m, which is calculated as a result of hollow brick wall material, using electricity during heating and cooling periods. The lowest insulation thickness is 0.016 m, calculated as a result of using block bims 4 wall type, natural gas as an energy source in the heating period, and electricity in the cooling period. For the aerogel insulation material, the optimum insulation thickness is 0.025 m, which is calculated as a result of the hollow brick wall material and the use of electricity during the heating and cooling periods. It has been determined that insulation is not necessary as a result of using the block bims 4 wall material, natural gas as an energy source in the heating period, and electricity in the cooling period. In Figure 1 optimum insulation thicknesses depending on the different external wall types, insulation materials and energy sources are given. As an energy source, electricity has a lower calorific value ($3,595 \text{ 106 J/kWh}$) and a low cost ($0.118 \text{ \$/kWh}$), and its thermal efficiency (99%) is very high. Natural gas has a high lower calorific value (34.485 106 J/m^3), a high cost ($0.385 \text{ \$/m}^3$), and an average thermal efficiency (93%). Hollow brick wall material has the highest heat conduction coefficient (0.450 W/m.K) but the lowest thickness (0.135 m). Block bims 4 wall material, on the contrary, has the lowest heat conduction coefficient (0.150 W/m.K) but the highest thickness (0.250 m). The cost of aerogel

insulation material is very high. This affects the insulation thickness. As a result of the use of hemp as insulation material for the outdoor temperature (-3) °C and electricity as an energy source in the heating and cooling period, the temperature difference between the indoor environment and the inner wall surface is the lowest value at 1.472 °C. This temperature difference is the most suitable situation in terms of thermal comfort in buildings. The highest value is 3.795 °C, calculated as a result of the use of aerogel as insulation material and electricity as an energy source in the heating and cooling period. This temperature difference is also unsuitable in terms of thermal comfort in buildings. It should be examined in terms of mold and moisture risk. As a result of the use of hemp as insulation material for the outdoor temperature (-10.5) °C and electricity as an energy source in the heating and cooling period, the temperature difference between the indoor environment and the inner wall surface is the lowest with 1.952 °C. This temperature difference is suitable for thermal comfort in buildings. The highest value is 5.023 °C, which is calculated as a result of using aerogel insulation material and natural gas as an energy source in the heating period and electricity in the cooling period. This temperature difference is also an unsuitable situation in terms of thermal comfort in buildings. It should be examined in terms of mold and moisture risk.

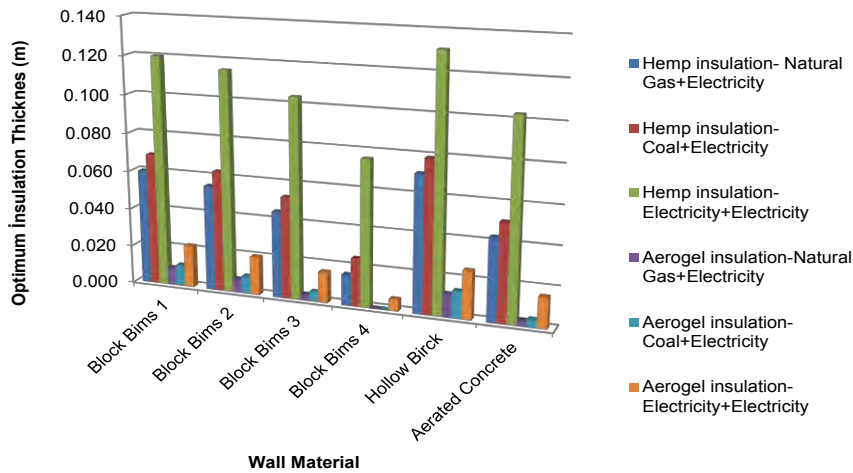


Fig. 1. Optimum insulation thicknesses depending on the different external wall types, insulation materials and energy sources

CONCLUSIONS

It has been determined that partial pressure is higher than saturation pressure depending on the 80% indoor relative humidity for the temperature values calculated as a result of using aerogel insulation material for the outdoor temperature (-3) °C, using natural gas as an energy source in the heating period and electricity in the cooling period thus there is a risk of mold and moisture growth. For the outdoor temperature (-10.5) °C, for the temperature values calculated as a result of firstly the use of aerogel insulation material and natural gas as an energy source in the heating period and electricity in the cooling period, and secondly the use of aerogel insulation material and coal as an energy source in the heating period and electricity in the cooling period. The partial pressure has been found to be greater than the saturation pressure and there is a risk of mold and moisture formation. The amount of moisture to be formed will be given in detail. In particular, mold and moisture risk are observed as a result of the use of aerogel insulation material on the outer wall. The reason for this is that the price of the insulation material is very high, so a very low optimum insulation thickness has been calculated. This thickness is not sufficient to prevent the risk of mold and moisture in the external wall structure. In future studies, mold and moisture content examinations will be carried out to include wood-derived exterior walls and different insulation materials with much higher moisture and mold content.

REFERENCES

- [1] Dlimi M, Iken O, Agounoun R, Zoubir A, Kadiri I, Sbai K, Energy performance and thickness optimization of hemp wool insulation and air cavity layers integrated in Moroccan building walls, *Sustainable Production and Consumption* 20 (2019) 273–288
- [2] Uygunoğlu T and Keçebas A, LCC analysis for energy-saving in residential buildings with different types of construction masonry blocks, *Energy and Buildings* 43 (2011) 2077–2085
- [3] Huang H, Zhou Y, Huang R, Wu H, Sun Y, Huang G, Xu T, Optimum insulation thicknesses and energy conservation of building thermal insulation materials in Chinese zone of humid subtropical climate, *Sustainable Cities and Society* 52 (2020) 101840
- [4] Cuce E, Cuce P M, Wood C J, Riffat S B, Optimizing insulation thickness and analysing environmental impacts of aerogel-based thermal superinsulation in buildings, *Energy and Buildings* 77 (2014) 28–39
- [5] Kurekci N A, Determination of optimum insulation thickness for building walls by using heating and cooling degree-day values of all Turkey's provincial centers, *Energy and Buildings* 118 (2016) 197–213
- [6] Lopez-Arce P, Altamirano-Medina H, Berry J, Rovas D, Sarce F, Hodgson S, Building moisture diagnosis: Processing, assessing and representation of environmental data for root cause analysis of mould growth, *Building Simulation* (2020) 13: 999–1008

EXPERIMENTAL STUDY OF RED PINE BIOCOAL AND SOMA LIGNITE BLENDS IN A CIRCULATING FLUIDIZED BED UNDER OXY-FUEL COMBUSTION

^{1*} Babak Keivani, ² Hayati Olgun, ³ Aysel.T Atımtay

¹Kırşehir Ahi Evran University, Department of Mechanical Engineering, 40200 Merkez, Kırşehir, Turkey

²Ege University, Solar Energy Institute, 35100 Bornova, Izmir, Turkey

³Middle East Technical University, Department of Environmental Engineering, 06800 Cankaya, Ankara, Turkey

*Corresponding author e-mail: bab20822000@gmail.com

ABSTRACT

Biocoal produced from red pine wood chips was co-combusted with Soma lignite in a circulating fluidized bed combustor (CFBC) system. The thermal capacity of the combustor was 30 kW, and the temperature was held at 850+50°C. Both air and oxygen enriched air was used during combustion tests of different ratios of lignite and biocoal mixtures. A screw type torrefaction system was used under 300 degrees C and 30 minutes to produce biocoal from red pine wood chips. The ratio of the fuel mixture was increased up to 50% by wt. Successful combustion was carried out with 50%/50% mixture of coal and biocoal. Keeping oxygen concentration in the oxidant between 21-28% by volume. The results of combustion tests showed that biochar can be a good additive to lignite coal to reduce SO₂, CO and N₂O flue gas emissions. Addition of oxygen to air increased the combustion efficiency and reduced CO emissions. Since biocoal does not have sulfur in it, replacement of coal with biocoal significantly reduced SO₂ emissions. However, emissions of NO_x increased with high oxygen concentrations and high levels of biocoal addition.

Keywords: Biocoal, Oxygen enriched combustion, Emissions

INTRODUCTION

The General Directorate of Forestry (GDF) estimates that Turkey has an annual sustainable forest residue potential of five to seven million tons [1]. It is crucial that these forest residues be converted to combustible solid fuels. However, conventional combustion technologies cannot be effectively used to fulfill the energy demands of the country. We are challenged to use wood biomass in general as a fuel for combustion / co-combustion systems because of its fuel properties compared to lignite [2]. To this end, the use of biomass with coal in power plants has its own limitations. For this reason, biomass and coal are not often used together in power plants. Torrefaction is a method that can be used to eliminate / reduce all these negative effects. Biomass co-firing also has the potential to reduce emissions [3]. Previous studies have widely proposed and reported on the use of biomass blends as feedstock in the oxy-combustion process [1]. However, there are very limited pilot studies on the use of biocoal mixtures as a raw material in oxygen combustion processes [4,5]. None of these studies has performed an oxy-combustion study of biocoal mixtures to further evaluate its properties as a potential solid fuel.

In this research torrefied pinewood chips were used for co-combustion with lignite. Detailed information about the torrefaction system is given elsewhere [6,7]. The purpose of this study is two-fold: Firstly, to use torrefied biomass (biocoal) with a lignitic coal for co-combustion, so that the emissions can be lowered as compared to the combustion of lignite coal alone in a power plant for energy generation. Secondly, to use oxy-fuel combustion system to produce a flue gas consisting of CO₂ and H₂O vapor, so that CO₂ in the flue gas can be captured with a CCS technology.

MATERIALS AND METHODS

Biocoal and Soma lignite were used as fuels for this study. Biocoal was prepared by torrefaction of red pine wood chips in a laboratory scale torrefaction system under nitrogen atmosphere at 300°C for 30 min. The details of the system is given in [6,7].

Experimental system and procedure

The experimental system used in this study is a pilot scale CFBC system consisting of feeder, combustor reactor, cyclones, down comer, return leg, primary and secondary air feeding systems, combustor heaters, ash hoppers, a flue gas cooling system, a bag filter and chimney [3,8].

RESULTS AND DISCUSSION

First of all, soma lignite was combusted alone in air and in the oxygen enriched atmosphere to see its combustion behaviour. The average bed temperature increased as the oxygen concentration levels increased in the experiments. The emissions of major pollutants (CO, NO, and SO₂) are considered in this study. CO emission is an indication of non-complete combustion. Therefore, as the oxygen concentration in the combustion air increases, CO concentration in the flue gas decreases due to better combustion with plenty of oxygen (Figure 1a). In contrary to CO emissions, as the oxygen concentration in the combustion air and biocoal amount in the fuel mixture increases, CO₂ emissions

increase as explained in CO emissions due to better combustion (Figure 1b). The results show It is the increase in the proportion of biocoal in the fuel composition that results in higher NOx emissions, although the nitrogen content of biochar (0.63% by weight) is lower than the amount of nitrogen present in lignite (0.84% by weight) (Figure 1c). when the oxygen concentration in the combustion air increases, the combustion efficiency also increases to 98.5% for oxygen concentration of 28% with better combustion (Figure 1d).

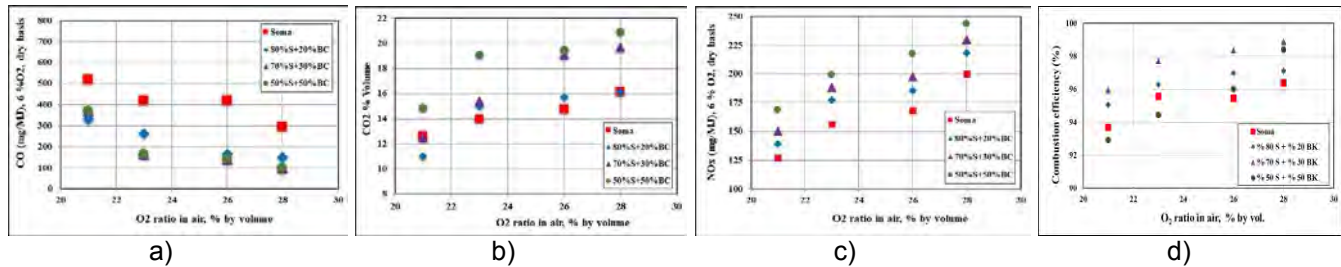


Fig. 1. Effect of O₂ concentration on a) CO emissions, b) flue gas CO₂ concentration, c) NO_x emission and d) combustion efficiencies

CONCLUSIONS

Oxygen enrichment decreased the CO formation and increased CO₂ concentration in all cases of combustion, either coal alone or with coal + biocoal, due to better combustion. As the share of the biocoal in the fuel mixture increased, emission of CO for the Soma lignite decreased. The highest CO emission was obtained with Soma lignite alone, while the CO emission decreased as the biocoal additive increased. In addition to decreased CO emission, the combustion efficiency increased with biocoal addition. As the oxygen content increased along with the addition of biocoal, Soma showed a faster increase in CO₂ concentration as well as the combustion efficiency.

Enriching oxygen concentration in air with O₂ up to 28%, increased NO_x emissions by promoting Fuel-N conversion in the temperature range of this study, and partly by promoting the Thermal-NO_x formation. Higher biocoal share in the fuel blend caused lower SO₂ emissions primarily due to the low S content of biocoal.

When Orhaneli and Soma lignites are compared, more NO_x formation takes place in Orhaneli case than Soma case with increase of oxygen in combustion air. With the addition of biocoal to these lignites, NO_x formation increased in both cases. Therefore, we may expect the synergistic effect can be attributed to the high alkaline and the earth alkaline metal oxide content of the biocoal as well as some formation of Thermal-NO_x in addition to Fuel-NO_x. However, this is for sure that co-combustion of Soma lignite with biocoal is a very good option to give support to a low-quality coal.

REFERENCES

- [1] Nedim S. Energy production from forest residues in Turkey. 3rd International Symposium and Innovative Technologies in Engineering and Science. Valencia. Spain. ISITES; 2015.
- [2] Aysel TA, Ufuk K, Alper U, Berrin E, Murat V, Hayati O, Hüsnü A. Co-firing of pine chips with Turkish lignites in 750 kWth circulating fluidized bed combustion system. *Bioresource Technology*. p. 601–10; 2017
- [3] Murat V, Aysel T.A, Hayati O, Hüsnü A. Emission characteristics of co-combustion of a low calorie and high sulfur–lignite coal and woodchips in a circulating fluidized bed combustor: Part 1, Effect of excess air ratio. *Fuel*. p. 792–80; 2014
- [4] Selçuk B, Sedat K, İkbâl S, Kamil K. A perspective for potential and technology of bioenergy in Turkey: Present case and future view. *Renew. Sustain. Energy Rev*. p. 48:228–239; 2015
- [5] Mehmet M. Vision 2023: Feasibility analysis of Turkey’s renewable energy projection. *Renew. Energy*. P. 570–75.
- [6] Hayati O, Babak K, Selin G, Arzu K. Experimental study on torrefaction of pine wood in a continuous screw conveyor. 6th International Symposium on Energy from Biomass and Waste. November 14-17. Venice, Italy; 2016
- [7] Babak K, Selin G, Hayati O, Aysel T.A. Torrefaction of pine wood in a continuous system and optimization of torrefaction conditions. *International Journal of Energy Research*. p. 4597-4609; 2018
- [8] Ufuk K. and Sibel O. Oxygen enriched combustion and co-combustion of lignites and biomass in a 30 kWth circulating fluidized bed. *Energy*. p. 317-328; 2016

POTENTIAL USE OF RENEWABLE ENERGY FOR RURAL ELECTRIFICATION IN PAKISTAN BY INCORPORATING BLOCKCHAIN TECHNOLOGY

Aqsa Rana^{a*}, Gyula Gróf^{a, b}

^a Department of Energy Engineering, Faculty of Mechanical Engineering, Budapest University of Technology, Műegyetem rkp. 3, Budapest 1111, Hungary

^b Center for Energy Research, Konkoly-Thege Miklós út 29-33, Budapest 1121, Hungary

*Corresponding author: aqsarana@energia.bme.hu

ABSTRACT

Significant innovations in technology and progressing use the renewable energy sources (RES) reinforce the demand for the sustainable, continuous, and abundant supply of energy to every consumer. As an emerging technology, blockchain promises to provide temper proof, secure, transparent, and decentralised energy trading mechanisms that help provide sustainable environmental solutions by the circulating economy to empower consumers and prosumers. The rapid development of blockchain technology has gained interest from energy start-ups, innovation developers, finance suppliers, academic institutions and government. This study outlines the potential significance, benefits and application of blockchain technology and analyses how Pakistan can integrate blockchain technology into its distribution system to cope with current challenges. After a detailed discussion of Pakistan's current financial position, digital market structure, energy policy and technology situation for the implication of blockchain technology, the Photographic Geographical Information System (PVGIS-5) database tool is used to estimate solar power generation capacity from the prosumer community in potential areas of the country like Baluchistan province. Then introduces a street scenario about domestic power generation and blockchain-based distribution into Pakistan's energy sector like the Brooklyn energy system by regulating laws, revising energy policies and suitable development subsidies.

Keywords: Electrification, Digitalization, Decentralising, Blockchain technology, Renewable energy.

INTRODUCTION

First of all, we provided an insight into the growing need for renewable energy at the global level due to continuously increasing industrialization and technology-dependent lifestyle (Electrification). The clean & green, secure and substantial amount of energy has become the foremost requirement of the time. A lot of smart and innovative initiatives and strategies are formulated from time to time to cope with energy challenges, so blockchain is one of those technologies. Background information related to the simplified technical structure of blockchain technology, with its core function, is explained in this research [1]. Blockchain is a game-changer technology with diverse applications in various grey areas, having several built-in essential features that can augment several traditional and imminent applications in the energy sector [2] Blockchain has enormous energy system applications due to its socio-economic and consumer-centric influences. Blockchain can reinforce three significant energy trends digitalisation, decarbonisation and electrification.

Secondly, we discussed an in-depth understanding of blockchain technology infrastructure and its practical importance, the general classification of its implementation areas and its overall application scenarios. Potential attributes and aspects in which blockchain technology might affect the operation and management of the energy system are resource sharing, transparency, billing, competitive nature, trading, market estimation, automatic control, grid management, swift communication & data transfer and so on [3]. Third, we focused mainly on blockchain technology in the energy sector and highlight its potential attributes to the energy sector. Then we review practical used case applications of blockchain technology in the energy sector in the world and contoured global experience for the development of blockchain technology in Pakistan's energy sector. Fourth, we discussed in detail Pakistan's current energy generation, transmission and distribution system, demand and supply structure, digital market situation and outlined position and adoption potential of blockchain technology in Pakistan's energy sector. Then with the help of the PVGIS-5 database tool, we identified the most suitable peripheral area of the country, Baluchistan province. The applicable scenario is suggested with real-time implementation strategies. Finally, we analysed barriers related to the implementation of blockchain technology with facts and figures, clarify its function mechanism, and make an in-depth discussion on possible ways, current risks, and future scope of integration of blockchain technology into Pakistan's energy sector.

CONCLUSION AND POLICY IMPLICATIONS

Integration of blockchain into the energy market enhances its capabilities into the main six dimensions: economic gadgets, reliable governance, deft environment, more mobility, effective dwelling, and smart human being. Keeping in view all outstanding feature of blockchain, we attempted to suggest its integration in Pakistan's energy sector, especially for the development and electrification of the rural areas. Currently, the country's centralised energy system faces many challenges that might be addressed and alleviated by blockchain technology. Presently all

circumstances like the growing use of renewable sources, promotion of distributed power generation, sustainable development goals, circular economy, secure and error-free energy transactions procedure are in favour of the successful implementation of blockchain technology in the energy sector, similar to health, finance, market, agriculture and many more sectors. Apart from its development into various sectors, blockchain technology in the energy sector is still in the exploratory phase. However, the major barrier is not just technology but maybe the energy policy.

PVGIS-5 is used to calculate the monthly PV energy and solar irradiation for the Baluchistan province. However, 211.4 kWh/m² average monthly sum of global irradiation per square meter received by the modules of the given system is quite suitable for local power generation. So, an implementation strategy like the Brooklyn energy system is proposed for decentralised domestic power project with detailed site allocation according to demand. Hence this study paved the way towards new sustainable development of RES in Pakistan. Hopefully, this case study provides considerable room for developers to explore this research domain and encourage the implementation of local energy generation and decentralised distribution to gain a double advantage. However, such the latest smart technologies are not common in practice, not just in Pakistan but around the globe. Few suggestions for Pakistan's energy system development are provided after a detailed analysis of current facts and figures.

- **Policy:** presently outdated system governs the energy sector, which does not seem to encourage blockchain technology in the energy sector. So, policies should be revised, more flexible rules for certifications and licenses should be regularised.
- **Individual production:** license provision system should be more prompt and simplified. Distributed power generation should be promoted to adjust the domestic energy need by mutual power assistance among household users.
- **Institutional framework:** government should support educational framework and research institutions to focus on relevant research. Domestic talent should train and upgrade to cope with real-time problems and their ultimate solutions.
- **Incentive mechanism:** current practices are not perfect to attract new users. More subsidies should provide to encourage new investors. Relevant regulation should be more convenient.
- **Management:** energy management system itself should be simple as well as improved and efficient.

REFERENCES

- [1] A. Ahl, M. Yarime, K. Tanaka and D. Sagawa, "Review of blockchain-based distributed energy: Implications for institutional development," *Renewable and Sustainable Energy Reviews*, vol. 107, pp. 200-211, 2019.
- [2] Q. Wang and M. Su, "Integrating blockchain technology into the energy sector — from theory of blockchain to research and application of energy blockchain," *Computer Science Review*, vol. 37, 2020.
- [3] M. Andoni, V. Robu, D. Flynn, S. Abram, D. Geach, P. McCallum, A. Peacock and D. Jenkins, "Blockchain technology in the energy sector: A systematic review of challenges and opportunities," *Renewable and Sustainable Energy Reviews*, vol. 100, pp. 143-174, 2019.

ANALYSIS OF ROOF THERMAL PERFORMANCE WITH INNOVATIVE TECHNOLOGY

¹Noelia Alchapar,¹Erica Correa

¹Affiliation (Institute of Environment, Habitat and Energy. National Council of Scientific and Technical Research. INAHE-CONICET) CCT-Mendoza. Av. Ruiz Leal s/n - Parque Gral. San Martín, M5500 Mendoza, Argentina

*Corresponding author e-mail: nalchapar@mendoza-conicet.gob.ar

ABSTRACT

The roof is the surface most exposed to solar radiation in a home; therefore, evaluating the thermal performance of different roofing technologies can significantly improve the building's thermo-energetic behavior. This work presents an experimental study that analyzes the thermal behavior of a single-family home that modifies the roof surface properties. Comparison of the thermal performance of the house is made under two roof solutions: (i) base case presents an albedo of 0.49 and thermal emissivity of 0.25; (ii) optimized case presents a cladding with smart technology that incorporates bituminous gas microspheres to its composition in addition to being a material with cool characteristics, the albedo of 0.85 and thermal emissivity of 0.90. During the evaluated summer period, the optimized roof solution shows a more efficient thermal performance than the base roof. Optimized roof achieves drops of up to 18°C in the outdoor surface temperature and up to 5°C in the indoor surface temperature, while the indoor air temperature goes down to 3°C.

Keywords: Building performance; Cool roof; Surface temperature; Indoor air temperature.

INTRODUCTION

In the 21st century, environmental and energy problems became more evident, which led to a greater interest in the international academy in investigating the scope, limitations, and potential of different construction materials as a measure of adaptation and mitigation of cities to the growing global warming [1].

It is known that buildings consume a large amount of energy throughout their useful life, from the manufacture of raw materials to their demolition. However, the use and maintenance (or operational) stage is the one with the greatest energy impact. In a building with a useful life of 50 years and an annual energy consumption of 50 kWh / year, operational consumption represents 83% of the total energy consumed by the building during its entire useful life. In response to this, the construction materials industry is directing its technological efforts to the development of smart materials through the incorporation of nanotechnology to increase their thermal and optical characteristics.

The application of cool materials - high albedo (α) and high thermal emissivity (ϵ) - on surfaces of roofs, walls, streets are at the forefront of building energy-saving techniques [2] and urban cooling [3]. Numerous theoretical models and field studies have quantified the benefits of such measures, including emission reductions and improvements in air quality and mitigation of the urban heat island effect [4].

The roof is the surface most exposed to solar radiation in a home, therefore evaluating the thermal performance of different roofing technologies can significantly improve the building's thermo-energetic behaviour [5,6]. This research presents an experimental study that analyzes the thermal behavior of a single-family home that modifies the surface properties (α and ϵ) of its roof. Comparison of the thermal performance of the house is made under two roof solutions: base and optimized (Figure 1)



Figure 1. Base roof with aluminum membrane and optimized with smart cladding.

EXPERIMENTAL STUDY

The sample unit studied corresponds to a type of social housing, with a compact and attached floor plan and with an east-west orientation, located in the city of Mendoza, Argentina (lat 32°54' 55"S, lon 68° 52' 19 "W). Base roof is made of a 3 mm aluminum membrane; 10 mm lightened mortar; 50 mm expanded polystyrene; pinewood boards 3/4" (U-value = 0.55 W/m²K), the wall is uninsulated brick (U-value= 2.08 W/m²K). Base roof presents an $\alpha=0.49$ and $\epsilon=0.25$. The optimized roof presents a cladding with smart technology that incorporates bituminous gas microspheres to its composition in addition to being a material with cool characteristics ($\alpha=0.85$ and $\epsilon=0.90$).

The thermal monitoring of the house was carried out from January 1 to 30, 2021. The environmental characteristics of the measurement days were recorded with a mobile meteorological station type ONSET Weather HOBO®, model H21 -001. Three points of the house were monitored: (i) outdoor surface temperature of the roof (T_{so}), with a data logger type Onset HOBO® UX120; (ii) roof indoor surface temperature (T_{si}), with LASCAR® EL-USB-TC type data loggers; and (iii) indoor air temperature (T_{ai}), with data logger type Onset HOBO® H08-003-02. Table 1 describes the thermal ranges monitored during the test.

Table 1. Thermal behavior of houses with base roof (left) and optimized (right). Indoor air temperature (T_{ai}), indoor surface temperature (T_{si}) and outdoor (T_{so}).

Statistics	Base Roof			Optimized Roof		
	T_{ai} (°C)	T_{so} (°C)	T_{si} (°C)	T_{ai} (°C)	T_{so} (°C)	T_{si} (°C)
Mean	29.9	34.1	31.1	28.1	25.4	27.5
Max	33	57.5	37	30.1	39.3	32
Min	26.2	17.5	25	25.7	12.6	22.5

CONCLUSIONS

During the tested summer period, the optimized roof solution shows a more efficient thermal performance than the base roof. The innovative cladding achieves drops of up to 18°C in the T_{so} and up to 5°C in the T_{si} of the inner wood ceiling. The T_{ai} drops to 3°C, this indoor reduction could improve the comfort conditions of homes without additional conditioning, or optimize the efficiency of air conditioning equipment, causing large savings in energy consumption for refrigeration. In future work, it is planned to develop a theoretical model through software building energy simulation to calculate the annual balance of the application of this technology, considering the benefits in summer and the penalties in winter.

REFERENCES

- [1] Zinzi M. Cool materials and cool roofs: Potentialities in Mediterranean buildings. Adv Build Energy Res [Internet]. 2010 Jan 1;4(1):201–66. Available from: <https://doi.org/10.3763/aber.2009.0407>
- [2] Kim H, Clayton MJ. Parametric behavior maps: A method for evaluating the energy performance of climate-adaptive building envelopes. Energy Build [Internet]. 2020 Jul; 219:110020. Available from: <https://doi.org/10.1016/j.enbuild.2020.110020>
- [3] Alchapar NL, Pezzuto CC, Correa EN. Análise multivariada como ferramenta para orientar o desenho de espaços urbanos termicamente aptos. Estudo de caso da cidade de Campinas e de Mendoza, Argentina. In: XIV Encontro Nacional e X Encontro Latinoamericano de Conforto no Ambiente Construído. 2017.
- [4] Manni M, Bonamente E, Lobaccaro G, Goia F, Nicolini A, Bozonnet E, et al. Development and validation of a Monte Carlo-based numerical model for solar analyses in urban canyon configurations. Build Environ [Internet]. 2020;170(November 2019):106638. Available from: <https://doi.org/10.1016/j.buildenv.2019.106638>
- [5] Santamouris M, Kolokotsa D. On the impact of urban overheating and extreme climatic conditions on housing, energy, comfort and environmental quality of vulnerable population in Europe. Energy Build [Internet]. 2015 Jul 1 [cited 2020 Mar 10]; 98:125–33. Available from: <https://www.sciencedirect.com/science/article/pii/S0378778814007877>
- [6] Alchapar NL, Colli MF, Correa EN. Albedo Quantification Using Remote Sensing Techniques. Cool Roof in the Metropolitan Area of Mendoza-Argentina. IOP Conf Ser Earth Environ Sci [Internet]. 2020 Jun 19; 503:012035. Available from: <https://iopscience.iop.org/article/10.1088/1755-1315/503/1/012035>

OUTDOOR PERFORMANCE OF AN IMPROVED THERMOELECTRIC HEAT PUMPING SOLAR AIR HEATER

¹ Josué Rock Segnon, ^{1,2*} Howard O. Njoku

¹ Applied Renewable and Sustainable Energy Group, Department of Mechanical Engineering, University of Nigeria, Nsukka 410001, Nigeria, lookmansegnon1998@gmail.com

² Department of Mechanical Engineering Science, University of Johannesburg, 2006 Auckland Park, South Africa

*Corresponding author e-mail: howard.njoku@unn.edu.ng; nwokoma@gmail.com

ABSTRACT

In this study, thermoelectric coolers (TECs) were used as heat pumps to improve the performance of a solar air heating system. Outdoor tests were carried out on two solar air collectors, one without TEC and the other with four TECs (model TEC1-12706) attached at the back of the absorber plate. The TECs were powered by a 40Wp mono-Si PV module to pump heat from the absorber plate in the collector. The heat collected and the energy conversion efficiency of the systems were analyzed and compared. The results showed that the performance of the solar air heater was improved by the incorporation of TE heat pumping. The heat collection and energy efficiency of the solar air heater were improved by 22.02% and 66.7%, respectively when TE heat pumping is applied.

Keywords: Solar air heating, Thermoelectric cooler, Heat pumping, Energy efficiency

INTRODUCTION

Combining solar energy conversion technologies considerably increases the systems output compared to standalone solar energy conversion technologies [1]. Thermoelectric modules (TEMs) can be combined with solar conversion systems to improve energy production. TE generators can be attached at the back of the PV module to convert the temperature difference between the PV module and the air into electricity and improve the system power output by up to 15% [2, 3]. Also, thermoelectric coolers (TEC) can be powered by PV modules to perform heating/cooling. This leads to reduction in size, easy mobility, etc. [4,5].

In this paper, a novel approach of improving the thermal performance of SAHs has been investigated experimentally. TE heat pumping having been proven as a substantial means of improving the performance of heating/cooling systems, no work, to date, is known to report TE heat extraction from the absorber plate in solar air heaters.

MATERIALS AND METHODS

The energy output of a 40Wp PV module was used to power four TECs (TEC1-12706) attached at the rear side of the absorber plate in a thermal collector adjacent to the PV module. The specifications of the different components of the solar air heater are presented in Table 1. The experimental setup is shown in Fig. 1. Figure 2 shows the TECs attached at the back of the absorber plate in a cross-sectional view of the TE heat pumping solar air heater (TE-SAH), with heat sinks for effective dissipation of the heat.

Table 1. TE-SAH materials

Designation	Specifications
Casing	Wood
Absorber plate	Steel; 430*430*2mm
Insulation	Polystyrene; 20mm thick
TE module	TEC1-12706; 40*40*4.2 mm
PV module	Mono-Si 40Wp



Figure 4. Experimental setup

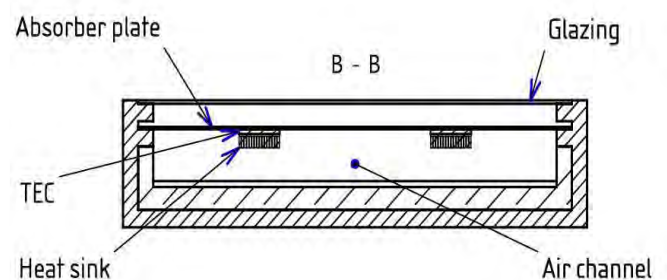


Figure 5. Cross-sectional view of TE-SAH

A reference prototype of the SAH, without any TEC was built in parallel to the TE-SAH to compare the thermal energy production (Eq. (1) and Eq. (2)) and the thermal energy efficiency (Eq. (3) and Eq. (4)). Experimental data were collected on the two prototypes at the same location (Nsukka, 6:8429°N; 7:3733°E. Nigeria).

$$Q_u = \dot{m}c(T_{out} - T_{in}) \quad (W) \quad (1)$$

$$Q_{u-cum} = \int \dot{m}c(T_{out} - T_{in}) dt \quad (J) \quad (2)$$

$$\eta_{th} = \frac{Q_u}{S A_c} = \frac{\dot{m}c(T_{out} - T_{in})}{S A_c} * 100\% \quad (3)$$

$$\eta_{cum} = \frac{\int Q_u dt}{\int S A_c dt} = \frac{\int \dot{m}c(T_{out} - T_{in})}{\int S A_c} * 100\% \quad (4)$$

where Q_u is the heat gain (W), \dot{m} is the air flow rate (kg/s), c is the heat capacity of air (J/kg K), T_{out} and T_{in} are the outlet and inlet air temperature (K), respectively, S is the solar irradiance (W/m^2), A_c is the absorbing surface of the collector (m^2), η_{th} and η_{cum} are the instantaneous and cumulative energy efficiency, respectively.

CONCLUSIONS

The outlet air temperature in the TE heat pumping solar air heater was higher than that in the reference solar air heater, though the intensity of the irradiance onto the reference SAH was higher than that onto the TE heat pumping SAH. The cumulative thermal energy of the collector was 463.43 kJ higher in the TE-SAH than in the reference SAH, representing an increase of 22.02% by application of TE heat pumping (Fig. 3a). The energy efficiency of the TE heat pumping solar air heater was 46.73%, 66.73% higher than that of the conventional solar air heater which achieved an energy efficiency of 28.03% (Fig. 3b). The performance of the TE heat pumping is also affected by the power input to the TECs which was directly dependent on the PV electrical energy output. Improvement of this system could be achieved by the use of a PV module of higher electrical output, hence higher power input to the TECs.

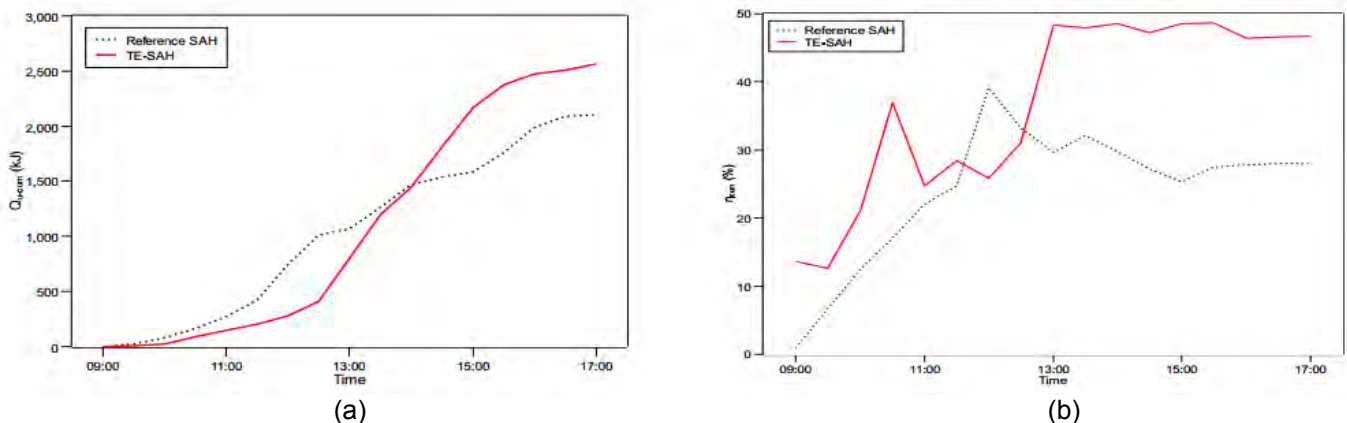


Figure 6. Performance of the SAH (a) Cumulative heat gain (b) Average efficiency

REFERENCES

- [1] Daniel Zenhausern, Evelyn Bamberger, Aleksis Baggenstos, and Andreas Haberle. PVT Wrap-Up: Energy systems with photovoltaic-thermal solar collectors. Technical report, 2017.
- [2] Neha Dimri, Arvind Tiwari, and GN Tiwari. Comparative study of photovoltaic thermal (PVT) integrated thermoelectric cooler (TEC) fluid collectors. *Renewable Energy*, 134:343–356, 2019.
- [3] Ahmet Z Sahin, Kehinde G Ismaila, Bekir S Yilbas, and Abdullah Al-Sharafi. A review on the performance of photovoltaic/thermoelectric hybrid generators. *International Journal of Energy Research*, 44 (5):3365–3394, 2020.
- [4] K.S. Ong. Review of solar, heat pipe and thermoelectric hybrid systems for power generation and heating. *International Journal of Low-Carbon Technologies*, 11(4):460–465, 2016.
- [5] Xiaoli Ma and Guiqiang Li. Building-integrated thermoelectric air conditioners: a potentially fully environmentally friendly solution in building services. *Future Cities and Environment*, 5(1), 2020

ACKNOWLEDGEMENT

The authors of this paper would like to thank the German Academic Exchange Service (DAAD) which funded this research through the In-Region scholarship programme at the University of Nigeria, Nsukka.

DEVELOPMENT OF HYBRID POWER SYSTEMS FOR NORTH INDIA RURAL AREAS

Gowtham Muthukumaran¹, Boris Kosoy²

¹Department of Energy Engineering, TU Berlin, Germany, ²Department of Thermodynamics and Renewable Energy, Institute of Refrigeration, Cryotechnologies and Ecoenergetics, Ukraine

e-mail: g.muthukumaran@campus.tu-berlin.de

ABSTRACT

This paper deals with the R&D of energy-efficient hybrid power systems for North India rural villages. The demand for energy in India is increasing because of the growing number of people and industries in society day by day. Over the years, meeting this demand has been a significant burden for utility providers. In the northern part of India, most of the rural villages need electricity. To solve this issue, one of the solutions is to implement a hybrid power system. The design and cost evaluation of the hybrid power system for the north India region is developed using Hybrid Optimization Model for Electrical Renewable (HOMER). HOMER replicates a system's functioning for the region by performing energy balance calculations at each time step (interval) throughout the year, with this Capital cost, operation, and maintenance cost, replacement cost, fuel cost, and interest are all factored into the system cost estimates. Through these various analyses, the proper design and cost evaluation of the hybrid system for the specific region were elaborated. The design of a hybrid power system is based on the peak load and load curve of the region. This research examines different renewable energy sources combinations for the specific region in north India, which may be used to provide a reliable and consistent supply of electricity.

Keywords: Hybrid power system, Cost analysis, Design, Renewable energy sources

INTRODUCTION

Energy is becoming necessary for increasing income and improving living quality for people regardless of where they are living. As per the statistics, still rural villages in India are not fully electrified and on the other side, carbon emissions are increasing day by day in India. So, to balance these two factors, the installation of a hybrid system is much essential. North Indian regions are a cluster of mountains, rivers, deserts, and forests. It is much difficult to connect a grid to every place, for that off-grid is one of the solutions. Off-grid hybrid systems have been drawing attention as a means of supplying power to rural regions in all aspects, including reliability, sustainability, and environmental protection, particularly for people living in remote places where grid extension is not feasible. In a hybrid power system, there are many combinations of potential resources, these systems will be developed with different renewable energy technologies such as PV, wind and battery, PV, biomass, and battery, etc... concerning the analysis, the best combination will be selected. Apart from local conditions, economic and financial considerations, the choice of which energy technology or combination of technologies to use for rural electrification is typically based on the number of people, number of houses, equipment usage, and considering various factors about the village. The main objective of this study is to utilize the renewable energy potential of the rural region by setting up a hybrid power system to provide an uninterrupted power supply. These technologies will entice investors and provide extra employment opportunities in the community. It will also produce revenue for the village's residents.

METHODOLOGY

The Hybrid energy system is fully designed with cost analysis in Hybrid Optimization Model for Electrical Renewable (HOMER) software. Firstly, a specific rural region will be selected, and a complete case study of the village will be done. The case study mainly focused on the number of people, number of houses, energy usage by each house, electricity rate, and renewable potential. After this analysis, we can decide the hybrid power system for the rural region according to their energy needs and the peak load of the village. In this study, two different combinations of the hybrid power system will be selected for the same region and analyse completely concerning the design, load, and cost. Finally, we can optimize the system with various factors and choose the best option for the specific rural region. In this way, the village has two different fully developed hybrid power system models. In the future or now, we can use both the design to another location by varying few important factors with regards to climatic conditions.

CONCLUSION

For developing countries like India, electrifying rural regions are and will continue to be a challenging task. Hybridizing renewable energy technology can provide long-term solutions to meet the country's energy needs. Renewable hybrid schemes are currently not financially competitive when compared to traditional fuel-fired facilities and grid-connected power systems. But Indian government providing a lot of subsidies to encourage implementation of renewable energy technology. Nonetheless, the need for environmental protection, as well as the current living standards of rural communities and the rising price of oil on the global market, have compelled the development of wise solutions that are environmentally friendly technologies, this brings renewable energy technologies on the cutting edge. In this study, the main finding is to be how the rural villages can use their energy potential and electrified without any grid

supply. The optimum combinations of hybrid systems could be defined based on thermal and economic factors analysis.

REFERENCE

- [1] Sinha S, Chandel S. Review of software tools for hybrid renewable energy systems. *Renewable and Sustainable Energy Reviews*. 2014; 32:192-205.
- [2] Abayomi Danlami B. Simulation of a Hybrid Power Generation System (A Case Study of Oke Eda, Akure, Ondo State, Nigeria). *American Journal of Modern Energy*. 2019;5(2):23.
- [3] Podder S, Khan R, Alam Mohon S. The Technical and Economic Study of Solar-Wind Hybrid Energy System in Coastal Area of Chittagong, Bangladesh. *Journal of Renewable Energy*. 2015; 2015:1-10.

CAUSAL INVESTIGATION OF ENERGY STORAGE TECHNOLOGY CRITERIA BY APPLYING A NOVEL INTEGRATED DECISION-MAKING METHODOLOGY

Ali Karasan, İhsan Kaya *

Yildiz Technical University, Department of Industrial Engineering, Besiktas, Istanbul, Turkey

*Corresponding author e-mail: ihkaya@yildiz.edu.tr

ABSTRACT

Energy storage technologies enable the ability to tackle the case of intermittency on the transmission of energy from an energy source by accumulating excess energy, which will be used when required. The concept itself holds many alternative storage technologies such as mechanical, electrical, electrochemical, chemical, and thermal [1]. Considering a selection problem for the most appropriate storage technology should be considered in a multicriteria evaluation perspective, and it should be designed based on a decision-making hierarchy, which involves many conflicting criteria that can be classified as containing qualitative and quantitative data. Moreover, the qualitative criteria assessments involve types of uncertainty such as impreciseness and/or hesitancy since the source of data is directly related to the expert knowledge and experience. So, some methods also should be inserted to overcome the uncertainties of the decision process. In this study, a novel methodology consists of the DEMATEL technique, and the cognitive mapping method is introduced to cope with the mentioned issues by extending it with z-numbers. Since the determining criteria may depend on each other, the DEMATEL technique is applied to reveal their relationship. Based on the obtained relationship diagram, the weight matrix for the cognitive map is constructed. Through the constructed weight matrix, the importance of each criterion has been calculated. We believe that the proposed decision-making methodology can be an efficient tool for prioritizing the energy storage technology criteria by considering both qualitative and quantitative data and promises results for the researchers or managers that can make inferences and valuable decisions for their systems based on the outputs.

Keywords: Energy storage, Z-numbers, Decision-making, DEMATEL, Cognitive mapping

INTRODUCTION

Since all kinds of energy sources are key elements for sustainable development for the countries, increment in energy demand and supply are the vital problems due to mass industrialization and exponential increase of the humankind population. On the other hand, as an energy alternative, non-renewable energy sources have significantly impacted humans and other living beings since their greenhouse gas emissions. Through that, renewable energy sources have been preferred as the primary sources of power by optimizing impacts to nature and energy supplements.

Renewable energy sources are the energy sources that may have intermittency during the transmission and characteristically stochastic processes [2]. Due to these uncertainties, it is hard to fulfill the required energy only from renewable energy since there should be a backup system to handle in case of an intermittency situation. As an alternative solution, energy storage technologies can be an efficient solution for this problem since they enable storing the excess energy and can operate it in case of need.

When the literature is briefly reviewed, it is seen that many studies are conducted to prioritize energy storage alternatives with a comprehensively constructed decision-making hierarchy. Most of the studies applied multi-criteria decision-making (MCDM) methods to obtain meaningful solutions [2-5]. Since the primary objective is to determine the most appropriate energy storage technology, they assume that the constructed decision-making framework consists of criteria, which are assessed independently from each other. This study mainly focused on criteria relationships with each other and their effect on criteria's importance. Through that, the decision-making context, which Çolak and Kaya [2] constructed, is considered for the evaluation process in a new decision-making perspective based on z-numbers.

For this aim, a two-phased methodology consists of decision-making trial and evaluation laboratory (DEMATEL) technique and cognitive mapping method is suggested during the evaluation process. Moreover, since the evaluation process contains both qualitative and quantitative data, z-numbers are conducted to extend the methodology to consider both impreciseness in the data and the decision-makers' decisions' reliability or hesitancy of decision-makers. The z-number fuzzy DEMATEL technique is applied to demonstrate the relations of the considered criteria. Then, the z-number fuzzy cognitive map method is used to obtain the importance of the criteria.

METHODOLOGY

In this paper, an integrated decision-making methodology consisting of the z-number fuzzy DEMATEL technique and z-number fuzzy cognitive mapping method is suggested to determine the importance of energy storage technology criteria by considering their casual relations. The flowchart of the suggested methodology for causal investigation of energy storage technology criteria is given in Figure 1. The considered evaluation hierarchy is also given in Figure 2.

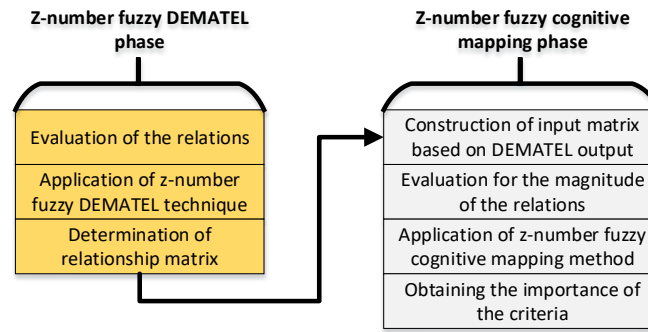


Figure 1. Flowchart of the suggested methodology

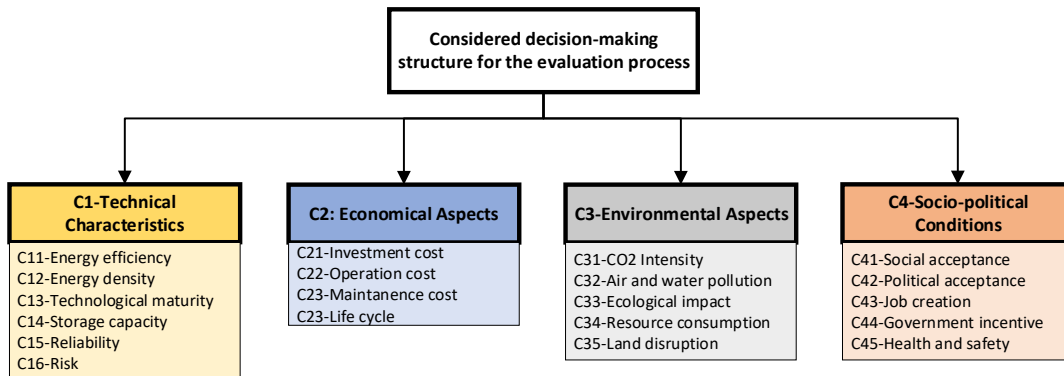


Figure 2. Considered decision-making structure for the problem [2]

CONCLUSIONS

In this paper, a preliminary study for the causal investigation of the energy storage technology criteria is considered. Through the analyses, it is aimed to find the answers to the following questions: (i) How could we calculate the interdependency weights of the identified main-criteria and sub-criteria by considering their possible influences on one another? (ii) How could build up a cause-and-effect relationship diagram illustrating the criticality of main-criteria and sub-criteria within the constructed system? (iii) What are the main-criteria and sub-criteria of more criticality, which demands careful attention by the concerned decision-makers?

Based on the ability to respond to the above questions, we believe that our proposed methodology can be used as a decision-making tool by the decision-makers or experts to make valuable inferences, assessments, and decisions to evaluate the energy storage technologies.

For further study, the considered decision-making structure can be extended by involving criteria such as related with national level importance, and cognitive functionality of the system. Moreover, after determining the importance of the criteria, the alternative energy storage technologies can be prioritized by using the z-number fuzzy TOPSIS method.

REFERENCES

- [1] Ren J, Ren X. Sustainability ranking of energy storage technologies under uncertainties. *Journal of cleaner production*. 2018 Jan 1; 170:1387-98.
- [2] Çolak M, Kaya İ. Multi-criteria evaluation of energy storage technologies based on hesitant fuzzy information: a case study for Turkey. *Journal of Energy Storage*. 2020 Apr 1; 28:101211.
- [3] Zhang C, Chen C, Streimikiene D, Balezentis T. Intuitionistic fuzzy MULTIMOORA approach for multi-criteria assessment of the energy storage technologies. *Applied Soft Computing*. 2019 Jun 1; 79:410-23.
- [4] Zhao H, Guo S, Zhao H. Comprehensive assessment for battery energy storage systems based on fuzzy-MCDM considering risk preferences. *Energy*. 2019 Feb 1; 168:450-61.
- [5] Murrant D, Radcliffe J. Assessing energy storage technology options using a multi-criteria decision analysis-based framework. *Applied Energy*. 2018 Dec 1; 231:788-802.

A SUPERVISED LEARNING-BASED METHOD USING A MODIFIED VOTING ALGORITHM FOR CLASSIFICATION OF COMPLEX POWER QUALITY DISTURBANCES IN A HYDROGEN ENERGY-BASED MICROGRID

¹Ahmet Küçüker, ²Alper Yılmaz, ^{2*}Gökay Bayrak

¹Sakarya University, Faculty of Engineering, Department of Electrical and Electronics Engineering, 54187, Sakarya, Turkey

²Bursa Technical University, Smart Grid Laboratory, Department of Electrical and Electronics Engineering, 16300, Bursa, Turkey

*Corresponding author e-mail: gokay.bayrak@btu.edu.tr

ABSTRACT

In this study, a multiple deep learning (DL) model-based classification methods using the modified Weighted Majority Voting (WMV) mechanism is proposed to classify complex PQDs in a hydrogen energy-based microgrid. Three different deep neural network models are investigated for the classification of PQDs: (1) Deep Convolutional Neural Network, (2) Deep Long Short Time Memory (DLSTM), and (3) DCNN-DLSTM. WMV method's weights were selected with an alternative method based on validation data set accuracy results. Existing machine learning (ML) methods are compared with the DL-WMV method under noisy and noise-free conditions. Results show that the combination of deep learning methods with the WMV method has the best accuracy rate. The classification accuracy under low-level noise and high-level noise conditions is 99.25% and 98.05%, respectively. The results also show that DL-WMV provides reliable and easily usable results in diagnosing PQDs in hydrogen energy-based microgrids.

Keywords: Deep Learning; Weighted Majority Voting; Power Quality Disturbances; Hydrogen Energy; Microgrid

INTRODUCTION

The power quality (PQ) has become a subject of interest for reasons such as the increase of nonlinear industrial loads and hydrogen energy-based microgrids, electrical vehicle (EV) charge stations, the spread of distributed generators (DGs), and microgrid structures, which are the main component of smart grid structures [1]. Traditionally, PQDs are classified by effective value conversion, harmonic analysis using Fourier transform (FT) [2], and visual inspection based on event waveform. It is decision-making based on operator knowledge and experience. Besides, intelligent automated methods can be developed to detect, identify, and analyze various disturbances with the enormous amount of data acquired in the field. In previous studies, automatic identification of PQDs was divided into three stages: a signal analysis using time-frequency analysis methods, feature selection using optimization methods, and event classification using multiclass classifiers [3]. Closed-loop feedback, which is not in the classical three-step process, and the desire to eliminate human involvement, have brought deep learning (DL) methods based on automatic feature selection [4]. In [5], a new approach based on single spectrum analysis, curvelet transform, and deep convolutional neural network (DCNN) has been performed to realize the classification of PQDs. A novel DL method was proposed using raw data for the classification of PQDs [4]. In Ref. [6], comparative analyses are given for PQD classifications using CNN, Long Short Time Memory (LSTM), and CNN-LSTM methods. It was seen that the performance rates of the compared methods differ for each class. The results obtained from the measurement data reveal the importance of an optimization requirement in the networks used. In this study, a new multiple deep learning architecture-based classification method using the modified Weighted Majority Voting (WMV) mechanism is proposed to classify complex PQDs in a hydrogen energy-based microgrid in the literature for the first time. Three different deep neural network models are used for classification: CNN, LSTM LSTM, and CNN-LSTM. WMV's weights were selected with an alternative method based on validation data set accuracy results. The designed WMV-based method uses an auto-updated weighting method by observing the validation results of DL classification models. The results show that the proposed DL-based multi-model ensemble method with modified WMV has a high prediction capability of PQD signals and useful for PQD classification for noisy and noise-free data.

PROPOSED METHOD

In this study, a hybrid model using a multiclass classifier, and the WMV was investigated for the classification of PQDs in a hydrogen energy-based microgrid. Its flowchart is shown in Fig. 1. For multiple deep learning model classification, we used three different DL methods and two voting methods as conventional majority voting (MV) and modified WMV. In MV, it is ensured that the class with the most votes is selected as the final assigned class. In WMV's weights were selected with an alternative method based on validation data set accuracy results. For every classifier, we analyzed the classification accuracy rate for every class. Most confused classes for every classifier are determined.

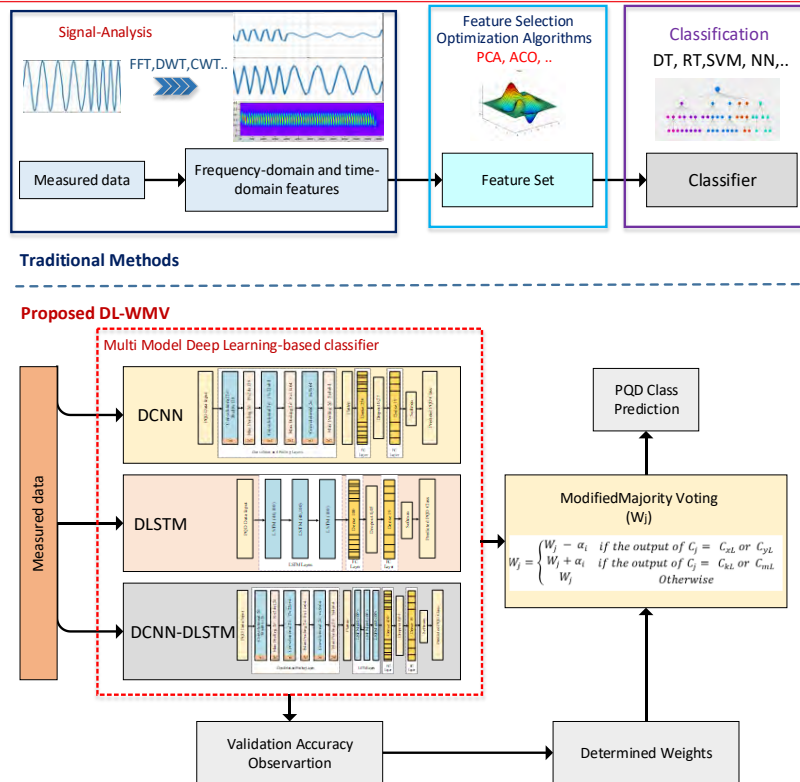


Figure 1. Proposed multiple DL model-based classification method using the modified WMV mechanism

CONCLUSIONS

The performance scores of deep learning methods are given in Table 1. 19 different class complex and single PQDs were classified by the proposed method. The proposed multi-model, which includes DCNN, DLSTM, and DLSTM-DCNN with the modified WMV mechanism, has the best score with a validation accuracy (Val Acc) 99.32% and with a test accuracy (Test Acc) of 99.25% without noisy data. Also, with a 40db noisy proposed model, it has the best score with a validation accuracy of 98.12% and a test accuracy of 98,05%. DL-WMV has significant advantages in noise immunity, accuracy, and computation load. It is also suitable for big data analysis of PQD data, considering the rapid growth of monitor devices in smart grids.

Table 1. Performance score of the DL methods under noisy and noise-free conditions

Model	Voting Method	Noise-free (%)		40dB (%)		30 dB (%)	
		Val Acc	Test Acc	Val Acc	Test Acc	Val Acc	Test Acc
DCNN	-	98.62	98.25	96.89	96.73	96.32	96.26
DLSTM	-	98.58	98.15	97.92	97.85	97.23	97.02
DCNN-DLSTM	-	98.60	98.23	98.25	98.01	97.61	97.58
DCNN, DLSTM, DCNN-DLSTM	MV	99.28	99.08	98.18	98.08	97.54	97.51
DCNN, DLSTM, DCNN-DLSTM	WMV	99.32	99.25	98.62	98.58	98.12	98.05

REFERENCES

- [1] Lin, R. H., Zhao, Y. Y., & Wu, B. D. (2020). Toward a hydrogen society: Hydrogen and smart grid integration. *International Journal of Hydrogen Energy*, 45(39), 20164-20175.
- [2] Deokar, S. A., & Waghmare, L. M. (2014). Integrated DWT-FFT approach for detection and classification of power quality disturbances. *International Journal of Electrical Power & Energy Systems*, 61, 594-605.
- [3] Bayrak, G., & Yılmaz, A. (2021). Detection and Classification of Power Quality Disturbances in Smart Grids Using Artificial Intelligence Methods. In *Artificial Intelligence (AI)* (pp. 149-170). CRC Press.
- [4] Wang, S., & Chen, H. (2019). A novel deep learning method for the classification of power quality disturbances using deep convolutional neural network. *Applied energy*, 235, 1126-1140.
- [5] Liu, H., Hussain, F., Shen, Y., Arif, S., Nazir, A., & Abubakar, M. (2018). Complex power quality disturbances classification via curvelet transform and deep learning. *Electric Power Systems Research*, 163, 1-9.
- [6] Garcia, C. I., Grasso, F., Luchetta, A., Piccirilli, M. C., Paolucci, L., & Talluri, G. (2020). A Comparison of Power Quality Disturbance Detection and Classification Methods Using CNN, LSTM, and CNN-LSTM. *Applied Sciences*, 10(19), 6755.

BIOCOMPOSITE AND POLYMERIC MATERIALS IN RADIATION SHIELDING APPLICATIONS: A REVIEW

^{1*} Ertuğrul Demir, ² Zeki Candan, ³ Matlab N. Mirzayev

¹Yeditepe University, Faculty of Arts and Sciences, Physics Department, İnönü Mahallesi Kayışdağı Caddesi 26 Ağustos Yerleşimi, 34755, Ataşehir, Istanbul, Turkey

²Istanbul University-Cerrahpaşa Research Information System, Faculty of Forest, Department of Forestry Industrial Engineering, Department of Forest Products Engineering, Faculty of Forestry, Istanbul University, Sariyer, 34473, Istanbul, Turkey

³Joint Institute for Nuclear Research, Flerov Laboratory of Nuclear Reactions, JINR, Joliot-Curie 6, 141980 Dubna, Moscow region, Russia

*Corresponding author e-mail: ertugrul.demir@yeditepe.edu.tr

Radiation can be defined as the emission of energy in the form of particles or electromagnetic energy [1]. It is also favourably classified into four general types as follows: 1- Charged particulate radiation: Fast electrons, and heavy charged particles, 2- Uncharged radiation: Electromagnetic radiation, and neutrons [2]. On the other hand, radiation can also be divided into two main categories according to its ability to ionize matter: 1- ionizing radiation and 2- non-ionizing radiation. Ionizing radiation is defined as high-energy radiation strong enough to cause displacement of electrons from atoms and breakage of chemical bonds. It has the ability to break DNA strands and create mutations and cause the death of cells [3]. Non-ionizing radiation such as radio waves, microwaves, infrared, can be defined as the energy required to excite atoms or electrons in sufficient amounts but is not enough to detach electrons from their orbits [4]. By contrast, X-rays and gamma rays or particles such as alpha, beta, and neutrons are a member of the ionizing radiation family. Gamma rays, which belong to the ionizing radiation family, are used in a wide variety of sectors. These sectors can be summarized as follows: sterilization and disinfection (food industry), nuclear medical diagnostic and therapy, space science, nuclear industry such as nuclear waste management, nuclear reactors, and radiation shielding applications [5-6] As it is known, high levels of ionizing radiation have harmful, undesirable effects on both living tissues and substances. When materials are exposed to high radiation doses, severe deteriorations in microstructure and physical properties are observed, as well as a significant increase in defect density. With regard to organisms, since ionizing radiation causes the ionization of biological molecules in living tissues, it can induce a number of genomic and chromosomal abnormalities that cause breaks in DNA sequencing and the death of cell structures [7-8-9].

As mentioned above, the use of radiation in our lives has become an inevitable issue. In this context, it is important to shield the radiation and use appropriate materials to protect against the harmful effects of radiation. In order to obtain an efficient radiation shielding material, it is necessary to consider several important aspects. First, the type of radiation such as photons or particles to be absorbed or attenuated, and secondly the type of interaction of the radiation with the target material should be determined [10]. Therefore, researchers have been conducting extensive studies to find the most suitable radiation shielding materials for different types of radiation. As conventional radiation shielding materials, lead, concrete, steel, tungsten, etc. come to the fore and these materials pose a problem in various applications due to their hardness, inflexibility, and high density. It may be appropriate to improve conventional radiation shielding materials for large volumes of structures such as nuclear reactors, but it is obvious that conventional shielding materials will be insufficient in space exploration, mobile nuclear devices, and clinics where maneuverability is limited, and lightweight materials are needed [10-11]. In conclusion, there is an increasing demand for the development of new radiation shielding materials that absorb or attenuate different types of radiation effectively, are light and flexible, and do not harm the environment and living tissues.

The purpose of this paper is to review recent researches into the evaluation of the situation of environmentally friendly biomaterials and polymers in radiation protection applications. In general, polymer materials have low mechanical properties and deform at high stresses, but mechanical properties such as tensile strength or hardness can be improved by reinforcing inorganic particles [12]. Polymer materials can be utilized as structural materials such as metals and alloys, especially in the aerospace industry, as they offer the flexibility conditions we seek. Moreover, since they are lighter than metals and alloys, they allow less fuel consumption to reach high altitudes. In this respect, polymer nanocomposite materials promise us many desirable properties that conventional radiation shielding materials cannot offer. When it comes to the radiation protection applications of biomaterials, we are stepping into an area where quite new and comprehensive studies are needed. In this context, even in the most recent workshop of NASA's Human Research Program (HRP) in 2020, no biomaterials session was held and there was only one study on the use of biomaterials [13].

On the other hand, radiation exposure in human space missions is considered to be one of the biggest challenges in this area. Space is home to unfavorable conditions for human life. Therefore, suitable habitats for biological systems should be provided during space missions. In deep space, the cosmic radiation dose is 104 Gy per year, which is about 500,000 times the Earth's annual sea level dose [14]. Although lead is effective material in shielding gamma

and x-rays, it is not preferred because it produces secondary x-rays when exposed to beta particles, is heavy, and most importantly, cannot fully keep safe astronauts from cosmic radiation. In this context, NASA has sought to explore to reduce the effects of ionizing radiation through the use of pharmacological and dietary supplements [15]. Here, biomaterials may introduce an excellent way out. Because melanized organisms are situated in high-radiation environments such as Chernobyl and on orbiting spaceships, melanin can behave as a radiation shielding material through attenuation and/or suppression of radical species [16-18]. Therefore, melanin synthesis and optimization is an important research topic for the protection of healthy tissue from ionizing radiation in radiation environments.

REFERENCES

- [1] James E. Martin, *Physics for Radiation Protection, A handbook*, 2006 WILEY-VCH Verlag GmbH & Co. KGaA, Weinheim. ISBN-10: 3-527-40611-5
- [2] Knoll, Glenn F., *Radiation detection and measurement*, 2000 John Wiley & Sons, Inc. ISBN 0-471-07338-5
- [3] Savage S.A, Schuz J., *Environmental Chemicals and Childhood Cancer*, DOI: 10.1016/B978-0-444-52272-6.00017-9
- [4] Omer Hiba, *Radiobiological effects and medical applications of non-ionizing radiation*, <https://doi.org/10.1016/j.sjbs.2021.05.071>
- [5] More, C.V., Alsayed, Z., Badawi, M.S. et al. *Polymeric composite materials for radiation shielding: a review*. *Environ Chem Lett* 19, 2057–2090 (2021). <https://doi.org/10.1007/s10311-021-01189-9>
- [6] Sayyed MI, Lakshminarayana G, Kityk IV, Mahdi MA (2017) Evaluation of shielding parameters for heavy metal fluoride-based tellurite-rich glasses for gamma ray shielding applications. *Radiat Phys Chem* 139:33–39. <https://doi.org/10.1016/j.radphyschem.2017.05.013>
- [7] Rahim Amirikhah, Nematollah Etemadi, Mohammad R. Sabzalian, Ali Nikbakht, Ali Eskandari, *Gamma radiation negatively impacted seed germination, seedling growth and antioxidant enzymes activities in tall fescue infected with Epichloë endophyte*, *Ecotoxicology and Environmental Safety*, Volume 216, 2021, 112169, ISSN 0147-6513, <https://doi.org/10.1016/j.ecoenv.2021.112169>.
- [8] S.V. Gudkov, M.A. Grinberg, V. Sukhov, V. Vodeneev *Effect of ionizing radiation on physiological and molecular processes in plants* *J. Environ. Radioact.*, 202 (2019), pp. 8-24, 10.1016/j.jenvrad.2019.02.001.
- [9] Xinghang Zhang, Khalid Hattar, Youxing Chen, Lin Shao, Jin Li, Cheng Sun, Kaiyuan Yu, Nan Li, Mitra L. Taheri, Haiyan Wang, Jian Wang, Michael Nastasi, *Radiation damage in nanostructured materials*, *Progress in Materials Science*, Volume 96, 2018, Pages 217-321, ISSN 0079-6425, <https://doi.org/10.1016/j.pmatsci.2018.03.002>.
- [10] *Polymer-Composite Materials for Radiation Protection*, Shruti Nambiar and John T. W. Yeow, *ACS Applied Materials & Interfaces* 2012 4 (11), 5717-5726, DOI: 10.1021/am300783d
- [11] F. Akman, H. Ogul, M.R. Kaçal, H. Polat, K. Dilsiz, O. Agar, *Gamma attenuation characteristics of CdTe-Doped polyester composites*, *Progress in Nuclear Energy*, Volume 131, 2021, 103608, ISSN 0149-1970, <https://doi.org/10.1016/j.pnucene.2020.103608>.
- [12] Bhattacharya M (2016) *Polymer nanocomposites—a comparison between carbon nanotubes, graphene, and clay as nanofillers*. *Materials* 9:262. <https://doi.org/10.3390/ma9040262>
- [13] 2020 NASA Human Research Program Investigator's Workshop Small Steps Lead to Giant Leaps: Translating Research into Space Exploration January 27-30 Galveston Island Convention Center Galveston, TX (2020).
- [14] P.A. Karam *Inconstant Sun: how solar evolution has affected cosmic and ultraviolet radiation exposure over the history of life on Earth* *Health Phys.*, 84 (3) (2003), pp. 322-333.
- [15] J. Rask, W. Vercoutere, B.J. Navarro, I. Krause *Space faring: the radiation challenge introduction and module 1: radiation educator guide* Nat. Aeronaut. Space Admin. (2008)
- [16] Schweitzer, A. D.; Howell, R. C.; Jiang, Z.; Bryan, R. A.; Gerfen, G.; Chen, C.-C.; Mah, D.; Cahill, S.; Casadevall, A.; Dadachova, E. *Physico-Chemical Evaluation of Rationally Designed Melanins as Novel Nature-Inspired Radioprotectors*. *PLoS One* 2009, 4 (9), No. e7229.
- [17] Dadachova, E.; Casadevall, A. *Ionizing radiation: how fungi cope, adapt, and exploit with the help of melanin*. *Curr. Opin. Microbiol.* 2008, 11 (6), 525–31.
- [18] Sinilova, N. G.; Pershina, Z. G.; Duplitseva, A. P.; Pavlova, I. B. *A radio-resistant pigmented bacterial culture isolated from atomic reactor water*. *Zh Mikrobiol Epidemiol Immunobiol* 1969, 46 (8), 94– 9.

Submission ID: 29

GEOHERMAL ENERGY PRODUCTION FROM ABANDONED OIL AND GAS WELLS: A TECHNICAL REVIEW

^{1*} *Abusalam Mukhtarov*, ² *Gulden Gokcen Akkurt*, ³ *Nurdan Yildirim*

¹ Politecnico di Torino, Department of Petroleum Engineering, Turin, Italy

² Izmir Institute of Technology, Faculty of Engineering, Department of Energy Systems Engineering, 35430, Urla, Izmir, Turkey ³ Yasar University, Department of Mechanical Engineering, Izmir, Turkey

*Corresponding author e-mail: s275131@studenti.polito.it

ABSTRACT

The utilization of abandoned oil and gas wells (AOGW) to harness geothermal energy is considered as one of the effective methods in order to enhance the total economic life of hydrocarbon wells. A downhole heat exchanger can be used to extract geothermal energy from abandoned petroleum wells. The paper is concentrated on the studies of recent researches for the achievement of the objective and prepared to give a comprehensive overview on the geothermal energy production from AOGW, including the application of other methods and types of heat exchangers.

Keywords: Abandoned oil and gas wells, geothermal energy extraction, downhole heat exchangers.

INTRODUCTION

Geothermal energy is a renewable energy source which is used to generate electricity and/or direct use applications such as heating/cooling and drying while producing low amount of greenhouse gases emissions. According to some recent researches, there are more than 20 countries that are using geothermal energy for electricity generation (73.7 TWh/year). In geothermal energy production, the energy can be obtained without burning fossil fuels such as oil, gas and coal [1].

There are nearly 20-30 million abandoned oil and gas wells (AOGW) in the World which cause serious environmental problems. Utilizing these wells to acquire geothermal energy can not only get rid of some risks and drilling costs but also tackle the pollution issues. Moreover, AOGW have a significantly high potential to be transformed into geothermal wells.

Using abandoned petroleum wells for the purpose of geothermal extraction is a good idea because of having the fact that hydrocarbon wells are generally located deeper that is enough to reach a high-temperature area. Geothermal power has the ability to decline dependence on non-renewable energy sources such as coal, oil, natural gas, and nuclear energy. Generally, due to its advantages and accessibility, geothermal energy extraction from abandoned hydrocarbon wells should be taken into consideration as an alternative energy source. The advantages are: 1. Due to having the wellbore of the well, that method does not require any drilling activities which makes it almost 50% cost-effective, 2. Current conditions are already known and also thermal and geological properties of wells, exploration data, reservoir and fluids properties, completion data and production history are available, 3. Corrosion, scaling problems, groundwater recession can be removed because of no extracting groundwater, 4. The casing, cement, and wellbore with equipping inner pipe can be used also in geothermal energy extraction, 5. Due to existing desirable thermodynamic properties, selection of circulating fluid can be chosen easily, 6. Geothermal energy extraction with a closed-loop system releases no dissolved gas into the atmosphere [2].

LITERATURE REVIEW

From the technical point of view, it can be observed that some of the researches had concentrated on open-loop system designs. On the other hand, the majority of researches that had been carried out is related to geothermal energy production from oil and gas wells with close loop design system. U-tube and Coaxial (double pipe) heat exchangers are the types of the closed-loop system [3-9].

One of the different approaches to produce geothermal energy with applying to AOGW is using 2 wells method. According to the investigation of Asif Mehmood et al. [10] the dual wells system can be addressed to abandoned oil and gas wells to get heat extraction. Thus, in that method, at least one injection well and one production well should be utilized. Using that approach, the energy can be harvested with high efficiency which is different from the traditional close loop systems. They presented that, the average final temperature has a fluctuation with changing the distance between production and injection wells. They concluded that when the distance between 2 wells is sufficiently high, the residence time will be high which allows enough time for energy transfer between hotter rocks and the fluids whereas it has the working fluid lost and that the outlet temperature can be affected by the injection pressure [10].

In another research, geothermal energy production from abandoned oil wells with utilizing in situ combustion has been represented. The explanation of that approach is that the air is injected into an oil reservoir to oxidize the heavy

oil for heating up. The burning of oil leads more heat to the reservoir, and it could make a way to produce high proportion of energy. The authors emphasized that subjecting in situ combustion to abandoned wells was highly beneficial, specially from economic side. Thus, appearing higher amount of heat helps to decrease the payback period. The computational results showed that outlet temperature raised up significantly after doing in situ combustions [11].

Pan (1985) paid attention to compare U-pipe, forward and reverse coaxial HEs. The result was that the reverse model is more effective than others due to having larger heat extraction [12].

There are several parameters which have impact on harnessing geothermal energy from AOGW. In the respect of pump power, Holmberg created a numerical model to study the performance of downhole heat exchangers (DHE) and carried out parametric study related to pressure drop and circulation pumping power [13]. Wight and Bennett studied the acquisition of electricity from abandoned oil and gas wells and evaluated the pump horsepower required to circulate the wellbore fluid [14]. Noorollahia et al. studied about extraction of geothermal energy by utilizing AOGW as low-temperature resources and concluded that well casing geometry and the size of injection and extraction pipes play a crucial role in the acquiring of heat output [15]. For optimizing the performance of DHE, Nian and Cheng researched the effects of pipe diameter, the rate of mass flow, working fluid inlet temperature, and insulation length on the extraction of heat. The wells which have high temperature and is deeper can require more insulation, even near the surface in order to minimize heat loss especially near the ground where there is a lower temperature than the bottom [16]. Moreover, the other investigation is addressed to know the effect of insulation by doing some measurement and simulation. The insulation cover was applied to the inner pipe, and the consequence showed that placing insulation on the pipe has a crucial impact on the heat extraction rate, thus when the pipe is insulated, the final(exit) temperature is higher than other circumstances in which there is not any insulation on the inner tube. So, it was obtained that applying insulation has great performance [17].

CONCLUSIONS

As a result, the extraction of geothermal energy from AOGW is very beneficial. Open-loop systems can make a way for heating, cooling, and other applications. The diameters, working fluid rate, and other properties are very crucial for the generation of heat. Closed-loop systems can be applied for electricity generation. Thus, fluid and wellbore parameters, selection of flow model play an important role in performance on DHEs. On the other hand, 2 wells method and combustion can be used to harness geothermal energy from AOGW. From a thermodynamics point of view, insulation is highly recommended to be applied on the DHE system in order to increase the temperature output by diminishing the heat loss.

REFERENCES

- [1] Coro G, Trumpy E. Predicting geographical suitability of geothermal power plants. Italy: Journal of Cleaner Production; 2020.
- [2] Templeton J. Abandoned petroleum wells as sustainable/renewable sources of geothermal energy. Energy 70; 2013.
- [3] Lund J, Freeston H, Boyd L. Direct application of geothermal energy. Geothermics; 2005.
- [4] Culver G, Reistad G.M. Testing and modeling of heat exchangers in shallow geothermal systems. USA; 1978.
- [5] Dominguez M. Thermodynamic optimization of downhole heat exchanger for geothermal applications. Geothermics ; 2010.
- [6] Horn A, Amaya A, Higgins B et al. Applications for Closed-Loop Geothermal Energy Systems. San Francisco; 2020.
- [7] Nalla G, Shook M, Bloomfield K. Parametric sensitivity study of operating and design variables in WHEs; 2005.
- [8] Morita K, Tago M, Ehara S. Case studies on small-scale power generation with the DHE. USA: Geothermics ; 2005.
- [9] Eliasson L, Valdimarsson P. Economic Evaluation of power production from a geothermal reservoir. Iceland; 2005.
- [10] Asif M, Jun Yao et al. Potential for heat production by retrofitting abandoned gas wells into geothermal wells. China: Journal of Energy; 2019.
- [11] Zhu Y, Li K, Liu C. Geothermal power production from abandoned oil reservoirs using in situ Combustion Technology. China: Energies; 2020
- [12] Pan H, Freeston D, Lienau P. Experimental performance of downhole heat exchangers model and full scale. New Zealand; 1983.
- [13] Holmberg H, Acuna J, Næss E, Sonju O. Thermal evaluation of coaxial deep borehole heat exchangers. Sweden: Renewable energy; 2016.
- [14] Wight NM, Bennett N. Geothermal energy from abandoned oil and gas wells using water in combination with a closed wellbore. Edinburg: Applied thermal engineering; 2015.
- [15] Noorollahi Y, Pourarshad M, Yousefi H. Numerical simulation of power production from abandoned oil wells in Ahwaz oil field in Iran. Iran: Geothermics; 2015.
- [16] Nian Y, Cheng W. Insights into Geothermal utilization of abandoned oil and gas wells. China: Renewable and sustainable energy reviews; 2017.
- [17] Guillaume F. Analysis of a novel pipe in pipe coaxial borehole heat exchanger. Sweden; 2011.

HIGHLY STABLE POUCH CELL SCALE QUASI-SOLID-STATE LITHIUM-AIR BATTERIES

Mustafa Çelik^{1,2}, Abdulkadir Kizilaslan^{1,2}, Tuğrul Çetinkaya^{1,2,3}, and Hatem Akbulut^{1,2,3}

¹ Sakarya University, Engineering Faculty, Department of Metallurgical and Materials Engineering, Esentepe Campus, 54187, Serdivan, Sakarya

² Sakarya University Research, Development and Application Center (SARGEM), Esentepe Campus, 54187 Sakarya, Turkey

³ NESSTEC Energy & Surface Technology A.S., Technology Development Zones, Sakarya University, 54050 Sakarya, Turkey

*Mustafa Çelik e-mail: mustafacelik@sakarya.edu.tr

ABSTRACT

Gel polymer electrolytes (GPEs) based on poly (vinylidene fluoride-co-hexafluoropropylene) (PVDF-HFP) are widely studied due to their high electrochemical stability and dielectric constants. Yet, their utilization is hindered due to low ionic conductivity, poor cycling stability, and low interfacial stability in contact with the anode. Most of the studies to increase the conductivity of polymer-electrolytes are linked to the incorporation of ceramic fillers such as Al₂O₃, SiO₂, and TiO₂ into the polymer matrix. In this study, we synthesized highly conductive gel polymer nanocomposite electrolytes with varying concentrations of LAMP, Al₂O₃, and TiO₂ nanopowders as ceramic fillers. 5%wt LAMP incorporated GPE were found to having 1.16x10⁻⁴ S/cm ionic conductivity and 0.82 lithium-ion transference number at room temperature. To increase the energy density and evaluate the scale-up potential, pouch cells were assembled utilizing Li, GPE and gas diffusion layer (GDL, Sigracet 24BC) as anode polymer electrolyte and cathode, respectively. Assembled all-solid-state pouch cells were displayed 2.9 V Li/Li⁺ open-circuit voltage and operated for 64 hours without any capacity fade which shows their promising potential to be utilized in high-energy-density flexible battery applications.

Keywords: PVDF-HFP, polymer electrolyte, ceramic filler, cycle life, Li-air pouch cell

INTRODUCTION

High energy density battery systems are of great importance due to the increasing demand for electronic devices and electric vehicles. Li-O₂ batteries are considered as the next-generation battery systems to meet the ever-increasing demand for energy storage with their specific energy density at 11400 Wh/Kg [1,2]. Yet, practical problems arising from the use of liquid electrolytes, e.g electrolyte leakage, flammability risks and narrow electrochemical stability window restricts their use in widespread applications [3–5]. Hence, the replacement of liquid electrolytes with (electro)chemically stable solid electrolytes is required not only to assemble stable batteries but also to obtain higher energy density [6,7].

Among solid electrolytes, many studies focused on the GPEs due to their flexible nature and easy fabrication. Yet, recent studies are directed into ceramic incorporated GPE due to the low ionic conductivity and better mechanical properties compared to bare GPEs [8].

Oxide based active and inactive nanoparticles are widely used as ceramic fillers in GPEs. Where the enhanced electrochemical performance is attributed to the increased amorphicity, chain mobility and electrochemical window. LAMP[9], LAGP [10] and LLTO [11] are studied as active fillers and SiO₂ [12,13], TiO₂ [14,15], Al₂O₃ [16,17], and Fe₃O₄ [18] are utilized as inactive fillers.

Although individual studies have been reported on the use of different ceramic powders and their electrochemical performances, a systematic and comparative approach to reveal the effect of ceramic powders in the polymer matrix on the electrochemical performance of Li-O₂ batteries has not yet been evaluated.

In this study, a systematic approach to evaluate the effect of ceramic in active filler incorporated into PVDF-HFP GPEs was pursued. Depending on the filler type and weight percentage, the electrochemical performance of GPEs was studied in the view of electrochemical impedance spectroscopy (EIS), linear sweep voltammetry (LSW), Li⁺ transference number and galvanostatic charge-discharge. In order to evaluate the scalable performance, all solid-state pouch cells were assembled, and their performance was studied as well.

MATERIALS AND METHODS

PVDF-HFP based composite GPEs were produced using the solvent casting method. Phase and morphological analysis of GPEs were characterized by XRD and FESEM respectively. Al₂O₃, TiO₂ and LAMP powders were added as ceramic additives in varying weight ratios (2.5-5-10-20 wt%). Electrochemical Impedance Spectroscopy (EIS), cyclic voltammetry (CV), linear sweep voltammetry (LSV) chronoamperometry and galvanostatic cycle tests were performed as electrochemical analysis techniques. Electrochemical performance of gel-polymer electrolytes was tested with ECC-air test cell and custom-made Li-air pouch cell.

CONCLUSIONS

We analyzed the effect of ceramic powders on various with varied ratios electrochemical performance of PVDF-HFP GPEs. Our results show that each ceramic additive has different merits on the electrochemical performance of GPE. The best ionic conductivity was obtained as $1.16 \times 10^{-4} \text{ S cm}^{-1}$ in the 5% wt LATP doped GPE. In terms of electrochemical stability window, our results display the feasibility of GPEs to be used with common oxide-based cathode as the stability window extends up to 6V vs Li/Li⁺. Best cycling stability was obtained in the 5%wt Al₂O₃ and LATP compositions which was attributed to the high Li⁺ number and wider electrochemical window. Upon testing at pouch-cell scale, 5%wt LATP doped GPEs were found to perform stable 16 cycles at 0.1 mA/cm² current density in 2h time-limited tests. With their lightweight and high energy density, Pouch Cell-Type Li-Air batteries have a high potential for flexible and wearable applications.

ACKNOWLEDGEMENTS

The authors thank the TUBITAK for supporting this work under the contract number 217M979.

REFERENCES

- [1] Leng L, Zeng X, Chen P, Shu T, Song H, Fu Z, et al. A novel stability-enhanced lithium-oxygen battery with cellulose-based composite polymer gel as the electrolyte. Vol. 176, *Electrochimica Acta*. 2015. p. 1108–15.
- [2] Jung HG, Hassoun J, Park JB, Sun YK, Scrosati B. An improved high-performance lithium-air battery. *Nat Chem*. 2012.
- [3] Xu W, Viswanathan V V., Wang D, Towne SA, Xiao J, Nie Z, et al. Investigation on the charging process of Li₂O₂-based air electrodes in Li-O₂ batteries with organic carbonate electrolytes. *J Power Sources*. 2011.
- [4] Padbury R, Zhang X. Lithium-oxygen batteries - Limiting factors that affect performance. *Journal of Power Sources*. 2011.
- [5] Balaish M, Kraysberg A, Ein-Eli Y. A critical review on lithium-air battery electrolytes. *Physical Chemistry Chemical Physics*. 2014.
- [6] Manthiram A, Yu X, Wang S. Lithium battery chemistries enabled by solid-state electrolytes. *Nature Reviews Materials*. 2017.
- [7] Tarascon JM, Armand M. Issues and challenges facing rechargeable lithium batteries. *Nature* [Internet]. 2001 Nov 15;414(6861):359–67. Available from: <http://www.nature.com/articles/35104644>
- [8] Jeon JD, Kim MJ, Kwak SY. Effects of addition of TiO₂ nanoparticles on mechanical properties and ionic conductivity of solvent-free polymer electrolytes based on porous P(VdF-HFP)/P(EO-EC) membranes. *J Power Sources*. 2006.
- [9] Li Y, Wang H. Composite Solid Electrolytes with NASICON-Type LATP and PVdF-HFP for Solid-State Lithium Batteries. *Ind Eng Chem Res* [Internet]. 2021 Jan 27;60(3):1494–500. Available from: <https://pubs.acs.org/doi/10.1021/acs.iecr.0c05075>
- [10] Liang T, Liang WH, Cao JH, Wu DY. Enhanced Performance of High Energy Density Lithium Metal Battery with PVDF-HFP/LAGP Composite Separator. *ACS Appl Energy Mater*. 2021.
- [11] Li J, Zhu L, Zhang J, Jing M, Yao S, Shen X, et al. Approaching high performance PVDF-HFP based solid composite electrolytes with LLTO nanorods for solid-state lithium-ion batteries. *Int J Energy Res*. 2021
- [12] Raghavan P, Choi JW, Ahn JH, Cheruvally G, Chauhan GS, Ahn HJ, et al. Novel electrospun poly (vinylidene fluoride-co-hexafluoropropylene)-in situ SiO₂ composite membrane-based polymer electrolyte for lithium batteries. In: *Journal of Power Sources*. 2008.
- [13] Capiglia C, Mustarelli P, Quartarone E, Tomasi C, Magistris A. Effects of nanoscale SiO₂ on the thermal and transport properties of solvent-free, poly (ethylene oxide) (PEO)-based polymer electrolytes. *Solid State Ionics*. 1999.
- [14] Croce F, Appetecchi GB, Persi L, Scrosati B. Nanocomposite polymer electrolytes for lithium batteries. *Nature*. 1998.
- [15] Croce F, Curini R, Martinelli A, Persi L, Ronci F, Scrosati B, et al. Physical and chemical properties of nanocomposite polymer electrolytes. *J Phys Chem B*. 1999.
- [16] Bruce PG. Energy storage beyond the horizon: Rechargeable lithium batteries. *Solid State Ionics*. 2008.
- [17] Krawiec W, Scanlon LG, Fellner JP, Vaia RA, Vasudevan S, Giannelis EP. Polymer nanocomposites: a new strategy for synthesizing solid electrolytes for rechargeable lithium batteries. *J Power Sources*. 1995.
- [18] Reddy MJ, Chu PP, Kumar JS, Rao UVS. Inhibited crystallization and its effect on conductivity in a nano-sized Fe oxide composite PEO solid electrolyte. *J Power Sources*. 2006.

Submission ID: 31

CHARACTERIZATION OF HYDROXYETHYL CELLULOSE/ACTIVE CARBON COMPOSITES

^{1*} Mustafa Zor, ² Ferhat Şen, ³ Barlas Oran, ³ Zeki Candan

¹ Zonguldak Bulent Ecevit University, Department of Design, 67900 Zonguldak, Turkey

² Zonguldak Bulent Ecevit University, Department of Food Processing, 67900 Zonguldak, Turkey

³ Istanbul University – Cerrahpasa, Department of Forest Industrial Engineering, Sariyer, 34473 Istanbul, Turkey

*Corresponding author e-mail: mstfzor@gmail.com

ABSTRACT

Thanks to its high crystalline nature and thermal, optical, electrical, and excellent mechanical properties, carbon and its derivatives are known as a preferred reinforcement material in many industrial applications such as science and engineering fields. In this study, it was aimed to improve the thermal and mechanical properties of hydroxyethylcellulose (HEC) by preparing hydroxyethyl cellulose/activate carbon composite materials. Composite materials containing hydroxyethyl cellulose and 1%, 3%, 5% active carbon were prepared. The thermal stability of the prepared composite materials was investigated by thermal gravimetric analysis (TGA) method. The samples were heated from 30°C to 750°C with a heating rate of 10°C/min under nitrogen atmosphere and their masses were measured. The mechanical properties of the composites were investigated by the tensile test. As a result, it has been concluded that the mechanical, thermal conductivity, and thermal resistance of HEC are increased with use of activate carbon as a filler and the obtained materials can be used in industries that need free film.

Keywords: Green Material, Active Carbon, UV-Curing, Coating, Wood Based Panel Material

EVOLUTION OF MICROCLIMATE EFFECT OF AN URBAN PARK OVER THEIR BUILT ENVIRONMENT

^{1*} María Angélica Ruiz, ¹ María Florencia Colli, ¹ Claudia Fernanda Martínez, ¹ Erica Norma Correa Cantaloube
¹ Consejo Nacional de Investigaciones Científicas y Técnicas (CONICET), Centro Científico Tecnológico CCT – Mendoza,
Instituto de Ambiente, Hábitat y Energía (INAHE), Av. Ruiz Leal s/n, Parque General San Martín, Mendoza, CP: 5500,
Argentina

*Corresponding author e-mail: aruiz@mendoza-conicet.gob.ar

ABSTRACT

Arid cities suffer the effects of urban heat island (UHI), with negative impacts on the environment, people and economies. Urban greening is a strategy for mitigating UHI. However, vegetation demands high scarce resources in cities on dry land. Hence, it is necessary to rethink the relationship between green spaces and its surrounding built environment. This work's objective is to evaluate the impact of Mendoza's Parque Central (Argentina) on the air temperatures of its built environment, taking as a measure the park cool island intensity (PCI) in the 2007-2017 period. Parque Central has a strategic value for the urban development of a residential area with a medium to high construction density. Methodologically, two monitoring campaigns were carried out during the summer periods of 2007-2008 and 2016-2017. In each campaign, temperature and relative humidity sensors were installed in the area. Satellite images from Landsat 7 were analyzed and the NDVI and NDBI indices were determined. The results indicate that over 10 seasons, the park's maximum NDVI has increased more than 8 times, while the maximum PCI intensities have increased 2.31 times.

Keywords: Urban Parks, Heat Island Mitigation, Park Cool Island, Digital Satellite Image, Built Environment.

INTRODUCTION

Greening is an efficient strategy for the adaptation and mitigation of the UHI and urban warming phenomena [1]. In particular, urban parks form the so-called Park Cool Island (PCI), which can effectively alleviate the negative influences of urban heat islands. However, it is important to highlight that in arid zones, urban greening demands a certain amount of water in a place where this resource is scarce. For this reason, it is necessary to plan the features of built-up areas around the park in order to guarantee their sustainability in terms of management, natural resource consumption, and thermal benefits. Thus, the objective of this work is to evaluate the impact of an urban park in the city of Mendoza, Argentina —Parque Central— on the air temperatures of its built environment, taking as a measure the intensity of park cool island. In addition, we analyzed the evolution of its cooling effect over time (ten years) in relation to the evolution of the park and the surrounding urban areas characterized by means of satellite image indices.

MATERIALS AND METHODS

Mendoza's Parque Central is the fourth green space on the surface of the city (approximately 14 hectares). It is located in the northwest area of the province capital (32° 52' 37.08" S and 68° 50' 28.03" W), in a residential area with medium to high construction density (2-4 m³/m²). It has a strategic value for urban development, given the numerous uses and artistic, sport, social and cultural activities provided. But several of those specimens incorporated in 2006 did not adapt to the environmental conditions of the growing site. At present, the most tolerant have been consolidated, integrating forested or aligned groups with the development of a dense vegetation cover (canopy) that provides important shading.

Two monitoring campaigns were developed during the summer periods of 2007-2008 and 2016-2017. In each campaign, temperature and relative humidity sensors of type HOBO H8-003-02 and UX100-003 (HOBO®; Onset; Cape Cod, MA) were installed, recording every 15 minutes. Two of them were located within the park in well differentiated structures: meadow and forest. In addition, four sensors were installed around the park (North, East, South and West) at an average distance of 450 m from the edge. Finally, a sensor was located in the center of the city.

Landsat 7 satellite images from 10/1/2008 and 1/18/2017 were analyzed in order to study the green areas, together with the evolution of their surroundings, and to evaluate their impact over the microclimate. NDVI [2] and NDBI [3] indices were determined as well. The QGIS software was used to process satellite images. The images were calibrated, corrected and projected onto POSGAR 2007–Argentina 2.

The definition of hourly PCI is the difference in air temperature between the surrounding urban areas and the park:

$$PCI = T_u - T_p \quad (1)$$

where, T_u is the hourly average temperature of urban surroundings (North, West, South and East), and T_p is the hourly average temperature inside the park (meadow and forest).

RESULTS AND DISCUSSION

In Mendoza's Parque Central, the increase in NDVI denotes the consolidation of biomass (Table 1), but the maximum temperature differences decrease from 2007-2008 to 2016-2017, during maximum temperature occurrence. This reduction shows the impact of urban growth throughout the period. The NDBI shows that along ten years the quantity of built-up areas has increased in all directions around the park. The maximum values of NDBI have increased in a range of 1.52 to 1.95 times. As the building mass increases, the thermal inertia of the environment increases as well and temperature differences with the cold structures within the park—the forests— decrease in the hours of sun. Based on [4] results, the cooling effect of the park would be expected to increase. However, this has not been the case, demonstrating that the thermal benefits of the park have been governed by the densification of its surroundings.

Table 1. NDVI values for Parque Central and NDBI values for each area of influence.

	NDVI		NDBI							
	2008	2017	North Point		South Point		East Point		West Point	
			2008	2017	2008	2017	2008	2017	2008	2017
<i>Minimum</i>	-0.20	0.02	-0.25	-0.25	-0.18	-0.21	-0.22	-0.26	-0.18	-0.30
<i>Average</i>	-0.05	0.26	-0.01	-0.01	-0.01	-0.01	-0.02	-0.04	-0.01	-0.02
<i>Maximum</i>	0.07	0.57	0.16	0.26	0.15	0.23	0.19	0.37	0.16	0.27

The cooling effect of the forest is more susceptible to the increase of NDBI than that of the meadow. In the South point the variation of the maximum NDBI has been the lowest whereas the cooling effect caused by the park is the greatest. On the contrary, the East point shows the highest increase in maximum NDBI and the lowest cooling effects.

Respect to PCI, during the 2007-2008 season, the maximum PCI is 1.3 °C, being relatively stable throughout the day. During the 2016-2017 summer, the maximum values of PCI occur during noon: the park is up to 3.0 °C colder than the urban surroundings. Although the cooling effects of greenspace are well known, the understanding on the roles of landscape inside and outside parks in PCI features is still not deeply explored.

CONCLUSIONS

This research highlights the challenges of reconciling the thermal benefits of an urban park placed in an arid zone with the built environment growth.

The forest structure is 37% cooler than the surroundings in 2016 vs. 2008. In contrast, the maximum PCI recorded between the meadow structure and its surroundings represents a 62% increase in its cooling effect.

Based on NDVI values, the forest area consolidation and the park evolution have allowed a more efficient behavior of the meadow structure, despite the temporary increase in anthropic pressure on the park, evidenced by the NDBI.

Over 10 seasons, the park's maximum NDVI has increased more than 8 times, while the maximum PCI intensities have increased 2.31 times. The high increase in vegetation is not directly proportional to the cooling effect of this urban park.

The cooling profile of the park has changed. NDVI and PCI grew but the evolution of the surroundings (measured as NDBI) has modified the role of the park as a thermal regulator. The thermal benefit of the park has moved from the night to the afternoon hours.

REFERENCES

- [1] Gómez-Navarro C, Pataki DE, Pardyjak ER, et al. Effects of vegetation on the spatial and temporal variation of microclimate in the urbanized Salt Lake Valley. *Agricultural and Forest Meteorology*, 296, 108211. 2021.
- [2] Rouse JW, Haas RH, Schell JA, et al. Monitoring the vernal advancement of retrogradation of natural vegetation. Greenbelt, MD: NASA/GSFC (Type III, Final Report). 1974.
- [3] Zha Y, Gao J, Ni S. Use of normalized difference built-up index in automatically mapping urban areas from TM imagery. *International Journal of Remote Sensing*, 24(3), 583–594. 2003.
- [4] García-Haro A, Arellano B, Roca J. Variaciones estacionales del efecto de enfriamiento de los parques urbanos de Barcelona: una aproximación mediante teledetección. In: *CTV 2019 Proceedings: XIII Int Conf on Virtual City: Challenges and paradigms of the contemporary city*. 2019 Oct 2-4, Barcelona, Spain. Barcelona: CPSV; 2019, p.8957-76.

METHYLENE BLUE ADSORPTION ON BIOCHAR PREPARED FROM PUMPKIN SHELL

Demet Bal^a, Çiğdem Özer*, Mustafa İmamoğlu^c

^a Bitlis Eren University, Faculty of Engineering & Architecture, Environmental Engineering Dept., 13000, Bitlis, Turkey

^b Bitlis Eren University, Faculty of Arts & Sciences, Chemistry Dept., 13000, Bitlis, Turkey

^c Sakarya University, Faculty of Arts & Sciences, Chemistry Dept., 54050 Sakarya, Turkey

*Corresponding author: e-mail: cozer@beu.edu.tr

ABSTRACT

In this study, methylene blue adsorption on biochar prepared with acid from pumpkin shell was studied. An ecological, environmentally friendly, green treatment alternative has been presented by creating a low-cost adsorbent from an agricultural waste. pH, contact time, MB initial concentration and adsorbent dose changes, which are effective parameters for adsorption, were examined. Equilibrium results were applied to Langmuir and Freundlich isotherms, and contact time results were applied to pseudo 1st and 2nd order kinetic models.

Keywords: Pumpkin, Biochar, Methylene Blue, Adsorption

INTRODUCTION

Dyes are organic complex molecules that give color to surfaces. Wastewater from plastic, paper and especially dyeing industries pollutes the water due to the discharge of these molecules [1]. In addition to aesthetic problems, it can negatively affect aquatic life by preventing the penetration of even small amounts of sunlight. MB is a very common pollutant in wastewater since its usage area is quite large. Long-term exposure to MB can cause health problems such as nausea, anemia, hypertension and vomiting [1]. For these reasons, the treatment of dye-contaminated wastewater remains an important problem [2]. Today, chemical methods such as ozonation, photocatalysis, fenton process and oxidation; Biological methods such as aerobic and anaerobic treatment and physical methods such as ion exchange, coagulation/flocculation, membrane filtration and adsorption are widely used to remove dyestuffs from wastewater [3]. Adsorption is an important separation process that is often preferred because it is both economical and effective in removing heavy metals, organic pollutants and dyes from wastewater. The range of adsorbents that can be used in the adsorption process is very wide [2]. Since the efficiency and cost of the process are determinant, the search for new alternatives is increasing in the selection of adsorbent with waste origin and effortless preparation process. Biochars are materials with high surface area, large pore volume, rich functional groups and wide application areas. They can be converted into cost-effective and easily available adsorbents by a series of chemical processes from different biomass. They are also preferred due to their low cost, porous structure and high efficiency [4]. In this study, biochar was prepared with sulfuric acid from pumpkin shell, which is an agricultural waste, and it was concluded that the obtained material is an effective adsorbent for MB.

MATERIALS AND METHODS

The biochar used as an adsorbent in the studies was prepared by thoroughly mixing the pumpkin shell with sulfuric acid at room temperature. After standing overnight, the washed material was dried and stored at room temperature. For the characterization of the prepared biochar, moisture and ash content determination, fixed carbon determination, elemental analysis, single and multi-point BET surface analyzes and FTIR analysis were performed, and SEM images were taken. Methylene Blue (MB) (Merck, Germany) solution was used as adsorbate. The required amount of MB was dissolved in distilled water.

The adsorption dynamics of MB on biochar prepared with sulfuric acid from pumpkin peel were evaluated by performing batch experiments. The effects of parameters such as pH, initial MB concentration, adsorbent dose and contact time were investigated. For the pH effect investigation, 0.050 g biochar was added to the dye solutions in volume of 50 mL and concentration of 400 mg L⁻¹ at various pH values and then was mixed using a magnetic stirrer at room temperature for 24 hours. 0.1 M HCl and NaOH solutions were used for pH adjustments. To investigate the effect of contact time on adsorption, dye solutions (50 mL) of 400 mg L⁻¹ at the original pH value (6.0) were mixed with 0.050 g biochar for 5 to 1440 minutes. To examine the effect of initial MB concentration on adsorption, dye solutions of 50 mL volume were prepared at pH 6.0 at concentrations ranging from 50 to 500 mg L⁻¹, and 0.050 g biochar was added to these solutions and mixed for 24 hours. At the end of the adsorption process, the biochar was separated from the suspension by centrifugation. MB concentrations remaining in solution were measured by UV-VIS spectrophotometer. Then, the amount of MB adsorbed per unit mass of biochar was calculated.

By using the data obtained from the experiments to examine the effects of initial MB concentration and contact time on adsorption, isotherm and kinetic model applications were carried out, respectively, Langmuir [5] and Freundlich [6] models were used for isotherm applications, while pseudo 1st order [7] and pseudo 2nd order [8] models were used for kinetic applications.

CONCLUSIONS

In this study, the adsorption behavior of methylene blue, which is frequently found in wastewater due to its wide usage area, was investigated from pumpkin shell on biochar prepared with sulfuric acid. An agricultural waste pumpkin shell has been used as a source of biochar to make it cost-effective for use as an adsorbent. The prepared biochar was characterized by BET surface area analysis, partial and elemental analysis, as well as FTIR analysis and SEM images. Although the multilayer surface area is low, biochar has the potential to be a good adsorbent due to its low moisture and ash content. The optimum pH of the adsorption of MB with biochar was determined as 6, the time to reach equilibrium was 16 hours, the initial concentration of MM was 400 mg L⁻¹, and the adsorbent dose was 50 mg. Equilibrium modeling was performed with Langmuir and Freundlich isotherm models, and it was seen that the study was more compatible with the Langmuir isotherm model, which indicates that monolayer adsorption is dominant. In order to evaluate the kinetic behavior of the adsorption mechanism of MB on biochar, the pseudo-first and second-order kinetic models were applied to the results of the contact time study, and the results showed that the mechanism consistent with both models could be better explained by the pseudo-second-order model in terms of q_e values. The obtained results showed that it is possible to evaluate the prepared biochar as an effective adsorbent in the removal of MB.

REFERENCES

- [1] Sahu S, Pahi S, Tripathy S, Sing SK, Behera A, Sahu UK, Patel RK, 2020. Adsorption of Methylene Blue on Chemically Modified Lychee Seed Biochar: Dynamic, Equilibrium, And Thermodynamic Study. *Journal of Molecular Liquids*, 315: 113743.
- [2] Altıntig E, Yenigun M, Sarı A, Altundag H, Tuzen M, Saleh TA, 2020. Facile Synthesis of Zinc Oxide Nanoparticles Loaded Activated Carbon as an Eco-Friendly Adsorbent for Ultra-Removal of Malachite Green from Water. *Environ. Technol. Innov.*, P. 101305.
- [3] Öztürk A, Çetintaş S, Bingöl D, 2020. The Use of Pomegranate Seed Activated by Mechanochemical Process as A Novel Adsorbent for The Removal of Anionic Dyes: Response Surface Method Approach. *Chem. Eng. Commun.*, 1–22.
- [4] Kaya N, Uzun ZY, 2020. Investigation of Effectiveness of Pinecone Biochar Activated with KOH for Methyl Orange Adsorption and CO₂ Capture. *Biomass Convers. Biorefinery*, 1–17.
- [5] Langmuir I, 1918. The Adsorption of Gases on Plane Surfaces of Glass, Mica and Platinum. *J. Am. Chem. Soc.*, 40: 1361–403.
- [6] Freundlich HMF, 1906. Over the Adsorption In Solution. *J. Phys. Chem*, 57: 1100–1107.
- [7] Lagergren S, 1898. About the Theory of So-Called Adsorption of Soluble Substances. *K. Sven. Vetenskapskad. Hand*, 24 (4): 1–39
- [8] Ho Y, Mckay G, 1999. Pseudo-Second Order Model for Sorption Processes. *Process Biochem.*, 34 (5): 451–465.

DETERMINING COMPENSATION RATE FOR WIND-SOLAR HYBRID ENERGY SYSTEM IN ISTANBUL BASED ON ANFIS MODELING

^{1*} Esra Gün, ² Ahmet Duran Şahin

¹Istanbul Technical University, Faculty of Aeronautics and Astronautics, Meteorology Department), Maslak, İstanbul, Turkey

²Istanbul Technical University, Faculty of Aeronautics and Astronautics, Meteorology Department), Maslak, İstanbul, Turkey

*Corresponding author e-mail: esragun03@gmail.com.tr

ABSTRACT

Hybrid energy applications should be considered now and in the next decades because of the discontinuity problems of renewable energy sources. In this study, wind and solar energy analyzes are made separately and together as hybrid systems based on the measurement wind velocity and solar irradiation data in Istanbul and its surroundings. Analysis of wind power, solar PV and hybrid generations are examined with monthly and hourly profiles and monthly hourly profiles were created by calculating the annual revenue value over the wholesale price of electricity.

It has been examined which source meets the monthly total electricity generation values of the hybrid system. Considering monthly rates, it is seen that sometimes the wind power coverage rate is high the PV is low, however, sometimes PV coverage rate is high, but the wind turbine electricity generation is low, and it is evaluated that, both systems have equal and close to equal generation rates.

Wind turbine and PV electricity generation estimated by using Openwind and PVSyst softwares respectively, and capacity factor for each renewable energy system calculated as for Ömerli dam region as 26% and 23%. The hybrid wind-solar system capacity factor calculated according to hourly electricity values of wind and PV as 24%. In the perspective of hybrid electricity generation profile, the scattering diagrams of hourly average values for each and all months for desired time are prepared and their correlations calculated. It is modelled that, the most significant highest relationship evaluated between July and August.

Wind power and PV electricity generation calculated as a result of the wind velocity and solar irradiation measurement data of Ormanlı, located on the European side of Istanbul, and capacity factor of wind power and PV is calculated as 34% and 23%, respectively. Wind-PV hybrid capacity factor calculated according to hourly production values of these renewable technologies as 28%.

Based on hybrid system electricity generations data of Ömerli and Ormanlı, An Adaptive Neuro-Fuzzy Inference System (ANFIS) modeling is applied, and monthly relationship between these sources are estimated for all locations. It is determined that the highest correlations evaluated between June and July.

Monthly total electricity generation values of the wind-solar hybrid system are analyzed by each source separately and together at different ratios and considering the monthly rates, it is found that wind power capacity is high while the sun potential is high, and sometimes hybrid system loads over the desired capacity. For all hours during the year compensation rates of considered wind-solar hybrid system is estimated.

Keywords: ANFIS, Energy, Hybrid energy system, Solar, Wind, Renewable

INTRODUCTION

The need for an ever-increasing energy is a fact that cannot be ignored. In order to meet the electricity demand, fossil resources were first used, and their use continued increasingly. However, the oil crisis that emerged in the early 70s and the global warming of oil in the 90s due to the excessive use of fossil fuels; energy to meet renewable and clean resources. Wind energy, which has been used for different purposes since the past, has been one of the energy sources which is seen as a renewable electrical energy source. Wind energy has become one of the most important energy sources today due to the high efficiency of wind turbines in the region with high wind speed potential and economic and technical constraints on fossil fuels. Solar energy has also been affected by these developments and has been in demand. Technological progress and cost reduction, as well as being able to be used in the feeding of small loads as well as being able to be used in the feeding of large loads positively affected the spread of solar energy systems. Wind and solar renewable energy sources can generate electricity independently of the grid or connected to the interconnected system. With the emergence of renewable systems based on wind and solar, hybrid systems have been developed which enable the use of two systems by combining them.

Turkey's highest sunshine hours due to the high solar energy is the region of South and Southeast Anatolia has the potential Mediterranean, Eastern Anatolia, Central Anatolia, Aegean, Marmara and Black Sea regions respectively following. Turkey Wind Atlas mean wind speed in the 50-meter-high residential areas, except by the Marmara and West Black Sea coastal areas from 6.0 to 7.0 m / s and the inner side of these regions 5.5-6.5 m / s, eastern Black Sea coast 5.0 m / s in the inner and inner parts, 7.0–8.5 m / s in the North West Aegean coast and 6.0–7.0 m / s in the inner parts of this region, 5.0–6 in the Western Mediterranean coast, 0 m / s and 4.5-5.5 m / s in the inner parts of this region.

Renewable energy sources are extremely attractive because they do not run out and do not have any significant harm to other sources in terms of environment and human health. The aim of hybrid systems is to increase the efficiency by providing the use of energy resources together and to ensure that others meet the energy needs of the system if one of the resources is not or decreases. The hybrid system components are formed by combining two or more sources.

DATA AND METHODS

Data used in this study were measured by İSKİ for five different stations located in and around İstanbul at least for one year (Figure 1).

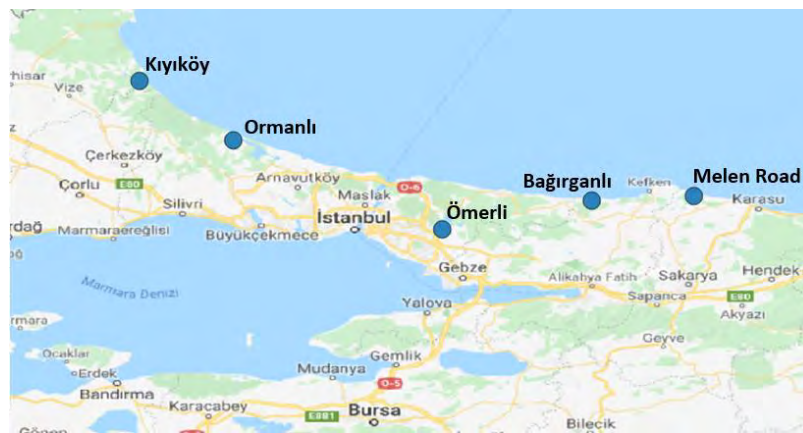


Figure 1. İSKİ measurement stations.

The wind and solar potentials for the identified regions were examined and the capacity factors for the wind-solar hybrid system were determined and modeled. Wind potentials of the sites determined by AWS Openwind program and hourly production analyzes are also performed. Solar analysis is performed with PVsyst program and hourly production results are obtained. The obtained productions are converted into one-year monthly and hourly data sets for hybrid systems and hybrid electricity generation analysis (compensation rates, capacity factors etc.) is evaluated (Figure 2).

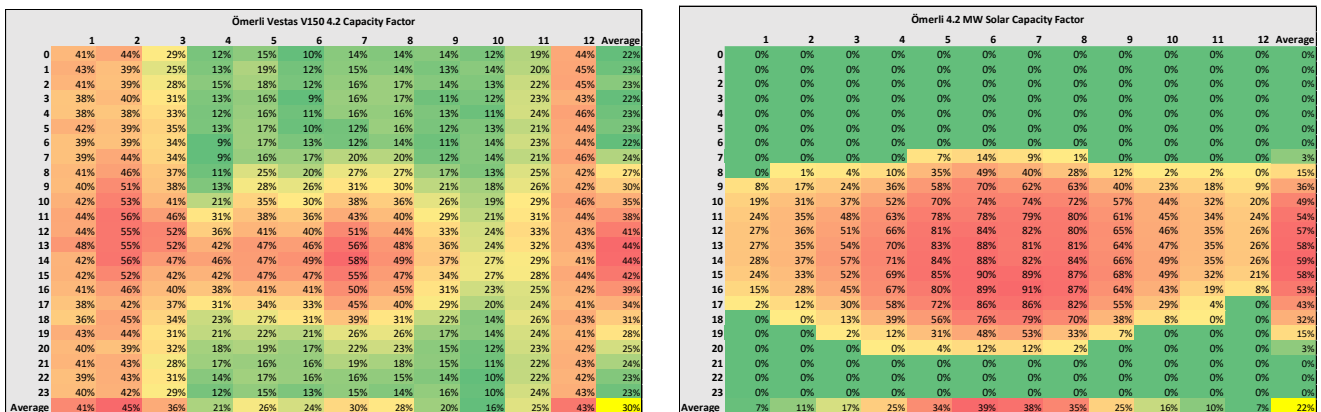


Figure 2. Wind and solar monthly and hourly capacity factor tables

In addition to energy production (wind, PV and hybrid) analysis, revenue analysis included two scenarios was performed for İSKİ (Table 1).

Table 1. Wind-PV hybrid generally summarize.

Project	Production (kWh)	Capacity Factor (%)	Electricity Sales revenue (TL)	Electricity Consumption Revenue (TL)
Ömerli	19,093,942	24	3,853,158	10,310,728
Ormanlı	21,002,490	29	4,238,302	11,341,344
Bağıranlı	18,351,502	25	3,703,333	9,909,811
Melen Yolu	19,435,586	26	3,922,101	10,495,216
Kıyıköy	16,065,659	22	3,242,050	8,675,456

CONCLUSIONS

In this research there are five stations that scattered all around İstanbul, according to the results wind turbines electricity generation capacity factor and revenue of these systems for Ormanlı is higher than others and lowest values evaluated in Kıyıköy. Ormanlı is followed by Ömerli, Melen Road, Bağıranlı and Kıyıköy, respectively, in the perspective of capacity factor and revenue. The regions with the highest solar capacity factor are Melen Road and Bağıranlı. The highest region in terms of hybrid production and capacity factor is Ormanlı and is followed by Melen Road, Bağıranlı, Ömerli and Kıyıköy respectively.

For Ormanlı, Melen Road, Bağıranlı, Ömerli and Kıyıköy hybrid systems, the ratio of the total production of the system is calculated by considering wind turbine and PV capacity and total energy generation of these systems. Hourly, monthly and annual energy production of the total hybrid system are also calculated for all regions.

Monthly and hourly production values for Ömerli were taken into consideration and the ratio of the total production value of the hybrid system was calculated. Monthly total electricity generation values of the hybrid systems are analyzed based on source and at compensation ratios. It is seen that mostly wind energy and PV complement each other as a renewable source.

ANFIS modeling is done with the relationships between the mean values and data sets and relations are evaluated and modeled using fuzzy logic. With ANFIS, annual-hour production values for wind turbine, PV and hybrid are evaluated with fuzzy logic. The relationship between the measured data and the modelled data by ANFIS is examined and it is seen that correlation between measurement and modeled values for the next month is very high.

REFERENCES

- [1] Gün, E., 2019. İstanbul ve Çevresinde Rüzgar-Güneş Hibrit Sisteminin Karşılama Oranlarının Belirlenerek Anfis Tabanlı Modellenmesi, Yüksek Lisans Tezi, İ.T.Ü. Fen Bilimleri Enstitüsü, İstanbul.
- [2] Url-1 <<https://www.enerji.gov.tr/tr-TR/Sayfalar/Gunes>>, 31.10.2019
- [3] Url-2<<https://www.mgm.gov.tr/kurumici/turkiye-guneslenme-suresi.aspx>>, 1.11.2019.
- [4] Altuntaşoğlu, Z. T. 2012. "Türkiye'de Rüzgâr Enerjisi, Mevcut Durum, Sorunlar," Mühendis ve Makine Dergisi, cilt 52, sayı 617, s. 56-63.)
- [5] Url-3<<https://www.mgm.gov.tr/genel/ruzgar-atlasi.aspx>>, 31.10.2019
- [6] Tudorache, T. and Morega, A. 2008. Optimum Design of Wind/PV/Diesel/Batteries Hybrid Systems, 2. International Conference on Modern Power Systems, Cluj-Napoca, Romania, 12-14 November, 261-264.
- [7] Salmanoğlu, F. 2009. Rüzgâr – Fotovoltaik Otonom Hibrit Güç Sistemlerinin Algoritmik Bir Yaklaşımla Optimal Tasarımı.Yüksek Lisans Tezi, Ege Üniversitesi, Fen Bilimleri Enstitüsü, İzmir
- [8] Dinçsoy, M.E. 2010. Orta Ölçekli Bir Otelin Elektrik Enerjisinin Hibrit Sistemler İle Modellenmesi Ve Optimizasyonu. Yüksek Lisans Tezi, İstanbul Teknik Üniversitesi, Fen Bilimleri Enstitüsü, İstanbul
- [9] Durna B., Şahin A.D, 2020. Mapping of daylight illumination levels using global solar radiation data in and around İstanbul, Turkey, Weather – January 2020, Vol. 75, No.
- [10] Ayhan, D. 2011. Bina Montajlı Güneş-Rüzgâr Hibrit Elektrik Güç Sistemlerinin Analizi. Yüksek Lisans Tezi, Marmara Üniversitesi, Fen Bilimleri Enstitüsü, İstanbul.
- [11] Başaran, K., Çetin, N.S., Çelik, H. 2011. Rüzgâr-Güneş Hibrit Güç Sistemi Tasarımı ve Uygulaması. 6th International Advanced Technologies Symposium (IATS'11), 114-119
- [12] Himri, Y., Stambouli, A. B., Draoui, B., Himri, S., 2008. Techno-economical study of hybrid power system for a remote village in Algeria, Energy, 33, 1128-1136.
- [13] Dalton, G. J., Lockington, D. A. and Baldock, T. E. 2009. Feasibility analysis of renewable energy supply options for a grid-connected large hotel, Renewable Energy, 34, 955-964.
- [14] Url 4 <<https://aws-dewi.ul.com/software/openwind/>>, erişim tarihi 9.11.2019.
- [15] Zadeh, L. (1965). Fuzzy sets, Information and Control, 8(3), 338–353
- [16] Kuvvetli, Y. (2017). Adaptif Sinir Ağına Dayalı Bulanık Çıkarım Sistemi İle Dönen Ürünlerin Fiyatlandırılması, Alphanumeric Journal, 5(2), 207–214.
- [17] Suparta,W. ve Alhasa, K.M. (2016). Adaptive Neuro-Fuzzy Interference System, Springer International Publishing 1.

HOT AIR DRYING OF SPHERICAL MOIST OBJECTS IN A 3D RECTANGULAR CHANNEL

¹ Seda Özcan Çoban, ¹ Fatih Selimefendigil, ² Hakan F. Öztop

¹Manisa Celal Bayar University, Engineering Faculty, Mechanical Engineering, Manisa, Turkey

² Firat University, Technology Faculty, Mechanical Engineering, Elazığ, Turkey

*Corresponding author e-mail: sedaozcan82@hotmail.com

ABSTRACT

Coupled heat and mass transport for convective drying of spherical shaped moist porous objects are investigated numerically. Six objects are placed in a rectangular channel as every two objects are side by side. Hot air flows through the channel over the objects, velocity and temperature of the air varied to see the change of moisture content inside the objects by time and the effects on drying performance. The finite element method was used to solve the nonlinear governing equations of the 3D Multiphysics problem. Results showed that the configuration of the objects is important due to drying air flows horizontally from the inlet of the channel. The moisture content of the objects is observed less on the front and top regions of the objects than other regions, especially for the object closer to the inlet of the channel. The simulations gave the result that temperature and velocity have important effects on drying which increasing the temperature and increasing velocity have positive effects on drying performance.

Keywords: Porous body, heat and mass transfer, multiphase flows, CFD

INTRODUCTION

Convective drying is a very conventional and common method for dehydration of moist products. Hot blowing air has been used as a favorable method for drying a wide variety of products since ancient times. This thermal drying method offers ease of use, low operational costs, and rapid processing, and used in a wide range of dryer types. Hot air flows through a drying chamber over the moist object and initially, moisture near the surface of the object starts to evaporate due to the thermal interaction between hot air and relatively cold object. After a period of time as the moisture content inside the object reaches a threshold value, the moisture diffuses from the interior parts of the object to the surface and then evaporates to air. The coupled transport mechanism of convective drying is considered a nonlinear Multiphysics problem and needs to be investigated. In most numerical and experimental studies, while the drying air is conditioned and given to the drying chamber with the help of a pump or fan [1–3], there are also studies in which the effect of wind on drying as hot airflow in the atmosphere or in a wind tunnel is examined [4–6]. The aim of the present paper is to investigate the coupled transport mechanism numerically by constructing a 3D simulation and see the effects of varying parameters in order to specify the optimum drying performance. It is important to determine the appropriate condition in drying for an effective process with energy-saving.

MATERIALS AND METHODS

Hot air flows in a rectangular channel and six identical spherical objects are placed at the center of the channel. Reduce of moisture content by time was investigated under the effect of varying air velocities as $u = 0.1, 0.2, 0.3, 0.4, 0.5$ m/s and varying air temperatures as $T = 303$ K, 313 K, 323 K, 333 K, 343 K. The schematical description of the problem is given in Figure 1. The height of the channel is $H = 0.05$ m. The length of the channel is $L = 20 \cdot H$. The radius of the spheres is $r = 0.2 \cdot H$ and the x-axis distance of the spheres are $l = 2 \cdot H$.

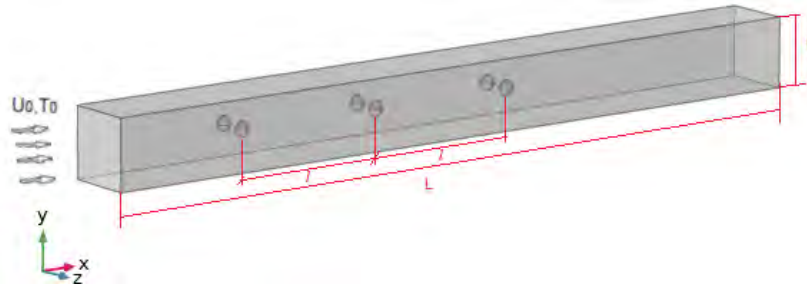


Figure 1. Schematical description of the problem (not to scale)

The air flowing through the channel is initially dry, and the moisture evaporates from the object to the surrounding air, so the channel air gets humidified after a time. Laminar 3D flow conditions are valid and conservation of mass, momentum and energy equations for transient channel flow are given as follows:

$$\frac{\partial p_a}{\partial t} + \nabla \rho_a \vec{u} = 0 \quad (1), \quad \rho_a \frac{\partial \vec{u}}{\partial t} + \rho_a \vec{u} \nabla \vec{u} = -\nabla \left[p \vec{I} + (\mu_a) \left((\nabla \vec{u}) + (\nabla \vec{u})^T \right) - (2/3) (\nabla \vec{u}) \vec{I} \right] \quad (2)$$

$$\rho_a \frac{\partial u}{\partial t} + \rho_a c_{p,a} \frac{\partial T}{\partial t} - \nabla (k_a \nabla T) + \rho_a c_{p,a} \vec{u} \nabla T = 0 \quad (3)$$

In the equations, ' p ' is the pressure (Pa), ' c_p ' is specific heat ($\text{kJ kg}^{-1} \text{K}^{-1}$), ' ρ ' is the density (kg m^{-3}), ' μ ' is the dynamic viscosity and subscript ' a ' denotes the air for all symbols. \vec{I} is the identity vector. Mass balance equations of water in two phases and air are described by a non-isothermal formulation of strong distributed evaporation from porous objects (Eq. 4), and energy equation for porous medium is described in Eq. 5.:

$$\frac{\partial c_v}{\partial t} + (\vec{u}_v) = R_{evap}, \quad \frac{\partial c_l}{\partial t} + (\vec{u}_l) = -R_{evap}, \quad \frac{\partial c_a}{\partial t} + (\vec{u}_a) = 0 \quad (4)$$

$$(\rho c_p)_{eff} \frac{\partial T}{\partial t} + \nabla \cdot (\vec{n}_g h_g + \vec{n}_l h_l) = \nabla \cdot (k_{eff} \nabla T) - H_{evap} R_{evap} \quad (5)$$

where ' c ' is the molar concentration (mol/m^3) with subscripts ' l ' liquid water and ' v ' water vapor. \vec{n} is the total mass fluxes ($\text{kg m}^{-2} \text{s}^{-1}$) of gas phase (g) and the liquid phase (l). ' R_{evap} ' is the rate of evaporation and ' H_{evap} ' is the latent heat of evaporation. ' S ' is the liquid saturation, and it is the dimensionless value describing the moisture content of the object. Thermophysical properties of air, water and porous matrix could be found in the referenced study [7].

Finite Element Method was used for solving the highly non-linear equations of the problem via a commercial CFD code COMSOL Multiphysics. Weak forms of the equations were obtained from Galerkin weighted residual method. Approximations of the flow field variables for the domain were done by Lagrange polynomials of different orders. A fine mesh was generated manually for the problem considering boundary layers in order to resolve all effects and for better convergence.

CONCLUSIONS

Effects of varying parameters on drying performance were investigated for convective drying of spherical porous objects in a 3D rectangular channel. Velocity and temperature of hot air were varied with five different values of each and moisture contents were evaluated for those parameters were simulated. Figure 2 shows the moisture content distribution by time (a) and local moisture content value with varying air velocities (b) for the vertical midline of the object in the right frontside of the channel (object 1). The moisture content decreases more sharply as time progresses, and it was seen that increasing air velocity causes a further reduction in moisture content. (Further information will be given in the full-text paper.)

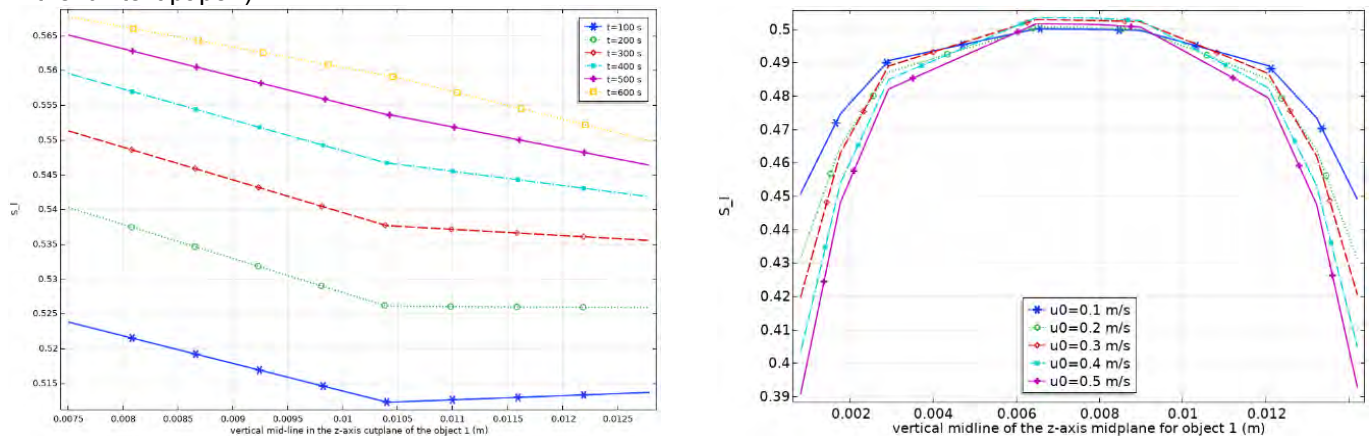


Figure 2. Moisture contents as S_l for object 1, by time(a) for varying air velocities ($t=300$ s)(b) $S_l(t=0) = 0.6$.

ACKNOWLEDGMENTS

This study is supported from the (THE SCIENTIFIC AND TECHNOLOGICAL RESEARCH COUNCIL OF TURKEY-TUBİTAK) under the grant no: 119M050 which is gratefully acknowledged.

REFERENCES

- [1] Castro AM, Mayorga EY, Moreno FL. Mathematical modelling of convective drying of feijoa (Acca sellowiana Berg) slices. *J Food Eng* 2019; 252: 44–52.
- [2] Defraeye T, Radu A. Convective drying of fruit: A deeper look at the air-material interface by conjugate modeling. *Int J Heat Mass Transf* 2017; 108: 1610–1622.
- [3] Esfahani JA, Majidi H, Barati E. Analytical two-dimensional analysis of the transport phenomena occurring during convective drying: Apple slices. *J Food Eng* 2014; 123: 87–93.
- [4] Lal S, Moonen P, Poulikakos LD, et al. Turbulent airflow above a full-scale macroporous material: Boundary layer characterization and conditional statistical analysis. *Exp Therm Fluid Sci* 2016; 74: 390–403.
- [5] Or D, Lehmann P, Shahraeeni E, et al. Advances in Soil Evaporation Physics-A Review. *Vadose Zo J* 2013; 12: vj2012.0163.
- [6] Lal S, Lucci F, Defraeye T, et al. CFD modeling of convective scalar transport in a macroporous material for drying applications. *Int J Therm Sci* 2018; 123: 86–98.
- [7] Selimefendigil F, Çoban SÖ, Öztop HF. Investigation of time dependent heat and mass transportation for drying of 3D porous moist objects in convective conditions. *Int J Therm Sci*; 162. Epub ahead of print 2021. DOI: 10.1016/j.ijthermalsci.2020.106788.

EFFECT OF AUXILIARY ACCEPTORS ON QUINOLINE-BASED DYE-SENSITIZED SOLAR CELLS

^{1*} Barış Seçkin Arslan, ¹ Nagihan Öztürk, ¹ Merve Gezgin, ¹ Yavuz Derin,
¹ Ahmet Tutar, ¹ Mehmet Nebioğlu, ¹ İlkay Şişman

¹Sakarya University, Department of Chemistry, Sakarya, TURKEY

*Corresponding author e-mail: barisseckin@gmail.com

ABSTRACT

In this study, three new D-A- π -A dyes were synthesized by introducing auxiliary acceptors to some D- π -A dyes containing quinoline π -system and the photovoltaic performances of these compounds were compared. The design of these compounds was used diphenylamine group as donor, cyanoacrylic acid as anchoring group and benzene, benzothiadiazole (BTD) or *N*-ethylhexyl benzotriazole (BTZ) as auxiliary acceptor. These compounds were also investigated by optical, electrochemical, and theoretical methods. The compound with BTD unit (BIM1) caused a large red shift in the UV-Vis spectrum compared to the dye bearing BTZ (BIM2) and produced higher short-circuit current density (J_{sc}). The device with BTZ dye slightly increases the open circuit voltage (V_{oc}) due to inhibition of charge recombination. Higher power conversion efficiency (5.21%) was achieved for the device based on BIM1. The D-A- π -A dyes obtained by adding the BTD group as auxiliary acceptor to the quinoline-based D- π -A dyes remarkably improved the photovoltaic performance of the dye-sensitized solar cell (DSSC).

Keywords: Dye-sensitized solar cells, D-A- π -A, quinolone, auxiliary acceptor.

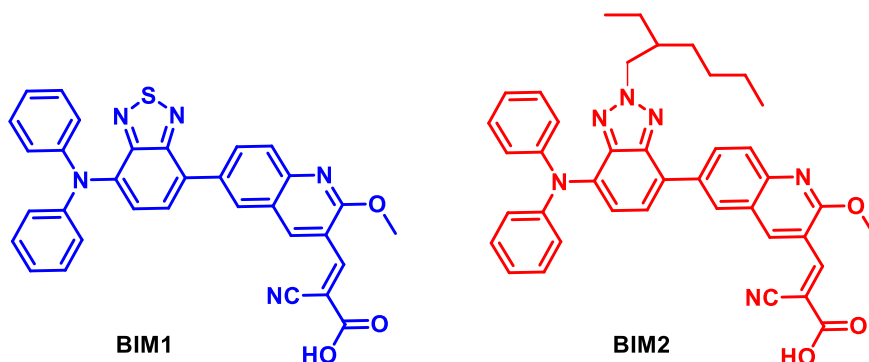
INTRODUCTION

As a cost-effective and environmentally friendly photovoltaic technology for using solar energy, DSSCs are promising in meeting the demand for clean and renewable energy sources [1]. Recently, significant progress has been made in DSSC research, thanks to the new D-A- π -A motif concept for molecular engineering of organic photosensitizers [2].

In this work, we synthesized two dyes (Scheme 1) bearing diphenylamine as electron donating group, BTD or BTZ as auxiliary acceptor unit, quinoline as π -bridge and cyanoacrylic acid as anchoring moiety. We report absorption characteristic and photovoltaic performances of dyes BIM1 and BIM2 in D-A- π -A skeleton [3]. We compare power conversion efficiencies when BTD and BTZ auxiliary acceptor is linked to the dyes.

RESULTS AND DISCUSSION

Acetylation of commercially available 4-bromoaniline followed by Vilsmeier reaction and the nucleophilic substitution reaction gave π -bridge of the dyes. This compound was converted to the boronic acid ester for use in coupling reactions. For coupling reactions, firstly, bromine-containing compounds were synthesized. Subsequently, D-A- π compounds were obtained by Suzuki-Miyaura coupling reaction of the boronic acid ester compound with the bromine-containing compounds. Finally, dyes BIM1 and BIM2 were obtained by Knoevenagel condensation.



Scheme 1. Chemical structures of the synthesized dyes.

The absorption wavelengths (λ_{max}) for dyes BIM1 and BIM2 are 476 and 400 nm (Fig. 1a). Remarkable red-shifts observed for dyes BIM1 and BIM2 can be attributed to the presence of stronger electron-withdrawing BTD and BTZ moieties on the dyes. The power conversion efficiency (PCE) of the DSSC based on BIM1 is much higher than that of BIM2 due to its broader absorption spectrum [4].

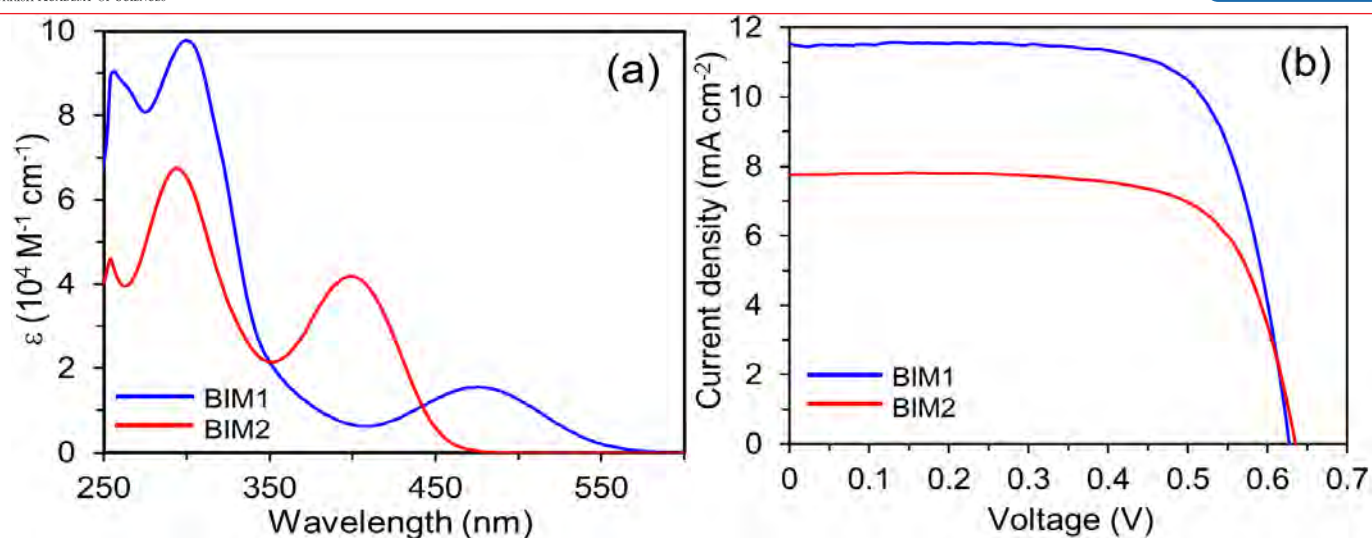


Figure 1. Absorption spectra (a) and J-V curves (b) of the dyes.

CONCLUSIONS

The DSSC based on the dye bearing BTD showed the PCE of 5.21%, which is better than that of 3.65% for the dye with BTZ. As a result, the insertion of a proper auxiliary acceptor to the sensitizers is an effective way to enhance the photovoltaic performance of the DSSCs.

REFERENCES

- [1] Zeng K, Tong Z, Ma L, et al. Molecular engineering strategies for fabricating efficient porphyrin-based dye-sensitized solar cells. *Energy Environ Sci.* 2020; 13:1617.
- [2] Wu Y, Zhu WH, Zakeeruddin SM, et al. Insight into D–A– π –A Structured Sensitizers: A Promising Route to Highly Efficient and Stable Dye-Sensitized Solar Cells. *ACS Appl Mater Interfaces.* 2015; 7:9307.
- [3] Arslan BS, Arkan B, Gezgin M, et al. The improvement of photovoltaic performance of quinoline-based dye-sensitized solar cells by modification of the auxiliary acceptors. *J Photochem Photobiol A.* 2021; 404:112936.
- [4] Zhang WQ, Li QY, Zhang Q, et al. Robust metal-organic framework containing benzoselenadiazole for highly efficient aerobic cross-dehydrogenative coupling reactions under visible light. *Inorg Chem.* 2016; 55:1005.

A NEW METHODOLOGICAL APPROACH FOR THE TECHNO-ECONOMIC ANALYSIS OF HYDROELECTRIC POWER PLANTS IN TURKEY

^{1*} Soner Çelikdemir, ² Mahmut Temel Özdemir

¹ Bitlis Eren University, Adilcevaz Vocational School, Electric and Energy, Bitlis, 13000, Turkey

² Fırat University, Engineering Faculty, Electrical and Electronics Engineering, Elazığ, 23000, Turkey

*Corresponding author e-mail: scelikdemir@beu.edu.tr

ABSTRACT

In this study, investment costs of hydroelectric power plants (HPP) in Turkey are analyzed. Equation model with 4 terms and 7 parameters is proposed for analysis. Archimedes Optimization Algorithm (AOA) is used to determine equation parameters. The study is handled in three stages. In the first stage, Turkey's 25 stream basins are divided into 8 groups according to precipitation and elevation values. In the second stage, separate equation parameters are determined for each group using a total of 67 HPP data. In the final stage, sensitivity analysis of the equation models developed is performed and the effect of the power, head and flow parameters of HPPs on cost is shown. With the proposed equation model, the average error value is calculated below a good value of 3.4902%. In this way, the cost of a HPP to be installed can be predicted with high accuracy using the proposed equation model.

Keywords: Hydroelectric Energy Potential, Techno Economic Cost Analysis, Basin Effect

INTRODUCTION

For our country, HPP has a great potential among Renewable Energy Resources (RES). Cost information is important for assessing this potential and converting it into investment. Equation model in the studies examined; It consists of power, head and flow parameters according to turbine types. This situation does not represent a general situation in the world geography. Because the costs of a HPP project with the same parameter values in different regions will also be different. This situation is due to the fact that the regions have different characteristics. In the studies reviewed, this situation is ignored. In addition, it has been stated in the studies that electromechanical costs constitute a large proportion of the total cost. Therefore, only electromechanical cost information is taken into account when conducting cost analyses of hydroelectric power plants [1–4]. However, considering the electromechanical costs, the proposed equation model does not cover the whole. This situation is seen as another deficiency in the literature. In the study, it is aimed to eliminate the deficiencies created by the situations that are ignored in the literature. For this purpose, both the characteristics of the regions and investment costs are taken into account in the proposed equation. For this, the data of 67 HPPs belonging to the last six years located in the stream basins of Turkey, which have not been used before in the literature, are used.

GROUPING OF TURKEY STREAM BASINS

The geography of Turkey consists of 25 stream basins. Although these basins have different stream arms when examined, the precipitation and elevation values of some basins are similar. Taking into account this similarity, grouping of stream basins is carried out. Thus, Turkey's stream basins are divided into 8 groups. Accordingly, basins with close rainfall and altitude values were included in the same group. The basin grouping made is given in Fig.1. In this way, an equation model is proposed for each basin group.

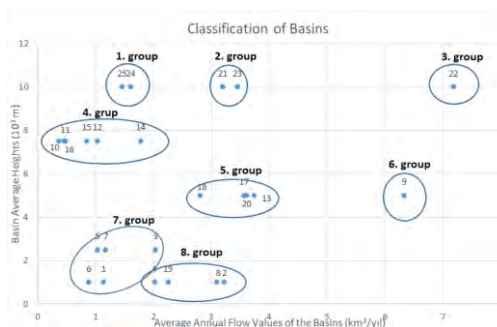


Figure 1. Grouping of Turkey Stream Basins

EQUATION MODEL DEVELOPMENT

In the literature, many analytical correlation methods are proposed for the cost calculation of electromechanical equipment [2–8]. In general, it is indicated by the following equation.

$$\text{Cost} = a.P^b + c.H^d + e.Q^f + g \quad (1)$$

In Equation 1, "a and b" are the constant coefficients of the P (KW) power expression, "c and d" are the constant coefficients of the H (m) head expression, and "e and f" are the constant coefficients of the Q (m) flow statement. HPP data, which has not been used before in literature studies in different regions of Turkey, are used in Eq. 1. Accordingly, the maximum error value is realized as approximately 16%. In addition, the average error is calculated as 3.4902 % and the standard deviation value as 5.9243. In his study, Ogayar developed an equation model for the turbine type. However the maximum error rate was calculated as 23.97% and the average error was 10.06% standard deviation 6.94 [4]. Filho, on the other hand, developed a single equation model in his study. But the maximum error rate was calculated as % 50.29% and the average error 21.33% standard deviation 16.67 [7]. Likewise, Cavazzini developed an equation model for the turbine type in his study. In this case the maximum error rate was calculated as -22.36% and the average error 8.24% standard deviation 7.39% [2]. According to these values, better results are obtained with the proposed equation model than the literature studies.

SENSITIVITY ANALYSIS

Sensitivity analysis is performed to see the effects of parameter values on cost in the proposed equation model. For this, the parameters in the equation model are examined respectively while performing the sensitivity analysis. Thus, the effect of the parameters on the cost will be seen more clearly. For the sensitivity analysis, the classification of the Turkey stream basins has been taken into account. Sensitivity analysis results are given in Fig. 2.

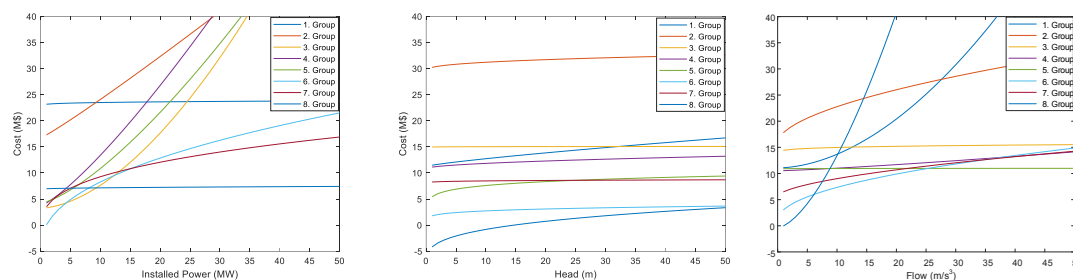


Figure 2. Installed Power / Head / Flow for Turkey Basin Classes – Cost Change Charts

CONCLUSIONS

The feasibility of projects belonging to HPPs can only be possible if cost analyzes are done correctly and if they are feasible. With the equation model proposed for the first time, percentage error rates were calculated below 19.965%. In addition, the average error is calculated as 3.4902% and the standard deviation value as 5.9243. According to these results, the cost is estimated with high accuracy. This indicates the effectiveness of the proposed equation model. In addition, in the study, the effects of change of parameters in the proposed equation model are examined for each basin class. Accordingly, it has been observed that the flow, head and installed power parameters are effective on the cost in the 1st and 8th Basin classes. however, it has been observed that the installed power parameter is more effective than the head and flow parameters in other basin classes. When turkey's basin classes are examined, the flow parameter on cost is more sensitive in the 1st and 8th Basin classes than the other basin classes. In other basin classes, on the other hand, it has been observed that the installed power parameter is more sensitive to cost than other basin classes. With this study, the cost of a HPP to be installed in any basin of Turkey can be predicted with high accuracy using the proposed equation model.

REFERENCES

- [1] Mishra S., Singal S.K., Khatod D.K. 2011. Approach for Cost Determination of Electro-Mechanical Equipment in Ror Shp Projects, Smart Grid and Renewable Energy.
- [2] Cavazzini G., Santolin A., Pavesi G., Ardizzon G. 2016. Accurate Estimation Model for Small and Micro Hydropower Plants Costs in Hybrid Energy Systems Modelling, Energy.
- [3] Aggidis G.A., Luchinskaya E., Rothschild R., Howard D.C. 2010. The Costs of Small-Scale Hydro Power Production: Impact on the Development of Existing Potential, Renewable Energy.
- [4] Ogayar B., Vidal P.G. 2009. Cost Determination of the Electro-Mechanical Equipment of a Small Hydro-Power Plant, Renewable Energy.
- [5] Mishra S., Singal S.K., Khatod D.K. 2013. Cost Analysis for Electromechanical Equipment in Small Hydropower Projects, International Journal of Green Energy.
- [6] Singal S.K., Saini R.P., Raghuvanshi C.S. 2010. Analysis for Cost Estimation of Low Head Run-of-River Small Hydropower Schemes, Energy for Sustainable Development.
- [7] Filho G.L.T., Santos I.F.S. dos, Barros R.M. 2017. Cost Estimate of Small Hydroelectric Power Plants Based on the Aspect Factor, Renewable and Sustainable Energy Reviews.
- [8] Celikdemir S., Yildirim B., Ozdemir M.T. 2017. Cost Analysis Of Mini Hydro Power Plant Using Bacterial Swarm Optimization, International Journal of Energy and Smart Grid.

EXTREME WINDS AND RISK ANALYSIS IN TURKEY FOR WIND ENERGY APPLICATIONS

¹Tolga Kara¹, Sena Ecem Yakut¹, Osman Tek², Metin Peköz², Merve Aksakal¹, and Ahmet Duran Şahin¹

¹Istanbul Technical University, Department of Meteorology, Energy and Climate Systems Lab, Maslak, İstanbul 34469, Turkey

² Turkish State Meteorological Service, Ankara 06830, Turkey

*Corresponding author e-mail: karat19@itu.edu.tr

ABSTRACT

Extreme atmospheric phenomena have been increasing due to the impacts of climate variability and change. Accurate estimation and evaluation of extreme events have become a critical issue to reduce its damage to economic values. From the perspective of wind energy applications, high wind speeds affect energy production, wind turbine stability, and its lifetime. Hence, it is crucial to have precise information about high wind speeds in wind farms. In this regard, the assessment of extreme wind conditions is an essential subject for each country. For the assessment of extreme wind conditions in Turkey, the 10-minute average wind speed data in 2016-2017 from the New European Wind Atlas Project was used. Both the Annual Maximum Method (AMM) and Peak Over Threshold Method (POTM) were applied for the regional analysis of extreme wind speeds in Turkey. Extreme wind speeds for the different return periods of 2, 20, and 50-years were predicted by using the AMM. As a result of the analysis made using the POTM, extreme wind speeds for different return periods of 10, 50, and 100-years were estimated. The maximum wind speeds were calculated as reference speed for each city in Turkey by applying the Constant Extreme Wind Speed Model (EWM) in IEC Standard 61400-1. Extreme winds that can repeat in a return period of 1-year and 50-years were calculated using these reference speeds. Extreme wind speeds with different return periods of 10, 50, and 100-years using POTM were found to be the highest in Van, Marmara, and Aegean Regions that are 40 and 45 m/s respectively. According to the EWM results, the highest wind speed in 2016 within the return period of 50-years was expected to occur in Antalya and estimated at 49.05 m/s. Similarly, for the period of 1-year, the maximum wind speed was expected to occur in Antalya and estimated at 39.24 m/s. Comparing the wind data of 2016 and 2017, there were no significant differences in estimated values of extreme wind speed. The highest wind speed in 2017 was expected to occur in Antalya, which is estimated at 37.68 m/s for the return period of 1-year, and 47.1 m/s for 50-years.

Keywords: Annual Maximum Method, Extreme Wind Speed, Risk Analysis, Peak over Threshold Value Method, Wind Energy

INTRODUCTION

Extreme atmospheric phenomena have been increased due to the impact of climate variability and change. Accurate estimation and evaluation of extreme events have become a critical issue to reduce its damage to economic values. Accurate estimation and evaluation of extreme events have become a critical issue to reduce its damage to economic values [1]. In this regard, the assessment of extreme wind conditions is an important subject for every country's agenda.

According to the IPCC AR5 (Intergovernmental Panel on Climate Change Fifth Assessment Report), it has been stated that the mid-latitude westerlies will increase based on the reanalysis data sets. There will be low-confidence changes in surface wind speeds [2]. Nevertheless, the frequency of high wind speeds over Europe will increase towards the end of the 21st century contrasting to the current climate conditions [3]. As a result of changes in the mean wind trends affecting evaporation, the presence of water and drought are also affected [4,5]. Continuous mid-latitude winds can increase coastal water levels [5, 6], long-term changes in the wind direction can affect wave climate and coastal stability [5, 7].

The extreme value approach needs long-term measurements for wind data, although the gathered datasets are short-term and low-confidence intervals [1]. From the perspective of wind energy applications, high wind speeds affect energy production, wind turbine stability, and lifetime, and hence, it's crucial to possess precise information about high wind speeds in wind farms. The low wind speeds can also cause low power generation depending on turbine types, whereas high wind speeds can change turbine stability. From the meteorological perspective, these extremes are directly linked to severe storms. If these risk values are known, it will be easier to reach a conclusion in the risk analysis. Calculation of probability transitions for wind intensities with different distributions (Weibull, Rayleigh, log normal, or Gamma frequency distribution functions) is of great importance in determining the occurrence of wind intensities [8,9].

Extreme wind conditions must be predicted prior to wind farm projecting for technical and economic aspects. In practice, the Constant Extreme Wind Speed Model and Turbulent Extreme Wind Speed Model in the IEC 61400-1 standard are used for determining the extreme conditions in a specific region [10].

EXTREME WIND SPEED ANALYSIS

The data used in this paper were collected from a database of New European Wind Atlas Project [11], created by a team behind NEWA consisting of 30 partners from 8 European countries. The publicly available mesoscale data in the atlas covers Europe with a resolution of 2-3 km. The generated 10-minute average wind speed data within the period of 2016-2017 used for the following 50-years wind analysis in this section. These calculations were applied for the regions and selected provinces of Turkey as study areas. The maximum wind speeds were calculated as reference speed for each city in Turkey by applying the EWM in IEC Standard 61400-1 [10].

The EWM is based on the reference wind speed (V_{ref}) and a constant turbulence standard deviation (σ_1) [10]. When the constant extreme wind model has first been examined; V_{e50} shows the extreme wind speed that has been repeated for 50 years. The extreme wind speed with a 1-year return period is shown with V_{e1} . V_{e50} is defined as the function of height (z) and V_{ref} . V_{e1} is the function of V_{e50} and height (z). The value of height, which is z level, is 100 m and hub height, which is referred to as z_{hub} in the equation in [10], is 80 meters. The Mediterranean region is selected as an example to represent the calculated maximum winds of selected provinces in Table 1.

Table 1. Extreme winds of provinces in Mediterranean Region

Provinces	Max $V_{(2016)}$	$V_{e50(2016)}$	$V_{e1(2016)}$	Max $V_{(2017)}$	$V_{e50(2017)}$	$V_{e1(2017)}$
Mediterranean Region						
Adana	37.71	38.65	30.92	36	36.89	29.52
Antalya	47.86	49.05	39.24	45.96	47.1	37.68
Burdur	22.67	23.23	18.59	24.74	25.35	20.28
Hatay	29.51	30.24	24.19	27.91	28.6	22.88
Mersin	28.86	29.58	23.66	27.01	27.68	22.14
Isparta	28.76	29.47	23.58	27.9	28.59	22.87
Kahramanmaraş	29.69	30.43	24.34	28.69	29.4	23.52
Osmaniye	28.91	29.63	23.7	28.8	29.52	23.61

In this study, both the AMM and POTM for the regional analysis of extreme wind speeds in Turkey were applied. Extreme wind speeds for various return periods of 2, 20, and 50-years were predicted using the AMM. As a result of the analysis made using the POTM, extreme wind speeds for various return periods of 10, 50, and 100-years were estimated to select the threshold, the POT package which has various tools to define an appropriate desired value, including the `tplot` and `mrplot` functions, were preferred [12]. Fig. 1 shows the threshold selection for the Mediterranean region using `tplot` function in R software, and it is determined clearly that a threshold of 25 m/s is an appropriate selection. For the foremost reasonable threshold selection, `mrplot` function could be additionally implemented. The mean residual life plot for the Mediterranean region using `mrplot` function, and it is evaluated that there is a non-linear behavior detected above 27 m/s in this figure. Hence, it is decided that the threshold value should be selected as 25 m/s as determined after the results of `tplot` function. The probability plot and Quantile-Quantile plot (Q-Q plot) were applied to the dataset and these methods represented quite well agreement with the data through the entire range. It is estimated that there will be 35 m/s as the extreme wind in 10 years, and additionally, approximately 37 m/s in 50 years and 39 m/s extreme wind in 100 years.

CONCLUSIONS

The maximum wind speeds as a reference value for each city in Turkey by applying the EWM in IEC Standard 61400-1 were calculated. Extreme winds which will be repeated in 1-year and 50-years were calculated using these reference values. It is estimated that, in the Marmara and Aegean Region, the highest extreme wind speeds with different return periods of 10, 50, and 100-years were estimated using POTM as 40 m/s and 45 m/s, respectively. Consistent with the EWM results, the highest wind speed in 2016 within the return period of 50-years was expected to occur in Antalya and estimated at 49.05 m/s. Similarly, for the period of 1-year, the maximum wind speed was expected to occur in Antalya and estimated at 39.24 m/s. Comparing the results of 2016 and 2017, there have been no significant differences in estimated extreme wind speeds. As mentioned above, the highest wind speed in 2017 was expected to occur in Antalya, which is estimated at 37.68 m/s for the return period of 1-year, and 47.1 m/s for 50-years.

REFERENCES

- [1] Şahin A. Hourly wind velocity exceedance maps of Turkey. Energy Conversion and Management. 2003;44(4):549-557.
- [2] Stocker TF, Qin D, Plattner GK, Tignor M, Allen SK, Boschung J, Nauels A, Xia Y, Bex V, Midgley PM. Contribution of working group I to the fifth assessment report of the intergovernmental panel on climate change. Climate change. 2013.

- [3] Kunz M, Mohr S, Rauthe M, Lux R, Kottmeier C. Assessment of extreme wind speeds from Regional Climate Models – Part 1: Estimation of return values and their evaluation. *Natural Hazards and Earth System Sciences*. 2010;10(4):907-922.
- [4] McVicar T, Van Niel T, Li L, Roderick M, Rayner D, Ricciardulli L et al. Wind speed climatology and trends for Australia, 1975–2006: Capturing the stilling phenomenon and comparison with near-surface reanalysis output. *Geophysical Research Letters*. 2008;35(20).
- [5] Vagenas C, Anagnostopoulou C, Tolika K. Climatic Study of the Marine Surface Wind Field over the Greek Seas with the Use of a High-Resolution RCM Focusing on Extreme Winds. *Climate*. 2017;5(2):29.
- [6] McInnes K, Macadam I, Hubbert G, O’Grady J. A modelling approach for estimating the frequency of sea level extremes and the impact of climate change in southeast Australia. *Natural Hazards*. 2009;51(1):115-137.
- [7] Pirazzoli P, Tomasin A. Recent near-surface wind changes in the central Mediterranean and Adriatic areas. *International Journal of Climatology*. 2003;23(8):963-973.
- [8] Sohoni V, Gupta S, Nema R. A comparative analysis of wind speed probability distributions for wind power assessment of four sites. *Turkish Journal of Electrical Engineering & Computer Sciences*. 2016; 24:4724-4735.
- [9] Natarajan A, Dimitrov NK, Madsen PH, Berg J, Kelly MC, Larsen GC et al. Demonstration of a Basis for Tall Wind Turbine Design, EUDP Project Final Report. DTU Wind Energy, 2016. 101 p. (DTU Wind Energy E; No. 0108).
- [10] International Electrotechnical Commission. Wind turbines-part 1: design requirements. IEC 614001 Ed. 3. 2006.
- [11] New European Wind Atlas Project (NEWA) [Internet]. <https://www.neweuropeanwindatlas.eu>. [cited 16 January 2021]. Available from: <https://www.neweuropeanwindatlas.eu>
- [12] Ribatet M, Dutang C. POT: generalized pareto distribution and peaks over threshold. R package version. 2009:1-.

NANOCELLULOSE IN ENERGY APPLICATIONS: CURRENT STATUS AND FUTURE PROSPECT

^{1*} Mert Yildirim, ¹ Zeki Candan
¹ Department of Forest Industrial Engineering,
Istanbul University-Cerrahpasa, Istanbul, Turkey

*Corresponding author e-mail: mert.yildirim@ogr.iu.edu.tr

ABSTRACT

With the increasing consumption of fossil fuels and environmental concerns, green energy development and storage technology has become a major topic. Nanocellulose gained tremendous interests in green energy applications due to its renewability, sustainability, biodegradability and environmentally friendly. Furthermore, the excellent physical, mechanical, and optical properties of lignocellulosic biomass originated nanocellulose allow it to be regarded as a substitute material to fulfill the increasing demand for fossil fuels and the environmental crisis. The main objective of this paper is to review the use of nanocellulose materials in energy devices such as supercapacitors, lithium-ion batteries and solar cells.

Keywords: Energy Device, Energy Storage, Nanocellulose, Solar Cell, Supercapacitor

INTRODUCTION

Fossil fuels have long been an important source of energy for fulfilling the increasing global energy needs. However, it has a lot of disadvantages, including pollution and global warming [1]. In the past decade, researchers have researched low-cost and energy-efficient green materials from renewable sources as candidates to replace some traditional materials in the manufacturing of energy devices in limiting negative impacts on the environment [2].

In this context, lignocellulosic biomasses are promising of green, renewable, and sustainable materials. Cellulose is the most ubiquitous and abundant biopolymer on the world. Nanocellulose is a type of cellulose with one dimension in the nanometer range (<100 nm). Nanocellulose materials are subdivided into three categories: cellulose-nanofibrils (CNF), cellulose nanocrystals (CNC) and bacterial nanocellulose (BNC). It can be derived from various of sources, including plants, trees, algae, bacteria, and even some animals. Among many other sustainable nanomaterials, nanocellulose is drawing increasing interest for use in energy due to its attractive properties [3].

This review focuses on the most recent developments in nanocellulose-based materials for energy storage applications.

APPLICATIONS OF NANOCELLULOSE IN ENERGY APPLICATIONS

Nanocellulose is used as a component in lithium-ion batteries, supercapacitors, solar cells, photoelectrochemical electrodes, and nanogenerators [4].



Figure 1. A schematic representation showing the use of nanocellulose to energy storage applications [5].

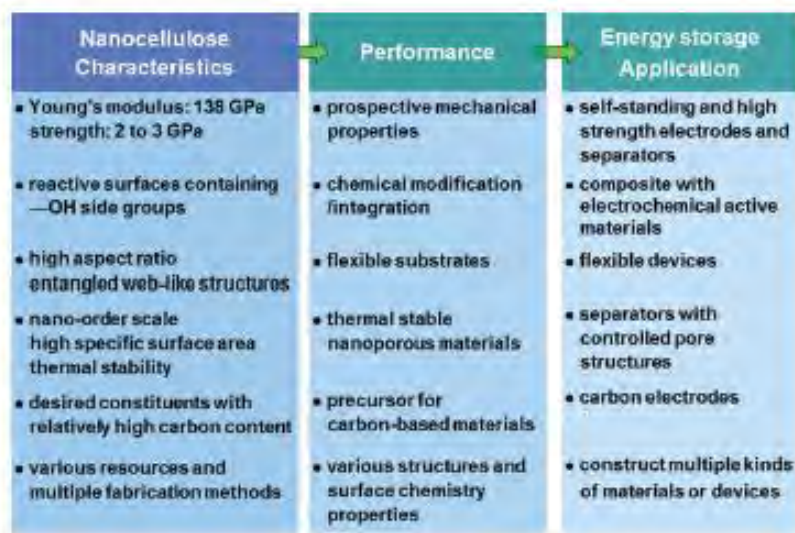


Figure 2. A summary of the properties of nanocellulose for energy storage applications [5].

CONCLUSIONS

The use of nanocellulose as a component in modern energy devices and systems may usher in a new era of material innovation. It has enormous materials application potential in a variety of energy-related areas. According to recent studies, nanocellulose is a potential piezoelectric material. Cellulose nanocrystals have the potential to improve the power conversion efficiency of solar cells. Although nanocellulose has unique properties for energy storage devices, there are several difficulties that must be solved in the future. It is currently difficult to produce nanocellulose on a large scale with high quality. The high manufacturing costs are a cause of concern in the production of nanocellulose. New methods for producing nanocellulose with large-scale production and low cost should emerge.

ACKNOWLEDGMENTS

The authors would like to thank TUBA Turkish Academy of Sciences for its support.

REFERENCES

- [1] Lasrado D, Ahankari S, Kar K. Nanocellulose-based polymer composites for energy applications—A review. *Journal of Applied Polymer Science*, 2020, 137(27):48959.
- [2] Du X, Zhang Z, Liu W, Deng Y. Nanocellulose-based conductive materials and their emerging applications in energy devices - A review. *Nano Energy*, 2017 35:299–320.
- [3] Yildirim M, Candan Z. Performance Properties of Particleboard Panels Modified with Nanocellulose/Boric Acid. *BioResources*, 2021, 16(1):1875-1890.
- [4] Wang X, Yao C, Wang F, Li Z. Cellulose-Based Nanomaterials for Energy Applications. *Small*, 2017, 13(42):1702240.
- [5] Chen W, Yu H, Lee SY, Wei T, Li J, Fan Z. Nanocellulose: a promising nanomaterial for advanced electrochemical energy storage. *Chemical Society Reviews*, 2018, 47(8): 2837–2872.

ANALYSIS OF URBAN SCALE ENERGY CERTIFICATION SYSTEMS FOR EFFICIENT COMMUNITIES

* *María Belén Sosa, Erica Norma Correa, María Alicia Cantón*
¹ *INAHE - CONICET, Ruiz Leal Avenue, Mendoza, Argentina*

*Corresponding author e-mail: msosa@mendoza-conicet.gob.ar

ABSTRACT

Cities have not been planned considering the energy they demand. The environmental crisis has led to center the attention in the energy conservation at building scale. But, the energy efficiency of the city does not depend on the sum of bioclimatic buildings. Being the planning of the urban form necessary to combine the performance of the buildings with the environment. In this frame, the urban certification systems incorporate the valuation of energy efficiency. This work analyzes four systems (BREEAM, LEED®, Green Star, and CASBEE), detects from the set that which in its categories emphasizes the relationship between urban form and energy consumption; and applies it to a set of cases in the study area. Analysis shows that LEED® places greater importance on urban form planning. However, when evaluating the performance between LEED® and the case studies, it is detected that the urban form-energy consumption relationship is not congruent between the certification requirements and the consumption obtained.

Keywords: Urban form, Urban scale certification, Energy efficiency

INTRODUCTION

Cities worldwide will demand 40% more energy resources by 2030 [1]. This projection is preoccupying, since in general terms cities have not been planned considering the energy they consume, or how the increasing cost or scarcity of this resource can affect development [2]. The energy efficiency on building scale is a topic commonly approached by the scientific community with several studies and application cases. However, this trend does not have been reflecting at the urban scale at the same magnitude. In this sense, working on the intermediate scale of the city, neighborhoods or communities, surpasses the analysis of buildings as units and of the city as a whole. This study scale can be a great advantage for sustainability, since it has been shown that actions at the local level tend to generate large-scale repercussions [3, 4].

That is why considering the energy component associated to the urban form is important during the design and planning stages in order to generate energy efficient urbanization's [5]. This consideration is very important to guarantee good standards in the urban form-energy consumption relationship. Previous studies in the Metropolitan Area of Mendoza, Argentina (AMM) show that there are strong correlations between variables of the urban form and the associated energy consumption. There were found optimal design combinations to reduce energy consumption by up to 37% between different alternatives [6]. These results shows that the form of the built environment can increase or decrease the effects of strategies associated with reducing energy consumption and the sustainability of a model urban.

In recent years, new tools have been developed and implemented from different perspectives to certify, under parameters of social, economic and environmental sustainability, the design of new neighborhoods and communities. These systems seek to improve the built environment through developments that value and respect the natural environment, that contribute to improving the quality life of citizens, and reduce the consumption of fossil resources. This is how certification systems, by targeting actions at the local level, can play an important role since having these tools allows urban planners to have a set of measures and parameters from which to implement actions to improve their development. The present work was developed based on three main objectives: (i) analyze the categories considered by the most widely used and implemented urban scale certification systems; (ii) detect the system that considers the urban form-energy consumption relationship within the categories; and (iii) apply this system to a group of cases in the study area (AMM) and verify if the certification system is consistent with the results previously obtained from the urban form-energy consumption relationship.

METHODOLOGY

First, we identified and selected urban scale certification systems. At international level, there are several certification systems that have developed and adapted their version for urban scale: "BREEAM" Communities (United Kingdom), "LEED®" Neighborhood Development (United States), Green Star Communities (Australia), "CASBEE" Urban Development (Japan), "DGNB" Urban Districts (Germany), "HQETM" (France), Pearl Community Rating System (United Arab Emirates). Within this group the most widely used worldwide were analyzed. This condition was determined by counting the number of certifications granted to date for each system in its urban-scale version, taking as a cut-off line those systems with more than ten certifications granted.

The next step was to analyze and contrast the categories considered in the selected certification systems. Each system evaluates the communities by categories, according to a check list that give a final score and the certification level achieved. To know and analyze the categories that make up each system, the official technical manuals were consulted. The categories with the associated credits of each system were systematized in a spreadsheet. With this information, the percentage weight of each category in each system was determined. It is important to clarify that in order to make a fair comparison, the total credits of each system were normalized to 100%, since there are variations between them. The quantitative analysis is presented in the conclusions section.

Finally, the design parameters determined by the selected certification system were applied to three neighborhoods of the AMM where energy performance is known empirically from previous studies [6]. These neighborhoods were monitored micro-climatically during the summer, they were adjusted in the ENVI-met simulation software, and with the output data the estimation of energy consumption was made considering only the performance of outer space for the summer condition. The three neighborhoods analyzed present the typical urban development model of the AMM and respond to three types of patterns -Rectangular, Multiazimutal, Cul-de-Sac-. The urban characteristics are: residential and commercial use, 20 m wide streets forested with 2nd magnitude trees, 3 m wide sidewalks, 3 m high single-family homes with homogeneous designs and materials.

CONCLUSIONS

The four most used urban scale certification systems are: BREEAM, LEED®, Green Star, and CASBEE. LEED® prioritizes the urban form-energy consumption relationship to a greater extent in the “Neighborhood Pattern and Design” category (37% of weight). But this certification system reflects that the energy efficiency prioritizes the rational use of transport, efficiency at the building scale, access to solar resources and the rational use of energy associated with urban infrastructure. And to a lesser extent, the design of the pattern of a community, since it leaves flexibility to the urban planners to define the morphology and orientation of blocks and street widths, without considering the micro-climatic context.

The application of all the requirements of the LEED® “Neighborhood Pattern and Design” to the three AMM neighborhoods shows that there is no direct relationship between the credits achieved and energy consumption estimated. This is because the requirements partially contemplate the variable related to urban form-energy consumption. This consideration is verified by observing the results obtained within the Cul-de-Sac and the Rectangular pattern. Both forms reached the same amount of credits (34.5), although the energy consumption is different (62592 versus 52921 kWh).

These findings addressed that certification systems are a first step to categorize a community. From the point of view of assessing the design of the urban form in relation to energy efficiency, LEED® system only considers partial aspects of a general nature. However, its regional application requires considering variables associated with the implantation site and microclimatic context. As well as specific aspects regarding the urban form that significantly impact energy consumption, in particular related to the urban canyon profile, the configuration of shadows in terms of guaranteeing homogeneous distributions, among others. In future stages we expect to give continuity to this theme in order to make a local contribution associated with the development of a certification system that deepens approaches related to the design of the energy efficient urban form, taking the LEED® system as a methodological reference.

REFERENCES

- [1] IEA, International Energy Agency (2016). Indicadores de Eficiencia Energética: Fundamentos Estadísticos.
- [2] Ko, Y. & Radke, J. (2014). The effect of urban form and residential cooling energy use in Sacramento, California. *Environment and Planning B*, vol. 41, n° 4, pp. 573-593.
- [3] Martínez, K. (2017). Comunidades y barrios sustentables: sistemas de certificación avanzando hacia la sustentabilidad de la escala urbana intermedia. *AUS [Arquitectura / Urbanismo / Sustentabilidad]*, vol. 10, pp. 18-21.
- [4] Middel, A., Häb, K., Brazel, A., Martin, C. & Guhathakurta, S. (2014). Impact of urban form and design on mid-afternoon microclimate in Phoenix Local Climate Zones. *Landscape and Urban Planning*, vol. 122, pp. 16-28.
- [5] Reinhard, J. (2017). Annex 51: Case studies and guidelines for energy efficient communities. *Energy and Buildings*, vol. 154, pp. 529-537.
- [6] Sosa, B., Correa, E. y Cantón, A. (2018). Neighborhood designs for low-density social housing energy efficiency: case study of an arid city in Argentina. *Energy and Buildings*, vol. 168, pp. 137-146.

ASSESSMENT OF THE FLOATING PHOTOVOLTAIC (FPV) SYSTEMS BUILD IN EXTREME WEATHER LOCATIONS AND COMPARISON WITH TERRESTRIAL SYSTEM

^{1*} Mustafa Kemal Kaymak, ² Ahmet Duran Şahin

¹ Istanbul Technical University, Faculty of Aeronautics and Astronautics, Meteorological Engineering Department, Ayazaga Campus, 34469, Maslak, Istanbul, Turkey

*Corresponding author e-mail: kaymak@itu.edu.tr

ABSTRACT

Greenhouse gas (GHG) emissions are primarily due to the exploitation of fossil fuel as an energy source, and one of the energy alternatives for the reduction of emissions is the use of renewable energy sources; one of these is solar irradiation conversion to useable clean energy. In the city of Istanbul, Floating PV (FPV) installation started in 2017, on one of the lakes with an extensive surface area and has extreme weather and wave conditions, Büyükçekmece, which supplies water to the city. To reduce evaporation losses and to generate electricity, two FPV prototypes were installed, with capacities of 90 kWp, 30 kWp. Additionally, near the lake coast a 30 kWp capacity terrestrial system was installed for comparison FPV electricity generation value with this.

FPV power plants are contemporary new alternatives for terrestrial PV's. Generally calm water bodies are preferred for this kind of systems. Because of extreme weather conditions in Büyükçekmece Lake wind driven waves up to 2 meters and this consequently let to an unbalanced load distribution on the system and hgh wave loads cause damage to the systems. One of the two systems called as semi-flexible, performed in the study failed due to the effects of these waves, however, a new designed called as full- flexible FPV survived in these severe conditions.

The total amount of electricity generated of the first 90 kWp FPV system is approximately 17,400 kWh and the capacity factor is around 42% for the 467-hours, between 19.05.2017 and 04.07.2017. As seen in here capacity factor is very high because of summer sunny weather conditions.

The electricity generation by the second system between 21-11-2018 and 22-12-2018 was measured as 309 kWh, while terrestrial PV was measured as 365 kWh and capacity factors are calculated 14.51% and 17.15%, respectively.

The most important result of these studies is in order to remain robust in severe weather conditions with unbalanced load distribution, each unit that forms the system must be single pare, but whole system connections must be flexible. Additionally, it is not easy to say that one of the systems that FPV or terrestrial PV, has great advantages in the perspective of electricity generation based on measured values.

Keywords: Floating Photovoltaic, Solar Energy, Severe Weather Condition, Sustainable Energy

INTRODUCTION

Floating Photovoltaic (FPV) systems are relatively new structures compared to its sister technology terrestrial PV. In the literature, the first FPV studies have started in 2007 with the installation of a 20 kWp with inclination of 1.3° South in the reservoir of a Hydroelectric Dam in Aichi, Japan. Designs and adaptations of FPV are made by taking PVs as an example. These similar designs can work in stagnant waters or regions with low wind speed for short fetch lengths. Previous review researches show that generally, FPV electricity generation systems are built at sheltered areas from the waves[1,2]. Incident wave effects on FPVs and their fixing elements have not been evaluated so far under actual atmospheric conditions. Beside that FPV rapidly growing technology in recent years and reached 1,314 GWp (Fig. 1).

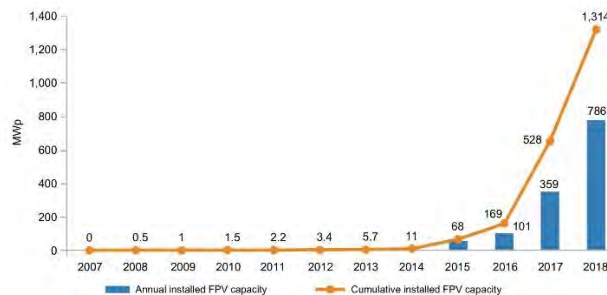


Figure 1. FPV Total installed capacity: World Bank Group, ESMAP and SERIS. 2019.

Since FPV and Floating Breakwater (FB) are similar structures, experiments for FB can also be used for FPV studies to understand response of these power systems under wind driven harsh wave conditions. The results obtained by Loukogeorgaki et al. [3] were found to be the same as the problems such as failure of connectors and failure of mooring lines faced by the authors of this study on the lake. Comparison between FPV and terrestrial PVs electricity generation is realized by Choi [4], who showed that the efficiency of floating is higher than terrestrial system.

MATERIALS AND METHODS

FPVs are generally divided into two types as a pure float and hybrid. Pure type is combined from Poliethilen (PE) pontoon and PV panel, hybrid type is combined from PE pontoon, metal frame and PV panels. However, as mentioned before projected area subjects to strong Northern and Southern winds on the lake surface, which reaches occasionally up 43 m/s. and so that hybrid type FPV is suitable for this location. Installation stage 90 kWp, called as semi-flexible, is given in Figure 2a and 3D drawing and general view of 30 kWp system, called as full flexible, is given in Figure 2b. These hybrid FPV systems are new designed and firstly applied to open sea lake conditions (Figure 2).

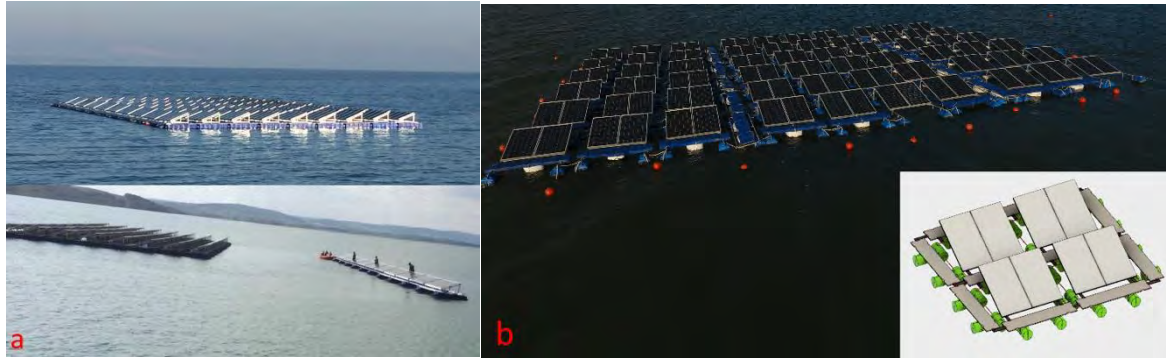


Figure 2. (a) 90kWp FPV System (semi-flexible) (b) 30 kWp FPV System (full-flexible)

The total amount of generated electricity at the same time period is measured as 5211 kWh for terrestrial PV and 5189 kWh for semi-flexible FPV in June 2017. After this time, period, severe weather condition and wind driven harsh wave damaged the first system then removed from lake.

Electricity generation comparison of second one in other words full-flexible FPV and terrestrial PV is given in Table 1. As seen that electricity generation of terrestrial PV is higher than FPV system. This situation could be explained for short time data and winter climate conditions that cause to harsh waves and these outcomes in dynamic fluctuations and as a result of these situations low electricity generation would occur. However terrestrial systems are fixed and there is no wave and wind effect, and these advantages result in higher electricity generation in winter conditions.

Table 1. The electricity generation by the second system between 21-11-2018 and 22-12-2018 (kWh) date.

Type	Mean (kWh)	Standad Deviation	Median (kWh)	Total Electriciy Generation (kWh)	Capaacity factor (%)
Terrastrial PV	5.14	3.55	4.21	365.45	17.15
FPV	4.35	3.44	3.19	309.09	14.51

CONCLUSIONS

Harsh waves cause to some unexpected problems during mooring, installation, maintains and survival of the systems. It is essential for this region to design and produce a wave-resistant system. FPV should be in harmony with the wave and maintains its integrity. Terrestrial PV and FPV systems do not have remarkable differences in the terms of electricity generation for Büyükçekmece Lake conditions. It is experienced that full-flexible hybrid design can be survival like this kind of severe weather condition other design cannot.

REFERENCES

- [1] Sahu A, Yadav N, Sudhakar K. Floating photovoltaic power plant: A review. *Renew Sustain Energy Rev.* 2016 Dec 1; 66:815–24.
- [2] Trapani K, Redón Santafé M. A review of floating photovoltaic installations: 2007-2013: A review of floating photovoltaic installations. *Prog Photovolt Res Appl.* 2015 Apr;23(4):524–32.
- [3] Loukogeorgaki E, Lentsiou EN, Aksel M, Yagci O. Experimental investigation of the hydroelastic and the structural response of a moored pontoon-type modular floating breakwater with flexible connectors. *Coast Eng.* 2017 Mar; 121:240–54.
- [4] Choi YK. A Study on Power Generation Analysis of Floating PV System Considering Environmental Impact. *Int J Softw Eng Its Appl.* 2014 Jan 31;8(1):75–84.

CAPITAL-ENERGY SUBSTITUTION IN TURKISH MANUFACTURING FIRMS: ROLE OF FIRM SIZE

Pınar Sezer

Hacettepe University, Department of Economics, Ankara, Turkey

Corresponding author e-mail: psezer@hacettepe.edu.tr

ABSTRACT

In this study, capital-energy substitutability is analyzed for Turkish manufacturing industry firms between 2005-2013 using firm-level microdata. To this end, translog cost function and cost-share equations are jointly estimated by the iterated seemingly unrelated regressions method. Using the estimated coefficients, Morishima and cross-price elasticities for capital-energy substitution are calculated. Estimations and elasticity calculations are carried out for all the firms and subsamples defined by firm size.

One of the observations of the study is Turkish manufacturing firms are sensitive to increases in energy prices. Moreover, the sensitivity increases as the size of the firm increases. Cross price elasticity, which reflects economic substitution possibilities, shows that a 1% increase in energy prices is associated with a 0.033% increase in capital demand in small firms and %0.038 increase in large firms. So, we can say that the cross-price elasticity of energy prices is not sensitive to firm size. On the other hand, Morishima substitution elasticities, which reflect technological substitution possibilities, show that a 1% rise in energy prices causes 0.916% increase in capital-energy ratio in small firms and 2.392% increase in large firms. As a result, we can say that technological substitution possibilities increases as the size of the firm increase.

Keywords: Energy Prices, Substitution, Morishima Substitution, Panel Micro Data

INTRODUCTION

The nature of the relationship between production factors determines the boundaries of production possibilities within alternative factor combinations. After the 1973 oil crisis, with the inclusion of energy as a production factor to the production function, sustainability & the complementary relation between capital and energy became a focus of interest. In micro and the macro-level relationship between capital and energy has important consequences regarding production process design, energy price shocks, rebound effects, energy, and environmental policies.

To this end, after the first inspirational article, a great number of articles investigated the relationship between energy and capital for several countries and country groups [1]. Although most of the studies share a common structure regarding preference about the functional form of production function/cost function and measure of substitution, we observe that the existing body of research did not reach a common conclusion about the relationship between energy and capital.

Statement of factor substitution as a microeconomic phenomenon gained much support and created a different path in the related literature [2]. As a result, in the past thirty years, the researchers have shown an increased interest in capital end energy substations at the firm level. However, this interest was limited by the access to firm-level data. The first study at the firm level investigated substitution possibilities between capital and energy for the Australasia manufacturing industry using cross-price elasticity and trans long cost function [3]. Following this work, there have been a limited number of studies for developed countries (USA, Denmark, Ireland, Italy, and Switzerland) [4,5,6,7,8].

The purpose of this paper is to contribute to the literature by estimating substitution between capital and energy at the firm level of a developing country, Turkey, for the first time. Previously in many studies, substitution elasticities have been calculated for developing and developed countries at the aggregate industry level, but this is the first study that calculates substitution elasticities for developing countries manufacturing industry at the firm level [9,10]. On the other hand, this study is also important for Turkey because aggregate level substitution estimations are also limited for Turkey. Former aggregate level estimations cover important information about the topic, but they should be updated with a more recent and more proper data set.

MATERIALS AND METHODS

In this study, capital-energy substitution is analyzed for the manufacturing industry firms grouped by firm size using the data acquired between 2005-2013. In order to estimate substitution elasticities, factor expenditures and factor prices are needed. For this purpose, Annual Industry and Service Statistics Micro Data Set (Turkstat), National Energy Tables, domestic producer price index at sector level were used to organize necessary data sets in the study.

Translog cost function and cost-share equations are estimated jointly by iterated seemingly unrelated regression method. Using the estimated coefficients, Morishima and cross-price elasticities for capital-energy substitution are calculated. Substitution elasticities are calculated for all manufacturing firms and also subsamples that were divided by the size of the firms.

CONCLUSION

One of the observations of the study is Turkish manufacturing firms are sensitive to increases in energy prices. Moreover, the sensitivity increases as the size of the firm increases. Cross price elasticity, which reflects economic substitution possibilities, shows that a 1% increase in energy prices is associated with a 0.033% increase in capital demand in small firms and a 0.038% increase in large firms. So, we can say that the cross-price elasticity of energy prices is not sensitive to firm size. On the other hand, Morishima substitution elasticities, which reflect technological substitution possibilities, show that a 1% rise in energy prices causes a 0.916% increase in capital-energy ratio in small firms and a 2.392% increase in large firms. As a result, we can say that technological substitution possibilities increase as the size of the firm increase.

REFERENCES

- [1] Berndt, E. R., & Wood, D. O. (1975). Technology, prices, and the derived demand for energy. *The review of Economics and Statistics*, 259-268.
- [2] Solow, J. L. (1987). The capital-energy complementarity debate revisited. *The American Economic Review*, 605-614.
- [3] Woodland, A. D. (1993). A micro-econometric analysis of the industrial demand for energy in NSW. *The Energy Journal*, 57-89.
- [4] Nguyen, S. V., & Streitwieser, M. L. (1999). Factor substitution in US manufacturing: does plant size matter? *Small Business Economics*, 12(1), 41-57.
- [5] Arnberg, S., & Bjørner, T. B. (2007). Substitution between energy, capital and labour within industrial companies: A micro panel data analysis. *Resource and Energy Economics*, 29(2), 122-136.
- [6] Haller, S. A., & Hyland, M. (2014). Capital–energy substitution: Evidence from a panel of Irish manufacturing firms. *Energy Economics*, 45, 501-510.
- [7] Bardazzi, Rossella, Filippo Oropallo, and Maria Grazia Pazienza. "Do manufacturing firms react to energy prices? Evidence from Italy." *Energy Economics* 49 (2015): 168-181.
- [8] Deininger, S. M., Mohler, L., & Mueller, D. (2018). Factor substitution in Swiss manufacturing: empirical evidence using micro panel data. *Swiss journal of economics and statistics*, 154(1), 6.
- [9] Dahl, C., & Erdogan, M. (2000). Energy and interfactor substitution in Turkey. *Opec Review*, 24(1), 1-22.
- [10] Bölük, G., & Koç, A. A. (2010). Electricity demand of manufacturing sector in Turkey: A translog cost approach. *Energy Economics*, 32(3), 609-615.

Pd-MODIFIED POLYRHODANINE FOR METHANOL ELECTROOXIDATION REACTION

^{1,2*} Ramazan Solmaz, ² Dursun Öztürk

¹Bingöl University, Health Sciences Faculty, Occupational Health and Safety Department, Bingöl 12000, Turkey

² Bingöl University, Renewable Energy Systems Division, Bingöl 12000, Turkey

³ Bingöl University, Engineering and Architecture Faculty, Electrical Engineering Department, Bingöl 12000, Turkey

*Corresponding author e-mail: rsolmaz@bingol.edu.tr; rsolmaz01@gmail.com

ABSTRACT

Conductive polyrhodanine (pRh) was electrochemically prepared on a Pt electrode and then modified with Pd particles for methanol electrooxidation reaction. Its electrochemical activity was tested in 0.5 M H₂SO₄ solution using cyclic voltammetry (CV) and chronoamperometry (CA) techniques. It was found that the pRh films are electroactive for methanol electrooxidation reaction. Modifying the surface of pRh with small amount of Pd enhances its activity. Moreover, the activity of the Pd-modified thin film was better than that of the Pt bulk electrode. The enhanced activity was related to the enlarged real surface area, synergistic effect between the conductive polymer and the Pd particles as well as high intrinsic activity of Pd for this reaction.

Keywords: Polyrhodanine, Pd-modified films, electrocatalysts, cathode, water electrolysis

INTRODUCTION

Direct methanol fuel cells (DMFCs) are one of the most promising energy converters of the future. However, their use in practical applications has not yet become widespread due to some important problems such as the slow anode and cathode kinetics not being at the desired level, the loss of effectiveness of the catalytic electrodes over operation time or the poisoning of anode by adsorption of intermediates [1]. The studies have been performed to improve better electrodes to overcome these disadvantages. The researchers have generally been focused on metallic electrocatalysts for this aim. Although, Pt has better initial activity for the electrooxidation of methanol this metal undergo deactivation due to poisoning by adsorption of intermediates such as carbon monoxide [2]. Also, this metal has limited sources on the earth and expensive. Some researchers suggested Pd for replacement for Pt in fabricating anode of the fuel cell due to relatively higher abundance and lower price [3]. However, there has still not been a solution to these drawbacks. Ni, Cu and some other metallic electrodes provide promising results for these metals. Unfortunately, many of them corrodes in the cell conditions especially numbers of metals are limited in acidic media. On the other hand, organic films provide enhanced corrosion protection ability. But organic films have been barely studied for this aim due to their stability in alkaline or acidic medium or their low activity as pure form. We have recently suggested self-assembled monolayer films of rhodanine for fabricating substrate for this process and reported promising results [4]. In this study, we have proposed polyrhodanine, which is a conductive polymer, as a novel substrate for preparing noble metal-based electrode. Metal particles can be distributed homogeneously over this film and results with high stability. For this aim, we deposited Pd particles over the pRh thin film to obtain an effective anode material for DMFCs. Some electrochemical techniques were used to test performance of the Pd-modified pRh composite thin coatings.

MATERIALS AND METHODS

The pRh films were electrochemically synthesised on a Pt electrode (10mmx10mmx1mm) from 0.01 M monomer containing 0.3 M ammonium oxalate solution using cyclic voltammetry technique by cycling the potential between 0.00 V and 1.40 V at a scan rate 100 mV s⁻¹. A Pt electrode and Ag/Ag/AgCl (1 M KCl) were used as counter and reference electrodes, respectively. Totally 200 segments were applied to the system. The details were given elsewhere [5].

1 mg cm⁻² Pd was deposited over the pRh surface from 5 mg PdCl₂ containing 0.1 M HCl solution as conductive electrolyte by applying 10 mA cathodic current for 363 s (Pt/pRh-Pd). Before the tests, -50 mA cathodic current was applied to the electrolysis system to clean and activate the surface as well as obtain a stable surface.

The modified surfaces were characterized by surface characterization and electrochemical techniques. Methanol electrochemical activity of the electrodes was investigated in 0.5 M H₂SO₄ solution in the absence and presence of 1.0 M CH₃OH using various electrochemical techniques. The temperature of solutions was thermostatically controlled at 298 K.

RESULTS AND DISCUSSIONS

CVs of the Pd-modified pRh electrode obtained in 0.5 M H₂SO₄ solution are shown on Figure 1a. For comparison, the same curves of Pt/pRh and the bulk Pt electrodes are comparatively given on the same figure. Apparently, the pRh films are active for the methanol electrooxidation reaction. On the other hand, modifying surface of the polymer

with small amount of Pd enhances its activity for this process. Moreover, the Pd-modified electrode has better activity for that of the bulk Pt electrode. The enhanced activity can be explained by enlarged surface area and possible synergism between the metal particles and the conductive polymer. The data provided on Figure 1b clearly show that the Pd-modified electrode has higher time-stability for the electrooxidation reaction.

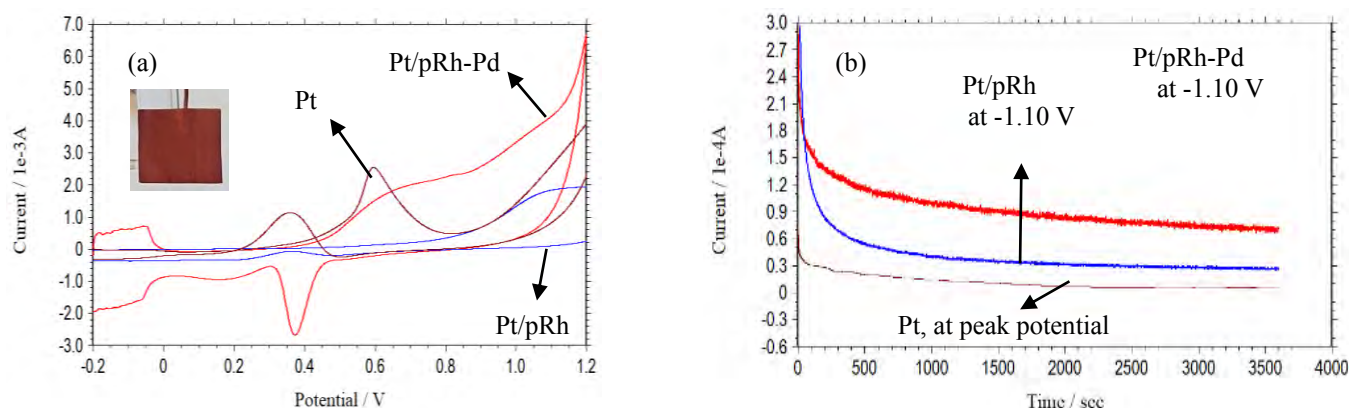


Figure 1. Cyclic voltammograms (a) and chronoamperometry curves (b) of the electrodes obtained in 0.5 M H_2SO_4 solution (Scan rate: 100 mV^{-1} , the potentials applied for chronoamperometric curves are provided on the figure)

CONCLUSIONS

Conductive polyrhodanine (pRh) was electrochemically prepared on a Pt sample and then modified with Pd particles for the methanol electrooxidation reaction. The thin metal-organic composite film was tested as possible anode material for DMFs in acidic solution. Very homogenous polymer films were prepared over the Pt surface and the Pd particles were almost homogeneously distributed over the film. It was found that modifying the surface of pRh with small amount of Pd enhances its activity. Moreover, the activity of the Pd-modified thin film was better than that of the Pt bulk electrode. The enhanced activity was related to the enlarged real surface area, synergistic effect between the conductive polymer and the Pd particles as well as high intrinsic activity of Pd for this reaction.

ACKNOWLEDGEMENTS

The author is greatly thankful to Bingöl University, Health Sciences Faculty, Occupational Health and Safety Department and Bingöl University Central Laboratory for characterization measurements.

REFERENCES

- [1] Yang X, Liu X, Meng X, Wang X, Li G, Shu C, Jiang Li, Wang C. Self-assembly of highly dispersed Pt and PtRu nanoparticles on perylene diimide derivatives functionalized carbon nanotubes as enhanced catalysts for methanol electro-oxidation, *J Power Sources* 2013; 240:536 – 543
- [2] Huang Y, Cai J, Zheng S, Guo Y, Fabrication of a high-performance Pb–PtCu/CNT catalyst for methanol electro-oxidation, *J Power Sources* 2012;21: 81 – 85
- [3] Qiu C, Shang R, Xie Y., Bu Y., Li C., Ma H., Electrocatalytic activity of bimetallic Pd–Ni thin films towards the oxidation of methanol and ethanol, *Mater Chem Phys* 2010;120: 323–330.
- [4] Salcı A, EA Şahin, R Solmaz, Methanol electrooxidation at nickel-modified rhodanine self assembled monolayer films: A new class of multilayer electrocatalyst, *International Journal of Hydrogen Energy* 2019; 44: 14228-14234.
- [5] Kardaş G, Solmaz R, Electrochemical synthesis and characterization of a new conducting polymer: Polyrhodanine. *Applied Surf Sci* 2007; 253: 3402–3407.

DETECTION OF TEMPERATURE ELEVATIONS IN ENCASED SMARTPHONES DUE TO MULTITASK PROCESSES

¹ Chibuzor Ndubisi, ^{2*} Howard Njoku

¹ Applied Renewable and Sustainable Energy Research Group, Department of Mechanical Engineering, University of Nigeria, Nsukka 410001, Nigeria. Email: chibuzor.ndubisi.197845@unn.edu.ng

² Applied Renewable and Sustainable Energy Research Group, Department of Mechanical Engineering, University of Nigeria, Nsukka 410001, Nigeria.

*Corresponding author e-mail: howard.njoku@unn.edu.ng

ABSTRACT

The ability of smartphones to perform multiple tasks has grown with technological advancements in software, design, and materials. But the capability of these devices is still being limited by their thermal management abilities. With an intent to deepen understanding of this problem, this work examines the temperature changes in encased smartphones while they perform more than one task simultaneously. The thermal profiles of the phone surfaces were obtained using an infrared camera, and the phones' inbuilt thermal sensors were used in ascertaining their battery and processor temperatures. To properly understand the effect of the number of tasks on phone temperature and performance, a single-task set, double-task set, and triple-task set of experiments were conducted. Results revealed that there is a positive correlation between the number of tasks being run and the increase in the phones' internal and surface temperatures. However, the test (i. e. encased) phone exhibited greater temperatures, mainly due to the insulating property of the case material.

Keywords: Heat, multitasking, phone case, smartphone, temperature.

INTRODUCTION

Smartphones have indeed become a notable feature of human life in the 21st century. From Xiaomi's Redmi Note 9 to Apple's iPhone 11, these technological marvels have thrived because of their ever-improving features and unrivalled usability. However, the design considerations that make the smartphone a 'handheld computer' have come at the cost of other engineering considerations. Chief among these are heat generation and dissipation, both of which are responsible for a large fraction of smartphone failures [1].

The major sources of heat within a smartphone are the battery and the components mounted on the circuit board—which include transistors, resistors, and integrated circuits. Heat is generated through their resistance to electric current when the phone is in use, and this heat travels to the smartphone surfaces via "cooling paths" [2]. With extra heat being generated by the battery due to entropy change [3], it becomes increasingly difficult to maintain a safe range of temperature for these internal components while keeping the phone surface temperature below the 45°C threshold [4] and preventing excessive, dangerous exposure to the infrared radiation [5].

Among other responses to this problem, Grimes et al. [6] integrated a fan into a mobile phone and achieved up to 60% increase in heat dissipation—an active cooling solution that would reduce phone portability. Gurrum et al. [7] successfully used 'gap filler pads' made of a silicone-ceramic mixture to establish contact between surfaces originally not in contact and accelerate heat transfer by conduction. And Tomizawa et al. [8] found that phase change materials, materials that absorb heat at constant temperature but change phase due to their latent heat of fusion, would be highly instrumental in thermal management.

All of these attempts point to an improvement in smartphone internal design. But it should also be remembered that smartphones generate heat due to the tasks run by their users. It is quite common nowadays to find smartphone users running many applications simultaneously, applications which have varying demands and levels of impact. Thus, this study focuses on this user-based facet of heat generation. Additionally, because phone cases have become a prominent accessory to smartphones, their impact on smartphone thermal behaviour shall also be investigated. Specifically, this study aims to evaluate the effect of multitasking (that is, running more than one app) on the thermal response from a mobile device while encased in a plastic smartphone case.

EXPERIMENTATION, RESULTS, AND DISCUSSIONS

The tests were conducted in a wooden cuboid-shaped chamber. The chamber had five of its inner surfaces lined with aluminium foil to prevent heat exchange with the external environment, while the sixth surface was made of glass. Two identical smartphones were placed adjacently in the box, one encased in a plastic case (test phone) and the other not encased (control phone). To adequately compare the effects of the number of apps being run, three sets of tests were executed: the single-task set, the double-task set, and the triple-task set. Each test lasted for 30 minutes, with the *Seek Compact* infrared camera being used to take thermal images (or thermograms) of the phones at the beginning and end of the tests. Additionally, the phones' inbuilt thermal sensors were used to obtain their

battery and processor temperatures. To reduce errors and improve accuracy, all background tasks were disabled on both smartphones, and their batteries were fully charged before each test.

A survey was conducted to determine the most frequently used apps by people in the local community. Consequently, the experiment involved the following tasks and corresponding applications: offline music playing (Muzio Player) for the single-task set; offline music playing (Muzio Player) & social media (Instagram) for the double-task set; and social media (Instagram), internet browsing (Google Chrome), & video streaming (YouTube) for the triple-task set.

Fig. 2 shows the thermograms obtained from the tests. In each case, the test phone is on the left while the control phone is on the right. The thermal images reveal an increase in heat zones after every experiment, with the largest increase being observed in the triple-task set. Especially in the double and triple-task sets, there is a clear difference between the thermograms of test and control phones.

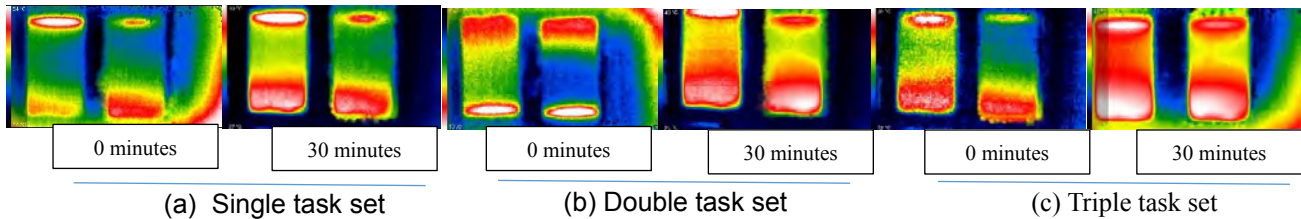


Figure 1. Thermograms of smartphones before and after running tasks.

Similarly, Fig.23 illustrates the changes in temperature for the processors and batteries of test and control phones. The test processor reached the highest temperature in all cases, passing 60°C during the triple-task set. Additionally, this test processor temperature did not increase in a linear fashion but surged up in the first three minutes and gradually increased to the maximum temperature.

CONCLUSION

The thermograms and graphs show that there is a positive relationship between the number of tasks being run and the smartphone temperature. And the encased phone exhibited higher temperatures than the non-encased phone in all cases, proving that the plastic casing inhibits heat dissipation at the detriment of the smartphone. Besides focusing on improvements in smartphone internal design, further research could seek to develop new casing materials that balance heat dissipation with optimal user experience.

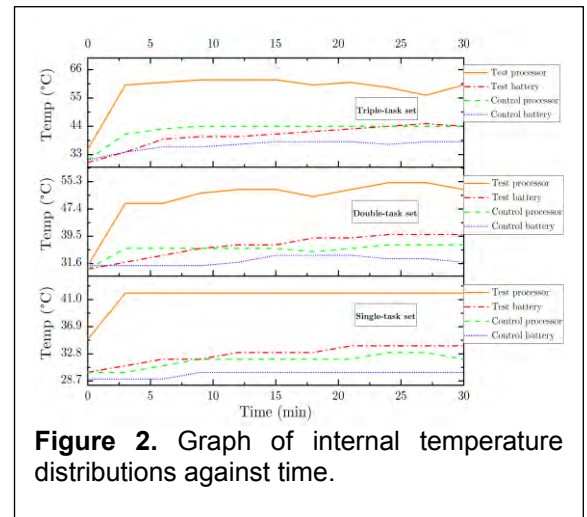


Figure 2. Graph of internal temperature distributions against time.

REFERENCES

- [1] McPherson JW. Reliability Physics and Engineering. Springer; 2005.
- [2] Luo Z, Cho H, Luo X, Cho K-i. System thermal analysis for mobile phone. Applied Thermal Engineering, 2008; 28(14-15):1889-95.
- [3] Xie Q, Kim J, Wang Y, Shin D, Chang N, Pedram M. Dynamic thermal management in mobile devices considering the thermal coupling between battery and application processor. In IEEE/ACM International Conference on Computer-Aided Design, Digest of Technical Papers, 2013; 242-7.
- [4] Berhe MK. Ergonomic temperature limits for handheld electronic devices. In ASME 2007 InterPACK Conference collocated with the ASME/JSME 2007 Thermal Engineering Heat Transfer Summer Conference, 2007: 1041-7.
- [5] International Commission on Non-Ionizing Radiation Protection. ICNIRP guidelines on limits of exposure to incoherent visible and infrared radiation. Health Physics, 2013; 105(1):74-96.
- [6] Grimes J, Walsh E, Walsh P. Active cooling of a mobile phone handset. Applied Thermal Engineering, 2010; 30(16):2363-9.
- [7] Gurrum SP, Edwards DR, Marchand-Golder T, Akiyama J, Yokoya S, Drouard J-F, Dahan F. Generic thermal analysis for phone and tablet systems. In 2012 IEEE 62nd Electronic Components and Technology Conference, 2012; 1488-92.
- [8] Tomizawa Y, Sasaki K, Kuroda A, Takeda R, Kaito Y. Experimental and numerical study on phase change material (PCM) for thermal management of mobile devices. Applied Thermal Engineering, 2016; 98:320-9.

INVESTIGATION OF LSTM FOR ENERGY DEMAND RESPONSE APPLICATIONS

¹ Merve GULER, ^{1,2*} Derya Betül UNSAL

¹Sivas Cumhuriyet University, Graduate Institute of Science, Department of Energy and Technology Engineering, Sivas, Turkey

² ¹Sivas Cumhuriyet University, Renewable Energy Research Center, Sivas, Turkey

*Corresponding author e-mail: dbunsal@cumhuriyet.edu.tr

ABSTRACT

Today, increasing energy demand in parallel with the increasing population and developing technology emerges as an important component of energy production planning and smart grids. The load estimation method chosen has a critical importance in energy production so that stability cannot be mentioned in a network structure where the supply-demand balance cannot be achieved, and the network balance can be provided. In this study, different load estimation methods based on machine learning are examined according to their advantages and disadvantages for short-term, long-term and medium-term forecasts. In order for the methods to be superior to each other, the missing points were specified, and when examined from many different points, attention was drawn to the superiority of LSTM's energy production estimation.

Keywords: Energy Demand, LSTM, Smart Grid

INTRODUCTION

In recent, machine learning-based forecasting methods are used in many areas such as weather, stock market, econometric forecasts, energy production and consumption forecasting. Despite the latest technological developments, the inadequacy of storage solutions for electrical energy has made it necessary to consume the energy as soon as it is produced and to provide the supply-demand balance in real time. This balancing has become a very important issue as it will provide great convenience for the economy of the countries in the interconnected network. In addition, energy saving has gained great importance in order to minimize environmental factors and foreign dependency. Therefore, any problem that may occur in the electricity market, Energy markets need supply-demand estimation methods applied by making arrangements in electricity transmission distribution systems in order to prevent them before they occur. In the literature, among the various electrical estimation methods developed in recent years, the most preferred methods have been selected and examined. In the studies examined, it has been observed that the estimation methods generally include the estimation of residential load in smart grids and the estimation of the electricity load provided to the grid by solar and wind from renewable energy sources. The literature studies examined in this context are discussed under two headings, namely, load estimation in Buildings and Renewable Energy sources. Among the various electricity estimation methods developed in recent years, the most preferred methods have been selected and examined. In the studies examined, it has been observed that the estimation methods generally include the estimation of residential load in smart grids and the estimation of the electricity load provided to the grid by solar and wind from renewable energy sources. The literature studies examined in this context are discussed under two headings: load estimation in Buildings and Renewable Energy sources. Among the various electricity estimation methods developed in recent years, the most preferred methods have been selected and examined. In the studies examined, it has been observed that the estimation methods generally include the estimation of residential load in smart grids and the estimation of the electricity load provided to the grid by solar and wind from renewable energy sources. The literature studies examined in this context are discussed under two headings, namely, load estimation in Buildings and Renewable Energy.

ANALYSIS OF METHODS

Based on the literature studies, a brief review and comparison of the most used prediction methods, deep learning method (CNN, LSTM), Support Vector Machines (SVM), Time Series Analysis (ARIMA) methods, are describes in this section.

For buildings, ARIMA and decomposition models were measured with the energy consumption of 100 commercial buildings every 5 minutes using AMI that allow energy companies to improve their energy management [1]. Designing the long, short-term memory (LSTM) model according to the rolling window method to estimate the energy consumption of a university as a deep learning framework and the model would perform better with the size of the data set [2]. A new deep learning model IoT-based system for load estimation aimed to increase the prediction sensitivity significantly with daily consumption forecast network (DCEN) and intraday load forecast network (ILFN) for use in regions with various climates and has valid efficiency [3]. A two-stage infrequent cyberattack model for smart grids proposed and developed an improvement defense mechanism based on time interval prediction in [4].

For renewables, new probability distribution model based on wind energy prediction error statistics is proposed to wind farm in Shandong provinces with Gauss function and Lagrangian multipliers to large-scale systems in [5]. Another new

short-term load prediction based on LSTM, different from existing wind energy estimation methods, is provided the layer training of the prediction system deep belief network (DBN) with a limited Boltzmann machine (RBM) [6]. Synthetic wind flow produced by Large Eddy Simulation (LES) was used as input, and hard parameter sharing imprinted on the turbine blade with multitasking learning (MTL) in [7]. Convolution Integral Based Multivariate Gray Model forecasting methods are investigated in [8]. For the PV system output power estimation, a deep neural network model called PVPNET and proposed model which based on LSTM is tested and the LSTM and Random Forest (RF) obtained better results than the other two systems [9].

Deep learning, which is one of the learning techniques developed with machine learning, is a product of rapidly developing technology. Deep learning is an important competitive in complex predictions, with strong learning ability, which can extract features from various training data [10]. Unlike a single neural network layer, LSTMs have four different layers. CNNs are a neural network similar to ordinary neural networks and are a learning algorithm that takes place in the input image, assigns various directions to various objects in the image and can differentiate and separate them from each other. For the LSTM network structure, the calculation formula for each LSTM unit is as follows with f_t input threshold i_t the previous cell status, \hat{C}_t cell status, C_t output threshold o_t and g_t current cell output [11] ;

$$f_t = \sigma(W_f \cdot [g_{t-1}, x_t]) + b_f \quad (1)$$

$$i_t = \sigma(W_i \cdot [g_{t-1}, x_t]) + b_i \quad (2)$$

$$\hat{C}_t = \tan h(W_C \cdot [g_{t-1}, x_t]) + b_C \quad (3)$$

$$C_t = f_t * C_{t-1} + i_t * \hat{C}_t \quad (4)$$

$$o_t = \sigma(W_o \cdot [g_{t-1}, x_t]) + b_o \quad (5)$$

$$g_t = o_t * \tan h(C_t) \quad (6)$$

Support vector machines (SVM) have come today as the preferred method for classification tasks. It is generally used on statistical learning theory and has been developed to minimize classification error. While using the SVM method in energy estimations; The proposed training model is applied to the data set. The reference vector of each training data is created and the desired day's load estimation is tried to be made with the past forecast data [12]. In SVM, the output values are trained to learn with known and current input values which serves to generate the output of future. When training an SVM model, the parameters to be selected for a good performance value are very important.

Time series is a set of sequential measurements over time of any quantity of interest and is frequently used in estimation methods. It includes several methods such as Autoregressive Integrated Moving Average (ARIMA) is basically a model consisting of autoregressive process (AR), regression (I) and moving average (MA) [12].

While ANN, SVM and time series analyzes can be preferred for very short-term forecasts, it is observed that in short-term forecasts, time series analyzes give good results up to weekly predictions, and SVM and ANN models perform well for hourly observations in medium-term forecasts. In long-term forecasts, SVM is preferred for analysis of annual estimates, while a significant decrease is observed in the bottom-up preference [13-15]. Overall, the LSTM architecture was able to classify a large percentage of cases correctly. As a result, it can be said that LSTM meets the estimation need to a great extent. Many estimation methods have been examined in literature studies and estimation variables; Accuracy analysis of many value estimation methods such as electricity price, temperature, time or income has resulted in different output results in [16].

CONCLUSIONS

In order to determine which model performs best when examined from various perspectives and randomly, the most cited scientific studies on deep learning in the literature between 2017 and 2020 and the estimation methods they used were examined and compared. Since there are many factors affecting the performance of each study, direct comparison was not made, and an average result was tried to be obtained. Although different comparisons were made, it was seen that the LSTM method obtained more efficient, faster and more accurate results in all of the results. In this context, it has been concluded that LSTM can be preferred as a more effective method for load estimation in buildings and estimation of energy to be given to the grid in renewable energy sources, especially solar and wind applications.

REFERENCES

- [1] R. Mohammad, "AMI Smart Meter Big Data Analytics for Time Series of Electricity Consumption," Proc. - 17th IEEE Int. Conf. Trust. Secur. Priv. Comput. Commun. 12th IEEE Int. Conf. Big Data Sci. Eng. Trust. 2018, pp. 1771-1776, 2018.
- [2] S. Aparna, "Long Short-Term Memory and Rolling Window Technique for Modeling Power Demand Prediction," Proc. 2nd Int. Conf. Intell. Comput. Control Syst. ICICCS 2018, no. Iccics, pp. 1675-1678, 2019.

- [3] L. Li, K. Ota, and M. Dong, "When Weather Matters: IoT-Based Electrical Load Forecasting for Smart Grid," *IEEE Commun. Mag.*, vol. 55, no. 10, pp. 46–51, 2017.
- [4] H. Wang et al., "Deep Learning-Based Interval State Estimation of AC Smart Grids Against Sparse Cyber Attacks," *IEEE Trans. Ind. Informatics*, vol. 14, no. 11, pp. 4766–4778, 2018.
- [5] P. Yang, L. Zhao, and Z. Li, "A practical method of unit commitment considering wind power," *Proc. 2010 World Non-Grid-Connected Wind Power Energy Conf. WNWEC 2010*, pp. 84–90, 2010.
- [6] S. Wang, Y. Sun, S. Zhai, D. Hou, P. Wang, and X. Wu, "Ultra-short-term wind power forecasting based on deep belief network," *Chinese Control Conf. CCC*, vol. 2019-July, pp. 7479–7483, 2019.
- [7] S. Woo, J. Park, and J. Park, "Predicting Wind Turbine Power and Load Outputs by Multi-task Convolutional LSTM Model," *IEEE Power Energy Soc. Gen. Meet.*, vol. 2018-Augus, pp. 1–5, 2018.
- [8] D. I. Jurj, D. D. Micu, and A. Muresan, "Overview of Electrical Energy Forecasting Methods and Models in Renewable Energy," *EPE 2018 - Proc. 2018 10th Int. Conf. Expo. Electr. Power Eng.*, pp. 87–90, 2018.
- [9] C. J. Huang and P. H. Kuo, "Multiple-Input Deep Convolutional Neural Network Model for Short-Term Photovoltaic Power Forecasting," *IEEE Access*, vol. 7, pp. 74822–74834, 2019.
- [10] J. Zhu, Z. Yang, Y. Chang, Y. Guo, K. Zhu, and J. Zhang, "A novel LSTM based deep learning approach for multi-time scale electric vehicles charging load prediction," *2019 IEEE Innov. Smart Grid Technol. - Asia (ISGT Asia)*, pp. 3531–3536, 1998.
- [11] R. Zazo, A. Lozano-Diez, J. Gonzalez-Dominguez, D. T. Toledano, and J. Gonzalez-Rodriguez, "Language identification in short utterances using long short-term memory (LSTM) recurrent neural networks," *PLoS One*, vol. 11, no. 1, 2016.
- [12] Y. Chen and K. Wang, "Prediction of Satellite Time Series Data Based on Long Short-Term Memory- Autoregressive Integrated Moving Average Model (LSTM-ARIMA)," *2019 IEEE 4th Int. Conf. Signal Image Process.*, pp. 308–312, 2019.
- [13] I. Kollia and S. Kollias, "A Deep Learning Approach for Load Demand Forecasting of Power Systems," *Proc. 2018 IEEE Symp. Ser. Comput. Intell. SSCI 2018*, pp. 912–919, 2019.
- [14] J. Wu, "Introduction to convolutional neural networks," *Natl. Key Lab Nov. Softw. Technol.*, pp. 1–31, 2017.
- [15] R. Jiao, X. Huang, X. Ma, L. Han, and W. Tian, "A Model Combining Stacked Auto Encoder and Back Propagation Algorithm for Short-Term Wind Power Forecasting," *IEEE Access*, vol. 6, pp. 17851–17858, 2018.
- [16] C. Kuster, Y. Rezgui, and M. Mourshed, "Electrical load forecasting models: a critical systematic review.," *Sustain. Cities Soc.*, 2017.

A SMART MONITORING AND PROTECTION SYSTEM DESIGN USING VISIBLE LIGHT COMMUNICATION FOR GRID INTEGRATION OF MICROGRIDS

¹Murat Das, ²Mehmet Sonmez, ^{1*}Gökay Bayrak

¹ Bursa Technical University, Smart Grid Laboratory, Department of Electrical and Electronics Engineering, 16300, Bursa, Turkey

² Osmaniye Korkut Ata University, Department of Electrical and Electronics Engineering, Osmaniye 80010, Turkey

*Corresponding author e-mail: gokay.bayrak@btu.edu.tr

ABSTRACT

In this paper, we propose a smart transmission protocol to monitor the voltage and frequency data of a microgrid system. Additionally, developed transmission protocol protects the systems against voltage and frequency fault conditions according to the grid code requirements of a microgrid defined in IEEE 929-2000. The grid code protection requirements include Over Voltage Protection (OVP), Under Voltage Protection (UVP), Over Frequency Protection (OFP), and Under Frequency Protection (UFP). Visible Light Communication (VLC), which is a wireless optical communication system, is used to transmit data from transmitter to receiver. An 8-IPPM data mapping method is improved to transmit fault conditions, voltage, and frequency values. Additionally, transmitter and receiver are implemented on a Field Programmable Gate Arrays (FPGA) board. First, the transceiver system is designed on the FPGA compiler. Afterward, it is observed that the simulation results for the proposed transmission protocol by using Modelsim Altera. In the last stage, the transceiver is implemented on the LabVIEW FPGA board to monitor and protect the grid system. The proposed VLC-based method prevents switching and data losses encountered in standard protection relays. Thus, it can be easily implemented for smart grids in practice, especially for innovative monitoring and protection methods required for microgrids.

Keywords: Visible Light Communication; 8-IPPM; Smart Grid; Power System Protection; Microgrid

INTRODUCTION

The Visible Light Communication (VLC) is a promising technology for Wireless Optical Communication Systems [1]. Compared with Radio Frequency (RF) communication, the VLC systems cannot affect from electromagnetic interference. Thanks to this characteristic, the VLC systems are very appropriate for Electrical Substations and electrical generating systems where include intense electromagnetic radiation.

An FPGA-based communication system was used to transmit the generated signal to the receiver. The BPSK (Binary Phase Shift Keying) technique is implemented on FPGA board [2]. In [3], a protection against cyber-attacks, which is used to monitor the IPFIX system, is improved for the smart grid. It is aimed to provide both security and monitoring in the paper. Another paper focuses on a communication infrastructure for Low Voltage (LV) grids by considering the state estimation since the Distribution System State Estimation (DSSE) has been considerable attention from many researchers [6]. In the paper, the idle times that are allocated by Smart Meters (SMs) are used to provide the monitoring of distribution systems. In recent decades, wireless sensor networks have been implemented on many applications due to its low power consumption. The power systems also consist of sensor devices; hence, references [4] carried out the communication connection among the power systems devices by using wireless sensor networks. The wireless network systems such as Zigbee and 802.11g are very useful for monitoring and transmission of data. Hence, some studies use wireless system standards to monitor both PV systems and smart grid [5].

In this paper, we improve a smart communication substructure for microgrid systems by using the VLC system instead of RF and Power line communication systems. The main contributions of this paper are summarized as follows

- We propose a VLC transceiver system that uses 8-IPPM technique to provide the data transmission. We describe a data mapping method for fault conditions, voltage, and current amplitudes.
- In our scenario, the fault detection is carried out at the transmitter side. The type of fault is transmitted to the receiver by using a data packet, which consists of eight bits. Four fault conditions, which are defined in IEEE 929-2000 [25] as OVP, UVP, OFP, and UFP, are registered a packet by using an improved fault coding method. Four code streams are generated to define the type of fault.
- We designed all monitoring system using our communication system instead of wireless system standards. This case provides flexibility to update the communication substructure for future grid systems.

PROPOSED METHOD

In this study, we propose a data transmission process with 8-IPPM technique. We select the 8-IPPM signal since the filled slot number is 7. Moreover, the technique can simultaneously transmit the data of three signals to the receiver side as one symbol of the 8-IPPM signal consists of three bits. The bit number is expressed by n if $2n$ denotes M

modulation order. The modulation order is 8 for the 8-IPPM technique so, the n is 3. Fig. 1 shows the general schematic of the proposed method.

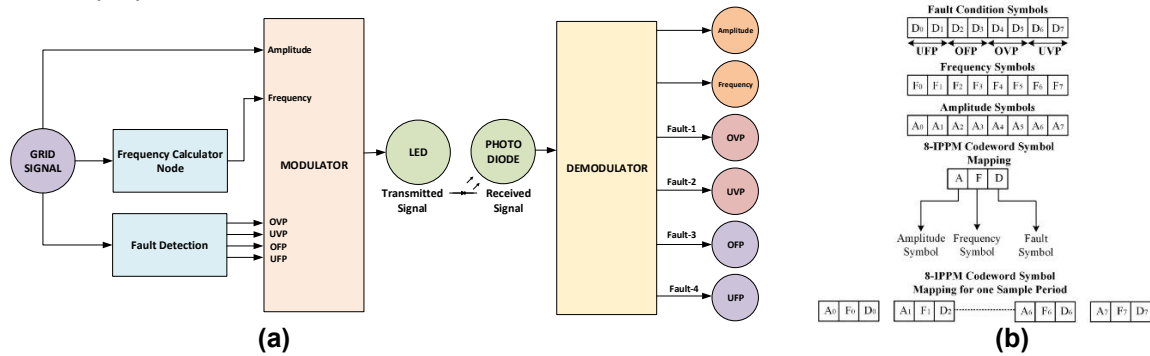


Figure 1. a) Proposed Data Transmission Process, b) Data Mapping for Fault Condition, Amplitude, and Frequency for Visible Light Communication

CONCLUSIONS

In this study, grid voltage and frequency data were obtained in real-time by VLC using the LabVIEW software interface developed based on FPGA. The voltage and frequency data obtained was experimentally performed with the modulator/demodulator designed based on VLC. A VLC transceiver system that uses 8-IPPM technique is presented to provide the data transmission. In the proposed method, fault detection is carried out at the transmitter side. The type of fault is transmitted to the receiver by using a data packet, which consists of eight bits. Four fault conditions, which are defined in IEEE 929-2000 as OVP, UVP, OFP, and UFP, are registered a packet by using an improved fault coding method. Four code streams are generated to define the type of fault. An innovative method that enables communication over light, which prevents switching and data losses, has been developed. Fig. 2 shows the developed VLC system for monitoring and detecting faults in a microgrid.

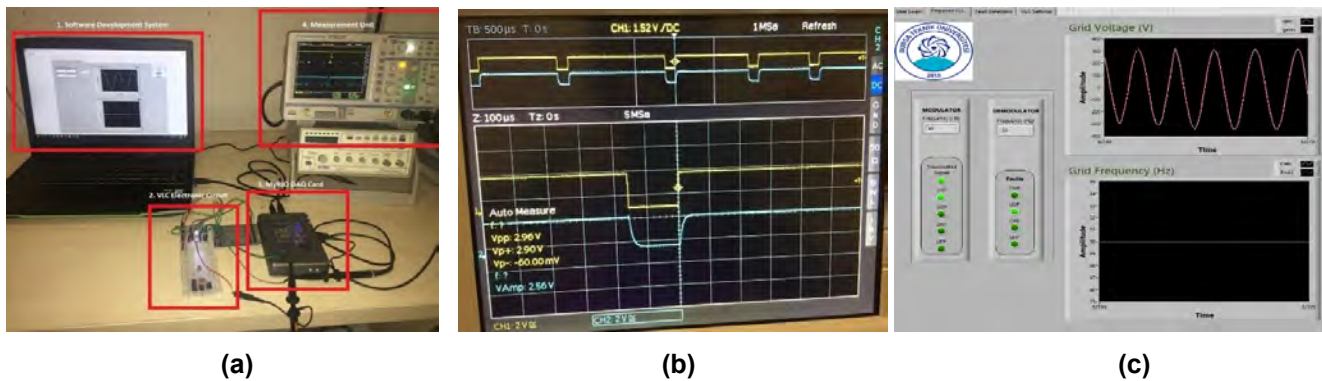


Figure 2. Developed VLC system for monitoring. a) Experimental setup for proposed monitoring system, b) The transmitted (Yellow line) and received (Blue line) signals, c) Under voltage protection condition

REFERENCES

- [1] T. Wang, F. Yang, J. Song, ve Z. Han, (2020). Dimming Techniques of Visible Light Communications for Human-Centric Illumination Networks: State-of-the-Art, Challenges, and Trends. *IEEE Wireless Communications*, 27(4), 88-95. doi: 10.1109/MWC.001.1900388.
- [2] J. E. Gancarz, H. Elgala, ve T. D. C. Little, (2015). Overlapping PPM for band-limited visible light communication and dimming. *J Sol State Light*, 2 (1), no. 3, May. 2015, doi: 10.1186/s40539-015-0022-0.
- [3] Bayrak, G., Yılmaz, A. (2021). Detection and Classification of Power Quality Disturbances in Smart Grids Using Artificial Intelligence Methods. In *Artificial Intelligence (AI)* (pp. 149-170). CRC Press.
- [4] Y. Yuan et al. (2017). SVM-based detection in visible light communications. *Optik*, 151, 55-64. doi: 10.1016/j.jilleo.2017.08.089.
- [5] M. Sönmez, (2020). Artificial neural network-based threshold detection for OOK-VLC Systems. *Optics Communications*. 460, 125107. doi: 10.1016/j.optcom.2019.125107.
- [6] J.-H. Yoo, B. W. Kim, ve S.-Y. Jung. (2015). Modelling and analysis of M-ary variable pulse position modulation for visible light communications. *IET Optoelectronics*, 9 (5), 184-190. doi: 10.1049/iet-opt.2014.0107.
- [7] M. Sönmez, (2018). Simplified and accelerated PPM receivers for VLC systems. *IET Optoelectronics*, 12(1), 36-43. doi: 10.1049/iet-opt.2017.0052.

SOLAR AND SONOLYSIS ASSISTED HYDROGEN RECOVERY FROM INDUSTRIAL SULPHIDE WASTEWATER USING CNT-ZnS/Fe₂O₃

Preethi Vijayarengan^{1*}, Shivkumar Maurya¹, Sathishkumar Manoharan^{2*}

¹Department of Civil Engineering, Hindustan Institute of Technology and Science, Chennai, India

¹Department of Aeronautical Engineering, Hindustan Institute of Technology and Science, Chennai, India

²Department of Chemical Engineering, Sethu Institute of Technology, Madurai, India

*Corresponding author e-mail: preethi_enviro@hotmail.com

ABSTRACT

The photocatalytic hydrogen production of Carbon nanotube (CNT) deposited ZnS/Fe₂O₃ photocatalyst is tested using a laboratory-scale Sonophotocatalytic reactor. The catalyst is characterized for crystallinity, band gap as well as particle shape and size. Feasibility studies are carried out by varying the operating parameters and it is found that maximum hydrogen production is obtained at their respective optimum values. The optimized concentration of SO₃²⁻, catalyst amount and photolytic volume of 0.2M, 0.5g/L and 150 mL, respectively are obtained using solar irradiation. The highest amount of hydrogen obtained from the sewage treatment plant (STP) sulphide wastewater is close to 6250 µmol/h. This high hydrogen production is due to the optimization of parameters coupled with uniform mixing achieved by the oxidation process of sonolysis of photocatalysts. The prepared photocatalyst is found to be photostable for up to 5 cycles.

Keywords: Hydrogen, Sonophotocatalysis, CNT, ZnS/Fe₂O₃, Sulphide Wastewater.

INTRODUCTION

Nowadays, nearly 85% of the global energy is derived from the non-renewable sources of fossil fuels. It is predicted that these fast-depleting non-renewable energy sources are likely to be completely exhausted within the next 60 years. Moreover, the main disadvantage in using these energy sources is the increased emission of harmful greenhouse gases, which are known to be the key cause of climate change and global warming. The need of the hour is therefore the production of renewable fuel in an economically and environmentally sustainable manner.

Solar photocatalytic hydrogen production is the cheapest and most sustainable way of recovering hydrogen from industrial sulphide containing wastewater. Several research studies have been conducted to explore the possibility to scale-up the Photocatalytic Hydrogen (H₂) Recovery. However, none of the research studies conducted so far have studied this at a large-scale level. The main hurdles to this scaling-up are: i) synthesis of an economical, sustainable and visibly active photocatalyst; ii) reactor design to keep the catalyst in suspension [1]. In the current research paper, the photocatalytic nanoparticles are kept under suspension using an ultrasonicator for good exposure to solar radiation for maximum and effective hydrogen recovery.

In this study, Zinc sulfide (ZnS) coated with iron oxide nanoparticles is used as the photocatalyst. This visible-active photocatalyst has the advantages of being non-toxic as well as cost-effective.

MATERIALS AND METHODS

A 500 mL cylindrical photocatalytic reactor is fabricated with plexiglass material. The reactor is kept immersed in the sonicator bath to keep the photocatalyst in dispersion. The sonicator has a frequency of 25 kHz. It has two tubes. One tube is used for nitrogen (N₂) gas flushing. Another tube is used to recover hydrogen through an inverted measuring cylinder by water replacement method. The experiments are performed using direct solar light. In the experiment, 0.05g of photocatalyst is added in 150 mL of reaction medium containing sulphide wastewater collected from a sewage treatment plant (STP) and Na₂SO₃ is used as the sacrificial agent. After flushing with nitrogen gas for one hour in each experiment, the sonophotocatalytic setup is kept under sunlight for one hour. The photographic view of the sonophotocatalytic reactor is shown in Figure 1.

CONCLUSIONS

This study has suggested / recommended / put forth a novel idea to recover hydrogen from sulphide wastewater using the sonophotocatalysis process. CNT deposited ZnS/Fe₂O₃ shows better hydrogen yield than plain ZnS/Fe₂O₃. After CNT deposition, the photocatalyst is found to have reduced band gap, particle size and is highly crystalline. The sonophotocatalysis process has the potential to give maximum hydrogen yield which is higher than that of photocatalytic method. Hence, this will be a suitable technology to scale-up the effective dispersion and exposure of the catalyst to sunlight for maximum H₂ recovery.

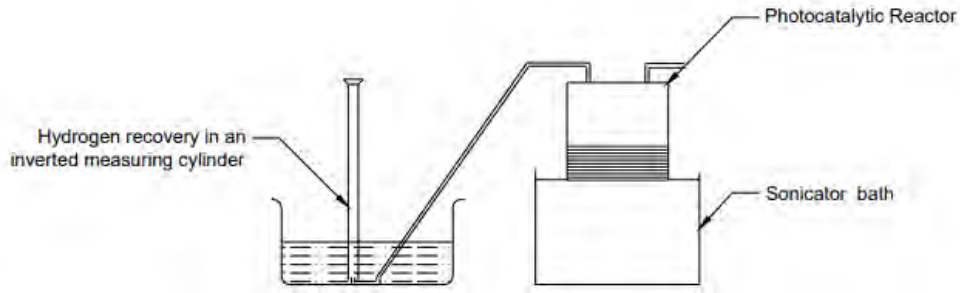


Figure 1. Sonophotocatalytic Reactor and Hydrogen Recovery

REFERENCES

- [1] Gentili P L, Penconi M, Ortica F, Cotana F, Rossi F, Elisei F. Synergistic effects in hydrogen production through water sonophotolysis catalyzed by new $\text{La}_{2x}\text{Ga}_y\text{In}_{2(1-x-y)}\text{O}_3$ solid solutions. *International Journal of Hydrogen Energy* 2009; 34:9042 – 9049.

SELECTION AND SYNTHESIS OF CERAMIC ELECTROLYTES FOR INTERMEDIATE TEMPERATURE SOLID OXIDE FUEL CELLS

^{1*} Handan ÖZLÜ TORUN

Kahramanmaraş İstiklal University, Elbistan Engineering Faculty, Energy System Engineering, Kahramanmaraş, 46000, Turkey

handan.ozlutorun@istiklal.edu.tr

ABSTRACT

In this study, electrolyte selection in solid oxide fuel cells is emphasized. The ceramic electrolyte, which can be used at intermediate temperature, was synthesized and characterized by the sol-gel method. It has been discussed whether the conductivity properties of the obtained compounds can be used in fuel cell application.

Keywords: Solid oxide fuel cell, Ceramic electrolyte, CeO₂

INTRODUCTION

Solid oxide fuel cells (SOFC) are systems that convert a chemical reaction into energy. The structure of a single cell: anode/electrolyte/cathode (Fig. 1) [1]. One of the most important parts in solid oxide fuel cells is the ceramic electrolyte. The choice of ceramic electrolyte affects the operating temperature and efficiency of the system. Until now, 8YSZ is mostly used as electrolyte. However, the efficiency of the cell made with this electrolyte is high at 1000 °C. Temperature increase limits the use of SOFC as it raises costs. The most important solution to eliminate this problem is to produce electrolyte with high efficiency at low temperature. It is desired that the electrolyte used is proton or oxygen ion conductor. Low temperature electrolytes are Bi₂O₃, CeO₂ and LaGaO₃ [2,3]. The common feature of these electrolytes is that they are compounds with oxygen-ion conductivity.

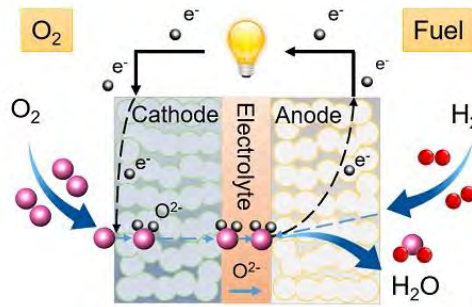


Fig.1 Solid oxide fuel cell part

Recently, CeO₂ has become the preferred electrolyte with its chemical stability and conductivity value. CeO₂ is a compound with a cubic crystal lattice that is abundant in nature. In order to increase the oxygen ion conductivity of CeO₂, it is necessary to form oxygen vacancies in the crystal structure. The amount of space facilitates ion movement. In general, the amount of space is increased by doping elements with different valence valences.

In this study, La-Er and La-Y elements were added to the crystal structure by sol-gel synthesis in order to increase the oxygen ion conductivity of pure CeO₂. The structural, morphological and electrical properties of the obtained compounds were investigated.

MATERIALS AND METHODS

The citric acid sol-gel method was used for the synthesis of the compounds. Pure CeO₂, Ce_{0.85}La_{0.10}Er_{0.05}O_{2-d} and Ce_{0.85}La_{0.10}Y_{0.05}O_{2-d} compounds were obtained. Precursors used were cerium (III) nitrate hexahydrate (Ce(NO₃)₃.6H₂O (sigma-Aldrich 99.99%), lanthanum (III) nitrate hexahydrate (La(NO₃)₃.6H₂O (sigma-Aldrich 99.99%), erbium (III) nitrate pentahydrate (Er(NO₃)₃.5H₂O (sigma-Aldrich 99.99%), ytterbium (III) nitrate hexahydrate (Y(NO₃)₃.6H₂O (sigma-Aldrich 99.99%) powders. X-ray powder diffractometry, scanning electron microscopy and impedance spectroscopy were used in characterization studies.

As seen in Figure 1, it was observed that all compounds had a cubic phase after the synthesis process.

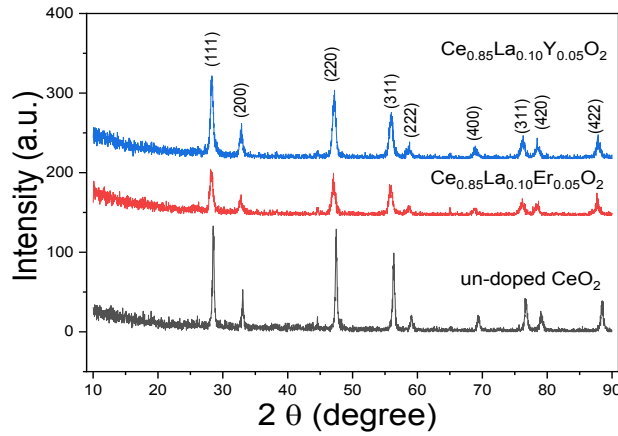


Fig. 2 X-ray diffraction pattern for all samples in which calcinated at 800°C

All samples were pressed before conductivity measurement. Pellet surfaces were painted with silver paste to provide contact. Impedance measurement curves are given in figure 2. It can be seen in Fig2 that the doping conductivity changes.

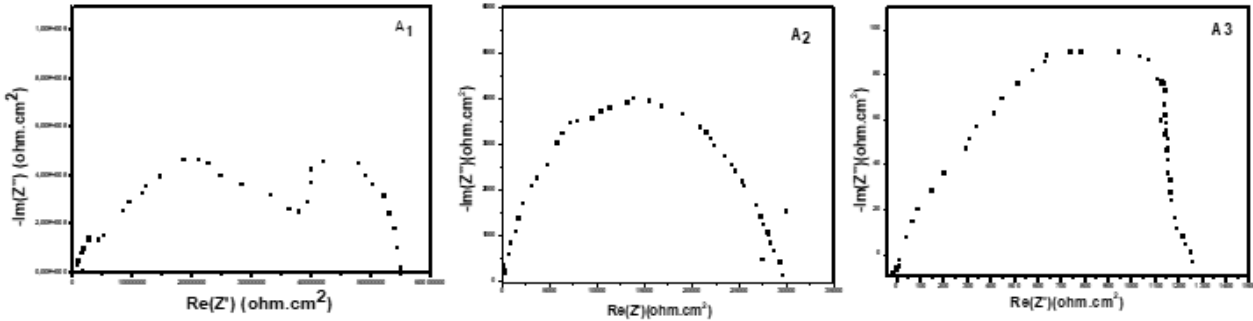


Fig.3. Impedance curce for all samples A1) pure CeO₂ , A2) Ce_{0.85}La_{0.10}Er_{0.05}O_{2-d} , A3) Ce_{0.85}La_{0.10}Y_{0.05}O_{2-d}

CONCLUSIONS

As a result, it was found that the conductivity of the obtained two compounds was high when compared to pure CeO₂.

ACKNOWLEDGEMENTS

We would like to thank Prof. Dr. T. Nejat Veziroglu Clean Energy Research Center for their support to conduct the impedance measurements within the scope of this research

REFERENCES

- [1]<https://www.nottingham.ac.uk/research/groups/advanced-materials-research-group/research/energy-materials/solid-oxide-fuel-cells.aspx>
- [2] Singh, B., Ghosh, S., Aich, S., & Roy, B. (2017). Low temperature solid oxide electrolytes (LT-SOE): A review. Journal of Power Sources, 339, 103-135.
- [3] Kharton, V. V., Marques, F. M. B., & Atkinson, A. (2004). Transport properties of solid oxide electrolyte ceramics: a brief review. Solid State Ionics, 174(1-4), 135-149.

ENVIRONMENTAL IMPACT ASSESSMENT OF A NOVEL PHOTOELECTROCHEMICAL REACTOR FOR HYDROGEN PRODUCTION

*Ali Erdogan Karaca, Ibrahim Dincer

Clean Energy Research Laboratory (CERL), Faculty of Engineering and Applied Science, Ontario Tech. University, 2000 Simcoe Street North, Oshawa, Ontario L1H 7K4, Canada

* E-mail: ali.karaca@ontariotechu.net

ABSTRACT

In this study, an environmental impact analysis is conducted on a newly developed photoelectrochemical (PEC) reactor for clean hydrogen production. For a cradle-to-grave type life cycle assessment (LCA) of the proposed reactor, SimaPro software is used as a powerful computational tool. The results are comparatively evaluated with three different hydrogen production options: natural gas steam reforming, wind-based PEM water electrolysis and solar-based PEM water electrolysis. The developed reactor comprises a membrane electrode assembly with a photosensitive stainless-steel cathode electrode coated with electrodeposited copper oxide and a TiO₂ coated stainless steel counter electrode. The material used for building the reactor and energy required for the chemical reaction are considered in the LCA analysis. In the light of conducted thermodynamic and electrochemical analyses, hydrogen production rate of the reactor is evaluated as 45.8 µg/s while operating with an energy efficiency of 6.2%. The LCA analysis results show that the proposed PEC reactor-based hydrogen production emits the lowest CO₂ emissions with a value of 1.05 kg CO₂ eq/kg H₂ that is followed by wind-based PEM water electrolysis (1.2 kg CO₂/kg H₂), whereas hydrogen production via natural steam reforming emits highest amount of CO₂ per kg of hydrogen (11.86 kg CO₂/kg H₂).

INTRODUCTION

Hydrogen is the lightest and most abundant chemical element in the universe that carries the greatest potential to be the key to the green energy sector for a more sustainable, cleaner and peaceful planet. As an energy carrier, hydrogen can significantly contribute to energy security by diversifying the energy mix and enhancing the resilience with different supply chains, markets and producers. Coal gasification and natural gas steam reforming together form majority of industrial hydrogen production [1]. On the other hand, the finite existence nature of the hydrocarbon-based fuels and the CO₂ emissions associated with consumption activities of these energy sources make a green transition in global hydrogen production crucial. Photoelectrochemical hydrogen production one of many methods to produce hydrogen in an environmentally benign manner, which uses free and abundant solar energy as primary energy source to split water into hydrogen and oxygen.

In the current study, the hydrogen production performance and environmental impact assessments of a novel PEC reactor are conducted. The environmental impact of the PEC-based hydrogen production process is evaluated by means of five impact categories namely abiotic depletion potential (ADP), acidification potential (AP), global warming potential (GWP), human toxicity potential (HTP) and ozone depletion potential (ODP). 1 kg of hydrogen production is defined as the functional unit for the conducted LCA study.

SYSTEM DESCRIPTION

A new photoelectrochemical reactor for hydrogen production is designed, developed and analyzed in the scope of the current study. Fig. 1 presents the system boundary of the conducted LCA study. The required external electrical energy for the chemical reaction in the PEC is provided from a PV-solar panel. Required material for reactor assembly and energy for hydrogen production are considered in the LCA of the proposed PEC reactor.

BRIEF ANALYSIS

The governing equations that are used in the analysis of the PEC reactor are as follows [2,3,4]:

$$\dot{m}_{H_2} = \dot{N}_{H_2} \times M_{H_2} \times 0.001 \quad (1)$$

$$\dot{N}_{H_2} = \frac{1}{2} \times \phi \times \dot{N}_{ph} \quad (2)$$

$$\dot{N}_{ph} = \frac{I_r \times A_i}{E_g} \quad (3)$$

$$E_g = \frac{hc}{\lambda} \quad (4)$$

$$\eta_{PEC} = \frac{\dot{m}_{H_2} \times LHV_{H_2}}{I_r \times A_e + \dot{W}_e} \quad (5)$$

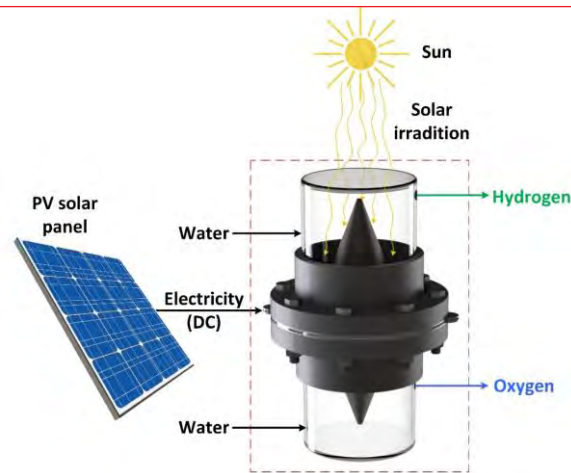


Fig.1 System boundary of the conducted LCA analysis of the PEC-based hydrogen production.

RESULTS AND DISCUSSION

The proposed PEC system thermodynamically and electrochemical analyzed. According to findings, hydrogen production rate of the PEC reactor at a solar irradiance of 600 W/m^2 and illuminated electrode area of 0.1125 m^2 is $45.8 \mu\text{g/s}$, and energy efficiency of the reactor is evaluated as 6.12%. Fig. 2 shows the impact of the illuminated area of photoactive electro on the reactor performance. It has been evaluated that increasing the solar incident area provides better utilization from solar energy; hence, both efficiency and hydrogen production rate of the reactor increase. A comparative environmental impact analysis is conducted on the PEC reactor. Since it associates with the CO_2 emissions, GWP is considered the most critical environmental impact criterion. In this regard, the GWP of the PEC reactor is evaluated as $1.052 \text{ kg CO}_2 \text{ eq/kg H}_2$. This ratio makes the proposed PEC-based hydrogen production the lowest CO_2 emitting hydrogen production method among investigated options. Fig. 3 presents the comparative LCA results of the corresponding hydrogen production methods. Fig. 4 shows the CO_2 emission rates of the investigated hydrogen production methods.

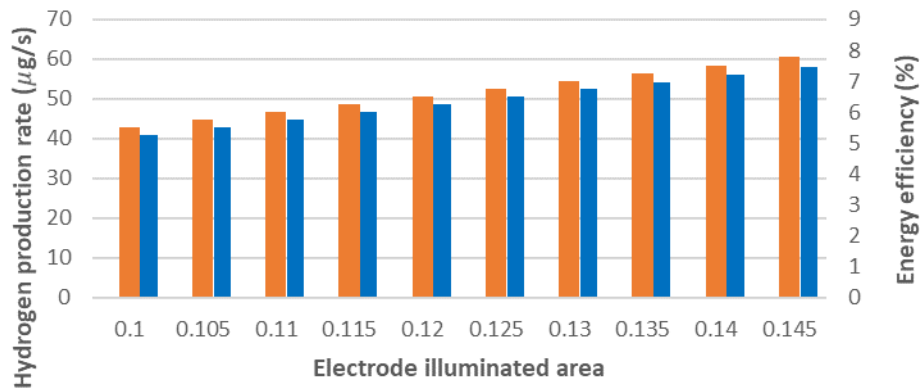
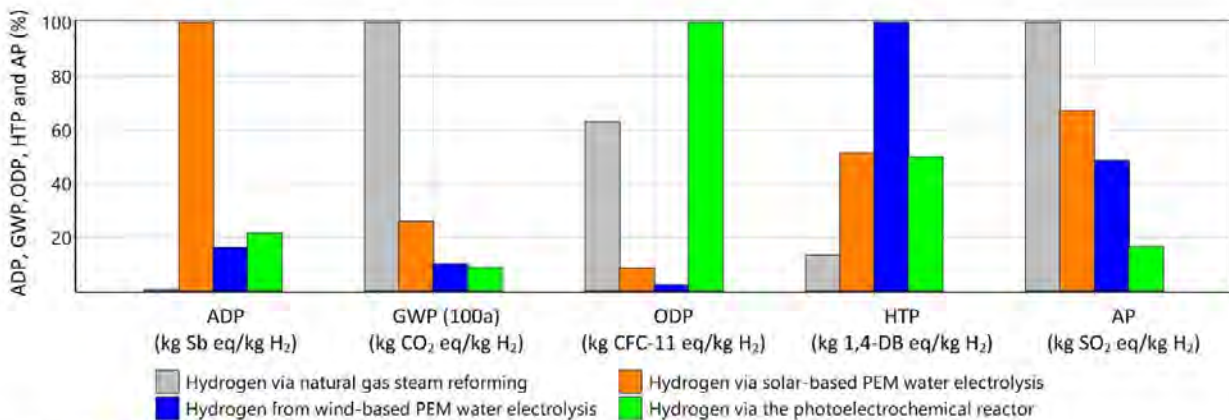


Fig. 2. Impact of photoactive electrode illuminated area on the PEC reactor performance.



Method: CML-IA baseline V3.06/EU25

SimaPro- Faculty- Faculty Ontario (9.1.0.11)

Fig. 3. Characterized LCA results of various hydrogen production methods.

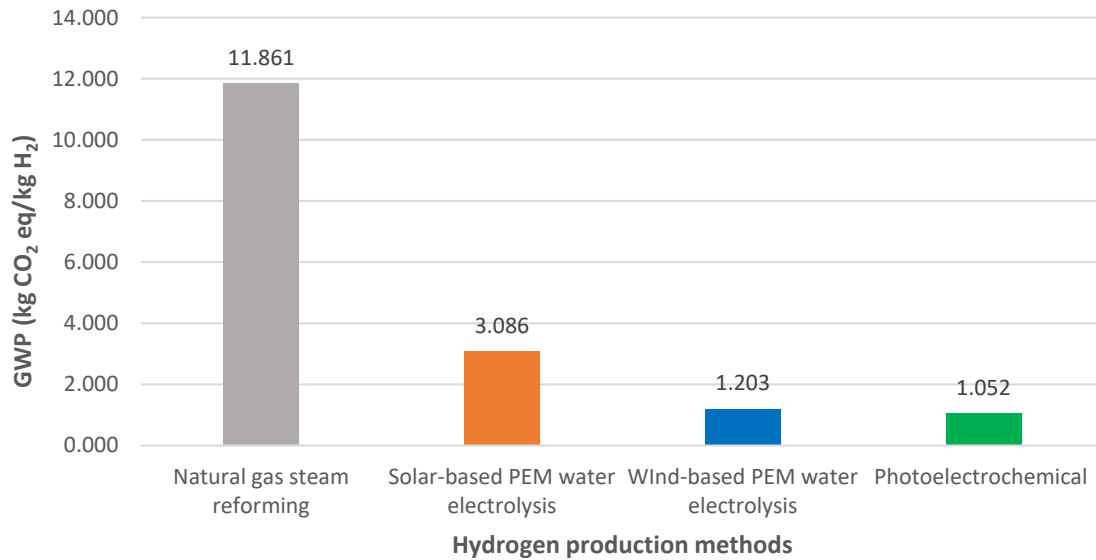


Fig. 4. Global warming potential (GWP) of various hydrogen production methods.

CONCLUSIONS

A new photoelectrochemical design is investigated for clean hydrogen production. The hydrogen production rate and energy efficiency of the reactor are evaluated as $45.8 \mu\text{g}/\text{s}$ and 6.12% respectively. The GWP of the PEC based hydrogen production is 1.052 kg CO₂ eq per kilogram of hydrogen, which makes the system the lowest CO₂ emitting option among the evaluated hydrogen production methods in the scope of the current study.

REFERENCES

- [1] Dincer, I., & Joshi, A. S. (2013). Solar based hydrogen production systems. New York: Springer. <https://doi.org/10.1007/978-1-4614-7431-9>
- [2] Falcão, D. S., & Pinto, A. M. F. R. (2020). A review on PEM electrolyzer modelling: Guidelines for beginners. *Journal of Cleaner Production*, 261, 121184. <https://doi.org/10.1016/j.jclepro.2020.121184>
- [3] Yan, Y., Crisp, R. W., Gu, J., Chernomordik, B. D., Pach, G. F., Marshall, A. R., ... & Beard, M. C. (2017). Multiple exciton generation for photoelectrochemical hydrogen evolution reactions with quantum yields exceeding 100%. *Nature Energy*, 2(5), 1-7. <https://doi.org/10.1038/nenergy.2017.52>
- [4] Chehade, G., Demir, M. E., Dincer, I., Yuzer, B., & Selcuk, H. (2018). Experimental investigation and analysis of a new photoelectrochemical reactor for hydrogen production. *International Journal of Hydrogen Energy*, 43(27), 12049-12058. <https://doi.org/10.1016/j.ijhydene.2018.04.110>

TECHNO-ECONOMIC AND ENVIRONMENTAL IMPACT ASSESSMENTS OF TRIGENERATION SYSTEMS WITH VARIOUS FUELS

^{1*}Fatih Sorgulu and ^{2,1}Ibrahim Dincer

¹Faculty of Mechanical Engineering, Yildiz Technical University, Besiktas, Istanbul, Turkey

²Faculty of Engineering and Applied Science, Ontario Tech. University, Oshawa, Ontario, Canada

*Correspondence: e-mail: fatih@sorgulu.edu.tr

ABSTRACT

In this study, renewable hydrogen production and blending with natural gas for the existing distribution pipelines is studied and evaluated in comparison with various fuels, such as diesel, coal, biogas, and biodiesel. In this regard, solar and wind energy-based power systems integrated with reverse osmosis units are designed and compared in energy, exergy, environment and cost, respectively. Solar PV panels and wind turbines are considered for electricity and heat. For hydrogen-based systems, an electrolyzer is utilized to produce hydrogen. The heat required for residential applications is also provided in an environmentally benign way. Here, electricity, heat, and freshwater needed in a community consisting of 100 houses are provided. The costs of capital, fuel, operation, and maintenance are calculated and evaluated in detail. An environmental impact assessment is performed by comparing carbon dioxide, carbon monoxide, unburned hydrocarbons, particulate matter, sulfur dioxide, and nitrogen oxides.

Keywords: Cost, Efficiency, Emission, Energy, Hydrogen, Natural Gas, Renewable Energy

INTRODUCTION

At present, environmentally, economically, and technically sustainable solutions require to overcome the increasing energy demand of today. Supplying diversity in energy systems to provide electricity, heat, and freshwater is vital. Energy reliability can be provided by employing various renewable energy sources and integrating energy storage options. Environmental awareness is more significant than ever. CO, CO₂, SO₂, NO_x emissions, and unburned hydrocarbons are recognized as the primary environmental problems. Fossil fuel-based energy systems produce these gases. Using fossil fuel resources wisely by integrating renewable energy and storage options will be critical. Here, injecting hydrogen into natural gas is a promising way to reduce emissions. This is the only study that presents a comprehensive cost and environmental analysis on hydrogen injection into natural gas pipelines compared with various fuels. The energy, environmental impact and cost assessment studies are undertaken for the seven integrated systems.

SYSTEM DESCRIPTION

Thermodynamic, techno-economic and environmental impact analyses of the integrated system are performed utilizing Engineering Equation Solver (EES) and Hybrid Optimization of Multiple Energy Resources (HOMER Pro) software [1-2]. Wind turbines, solar PV panels, fossil fuel-based generators, a boiler, and a reverse osmosis unit are utilized to produce electricity, heat, and freshwater. For the hydrogen-based systems, the electrolyzer is also considered. Here, hydrogen injection into natural gas and use in gas cooktops and combi boilers is focused. The average daily electricity consumption is considered as 838.3 kWh [3]. In the summer, solar radiation is determined as 6.5 kWh/m² per day. The yearly average wind speed is defined as 4.73 m/s, reaching 5.3 m/s in February [4].

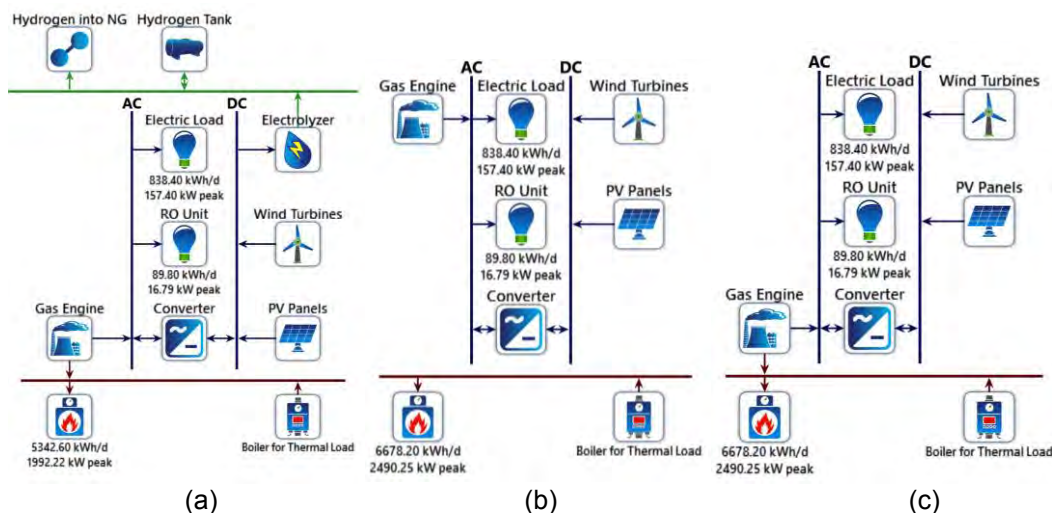







Fig. 1. Schematic illustrations of a) hydrogen natural gas blend b) fossil fuel c) biofuel-based systems.

RESULTS AND DISCUSSION

The main components of the proposed systems, such as PV panel, wind turbine, generator, boiler, and electrolyzer, and their capacities, including hours of operation, are tabulated in Table 1. In comparison, the rated power of the PV panel changes between 135 kW to 2.4 MW, rated power of the wind turbine changes between 100 kW to 2.4 MW. As expected, the power required for the electrolyzer increase with the increase of hydrogen requirement.

Table 1. Main components and their utilizations in the integrated system.

						
1. Case (NG-80% H ₂ -20%)	Capacity (kW)	369	350	130	200	170
	Hours of Operation	4352	8205	3908	7203	8216
2. Case (NG-20% H ₂ -80%)	Capacity (kW)	2428	2400	110	479	1350
	Hours of Operation	4352	8205	1330	8149	8497
3. Case (Natural Gas)	Capacity (kW)	155	100	200	278	-
	Hours of Operation	4352	8205	4754	8760	-
4. Case (Biogas)	Capacity (kW)	135	100	200	273	-
	Hours of Operation	4352	8205	4850	8462	-
5. Case (Biodiesel)	Capacity (kW)	194	250	200	278	-
	Hours of Operation	4352	8205	3362	8760	-
6. Case (Diesel)	Capacity (kW)	194	250	149	278	-
	Hours of Operation	4352	8205	3362	8760	-
7. Case (Coal)	Capacity (kW)	135	100	150	262	-
	Hours of Operation	4352	8205	4850	7971	-

Fossil fuel-based energy systems produce carbon dioxide, carbon monoxide, sulfur dioxide, and nitrogen oxides. In addition to these gases, unburned hydrocarbons and particulate matter are emitted. Natural gas is cleaner than coal because of the sulfur content of coal and the higher heating values of natural gas. However, CO and CO₂ are produced with natural gas combustion. With the hydrogen injection, up to 80%, CO₂ emissions can be decreased from 812 ton/yr to 14 ton/yr.

Table 2. Emissions generated under different cases.

	Unit	1. Case	2. Case	3. Case	4. Case	5. Case	6. Case	7. Case
Carbon Dioxide (CO ₂)	kg/yr	360,157	13,996	620,783	443,437	0	812,369	879,246
Carbon Monoxide (CO)	kg/yr	1,400	410	1,406	2.61	989	989	2,044
Unburned Hydrocarbons	kg/yr	61.7	18.1	61.4	0.114	43.2	43.2	90
Particulate Matter	kg/yr	8.4	2.46	8.52	0.0158	6	6	12.3
Sulfur Dioxide (SO ₂)	kg/yr	0	0	0	0	0	2,009	11,358
Nitrogen Oxides (NO _x)	kg/yr	1,316	385	1,321	2.45	929	929	1,921

CONCLUSIONS

In the presented systems, renewable energy and fossil fuel-based power systems are analyzed and compared. Thus, a blend of hydrogen and natural gas is compared with various fuels. In addition, PV panels and wind turbines are considered as primary power suppliers. In this regard, the main findings obtained in this study are listed as follows:

- The levelized costs of electricity are calculated between 0.28 and 4.01 \$/kWh for seven cases.
- The total net present costs are calculated between \$1.78 million and \$17.9 million for the different scenarios.

REFERENCES

- [1] EES. Engineering Equation Solver Software. Available at: www.fchart.com. (Accessed on: 24/05/2021).
- [2] Mepas Energy. Available at: <https://www.mepasenerji.com> (Accessed on: 02/06/2021).
- [3] HOMER Pro. Available at: <https://www.homerenergy.com>. (Accessed on: 11/06/2021).
- [4] The Prediction of Worldwide Energy Resources, NASA. Available at: <https://power.larc.nasa.gov>. (Accessed on 09.05.2021).

IRON OXIDE-BASED PHOTOCATALYSTS FOR HYDROGEN PRODUCTION AND DYE DEGRADATION UNDER NATURAL SUNLIGHT

^{1*} Preethi V, ² Ananth S, ^{3*} Sri Chandana P, ¹ Gokul Krishnan M, ⁴ Subramanyam Sarma L

¹ Department of Civil Engineering, Hindustan Institute of Technology and Science, Chennai 603103

² Department of Physics, KPR Institute of Engineering and Technology, Coimbatore 641407

³ Department of Civil Engineering, Annamacharya Institute of Technology and Sciences, Kapdapa, 516003

⁴ Nanoelectrochemistry Laboratory, Department of Chemistry, Yogi Vemana University, Kapapa, 516003

*Corresponding author e-mail: vpreethi@hindustanuniv.ac.in, srichandanaloka@gmail.com

ABSTRACT

Nanomaterials are challenging in simultaneous degradation of pollutants and hydrogen production. This present research work focuses on various visible light active iron oxide nanophotocatalysts for H₂ production and dye degradation. The prepared photocatalysts were characterized for structure (XRD), and morphology (SEM). The efficiency of various iron oxide-based photocatalysts for hydrogen recovery from highly toxic sulphide-containing wastewater is described in this paper. Among the various iron oxide photocatalysts, Yt/Fe₂O₃ shows maximum activity. Effect of operating parameters such as sulphite ion concentration, catalyst dosage, photolytic solution volume, reusability studies were conducted for hydrogen production. The dye degradation studies were conducted for the prepared iron-based catalytic materials using Rhodamine B as the model dye.

Keywords: H₂ production, Yt/Fe₂O₃, Sunlight, dye, Photodegradation.

INTRODUCTION

Industrialization and urbanization pushed us to focus more on research related to environment and energy. Photocatalytic process using direct solar irradiance helps to achieve the generation of renewable energy, H₂ and degradation of pollutants [1]. Research is being done to explore visible light active, stable photocatalyst for maximum hydrogen production and complete mineralization of pollutants. Fe₂O₃ is a promising material for photocatalytic process because of its narrow band gap (2.1 eV), it promises a wide optical absorption in the visible light area. In real-time applications, Fe₂O₃ can increase photocatalytic activity. Incorporation of other metal oxides with Fe₂O₃ is expected to improve the photocatalytic performance several fold. Iron oxide acts as a sinker of photogenerated electrons and hole pairs in it co-catalyst lattice and increases the charge separation and improves the photoactivity [2]. In addition, co-catalyst had maximum active sites than pristine catalyst, thus enhances the hydrogen production as well as degradation [3, 4]. In this study, the iron oxide composites like Al₂O₃/Fe₂O₃, Sm₂O₃/Fe₂O₃ and Y₂O₃/Fe₂O₃ were prepared to recover hydrogen from sulphide wastewater and to destroy the Rhodamine B dye by photocatalysis using natural solar irradiation. Focus was on preparation and characterization of iron oxide based photocatalysts, effect of various factors for achieving maximum hydrogen production and degradation of Rhodamine B dye and its kinetics.

MATERIALS AND METHODS

For synthesis of Pure Iron Oxide, the iron oxide nanoparticles were prepared by combustion process by using natural urea source (Cow urine). For this, 40.4 grams of ferric nitrate (Fe(NO₃)₃·9H₂O) was dissolved in 100 mL natural urea solution and stirred for 30 minutes. Then, this homogeneous solution was heated using a hot plate continuously. The urea- iron nitrate solution turns into a transparent viscous gel after an hour of heating which auto ignited to form voluminous foam. Further heating resulted drying of the nanoparticles due to the combustion process.

By following the above combustion process and natural urea fuel, the Iron Oxide: Aluminum Oxide nanoparticles were synthesized. The ferric nitrate and aluminum nitrate (Al(NO₃)₃·9H₂O) were taken in equal molar ratio and dissolved separately in 50 mL fuel. After making complete dissolvent, both the solutions are transformed into a single container and mixed thoroughly. Then, the homogeneous solution was heated using a hot plate to precede the combustion process.

For the Iron Oxide: Yttrium Oxide synthesis, equal quantities of ferric nitrate and Yttrium nitrate (Y(NO₃)₃·6H₂O) were taken as precursor materials and dissolved separately in 50 ml natural urea. The Iron Oxide: Samarium Oxide synthesis process, the ferric nitrate and Samarium nitrate Sm(NO₃)₃·6H₂O were taken in 1:1 ratio as base materials and dissolved in 50 mL natural urea separately. All the processes have yielded very fine particles which were dried and powdered well for further studies and characterization. XRD and SEM analyses were performed.

Photocatalytic solar hydrogen production: Trapezoidal photocatalytic reactor with working volume of 1L was used to recover hydrogen from simulated sulphide wastewater of 0.2M sulphide ion concentration. The reactor is made up of acrylic material. The activities of various iron oxide (Fe₂O₃) photocatalysts were used to check the photocatalytic activity.

The produced hydrogen was collected for one hour in an inverted measuring cylinder. All the experiments were conducted during the daytime between 12 to 2 pm. The solar light intensity was measured using lux meter and the intensity of sunlight was found to be 75000 to 82000 lux. Synthetic sulphide of 0.2M concentration and 0.1g of Y_2O_3/Fe_2O_3 were used to study the effect of sulphite ion concentrations (as sacrificial agent) for maximum hydrogen production. The effect of Y_2O_3/Fe_2O_3 amount on recovery of H_2 from synthetic sulphide wastewater was studied by varying catalyst dose from 0.05 to 0.25 g/L. The effects of volume of photolytic solution on the recovery of hydrogen from sulphide wastewater were analysed by increasing the volume of photolytic solution from 1 L to 3 L. For large-scale hydrogen recovery from industrial sulphide wastewater, photocatalyst stabilisation is critical. As a result, the prepared Y_2O_3/Fe_2O_3 photocatalyst was reused for multiple runs to ensure its stability.

Photocatalytic degradation of RhB:

A 50 mg/L of stock solution of RhB was prepared. The quantification of RhB was achieved by a UV-Vis double beam Spectrophotometer (Systronics Model No. 2203). The peak absorbance wavelength of RhB used in the study is 554.8 nm. Photocatalytic degradation of RhB was evaluated under the irradiation of 125W Vis Lamp with built in safety resistor in a double jacketed quartz reactor of 1L volume with inlet and outlet openings. The lamp was placed in the quartz sleeve that can be inserted in the reactor at the given provision. In a typical experiment unless until mentioned, the initial concentration of RhB was 5 mg/L and the catalyst dose was 200 mg/L. Prior to irradiation, the reaction suspensions were stirred in darkness for 30min to attain adsorption-desorption equilibrium. The solution was irradiated for a total of 4h while drawing the sample at regular intervals of 15min. The samples are centrifuged at 5000rpm with Remi make model number R-24 centrifuge and measured absorbance. The whole reaction solution was continuously stirred at 600 rpm on a magnetic stirrer while the temperature was maintained at $25\pm 2^\circ C$ using cooling tank with pump.

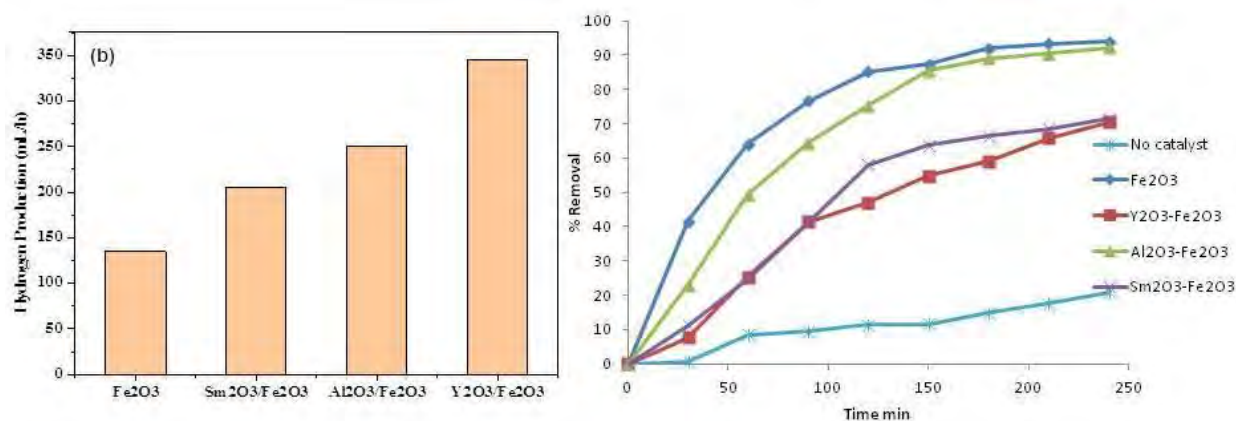


Fig 1. Photocatalytic activity of iron oxide based photocatalysts for H_2 production and dye degradation

CONCLUSIONS

Direct solar study was conducted with Fe_2O_3 based photocatalysts on sulphide wastewater and achieved maximum H_2 production of 365 mL/h. The photocatalyst that has been prepared is stable for up to 6 cycles. In this study, the synthesized photocatalyst Y_2O_3/Fe_2O_3 and photocatalytic reactors were found to be effective in decomposing the sulphide wastewater along with generation of clean gas fuel (H_2) under solar irradiation (Fig.1). These optimization experiments would aid in the commercialization of this technology for photocatalytic hydrogen recovery on a wide scale by using solar light. The as-prepared photocatalysts were also evaluated for the photocatalytic degradation efficiency using Rhodamine B as the model compound and the study demonstrates that the Photocatalytic degradation efficiencies of the iron oxide-based photocatalysts were significant under the visible light irradiation in the laboratory Photocatalytic reactor with pseudo-first order kinetic rates constants from 0.0051 to 0.0133 h^{-1} . Even under sunlight irradiation similar trend in the degradation efficiencies were observed. In conclusion iron oxide-based photocatalysts demonstrate their ability in both H_2 production and dye degradation efficiencies under sunlight.

REFERENCES

- [1] Muninathan S and Arumugam S, Enhanced photocatalytic activities of NiS decorated reduced graphene oxide for hydrogen production and toxic dye degradation under visible light irradiation, International Journal of Hydrogen Energy, 46, 2021, 6532-6546.
- [2] Ismael M, Enhanced photocatalytic hydrogen production and degradation of organic pollutants from Fe (III) doped TiO_2 nanoparticles, Journal of Environmental Chemical Engineering 8 (2020) 103676.
- [3] Lakshmanareddy N, Navakoteswara Rao V, Cheralathan K K, Subramaniam E P, Shankar MV, Pt/ TiO_2 nanotube photocatalyst – Effect of synthesis methods on valance state of Pt and its influence on hydrogen production and dye degradation, Journal of Colloid and Interface Science 538 (2019), 83-98.
- [4] Phivilay S.P, Poretzky A.A., Domen K., Wachs I.E., Nature of catalytic active sites present on the surface of advanced bulk tantalum mixed oxide photocatalysts, ACS Catal. 3 (2013) 2920–2929.

LOCATION SELECTION OF THE HYDROGEN REFUELING STATIONS: AN ISTANBUL CASE

^{1,2*} Ebru Geçici, ² Mehmet Güray Güler, ¹ Taner Bilgiç

¹ Boğaziçi University, Engineering Faculty, Industrial Engineering Department, Bebek, İstanbul, Turkey

² Yıldız Technical University, Faculty of Mechanical Engineering, Industrial Engineering Department, Beşiktaş, İstanbul, Turkey

*Corresponding author e-mail: egecici@yildiz.edu.tr

ABSTRACT

The energy sources, which we use today, will not be sufficient in the near future. The transportation sector is also affected by this lack of energy. Therefore, the availability of alternative energy sources has a critical role in the future. Hydrogen energy, which can be used in the chemical industry, transportation, the housing sector, is one of these alternative energy sources, and especially in the transportation sector, hydrogen fuel cell vehicles (HFCV) constitute an important alternative. However, the spread of the HFCV depends on the construction of the hydrogen refueling stations (HRS). In this study, the location selection of the HRS in İstanbul is examined for the long-term planning horizon. For this purpose, the multi-period p-median model is used, and several scenarios are implemented. According to the results, the HRSs are opened in the city center at the initial periods, whereas, at the end of the planning horizon, the HRSs are spread over the region.

Keywords: Hydrogen Refueling Station, P-Median Model, Optimization, Technology Diffusion, Multi-Period

INTRODUCTION

Since the current energy sources will not be enough for the future, the researchers look for alternative energy sources. One of these energy sources is hydrogen energy which has several advantages such as low polluting fuel [1], providing long-term transportation [2] and storage possibilities [3], etc. Hydrogen energy, which can be used in different fields such as the chemical industry and housing, will have an important role in the transportation sector as hydrogen fuel cell vehicles (HFCV), together with electrical vehicles. Since HFCVs provide a longer range and less fueling time, they will be more preferable to electrical vehicles [4]. However, to increase the number of HFCVs in the future, it is necessary to open the required number of hydrogen refueling stations [5]–[8]. This raises the question of where to open the hydrogen refueling stations (HRS). To find an answer to this question, there are different studies in the literature, which are obtained by using various solution approaches. These approaches are classified as set covering models, flow-refueling location model, and p-median model ([7], [9]–[11]) by Lin et al. [12]. In this study, location selection of the HRS in İstanbul is examined. For this purpose, a multi-period p-median model is proposed. In general, p-median models requires three different parameters: supply points, demand points, and distance between the supply and demand points. Here, the neighborhood of the İstanbul is selected as demand points, whereas existing gas stations are chosen as (potential) supply points. In order to determine the hydrogen demand, the number of HFCV on a neighborhood has been estimated. However, it is assumed that the adaptation to hydrogen energy, which is a new technology, is not the same in every district. Therefore, the development index of the districts, which is calculated by using education index, income index, and life expectancy index, is calculated and adaptation levels of districts to different technology are reflected in the demand. Then, by using the demand of the neighborhoods with the distance between the neighborhoods and existing gas stations, the objective function minimizes the weighted distance traveled by vehicle users to buy fuel.

ANALYSIS AND RESULTS

We study the location selection of HRS in İstanbul, which is the most crowded city in Turkey, for a planning horizon of 30 years where each period consists of six years. As we mentioned before, the neighborhoods are selected as demand points. To calculate the demands of neighborhoods, the following steps are used: (i) the number of vehicles is calculated for Turkey by using exponential smoothing function, (ii) the number of vehicles in İstanbul is calculated, (iii) by using current vehicle ratio of districts, the number of vehicles in districts are calculated, (iv) then to reflect technology diffusion of districts with different characteristics, the human development index is calculated and employed through an S-curve, (v) by using S-curve values, the number of HFCV in districts are calculated, (vi) with the number of HFCV and flows between districts, the district demand is obtained, and (vii) in the last step, by multiplying district demand with a population ratio of neighborhoods, the demand of 954 neighborhoods is obtained for all periods. To define candidate sites for HRS, existing 734 gas stations in İstanbul are selected. After the preparation of the parameters of the model, the multi-period model is run by using in an Intel® Core™ i5-10210U CPU with 8 GB RAM computer.

The obtained results constitute the results of the base scenario. According to the base scenario results, the stations to be converted to HRS in the beginning periods are selected from the city center, whereas, at the end of the periods,

the opened stations spread over the city. This scenario was obtained through the current utilization of the fuel stations. Several alternative scenarios were analyzed using different performance measures such as maximum distance, the maximum number of the neighborhood and the maximum number of vehicles served by stations, and the total distances traversed by the system. It's shown that 85 stations perform very well. Then, the multi-period model is run, and then the results are compared with the base scenario which has 126 stations. It is observed that the base scenario shows more improvement for the performance measures in the initial periods, but similar results were obtained for both scenarios in the final periods. According to these results, it is evaluated that if it is desired to reach users faster, the base scenario with a high number of stations should be preferred, and when the installation cost is considered, the second scenario in which fewer facilities are opened should be preferred.

CONCLUSIONS

Since the available energy sources will not be enough to fulfill demand, alternative energy sources are being investigated. Hydrogen is one of these alternative energies, especially for the transportation sector. HFCV will be used in the near future in addition to the electrical vehicles. However, to increase HFCV, the HRS should be opened, and location of these stations should be defined. For this purpose, location selection of HRS in İstanbul is examined by using a multi-period p-median model for the next 30 years where each period consists of six years. The results show that transformation of the existing gas stations to HRS start from the center and then continue far from the city center. In addition, to analyze effect of the number of opened stations, different scenarios are analyzed, and the optimal value is selected. After that the multi-period model is run and these two scenarios are compared. Although the improvements observed in performance measures are close in the last periods, it is stated that a faster improvement achieved for the base scenario in the initial periods.

REFERENCES

- [1] I. Dincer, "Technical, environmental, and exergetic aspects of hydrogen energy systems," *Int. J. Hydrogen Energy*, vol. 27, no. 3, pp. 265–285, 2002.
- [2] Ş. Şeker and N. Aydın, "Hydrogen production facility location selection for Black Sea using entropy based TOPSIS under IVPF environment," *Int. J. Hydrogen Energy*, 2020.
- [3] M. Yáñez, A. Ortiz, B. Brunaud, I. Grossmann, and I. Ortiz, "Contribution of upcycling surplus hydrogen to design a sustainable supply chain: The case study of Northern Spain," *Appl. Energy*, vol. 231, pp. 777–787, 2018.
- [4] M. D. Üçok, "Hydrogen Fuel Cell Vehicles," in *IICEC Energy And Climate REsearch Paper*, 2019, pp. 1–40.
- [5] J. E. Kang, T. Brown, W. W. Recker, and G. S. Samuelsen, "Refueling hydrogen fuel cell vehicles with 68 proposed refueling stations in California: Measuring deviations from daily travel patterns," *Int. J. Hydrogen Energy*, vol. 39, no. 7, pp. 3444–3449, 2014.
- [6] M. Muratori, H. Bush, B. C. Hunter, and M. W. Melaina, "Modeling hydrogen refueling infrastructure to support passenger vehicles," *Energies*, vol. 11, no. 5, p. 1171, 2018.
- [7] H. Kim, M. Eom, and B.-I. Kim, "Development of strategic hydrogen refueling station deployment plan for Korea," *Int. J. Hydrogen Energy*, vol. 45, no. 38, pp. 19900–19911, 2020.
- [8] M. Fuse, H. Noguchi, and H. Seya, "Near-term location planning of hydrogen refueling stations in Yokohama City," *Int. J. Hydrogen Energy*, vol. 46, no. 23, pp. 12272–12279, 2021.
- [9] M. A. Nicholas, S. L. Handy, and D. Sperling, "Using Geographic Information Systems to Evaluate Siting and Networks of Hydrogen Stations," *Transp. Res. Rec.*, vol. 1880, no. 1, pp. 126–134, 2004.
- [10] M. A. Nicholas and J. Ogden, "Detailed Analysis of Urban Station Siting for California Hydrogen Highway Network," *Transp. Res. Rec.*, vol. 1983, no. 1, pp. 121–128, 2006.
- [11] K. Itaoka, S. Kimura, and K. Hirose, "Methodology Development to Locate Hydrogen Stations for the Initial Deployment Stage," in *E3S Web of Conferences*, 2019, p. 01014.
- [12] R.-H. Lin, Z.-Z. Ye, and B.-D. Wu, "A review of hydrogen station location models," *Int. J. Hydrogen Energy*, 2020.

PERFORMANCE EVALUATION OF SOLAR DRYER WITH AND WITHOUT SOLAR PHOTOVOLTAIC HEAT EXTRACTION (PVHE) DUCT

¹Monesh S, ¹Ashwin Shankar, ¹S Ezhilarasan, ^{1,*}Sumit Tiwari

¹Shiv Nadar University, Department of Mechanical Engineering, Tehsil Dadri, Gautam Buddha Nagar, Uttar Pradesh, India

*Corresponding author e-mail: tiwsumit@hotmail.com

ABSTRACT

Solar drying systems have been an economical and eco-friendly mode for drying products and have been used in plenty in the agricultural sector. Use of renewable energy in different sectors not only leads to promote sustainable development but also support in environment protection. This paper deals with a comparative study on the temperature difference of a greenhouse tunnel drying system with and without the integration of a solar photovoltaic module heat extraction (PVHE) duct to pre-heat the ambient air before entering the drying chamber. An extensive theoretical analysis for agricultural produce like cotton, banana and chilli were observed. With the inclusion of the PVHE module, there was a gradual rise in the temperature of air inside the drying cabinet resulting in an average increase in 8°C improving the drying performance with respect to the decrease in moisture content. It is concluded that with PVHE gives better solar drying performance than without PVHE.

Keywords: Solar drying, Solar photovoltaic module heat extraction duct, Moisture ration, Drying efficiency

INTRODUCTION

Agriculture accounts for about 18% of the Indian economy and hence plays a vital cog in the development of the nation [1]. About 50% of the Indian population thrive on agriculture directly and the sector has seen major advancements over the past few years towards sustaining agricultural products. There has been a major waste in the product due to various factors like improper transportation, fertilization, exposure to dust and pests. Barring these factors, moisture content catalyses fungal and bacterial infections and hence decreases the shelf life of the crops making them easily perishable. To prevent this issue, drying of crops is employed to minimize the moisture content and improve its life. In closed drying, electricity and fuel were initially used to dry crops but they were non-renewable, expensive and harmful to the environment. This led to the use of solar panels, which were more effective and sustainable than previous practices [2-4]. A comparative study has been explored between greenhouse drying with or without PVT air collector with the help theoretical thermal modelling. In present analysis, mathematical equations have been taken from previous literature and coupled with some new one for exploring sustainable solar drying system able to run in forced mode.

THERMAL MODELING

Case 1 Thermal modelling for solar dryer

As mentioned by Rathore and Panvar [5], the energy balance equations are as follows

Energy balance on the cover,

$$m_c C_{pc} \left(\frac{dT_c}{dt} \right) = A_c h_{c,c-a} (T_a - T_c) + A_c h_{r,c-s} (T_s - T_c) + A_c h_w (T_o - T_c) + A_p h_{r,p-c} (T_p - T_c) + \alpha_c A_c I_s \quad (1)$$

Energy balance on the air inside the dryer,

$$m_a C_{pa} \frac{dT_a}{dt} = A_p h_{c,p-a} (T_p - T_a) + A_f h_{c,f-a} (T_f - T_a) + D_p A_p C_p \omega \rho_p (T_p - T_a) \frac{dM_p}{dt} + \rho_a V_{out} C_{pa} T_{out} - \rho_a V_{in} C_{pa} T_o + U_c A_c (T_o - T_a) + [(1 - F_p)(1 - \alpha_f) + (1 - \alpha) F_p] I_s A_c \tau_c \quad (2)$$

Energy balance on the product,

$$m_p (C_{pp} + C_{pl} M_p) \frac{dT_p}{dt} = A_p h_{c,p-a} (T_a - T_p) + A_p h_{r,p-c} (T_c - T_p) + D_p A_p \rho_p L_p dM_p/dt + F_p \alpha_p A_c \tau_c \quad (3)$$

Energy balance on the floor,

$$m_f C_{pf} \left(\frac{dT_f}{dt} \right) = A_f h_{c,f-a} (T_a - T_f) + (1 - F_p) \alpha_f A_f I_s \tau_c \quad (4)$$

Mass balance equation,

$$\rho_a V \left(\frac{dT_h}{dt} \right) = A_{in} \rho_a H_{in} v_{in} - A_{out} \rho_a H_{out} v_{out} + D_p A_p \rho_p \frac{dM_p}{dt} \quad (5)$$

Case 2 Thermal modelling for PV module duct integrated solar dryer

Energy Balance equation for PV [19-24],

$$\tau_g [\alpha_c \beta_c I_t + (1 - \beta_c) \alpha_f I_t] A_m = [U_{tca} A_m (T_c - T_a) + U_{bcf} A_m (T_c - T_f)] + \tau_g \eta_c \beta_c I_t A_m \quad (6)$$

$$\tau_g [\alpha_c \beta_c + (1 - \beta_c) \alpha_T] I_t = U_{tca} (T_c - T_a) + U_{bcf} (T_c - T_f) + \tau_g \eta_c \beta_c I_t \quad (7)$$

Energy equation for air duct,

$$\dot{m}_f C_f \frac{dT_f}{dx} = U_{bcf} (T_c - T_f) + U_{bda} (T_d - T_a) \quad (8)$$

METHODOLOGY

Thermal model for drying system has been taken from the reference Rathore and Panvar [5] and modified for PVT air collector integrated solar drying.

1. Thermal model has been solved with the help of MATLAB2016.
2. Different temperatures (drying chamber, cell, crop) have been calculated from the MATLAB program.
3. Further, moisture ratio over time for different crops in greenhouse dryer and PVT integrated greenhouse dryer have been explored.

CONCLUSIONS

Three crops namely, cotton, banana and chilli have been compared and found following results

1. Cotton and chili-drying needs 2-3 days of complete drying compared to 1 day for banana.
2. For PVT integrated greenhouse dryer, all three crop's moisture ratio decrement slopes increased which may help in fast drying.
3. There is an improvement in the temperature of air inside the drying system with the incorporation of PV module duct that helps in preheating the ambient air and circulating it inside the greenhouse dryer.
4. Application of PVT air collector makes the system self-sustainable for working under forced mode.

REFERENCES

- [1] Madhusudhan L (2015) Agriculture Role on Indian Economy. *Bus Eco J* 6:176. doi:10.4172/2151-6219.1000176.
- [2] Hegde Vinay Narayan, Hosur Viraj Shrikanth, Rathod Samyukthkumar K, Harsoor Puneet A, Narayana K Badari. Design, fabrication and performance evaluation of solar dryer for banana. *Energy, Sustainability and Society* (2015) 5:23.
- [3] Saini Vineet, Tiwari Sumit, Tiwari GN. Environ economic analysis of various types of photovoltaic technologies integrated with greenhouse solar drying system. *Journal of Cleaner Production* 2017; 156:30-40.
- [4] Tiwari Sumit, Tiwari G.N. Exergoeconomic analysis of photovoltaic-thermal (PVT) mixed mode greenhouse solar dryer. *Energy* 2016b; 114: 155-164.
- [5] Janjai S, Lamler N, Intawee P. Experimental and simulated performance of a PV-ventilated solar greenhouse dryer for drying of peeled longan and banana. *Solar Energy* 2009; 83:1550-65.
- [6] Hossain MA. Forced convection solar drying of chilli, Ph.D. thesis. Bangladesh Agricultural University, Bangladesh, Mymensingh; 2003.
- [7] Tiwari, S., Tiwari, G.N. Grapes (*Vitis vinifera*) drying by semitransparent photovoltaic module (SPVM) integrated solar dryer: an experimental study. *Heat Mass Transfer* 54, 1637-1651 (2018).
- [8] Tiwari Sumit, Tiwari GN. Thermal analysis of photovoltaic thermal integrated greenhouse system (PVTIGS) for heating of slurry in potable biogas plant: An experimental study. *Solar Energy* 2017; 155:203-211.
- [9] Tiwari GN, Tiwari S, Dwivedi VK, Sharma S and Tiwari V. Effect of water flow on PV module: A case study. 2015 International Conference on Energy Economics and Environment (ICEEE), Noida, 2015; 1-7. doi: 10.1109/EnergyEconomics.2015.7235080.
- [10] Sumit Tiwari, G.N. Tiwari, I.M. Al-Helal, Performance analysis of photovoltaic-thermal (PVT) mixed mode greenhouse solar dryer. *Solar Energy* 2016; 133: 421-428.

ESTIMATION OF CRUDE OIL PRODUCTION IN TURKEY VIA HOLT-WINTERS METHOD

^{1*} Ezgi Guler, ² Suheyla Yerel Kandemir

¹Bilecik Şeyh Edebali University, Faculty of Engineering, Industrial Engineering, Bilecik, Turkey

²Bilecik Şeyh Edebali University, Faculty of Engineering, Industrial Engineering, Bilecik, Turkey

*Corresponding author e-mail: ezgi.guler@bilecik.edu.tr

ABSTRACT

In this study, the Holt-Winters method, one of the seasonal adjustment techniques, is used for crude oil production forecasting in Turkey. First, forecasting models are created, and the fit values of the periods are obtained via Holt-Winters Additive (Ho-WA) and Holt-Winters Multiplicative (Ho-WM) methods. Then, predictions are made for the future data with these approaches and predicted data for the 36 months between May 2021 and April 2024 are obtained. When the prediction model successes of the models are evaluated with the metric values of coefficient of determination, Root Mean Square Error and Mean Absolute Percentage Error. It is concluded that the Ho-WA method is advantageous in terms of all metrics and is more suitable for model success. The predicted values obtained are intended to be a guide for decision makers.

Keywords: Crude Oil, Energy, Forecasting, Holt-Winters Method

INTRODUCTION

Energy is one of the production inputs that plays a vital role in the progress of countries. Energy sources are divided into two as renewable energy sources and non-renewable energy sources [1]. Despite the widespread use of renewable energy sources in recent years, it has been estimated that the share of fossil fuels in energy will gradually increase, and this share will reach 58% in 2030 [2]. Crude oil, one of the non-renewable energy sources, has an essential share in the world economy for the energy sector. Disruptions in the supply chain of oil have significant effects on society and the economy [3]. In this context, controlling the production and supply of crude oil has become an essential issue. Estimating crude oil production data for future periods helps produce necessary information and plans for decision makers.

There are some studies on this subject in the literature. Li and Wang [4] proposed forecasting models for crude oil production and consumption in their study. They estimated the data for India from 2018-2030 by integrating the Auto Regressive Integrated Moving Average (ARIMA) models. Ozturk and Ozturk [5] estimated the energy consumption (coal, oil, natural gas, renewable energy, and total energy) in Turkey using the ARIMA method in their study. Abdullahi [6] proposed a production forecasting model using Structural Time Series Models (STSMs) that considers structural changes in energy for the five main petroleum products consumed and aggregates in Nigeria. In this study, forecast data for the future periods are obtained using the crude oil data of the past months in Turkey. When the literature has been searched, no estimation study with a time series approach was found for crude oil production data in Turkey.

MATERIALS AND METHODS

In this study, monthly crude oil production data covering May 2006-April 2021 (180 months) in Turkey are used. The required dataset is obtained from the JODI-Oil World Database [7]. The Holt-Winters method is used to forecast crude oil production data for future periods. In addition, Holt-Winters additive and multiplicative methods are used for additive seasonality and multiplicative seasonality, respectively [8]. The formulas of approaches are given in Table 1.

Table 1. Holt-Winters Methods

	HoWA	HoWM
L_t	$\alpha(Y_t - S_{t-s}) + (1 - \alpha)(L_{t-1} + B_{t-1})$	$\alpha \frac{Y_t}{S_{t-s}} + (1 - \alpha)(L_{t-1} + B_{t-1})$
B_t	$\beta(L_t - L_{t-1}) + (1 - \beta)B_{t-1}$	$\beta(L_t - L_{t-1}) + (1 - \beta)B_{t-1}$
S_t	$\gamma(Y_t - L_t) + (1 - \gamma)S_{t-s}$	$\gamma \frac{Y_t}{S_{t-s}} + (1 - \gamma)S_{t-s}$
F_{t+m}	$L_t + B_t m + S_{t-s+m}$	$(L_t + B_t m) S_{t-s+m}$
L_t : Level of the series at period t , Y_t : Actual value, S_t : Seasonal component, B_t : Trend component, α : Level constant β : Trend correction constant, γ : Seasonal correction constant, F_{t+m} : Forecast value for m .		

Applying the HoWA and HoWM methods, the fit values of the periods are obtained. After, R^2 , MAPE and RMSE metrics are used to evaluate the model success of the methods. These metrics are given in Eq. (1), Eq. (2), and Eq. (3), respectively [9].

$$R^2 = 1 - \frac{\sum_{j=1}^N (Y_j - \hat{Y}_j)^2}{\sum_{j=1}^N (Y_j - \bar{Y})^2} \quad (1)$$

$$MAPE = \frac{100}{N} \sum_{j=1}^N \left| \frac{Y_j - \hat{Y}_j}{Y_j} \right| \quad (2)$$

$$RMSE = \sqrt{\frac{1}{N} \sum_{j=1}^N (Y_j - \hat{Y}_j)^2} \quad (3)$$

Where, Y_j and \hat{Y}_j are the actual and fitted values, respectively, \bar{Y} is the average value of the dataset, N represents forecast horizon. Finally, the necessary evaluations are made between the methods according to the values obtained, and the 36-month (3 years) crude oil data between May 2021 and April 2024 is estimated.

CONCLUSIONS

Crude oil is a natural and combustible mineral oil extracted from the ground consisting of a combination of various hydrocarbons. In this study, crude oil production in Turkey is examined with the estimation approach. For this purpose, the Holt-Winters method is used for monthly estimation. The predicted values for the 36 months between May 2021 and April 2024 are obtained with the HoWA and HoWM methods. Fit values for past periods are obtained with additive and multiplicative models. Afterward, R^2 , MAPE, and RMSE values are calculated to evaluate model success. In the HoWA method, the metric values are obtained as R^2 : 0.969; MAPE: 1.767; RMSE: 34.705, respectively. In the HoWM method, the metric values are obtained as R^2 : 0.964; MAPE: 1.894; RMSE: 37.312, respectively. According to the metric values (R^2 , MAPE, RMSE), the estimation success is extremely high. When the results are examined, it is seen that there is no significant difference between the two approaches, but the HoWA method is more convenient in terms of model success. In this context, it can be said that the seasonality in the crude oil data set is independent of the trend.

REFERENCES

- [1] Guler E, Yerel Kandemir S, Acikkalp E, Ahmadi MH. Evaluation of sustainable energy performance for OECD countries. *Energy Sources, Part B: Economics, Planning, And Policy*. 2021: 1-24.
- [2] Akpınar E. Baku-Tbilisi-Ceyhan pure oil pipeline (BTC) and its effects on Turkey's geopolitics. *Gazi University Journal of Gazi Educational Faculty*. 2005; 25(2): 229-248.
- [3] Lima C, Relvas S, Barbosa-Póvoa APF. Downstream oil supply chain management: A critical review and future directions. *Computers and Chemical Engineering*. 2016; 92: 78-92.
- [4] Li S, Wang Q. India's dependence on foreign oil will exceed 90% around 2025-the forecasting results based on two hybridized NMGM-ARIMA and NMGM-BP models. *Journal of Cleaner Production*. 2019; 232: 137-153.
- [5] Ozturk S, Ozturk F. Forecasting energy consumption of Turkey by ARIMA model. *Journal of Asian Scientific Research*. 2018; 8(2): 52-60.
- [6] Abdullahi AB. Modeling petroleum product demand in Nigeria using structural time series model (STSM) approach. *International Journal of Energy Economics and Policy*. 2014; 4(3): 427-441.
- [7] JODI-Oil World Database [Internet]. 2021 May 5. Available from: <http://www.jodidb.org/>
- [8] Ribeiro RCM, Marques GT, dos Santos PC. Holt-Winters forecasting for Brazilian natural gas production. *International Journal for Innovation Education and Research*. 2019; 7(6), 119-129.
- [9] Kafieh R, Arian R, Saeezadeh N, Amini Z, Serej ND, Minaee S, Yadav SK, Vaezi A, Rezaei N, Javanmard SH. COVID-19 in Iran: forecasting pandemic using deep learning. *Computational and Mathematical Methods in Medicine*. 2021: 1-16.

ENERGY CONSUMPTION FOR SILAGE MAIZE PRODUCTION IN KOCAELI PROVINCE OF TURKEY

^{1*} Hasan Huseyin Ozturk, ¹ Hakan Goker

¹ Univ. of Cukurova, Fac. of Agriculture Dept. of Machinery and Technologies Engineering, 01330, Balcali, Saricam, Adana, Turkey

*Corresponding author e-mail: hhozturk@cu.edu.tr

ABSTRACT

In this study, total fuel (diesel + motor oil) consumption, energy consumption and carbon dioxide (CO₂) emission in silage maize production in Kocaeli region were evaluated. 195.145 L/ha fuel (Diesel + lubricant oil) is consumed in usage of tools and machinery in silage maize production. For this process, a total of 7241.62 MJ/ha of diesel and motor oil consumption is made. In silage maize production, 535.92 kg CO₂ emission is produced regarding the consumption of 193.28 L/ha diesel and 1.864 L/ha motor oil. In this region, 4.8447 L total fuel (Diesel+lubrication oil) and 179.782 MJ energy were consumed to produce 1 ton of silage maize. In result of total fuel consumption, 13.3049 kgCO₂ is released for 1 ton of silage maize production.

Keywords: Kocaeli, Silage maize, Fuel consumption, Energy consumption, CO₂ emission.

INTRODUCTION

In this study, it was aimed to determine the total energy consumption (diesel+ motor oil) in silage maize production in Kocaeli and to determine the energy efficiency of the production. For this purpose, the processes and fuel consumption in the production of silage maize in the districts of Kocaeli region were examined in detail. The diesel consumption values of the tools and machinery used in the production of silage maize were determined by surveys conducted with experts in the Agriculture and Forestry District Directorates. During the process of silage maize production, efficiency criteria for total fuel (Diesel + lubrication oil) consumption for the tractor engine in the use of equipment and machinery are defined as follows, based on production and consumption and CO₂ emission values.

MATERIALS AND METHODS

Calculation of Total Fuel Consumption: The diesel and engine oil values per unit production area (da) consumed by tractor during silage maize production processes were evaluated as total fuel consumption.

$$TFC=DC+MYT \dots \dots \dots (1)$$

where *TFC*- Total fuel consumption (L/ha), *DC*- Diesel consumption (L/ha), *LOC*- Lubrication oil consumption (L/ha)

Calculation of Lubricant Consumption: Lubrication oil (lubricant) consumption per hour for tractor used in silage maize production operations was determined as follows, depending on the tractor's highest PTO power.

$$LOC=0,00059 \times PTO_{max} + 0.02169 \dots \dots \dots (2)$$

where *LOC*- Tractor lubrication oil consumption per hour (L/h), *PTO_{max}*- Tractor's highest PTO power (kW).

Determination of Total Energy Consumption: The total energy consumption (*TEC*, MJ/ha) pertaining to the consumption of diesel and engine oil per unit production area (da) was determined by the tractor used during silage maize production processes are as follows.

$$TEC=DEC+LEC \dots \dots \dots (3)$$

where *TEC*- The total energy consumption (MJ/ha), *DEC*- Diesel energy consumption (MJ/ha), *LEC*- Lubrication oil energy consumption (MJ/ha)

Calculation of Diesel Energy Consumption: The diesel energy consumption (*DEC*, MJ/ha) related to diesel consumption consumed per unit production area (ha) by the tractor used during silage maize production processes is determined as follows.

$$DEC=DC \times LHV_D \dots \dots \dots (4)$$

where *DEC*- Diesel energy consumption (MJ/ha), *DC*- Diesel consumption (L/ha), *LHV_D*- Lower Heating Value of Diesel (MJ/L).

Calculation of Lubrication Oil Energy Consumption: The lubrication oil energy consumption (*LEC*, MJ/ha) per unit production area (ha) consumed by tractor used during silage maize production processes was determined as follows.

$$LEC=LOC \times LHV_L \dots \dots \dots (5)$$

where *LEC*- Lubrication oil energy consumption (MJ/ha), *LOC*- Lubrication oil consumption (L/ha), *LHV_L*- Lower Heating Value of lubrication oil (MJ/L).

Calculation of CO₂ Emissions: Taking into consideration the lubrication oil consumption value of the tractor engine, CO₂ emissions related to oil consumption can also be calculated. The values given in Table 1 are used for the thermal values of diesel fuel and engine oil and CO₂ emission factors depending on the type of fuel.

Table 1. Thermal Values and CO₂ Emission Factors [1]

Fuel	Lower heating value (MJ/L)	CO ₂ Emission factor (kgCO ₂ /MJ)
Diesel	37.1	0.07401
Lubricant oil	38.2	0.07328

Calculation of total CO₂ Emissions: In calculating the CO₂ emissions released in result of silage maize production, the fuel-based CO₂ emission calculation method proposed in the Intergovernmental Panel on Climate Change was taken into account [1]. The total CO₂ emission (TCO_2E , kgCO₂/ha) pertaining to the consumption of diesel and engine oil per unit production area (da) was determined by the tractor used during production processes as follows.

$$TCO_2E = CO_2E_D + CO_2E_L \dots \dots \dots (6)$$

where TCO_2E - Total CO₂ emission (kgCO₂/ha), CO_2E_D - CO₂ emission related to Diesel consumption (kgCO₂/ha), CO_2E_L - CO₂ emission related to lubricant oil consumption (kgCO₂/ha)

RESULTS AND DISCUSSIONS

The total fuel consumption values are in parallel with the change in the usage time of the tools and machines used in the silage maize production processes and the loading rates of the tractor engine. The highest total fuel consumption occurs in silage maize harvesting operations with value of 33.422 L per unit area (ha). The second place in total fuel consumption is plough tillage applications with a value of 26.695 L/ha. The total fuel consumption in silage maize production, 23.61 L/ha in sowing process with planting machine, 21.77 L/ha in fertilizer intermediate hoeing process, 20.69 L/ha in sprout with disc harrow, 21.98 L/ha in fertilizer distribution process is 19.816 L/ha in cultivation with cultivator, 18.559 L/ha in spraying with sprayer, and 10.283 L/ha in scaling. A total of 195.145 L/ha fuel (diesel + lubrication oil) is consumed in the use of tools and machinery in silage maize production [2]. The total energy consumption values related to the total fuel consumption are in parallel with the change in the usage time of the tools and machines used in the silage maize production processes and the loading rates of the tractor engine. Total energy consumption related to the highest total fuel consumption is realized in silage maize harvesting with 1240.35 MJ per unit area (ha). The second place in energy consumption regarding total fuel consumption is plough tillage applications with a value of 990.8 MJ/ha. Total energy consumption for total fuel consumption in silage maize production is 876.12 MJ/ha, respectively in cultivation process 815.27 MJ/ha, in fertilizer intermediate hoeing process, 775.32 MJ/ha, in cultivation of the disc harrow, 738 MJ/ha, in the fertilizer distribution process, 31 MJ/ha, 735.37 MJ/ha in cultivation with cultivator, 688.67 MJ/ha in spraying with sprayer, and finally 381.41 MJ/ha in plough cultivation. For the use of tools and machinery in silage maize production, a total of 7 241.62 MJ/ha of Diesel and lubrication oil consumption is made [2]. It is observed that the total CO₂ emission values related to the total fuel consumption are in parallel with the change in the usage time of the tools and machines used in the process of silage maize production and the loading rates of the tractor engine. The highest total CO₂ emission related to total fuel consumption is realized in silage maize harvesting processes with 91.79 kgCO₂ per unit area (ha). The second place in CO₂ emission related to total fuel consumption is plough tillage applications with a value of 73.33 kgCO₂/ha. Total CO₂ emission related to total fuel consumption in silage maize production, 64.84 kgCO₂/ha in sowing process, 60.33 kgCO₂/ha in fertilizer intermediate hoeing process, 57.38 kgCO₂/ha in soil cultivation with disc harrow, 54 in fertilizer distribution process, 64 kgCO₂/ha, 54.22 kgCO₂/ha in tillage, 50.96 kgCO₂/ha in spraying with sprayer and 28.23 kgCO₂/ha in tillage. In the use of tools and machinery in the production of maize silage, 535.92 kg of CO₂ emission is realized regarding the consumption of 193.28 L/ha Diesel and 1.864 L/ha lubrication oil [2].

CONCLUSIONS

The total energy consumption for total fuel consumption in silage maize production is 1240.35 MJ/ha in harvesting process with silage machine, 990.8 MJ/ha in tillage with plough, 876.12 MJ/ha in sowing with seed drill, intermediate hoeing with fertilizer 815.27 MJ/ha, 775.32 MJ/ha in tillage with disc harrow, 738.31 MJ/ha in fertilizer distribution, 735.37 MJ ha in tillage, 688.67 MJ/ha in spraying with sprayer and in land cultivation, it is 381.41 MJ/ha.

REFERENCES

- [1] IPCC. Climate Change, 1995: The Science of Climate Change. Contribution of Working Group I to the Second Assessment Report of the Intergovernmental Panel on Climate Change [Houghton., J.T., et al. (eds.)]. Cambridge University Press, Cambridge, United Kingdom and New York, NY, USA, 572 pp;1996.
- [2] Goker H. A Research on Fuel Consumption for Silage Maize Production in Kocaeli Region. C.U. Institute of Natural and Applied Sciences Dept. of Agricultural Machinery and Technologies Engineering, Adana; 2019.

SOLAR ENERGY USE FOR DRIP IRRIGATION OF MAIZE PRODUCTION IN HARRAN PLAIN OF TURKEY

^{1*} Hasan Huseyin OZTURK, ² Hasan Kaan Kucukerdem

¹ Univ. of Cukurova, Fac. of Agriculture Dept. of Machinery and Technologies Engineering, 01330, Balcalı, Sarıcam, Adana, Turkey

² Iğdir University Faculty of Agriculture Dept. of Biosystem Engineering, Iğdir, Turkey

*Corresponding author e-mail: hhozturk@cu.edu.tr

ABSTRACT

In this study, it was aimed to determine the design variables of solar powered drip irrigation systems for maize irrigation under Harran plain conditions. The number of drippers per deca (da) has been determined as 3571 and irrigation period will be done in a way that ends during the day. The power and flow rate of the irrigation pump is calculated as 3 kW and 5.5 m³/h, respectively. The total installed power of the solar energy system is 5 kW.

Keywords: Solar energy, Maize, Drip irrigation, Harran

INTRODUCTION

The main method of supplying water for irrigation purposes is to transport water between the water source and the irrigation area. This movement of water requires some energy. The main purpose of irrigation applications is to provide the water required by the plant in a timely and sufficient amount, with minimum energy and operating costs. The methods used for water pumping use various power sources such as human and animal power, wind, sun and fossil fuels. PV systems are designed specifically for the drinking water supply and agricultural irrigation where electricity cannot be delivered. One of the most promising areas of application for PV systems in countries with a lot of solar radiation, such as Turkey, is to be used as a source of power for the pumping of required water for the sake of a given product. The main advantages of solar powered irrigation (SPI) systems compared to irrigation systems operated by internal combustion engines are that they do not have practical maintenance requirements, they have a long service life, and they do not pollute the fuel requirements and therefore the environment. Another advantage of these systems is that they use solar energy as a source of energy. In irrigation applications, water is most needed when solar radiation is the maximum. This can be considered as an advantage for these systems. SPI systems are being used efficiently for low-pressure drip irrigation applications, which enable efficient use of irrigation water. In this study, it was aimed to determine the design variables of solar powered drip irrigation systems for maize irrigation under Harran plain conditions. The calculations were made for 2 decares (da) production area, total depth 100 m for water source and 1 atmosphere (atm) operating pressure.

MATERIALS AND METHODS

Power of electric motor and pump unit: The power of the electric motor-pump unit in the SPD system (P_{MP}) was calculated as follows [1,2]:

$$P_{MP} = \frac{Q \times H_m \times \gamma}{102 \times \eta_p \times \eta_m} \dots \dots \dots (1)$$

where H_m - total manometric height (m), Q - water flow rate (L/s), P_{MP} - brake power of the pump (kW), γ - specific mass of irrigation water (kg/L), η_p - efficiency of pump (%) and η_e -efficiency of electric motor (%).

The power of the photovoltaic system: The power of the PV system (P_{PV}) that will generate daily required electricity for the drip irrigation system was determined as follows:

$$P_{PV} = \frac{E_{el}}{h} \dots \dots \dots (2)$$

where P_{PV} - power of PV system (kW), E_{el} - the daily electricity generation of the PV system (kWh/day) and h - the daily sunshine duration (h).

RESULTS AND DISCUSSION

For maize production, row spacing distances are taken into account as 0.7 × 0.15 m, and evapotranspiration value as 7 mm/day. The effective root depth for maize plants is 0.9 m, the usable water allowed to be consumed is 30%, the infiltration rate is 8 mm/h and the dripper flow rate is 1.6 l/h for medium-textured soils. The irrigation interval is determined as 7 days, the net irrigation water need for the area to be wetted is 46.47 mm, the net irrigation water need for each irrigation is 6.59 mm/day and the total irrigation water need for each irrigation is 54.67 mm/2 da. The lateral pipe length is 50 m, the number of drippers on each row is 125, one lateral flow rate is 200 l/h and the total lateral flow is 11,42 m³/h for 2 da. The laterals will be arranged as 1 per row. The number of drippers per unit area

(da) has been determined as 3571 and irrigation period will be done in a way that ends during the day. The power and flow rate of the irrigation pump is calculated as 3 kW and 5.5 m³/h, respectively. The pump with 33 stages with a diameter of 1^{1/2} inches should be used. The total installed power of the solar energy system is 5 kW.

CONCLUSIONS

In a growing season in the Harran plain, since the corn is irrigated with the furrow irrigation method, the fertile layer in the upper layer of the soil flows into the drainage channels together with the irrigation water. Considering that the formation of the fertile soil layer at the top of the soil takes 100 thousand years, this situation can be considered as a great loss. In the Harran plain, it has been determined that the ground water rises, and the salinity increases in some production areas due to wild irrigation (furrow and pan). Modern irrigation methods (drip and sprinkler system) should be adopted in all production areas immediately. The tassel flowering period is the most sensitive period in the corn plant. During this period, it was determined that the production areas in the region were not sensitive to irrigation. In order to maintain the vitality of the pollen in the tassel flowers, the plant must be watered during this critical period and the root zone must be moist. In order for the plant to meet the moisture lost by transpiration due to the air temperatures through the roots, the humidity in the root zone must be high. In this regard, the regional farmer should follow up technically.

REFERENCES

- [1] Cuadros F, Rodriguez FL, Marcos A, Coello J. A procedure to size solar-powered irrigation (photoirrigation) schemes. *Solar Energy* 2004, 76, 465–473.
- [2] Glasnovic Z, Margeta J. A model for optimal sizing of photovoltaic irrigation water pumping systems. *Solar Energy*, 2007, 81:904–916.

EXERGY ANALYSIS OF A STEAM POWER PLANT AT FULL AND PARTIAL LOAD CONDITIONS

^{1*} Uchenna G. Azubuikwe, ² Howard O. Njoku, ³ Onyemaechi V. Ekechukwu

^{1, 2, 3} Applied Renewable & Sustainable Energy Research Group, Department of Mechanical Engineering, University of Nigeria, Nsukka 410001, Nigeria.

*Corresponding author e-mail: uchennaazubuikwe009@gmail.com

ABSTRACT

An exergy analysis of a 220MW steam power plant was performed in order to compare performances under full and partial operating load conditions. Design data for four different operation loads, i.e., 220MW load (100%), 165MW load (75%), 110MW load (50%) and 55MW load (25%) were obtained from the plant and used for the exergy computations. The results showed that at 25% load, condenser has the lowest exergetic efficiency of 40.29% compared to other components, whereas at 25% load the drain cooler has the highest exergetic efficiency of 53.61% compared to other loads in the component. The boiler has the lowest exergetic efficiencies across the four loads, i.e., 41.7% (25% load) to 42.8% (100% load), and the highest exergy destructions, followed by the turbines. For the entire plant, overall exergy destructions decreased as operation loads decreased. Exergetic efficiencies similarly decreased from 33.18% at 100% load to 28.29% 25% load.

Keywords: exergy efficiency, steam power plant, plant loads.

INTRODUCTION

Thermal power plants generate electrical energy by the conversion of primary energy. Due to the inefficiencies of installed power plants and the high demands for electrical energy, exergy analyses are frequently required for the plant's improvement. Dang et al. [1] carried out exergy analysis on a 600MW steam power plant for two different loads, i.e., at design load (100% load) and off load (70% load). The results showed that decreasing the load from the design load decreases the exergetic efficiency of the plant. Akilu and Syed [2] studied the performance of a 4.2MW gas turbine plant for varied load of 50% less than the design load. The results showed that the exergy destruction in the components of the plant increases from the 50% off load to full load, except for the compressor. In this study, the partial operating loads of a 220MW steam power plant will be varied from the design operating load to 25% off operating load to analyze the performances of the individual components and the overall power plant.

ANALYSIS

The plant considered is a 220MW unit at the Egbin Thermal Power Plant (ETPP) located in Lagos (Nigeria). The condensate pump (P1), feedwater pump (P2), drain cooler (DC), low pressure heaters (LPH1, LPH2 and LPH3), deaerator (DE), high pressure heaters (HPH5 and HPH6), boiler (Bo), turbines (HPT, IPT and LPT) and condenser (CD) of the unit were considered. The governing equations used were Eqs. (1) to (3) as stated by Bejan et al. [3]. Eq. (1) is the exergy flow rate in a k^{th} component. Eq. (2) is the exergy balance given in terms of fuel ($\dot{\Xi}_{F,k}$) and product ($\dot{\Xi}_{P,k}$) exergies, where $\dot{\Xi}_{D,k}$ is the exergy destruction. While Eq. (3) is the exergetic efficiency (ϵ_k) of the k^{th} component.

$$\dot{\Xi}_k = m[(h - h_0) - T_0(s - s_0)] + (\sum x_n \epsilon_{ch,n} + RT_0 \sum x_n \ln x_n) \quad (1)$$

$$\dot{\Xi}_{F,k} = \dot{\Xi}_{P,k} + \dot{\Xi}_{D,k} \quad (2)$$

$$\epsilon_k = \frac{\dot{\Xi}_{P,k}}{\dot{\Xi}_{F,k}} = \frac{\dot{\Xi}_{P,k}}{\dot{\Xi}_{P,k} + \dot{\Xi}_{D,k}} \quad (3)$$

Data of pressure, temperature, mass flow rates of (steam, natural gas), enthalpies entering and exiting the components of the unit were obtained for full load (i.e., 100%), $\frac{3}{4}$ load (75%), $\frac{1}{2}$ load (50%) and $\frac{1}{4}$ load (25%). The computations were carried out using the Scilab computational software. Fig. 1 shows the $\dot{\Xi}_{D,k}$ and ϵ_k for the different loads. The figure shows that $\dot{\Xi}_{D,k}$ at design load are highest compared to that of the partial loads for all the components except in HPT where $\dot{\Xi}_{D,k}$ is highest at 50% load. $\dot{\Xi}_{D,k}$ at 25% load are lowest in all the components except P2 and HPT. The boiler has the highest $\dot{\Xi}_{D,k}$ and lowest ϵ_k across the loads, i.e., 41.7% (25% load) to 42.8% (100% load). P1 and DC have the lowest $\dot{\Xi}_{D,k}$ while P1 and HPH6 are the most efficient components across the loads. At 25% load, CD has the lowest ϵ_k of 40.29%, whereas at 25% load DC has the highest ϵ_k of 53.61% compared to other loads in the component. Fig. 2 shows the overall fuel exergy ($\dot{\Xi}_{F,ov}$), overall product exergy ($\dot{\Xi}_{P,ov}$), overall exergy destruction ($\dot{\Xi}_{D,ov}$), and overall exergetic efficiencies (ϵ_{ov}) of the various loads. From the figure it is shown

than $\dot{\Sigma}_{F,ov}$, $\dot{\Sigma}_{P,ov}$, $\dot{\Sigma}_{D,ov}$ and ϵ_{ov} decrease as the loads decreases where ϵ_{ov} decreased from 33.18 % (100% load) to 28.29% (25% load).

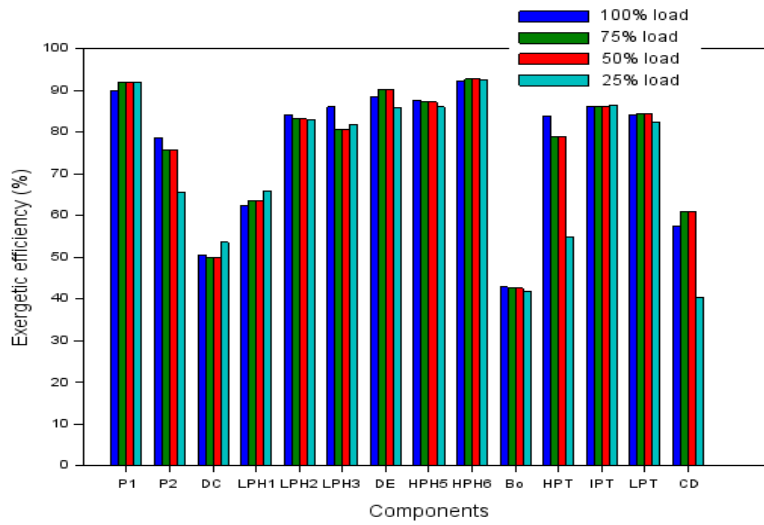


Figure 1: Exergy destructions and exergetic efficiencies of the components.

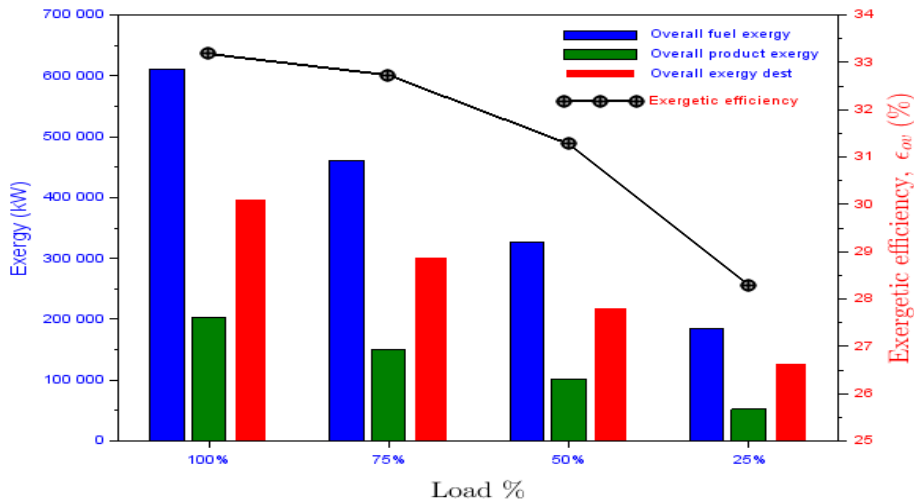


Figure 2. Overall exergy destructions, fuel exergy, product exergy at design (100%) and partial loads of ETPP.

CONCLUSIONS

In the component level, P1 and DC have the lowest $\dot{\Sigma}_{D,k}$ while P1 and HPH6 are the most efficient components across the loads. The boiler has the highest $\dot{\Sigma}_{D,k}$ with about 87% of the total $\dot{\Sigma}_{D,k}$ and also the lowest ϵ_k of about 41.7 – 42.8% across the different loads. This is followed by HPT and LPT. In the overall plant, $\dot{\Sigma}_{D,ov}$ and ϵ_{ov} decreases as the load decreases with ϵ_{ov} decreased from 33.18 % (100% load) to 28.29% (25% load).

REFERENCES

- [1] Dang R, Mangal S.K, Gaurav S. Energy and exergy analysis of thermal power plant at design and off design loads. *International advanced research journal in science, engineering and technology* 3(5) 29-36, 2016.
- [2] Aklilu T.B, Syed I.G. Exergy based performance analysis of a gas turbine at part load conditions. *Journal of applied sciences* 11(11) 1994-1999, 2011.
- [3] Bejan A, Tsatsaronis G, Moran M. Thermal design and optimization. John Wiley & Sons, Inc., New Jersey, 4th edition, 1996.

ACTIVATED CARBON-DECORATED SPHERICAL TITANIUM OXIDE NANOPARTICLES FOR ENHANCED HYDROGEN PRODUCTION

Sankar Sekar^{1, 2}, Deuk Young Kim^{1, 2}, and Sejoon Lee^{1, 2, *}

¹Quantum-functional Semiconductor Research Center, Dongguk University-Seoul, Seoul 04620, Republic of Korea

²Department of Semiconductor Science, Dongguk University-Seoul, Seoul 04620, Republic of Korea

*Corresponding Author: sejoon@dongguk.edu

ABSTRACT

The high-performance photocatalysts are dynamic for enhancing the hydrogen production for solar energy-driven sulphide wastewater degradation. Herein, we report the synthesis of narthangai leaves (*Citron Sp.*) derived activated carbon (AC)-decorated titanium oxide nanoparticles (TiO₂@AC) nanocomposites via simple sol-gel technique tailed by ultrasonication process. The TiO₂@AC nanocomposites reveal accumulated particle-like structure with anatase phase of TiO₂. The TiO₂@AC nanocomposites show an improved hydrogen production activity (400 mL/h), because of the synergic effect between the high conductivity AC and the interconnected TiO₂ nanoparticles. The results support that the TiO₂@AC nanocomposites are beneficial for future green energy conversion applications.

Keywords: TiO₂, Biomass, Activated carbon, Hydrogen production, wastewater.

INTRODUCTION

Hydrogen is one of the most prominent renewable and green energy resources because of its high combustion efficiency, carbon-free emission, and eco-friendliness. Among the various hydrogen production techniques, solar photocatalytic hydrogen production is one of the cost-effective and sustainable methods for generating hydrogen from industrial sulphide-containing wastewater [1].

Recently semiconductor metal oxides-based photocatalyst has gained significant attention because of their simple structure, mild reaction conditions, low energy consumption, and high catalytic activity. TiO₂ is used as an effective photocatalyst because of its chemically stable, inexpensive, strong oxidizing power, high photocatalytic stability, and non-toxic. Currently, carbon-based materials were used as composite materials for improving photocatalytic hydrogen production activity. Despite such enormous benefits, the nanocomposites of narthangai leaves-derived AC-decorated titanium oxide have not been studied for hydrogen production from the sulphide wastewater through solar irradiation.

Herein, we report on the synthesis of TiO₂@AC nanocomposites via the sol-gel method and subsequently by the ultrasonication process using TiO₂ nanoparticles and AC nanoflakes. The TiO₂@AC nanocomposites showed an excellent photocatalytic hydrogen production performance (400 mL/h) compared with pristine TiO₂ nanoparticles (275 mL/h).

MATERIALS AND METHODS

For the fabrication of TiO₂@AC, firstly, the TiO₂ nanoparticles (1 g) and AC nanoflakes (0.5 g) were mixed with 100 ml of DI water. Then, the mixture solution was sonicated for 1 h (UD-211 ultrasonic disruptor). After sonication, the solution was washed with DI water and dried at 130 °C in an electric oven for 10 h. Finally, the fine TiO₂@AC nanocomposites were achieved.

The photocatalytic hydrogen production of TiO₂ nanoparticles and TiO₂@AC nanocomposites was performed by a trapezoidal reactor under solar irradiation as shown in Figure 1. All the investigation were carried out for 1 h. The average solar irradiance was calculated to be 850 W/m² through using an LX-101A lux meter. The synthetic sulphide wastewater (1 L) was used as a photolytic solution. After that, the prepared photocatalysts were mixed with the photolytic solution. The effects of the sulphide ion (0.1–0.3 M), sulphite ion (0.1–0.3 M), and photocatalyst concentrations (0.05 to 0.25 g/L) on the superior production performance of hydrogen were determined. The inverted measuring cylinder was used to calculate the hydrogen production rate [2]. The peristaltic pump was used to hold the photocatalyst under suspension.

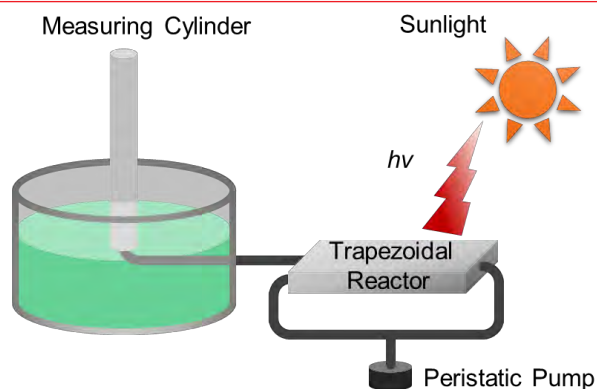


Figure 1. Schematic illustration of the photocatalytic trapezoidal reactor.

CONCLUSIONS

The nanocomposites of $\text{TiO}_2@\text{AC}$ were effectively synthesized *via* the sol-gel process and trailed by ultrasonication technique. The $\text{TiO}_2@\text{AC}$ nanocomposites revealed an aggregated structure of TiO_2 nanoparticles-anchored AC nanoflakes. The $\text{TiO}_2@\text{AC}$ photocatalysts exhibited an excellent hydrogen production rate performance (400 mL/h) with excellent reusability. These consequences describe that the $\text{TiO}_2@\text{AC}$ nanocomposites are beneficial for recycling sulphide wastewater through photocatalytic hydrogen production.

ACKNOWLEDGEMENTS

This research was supported by National Research Foundation (NRF) of Korea through the basic science research programs (2016R1A6A1A03012877 and 2019R1A2C1085448) funded by the Korean Government.

REFERENCES

- [1] Ahmad, H., et al., Hydrogen from photo-catalytic water splitting process: A review. *Renew. Sust. Energ. Rev.*, 2015. 43: p. 599-610.
- [2] Sekar, S., et al., Upcycling of Wastewater via Effective Photocatalytic Hydrogen Production Using MnO_2 Nanoparticles—Decorated Activated Carbon Nanoflakes. *Nanomaterials*, 2020. 10(8): p. 1610.

BIOCHAR: PHYSICAL PROPERTIES AND EFFECTS ON THE SOIL

^{1*} Mehmet Hakkı Alma, ¹ Alperay Altıkat, ¹ Sefa Altıkat

¹İğdır University Agricultural Faculty Department of the Biosystems Engineering, İğdır University, İğdır, Turkey

*Corresponding author e-mail: mhalma46@gmail.com

ABSTRACT

Biochar is a material with high carbon content produced thermochemical transformation processes of feedstock. It has been used industrial and environmental sectors and as a soil conditioner for problematic soils. Among the physical properties of biochar, the features such as surface area, bulk density, porosity, and water holding capacity come to the fore. These features interact with each other. The factors such as pyrolysis temperature, heating rate, residence time and gas flow rate used in the production phase of biochar change the properties of biochar. The positive changes occur in the physical quality of the soil if mixing of biochar into the soil. In addition, due to biochar, the carbon is added into the soil and this carbon can remain intact for years. Besides, biochar leads to an increase in the crop yield and the rate of CO₂ emitted from the soil to the atmosphere decreases. In this study, some physical properties of biochar and its effects on soil were investigated.

Keywords: Biochar, Phyrolysis, Surface area, Porosity, Soil

INTRODUCTION

Biochar is a carbon-rich and dissolution-resistant material obtained from thermal degradation of organic material under oxygen-free or low oxygen conditions and generally at low temperatures. Biochar is a combustion product with a high carbon content that is formed by burning organic material in thermochemical conversion processes under oxygen-free or limited oxygen conditions. Thermochemical transformation can be defined as controlled heating or oxidation of biomass using intermediate energy carriers or various methods for generating heat. The concept of thermochemical conversion of biomass covers many different methods, from burning biomass, which is one of the simplest and oldest examples of energy use, to technologies used for the production of liquid vehicle fuels and chemical raw materials. Thermochemical processes can be classified into various methods that can vary from heating biomass in an endothermic to full exothermic oxidation of biomass. Although biochar depends on the production conditions, it contains between 60% and 80% C in its content. Because of this feature, it can be applied as a soil regulator to agricultural soils with low carbon content. Many studies have examined the effects of biochar on agricultural soils. According to the obtained results, the application of the biochar into the soil increases the carbon content of soil [1] and crop yield [2], reduces the emission of CO₂ from soil to the atmosphere. In addition, the application of the biochar increases the physical, biological, and chemical quality of soil [3]. Aggregate size distribution of soil is an important factor that allows biochar to be effective on soil properties. Studies have determined that the effect of biochar on soil physical properties is more pronounced in coarse-textured soils than in normal textured soils [4]. In this study, the basic physical properties of biochar and its effects on soil were examined.

SURFACE AREA OF THE BIOCHAR

The surface area (SA) of biochar is determined by BET analysis. In most of the studies, it has been determined that there is a positive relationship between the SA and the pyrolysis temperature. However, for some raw materials, an increase in temperature may not cause an increase in SA. The reason for this is the deterioration of the micropore structure of some raw materials at high phrolysis temperatures. Therefore, carbonization temperature is not the only factor affecting SA. Heating rate, pressure and residence time in the reactor also have an effect on SA during the production phase.

POROSITY OF THE BIOCHAR

Biochar has macro and micropores. Macropores (1000–0.05 μm) are observed due to the vascular nature of the biomass used. Micropores (0.05–0.0001 μm) are formed as a result of operating parameters such as heating rate, residence time and gas flow rate used in the production phase. Micropores constitute 80% of the porous structure of biochar. The excess of micropores on biochar cause an increase in sorption properties. As the temperature increases, the porosity of the biochar increases. There is a positive relationship between the SA of biochar and the micropore ratio.

WATER HOLDING CAPACITY (WHC) OF THE BIOCHAR

Changes in the functional groups of the biomass during pyrolysis lead to the formation of a porous structure and increase the WHC. In the researches, it was concluded that the increase in the pyrolysis temperature will also increase the WHC of biochar. However, in some studies, no increase in the WHC of biochar was observed at temperatures >500°C. This result is thought to be caused by the degradation of aliphatic functional groups at temperatures >500°C.

EFFECTS OF BIOCHAR ON THE SOIL

Today, livestock and poultry manures whose disposal is difficult and expensive, agricultural wastes, wood wastes from forestry, pulp production, packaging or carpentry, agricultural enterprise wastes, and plants that are specially grown for biochar are among the raw materials of biochar. In the studies conducted, it was determined that the biochar produced as a result of different thermochemical conversion processes has many advantages.

Biochar helps plant growth and increases crop yield. It improves the physico-chemical, and biological quality criteria of the soil and increases its nutritional values when applied and mixed in certain proportions to problematic soils. It reduces greenhouse gas emissions from crop production, helps the soil store carbon, and ensures that the stored carbon remains stable in the soil for years. By adsorbing chemicals used in agricultural production, it prevents their mixing into streams and groundwater, thus helping sustainable agricultural production. It plays an important role in reducing the use of compost with chemical and organic fertilizers. It prevents plants from taking pesticides in the soil at the stage of development. In soils with low porosity, it prevents the washing of nutrients, especially in rainy weather conditions. It helps to consume less water by improving the ability of soil to retain moisture. It increases the proportion of some fungi that positively affect plant development in the soil and improve soil quality. In processed soils, CO₂ reduces the emission of CH₄ and N₂O gases into the atmosphere, thus making a positive contribution to global warming.

To make maximum use of these advantages of biochar, it is necessary to mix them into the lower layers of the soil using appropriate methods. The number of scientific studies on mixing biochar with soil is quite limited. The general practice is to lay on the soil surface manually and mix it with disc harrow and soil milling machines. In cases of the obligation to mix in sowing depth, there are studies in which direct sowing machines to the stubble have been used. In the application of biochar in gardens, biochar is usually added to the furrows that open to the roots of trees and they are covered with soil. Mixing biochar with organic fertilizers or different composts and soil assures the increase of its effectiveness.

The number of field experiments conducted to study the effects of biochar on soil properties is quite limited. Most of the research conducted was managed in laboratory or greenhouse conditions. It will not be possible to determine the effects of biochar on soil physical properties without researching field conditions. In addition, different soil conditions (different C content and soil temperature), different management practices biochar (new or old biochar, volume, weight, and raw materials), involving interactions with organic or inorganic fertilizer research is also needed. In most of the studies, the biochar was mixed to a depth of about 15 cm in the soil and the changes in the soil physical properties were studied. The effects of biochar, which will be applied to different soil depths, are unknown. This is a very important issue for determining the effects of water stored in soil lower layers and nutrients necessary for plant development. In addition, further research into the economic analysis and environmental effects of biochar application is an important issue for the effectiveness and sustainability of the system.

CONCLUSIONS

Biochar is a product with high carbon content obtained as a result of different thermochemical processes of the biomass. It increases the soil carbon content. Biochar-derived carbon can remain in the soil for many years without decomposition. Its physical properties vary depending on some factors. Among these factors, pyrolysis temperature, heating rate, residence time and gas flow rate are important operating parameters and have a direct effect on the biochar properties. In addition, the type of raw material, particle size and moisture content of the raw material are among the factors that affect the properties of the biochar. Especially the pyrolysis temperature used in the production stage effective on the physical properties of it. It has been concluded that the increase in pyrolysis temperature improves the physical properties. Due to the high adsorbent property and porous structure, it is able to adsorb pollutants in both water and soil. Furthermore, it reduces soil compaction due to the size of the surface area and low bulk density. When mixed into the soil, it improves the WHC, infiltration rate, aggregate stability and porosity of the soil.

REFERENCES

- [1] Lehmann J, Rillig MC, Thies J, Masiello CA, Hockaday WC and Crowley D (2011). Biochar effects on soil biota: a review. *Soil Biol. Biochem.*, 43:1812–1836.
- [2] Brassard P, Stephane G and Vijaya R (2016). Soil biochar amendment as a climate change mitigation tool: key parameters and mechanisms involved. *J. Environ. Manage.*, 181:484–497.
- [3] Ding Y, Liu YG, Liu SB, Li ZW, Tan XF and Huang XX (2016). Biochar to improve soil fertility: A review. *Agron. Sustain. Dev.*, 36:12-18.
- [4] Omondi MO, Xia X, Nahayo A, Liu X, Korai PK and Pan G (2016). Quantification of biochar effects on soil hydrological properties using meta-analysis of data. *Geoderma* 274:28–34.

BIO-OIL SEPARATION AND UPGRADING TECHNIQUES

^{1*} Mehmet Hakkı Alma, ¹ Alperay Altıkat, ¹ Sefa Altıkat

¹İğdir University Agricultural Faculty Department of the Biosystems Engineering, İğdir University, İğdir, Turkey

*Corresponding author e-mail: mhalma46@gmail.com

ABSTRACT

Bio-oil produced from agricultural wastes, organic urban wastes and forest wastes can be used instead of fossil fuels thanks to various separation and upgrading methods. The pyrolysis oil releases during the production phase uses in many applications as a renewable fuel. Bio-oil has high water content and viscosity. In addition, the pH value of bio-oil is low. For these reasons, it is not suitable for direct use as fuel. Some separation and upgrading methods must be applied for uses as a fuel. In this study, the separation and upgrading methods applied to use bio-oil as an alternative to conventional fuels were investigated. For this purpose, in the separation of bio-oil; distillation, solvent extraction and column chromatography methods were investigated. As upgrade methods: filtration, solvent addition, emulsification, esterification, zeolite, hydrodeoxygenation, steam reforming and supercritical fluids methods were investigated.

Keywords: Bio-oil, Upgrading, Separation, Fuel, Biomass

INTRODUCTION

Bio-oil composes of liquid and solid particles and contains multitude of organics [1]. The calorific value of bio-oil varies between 16-19 MJkg⁻¹ [2]. Bio-oil is obtained from the pyrolysis of biomass, if properly produced and processed, can replace fossil fuel [3]. The proportional distribution of the cellulose, hemicellulose and lignin in the raw material affects the bio-oil quality. Generally, the fast pyrolysis and hydrothermal liquefaction (HTL) methods use for biochar production. The most common and economical use among these is the fast pyrolysis process. Although fast pyrolysis is frequently used in production, HTL method has become a preferred method against fast pyrolysis, especially in parallel with the improvement in bio-oil quality. Besides the method is still in development stage. The temperature and pressure in the HTL are in the range of 250°C-374°C, 4MPa-22 MPa, respectively. However, especially the high-pressure requirement of the HTL process reduces the possibility of widespread use and preference of the method. In this study, the separation and upgrade methods of bio-oil to be used as an alternative fuel were examined in detail.

THE SEPARATION OF THE BIO-OIL

Conventional methods such as solvent extraction, distillation, and column chromatography are mostly used for the separation of the bio-oil.

DISTILLATION

The purpose of distillation is to remove the water from the bio-oil. In distillation processes, azeotropic [52], atmospheric pressure, steam and vacuum distillation methods [53,54] are used. Another distillation method is molecular distillation. The molecular distillation method has advantages such as low operating temperature, low heating rate and high efficiency.

SOLVENT EXTRACTION

Biooil contains many different chemical compounds. Solvent extraction method is used to separate these compounds. For this purpose, solvents with different properties such as water, acetate, ketone are used. Solvents such as diethyl ether and dichloromethane are used to separate acetic acid and phenolic compounds in bio-oil. The separated acetic acid is used in the production of hydrogen.

COLUMN CHROMATOGRAPHY

In this method, the components are separated by adsorption. The polarity of the components is taken into account in the selection of the carrier. In this method, eluent is used as a mobile phase carrier. Different eluents such as hexane, toluene, benzene, pentane, ethyl acetate, and methanol can be used. Eluent selection is made by considering the polarity of the compounds.

BIO-OIL UPGRADE METHODS

Bio-oil upgrading methods can be examined in 3 categories as physical, chemical and other (fig.1.). Information about the methods and their limitations is given in Table 1.

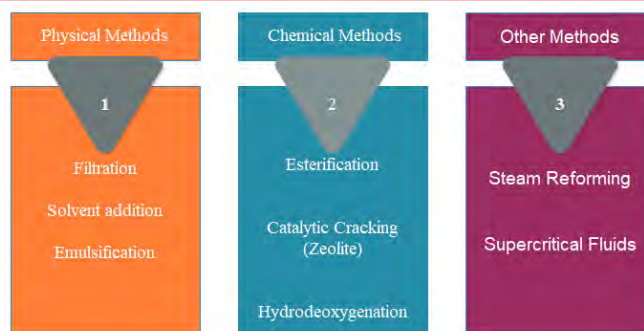


Figure 1. Bio-oil upgrading methods

Table 1. Bio-oil upgrading methods and limitations [4]

Upgrading method and decription	Liimitation
1. Hot vapor filter: Ash particles are separated from steam	In this method, the oil yield decreases and iron concentration increases. Fluctuations in pressure level occur at the processes.
2. Solvent addition: More homogeneous bio-oil is obtained. The viscosity and density of the oil decreases	Flash point decreases. Solvent addition is a rather complicated process.
3. Emulsification: In this method, the calorific value of the bio-oil increases and the water content decreases.	Corrosion is a major problem. The cost of refining emulsifiers from bio-oil is high.
4. Esterification: Carboxylic acids are removed from the bio-oil. The stability of the bio-oil increases, its corrosive effect and acidity decrease.	In this method the bio-oil yield is low.
5. Catalytic Cracking (zeolite): In this method, oxygen-containing compounds are removed from the bio-oil.	The H/C ratio in bio-oil is reduced. Blockages occur in the reactor.
6. Hydrodeoxygenation: The oxygen in the bio-oil is removed by pressurized hydrogen. The viscosity of the bio-oil decreases and its heating value increases.	High pressure hydrogen is needed. It is a costly method.
7. Steam reforming: It is a method used for the production of hydrogen	The stability of the catalyst is very short.
8. Supercritical fluids: In this method, the heating value of the bio-oil is increased, and its acidity is reduced.	Solvents are expensive.

CONCLUSIONS

Different techniques are used to separate specific compounds in biooil. Distillation, solvent extraction, column chromatography methods are used as traditional separation techniques. Molecular distillation and supercritical liquid extraction techniques are classified as new methods and their efficiency is higher than traditional methods. To use bio-oil as an alternative fuel to conventional fuels, it must undergo a series of processes involving physicochemical and catalytic processes. For example, solvent addition and emulsification methods can be used to improve the stability of bio-oil. While choosing these methods, economy and efficiency should be kept in the foreground. For example, although the esterification method is economical, its efficiency is low. Catalytic cracking methods (such as hydrodeoxygenation, zeolite cracking and steam reforming) can be listed among the new methods used in the upgrading of bio-oil. Steam reforming can be used to produce syngas and H₂ from the hydrocarbon fuels.

REFERENCES

- [1] Lu Q, Li WZ, Zhu XF. (2009). Overview of fuel properties of biomass fast pyrolysis oils. *Energy Convers. Manag.* 50(5):1376-83.
- [2] Mohan D, Pittman Jr CU, Steele PH. (2006). Pyrolysis of wood/biomass for bio-oil: a critical review. *Energy Fuels.* 20(3):848-889.
- [3] Yang Y, Brammer JG, Samanya J, Hossain AK, Hornung A. (2013). Investigation into the performance and emissions of a stationary diesel engine fuelled by sewage sludge intermediate pyrolysis oil and biodiesel blends. *Energy*, 62:269-276.
- [4] Panwar N.L., Paul A.S. (2021). An overview of recent development in bio-oil upgrading and separation techniques. *Environ. Eng. Res.*,26(5): 200382

INFLUENCE OF BIOHYDROGEN PRODUCTION ON THE RATIO OF GENERATED ACIDS AND REGULATION OF ΔpH IN *E. coli* DURING FERMENTATION OF MIXED CARBON SOURCES AT pH 7.5

Heghine Gevorgyan^{*1,2,3} and Karen Trchounian^{1,2,3}

¹ Yerevan State University, Faculty of Biology, Department of Biochemistry, Microbiology and Biotechnology, Faculty of Biology, 1 Alex Manoogian, 0025 Yerevan, Armenia

² Yerevan State University, Faculty of Biology, Scientific-Research Institute of Biology, 1 Alex Manoogian, 0025 Yerevan, Armenia

³ Yerevan State University, Microbial Biotechnologies and Biofuel Innovation Center, 1 Alex Manoogian, 0025 Yerevan, Armenia

*Corresponding author e-mail: heghine.gevorgyan@ysu.am

ABSTRACT

In this study the role of H₂ in the ratio of generated acids and ΔpH regulation in *Escherichia coli* during the mixed carbon sources (glucose, glycerol, formate) fermentation was investigated. Externally added formate (10 mM) was utilized by wt cells ~2.6 mM during the lag phase, which decreased the value of intracellular pH (pH_{in}) by ~0.1 units at 3 h of growth, compared to *fdhF* mutant (Fig. 1, Table 1). Meanwhile, ΔpH maintained similar -0.26 in both wt and *fdhF* strains. Due to H₂ generation produced from 3 h internal formate was neutralized in wt. Whereas, in *fdhF* formate excreted out, which led to acidification of pH_{ex} by ~0.1 and pH_{in} by ~0.28 units at 6 h. This resulted in the vital perturbation of ΔpH in *fdhF*, compared to wt (by ~0.29 units). The external formate concentration remained elevated by ~16 mM and ~50 mM in *fdhF* at 20 h and 72 h, accordingly. This phenomenon was coupled by the low generation of acetate and lactate. As a result, changes in the ΔpH perturbation were decreased at 24 h (by ~0.08 units) and 72 h (by ~0.02 units).

Keywords: molecular hydrogen, fermentation, ΔpH , formate dehydrogenase H

INTRODUCTION

Nowadays, molecular hydrogen (H₂) generation by biological means is remarkable, as the optimization of the medium conditions during bacterial growth will provide with alternative and renewable source of energy [1]. *Escherichia coli* utilize the mixture of carbon sources and produce H₂ via formate hydrogen lyase (FHL) complexes [2]. FHL-1 and FHL-2 are composed of formate dehydrogenase H (Fdh-H) with hydrogenase-3 and hydrogenase-4, accordingly. During fermentation of glucose and glycerol the same end-products, such as formate, acetate, lactate, succinate and ethanol are generated in different ratios [2]. It is important to understand the role of H₂ in metabolic flux formation to regulate and improve H₂ generation technology.

MATERIALS AND METHODS

In this study *E. coli* BW 25113 wt (*rrnB* $\Delta\text{lacZ4787}$ *HsdR514* $\Delta(\text{araBAD})567$ $\Delta(\text{rhaBAD})568$ *rph-1*) and JW2701 (ΔfdhF) mutant defective in Fdh-H strains were used [3]. Bacterial growth medium consists of 20 g L⁻¹ peptone, 15 g L⁻¹ K₂HPO₄, 1.08 g L⁻¹ KH₂PO₄, 5 g L⁻¹ NaCl (pH 7.5) with addition of glucose (11.1 mM), glycerol (137 mM) and sodium formate (10 mM) [2]. Overnight anaerobically grown cultures were added into the growth medium and were cultivated at 37°C for 3, 6, 24 and 72 h.

Utilization of substrates and generation of fermentation end-products were determined by the HPLC [2]. The system used was Agilent 1260 Infinity II LC Bio-inert with a refractive index detector (Agilent RID, G1362A, set on positive polarity and optical unit temperature of 55°C). Using Agilent OpenLAB CDS data processing was carried out. Macherey-Nagel EC 250/4.6 NUCLEOSIL 120-5 C18 column (250 x 4.6 mm, MN720041.46, Düren, Germany) was selected for analysis. The column was purged with acetonitrile/ water (80/20) at 60°C overnight and then regenerated with a mobile phase (5mM sulfuric acid in ddH₂O) for a few hours to make experimental condition.

For the measurement of external media pH (pH_{ex}) during bacterial growth pH-meter with selective pH-electrode (HI1131, Hanna Instruments, Portugal) was used. Intracellular pH (pH_{in}) was determined using 9-aminoacridine fluorescent dye (9-AA, with excitation at 390 nm and emission at 460 nm) [2]. The uptake of 9-AA by bacterial cells was determined from the quenching of fluorescence (Cary Eclipse, Agilent Technologies, USA). ΔpH was calculated as the difference of pH_{in} and pH_{ex} [2].

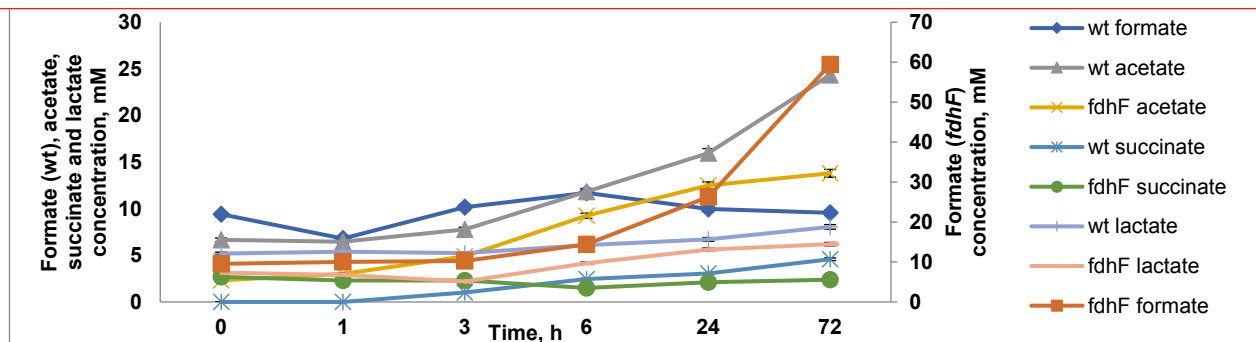


Figure 1. Generation of fermentation end-products by *E. coli* wt and *fdhF* mutant strain grown at pH 7.5. For others see Materials and Methods.

Table 1. Values of pH_{in} , pH_{ex} and ΔpH in *E. coli* wt and *fdhF* mutant strain grown at pH 7.5. For others see Materials and Methods.

Time, h	wt			<i>fdhF</i>		
	intracellular pH	extracellular pH	ΔpH	intracellular pH	extracellular pH	ΔpH
3	6.85	7.114	-0.264	6.75	7.003	-0.253
6	6.49	6.72	-0.23	6.21	6.81	0.06
24	6.77	6.665	0.105	6.784	6.6	0.184
72	7.267	6.532	0.735	7.15	6.433	0.717

CONCLUSIONS

In this study generation of fermentation end-products, ΔpH regulation and the role of H_2 production in the mentioned processes were studied. The lack of external formate absorption in *fdhF* is explained by the absence of the enzyme responsible for the formate degradation. Data received show that H_2 generation has a vital impact on the formation of both metabolic fluxes and ΔpH regulation. Moreover, bacteria regulate ΔpH through the variation of the concentration of the generated acids.

REFERENCES

- [1] de Valladares. Global Trends and Outlook for Hydrogen, *IEA Hydrogen Technology Collaboration Program (TCP)*, 2017.
- [2] Gevorgyan H., Khalatyan S., Vassilian A., Trchounian K. The role of *Escherichia coli* FhIA transcriptional activator in generation of proton motive force and F_0F_1 -ATPase activity at pH 7.5. *IUBMB Life*. 2021, 73 (6): 883-892.
- [3] Gevorgyan H., Trchounian A., Trchounian K. Formate and potassium ions affect *Escherichia coli* DCCD-sensitive ATPase activity at low pH during mixed carbon fermentation. *IUBMB Life*. 2019, 72, 915-921.

MATHEMATICAL MODELLING OF ADSORPTION ISOTHERMS FOR POROUS BED WITH AXIAL DISPERSION MODEL

¹Manigandan Sidhareddy, ^{1,*}Sumit Tiwari

¹Shiv Nadar University, Department of Mechanical Engineering, Tehsil Dadri, Gautam Buddha Nagar, Uttar Pradesh, India

*Corresponding author e-mail: tiwsumit@hotmail.com

ABSTRACT

In this work, the transient analysis of adsorption of zeolite water-pair has been presented using PDE interface of commercial COMSOL package. The Axial Dispersion model with combination of Linear Driving Force (LDF) model is applied with different isotherms like Langmuir, Freundlich and Sips isotherm and the comparison study is carried out. From the Study its seen that the Langmuir isotherm predicts good compared to other isotherms. The study is to be further extended to perform adsorption with different modified isotherms. The regeneration of desiccant with integration of ultrasonic energy and heat (solar/waste) energy is to be carried out. As a special case ultrasonic assisted regeneration is to be carried in vacuum conditions to study its effects and efficiency. The different desiccants namely, silica gel, activated carbon, zeolites have been compared on the basis of adsorption isotherms.

Keywords: Regeneration, Ultrasound Energy, Heating, Vacuum

INTRODUCTION

The growing need for cooling and drying applications has boosted the use of refrigeration and dehumidifying systems. The increased energy consumption of vapour compression refrigeration systems had intensified interest in prominent technologies such as adsorption cooling and drying systems. Adsorption cooling based on desiccant is efficient owing to its capability to utilize low grade heat energy such as waste heat from industries, power plants, and solar energy which improves the system's efficiency. The adsorption system's effectiveness is determined by both the adsorption and desorption processes. The emphasis on desiccant regeneration has increased by using various energy sources such as heating, microwave, ultrasonic, and solar, among many others, to make the system more efficient. The work done by Yao et al. (1–5) on regeneration of Silica gel using Ultrasonic Energy showed the efficiency of ultrasound in regeneration. It has been stated that the regeneration efficiency is increased due to the factors like microstreaming, alternative pressure bubbles and turbulence which enhances the moisture diffusivity and also part of ultrasound energy is converted to heat which enhances the temperature of the desiccant bed. Many theories have been proposed for the reason for ultrasonic assisted regeneration but mechanism which enhances the process is not clear. So to study the effect Daghooghi et al. [6] performed experiment on desorption of zeolite- water pair by varying the power supply of ultrasonic and heating power and maintaining total power constant. The work is to be carried similar but the regeneration of desiccant is to be carried in vacuum conditions, because the boiling point of the water decreases with decrease in pressure.

MATERIALS AND METHODS

The Adsorption isotherms of the zeolite water pair was numerically analysed with different input conditions and compared with the experimental results (7). The axial dispersion model with Linear driving force (LDF) as shown in Eqs. (1-5) was numerically solved using COMSOL PDE Interface. The comparison plot for different isotherms is shown in the fig. 2. As the next step the adsorption of desiccant pair is to be carried out in vacuum conditions. The combination of heating and ultrasonic is to be used as main source of energy. The experiment is to be carried out in normal conditions and in vacuum conditions with different desiccants. The regeneration is to be carried to with different ultrasonic frequency like 25kHz, 33kHz, 40kHz, 80kHz with total input power of 40W. The schematic diagram of the proposed experimental setup is shown in Fig.1.

Axial Dispersion Model:

$$D_{ax} \frac{\partial^2 C}{\partial z^2} - v \frac{\partial C}{\partial z} - \frac{(1-\varepsilon_b)}{\varepsilon_b} \frac{\partial q}{\partial t} = \frac{\partial C}{\partial t} \quad (1)$$

Linear Force Driving Model:

$$\frac{dq}{dt} = k(q^* - q) \quad (2)$$

Langmuir Isotherm:

$$q^* = q_s \frac{bc}{1+bc} \quad (3)$$

Freundlich Isotherm:

$$q^* = KP^{1/n} \quad (4)$$

Sip Isotherm

$$q^* = q_s \frac{(bP)^{1/n}}{1+(bP)^{1/n}} \quad (5)$$

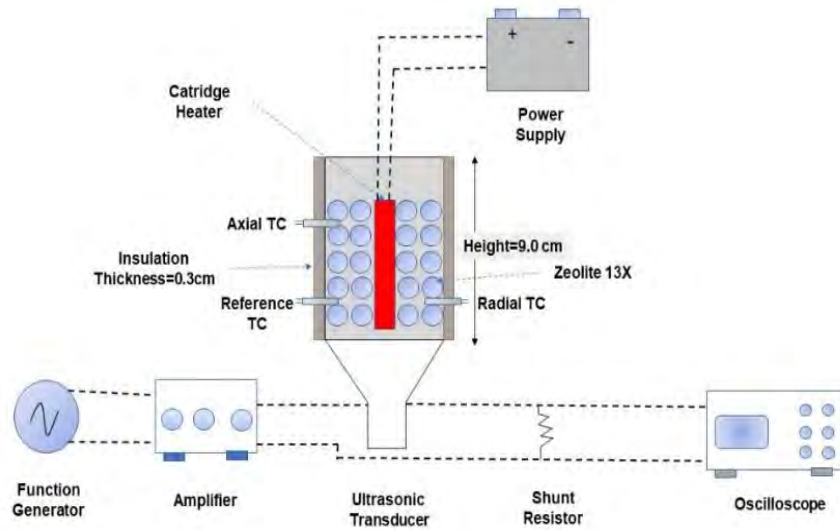


Fig. 7. Schematic Diagram of Experimental Setup (6)

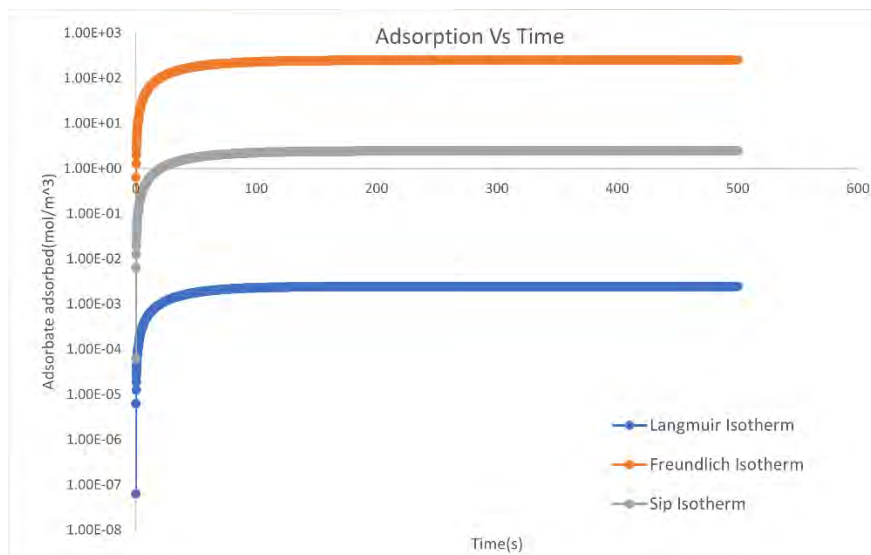


Fig. 2. Comparison of Adsorption with Different Isotherms

CONCLUSIONS

In this study, the Numerical analysis done on Adsorption using Axial dispersion model with different isotherm showed that the Langmuir adsorption isotherm predicts good compared to other isotherms in range of given pressure and inlet mass flow rate of water. The Freundlich Isotherm predicts with more error similar to sips equation. So, further study is to be carried with different pressure range and the flow rate and different isotherms. As the analysis is done as Initial step, the major concentration is to be kept on the experimental work and integrating the ultrasonic and heating power to perform regeneration process in vacuum condition. The study will give some idea on the effect of ultrasonic power and the effect of frequency on Regeneration process in vacuum condition.

REFERENCES

- [1] Yao Y, Yang K, Liu S. Study on the performance of silica gel dehumidification system with ultrasonic-assisted regeneration. Energy [Internet]. 2014; 66:799–809. Available from: <http://dx.doi.org/10.1016/j.energy.2014.01.061>
- [2] Yang K, Yao Y, Liu S, He B. Investigation on applying ultrasonic to the regeneration of a new honeycomb desiccant. Int J Therm Sci [Internet]. 2013; 72:159–71. Available from: <http://dx.doi.org/10.1016/j.ijthermalsci.2013.05.007>
- [3] Yao Y, Yang K, Zhang W, Liu S. Parametric study on silica gel regeneration by hot air combined with ultrasonic field based on a semi-theoretic model. Int J Therm Sci [Internet]. 2014; 84:86–103. Available from: <http://dx.doi.org/10.1016/j.ijthermalsci.2014.05.005>

- [4] Zhang W, Yao Y, Wang R. Influence of ultrasonic frequency on the regeneration of silica gel by applying high-intensity ultrasound. *Appl Therm Eng* [Internet]. 2010;30(14–15):2080–7. Available from: <http://dx.doi.org/10.1016/j.applthermaleng.2010.05.016>
- [5] Yao Y, Liu S. Ultrasonic technology for desiccant regeneration. *Ultrason Technol Desiccant Regen*. 2014;1–311.
- [6] Daghooghi-Mobarakeh H, Campbell N, Bertrand WK, Kumar PG, Tiwari S, Wang L, et al. Ultrasound-assisted regeneration of zeolite/water adsorption pair. *Ultrason Sonochem* [Internet]. 2020;64(February):105042. Available from: <https://doi.org/10.1016/j.ultsonch.2020.105042>
- [7] Czepirski L, Komarowska-Czepirska E. Adsorption of Water Vapours in Natural and Modified Zeolites. *Stud Surf Sci Catal*. 1993;80(C):121–7.

NOMENCLATURE

C	Concentration of the Adsorbate(mol/m ³)
D_{ax}	Axial Dispersion Coefficient(m ² /s)
ε_b	Voidage Fraction of Bed
q	Adsorbed Concentrated Species
q_s	Adsorbed Concentrated species at Saturated Equilibrium
K	Freundlich Constant

WORKING FLUID SELECTION AND PERFORMANCE ANALYSIS OF A GEOTHERMAL BINARY POWER PLANT

Zeynep Ozcan^{1,*}, Prof. Dr. Gulden Gokcen Akkurt²

¹Izmir Institute of Technology, Energy Engineering MSc. Programme, 35430, Urla, Izmir, Turkey.

²Izmir Institute of Technology, Faculty of Eng., Dept. of Energy Systems Engineering, 35430, Urla, Izmir, Turkey.

*Corresponding author e-mail: zeynepozcan@iyte.edu.tr

ABSTRACT

Energy and exergy analysis of a binary geothermal power plant was carried out using actual plant data for various working fluids and performance of working fluids are compared. As a result, the plant using isobutane has the highest energy and exergy efficiencies and turbine work.

Keywords: Binary power plants, Working fluid selection, Energy analysis, Exergy analysis

INTRODUCTION

Geothermal energy is used for electricity generation or direct use applications such as heating, cooling, drying and industrial applications based on its temperature and flowrate. Most common geothermal power generation systems are flash steam, dry steam and binary cycle plants [1]. Design, environmental impact and efficiency of a binary cycle plant is influenced by working fluid properties [2]. Working fluid selection criteria are based on thermodynamic properties of fluids, as well as health, safety, and environmental impacts. Environmental criteria are ozone depletion potential, toxicity, flammability, and global warming potential. Since all hydrocarbon fluids are flammable, additional fire prevention equipment is required on site in addition to the regular standards for any power plant [3]. From the thermodynamics point of view, critical temperature and pressure of the working fluid should be competitive with the geothermal fluid temperature and effects the choice of the cycle (subcritical/supercritical) [4]. Exergy analysis based on the 2nd law of thermodynamics has proven to be an effective method in energy system performance evaluation and thermodynamic analysis [1]. There is extensive literature on energy and exergy analysis of geothermal power plants [1-4]. In this study, thermodynamic performance of an existing binary power plant which employs isobutane as working fluid is analyzed for various working fluids.

MATERIALS AND METHODS

A binary power plant located in Reno-Nevada-USA is operated with isobutane as the working fluid and generates 27 MWe. Fig.1 shows a schematic diagram of the plant [1]. In addition to isobutane, several other working fluids such as n-butane, R-152A, R-124 and isopentane were also selected and, energy and exergy analysis were conducted through EES software [5] based on the data given in [1]. The turbine inlet temperature of the plant is 146.8°C which is higher than the critical temperature (135.9°C [6]) of isobutane while inlet pressure remained lower than critical pressure.

The equations for energy and exergy analysis are given in Eq.1-8.

Energy balance; [1,2]

$$\dot{Q} + \dot{W} = \sum \dot{m}_{out} h_{out} - \sum \dot{m}_{in} h_{in} \quad (1)$$

$$\dot{W}_T = (h_3 - h_4) \times \dot{m}_{wf} \quad (2)$$

Exergy balance; [1,2]

$$\dot{E}_{heat} + \dot{W} = \sum \dot{E}_{out} - \sum \dot{E}_{in} + \dot{I} \quad (3)$$

$$\dot{E} = \dot{m} \times ((h - h_0) - T_0(s - s_0)) \quad (4)$$

$$\dot{E}_{heat} = \sum \left(1 - \frac{T_0}{T}\right) \dot{Q} \quad (5)$$

Exergy destruction of the plant: [1,2]

$$\dot{I}_{plant} = \dot{E}_6 - \dot{W}_{net,out} \quad (6)$$

Energy and exergy efficiencies: [1,2]

$$\eta = \dot{W}_{net,out} / \dot{Q}_{ri} \quad (7)$$

$$\eta_{ex} = \dot{W}_{net,out} / \dot{m}_{wf} \times ((h_3 - h_2) - T_0(s_3 - s_2)) \quad (8)$$

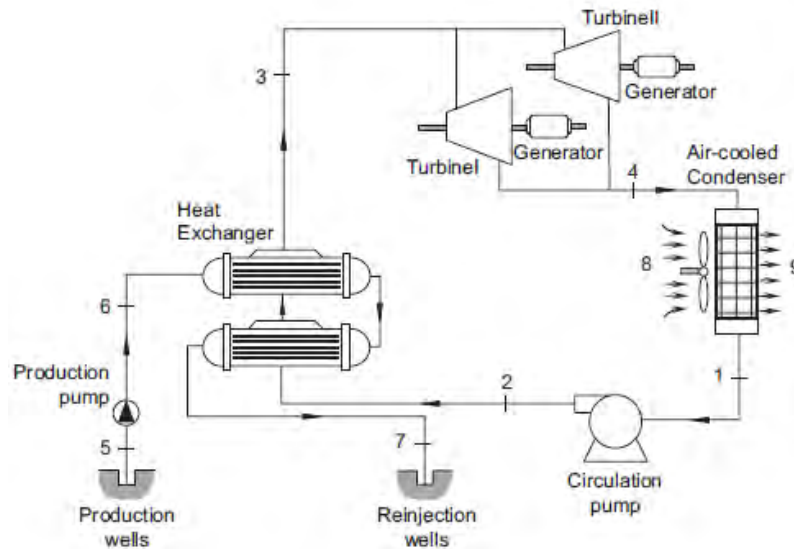


Fig.1. System schematic of the plant [1].

RESULTS AND DISCUSSION

Energy and exergy analysis for given power plant data and various working fluids are conducted using EES software and the results are presented in Table 1. The Table exhibits that isobutane has the highest energy and exergy efficiencies and turbine work output for given turbine inlet temperature of 146.8°C. On the other hand, for the same turbine inlet temperature, isopentane gave negative values for work output and efficiencies. The reason is the given turbine inlet temperature (146.8°C) is lower than isopentane critical temperature (187.8°C [6]). Therefore, turbine inlet temperature is increased to 184.8°C which is the closest value to the critical temperature of isopentane that obtain convenient and optimum EES results, then the results are given in Table 1. For the total plant exergy destruction rate, isobutane resulted in 60,703 kW which is the lowest value while R-124 and isopentane encountered highest exergy destruction rates.

CONCLUSIONS

Isobutane has the highest energy and exergy efficiencies which are 4% and 38%, respectively. Also, the highest total turbine work (21,745 kW) and lowest total exergy destruction rate (60,703 kW) were encountered for isobutane. Moreover, isopentane has the lowest energy and exergy efficiency while R-124 has the lowest energy efficiency, turbine work output and highest total loss value (71,635 kW). Therefore, it is proper to state that isobutane is the optimum working fluid among other fluids in this study.

Table 1. Comparison of results for different working fluids

Turbine inlet temp. (°C)	Working fluids	Energy eff. (%)	Exergy eff. (%)	Turbine work (kW)	Total exergy destruction (kW)
146.8	Isobutane	4.1	38	21,745	60,703
	n-butane	2.7	21	15,393	67,137
	R-152A	2.2	28	14,246	67,476
	R-124	1.1	23	9,654	71,635
	Isopentane	-0.10	-1.72	-32,756	115,272
184.8	Isopentane	2	18	14,205	68,311

REFERENCES

- [1] Kanoglu M, Bolatturk A. Performance and parametric investigation of a binary geothermal power plant by exergy. *Renew Energy*. 2008;33(11):2366–74.
- [2] Zeyghami M. Performance analysis and binary working fluid selection of combined flash-binary geothermal cycle. *Energy*. 2015;88:765–74.
- [3] Nalevankova J. Comparison of working fluids for ORC geothermal power plant comparison of working fluids for ORC. *Conference Paper*. 2015;(February 2016).
- [4] Karellas S, Schuster A. Supercritical fluid parameters in organic rankine cycle applications. *Int J Thermodyn*. 2008;11(3):101–8.
- [5] F-Chart Software, EES, engineering equation solver. In: F-Chart Software, 2015. Internet Website, Available from: <http://fchartsoftware.com/ees/index.php/>
- [6] Sierra ALM, Garcia NA. Criteria for the selection of working fluids for geothermal power plants: a case study in Spain. *Proceedings*. 2018;2(23):1424.

PRECASTED TIMBER-CONCRETE COMPOSITE AS A COMPONENT OF SUSTAINABLE CONSTRUCTION

^{1*} Paweł Mika, ² Sabina Kuc, ³ Łukasz Wesołowski

^{1,2,3} Cracow University of Technology, Faculty of Architecture, Podchorążych 1, 30-084 Cracow, Poland

*Corresponding author e-mail: pmika@pk.edu.pl

ABSTRACT

Two building materials have been introduced at the end of XIX century - steel and concrete. They replaced traditional and locally produced structural materials, especially wood. According to the latest research, steel and concrete represent 3% and over 5% of human green-house emissions on Earth, respectively. 8% of the entire human gas emissions come from these two materials only.

The article presents construction systems that combine traditional sustainable material (wood) with modern material (concrete). Hybrid solutions such as timber-concrete composites (TCC) become more and more common type of technology. The combination of high concrete compressive strength and wood tensile strength gives good results, especially in the case of floor slabs. This technology is often used in the buildings with engineered wood structure. The research presents solutions that introduce such a hybrid solution to other partitions of the building. An analysis was made in terms of the problems that may arise and the advantages that this solution can bring, mainly in terms of energy efficiency and environmental impact.

Keywords: timber-concrete composites, hybrid structures, timber, engineered wood, concrete prefabrication

INTRODUCTION

Joining materials with different properties together often brings interesting or even breakthrough results, as was the case, for example, when concrete and steel were joined. There has been a revolution in the construction industry all over the world that has changed modern architecture both in terms of design and aesthetics. However, cement is a very energy-consuming material to produce. A reduction in cement production will mean less exploitation of the planet, less CO₂ in the atmosphere and less pollution. Modern wooden construction can be very energy-efficient and can be a perfect counterpoint for heavy reinforced concrete structures. Wood is a natural storehouse of CO₂. However, even the most modern wooden structures made with the use of Cross Laminated Timber, Glue Laminated Timber or Laminated Veneer Lumber often need concrete, e.g. as a foundation or to add additional weight to the structure, and stiffen it. Combining these two materials is nothing new. Research on such composite systems has been conducted for years [1]. However, it is only now that there is a sudden increase in interest in high-performance timber construction. Therefore, the use of hybrid systems combining wood with concrete has become common. The combination of high concrete compressive strength and wood tensile strength gives good results [2], especially for ceilings. Therefore, an attempt was made to analyze the use of such solutions as prefabricated wall panels.

MATERIALS AND METHODS

The research was carried out on the basis of exemplary TCC solutions used in existing buildings. Theoretical research was also carried out on the possibilities offered by the combination of concrete with wood in terms of thermal insulation. Experimental research involving the use of TCC in partitions other than internal ceilings is currently under development.

CONCLUSIONS

Joining concrete with wood gives excellent results for internal ceilings in timber-framed buildings. Such ceilings are lighter, have good sound insulation, do not require additional finishing because wood is a material with high aesthetic parameters. Lighter construction also means less energy expenditure on transport and assembly, which results in lower emissions of carbon dioxide into the atmosphere. The use of such hybrid solutions in external walls or roofs can also bring a number of benefits for investors, users and the environment.

The conducted research is part of the EU Erasmus+ project "Sustainable, High-Performance Building Solutions in Wood". Aim of the project is to develop a new trans-disciplinary module and e-learning platform in order to bring technical knowledge about engineered wood to design offices and to make wood industry more innovative and sustainable.

REFERENCES

- [1] Girhammar UA. Composite Timber and Concrete Components for Walls. Proceedings of the 12th IABSE Congress. 1984 Sep 3-7; Vancouver, Canada; 1984. p.369-376.
- [2] Fragiaco M, Gregori A, Xue J, Demartino C, Toso M. Timber-concrete composite bridges: Three case studies. Journal of Traffic and Transportation Engineering (English Edition). 2018;5(6):429-38.

BIOCLIMATE OF URBAN AREAS AT THE RUSSIAN FAR NORTH IN THE CONTEXT OF CLIMATE CHANGE: ENERGY AND HUMAN HEALTH

Elena A. Grigorieva*

Institute for Complex Analysis of Regional Problems, Far-Eastern Branch, Russian Academy of Sciences (ICARP FEB RAS), Birobidzhan, Russia

*Corresponding author e-mail: eagrigor@yandex.ru

ABSTRACT

Extreme climatic environments at the Russian Far North (RFN) produce increase demand on human health, especially among climate-sensitive groups of the population – those with respirator and cardiovascular problems, particularly children and elderly. The study aims at estimation of thermal discomfort of urban areas at the RFN in bioclimatic indices, expressed in calorific terms. Generally, northern cities with low temperatures and strong winds are more uncomfortable, especially in January. No obvious changes in thermal extremity is found due to the growing temperature in 1980-2010 compare to 1960-1990. Cold environments cause direct and indirect impact on human health.

Keywords: bioclimate, urban, Russian Far North, human health, climate change

INTRODUCTION

The Extreme North or Far North of Russia (RFN) is a large part of the country located mainly north of the Arctic Circle. Its total area is about 5,500,000 km², comprising about one-third of Russia. The southern border of the Far North passes: in the European part of Russia and in the Western Siberia – about latitude 62° N, in the Eastern Siberia – at latitude 60° N, in the Russian Far East – at latitude 55° N. This part of Russia is located in very harsh environment characterized by extremely low ambient temperatures, particularly in the northern areas of Krasnoyarski Krai, Tyumen Region and Salkha (Yakutiya). Cold climates conditions are combined with high air humidity and strong wind, especially in Magadan Region, which sharply aggravates the effect of low temperatures on human body and its thermoregulation system, as well as worsens human health and well-being. Many bioclimatic indices are designed to display the complex influence of climate and weather on thermal (dis)comfort, which are used for both cold and warm seasons, and for the bioclimatic estimations during the year as a whole [1,2]. Climatic and weather conditions of the northern latitudes themselves, reinforced by recent dramatic climate changes, contribute to social and economic changes in urban and rural areas. The current study is aimed at assessing changes in the outdoor thermal environment in urban areas of the Russian Extreme North from the point of view of energy supply for human health and well-being using bioclimatic indices.

MATERIALS AND METHODS

To determine the level of thermal load of weather and climate as a whole on the human body or the risk to human health, special bioclimatic indices are used, which characterise the ambient thermal environment in calorific terms, showing the energy supply (or deficit) of ambient conditions. They are mainly designed on the basis of parallel physiological and meteorological observations, including Hill wind wet cooling index and Wind Chill Index [1-7].

In Russia and the former USSR, the Hill wind wet cooling index (H , $\text{mcal cm}^{-2} \text{s}^{-1}$) is widely used in bioclimatic studies of both cold and warm periods, which takes into account the air temperature and humidity, and wind speed [1,6]. During cold season, $H > 70 \text{ mcal cm}^{-2} \text{s}^{-1}$ characterizes absolutely uncomfortable conditions, 51–70 – extremely uncomfortable, 41–50 – uncomfortable; summer conditions with index values from 14 to 22 are estimated as comfortable, and with a value $< 8 \text{ mcal cm}^{-2} \text{s}^{-1}$ as hot [6].

Wind Chill Index (W , $\text{kcal m}^{-2} \text{h}^{-1}$) indicates thermal sensation of temperature enhanced by wind speed [4,6,7]. W is used for estimation of a possible hypothermia: a person dressed in winter clothing is hypothermized at $W=1190-1547$, $W>2500$ means “intolerably cold”. $W<762 \text{ kcal m}^{-2} \text{h}^{-1}$ indicates comfortable conditions [6].

Estimation of the spatial and temporal dynamics of the thermal (dis)comfort was carried out for the main urban areas of RFN, including Murmansk, Arkhangelsk, Vorkuta, Surgut, Noyabrsk, Novy Urengoy, Norilsk, Yakutsk, Magadan, Petropavlovsk–Kamchatsky, where Surgut is the largest city, Petropavlovsk–Kamchatsky – more southern, and Norilsk – more northern city. The average monthly and yearly data on air temperature, absolute humidity, and wind speed, for two periods: from 1960 to 1990, and from 1980 to 2010, presented by World Data Centre in Obninsk at <http://meteo.ru/data>, were used.

RESULTS AND DISCUSSION

Wind speed and air humidity modify effect of cold temperatures, which is expressed in bioclimate indices. The calculations show the least severe conditions of the cold season are observed in locales protected from the wind, with very low temperatures and almost complete windlessness. Despite the higher winter temperatures, cities with a strong wind speed close to the Arctic and Far Eastern seas are characterized by increased severity throughout the whole year. The weather severity here is 1.5–2 times higher than at the spots located inside the continent or much further north. In general, more severe conditions are observed in cities located in Krasnoyarski Krai, Tyumen and Magadan.

According to the Hill wind wet cooling index, all cities are located in a severely cold zone during January, with H index above $50 \text{ mcal cm}^{-2} \text{ s}^{-1}$ in the category of “extremely uncomfortable” conditions, and “absolutely uncomfortable” conditions are indicated in Norilsk, up to 88 in January and $83 \text{ mcal cm}^{-2} \text{ s}^{-1}$ during the cold season (from November to March). Vorkuta and Magadan have the same thermal harshness during winter – near $75 \text{ mcal cm}^{-2} \text{ s}^{-1}$. These cities have very strong winds during the whole year, and especially during the winter season – up to $6.0\text{--}6.6 \text{ m s}^{-1}$. The coldest Yakutsk has much lower values of thermal discomfort expressed by Hill index – near $50 \text{ mcal cm}^{-2} \text{ s}^{-1}$, although these values are still characterized as “extremely uncomfortable”, which is explained by calm conditions with wind speed near 1.0 m s^{-1} .

The Wind Chill Index shows that outdoor climate in RFN is extremely and intolerably cold, with values for the period from January to February higher than $1190 \text{ kcal m}^{-2} \text{ h}^{-1}$ at the whole area, whilst in Vorkuta and Norilsk these conditions are observed during months from November to April. The more severe environments are noticed in the northern Norilsk – higher than $1700 \text{ kcal m}^{-2} \text{ h}^{-1}$ in months from December to February. Extreme values of wind Chill index have the same spatial distribution as Hill index estimations. During months from June to September Wind Chill index indicates comfortable conditions with $W < 762 \text{ kcal m}^{-2} \text{ h}^{-1}$ everywhere in the cities at the RFN.

Climate change is objectively manifested in ambient temperatures – $0.4\text{--}2.0 \text{ }^\circ\text{C}$ of mean year values, and up to $4.0 \text{ }^\circ\text{C}$ in January in Yakutsk. Despite the increase in temperature, climatic discomfort expressed by bioclimatic indicators in calorific terms, practically does not change, remaining in the same grades of thermal extremity throughout the year.

The effect of a cold thermal environment aggravated by strong winds, can be expressed on human health directly (damage to the extremities, chills, frostbite, cooling trauma) and indirectly (an increase in respiratory and cardiovascular morbidity, particularly in children and elderly) [8,9]. Special plans for cities should guarantee safety of people, especially for those who work outside: high-calorific food, proper clothing insulation, working regimes [9].

CONCLUSIONS

Bioclimatic indices Hill wind wet cooling index and Wind Chill Temperature express cold environments of cities at the Russian Far North regions in calorific terms. Generally, northern cities with low temperatures and strong winds are more uncomfortable, especially in January. No obvious changes in thermal extremity is found due to the growing temperature in 1980-2010 compare to 1960-1990. Cold environments cause direct and indirect impact on human health, manifesting itself in an increase of respiratory and cardiovascular morbidity.

REFERENCES

- [1] de Freitas CR, Grigorieva EA. A comprehensive catalogue and classification of human thermal climate indices. *Int J Biometeorol* 2015; 59:109–120. doi:10.1007/s00484-014-0819-3.
- [2] de Freitas CR, Grigorieva EA. A comparison and appraisal of a comprehensive range of human thermal climate indices. *Int J Biometeorol* 2017; 61:487–512. doi:10.1007/s00484-016-1228-6.
- [3] Hill L, Griffith OW, Flack M. The measurement of the rate of heat loss at body temperature by convection, radiation and evaporation. *Physiol Transact Royal Soc B* 1916; 207:183–220.
- [4] Siple PA, Passel CF. Measurements of dry atmospheric cooling in sub-freezing temperatures. *Proc Amer Philos Soc* 1945; 89:177–119.
- [5] Osczevski R, Bluestein M. The new wind chill equivalent temperature chart. *Bull Am Meteorol Soc* 2005; 86:1453–1458. doi:10.1175/BAMS-86-10-1453
- [6] Kobysheva NV, editor. Guide to specialized climatological services of the economy. St. Petersburg: State University named after A.I. Voeikov; 2008. (In Russ.).
- [7] Korobeynikova A, Danilina N, Makisha N. Sustainable Development of the Slope Lands of the Russian Arctic: Investigation of the Relationship between Slope Aspects, Wind Regime and Residential Wind Comfort. *Land* 2021;10(4):354. <https://doi.org/10.3390/land10040354>.
- [8] Grigorieva EA, Khristoforova NK. Climate and Human Health at the Russian Far East. *Ekologiya cheloveka [Human Ecology]* 2019; 5:4-10. doi:10.33396/1728-0869-2019-5-4-10.
- [9] Revich BA, Grigorieva EA. Health risks to the Russian population from weather extremes in the beginning of the XXI century. Part 1. Heat and cold waves. *Issues Risk Analysis*. 2021; 18:12–33 (In Russ.).

PERFORMANCE ANALYSIS OF DOUBLE SLOPE PASSIVE AND ACTIVE SOLAR STILL FOR INDIAN CLIMATIC CONDITION

¹Tunuguntla Arun Sri Sai Krishna, ^{1*}Sumit Tiwari, ²Rakhi Sharma, ³Desh Bandhu Singh

¹Department of Mechanical Engineering, Shiv Nadar University, Dadri, Gautam Budha Nagar, Uttar Pradesh, India

²School of Engineering & Technology, Indira Gandhi National Open University, New Delhi, India

³Department of Mechanical Engineering, Graphic Era Deemed to be University, Dehradun, India

*Corresponding author e-mail: tjwsumit@hotmail.com

ABSTRACT

Over the years, the demand for freshwater is increasing rapidly. In the present communication, the performance of double slope solar still has been analyzed for a clear day of March month in Delhi. Thermal modeling has been analyzed for passive and active double slope solar still. Further, results were compared for both cases based on input data (solar radiation and ambient temperature) provided from IMD, Pune. The average efficiency for solar still with and without parabolic dish was found to be 24.52% and 19.77%, respectively. The yield of passive solar still is observed to be 8.48 kg and 14.16 kg from active solar still having a 2m² basin area.

Keywords: Double slope solar still, Evaporative heat transfer coefficient, Overall thermal efficiency, Parabolic dish, Yield

INTRODUCTION

Water is the most important resource of nature [1]. Freshwater is a necessity for every living being on this earth. About 70 percent of the earth's surface is covered with water. Over 97 percent of this water is saline, which is present in oceans, 2 percent is in form of ice in the polar region, and the remaining is fresh water in the form of lakes, rivers, and groundwater [2]. As there is a rapid growth of population, industrialization's need for water is also increasing. Most of the domestic and industrial purposes are fulfilled by ground and river waters [3]. After these two, the major sector using freshwater is the agricultural sector. The water demand is drastically increasing over years. Therefore, purification of saline water takes its role. The most common method of desalinating saltwater is solar desalination [4].

From the review very, little work has been found for solar still with the parabolic dish. In the present analysis, solar still with the parabolic dish has been explored and compared with passive solar still without collector in terms of mass output.

PROPOSED SETUP AND METHODS

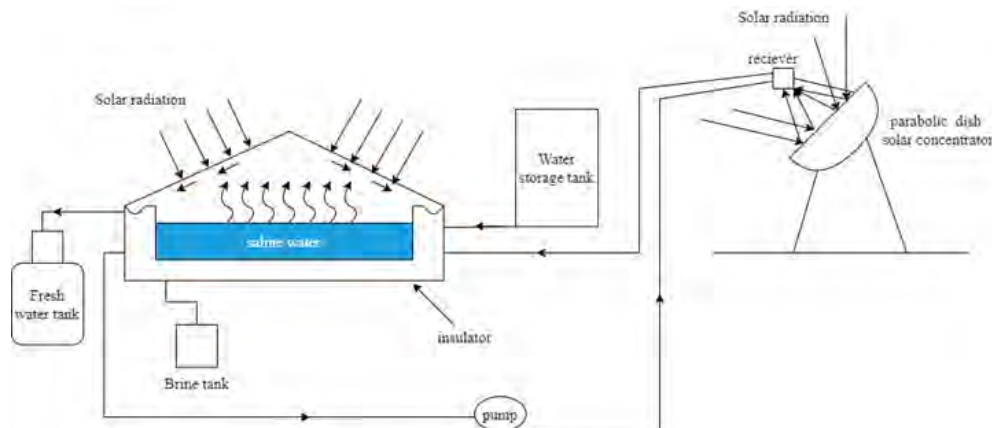


Fig. 1. Schematic view of solar still (double slope) having parabolic dish for energy collection

A schematic view of solar still (double slope) having a parabolic dish for energy collection is shown in Fig. 1. The solar still and parabolic dish collector is integrated in such a way that the water flows between them in forced mode. The heated water from the receiver goes to the bottom of the still using pipes. The beauty of the setup is to receive heat in two ways: one from the double slope glass of solar still and the second through dish collector. The principle of producing clean energy is that solar still gets radiation at the top glass. Further, radiation is absorbed to the solar still basin through water, and due to increased basin temperature; heat is transferred to water due to convection. Also, some of the heat given to solar still basin water from dish type concentrator. Solar dish contains a receiver

having water flow. The solar radiation will be reflected through the dish and concentrated on the solar receiver and takes the heat.

Finally, heated water transfers the heat to glass with the help of conductive, convective, radiative, and evaporative heat transfer coefficients. Due to heat, water gets evaporate and condense on the glass due to cooling. The condensed water glide through the inclined glass and collect in a freshwater tank via the corners of east and west walls.

THERMAL MODELLING

Parabolic Dish Equations (Alarcón et al. [5])

$$\text{Heat removal factor- } F_R = \frac{\dot{m}C_p}{A_w U_L} \left[1 - \exp \left(-\frac{A_w U_L F'}{\dot{m}C_p} \right) \right] \quad (1)$$

$$\text{Useful gain } \dot{Q}_u = F_R A_a \left[I_s \eta_0 - \frac{A_r}{A_a} U_L (T_w - T_a) \right] \quad (2)$$

Thermal modeling of solar still

Heat equation for east side glass:

(a) Inner east glass

$$\alpha'_g I_E + h_{tE}(T_w - T_{ciE}) - U_{EW}(T_{ciE} - T_{ciW}) = \frac{K_g}{L_g}(T_{ciE} - T_{coE}) \quad (3)$$

(b) Outer east glass

$$\frac{K_g}{L_g}(T_{ciE} - T_{coE}) = h_{aE}(T_{coE} - T_a) \quad (4)$$

where, $h_{tE} = h_{cWE} + h_{eWE} + h_{rWE}$

Heat equation for west side glass:

(c) Inner west glass

$$\alpha'_g I_W + h_{tW}(T_w - T_{ciW}) + U_{EW}(T_{ciE} - T_{ciW}) = \frac{K_g}{L_g}(T_{ciW} - T_{coW}) \quad (5)$$

(d) Outer west glass

$$\frac{K_g}{L_g}(T_{ciW} - T_{coW}) = h_{aW}(T_{coW} - T_a) \quad (6)$$

where, $h_{tW} = h_{cWW} + h_{eWW} + h_{rWW}$

Heat equation at Basin liner:

$$\alpha'_b \tau_g (I_E + I_W) = 2U_{bw}(T_b - T_w) + 2U_{ba}(T_b - T_a) \quad (7)$$

Energy balance for water mass:

$$(MC_w) \frac{dT_w}{dt} = (I_E + I_W) \tau_g \alpha'_w + 2U_{bw}(T_b - T_w) - h_{tE}(T_w - T_{ciE}) - h_{tW}(T_w - T_{ciW}) + \dot{Q}_u \quad (8)$$

After solving all the energy balance equations, MATLAB program has been used to solve first order differential equation for different temperatures. Further, energy and mass evaporated can be evaluated on the data generated by MATLAB.

CONCLUSIONS

The following conclusions can be drawn,

- The average efficiency for parabolic dish type solar concentrator was found to be 48.12%.
- From the analysis, a 78.77% increment in terms of distilled mass in the case of solar still with parabolic dish collector is found.
- The average efficiency for solar still with and without parabolic disc was found to be 24.52% and 19.77% respectively.
- The yield of passive solar still is observed to be 8.48 kg and 14.16 kg from active solar still having a 2m² basin area.

From the results, it can be concluded that active solar still can be the right choice for the mass production of clean water. Further, a study is required to utilize solar heat in nighttime also through different thermal storage options namely, sensible heat storage material and phase change materials.

REFERENCES

- [1] Malik MAS, Tiwari GN, Kumar A, Sodha MS. Solar distillation. first edition UK: Pregamon Press; 1982.
- [2] Fathy Mohamed, Hassan Hamdy, Ahmed M. Salem. Experimental study on the effect of coupling parabolic trough collector with double slope solar still on its performance. Solar energy 2018; 163:54–61.
- [3] Progress on Sanitation and Drinking Water. Update and MDG assessment. UNICEF-WHO; 2015:1–90.
- [4] Sathyamurthy R, Harris Samuel DG, Nagarajan PK, El-Agouz SA. Review of different solar still for augmenting freshwater yield. J Environ Sci Technol 2015; 8(6):244–65.
- [5]. Alarcón Jorge Alexander, Hortúa Jairo Eduardo, Andrea López G. Design and construction of a solar collector parabolic dish for rural zones in Colombia. TECCIENCIA 2013; 7(14): 14-22. DOI: <http://dx.doi.org/10.18180/tecciencia.2013.14.2>.

NOMENCLATURE

- A_s : Surface area of condensing cover (m^2)
 h : Total internal heat transfer coefficient (HTC) ($W/m^2\text{ }^\circ C$)
 h_{cw} : Internal convective HTC ($W/m^2\text{ }^\circ C$)
 h_{ew} : Internal evaporative HTC ($W/m^2\text{ }^\circ C$)
 h_{rw} : Internal radiative HTC ($W/m^2\text{ }^\circ C$)
 h_a : HTC between outer condensing cover and ambient air ($W/m^2\text{ }^\circ C$)
 I : Solar intensity on the condensing cover (W/m^2)
 k_g : Thermal conductivity of condensing cover ($W/m\text{ }^\circ C$)
 L_g : Thickness of condensing cover (m)
 L : Latent heat of vaporization (J/kg)
 M : Mass of water in the basin of solar still (kg)
 \dot{m} : Hourly distillate yield (kg/m^2)
 P : Partial saturated vapor pressure (N/m²)
 \dot{Q}_u : Useful thermal energy gain from the collector (W/m^2)
 q_{EW} : Evaporative heat transfer rate (W/m^2)
 T : Temperature ($^\circ C$)
 U_L : Overall HTC for flat plate collector ($W/m^2\text{ }^\circ C$)
 U_{EW} : Internal radiative HTC between east and west condensing cover ($W/m^2\text{ }^\circ C$)
 U_{bw} : HTC between basin liner and water ($W/m^2\text{ }^\circ C$)
 U_{ba} : HTC between basin liner and ambient air ($W/m^2\text{ }^\circ C$)
 U_a : Overall HTC between outer condensing cover and ambient air ($W/m^2\text{ }^\circ C$)
 V : Air velocity (m/s)

Subscripts

- E: East side
 W: West side
 C: Collector plate
 w: Water
 ci: Inner condensing cover
 co: Outer condensing cover
 a: Ambient
 b: Basin liner

Greek Letters

- α'_g : Fraction of solar energy absorbed by glass cover
 α'_b : Fraction of solar energy absorbed by basin water
 ϵ_g : Emissivity of glass cover
 ϵ_w : Emissivity of water
 τ_g : Transmittivity of glass

A SENSITIVITY STUDY OF N ALIKE PARTLY ENCLOSED WITH PHOTOVOLTAIC THERMAL COMPOUND PARABOLIC CONCENTRATORS HAVING SERIES CONNECTION

¹Raj Vardhan Patel, ²Ram K Sharma, ³Sumit Tiwari, ⁴Anuj Raturi, ⁴Desh Bandhu Singh, ⁵Navneet Kumar

¹Department of Mechanical Engineering, Sherwood College of Engineering Research and Technology, Barabanki, Uttar Pradesh 225003, India

²University of Petroleum and Energy Studies (UPES), Bidholi, Premnagar, Dehradun - 248007, Uttarakhand, India

³Department of Mechanical Engineering, Shiv Nadar University, Dadri, Gautam Budha Nagar, Uttar Pradesh, India

⁴Department of Mechanical Engineering, Graphic Era Deemed to be University, Bell Road, Clement Town, Dehradun 248002, Uttarakhand, India

⁵Galgotias College of Engineering and technology, Greater Noida, Uttar Pradesh, India

*Corresponding author e-mail: tiwsumit@hotmail.com

ABSTRACT

The world is facing a scarcity of energy as conventional resources are limited. The solar collectors with PV module have proved the effective solution towards electricity along with thermal energy. The present study is focused on the sensitivity study of N alike partly enclosed with photovoltaic thermal compound parabolic concentrators having series connection for the summer climatic condition of New Delhi, India. The sensitivity analysis has been done by using one-at-a-time (OAT) method. The outcome of changing mass flow rate, numbers of collectors, packing factor, the inclination of collectors and concentrator ratio on heat gain have analyzed. The study shows the concentrator ratio is more sensitive, followed by numbers of collectors, mass flow rate, inclination angle and packing factor. The average sensitivity figure for the proposed system has been found to be 1, 0.91, 0.31, 0.17 and 0.08 with respect to mass flow rate, numbers of collectors, packing factor, inclination of collectors and concentrator ratio.

Keywords: Sensitivity figure; Sensitivity analysis; solar collector; solar system; Series connection

INTRODUCTION

Power development plays an essential role in the country's economic growth. The world faces the issue of scarcity of fossil fuels, petroleum products, etc., as these also have carbon emissions. Solar-driven technology has attained greater attention because of its cost-effectiveness, along with its highly efficient methods. The solar collectors have been used to heat the water, air, space heating, seasoning of timbers etc., for domestic as well as industrial purposes. Apart from this, solar collectors have also been used for electrical power generation, which could replace the conventional way of producing power. The photo-voltaic thermal (PVT) collectors are capable of generating electricity along with heat energy. The parabolic trough collectors (PTC) concentrate the solar radiation on its focal. The compound parabolic concentrators (CPCs) are the non-imaging trough concentrators, which works on the principle of edge optics. These collectors have the potential to reflect all radiations falling over it to the absorber of the collectors [1-4]. The main aim of the study is too focused on the following objectives:

- To investigate the heat gain of the N-PVT-CPCs connected in series by varying the MFR keeping all other parameters constant.
- To investigate the effect on the heat gain of the N-PVT-CPCs by changing the area covered keeping all other parameters constant.
- To examine inclination angle effect on the heat gain of the N-PVT-CPCs for the fixed values of collectors, PF and CR keeping all other parameters constant.
- To estimate values of sensitivity figures for N-PVT-CPCs.
- To explore effect of PF and CR on heat gain of N-PVT-CPCs for given values of N and MFR keeping all other parameters constant.

PROPOSED SETUP AND METHODS

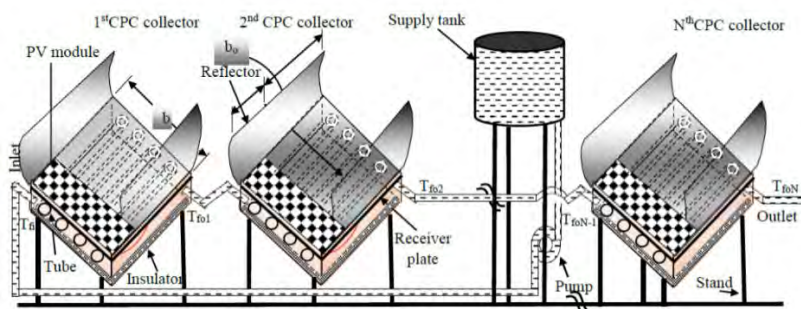


Fig. 1. N identical partly covered CPCs (N-PVT-FPCs) connected in series

THERMAL MODELLING

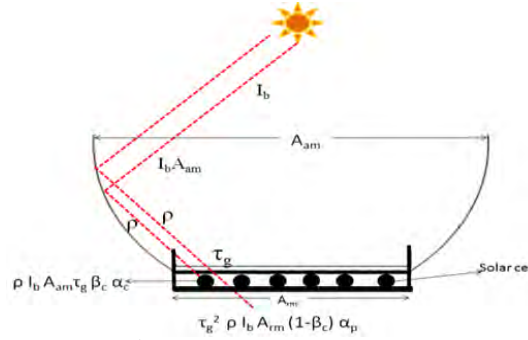


Fig. 2. XX' view (cut section) of 1st PVT-CPC along width (heat interaction)

The equations based on equating input heat to output heat can be written as:

For solar cell of semitransparent PV module (Fig.2)

$$\rho \alpha_c \tau_g \beta_c I_b A_{am} = [U_{tc,a}(T_c - T_a) + U_{tc,p}(T_c - T_p)] A_{rm} + \rho \eta_m I_b A_{am} \quad (1)$$

The expression for solar cell temperature from equation (1) can be found as

$$T_c = \frac{(\alpha\tau)_{1,eff} I_b + U_{tc,a} T_a + U_{tc,p} T_p}{U_{tc,a} + U_{tc,p}} \quad (1a)$$

The electrical efficiency of the cell can be written as:

$$\eta_c = \eta_0 \{1 - \beta_0 (T_c - T_0)\} \quad (1b)$$

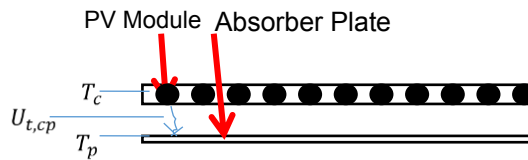


Fig. 3. Heat interaction for absorber plate

For absorber plate (Fig. 3)

$$\rho \alpha_p \tau_g^2 (1 - \beta_c) I_b A_{am} + U_{t,cp}(T_c - T_p) A_{rm} = F' h_{pf}(T_p - T_f) A_{rm} + U_{t,pa}(T_p - T_f) A_{rm} \quad (2)$$

Eliminating T_c from equation (1) and (2) and rearranging, one can find expression for T_p as

$$T_p = \frac{[(\alpha\tau)_{2,eff} + PF_1 (\alpha\tau)_{1,eff}] I_b + U_{L2} T_a + h_{pf} T_f}{(U_{L2} + h_{pf})} \quad (3)$$

For fluid (water) flowing through tubes made of copper (Fig. 4)

$$\dot{m}_f c_f \frac{dT_f}{dx} = F' h_{pf}(T_p - T_f) b \quad dx \quad (4)$$

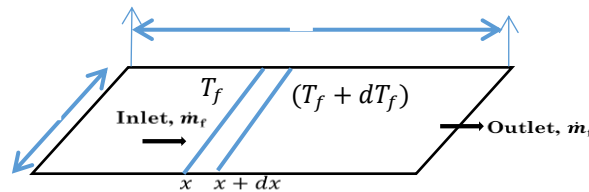


Fig. 4. Fluid flow through tubes below absorber plate

CONCLUSIONS

The following conclusions have been drawn from the study:

- i. The daily heat gain from the series connection of the N-PVT-CPCs collectors increases with CR, numbers of collectors and MFR. The increment rate in daily heat gain is higher with an increase in CR, numbers of collectors, and MFR.
- ii. The increase in MFR beyond 0.04 kg/s is not significant to the heat gain, as the heat gain not increases as it increases when MFR changes from 0.01 to 0.04 kg/s.
- iii. With the increase in PF and the inclination angle of collectors from horizontal, the heat gain of the proposed system decreases, the rate of decrement has been higher with the inclination than PF.
- iv. The sensitivity analysis of the N-PVT-CPCs series connections found that the CR is the most sensitive parameter followed by the numbers of collectors, MFR, inclination angle and PF, respectively. The average

values of sensitivity figure are 1, 0.91, 0.31, 0.17 and 0.08 for the input variables CR, numbers of collectors, MFR, inclination, and PF respectively.

REFERENCES

- [1] C. Jiang et al., "A review of the compound parabolic concentrator (CPC) with a tubular absorber," *Energies*, vol. 13, no. 3, 2020, doi: 10.3390/en13030695.
- [3] R. V. Patel, G. Singh, K. Bharti, R. Kumar, and D. B. Singh, "A mini review on single slope solar desalination unit augmented with different types of collectors," *Mater. Today Proc.*, vol. 38, pp. 204–210, 2021, doi: 10.1016/j.matpr.2020.06.580.
- [3] R. V. Patel, K. Bharti, G. Singh, G. Mittal, D. B. Singh, and A. Yadav, "Comparative investigation of double slope solar still by incorporating different types of collectors: A mini review," *Mater. Today Proc.*, vol. 38, pp. 300–304, 2021, doi: 10.1016/j.matpr.2020.07.338.
- [4] A. Fernández-García, E. Zarza, L. Valenzuela, and M. Pérez, "Parabolic-trough solar collectors and their applications," *Renew. Sustain. Energy Rev.*, vol. 14, no. 7, pp. 1695–1721, Sep. 2010, doi: 10.1016/j.rser.2010.03.012.

ABBREVIATIONS

PVT	photovoltaic thermal
PTC	parabolic trough collector
CPCs	compound parabolic collectors
N	Number of collectors
PV	photovoltaic
HTFs	heat transfer fluids
MFR	mass flow rate
N-PVT-CPCs	N identical partly covered compound parabolic collectors
PF	packing factor
OAT	one-at-a-time
CR	concentration ratio

EFFECT OF WATER DEPTH ON EFFICIENCIES AND PRODUCTIVITY OF N ALIKE EVACUATED TUBULAR SOLAR COLLECTORS COUPLED TO SOLAR STILL OF SINGLE SLOPE TYPE BY INCORPORATING EXERGY

Desh Bandhu Singh^{1*}, Rakesh Kumar Yadav², Yatender Chaturvedi³, Gaurav Kumar Sharma⁴, Sanjeev Kumar Sharma⁴, Navneet Kumar⁶

¹Department of Mechanical Engineering, Graphic Era Deemed to be University, Dehradun, India

²KCC Institute of Technology and Management, Greater Noida – 201306, G.B. Nagar, Uttar Pradesh, India

³Department of Electrical and Electronics Engineering, KIET Group of Institutions, Ghaziabad – 201206

⁴Department of Mechanical Engineering, Indian Institute of Technology (ISM), Dhanbad, Jharkhand, India

⁵Galgotias College of Engineering and Technology, Greater Noida – 201306, G.B. Nagar, Uttar Pradesh, India,

*Corresponding author e-mail: deshbandhusingh.me@geu.ac.in

ABSTRACT

This research paper focuses on the effect of water depth on efficiencies and productivity analyses of N alike evacuated tubular collectors (ETCs) coupled to solar still of single slope type by incorporating exergy. The investigation for the proposed system has been done for typical days of June and January for the complex climatic situation of New Delhi. The hourly thermal efficiency, hourly exergy efficiency and hourly productivity have been computed and they have been 2D plotted for different values of water depth. Based on the hourly values of different efficiencies and productivity, their values on daily basis have been computed followed by the evaluation of average values on daily basis for different values of water depth. It has been concluded that the optimum values of water depth are 0.56 m, 0.56 m and 0.42 m on the basis of thermal efficiency, exergy efficiency and productivity respectively.

Keywords: Exergy, Efficiency, productivity, ETC, single slope solar still

INTRODUCTION

The design and study of single slope type solar energy operated system is the requirement of contemporary global environment as the conventional source of energy is depleting day by day; whereas renewable source of energy seems to exist for long and the use of renewable energy does not produce any negative effect on the surroundings as polluting elements are not present. The performance analysis of active solar still was first of all reported in 1983 [1] and a lot of works on the performance analysis of active solar still has been reported since then. Issa and Chang [2] did experimentation on solar still of single slope type by incorporating evacuated tubes in mixed mode and it was concluded that the freshwater production of the reported system was 2.36 times more than the solar still of passive type because of the addition of extra heat to the basin in the case of active mode of operation. It was further reported that the life cycle conversion efficiency for solar still of single slope type included with evacuated tubular collector was higher than solar energy-based water purifier in passive mode due to higher exergy gain by system consisting of evacuated tubular collector as heat was added to the basin in the case of active mode. [3]. Singh and Tiwari [4] reported the development of typical equations for solar still of double slope type by incorporating evacuated tubular collectors. Further, Kumar et al. [5] reported the developed typical equations for solar still of single slope type included with compound parabolic concentrators integrated evacuated tubular collectors and it was concluded that the performance of solar still of single slope type included with compound parabolic concentrators integrated evacuated tubular collectors was better than solar still of single slope type included with evacuated tubular collectors because of the enhancement in heat collection region. From the extant research, it is clear that the effect of dissimilarity of water depth on the performance of solar still of single slope type included with evacuated tubular collectors has not been reported. Hence, this work reveals the effect of dissimilarity of water depth on the performance of solar still of single slope type included with evacuated tubular collectors.

SETUP EXPLANATION

A schematic view of solar still (single slope) having evacuated tubular collectors is shown in fig. 1. The solar still and evacuated tubular collectors are integrated in such a way that the water flows between them in forced mode. The heated water from collectors goes to the bottom of the still using pipes. The beauty of the setup is to receive heat in two ways: one from the single slope glass of solar still and the second through evacuated tubular collectors. The principle of producing clean energy is that solar still gets radiation at the top glass. Further, radiation is absorbed to the solar still basin through water, and due to increased basin temperature; heat is transferred to water due to convection. Also, some of the heat given to solar still basin water from evacuated tubular collectors. The evacuated tubular collector contains vacuum in annular space between two glass tubes which prevents heat loss by convection. Finally, heated water transfers the heat to glass with the help of convective, radiative, and evaporative heat transfer coefficients. Due to heat, water gets evaporate and condense on the glass due to cooling. The condensed water glide through the inclined glass and collect in a freshwater tank. Fundamental equations have been presented as Table 1.

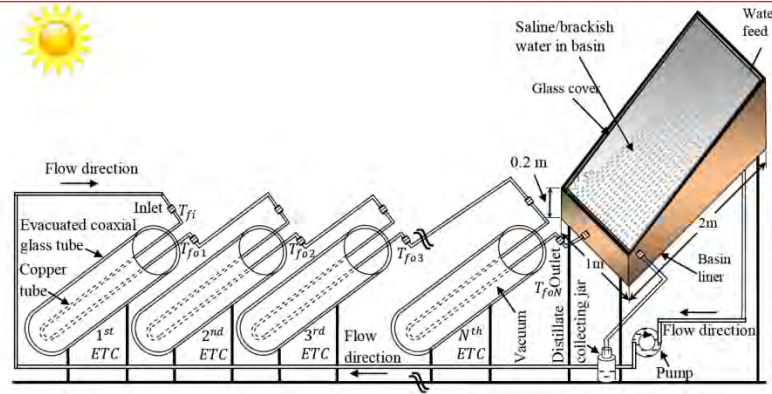


Fig. 1. Schematic view of solar still (single slope) having evacuated tubular collectors in series

Table 1. Mathematical equations

Parameters	Expression	Remarks
\dot{Q}_{uN}	$\dot{Q}_{uN} = \frac{(1-K_k^N)}{(1-K_k)} (A F_R (\alpha\tau))_1 I(t) + \frac{(1-K_k^N)}{(1-K_k)} (A F_R U_L)_1 (T_{fi} - T_a)$	Mishra et al. [6]
T_{foN}	$T_{foN} = \frac{(A F_R (\alpha\tau))_1 (1-K_k^N)}{\dot{m}_f C_f (1-K_k)} I(t) + \frac{(A F_R U_L)_1 (1-K_k^N)}{\dot{m}_f C_f (1-K_k)} T_a + K_k^N T_{fi}$	Mishra et al. [6]
T_w	$T_w = \frac{\tilde{f}(t)}{a} (1 - e^{-at}) + T_{w0} e^{-at}$	Singh et al. [7]
T_{gi}	$T_{gi} = \frac{\alpha_g' I_s(t) A_g + h_{1w} T_w A_b + U_{cga} T_a A_g}{U_{cga} A_g + h_{1w} A_b}$	Singh et al. [7]
\dot{m}_{ew}	$\dot{m}_{ew} = \frac{h_{ewg} A_b (T_w - T_{gi})}{L} \times 3600$	Singh et al. [7]
$\dot{E}x(t)$	$\dot{E}x(t) = A_b \times h_{ewg} \times \left[(T_w - T_{gi}) - (T_a + 273) \times \ln \left(\frac{T_w + 273}{T_{gi} + 273} \right) \right]$	Nag [8]
$\dot{E}x_c(t)$	$\dot{E}x_c(t) = \dot{m}_f \times C_f \times \left[(T_{foN} - T_{fi}) - (T_a + 273) \times \ln \left(\frac{T_{foN} + 273}{T_{fi} + 273} \right) \right]$	Nag [8]
$\eta_{daily,thermal}$	$\eta_{daily,thermal} = \frac{\sum_{t=1}^{24} \dot{m}_{ew} \times L}{\sum_{t=1}^{24} [\dot{Q}_{uN}(t) + A_b \times I_s(t) + \frac{P_u}{0.38}] \times 3600} \times 100$	Singh and Tiwari[9]
$\eta_{daily,exergy}$	$\eta_{daily,exergy} = \frac{\sum_{t=1}^{24} [\dot{E}x_{out,s}(t)]}{\sum_{t=1}^{24} [\dot{E}x_c(t) + 0.933 \times (A_b \times I_s(t) + P_u)]} \times 100$	Singh and Tiwari[9]
Daily productivity	$Daily\ productivity = \frac{[Daily\ yield \times (SP)_w]}{Daily\ cost + (Daily\ pump\ work \times (SP)_e)} \times 100$	Singh and Tiwari[9]

All unknown terms in equation can be seen in the reference provide. All relevant equations have been fed to the computer code in MATLAB-2015a. Data have been taken from Indian Meteorological Department, Pune, India. The output obtained from the system has been analysed and average daily thermal efficiency, average daily exergy efficiency and average daily productivity have been estimated for different values of water depth. The average values are based on the output obtained for January (winter) and June (summer). The selling price of water has been taken as Rs 5 per kg. The daily cost has been estimated by dividing uniform end of year annual cost by number of days in a year.

CONCLUSIONS

The following conclusions can be drawn,

- The average daily thermal and exergy efficiencies first rise and then become almost constant beyond 0.56 m.
- The average daily productivity first increases till 0.42 m and then decreases beyond 0.42 m. The optimum value of average productivity is found corresponding to 0.42 m water depth.

REFERENCES

- [1] Rai S.N. and Tiwari G.N., (1983), Single basin solar still coupled with flat plate collector, Energy Conversion and Management Vol. 23(3) p.145–149.
- [2] Issa R.J. and Chang B., (2018), Performance study on evacuated tubular collector coupled solar still in West Texas climate, International Journal of Green Energy, vol. 14, issue 10, pp. 793-800.
- [3] Singh D.B., (2018a), Energy metrics analysis of N identical evacuated tubular collectors integrated single slope solar still, Energy, vol. 148, pp. 546-560.
- [4] Singh D.B. and Tiwari G.N., (2017), Analytical characteristic equation of N identical evacuated tubular collectors integrated double slope solar still, Journal of Solar Energy Engineering: Including Wind Energy and Building Energy Conservation, ASME, Vol. 135, issue 5, pp. 051003(1-11).

- [5] Kumar R., Sharma R., Kumar D., Singh A.R., Singh D.B., Tiwari G.N., (2020), Characteristic equation development for single-slope solar distiller unit augmented with N identical parabolic concentrator integrated evacuated tubular collectors, Journal of Solar Energy Engineering: Including Wind Energy and Building Energy Conservation, ASME, vol. 142, pp. 021011-(1-11).
- [6] Mishra R.K., Garg V., Tiwari G.N., (2015), Thermal modeling and development of characteristic equations of evacuated tubular collector (ETC), vol. 116, pp. 165-176.
- [7] Singh D.B., Dwivedi V.K., Tiwari G.N., Kumar N., (2017), Analytical characteristic equation of N identical evacuated tubular collectors integrated single slope solar still, desalination and Water Treatment, 88, 41-51.
- [8] Nag P.K., Basic and Applied Thermodynamics, Tata McGraw-Hill, 2004, ISBN 0-07-047338-2.
- [9] Singh D.B., Tiwari G.N., (2017), Performance analysis of basin type solar stills integrated with N identical photovoltaic thermal (PVT) compound parabolic concentrator (CPC) collectors: A comparative study, Solar Energy, 142, 144-158.

NOMENCLATURE

- \dot{Q}_{uN} : Heat gain of collectors (kWh)
 T_w : Temperature of water (°C)
 T_w : Internal convective HTC (W/m²°C)
 T_{gi} : Temperature at the inner surface of condensing cover (°C)
 T_a : Temperature of surrounding/ambient (°C)
 T_{foN} : Temperature at the end of Nth collector (°C)
 T_{fi} : Temperature at the end of 1st collector (°C)
 \dot{m}_{ew} : Hourly fresh water yielding (kg/h)
 $\dot{E}x(t)$: Hourly exergy obtained from the system (kWh)
 $\dot{E}x_c(t)$: Hourly exergy obtained from series connected collectors (kWh)
 η : Efficiency (%)
 h_{ewg} : Evaporative heat transfer coefficient between water surface and inner surface of condensing cover (W/m²-K)
 A_b : Area of basin (m²)
 SP_w : Selling price of water (Rs/kg)
 P_u : Pump work
 $I_s(t)$: Solar intensity for solar still (W/m²)
 $I(t)$: Solar intensity for collector (W/m²)
 t : Time (s)

COMPARATIVE ANALYSIS OF SOLAR ENERGY-BASED WATER PURIFICATION SYSTEMS BASED ON VARIOUS DESIGNS

¹Navneet Kumar, ²V. K. Dwivedi, ³Desh Bandhu Singh

¹Galgotias College of Engineering and technology, Greater Noida, Uttar Pradesh, India

²Madan Mohan Malviya University of Technology, Gorakhpur, U.P., India

³Department of Mechanical Engineering, Graphic Era Deemed to be University, Bell Road, Clement Town, Dehardun 248002, Uttarakhand, India

*Corresponding author e-mail: navneet.kumar@galgotiacollege.edu

ABSTRACT

In this research work, a comparative analysis of various designs of solar energy-based water purification systems as single basin single slope passive (SBSSP), single basin double slope passive (SBDSP), and single basin double slope active solar still under natural mode (SBDSAN)] was performed by conducting experiments on these systems at various water depths throughout the year. Double slope active solar energy-based system yields nearly 50% more than the double slope passive solar energy-based system in the natural mode, whereas single slope passive water purification system yields more (259.5 kg/m²) than double slope passive system (232.3 kg/m²). The exergy efficiency of double slope active solar energy-based system is higher than the exergy efficiency of double slope passive solar energy-based system whereas vice versa is the case of energy efficiency. The thermal model of double-slope solar based in this paper has also checked with the help of derived equations. There is closer agreement between experimental and theoretical data for internal and external cover temperatures, water temperatures and distillates yield output of fresh water.

Keywords: Single slope, Double slope; Thermal modeling; Energy; Exergy

INTRODUCTION

Researchers are working diligently to solve the drinkable water issue, which is critical for humanity's survival. There is a drinking water crisis in many countries. Various methods for producing clean water are now being tried by scientists. Solar energy-based water purification systems could be proven to be one of best solutions to solve the water problem in society due to its simple technology and without the use of electrical power. Several scientists have shown that the passive solar energy best water purify system is a slow water purification technique. The daily yield is improved by plastic condensing coverings, solar energy-based water purify system with parabolic concentrator, evacuated tube collector, and flat plate collectors. Usage of flat plate collector is the most common choice because of low maintenance costs and simple nature to increase the productivity of solar energy-based water purifying system. Flat plate collector provides the basin water with extra heat capacity, and hence the water temperature rises further relative to passive solar water purifying system. A Swedish engineer Wilson has been credited to design first solar still, to produce potable water in Chile. Malik et al. [1] reported passive solar energy-based water purifying system. Tiwari [2] checked later the research performed on passive and active solar energy-based water purifying system until 1992. Eduardo Rubio et al. [3] proposed a different mathematical model to examine the results of a passive solar energy based double-slope. Sandeep et al. [4] have still studied the thermal efficiency of the updated active solar basin type. The current research intended to assess the annual yield of various designs of solar energy-based water purifying systems, as well as the analysis of energy and exergy, and the validation of the thermal model with annual experimental data obtained through outdoor experiments.

DESCRIPTION OF EXPERIMENTAL SETUP

The single basin single slope passive solar system (SBSSP), single basin double slope passive solar system (SBDSP) and single basin double slope passive solar system (SBDSAN) under natural mode (SBDSAN) were planned to assess the efficiency of different designs of solar energy-based water purification systems according to the descriptions given in Table 1. In Figure 1, 2 and 3 respectively, photos of three types of systems were given. There is basin area of solar stills of 1 & 2 m², both in single and double slope respectively. In order to make a body of solar silks, the glass reinforced plastic (GRP) was used. The thickness of glass condensing cover is 4 mm to prevent it from breakage in normal conditions and is inclined at 15° for both active and passive solar energy-based water purifying system. To get maximum solar radiation, the bottom surface had been painted black. The entire structure was installed as seen on iron platform in the Figs. 1, 2 and 3. Experiments on passive solar stills were conducted in the campus of IIT Delhi whereas an experiment on active system was done in Ghaziabad, UP, India. All experimental measurements were taken on an hourly basis from morning in a day to morning next day for continuous 24 hours.

Table 1: Dimensions of the various designs of solar still

Parameters	SBSSP	SBDSP	SBDSAN
Basin area	1.0 m ²	2.0 m ²	2.0 m ²
Basin height	0.19 m (sides) 0.47 m (sides)	0.22 m (sides) 0.48 m (center)	0.22 m (sides) 0.48 m (center)
Condensing cover area	1.03x1.06 m ²	1.03x1.06 m ²	1.03x1.06 m ²
Condensing cover thickness	0.004 m	0.004 m	0.004 m
Condensing cover angle	15°	15°	15°
Insulation thickness	0.006 m	0.006 m	0.006 m
Number of FPC	0	0	1
FPC Area	0	0	2.0 m ²



Fig. 1. Single Slope Passive Solar Energy Based System



Fig.2. Double Slope Passive Solar Energy Based System



Fig. 3. Double slope active Solar Energy Based System in natural mode

FORMULAE USED

(a) The daily yield was determined by summing the per day (24 hours) hourly yield:

$$M_{ew} = \sum_{i=1}^{i=24} m_{ewi} \quad (1)$$

(b) For passive solar energy-based system, the overall thermal efficiency is determined by:

$$\eta_{passive} = \frac{\sum \dot{m}_{ew} \times L}{(\sum (I(t))_t \times A_s \times 3600)} \quad (2)$$

(c) For active solar energy-based system, the average thermal output is determined by:

$$\eta_{active} = \frac{\sum \dot{m}_{ew} \times L}{\sum (I(t))_s \times A_s \times 3600 + \sum (I)_C \times A_C \times 3600} \quad (3)$$

Exergy efficiency of solar energy-based system is also calculated as:

$$\eta_{EX} = \frac{\text{Exergy Output of solar still } (\dot{E}x_{evap})}{\text{Exergy Input to solar still } (\dot{E}x_{in})} \quad (4)$$

Passive solar energy-based exergy input ($\dot{E}x_{in}$) determined as:

The passive solar energy-based system ($\dot{E}x_{in}$) exergy input is given in the following equation (5).

$$\dot{E}x_{in} = \dot{E}x_{sun} = A_s \times I(t) \times \left[1 - \frac{4}{3} \times \left(\frac{T_a + 273}{T_s} \right) + \frac{1}{3} \times \left(\frac{T_a + 273}{T_s} \right)^4 \right] \quad (5)$$

The exergy input of active solar energy-based system remains the sum of exergy input to solar still and exergy input to flat plate collector and is represented by Equation 6.

$$\dot{E}x_{in} = \dot{E}x_{sun} (solar\ still) + \dot{E}x_{sun} (FPC) \quad (6)$$

where

$$\dot{E}x_{sun} (FPC) = Q_u \times \left[1 - \frac{T_a + 273}{T_w + 273} \right] \quad (7)$$

The exergy output of a solar energy-based system can be expressed as follows:

$$\dot{E}x_{evap} = A_s \times h_{ew} (T_w - T_{cie}) \times \left[1 - \frac{T_a + 273}{T_w + 273} \right] \quad (8)$$

CONCLUSIONS

The study draws the following conclusions:

- i. The daily yield of an SBDSP was found to be 1.838 kg/m² for a day in the month, while the daily yield of an SBDSAN was found to be 2.791 kg/m².
- ii. In comparison to the SBDSP, the SBDSAM yields 1.5 times more.
- iii. SBDSAN's thermal efficiency is lower than SBDSP's thermal efficiency. SBDSAN, on the other hand, exceeds SBDSP in terms of exergy efficiency.

REFERENCES

- [1] M.A.S. Malik, G.N. Tiwari, A.Kumar, M.S. Sodha, Solar distillation. 1st edn. UK: Pergamon Press, 1982.
- [2] G.N. Tiwari. Recent advances in solar distillation. Contemporary Physics-Solar Energy and Energy Conservation, Wiley Eastern Ltd, New Delhi, India, 1992, Chapter II.
- [3] Eduardo Rubio, L. Jose Fernandez, A. Miguel, Porta-Gandara, Modeling thermal asymmetries in double slope solar stills. Renewable Energy 29 (2004) 895-906.
- [4] Sandeep, Sudhir Kumar & V.K. Dwivedi. Evaluating thermal performance of a basin type modified active solar still. Desalination and Water Treatment, 72 (2017) 100–111.

AN ON-BOARD ENERGY AND ENVIRONMENTAL ANALYSIS WITHIN THE COVID-19 EFFECTS

¹ Alperen Sari, ^{2*} Egemen Sulukan, ² Doğuş Özkan, ³ Tanay Sıdkı Uyar
¹Marmara University, Mechanical Engineer Department, 34722 Istanbul, Turkey
² National Defence University, Mechanical Engineering Department, 34942 Istanbul, Turkey
³ Beykent University, Department of Mechanical Engineering, 34398 Istanbul, Turkey

*Corresponding author e-mail: esulukan@dho.edu.tr

ABSTRACT

The maritime transport sector, which has taken important measures in recent years in the fight against climate change and global warming, is greatly affected by regional and global economic developments. In 2019, the economic stagnation caused by the regional events, especially the US-China economic tension and the Brexit crisis in Europe, had an impact throughout the world. The covid-19 pandemic, which emerged in China at the end of 2019 and was effective worldwide in the first quarter of 2020, caused the world economy and maritime transport to contract by 4.1% in 2020. In this study, it is planned to analyze possible situations by modeling this situation that has suddenly emerged via decision support tools. In this context, energy and environmental analysis of a chemical tanker ship was carried out with the Reference Energy System (RES) concept between 2017 and 2030 via The Low Emission Analysis Platform (LEAP).

Keywords: Reference Energy System, Energy Analysis, Energy Modelling, LEAP, Greenhouse Gas Emissions

INTRODUCTION

Transport, especially maritime transport, is a sector that is greatly affected by the developments in the world economy and trade [1]. In 2019, the trade war between the USA and China, and regional crises such as the Strait of Hormuz and Brexit, etc., caused a great recession in the world economy [2]. The Covid-19 epidemic, which emerged in China in December 2019 and was described as a global pandemic by the World Health Organization (WHO) on March 11, 2020, continues to be effective worldwide in 2021 [3]. The Covid-19 crisis, which is considered to have effects beyond the great social and economic crises that have taken place in world histories such as the Great Depression and the 2008 Financial Crisis, is undoubtedly the main parameter that should be considered in all development policies [4].

The pandemic process has brought maritime transport to the forefront with its critical role in ensuring the continuity of global trade and supply in the crisis phase and the following period [2]. This has been demonstrated by the recommendations of many international organizations around the world to protect port workers and sailors, but to keep ports open for ships and related operations [5]. According to UNCTAD (2020), unfavorable economic conditions strengthened by the pandemic in 2020 caused a 4.1% decrease in international maritime trade [2]. In 2019 followed by 2020, a year in which the growth momentum slowed down, severe pressure on international shipping continued.

Although the development of the vaccine and the start of the vaccine process is promising, it is clear that the pandemic has not yet come to an end. With globalization, the economies of countries that are more dependent on each other make total normalization more difficult. The timing and scale of the recovery are difficult to predict, as many factors can significantly influence the outlook for world trade and the shipping that makes it possible. UNCTAD forecasts (UNCTAD, 2020:24) indicate that maritime trade will recover with a growth of 4.8% in 2021 [2].

MATERIALS AND METHODS

In this study, energy and environmental analyzes are made by modeling a chemical tanker ship with the Reference Energy System (RES) concept and the Decision Support Tool. LEAP (The Low Emission Analysis Platform), developed by the Stockholm Environment Institute and used by many governments, universities, academies and international organizations around the world, is used as a decision support tool [6].

In the analyzes made, 2017 data of the Diamond-T chemical tanker ship belonging to Transal Denizcilik company are used. After entering the 2017 values determined as the reference year, 3 different scenarios were developed and energy and environmental analyzes were made. In the first scenario, Business-as-Usual (BAU) scenario values were taken into consideration and analyzes were made assuming that the demand for the maritime sector would increase by 3 percent as of 2018, in line with UNCTAD data [7].

In the last scenario, while the demand for the maritime sector increases by 3% every year, analyzes were made to reduce the greenhouse gas emissions from a chemical tanker ship by 55% in 2030.

CONCLUSIONS

In the analyzes made, it has been determined that the amount of greenhouse gas emissions originating from a chemical tanker ship in the BAU scenario will be 874,795 thousand metric tons of CO₂ in total until 2030. According to the results of the BAU scenario, it is seen that the total amount of greenhouse gas emissions to be emitted in 2030 will be 73,420 thousand metric tons of CO₂. It has been observed that the total amount of greenhouse gas emissions to be emitted from a chemical tanker ship until 2030 due to the covid-19 effect evaluated in the second scenario and the contraction experienced in economic and maritime transport is 809,508 thousand metric tons of CO₂ equivalent. It has been determined that the shrinkage experienced in the maritime sector due to the economic recession and pandemic effect prevents the emission of greenhouse gas emissions for approximately 1 year.

In the last scenario, greenhouse gas emissions from a chemical tanker ship until 2030 were analyzed in line with the targets of reducing greenhouse gas emissions from the maritime sector determined by IMO (International Maritime Organization) and EU (European Union). In order to achieve these goals, by 2030; It is clearly seen that there is a need for a coordinated study in which all actors of the maritime industry will take part, such as the development of alternative fuel technologies, the introduction of scrubber, etc. filtering systems, operational improvements, innovations and improvements in the shipbuilding phase.

REFERENCES

- [1] Thomas T.A. and Atkins W.A. Transportation [Internet]. Water Encyclopedia; 2010. Available from: <http://www.waterencyclopedia.com/St-Ts/Transportation.html>. [Erişildi: 30 03 2021].
- [2] United Nations Conference on Trade and Development (UNCTAD). Review of Maritime Transport 2020. United Nations Publications. Geneva; 2020.
- [3] Dinçer I. Covid-19 coronavirus: closing carbon age, but opening hydrogen age. *International Journal of Energy Research*; 44 (8); p. 6093; 2020.
- [4] McAleer M. Wang Y-A. Chang C-L. Herding behavior in energy stock markets during the Global Financial Crisis, SARS, and ongoing COVID-19. *Renewable and Sustainable Energy Reviews*; 134; p. 110349; 2020.
- [5] Stannard S. COVID-19 in the maritime setting: The challenges, regulations and the international response. *International Maritime Health*; 71 (2); pp. 85-90; 2020.
- [6] Heaps C. LEAP: The Low Emissions Analysis Platform. [Software version: 2020.1.33]. Stockholm Environment Institute. Somerville; MA; USA.; 2021. [Internet]. Available from: <https://leap.sei.org>.
- [7] United Nations Conference on Trade and Development (UNCTAD). Review of Maritime Transport 2018. United Nations Publications. Geneva; 2018.

TECHNO-ECONOMIC ANALYSIS OF ONSHORE/ OFFSHORE WIND POWER PLANTS

^{1*} Soner Çelikdemir, ² Mahmut Temel Özdemir

¹Bitlis Eren University, Adilcevaz Vocational School, Electric and Energy, Bitlis, 13000, Turkey

²Firat University, Engineering Faculty, Electrical and Electronics Engineering, Elazig, 23000, Turkey

*Corresponding author e-mail: scelikdemir@beu.edu.tr

ABSTRACT

In this study, an equation model is proposed for the first time to estimate the costs of wind power plants (WPP) by analyzing the investment costs of WPP in Turkey. In addition, a case preliminary study is carried out in Adilcevaz region with the proposed equation model. The costs of the wind energy farm to be established in the designated area are calculated for different turbine models and the appropriate turbine model is selected. In addition, an equation model has been developed for the estimation of the costs of offshore wind power plants (WPP) by analyzing the investment costs of the existing offshore WPP in the literature. For the equation model, unlike the literature, distance from the shore and depth parameters are also added. By analyzing the sensitivity of the models, cost changes in different parameter values are expressed. In addition, in the study, a preliminary case study is carried out for different zones in the Bozcaada zone with the proposed offshore equation model. The costs for the different turbine models of the wind energy farm to be established in the determined zone has been calculated and the appropriate zone selection has been made.

Keywords: Onshore and Offshore Wind Energy Potential, Techno Economic Cost Analysis, Sensitivity Analysis

INTRODUCTION

The primary type of energy source in which electrical energy is produced has gained importance today and has become a choice for consumers. This case increases the importance of renewable energy sources (RES) with little environmental impact. Among RESs, WPP has a large share [1]. Turkey; It has significant potential due to its geographical location, pressure centers under its influence, the fact that its three sides are surrounded by seas and the ground shapes [1–3]. Cost information is important for assessing the potential of a region and converting it into an investment. Of this importance, techno-economic cost analysis is a topic addressed by researchers [4–6]. Cost analyzes have been performed for offshore WPPs and equation models have been proposed [3–5]. However, all of the studies carried out cover offshore WPPs. There is no study in the literature where cost analyses are carried out for onshore wind power plants. This situation is seen as a deficiency. The main motivation of this study is to eliminate this gap in the literature. In the first phase of the study, data belonging to 15 WPP in Turkey, which has not been used before in the literature, are used. In the second phase, the resulting equation model is tested using RESs with different parameter values whose data has not been used before. Thus, the proposed equation model is shown to have general validity. At the other stage, sensitivity analysis is performed to examine the changes of the proposed equation model depending on parameter values. In this way, the effect of parameters is seen on the proposed equation model. In the final stage, a case study is carried out for Adilcevaz region using the proposed equation model. Similarly, cost analyzes have been made for offshore WPPs and equation models have been proposed [3,6]. However, studies have been conducted using limited data in the literature. Therefore, the proposed equation models do not have general validity. This situation is seen as a deficiency. The main motivation of this study is to eliminate this gap in the literature. In the first stage of the study, the offshore RES data pool available in the literature has been created. For the proposed equation coefficients of the cost analysis, the Archimedes Optimization Algorithm (AOA) available in the literature has been preferred. In this preference, convergence rate and performance criteria has been effective in problem solving. Thus, it has been shown that the proposed equation model is more comprehensive. In the second stage, in addition to the literature, depth and distance from shore parameters are added for equation development. At the other stage, sensitivity analysis was performed to examine the changes of the proposed equation model depending on parameter values. In this way, the effect of parameters is seen on the proposed equation model. In the final stage, a case study has been carried out for different zones in bozcaada zone using the proposed equation model.

EQUATION MODEL DEVELOPMENT

There are different equation correlations in the literature. Studies have been conducted using limited number of data for equation correlation. The power expression of a wind power plant depends on the rotor blade diameter, the wind speed and therefore the hub height. These expressions are also considered as parameters affecting the cost of WPPs. In light of this information, the proposed equation model for onshore WPP cost is given in Eq. 1. In this study, in addition to the equation model available in the literature, depth expressions and distance to shore are also added. In the light of this information, the proposed equation model for the offshore WPP cost is given in Eq. 2.

$$\text{Cost} = a.P^b + c.H^d + e.R^f + g \quad (1)$$

$$\text{Cost} = a.P^b + c.H^d + e.R^f + g.D^h + i.X^j + k \quad (2)$$

In Eq. 1 and Eq. 2, “a and b” are the constant coefficients of the P (KW) power expression, “c and d” are the constant coefficients of the H (m) hub height, “e and f” are the constant coefficients of the R (m) rotor diameter expression, “g and h” are constant coefficients of D (km) distance to shore, “i and j” are constant coefficients of X (m) depth expression. Onshore parameter values are given in the first row of Tab. 1. Offshore parameter values are given in the second row of Tab. 1.

Table 2. Parameter Values

A	B	C	D	E	F	G	H	I	J	K
0,13847	1,37984	0,04267	0,21425	0,17448	0,08659	1,39859	-	-	-	-
6,28682	0,74735	0,14702	1,34074	1,72841	0,71273	0,48269	1,22683	1,54236	0,39714	-148,032

EQUATION VALIDATION

The proposed equation parameters are calculated by referencing onshore WPPs with uniform rotor diameter and hub height. However, today some wind energy farms have different hub height and rotor diameter values. This case affects the cost value. The proposed equation model is applied to onshore WPPs with different parameters. In this case, values close to the error rates in the proposed equation model are obtained. The maximum percent error value is calculated as -10.8234%, the average error is 6.7683% and the standard deviation value is 6.8693.

SENSITIVITY ANALYSIS

Sensitivity analysis is carried out to see the effects of the parameters in the proposed equation model on the cost. The parameters in the equation model for sensitivity analysis are examined respectively. The results of the sensitivity analysis study for onshore wind farms are given in Figure 1. For offshore wind farms, the results of the sensitivity analysis study are given in Figure 2. In this way, the effect of the parameters on the cost can be clearly seen.

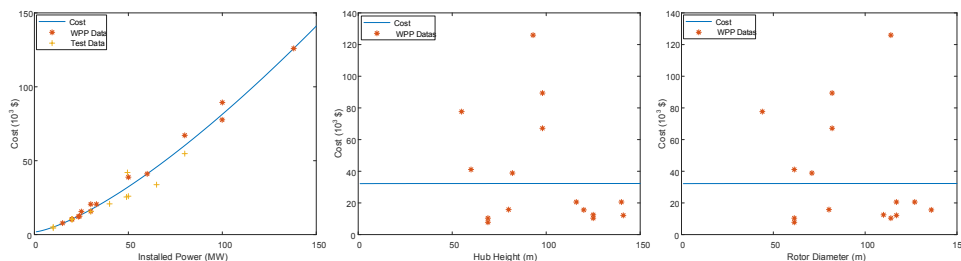


Figure 8. Sensitivity Analysis for Onshore Wind Power Plants

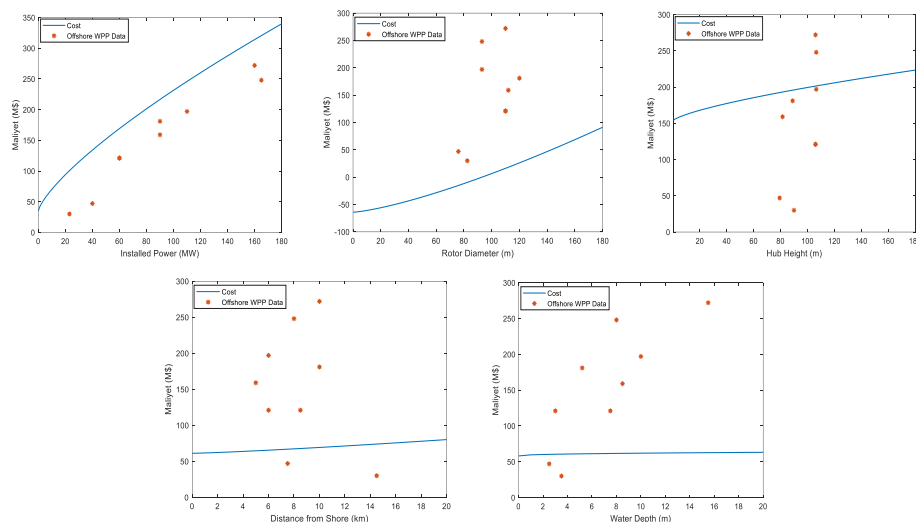


Figure 9. Sensitivity Analysis for Offshore Wind Power Plants

CASE STUDY

In this section, the cost of a wind energy farm to be established in Adilcevaz region has been estimated. In the study, 14 wind turbine models belonging to different brands are examined. According to the data obtained, the most suitable model for the wind farm to be established in the region will be Nordex N117-3/3 with the lowest unit energy cost and the worst model Enercon E82-2.3/1 with the highest unit energy cost. In addition, as the hub height increases, the average wind speed value, scale parameter, capacity factor and power density values increase. The actual runtime and the amount of energy produced vary according to the characteristics of the wind turbine. The unit energy cost is

calculated by the ratio of wind power plant cost to the amount of energy produced. The case study results are given in Tab. 2.

Table 3. Case Study Results

Turbine	Average Wind Speed (m/s)	Power Density (W/m ²)	Actual Operation (%)	E (kWh)	Cost (M\$)	COE (\$/Wh)
Nordex N117-3/3	5.590438059	354.4550629	0.823636778	5409317	33.23136592	0.00614336
Enercon E82-2.3/1	4.659090909	197.1275828	0.732032854	2005540	32.86892498	0.01638906

Offshore wind energy potentials were determined using 6 different measurement station data in Bozcaada and Gökçeada zone on the Aegean coast. The study results for these zones are given in Tab. 3. Taking into account the distance of these zones to the shore and depth data, the most suitable model selection has been made for the wind energy farm to be established in the zone with high energy potential. In the study, 8 wind turbine models belonging to different brands are examined.

Table 4. Case Study Results

Zone	Average Wind Speed (m/s)	Power Density (W/m ²)	Actual Operation (%)	Cost (M\$)	COE (\$/Wh)
1	4.513208	114.5036	0.616473	300.8802	0.050064
2	8.866467	1106.692	0.530345	302.0739	0.009678
3	7.777126	833.3565	0.778462	298.4601	0.012879
4	8.525389	1013.357	0.611567	376.8492	0.012908
5	5.944288	367.2117	0.536048	306.1251	0.021193
6	6.736872	545.4119	0.514716	311.7892	0.017305

CONCLUSIONS

With the equation model proposed for the first time, percentage error rates were calculated below 17.87%. In addition, the average error is calculated as 6.3674% and the standard deviation value as 7.9112. The proposed onshore equation model has been tested with 9 WPP data with different power, rotor diameter and hub height. In this case, percentage error rates are calculated below 10.8234%. In addition, the average error is calculated as 6.7683% and the standard deviation value as 6.8693. According to the results obtained, the cost is estimated with high accuracy. This indicates the effectiveness of the proposed equation model. In addition, the change effects of the parameters in the proposed equation model are examined in the study and it is observed that the effect of system power in the equation is much greater. In the case study conducted for the Adilcevaz region, calculations are made for different turbine models. According to these calculations, the most suitable turbine model selection is found to be Nordex N117-3/3 with the lowest unit energy cost value. With this study, a cost equation is proposed for the first time for onshore WPPs and contribute to the calculation of cost equation parameters using AOA. A new cost equation model has been proposed for offshore and percentage error rates have been calculated below 6.96%. In addition, the average error has been calculated as 2.12335 %. In the case study conducted for Bozcaada zone, calculations have been made using different turbine models for different zones. According to these calculations, the most suitable zone is the 2nd zone, which is indicated as the northern zone of Bozcaada. In addition, SWT-7.0-154 with the lowest unit energy cost value has been found as the most suitable turbine model. With this study, a new cost model for offshore wind power plants has been developed and contributed to the literature. In addition, this developed equation model has been used in a case study.

REFERENCES

- [1] Cali U.,Erdogan N.,Kucuksari S.,Argin M. 2018.Techno-Economic Analysis of High Potential Offshore Wind Farm Locations in Turkey,Energy Strategy Reviews.
- [2] Argin M., Yerci V.,Erdogan N.,Kucuksari S.,Cali U. 2019.Exploring the Offshore Wind Energy Potential of Turkey Based on Multi-Criteria Site Selection,Energy Strategy Reviews.
- [3] Satir M.,Murphy F.,McDonnell K. 2018.Feasibility Study of an Offshore Wind Farm in the Aegean Sea, Turkey,Renewable and Sustainable Energy Reviews.
- [4] Dicorato M.,Forte G.,Pisani M.,Trovato M. 2011.Guidelines for Assessment of Investment Cost for Offshore Wind Generation,Renewable Energy.
- [5] Çelikdemir S., Özdemir M.T. 2020.Adilcevaz Bölgesinde Rüzgar Enerji Potansiyelinin İncelenmesi,Bitlis Eren Üniversitesi Fen Bilimleri Dergisi.
- [6] Ioannou A.,Angus A.,Brennan F. 2018.Parametric CAPEX, OPEX, and LCOE Expressions for Offshore Wind Farms Based on Global Deployment Parameters,Energy Sources, Part B: Economics, Planning and Policy.

ADAPTIVE CONTROL TECHNIQUE FOR GRID INTEGRATED SPV GENERATING SYSTEM FOR POWER QUALITY ENRICHMENT

^{1*} Dinanath Prasad, ² Narendra Kumar, ³ Rakhi Sharma

¹Delhi Technological University, Electrical engineering Dept., Bawana Rd, Shahbad Daulatpur, Rohini, Delhi, 110042

²Delhi Technological University, Faculty, Electrical engineering Dept., Bawana Rd, Shahbad Daulatpur, Rohini, Delhi, 110042

³Indira Gandhi National Open University, Faculty, Electrical engineering Dept., Maidan Garhi Rd, New Delhi, Delhi 110068

* e-mail: prasaddinanath@akgec.ac.in

ABSTRACT

This paper bestows the adaptive control technique for grid-interfaced double stage solar photovoltaic (SPV) system. In the first stage, system includes DC-DC boost converter, the duty ratio of boost converter is regulated by maximum power point tracker (MPPT) system. A fuzzy logic based MPPT controller is incorporated for maximum power extraction from SPV system. However, in second stage, 3-leg voltage source converter (VSC) is connected with SPV array via DC link capacitor. Proposed fuzzy logic based adaptive control scheme is designed to generate reference currents. Moreover, the generated reference currents and sensed AC grid current is utilized to provide switching pulses to VSC. The proposed system exhibits for multifunctional applications such as, power quality enrichment, balancing of load, reactive power compensation, voltage regulation etc. A rule based fuzzy logic controller is utilized for maintaining DC link voltage. The PV feed-forward technique is incorporated in proposed controller for dynamic performance enhancement. The above-mentioned work is simulated in MATLAB/Simulink environment for power quality enrichment.

Keywords: Fuzzy logic, Harmonics, SPV array, MPPT, Adaptive control.

INTRODUCTION

There is an increasing emission of greenhouse gases become substantial issue globally to choose dispersed energy sources. Therefore, the emphasis on the clean energy generating units increased in the distribution end significantly. The smaller size generating units such as solar photovoltaic is the emerging sources chosen because of abundance availability and generation of clean energy. Solar arrays require large area as well as considerable investments, they can be utilized by installing rooftop photovoltaic systems in apartments, commercial buildings, etc. [1], [2]. Moreover, solar photovoltaic generating system widely used in grid integrated mode. For grid integration mode single and double stage configured topology of SPV system are reported in many literatures [3],[4]. The performance comparative analysis between single and double stage topology has been incorporated in literature [5]. The maximum active power from SPV array can be extracted by maximum power point tracker (MPPT). The accurate tracking of maximum power from SPV system is itself a very tedious task. Various important points are to be kept in mind while selections of MPPT such as accuracy, reliability, structure, speed of convergence and cost. Therefore, several MPPT algorithms such as P&O, fuzzy logic control, ANN, current sweep, RCC, array reconfiguration, BFV, LRCM, sliding mode control, etc, have been reported in literature [6].

In recent times researchers are showing more interest in (SOGI) Second order generalized integrator and (DSOGI) damped second order generalized integrator [25], [26]. The SOGI control scheme has inferior DC offset rejection capability and poor dynamic response deteriorated under nonlinear load conditions. However, SOGI scheme is designed by incorporating orthogonal signal generator (OSG) for estimation of input signal. In the DSOGI control scheme a damping factor is incorporated to damping out the oscillation, which possess better convergence rate and good frequency response compared to SOGI algorithm. The fuzzy logic rule-based control algorithm is reported in the literature [27] for grid integrated solar PV system on PWM signals generation for the inverter.

MATERIALS AND METHODS

The following attributes of the proposed work are summarized here.

1. The proposed fuzzy logic-based scheme is better harmonic filtering capability under variable system frequency.
2. The system shows better performance for load balancing with variable irradiance and under load unbalancing.
3. An error between DC link voltages is computed through rule based fuzzy logic controller which eliminates the dependency on PI controller.
4. The proposed controller is independent from the trigonometric function for fundamental component of load current extraction. Therefore, this control scheme possesses better dynamic response compared to the conventional controllers.

- The proposed controller showing excellent dynamic characteristics during the transition from SPV system to DSTATCOM and vice-versa.

The Proposed System Layout And control technique algorithm Is shown in Figure1 and Figure 2

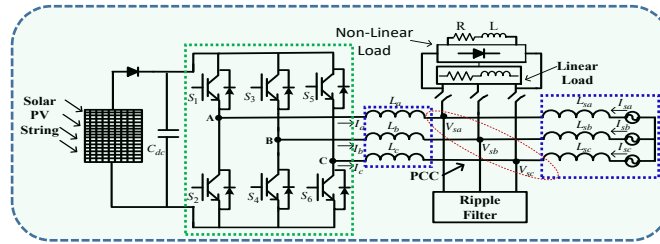


Figure 1

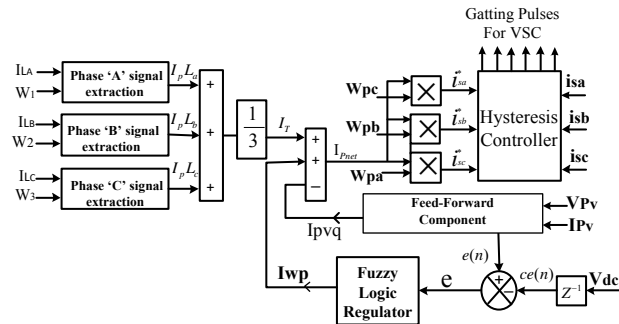


Figure 2.

CONCLUSIONS

A three-phase grid interfaced, double stage solar photovoltaic system (SPV) has been implemented and controlled using fuzzy based adaptive control scheme. This scheme has been effectively used to extraction of reference currents and providing gating pulses for VSC. The performance of control scheme for SPV system has been found satisfactory under the linear/nonlinear loads as well as in load unbalancing conditions under varying system frequency. The mentioned system along with fuzzy logic based adaptive control scheme has shown better performance in power quality enhancement. The effectiveness of feed-forward component has been presented for dynamic performance improvement. Rule based fuzzy logic controller is incorporated accurately with adaptive control scheme for converter loss component estimation. The complete system was incorporated in MATLAB/Simulink environment for power quality enrichments.

REFERENCES

- [1] B. Mountain and P. Szuster, "Solar, solar everywhere: Opportunities and challenges for Australia's rooftop PV systems," IEEE Power and Energy Magazine, vol. 13, no. 4, pp. 53–60, July 2015.
- [2] A. M. Rauf and V. Khadkikar, "Integrated photovoltaic and dynamic voltage restorer system configuration," IEEE Transactions on Sustainable Energy, vol. 6, no. 2, pp. 400–410, April 2015.
- [3] M. A. Hannan, Z. A. Ghani, A. Mohamed and M. N. Uddin, "Real-time testing of a fuzzy logic controller-based grid-connected photovoltaic inverter system," 2014 IEEE Industry Application Society Annual Meeting, Vancouver, BC, 2014, pp. 1-8, doi: 10.1109/IAS.2014.6978394.
- [4] B. Singh, S. Kumar and C. Jain, "Damped-SOGI-Based Control Algorithm for Solar PV Power Generating System," in IEEE Transactions on Industry Applications, vol. 53, no. 3, pp. 1780-1788, May-June 2017, doi: 10.1109/TIA.2017.2677358.
- [5] M. A. Hannan, Z. A. Ghani, A. Mohamed and M. N. Uddin, "Real-time testing of a fuzzy logic controller-based grid-connected photovoltaic inverter system," 2014 IEEE Industry Application Society Annual Meeting, Vancouver, BC, 2014, pp. 1-8, doi: 10.1109/IAS.2014.6978394.

STATE-OF-ART GREEN CRYPTOCURRENCY MINING MODELS

^{1*} Nazenin Gure

¹Beykent University, Faculty of Engineering-Architecture, Mechanical Engineering Department, Ayazaga Campus, Istanbul, Turkey

[*nazeningure@beykent.edu.tr](mailto:nazeningure@beykent.edu.tr)

ABSTRACT

Cryptocurrency mining is profitable investment with ever-increasing energy demand. Renewables pose advantage to miners. Besides, mining income covers renewable power plant costs as well as providing further finance. Mining hardwares produce excessive heat during processing. State-of-art systems utilizing excessive mining heat into energy and for heating households, drying or greenhouse crops along with renewable energy supply are investigated. Unique token economy finance based on finding, using and founding of energy solutions is covered. Further novel proposal of excessive mining heat use cases for saline water treatment is proposed in this study.

Keywords: Blockchain, Cryptocurrency, Climate Change, Green-Mining, Renewable Energy

INTRODUCTION

Among blockchain consensus mechanisms, proof-of-work (PoW) requires computational power, also known as mining. Greener and cheaper energy supply of mining has become fundamental features of cryptocurrency mining. While renewable empowered mining ratio is generally stated as 76%, revised estimations lead that this ratio is actually 39%. According to Digiconomist's and Cambridge's surveys in the pool of 280 major crypto companies in 59 countries, the distributions of renewable sourced mining are 62%, 17%, 15% and 6% for hydropower, wind, solar and geothermal, respectively. Additionally, fossil fuel sourced electricity distribution used by miners are 38% for coal, 36% for natural gas and rest for other resources. River sourced hydropower plants are preferred for small-scale mining facilities due to stable energy feed stem from snows instead of rainfall. Weather dependency of hydropower plants shifts miners to coal fuelled stable energy feed [1], [2]. Although miners are tend to use stable and cheaper energy, renewable power plant investors prefer to embed mining facility to cover investment costs and earn additional income [3]. Mining integration into renewable power plants drops the period of redemption from 5 to 1 year. There exists state-of-art researches and applications for green-mining. Malfuzi et al. and Rusovs et al. proposed renewable embedded mining plant designs. Malfuzi's novel green solution biogas fed solid oxide fuel cell is estimated as the least profitable but the greenest option [4]. State-of-art challenges extend the green perspective upon excess heat of mining hardwares. Studies of Nguyen and Hoang, and the products of Heatmine [5] and Qarnot [6] focuses on heating upon mining. Another state-of-art model to shift global renewable use cases and application of energy solutions is initiated by Steve Wozniak via Eforce. Eforce token with the symbol WOZX generated 1 Billion [7] and its WOZX economy is based on blockchain based energy projects and rewarding the peers upon energy solutions [8]. Finally, waste heat is further used to grow crops in green houses. State-of-art application in this case is that renewable empowered mining facility's waste heat to be used to grow vegetables like tomatoes and strawberries.

STATE-OF-ART SYSTEMS GENERATING AND HARVESTING HEAT FROM MINING

A sophisticated study performed by Rusovs et al. on novel bio-generation plant with tri-generation station merged with mining equipments. Tri-generation station has three different energy output with one feeds mining and a loop to cool down both the plant and the waste-heat of mining by adsorption unit [9]. The latter protects ASICs and components from waste-heat related breakages. As a different perspective, inverse approach of heating from mining is also studied [10]. Hotmine and Qarnot are the leading brands for mining induced heaters on sale. Qarnot provide two solution products that both mines while one for heating homes and the other for heating domestic water. Their offer rewire heating with a profit that is more profitable than traditional or renewable alternatives. However, to heat 100 m²-house, four units of Hotmine or five units of Qarnot are required [6], [11]. Meanwhile, the methodologies to exploit heat from mining are wide-ranging. In literature proposed heating systems containing mining rig as heat source are used to heat domestic houses, buildings, HVAC systems, domestic hot water as well as facilities, schools, public water-based structures such as pools, spas, Turkish bath and similar [10], warehouses [5], churches, campuses, and most of all greenhouses [3], [5], [12]. Regarding methodologies to achieve these scenarios are listed as: Canadian well ventilation [12], floor heating upon mineral oil submersed mining processors of Bitmain, boiler heating [13] and adsorption. Sophisticated state-of-art systems composed of air-to-water heat pump, connecting waste heat to exhaust air duct and then exhaust-air heat pump, delivering waste heat to compact unit. Last, for low heat demand buildings, compact unit connected to solar thermal panel integrated hydronic heating system [10]. Applications such as heat pump and Canadian well ventilation have chilled circulation output, which is returned back to cool the mining processors. Pilot scale tests are performed with two Antminer S9 mining rigs having monthly heat capacity of 2.3 MWh as well as heat pump having monthly power consumption of 78 kWh. Resultant hybrid system

managed to heat Hyrsylä Co-housing multi-family house that is renovated from primary school in Lohja, Finland while cooling mining rigs. In separate analysis, it is represented that the same hybrid system is capable to meet domestic hot water need of Hyrsylä.

Finally, pioneer project for the state-of-art greenhouse application is 'cryptotatoes' by Brejcha. Mining facility is powered by bio-waste and use waste heat for greenhouses that resulted successful growth of tomatoes [3]. Heatmine on the other hand, supply 75% of heating of Canadian strawberries from mining [5]. UnitedCorp's unique hybrid Blockchain Dome Heat Station system heats greenhouses stable at 20°C regardless of the seasons [12].

CONCLUSIONS

As crypto-mining become more profitable, state-of-art projects to harvest or reuse excess heat also peaks. Moreover, advantages of renewable integration not only profit miners. Mining integration into renewable power plants is also profitable for the investors since costs are covered withing a year and further supply income afterwards. Heating upon mining is found that sufficient to heat households even in coldest regions such as Finland and Siberia [14]. Alternative use cases for hot seasons cover dryers, drying moist buildings to prevent mold, and other facilities that require heat like pools and spas [10]. As a unique suggestion, mining waste heat is ideal for the desalination of sea water. Possible green mining loop for hot regions with lack of fresh water can be solar power plant fed mining [15] and using resultant mining and solar waste heat for desalination of sea water, followed by irrigation of crops.

REFERENCES

- [1] DIGICONOMIST, "Bitcoin Energy Consumption Index CO2," 2020. <https://digiconomist.net/bitcoin-energy-consumption> (accessed Nov. 20, 2020).
- [2] Cambridge, "Bitcoin Mining Map," *University of Cambridge judge business school, Cambridge Center for Alternative Finance*, 2020. https://cbeci.org/mining_map.
- [3] J. Redman, "'Cryptotatoes' Using Excess Mining Heat to Grow Produce," *NEWS BITCOIN*, 2018. <https://news.bitcoin.com/cryptotatoes-using-excess-mining-heat-to-grow-produce/> (accessed Nov. 28, 2020).
- [4] A. Malfuzi, A. S. Mehr, M. A. Rosen, M. Alharthi, and A. A. Kurilova, "Economic viability of bitcoin mining using a renewable-based SOFC power system to supply the electrical power demand," *Energy*, vol. 203, p. 117843, 2020, doi: <https://doi.org/10.1016/j.energy.2020.117843>.
- [5] HEATMINE GROUP, "Heatmine announces new heating unit powered by cryptocurrency miners," *openPR*, 2018. <https://www.openpr.com/news/1337992/heatmine-announces-new-heating-unit-powered-by-cryptocurrency-miners.html> (accessed Nov. 28, 2020).
- [6] Qarnot, "QB1 ECOLOGICAL AND FREE HOT WATER THANKS TO COMPUTERS' WASTE HEAT," *Qarnot*, 2020. <https://qarnot.com/en/heating-water/>.
- [7] J. V. J. Vanetti and S. Wozniak, "Transfer of energy savings," 2020. [Online]. Available: https://www.efforce.io/uploads/op/EFFORCE_ONE_PAGER.pdf.
- [8] EFFORCE, "EFFORCE White paper," 2020. [Online]. Available: https://efforce.io/WP_ENG_V1.pdf.
- [9] D. Rusovs, S. Jaundālders, and P. Stanka, "BLOCKCHAIN MINING OF CRYPTOCURRENCIES AS CHALLENGE AND OPPORTUNITY FOR RENEWABLE ENERGY," in *2018 IEEE 59th International Scientific Conference on Power and Electrical Engineering of Riga Technical University (RTUCON)*, 2018, pp. 1–5, doi: 10.1109/RTUCON.2018.8659867.
- [10] T. Nguyen and A. Hoang, "Reusing Waste Heat from Cryptocurrency Mining to Heat Multi-Family House," *Metropolia University of Applied Sciences*, 2018.
- [11] T. Breunig, "Home Heating with Crypto Mining," *Efficiency, Energy Harvesting, Green Building, Innovative Business Model-CLEANTECH CONCEPTS*, 2018. <http://www.cleantechconcepts.com/2018/06/home-heating-with-crypto-mining/> (accessed Nov. 20, 2020).
- [12] UnitedCorp, "Second Greenhouse Heated By Cryptocurrency Mining- iGrow," *iGROW*, 2018. <https://www.igrow.news/igrownnews/second-greenhouse-heated-by-cryptocurrency-mining> (accessed Nov. 28, 2020).
- [13] A. Baydakova, "Bitcoin Miners Are Heating Homes Free of Charge in Frigid Siberia," *Coin Desk*, 2019. <https://www.coindesk.com/bitcoin-miners-are-heating-homes-for-free-in-frigid-siberia> (accessed Nov. 20, 2020).
- [14] A. PETERS, "A solution to bitcoin's energy waste: Use it to warm buildings," *FASTCOMPANY*, 2018. <https://www.fastcompany.com/90268985/a-solution-to-bitcoins-energy-waste-use-it-to-warm-buildings> (accessed Nov. 20, 2020).
- [15] J. P. Buntinx, "Will Mining Cryptocurrency in the Desert Using Solar Power Make You Rich?," *The Merkle News*, 2017. <https://themerke.com/will-mining-cryptocurrency-in-the-desert-using-solar-power-make-you-rich/> (accessed Nov. 20, 2020).

DESIGN OF A FUTURE HYDROGEN SUPPLY CHAIN: A MULTI-OBJECTIVE MODEL FOR TURKEY

¹ Ebru Geçici, ² Ahmet Erdoğan, ^{3*} Mehmet Güray Güler
Department of Industrial Engineering, Faculty of Mechanical Engineering, Yıldız Technical University, Istanbul, Turkey

*Corresponding author e-mail: mgguler@yildiz.edu.tr

ABSTRACT

Fossil fuel reserves, which are the the main energy source in the transportation sector today, are being depleted very fast. In addition, they are the main source of carbon emissions as well. Researchers, therefore, are trying to exploit efficient energy resources and hydrogen is one of the best alternatives. However, usage of hydrogen depends heavily on infrastructures which is not well developed today. The lack of existing infrastructure has been identified as one of the main obstacles to developing hydrogen economy. This study addresses the design of Hydrogen Supply Chain (HSC) design problem of Turkey. The problem is modeled using a multi objective mixed integer programming (MIP) model and solved using the epsilon constraint method. The aim is to balance three objectives: (cost, carbon emission and safety risk). The results reveal that, it's better to design a decentralized to develop a supply network that includes electrolysis production facilities to balance the cost, carbon emission and safety risk.

Keywords: Hydrogen supply chain design, multi-objective optimization, Mixed integer linear programming

INTRODUCTION

The need for energy in the transportation sector, is increasing every day. With this growing need, existing energy resources such as oil will not be sufficient to meet the demand in the medium and long term. Also, the use of oil as a fuel causes carbon emissions (CO₂), which is one of the main causes of global warming [1]. For this reason, the number of researches on alternative energy sources is increasing. One of these alternatives is hydrogen energy, which can be produced from various energy sources [2]. In order to deliver hydrogen energy, which has not yet become widespread, to the consumer, harmless to the environment, safely and cost-effectively a sustainable hydrogen supply chain network (HSC) must be established. HSC consists of four parts: (i) primary energy sources, (ii) production, (iii) storage and (iv) transportation. Figure 1 shows the link between these stages [2].

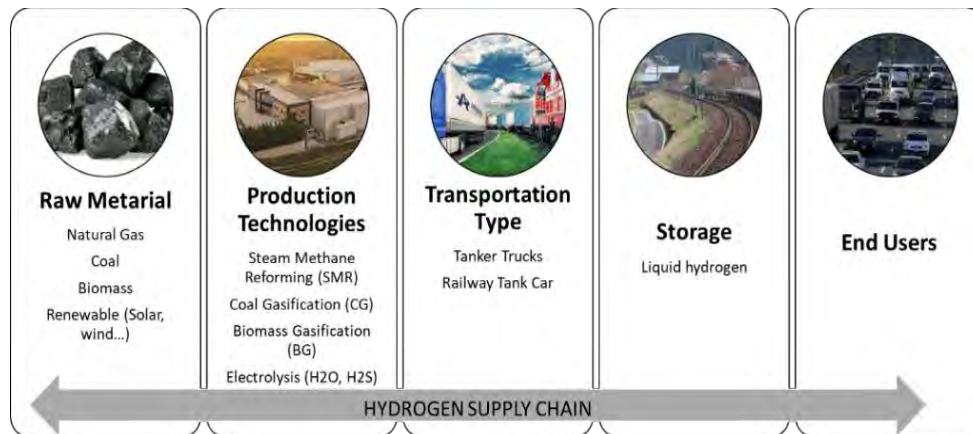


Figure 1. Hydrogen Supply Chain (Adopted from [2])

In this study, the design of HSC to meet the energy demand of transportation sector in Turkey in the future is addressed. The problem is modeled with a MIP model and in addition to cost minimization, minimization of risk and carbon emissions are also addresses in the proposed model. The epsilon constraint method is used to solve the multi-objective structure. The combination of multiple objectives and all parts of the HSC constitutes the motivation of this study.

MATHEMATICAL MODEL, METHODS AND CASE STUDY

Almansoori and Shah, with their seminal studies in 2006 has studied HSC of England. They formulate the problem using a MIP model with an objective of minimizing the average cost that consists of production, storage and transportation costs. In terms of duration, there are operating costs that incur on yearly basis and capital costs that incur once in a planning horizon. The region is divided into smaller sub-regions, called grids and the aim is to find the location and type of the production facilities and the flow of hydrogen from these facilities to the grids while minimizing

the cost [5]. This model is later extended to cover several different goals. Kim et al. [4], for example, added risk levels of production, storage and transportation and proposed a model that minimize the risk level of the total HSC. Later Almaraz et al [3] and Bique et al [1] added CO₂ emission minimization to the model as the third objective.

In this study, the HSC model of Turkey studied in [2] is extended to cover three different objectives (cost, risk, CO₂ emission). The country is divided into 33 grids and the hydrogen demand of each grid in 2050 (the expected saturation period) is calculated. It is assumed that hydrogen vehicles will constitute 25% of the total vehicles in parallel with the literature ([1]). Four different optimization scenarios are created: (i) cost minimization, (ii) carbon emission minimization, (iii), risk minimization, and (iv) multi-objective.

In scenario 1, it is observed that a total of 10 large-size steam methane reforming (SMR) facilities and six small-size electrolysis production facilities are opened in nine different grids. Long transport links are established between grids due to the small number of facilities. In scenario 2 and scenario 3, the model opens maximum number of small facilities since it minimizes transportation in and between grids and sets the lowest risk and CO₂ emission. The establishment of 979 small-scale electrolysis plants in total shows that it is the best option for risk and carbon emission values. Therefore, it is seen that a local solution is obtained, in contrast to scenario 1. In scenario 4, using the epsilon constraint method, the cost is minimized while the CO₂ emission and the risk levels are limited with additional constraints added to the model. Thus, it was ensured that the other two objectives are kept at certain levels. These levels are found to be 578.10 thousand tons/day for carbon emissions and 1,323 units for risk. The results reveal 83 small scale, 19 medium scale and 2 large scale electrolysis production facilities and 5 large scale SMR manufacturing facility in 17 different cities. While the last scenario offers a more centralized network design than the solutions of the risk and carbon scenarios, it offers a more localized network design than the solution of the cost scenario. The results obtained for all scenarios are shown in Table 1. The solution with an increase of 60% from the best cost value, 15% from the best carbon emission value and 3% from the best risk value was chosen as the most balanced multi-purpose optimization solution.

Table 1. Solutions of Scenarios

Scenario \ Objective	Cost (M\$/day)	Carbon Emission (Thousand tons/day)	Risk (unit)
Cost Minimization	8.83 (%0)	653.72 (%30)	1.421 (%10)
Carbon Emission Minimization	21.10 (%139)	502.48 (%0)	1.290 (%0)
Risk Minimization	21.10 (%139)	502.48 (%0)	1.290 (%0)
Multi-Objective Minimization	14.17 (%60)	578.10 (%15)	1.323 (%3)

CONCLUSIONS

Although hydrogen is one of the best alternatives for future energy sources, the supply chain infrastructure of hydrogen is still immature. In this study, considering the demand of the transportation sector in 2050, a multi-objective optimization approach is applied to develop a sustainable HSC network in Turkey. In the study, three objectives considered are cost, carbon emission and safety risk. The epsilon-constraint method is used to examine the three objectives together. When the established production facilities are examined, it is observed that in the scenario where the cost is minimized, a central distribution network is formed by establishing large-sized SMR facilities. In the multi-objective scenario, it is observed that many small-sized electrolysis plants are established. This results in a decentralized network configuration to develop a sustainable HSC network based on electrolysis, addressing to minimize cost, carbon emissions and risk.

REFERENCES

- [1] Bique, A. O., Maia, L. K., La Mantia, F., Manca, D., & Zondervan, E. Balancing costs, safety and CO₂ emissions in the design of hydrogen supply chains. *Computers & Chemical Engineering*, 2019; 129, 106493.
- [2] Güler, M. G., Geçici, E., & Erdoğan, A. Design of a future hydrogen supply chain: A multi period model for Turkey. *International Journal of Hydrogen Energy*, 2021; 6(30), 16279-16298.
- [3] Almaraz, S. D. L., Azzaro-Pantel, C., Montastruc, L., Pibouleau, L., & Senties, O. B. Assessment of mono and multi-objective optimization to design a hydrogen supply chain. *international journal of hydrogen energy*, 2013; 38(33), 14121-14145.
- [4] Kim, J., Lee, Y., & Moon, I. (2011). An index-based risk assessment model for hydrogen infrastructure. *International journal of hydrogen energy*, 36(11), 6387-6398.
- [5] Almansoori A, Shah N. Design and operation of a future hydrogen supply chain: snapshot model. *Chem Eng Res Des* 2006; 84:423e38.

THE LIGHTWEIGHT DEEP LEARNING MODEL FOR SMART GRID STABILITY PREDICTION

¹Ferhat Ucar

¹Firat University, Faculty of Technology, Electrical and Electronics Engineering, Elazig, Turkey

*Corresponding author e-mail: fucar@firat.edu.tr

ABSTRACT

Today, energy providers are more stressed with the need for flexible demand management with renewable energy integration. In the smart grid (SG) structure, clients do not only consume the electricity but also gain the ability to produce it. This dynamic situation reveals a bidirectional energy flow. Besides, complex power flow composes a challenge for deciding to buy or sell the energy optimum. The big picture highlights only one item: SG stability. Decentral Smart Grid Control (DSGC) promises to implement the demand response with a concise framework. DSGC does not sense the major behaves of the grid; it only binds the electricity price to the electrical frequency. Although DSGC offers dynamically and economically feasible grid stability, it still has deficiencies based on the simplifying assumptions. One of the most prominent assumptions indicates that all players of the grid are assumed as identical. In this work, we attempt to introduce how data analytics may help overcome the assumptions in the DSGC system to build a grid stability model. With an enhanced dataset, this work proposes a deep learning-based SG stability model with a lightweight structure. The performance of the deep learning model provides a robust grid stability recognition with a 99.16% accuracy.

Keywords: Smart grid, Grid stability, Deep learning, Convolutional neural networks, DSGC

INTRODUCTION

The smart grid (SG) is a state-of-the-art power grid framework that attempts to have solutions to energy management problems. The SG technology has been developed rapidly and is still growing. Various challenges still exist to be considered when pushing SG to the forefront. The integration of renewable energy resources to the grid seamlessly, and facing a new type of consumer are among urgent issues. This situation constructs the most prominent difference of SG to the conventional grid: two-way electricity power flow. While the conventional grid design includes one-direction electricity flow, from the point it is produced to the point it is consumed, in the SG framework, electricity is allowed to flow in both directions. This bi-directional energy flow comes with a new term called "prosumers". The prosumer definition combines the "producer" and "consumer". The prosumers both supply the energy and consume it at the same time [1]. The demand management and planning the generation, distribution, and monitoring of the consumptions are more complex than before. The economic management of electrical energy tightly dependent on the option of whether buying or not buying the energy at a certain price. Today's industrial and residential environments also involve more distributed energy resource centers compared to yesterday. On top of that SG is equipped with advanced self-monitoring and self-healing systems [2]. All those concerns and decision-makings has developed an attention to the smart grid stability [3].

The stability analysis involves some data processing in the way of determining the price value for the consumers. So a decision-making could be progressed about the usage and the whole process is a time dependent and dynamically estimated. The stability analysis involves some data processing in the way of determining the price value for the consumers. So a decision-making could be progressed about the usage and the whole process is a time dependent and dynamically estimated. The stability assessment is not only important as a technical assignment but also as an economic climate of the electrical energy prices. Decentral Smart Grid Control (DSGC) systems takes just the frequency of the grid to the scene. Because an oversupply situation increases the frequency of the grid and the vice versa, an underproduction situation decreases the frequency of the grid. This scenario points out that the measured frequency has all the information we need to determine the electrical energy prices [4,5]. The DSGC method resolves the grid stability problem with mathematical models based on differential equations. Grid architecture is considered as a four-node star type with a generation node for three consumption nodes. The power balance in total (produced or consumed at each node), the response time of each participant to set the production and/or consumption according to price changes, and the elasticity of energy price is pictured with features (inputs) [5,6]. With the help of mentioned parameters, we have a design of a mathematical model for a prediction tool of grid instability. The end game is to solve the binary classification with the labels of "stable" and "unstable". On the other hand, the solution of this model has recourse to significant assumptions. As splendidly described in [6], a mathematical model based on differential equations can be handled in a number of ways, and some issues like "fixed input" and the "equality" may have been faced. So, it can be argued that a robust intelligent classifier with a state-of-the-art deep learning-based methodology could let us cope with those issues.

In this study, a lightweight convolutional neural network-based deep learning structure is proposed to predict the grid stability using a comprehensive SG stability dataset. The contributions of the proposed model can be listed in the following manner:

- A lightweight 1D-Convolutional Neural Network (CNN) is designed from scratch according to specific requirements of the SG stability prediction. The ad hoc designed deep learning-based model performs well in the stability assessment.
- Using the comprehensive SG stability datasets of [4] and [6] helps to picture the performance in a good manner.

The proposed work takes the study [4] as the benchmark and differs from it in such a way that the proposed lightweight CNN structure is computationally effective with its specific structure from scratch.

MODELING AND ANALYSIS

Deep learning (DL) models have been widely used in a variety of applications in the electricity energy field since the last decade [7]. After it is first proposed in the current network model, CNN structures are swiftly developed in various types. Although generally usage of the CNN relies on a 2D image input, there are specific types in which the 1D signals could be processed [8]. In the proposed SG stability deep learning model, a 1D-CNN is designed from scratch with a lightweight structure. Figure 1 shows the proposed deep learning model with its specific layers. The comprehensive SG stability dataset is a public one and composed with grid stability simulations with an augmented type as in [4]. In Table 1, we can see the details of the dataset and its features.

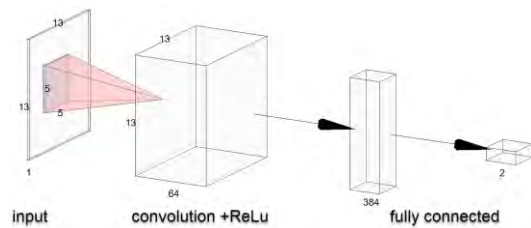


Figure 1. The proposed lightweight CNN structure

Table 1. The proposed lightweight CNN structure

Type	Features	Description
Inputs	tau1 to tau4	the reaction times
	p1 to p4	produced power (+) or consumed power (-)
	g1 to g4	price elasticity coefficient
	stab	differential equation root
Outputs	stabf	stable or unstable classes (categorical binary label)

CONCLUSIONS

Table 2. Performance values

Metric	Performance
Accuracy	0.9925
Sensitivity	0.9948
Specificity	0.9912
Precision	0.9847
F1 Score	0.9897

The experimental analyses have been done in Python - PyTorch DL package with hyperparameter tuning through the process. The performance results are shown in table 2 with selected evaluation metrics. The proposed model reached an accuracy value of 0.9925 with a lightweight 1D-CNN structure. Using the same SG stability dataset, the benchmark study reaches 0.9962 accuracy value with a more complex classifier model. The proposed model solves the DSGCs assumption issues with a deep learning-based prediction model of grid stability and reaches high performance values in very known performance criteria.

REFERENCES

- [1] Tsaousoglou G, Pinson P, Paterakis NG. Transactive Energy for Flexible Prosumers Using Algorithmic Game Theory. IEEE Trans Sustain Energy. 2021;
- [2] Yang L, Xie P, Zhang R, Cheng Y, Cai B, Wang R. HIES: Cases for hydrogen energy and I-Energy. Int J Hydrogen Energy. 2019 Nov 12;44(56):29785–804.
- [3] Guizani M, Anan M. Smart grid opportunities and challenges of integrating renewable sources: A survey. In: IWCMC 2014 - 10th International Wireless Communications and Mobile Computing Conference. Institute of Electrical and Electronics Engineers Inc.; 2014. p. 1098–105.
- [4] Breviglieri P, Erdem T, Eken S. Predicting Smart Grid Stability with Optimized Deep Models. SN Comput Sci. 2021 Apr 4;2(2):73.
- [5] Schäfer B, Grabow C, Auer S, Kurths J, Witthaut D, Timme M. Taming instabilities in power grid networks by decentralized control. Eur Phys J Spec Top. 2016 May 1;225(3):569–82.
- [6] Arzamasov V, Bohm K, Jochem P. Towards Concise Models of Grid Stability. In: 2018 IEEE International Conference on Communications, Control, and Computing Technologies for Smart Grids, SmartGridComm 2018. Institute of Electrical and Electronics Engineers Inc.; 2018.
- [7] Ekici S, Ucar F, Dandil B, Arghandeh R. Power quality event classification using optimized Bayesian convolutional neural networks. Electr Eng [Internet]. 2020 Jul 20; Available from: <http://link.springer.com/10.1007/s00202-020-01066-8>
- [8] Lecun Y, Bengio Y, Hinton G. Deep learning. Vol. 521, Nature. Nature Publishing Group; 2015. p. 436–44.

HYDROGEN ENERGY UTILIZATION – A REVIEW

^{1*}Emre Akiskalioglu

¹Research Assistant, Beykent University, Mechanical Engineering Department, Ayazağa Campus, Istanbul, Turkey

*Corresponding author e-mail: emreakiskalioglu@beykent.edu.tr

ABSTRACT

Hydrogen production methods and different hydrogen energy utilization methods stands out as potential clean energy generation alternative. In this study, energy generation capacities and cost-effective feasibility analysis of current hydrogen production methods and hydrogen decarbonisation are presented. To overcome present energy storage challenges, potential renewable energy alternative is proposed as hydrogen decarbonization methods with promising zero CO₂ emission.

Keywords: Hydrogen Energy, Hydrogen Production Methods, Fuel Cells, Hydrogen Decarbonization, Zero Emission

INTRODUCTION

Hydrogen is easy to find. Despite its simplicity and abundance, it is not found naturally and compound with other elements. It can be obtained from biomass, oil, natural gas, electricity etc. According to IRENA Global Renewables Outlook 2020 [1], blue hydrogen costs are way cheaper than green hydrogen. But it can be compatible soon as reduce of electrolyser cost and green power.

CURRENT ADVANCED TECHNOLOGIES OF IN HYDROGEN ENERGY UTILIZATION

Manabu Tange, Tetsuhiko Maeda et al., [2] researched a system that uses metal hydride. This metal hydrides can balance the energy demand between night and day. This system designed to maximize the efficiency and aimed to reduce cost of electricity. It can be useful for both power suppliers and end users.

Baptiste Delhomme, Andrea Lanzini et al. [3], pointed out that hydrogen is fully renewable, reliable than the other RES (such as wind, solar) and practically this system can be stored anywhere in the World. In this research, a solid oxide fuel cell (SOFC) based combined heat and power (CHP) system.

Nazim Muradov [4] researched about decarbonization of fossil fuels. Figure 1 explains his concept.

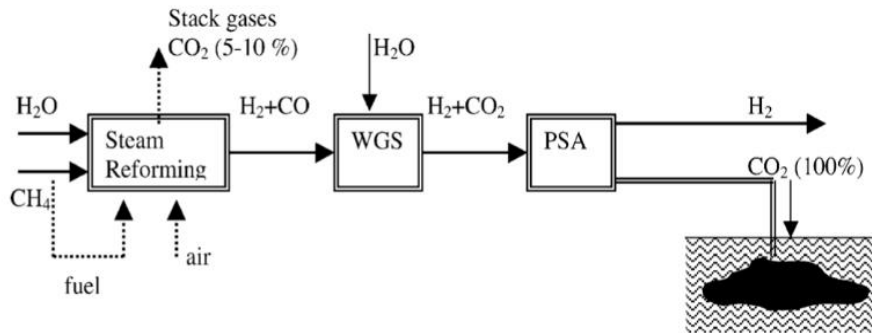


Fig. 1 A fuel-gas decarbonization concept.

Hydrogen also can be obtained from solar decarbonisation of fossil fuels. These processes are usually listed as, the solar thermal decomposition, the steam-reforming, and the steam-gasification.

CONCLUSIONS

To achieve zero CO₂ emission rates, it is fundamental to reduce cost of hydrogen production methods. Today's global production of hydrogen is coming from mainly carbon-based methods [6]. Decarbonization of hydrogen from metals and using fuel cell applications, we can use hydrogen as a fully renewable and cheaper energy source.

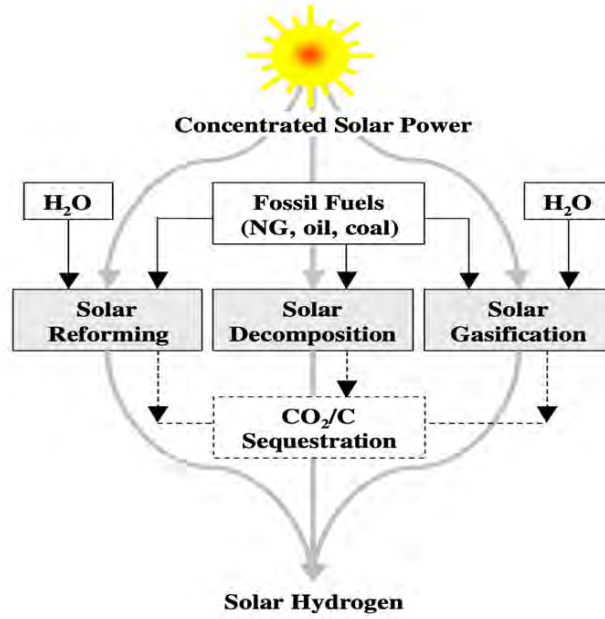


Fig. 2. Scheme of solar thermochemical routes [5]

REFERENCES

- [1] [internet] IRENA Global Renewables Outlook 2020. (Link: <https://irena.org/publications/2020/Apr/Global-Renewables-Outlook-2020>)
- [2] Tange, Manabu & Maeda, Tetsuhiko & Nakano, A. & Ito, Hiroshi & Kawakami, Yoshiaki & Masuda, Masao & Takahashi, Toru. (2011). Experimental study of hydrogen storage with reaction heat recovery using metal hydride in a totalized hydrogen energy utilization system. *International Journal of Hydrogen Energy*. 36. 11767-11776. 10.1016/j.ijhydene.2011.06.023.
- [3] Coupling and thermal integration of a solid oxide fuel cell with a magnesium hydride tank. Baptiste Delhomme, Andrea Lanzini, Gustavo A. Ortigoza-Villalba, Simeon Nachev, Patricia de Rango, Massimo Santarelli, Philippe Marty, Pierluigi Leon. *International Journal of Hydrogen Energy* 38 (2013) 4740-4747.
- [4] Hydrogen via methane decomposition: an application for decarbonization of fossil fuels. Nazim Muradov. *International Journal of Hydrogen Energy* 26 (2001) 1165-1175.
- [5] Hydrogen production via the solar thermal decarbonization of fossil fuels. P.v. Zedtwitz, J. Petrasch, D. Trommer, A. Steinfeld. *Solar Energy* 80 (2006) 1333-1337.
- [6] Parra, D.; Valverde, L.; Pino, F.J.; Patel, M.K. A Review on the Role, Cost and Value of Hydrogen Energy Systems for Deep Decarbonisation. *Renew. Sustain. Energy Rev.* 2019, 101, 279-294.

BID OPTIMIZATION IN ELECTRICITY MARKETS

^{1*} Ezgi Polat, ² Mehmet Güray Güler, ³ Mehmet Yasin Ulukoş

¹ Yıldız Technical University, Department of Industrial Engineering, Faculty of Mechanical Engineering, Besiktas, Istanbul, Turkey

² Yıldız Technical University, Department of Industrial Engineering, Faculty of Mechanical Engineering, Besiktas, Istanbul, Turkey

³ Istanbul Technical University, Department of Industrial Engineering, Faculty of Management, Macka, Istanbul, Turkey

*Corresponding author e-mail: eezgipolat@gmail.com

ABSTRACT

The Turkish Electricity Market has rapidly become a competitive market with the privatization and liberalization policies and the increasing efficiency of renewable power plants. When producers in the electricity market generate more or less than they have committed to supply to the market, they are subject to financial sanctions. Therefore, the increasing competition in electricity markets has revealed the necessity of developing accurate forecasting tools and effective bidding strategies for electricity producers. The main aim of this study is to optimize the bid of a solar power plant operating in Turkey to the day ahead market, using Artificial Neural Networks (ANN). Unlike previous studies, the loss function used in ANN has been customized to address the costs that will be caused by underproduction or overproduction.

Keywords: Electricity markets, bid optimization, artificial neural networks

INTRODUCTION

Turkey's installed capacity and electricity generation are increasing day by day with the privatization policies and the penetration of renewable energy plants into the market. In addition, the electricity demand is growing rapidly due to factors such as industrialization and population growth. The Turkish Electricity Market operates to instantly balance this supply and demand. In the Day-Ahead Market, an independent system operator determines hourly Market Clearing Prices (MCP) by matching the supply and price offers of electricity producers and the demand and price offers of electricity consumers for the next day. When producers generate more than the submitted bid (*overproduction*), they sell the excess production at a *lower* price. On the other hand, they are subject to financial sanctions if they cannot meet their bid (*underproduction*). In renewable power plants, supply-demand imbalances occur as a result of forecasting electricity generation with high error due to the direct effect of weather changes. The difference between the actual generation and the forecasted generation is balanced in the Balancing Power Market and this imbalance causes financial losses for electricity producers. Therefore, it is crucial for the power plants to predict the next day's production with the least error. The renewable power plants usually place these forecasts directly as their bids, however this may not bring the highest profit. In this study our aim is to find a bid that maximizes the profit and that is not necessarily the same with the forecast.

In the literature, there are studies on the optimization of production forecast and bid, separately. In general, for production forecast in renewable energy power plants, statistical or machine learning forecasting methods are developed in which weather and calendar variables are used as inputs. There are also studies on bid optimization in the literature. Bhaskar and Singh [1] propose a stochastic model for the optimum bid of wind energy in the day ahead electricity market. First of all, uncertainties arising from wind energy production and market prices are determined by advanced statistical methods, then possible scenarios are produced using the kernel density estimation method. Matevosyan and Soder [2] use stochastic programming to minimize imbalance costs and develop a new method that generates optimum bid for the short-term electricity market. Herranz et al. [3] propose a method that minimizes an electricity purchase cost to determine the optimum bidding strategy. A genetic algorithm model is designed to optimize the parameters that define the best purchasing strategy. Zhang et al. [4] mention that the uncertainties in renewable energy production make the market bid risky, and develop different strategies with the newsvendor approach to reduce this risk and the costs of imbalance.

We propose an Artificial Neural Network with a customized loss function, which considers the impact of costs incurred due to imbalances between supply and demand. Thus, the electricity producer will bid the amount that it will return a maximum profit instead of the production forecast.

MATERIALS AND METHODS

In this study, we develop a bid forecasting model for a solar power plant operating in Turkey. The predictor variables include half-hourly temperature, humidity, pressure, wind speed, solar radiation, day of the week, hour of the day, electricity prices for the period between 01-09-2016 to 31-12-2016. 80% of data is used for training data and the remaining 20% for testing.

We propose a bid optimization strategy based on ANN. ANN aims to build a relationship between inputs and outputs by changing the weights of the nodes that comprises the network. ANN uses a loss function to measure the closeness

between the outputs and the actual values. The aim of the network is to provide a small loss value. The Mean Squared Error is commonly used as a loss function for regression problems. Oroojlooyjadid et al. [5] present a new revised loss function (1) for deep learning algorithms. The authors state that “The revised loss function allows the deep learning algorithm to obtain the minimizer of the newsvendor cost function directly, rather than first estimating the demand distribution and then choosing an order quantity.” We adapted their approach in our model. Let y_i be the bid value for a given period i , q_i be the amount of electricity produced in period i . Also let c_p and c_h be the System Marginal Price and Market Clearing Price, respectively. Finally let E_i denote the loss value of period i .

$$E_i = \min_{y_i} \left[(c_h(y_i - q_i))^+ + (c_p(q_i - y_i))^+ \right], \quad (1)$$

where $(c_h(y_i - q_i))^+$ and $(c_p(q_i - y_i))^+$ are the holding cost (*overproduction*), shortage cost (*underproduction*), respectively. Since the loss function we use in the ANN must be differentiable, we revised the loss function (1) by squaring each cost term. Then we have a Euclidean revised loss function:

$$E_i = \begin{cases} \frac{1}{2} \|c_p(d_i - y_i)\|_2^2, & \text{if } y_i < d_i, \\ \frac{1}{2} \|c_h(y_i - d_i)\|_2^2, & \text{if } d_i \leq y_i. \end{cases} \quad (2)$$

Our model uses the gradient of the loss function in defined in Equation (2) to iteratively update the weights of the networks.

CONCLUSIONS

In this study, we proposed an optimization method to determine electricity producers' bidding strategy in the day-ahead electricity markets. We established an ANN with a customized loss function, which considers the effect of shortage cost and holding cost. Fig. 1 shows the comparison of the actual data of electricity generation with the bid values produced by our model. It can be observed that although the bid values generated with the ANN are meaningful, there is still room for improvement with different customized loss functions.

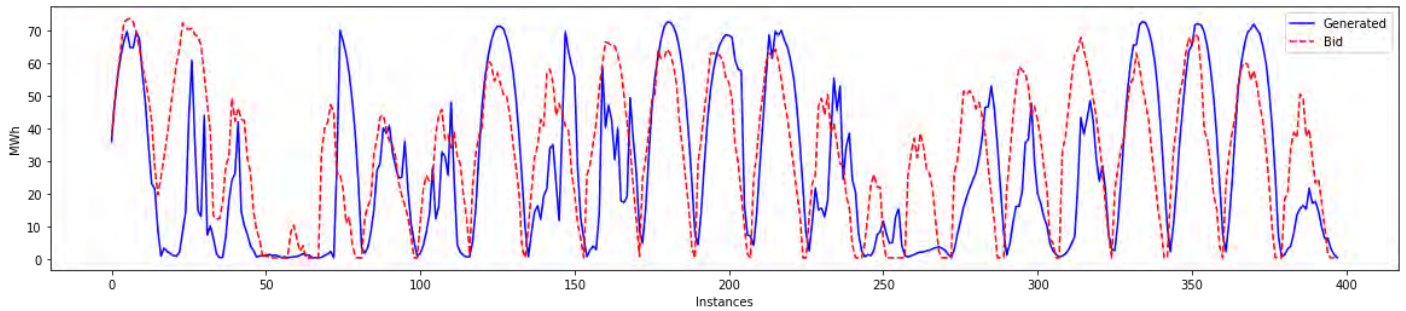


Fig. 1. Comparison of electricity generation and bid values

REFERENCES

- [1] Bhaskar K, Singh SN. Wind power bidding strategy in a day-ahead electricity market. In 2014 IEEE PES General Meeting| Conference & Exposition 2014 Jul 27 (pp. 1-5). IEEE.
- [2] Matevosyan J, Soder L. Minimization of imbalance cost trading wind power on the short-term power market. IEEE Transactions on Power Systems. 2006 Jul 31;21(3):1396-404.
- [3] Herranz R, San Roque AM, Villar J, Campos FA. Optimal demand-side bidding strategies in electricity spot markets. IEEE Transactions on power systems. 2012 Mar 2;27(3):1204-13.
- [4] Zhang H, Gao F, Wu J, Liu K, Liu X. Optimal bidding strategies for wind power producers in the day-ahead electricity market. Energies. 2012 Nov;5(11):4804-23.
- [5] Oroojlooyjadid A, Snyder LV, Takáč M. Applying deep learning to the newsvendor problem. IIEE Transactions. 2020 Apr 2;52(4):444-63.

PRODUCTION SCHEDULING OF A NATURAL GAS POWER PLANT

^{1*} Mehmet Güray Güler, ² Ebru Geçici, ³ Saliha Büşra Gündüz
^{1, 2, 3} Yıldız Technical University, Department of Industrial Engineering, Beşiktaş, Istanbul, Turkey

*Corresponding author e-mail: mgguler@yildiz.edu.tr

ABSTRACT

Natural Gas Combined Cycle Power Plants (CCPP) produce are very significant producers of electricity. They incur significant costs during their production process. In addition to the cost of natural gas, each plant is subject to very high start-up cost and shut down costs. Electricity, on the other hand, cannot be stored efficiently, and hence it is sold as soon as it is produced. Moreover, it's a commodity which is traded in the electricity markets and its price is subject to change at each hour. Therefore, scheduling the electricity production of a CCPP is not very straightforward. In this study, we model the electricity production of a CCPP using a mixed integer programming (MIP) model. The results show that number of starts ups and shutdowns reduces as the costs increases.

Keywords: mixed integer programming, optimization, electricity production, natural gas power plants

INTRODUCTION

Electricity is a commodity that can be traded in the electricity markets with sales prices, or market clearing prices (MCP) that changes hourly. Therefore, electricity producers decide on their production schedule with respect to their production costs and the MCP. Some electricity producers have negligible production costs. Solar panels or windmills, for example, can make profit by electricity production at any hour since they don't have any cost at all. Natural Gas Combined Cycle Power Plants (CCPP), on the other hand, produces electricity with natural gas and has a significant (variable) production cost. Therefore, their production schedule is more sensitive to MCP. In other words, if the prices are sufficiently high, they can make profit, but they can make a loss if the prices are low since electricity cannot be stored to be sold later efficiently at the scale of a CCPP. There are also some significant factors about starting and stopping production. First, there are significant costs associated with both starting (startup cost) and stopping (shut down cost) production. Second, a CCPP cannot immediately start production at full capacity in an hour, i.e., it takes time to boost the production to full power. Third, the efficiency of a CCPP increases as the power of the system increases which results in a reduced production cost, therefore it is not straight forward to take decision on the production for a CCPP. For example, although it may be profitable to produce electricity in an hour, it may not be justified if the startup cost is too high or even if it's not profitable to produce electricity in an hour, it could be better to start in that period to boost the production in the subsequent periods. In this study we address the production scheduling of a CCPP. We model the problem using a mixed integer programming (MIP) model and minimize total cost of production which consists of (variable) production cost, startup cost and shut down costs.

METHODS

There are two widely used methods for scheduling natural gas power plants: in the literature (i) mixed integer programming and (ii) dynamic programming. Three main reasons are stated for the use of MIP models (i) Gotzman, Ziółkowski and Badur state that MIP models, shows significant acceleration in terms of development in the past periods with additional improvements like branch-and-cut algorithms. [1]. (ii) Simoglou, Biskas, and Bakirtzis state that the main advantage of an MIP model is a global and demonstrable optimal solution, emphasizing that its optimality is more accurate than other models [2]. (iii) Morales-España, Latorre, and Ramos state that the MIP formulation offer the solution faster than the other solution techniques [3]. At the same time, Prina, Fanali, Manzolini et al. prefer this method in their case studies, while Marquant, Evins and Carmeliet added their own approaches over an MIP model. [4]-[5]. On the other hand, the reason for using dynamic programming is that the dynamic programming solution provides convenience in modeling in case of a small number of operating states, that is, in switchboard models that are either open or closed. Lopez, Gomez and Moya preferred dynamic programming in line with this convenience [6]. In this study, an MIP model is employed to schedule the production plan of a CCPP.

CONCLUSIONS

The proposed model addresses the scheduling problem of a hypothetical CCPP. The efficiency of a CCPP has a non-linear relationship between the state of power and the amount of used natural gas. Non-linearity, however, makes it very hard, sometimes impossible to solve a MIP model. Therefore, as an initial step, the production is assumed to binary, i.e., the CCPP either works at full capacity or does not work at all. The problem is solved over a week using the MCP of the last week of June 2021. Two different scenarios are analyzed. The first scenario has low start up and shut downs costs, on the other hand the second scenario has higher costs. The resulting schedule is given in Figure 1.

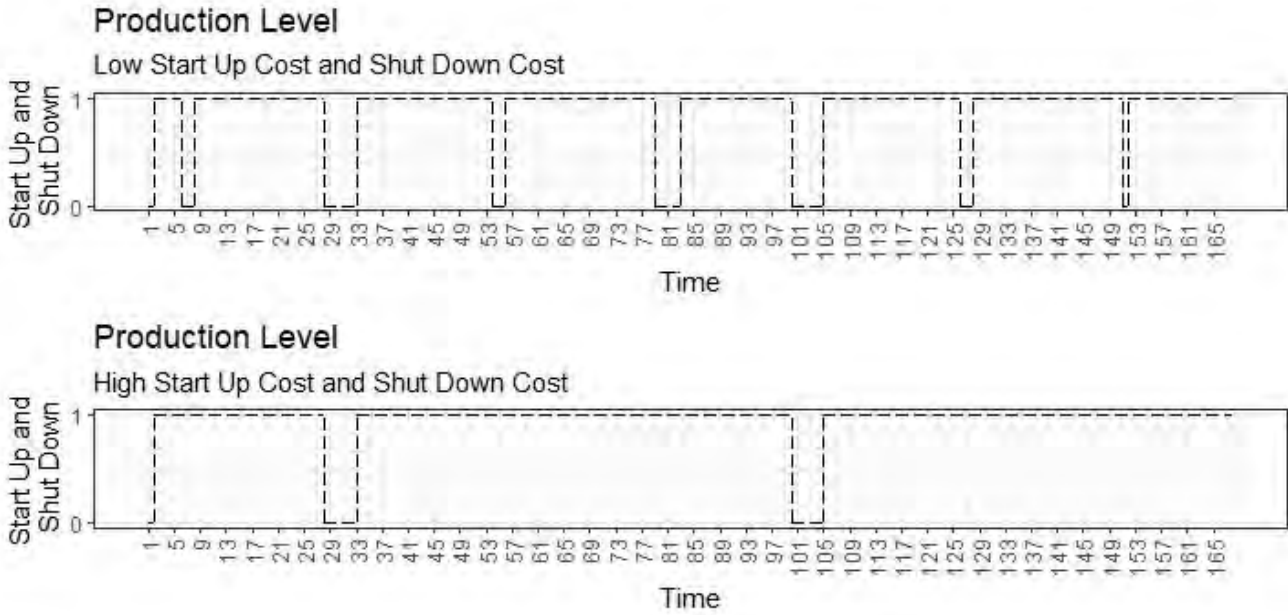


Fig. 1. Production schedule of a CCGP for two different cost scenarios.

It can be observed that when the costs are low, the system shuts down and starts to operate more frequently than the other scenario where the costs are high. The model will be extended to different levels of production at the first step, i.e., the system will have some intermediate steps (in addition to open and closed) for production. The next step is to extend the model to continuous production levels and utilize the non-linearity of the efficiency to the solution.

REFERENCES

- [1] Gotzman S, Ziolkowski P, Badur J. Evaluation of long-term startup costs impact on short-term price based operational optimization of a CCGT using MILP. In: E3S Web of Conferences. EDP Sciences, 2019. Epub ahead of print December 16, 2019. DOI: 10.1051/e3sconf/201913701012.
- [2] Simoglou CK, Biskas PN, Bakirtzis AG. Optimal self-scheduling of a thermal producer in short-term electricity markets by MILP. IEEE Transactions on Power Systems 2010; 25: 1965–1977.
- [3] Morales-España G, Latorre JM, Ramos A. Tight and compact MILP formulation for the thermal unit commitment problem. IEEE Transactions on Power Systems 2013; 28: 4897–4908.
- [4] Prina MG, Fanali L, Manzolini G, et al. Incorporating combined cycle gas turbine flexibility constraints and additional costs into the EPLANopt model: The Italian case study. Energy 2018; 160: 33–43.
- [5] Marquant JF, Evins R, Carmeliet J. Reducing computation time with a rolling horizon approach applied to a MILP formulation of multiple urban energy hub system. In: Procedia Computer Science. Elsevier B.V., 2015, pp. 2137–2146.
- [6] Lopez JA, Gomez RN, Moya IG. Practical Commitment of Combined Cycle Plants using Dynamic Programming. IEEE, 2010.

EXPERIMENTAL INVESTIGATION AND THEORETICAL MODEL OF R718/LiBr BUBBLE PUMP OPERATED ABSORPTION REFRIGERATION MACHINE

^{1,2*} Nizar Ben Ezzine, ² Raoudha Garma, ² Monia Chatti, ² Ahmed Bellagi

¹University of Carthage, Faculty of Sciences of Bizerte, 7021 Zarzouna, Tunisia

² University of Monastir, National Engineering School of Monastir, LRTTPI, Av. Ibn Jazzar, 5060 Monastir, Tunisia

*Corresponding author e-mail: n_benezzine@yahoo.fr

ABSTRACT

This paper reports on the results of an experimental study and theoretical thermodynamic simulation of a prototype of self-circulation of R718/LiBr absorption refrigerator based on thermally bubble pumps. The first test results showed that cold at 5°C is effectively produced by the machine for heating temperature of about 82°C and an ambient air of 20°C. The experimental results were very useful for the determination of the starting bubble pumping as well as the effect of the operating parameters on the level of cold produced and the efficiency of this system. The comparison of the experimental data with the theoretical model showed a good agreement.

Keywords: R718, LiBr, Bubble pump, absorption refrigeration cycle, design

INTRODUCTION

The absorption refrigeration technology operated with natural refrigerant has seen renewed interest in the recent years due to the growing awareness of global warming, climate change, and energy and environmental problems. Ammonia-water and water-lithium bromide are the most useful working fluids in these kind of refrigeration machine [1-4].

Conventional absorption refrigeration machine utilizes an electrical solution pump between absorption and desorption process. Substitution of mechanical pump by thermally bubble pump makes this machine suitable for 100% solar absorption cooling applications.

In our research laboratory, a prototype was built to demonstrate the feasibility of a water-lithium bromide vapor absorption refrigeration cycle which uses a thermally activated solution pumping mechanism. It was charged with a prepared aqueous concentrated solution of lithium bromide (50% mass.). The experimental results were used as input data for the theoretical model. The thermodynamic analysis was performed based on a mathematical model of the machine.

EXPERIMENTAL PROTOTYPE

A schematic view of the designed and fabricated experimental refrigerator is shown in Fig.1. The system design allows investigating the bubble pump behaviour and the absorber efficiency.

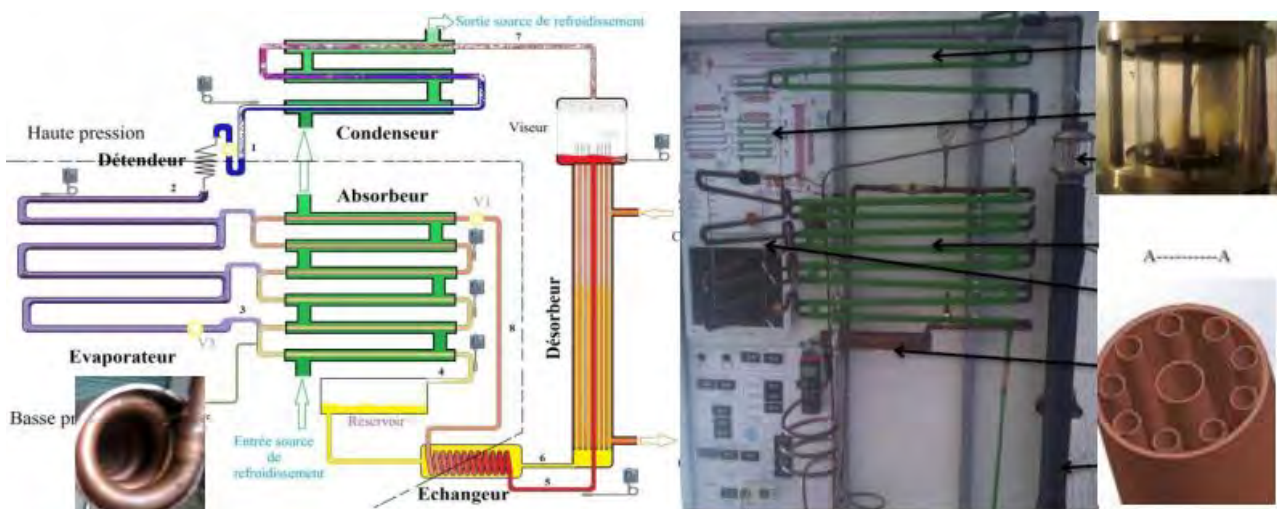


Fig.1. Schematic of the experimental prototype

Experimental temperatures of the evaporator, absorber, desorption and heat source are shown in Fig.2. At the starting all the temperatures are equal to about 21°C which correspond to the ambient temperature. During the first minutes (30 mn) both of the desorption and generator temperature increase sharply but no cooling effect is produced

yet. This is due to the start-up of the bubble pump. When the generator heat source inlet temperature reaches 82°C, the bubbles pump flow is started and then R718 liquid begin drain from condenser to evaporator. The evaporator starts to produce cold, and its temperature starts to decrease. After about 10mn, the machine is at steady state operation and the evaporator temperature is stabilized at about 7°C.

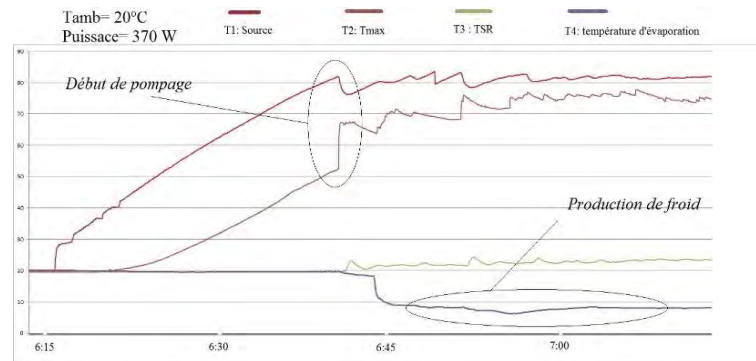


Fig. 2 Experimental temperatures of the evaporator, absorber, desorption and heat source.

THERMODYNAMIC ANALYSIS

A schematic the mass and energy conservation equations for each component of the machine are established. The obtained large set on non-linear equations of simulation model are solved simultaneously. The cycle is simulated with four cooling medium temperatures as presented in Fig.3 that represents the evolution of coefficient of performance vs. the driving heat and cooling medium temperatures.

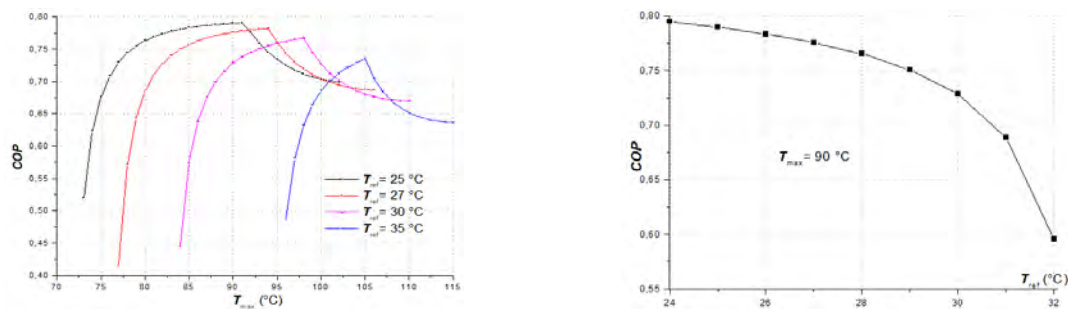


Fig.3 COP vs. driving and cooling medium temperatures.

CONCLUSIONS

An experimental prototype of a thermally driven bubbles pumps operated absorption refrigeration cycle charged with lithium bromide and water was fabricated based and tested. The experimental results showed the feasibility of this cycle and cold was effectively produced at about 7°C for a relatively low driving temperature of 82°C. The experimental results were used as input data for the thermodynamic simulation model.

Experimental and numerical results confirm that R718/LiBr is a good potential mixture for absorption refrigeration cycles which can be operated at low generation temperatures that allow the solar heat source coupling.

REFERENCES

- [1] A. Koyfman, M. Jelinek, A. Levy, I. Borde, An experimental investigation of bubble pump performance for diffusion absorption refrigeration system with organic working fluids, Applied Thermal Engineering 23 (2003) 1881-1894.
- [2] N. Ben Ezzine, R. Garma, A. Bellagi, A numerical investigation of a diffusion absorption refrigeration cycle based on R124-DMAC mixture for solar cooling. Energy, 5 (2010), 1874-1883.
- [3] R. Saravanan, M.P. Maiya, Experimental analysis of a bubble pump operated H₂O-LiBr vapour absorption cooler, Applied Thermal Engineering 23 (2003) 2383-2397.
- [4] Y. He, G. Chen, Experimental study on an absorption refrigeration system at low temperatures, International Journal of Thermal Sciences, 46 (2007) 294-299.
- [5] M. Barhoumi, A. Snoussi, N. Ben Ezzine, A. Bellagi, Modelling of the thermodynamic properties of the ammonia –water mixture, International Journal of Refrigeration 27(3) (2004) 271-283.
- [6] G. Alefeld, R. Radermacher, Heat conversion systems, CRC Press, Boca Raton, FL, 1993.
- [7] N. Ben Ezzine, Kh. Mejri, M. Barhoumi, A. Bellagi, Thermodynamic analysis and multi-parametric optimisation of double effect absorption chiller, International Journal of Exergy, Vol. 3, N°1, 2006, 68-86.
- [8] M. Shacham, Int. J. Num. Methods in Engineering, 23 (1986), pp.1455-1481.

SUITABILITY OF SIDERITE AS OXYGEN CARRIER IN CHEMICAL LOOPING COMBUSTION

¹ Merve Durmaz, ^{2,*} Nesibe Dilmaç, ³ Ömer Faruk Dilmaç
^{1, 2, 3} Çankırı Karatekin University, Chemical Engineering Department, Uluyazı, Çankırı, Turkey

*Corresponding author e-mail: ndilmac@karatekin.edu.tr

ABSTRACT

In this study the performance of siderite as oxygen carrier (OC) in a bench-scale Chemical Looping Combustion (CLC) set-up was evaluated by using various blends of CO and H₂ in N₂ as fuel. 92% fuel conversion was obtained as mean of four tests performed at 850°C. Siderite kept its reactivity and durability for approximately 8 hours throughout the tests. It was concluded that, siderite may be a proper OC for pilot or sub-pilot applications since the cost of the OC is a key factor in commercial scale units in which vast amount of OC is required.

Keywords: Chemical Looping Combustion, Oxygen Carrier, Siderite

INTRODUCTION

Chemical Looping Combustion (CLC) is a promising combustion technology which offers low energy penalty compared to the competing clean energy processes. The air-isolated combustion of fuel in this technology leads to inherent CO₂ capture, while the continuity of the process is enabled by rotating a solid media *i.e* the oxygen carrier (OC), between two distinct reactors, one for oxidizing the fuel by the solid-state oxygen (the fuel reactor), and the other for recharging the depleted OC with air oxygen (the air reactor). Thus, the OC is of vital importance on the success of the process. In general, it is demanded from the OC to be sufficiently reactive, durable, and environmentally benign. However, as solid fuels –especially coal– are likely to have an important role in future energy scenarios, the availability and the cost of the material are being more determinative on OC selection. Due to this fact, in recent CLC studies, the oxygen carrying performance of natural ores and metallurgical wastes has been intensively investigated. Among many tested materials, iron-based OCs exhibited substantial potential as OC since they mostly satisfied the abovementioned expectations [1]. Especially hematite and ilmenite, two main iron ores yielded promising results [2]. However, hematite is the primary raw material of iron and steel industry, and ilmenite is mainly used for titanium dioxide manufacturing. Thus, searching alternative OCs is inevitable. In this context, we investigated the performance of siderite as OC in CLC since siderite has not been evaluated as OC before. Besides, it is very common and affordable mineral which can be easily transformed into its oxide form by a simple pretreatment such as calcination.

MATERIALS AND METHODS

The siderite sample whose chemical composition is 56.6% Fe, 7.4% MnO, 4.6% CaO, 2.5% MgO, and 28.9% others, was supplied from Hekimhan mine (Malatya, Turkey) via Hekimhan Madencilik AŞ. After being crushed, the samples were sieved and the portion with 0.20 mm diameter was calcined at 900°C for 12 hours. 5 g calcined siderite was loaded into reactor for each CLC test.

The experimental set-up was composed of a vertical electric furnace, a quartz fluidized bed, a real-time gas analyser, gas lines, mass flow controllers (MFCs) and a programmable logic controller (PLC). The CLC loops were established by the PLC unit via alternating the atmosphere sent to the reactor with the sequence of "fuel flow, purging flow, and air flow" throughout 50 full cycles. Gas mixtures at various proportions of H₂ and CO were used as fuel for CLC tests and the flue gas concentration was continuously analyzed and recorded by the gas analyzer. Tests were conducted at 850°C and 6 times of the minimum fluidization velocity. Further details about the set-up can be found in our previous studies [3], [4], [5].

The time intervals of the full cycles during the fuel gas flow were referred as reduction half cycle (RHC), while the remaining sections including reoxidation of OC under air flow were referred as oxidation half cycle (OHC). The time-dependent conversion of OC during any RHC was calculated by Eq. (1), while mean fuel conversion efficiency values for CO and H₂ was determined by Eq. (2).

$$X_{i^{\text{th}}}^{\text{RHC}} = X_{(i-1)^{\text{th}}^{\text{OHC}}} - \left(\frac{(M_A)_{\text{O}} \cdot \dot{n}_{\text{in}}}{m_{\text{O}} \cdot R_{\text{OC}}} \right) \cdot \int_{t_{4i-4}}^{t_{4i-3}} \left(1 - \frac{y_{\text{CO}_{\text{in}}} \cdot (y_{\text{CO}_{\text{out}}} + y_{\text{H}_2_{\text{out}}})}{(y_{\text{CO}_{\text{out}}} + y_{\text{CO}_{2\text{out}}})} \right) \cdot dt \quad (1)$$

$$\overline{(Y_{\text{CO}})}_{i^{\text{th}}}^{\text{RHC}} = \left[1 - \frac{\int_{t_{4i-4}}^{t_{4i-3}} (\dot{n}_{\text{out}} \cdot y_{\text{CO}_{\text{out}}}) \cdot dt}{\int_{t_{4i-4}}^{t_{4i-3}} (\dot{n}_{\text{in}} \cdot y_{\text{CO}_{\text{in}}}) \cdot dt} \right] \quad \text{while} \quad \overline{(Y_{\text{H}_2})}_{i^{\text{th}}}^{\text{RHC}} = \left[1 - \frac{\int_{t_{4i-4}}^{t_{4i-3}} (\dot{n}_{\text{out}} \cdot y_{\text{H}_2_{\text{out}}}) \cdot dt}{\int_{t_{4i-4}}^{t_{4i-3}} (\dot{n}_{\text{in}} \cdot y_{\text{H}_2_{\text{in}}}) \cdot dt} \right] \quad (2)$$

RESULTS

Fig. 1 shows the variation of the fuel conversion efficiency during CLC tests, while the mean values were as 88.85%, 96.68%, 93.75%, and 89.31% for "Test 1", "Test 2", "Test 3", and "Test 4", respectively.

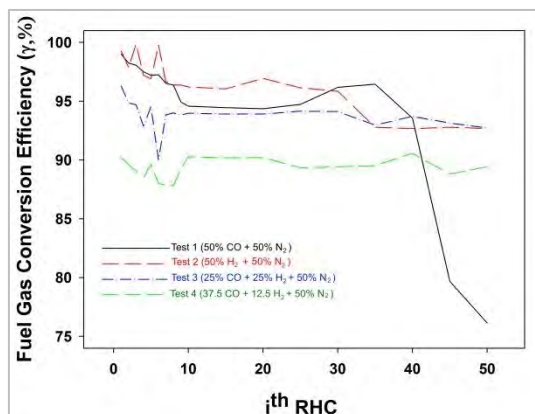


Figure 1. Variation of fuel conversion efficiency during CLC tests

As can be seen from Fig. 1, the fuel conversion efficiency dramatically decreased after 40th RHC in "Test-1" in which the fuel was H₂ free. However, the conversion efficiency was almost stable for 50 RHCs –approximately for 8 hours– during the remaining tests in which the fuel was blended with various amounts of H₂. Since satisfying results were obtained during "Test-3" fueled by synthetic syngas *i.e* CO:H₂ with 1:1 molar ratio, the variation of the reduction rate of OC throughout in this test was also graphed. Fig. 2 implies that siderite kept its reactivity for almost whole test since no considerable decrease on reaction rate was occurred. This fact clarifies the stable trend of fuel conversion efficiency during "Test-3" seen on Fig. 1.

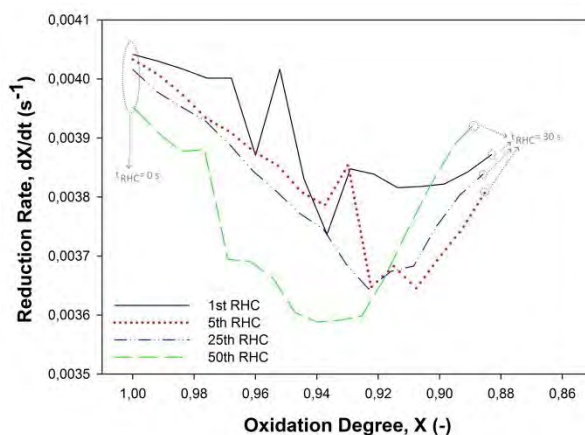


Figure 2. Variation of reduction rate of siderite OC throughout "Test-3"

CONCLUSIONS

Siderite is a proper and cost-effective iron-based OC for CLC process with sufficient reactivity and durability as it accompanied 92% fuel conversion as mean of 4 tests each lasted for 8 hours. It may be considered as a suitable OC for pilot scale CLC applications especially during the conversion of coal derived syngas into energy.

REFERENCES

- [1] Hildor F, Mattisson T, Leion H, Linderholm C, Rydén M. Steel converter slag as an oxygen carrier in a 12 MWth CFB boiler– Ash interaction and material evolution. *Int J Greenh Gas Control* 2019;88:321–31. doi:10.1016/j.ijggc.2019.06.019.
- [2] Yu Z, Yang Y, Yang S, Zhang Q, Zhao J, Fang Y, et al. Iron-based oxygen carriers in chemical looping conversions: A review. *Carbon Resour Convers* 2019. doi:10.1016/j.crcon.2018.11.004.
- [3] Dilmaç N, Dilmaç ÖF, Yardımcı E. Utilization of Menteş iron ore as oxygen carrier in Chemical-Looping Combustion. *Energy* 2017;138. doi:10.1016/j.energy.2017.07.126.
- [4] Dilmaç ÖF, Dilmaç N D TE. Performance of EAF slag as oxygen carrier in Chemical Looping Combustion. 14th Int. Combust. Symp. (INCOS-14 , April 25-27), Karabük-Türkiye: 2018.
- [5] Durmaz M, Dilmaç N, Dilmaç ÖF. Evaluation of performance of copper converter slag as oxygen carrier in chemical-looping combustion (CLC). *Energy* 2020;196. doi:10.1016/j.energy.2020.117055.

NEW ENHANCED DESIGN OF HYDROGEN BASED THERMALLY DRIVEN R717 ABSORPTION REFRIGERATION SYSTEM

^{1,2*} Nizar Ben Ezzine, ² Monia Chatti, ² Raoudha Garma, ² Ahmed Bellagi

¹University of Carthage, Faculty of Sciences of Bizerte, 7021 Zarzouna, Tunisia

² University of Monastir, National Engineering School of Monastir, LTTPI, Av. Ibn Jazzar, 5060 Monastir, Tunisia

*Corresponding author e-mail: n_benezzine@yahoo.fr

ABSTRACT

In this study new enhanced and modified hydrogen-R717-water diffusion absorption cycle MHDAR with increasing internal heat recovery has investigated and compared by numerical simulation to the Pluten-Munters common basic configuration BDAR. Simulations are performed for two cooling medium temperatures, water at 27°C and air at 35°C, and four driving heat temperatures in the range [90°C - 180°C]. The cycle performance characteristics are analyzed parametrically by computer simulation. Simulation results allow to conclude that the coefficient of performance and the minimum evaporator temperature reached largely depend on the maximum driving temperature and the absorber efficiency. In the air-cooled case, the conventional BDAR cycle COP cannot exceed 0.22 with a generator driving temperature of about 140°C. While the new enhanced MHDAR cycle reaches a maximum COP of 0.38 and minimum evaporation temperature of -24°C for the same operating conditions.

Keywords: Hydrogen, Absorption Refrigeration, R600, Enhancement design

INTRODUCTION

In recent years, energy consumption of refrigeration and air-conditioning applications is increasing significantly, which poses technical problems in electricity production plants. In addition, they create two sources of environmental pollution: direct emission of greenhouse gases, especially for HFC working fluids, and emission of the greenhouse gases during generation of electric power. Absorption refrigeration systems mainly powered by solar energy and using natural refrigerants are among the best alternatives to overcome these problems. Hydrogen Diffusion absorption refrigeration (HDAR) cycle [1] has been recognized as one of the most promising technologies in refrigeration and air-conditioning applications. The corresponding thermodynamic cycle is based on refrigerant/absorbent pair mixture as working fluids and an inert gas for pressure equalization.

Numerous researches in this field have been done and a lot more is still undergoing. Most of the work on hydrogen diffusion absorption refrigerators reported in the literature involves thermodynamic modelling and looking for new fluids associated or not to experimental tests. Ben Ezzine et al. [2] presented an experimental investigation of an air-cooled diffusion absorption machine operating with a binary light hydrocarbon mixture (C₄H₁₀/C₃H₈) as working fluids and helium as pressure equalizing inert gas. Zohar et al. [3] examined numerically the performance of a HDAR system working with an organic absorbent (DMAC-dimethylacetamide) and five different refrigerants. Ben Ezzine et al. [4] investigated the feasibility of a HDAR operating with the working fluid system DMAC-R124 and coupled to a solar collector. Few research has been performed on theoretical and practical enhancement design of the basic conventional HDAR. The present paper is a contribution to enhancement and research for new enhanced HDAR configurations. Numerical investigations are then performed for a new MHDAR operated with hydrogen-R717-water mixtures with hydrogen as the auxiliary gas. The effects of different operating parameters on the system performances are analysed and discussed.

DESCRIPTION OF THE NEW MODIFIED MHDAR

As shown in Fig.1 the new enhanced MHDAR configuration, is also an extension of the BHDAR. The novel enhancement consists to integration of three-fluid-ways heat exchanger RECT-SHX. When passing through the RECT-SHX the rich solution (6) is preheated simultaneously by the hot weak solution (9) leaving generator and vapor (10) containing some amount of absorbent vapor to be purified.

MODELING AND SIMULATION

In the same operating conditions simulation was then performed for the different case study. Based on the simulated results, the thermodynamic cycle of the air-cooled HDAR is represented on the OLDHAM diagram shown in fig.2. In the case of 35°C air-cooling medium the three investigated cycles are simulated and compared as presented in fig.3 that reports the results of the comparison between the basic Platen-Munters hydrogen diffusion absorption refrigerator cycle BHDAR and the two enhanced cycle MHDAR1 and MHDAR2 investigated in this work for varying driving heat temperatures. It shows clearly that the second modified cycle MDAR2 is more performing. For the air cooled MDAR2 and when the driving temperature reaches a value of 150°C and beyond, the COP is at maximum with a value of 0.37, that is approximately 68% higher than that of the basic diffusion absorption refrigerator.

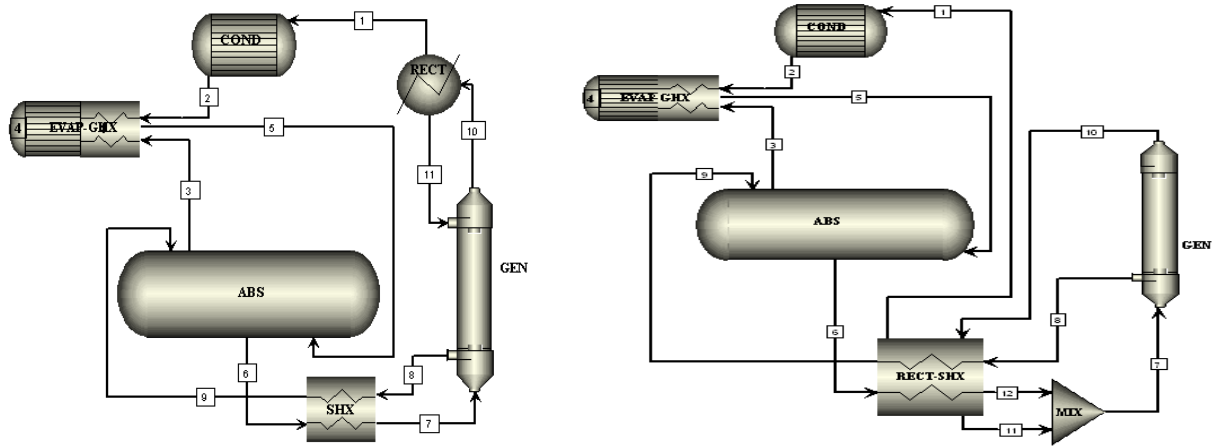


Fig. 1. Schematic of the basic BHDAR and the new MHDAR hydrogen diffusion absorption refrigeration systems

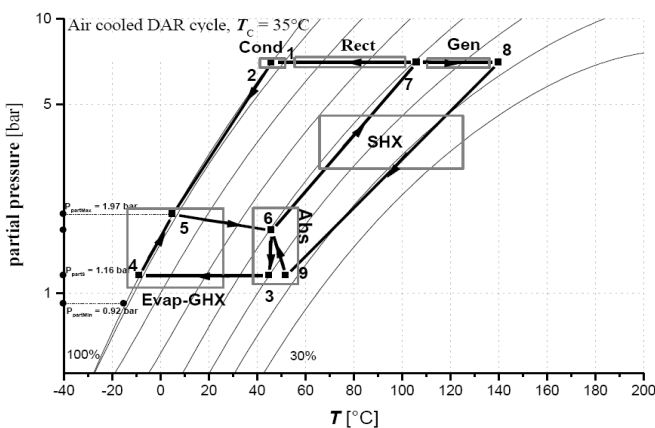


Fig. 2. Thermodynamic Cycle on the Oldham diagram

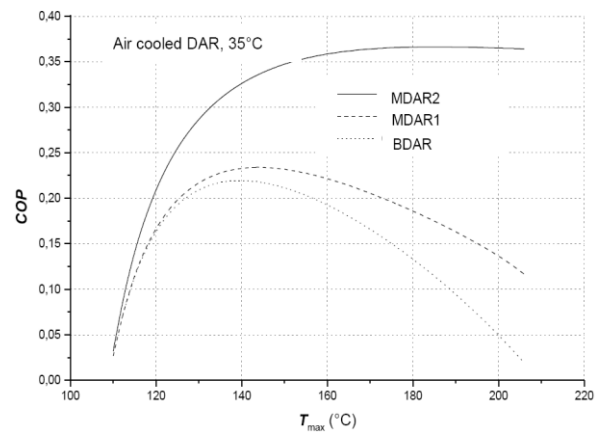


Fig. 3. COP vs. driving temperature

CONCLUSIONS

The new enhanced configurations of Hydrogen Diffusion Absorption Refrigeration system proposed in this investigation and based on internal heat recovery are simulated and compared to the basic conventional Pluten-Munters cycle BHDAR.

Parametric analysis and simulation results show that the driving temperature and the absorber efficiency have the largest effect on the COP and the minimum evaporation temperature. The maximum reached COP of new MHDAR is 68% higher than that of the basic hydrogen diffusion absorption refrigerator BHDAR.

REFERENCES

- [1] B.C. Von Platen, C.G. Munters. US Patent 1, 685,764, 1928.
- [2] N. Ben Ezzine, R. Garma, M. Bourouis, A. Bellagi, Experimental studies on bubble pump operated diffusion absorption machine based on light hydrocarbons for solar cooling, *Renew. Energ.* 35 (2010) 464-470.
- [3] A. Zohar, M. Jelinek, A. Levy, I. Borde, Performance of diffusion absorption refrigeration cycle with organic working fluids, *Int. J. Refrigeration*, 32 (2009), pp. 1241–1246.
- [4] N. Ben Ezzine, R. Garma, A. Bellagi, A numerical investigation of a diffusion absorption refrigeration cycle based on R124-DMAC mixture for solar cooling. *Energy*, 5 (2010), 1874-1883.
- [5] M. Barhoumi, A. Snoussi, N. Ben Ezzine, A. Bellagi, Modelling of the thermodynamic properties of the ammonia –water mixture, *International Journal of Refrigeration* 27(3) (2004) 271-283.
- [6] Kh. Mej bri, N. Ben Ezzine, A. Bellagi, Modélisation numérique des propriétés thermodynamiques du mélange frigorifique ammoniac-eau, *Journal de la Société Chimique de Tunisie*, 6(2) (2004) 213-228.
- [7] G. Alefeld, R. Radermacher, *Heat conversion systems*, CRC Press, Boca Raton, FL, 1993
- [8] N. Ben Ezzine, Kh. Mej bri, M. Barhoumi, A. Bellagi, Thermodynamic analysis and multi-parametric optimisation of double effect absorption chiller, *International Journal of Exergy*, Vol. 3, N°1, 2006, 68-86.

UTILIZATION OF SOFT DRINK INDUSTRY WASTE AS ENERGY FEEDSTOCK

^{1*} Ismail Cem Kantarli

¹ Ege University, Ataturk Medical Technology Vocational Training School, Izmir

*Corresponding author e-mail: ismail.cem.kantarli@ege.edu.tr

ABSTRACT

In this study, conversion of brewed tea waste into hydrochars was investigated with the aim of obtaining an improved energy feedstock. It was hydrothermally carbonized in sub-critical water at four different temperatures: 220, 240, 260 and 280 °C. Fuel characteristics and chemical properties of derived hydrochars were determined using standard fuel analysis and spectroscopic methods. The combustion behavior of brewed tea waste and hydrochars was examined via non-isothermal thermogravimetric analysis under air atmosphere. Hydrochar yields decreased with increasing carbonization temperature. Hydrochar yield was lower than biochar yield at the same temperature and duration. 25-35% of initial ash in biomass was removed by hydrothermal carbonization. Hydrothermal carbonization converted brewed tea waste to hydrochars with improved fuel and combustion characteristics observed by properties such as higher calorific value and lower burnout temperature. Acid-base ratio values indicates high risk of slagging for both brewed tea waste and hydrochars during their combustion, while fouling index values indicated that hydrothermal carbonization was very effective in lowering the fouling tendency of brewed tea waste.

Keywords: hydrothermal carbonization, brewed tea waste, combustion, slagging, fouling

INTRODUCTION

Fermented black tea is a very popular hot drink in Turkey. It has an annual per capita consumption of approximately 3.5 kg in Turkey. After the extraction (brewing) of fermented black tea, brewed tea waste (BTW) remains as a waste with a high water content. BTW is also produced as waste of soft beverage industry during the production of iced tea. Therefore, BTW can be classified both as domestic waste and beverage industry waste. Utilization of this waste is possible by converting it to a energy densified product, biochar/hydrochar by carbonization. Being a wet waste, BTW can be converted to hydrochar by hydrothermal carbonization (HTC) which is applied to wet biomass with water content up to 80% under inert conditions in the temperature range of 180–280 °C. In this study, utilization of BTW as energy feedstock was aimed and the fuel and combustion characteristics of derived hydrochars was investigated. In addition, slagging and fouling indices of hydrochars were calculated in order to foresee potential problems related with their combustion.

MATERIALS AND METHODS

BTW was supplied by a local cafe in Bornova, Izmir. BTW had a solid content of 13.4 % as received. It has a calcium content of 1.33% and a potassium content of 0.87% on dry basis. HTC system and characterization of hydrochars were described elsewhere [1]. Hydrochars were defined as following the “HC-temperature” sequence (HC-220 stands for hydrochar obtained from HTC of BTW conducted at 220 °C for 60 min). Torrefaction of BTW was also carried out at 260°C for a duration of 60 min for comparison purpose and the resultant biochar was defined as BC-260. Combustion behavior of BTW, its hydrochars and BC-260 were determined using a thermogravimetric analyzer under air with a flow rate of 200 mL/min. The ignition temperature (T_i), burnout temperature (T_b), and average combustion reactivity (R_m) of BTW, its hydrochars and BC-260 were calculated from the thermogravimetry (TG) / derivative thermogravimetry (DTG) curve according to the literature [2].

RESULTS AND CONCLUSIONS

The effect of HTC temperature on the fuel and combustion characteristics of the BTW derived hydrochars is given in Table 1. Hydrochar yield decreased sharply with the increase of temperature due to the enhanced degradation of BTW [3]. The mass yield of HC-260 was found to be lower than that of BC-260 possibly due to the decreased stability of biomass components under supercritical water conditions. Ash contents of hydrochars were higher than that of BTW. This was attributed to the existence of most of the inorganics, mainly calcium salts (Table 2), of BTW in less soluble form. Therefore, only 25-35% of ash in BTW was dissolved in subcritical water. The volatile content (VC) of hydrochar decreased and its fixed carbon (FC) content increased with increasing temperature. The higher heating values (HHV) of hydrochars increased due to the increase of C content and decrease of O content with increasing temperature. Energy yield (EY) of hydrochars decreased with increase of temperature mainly due to the decrease in mass yield for higher temperatures.

T_i of hydrochars obtained did not change much with HTC temperature. T_b of all hydrochars were found to be lower than that of BTW. Low temperature hydrochars had higher R_m than high temperature hydrochars.

Table 1. Proximate analysis, elemental analysis, fuel properties and combustion parameters of hydrochars

	Proximate analysis, %wt., dry basis			Elemental analysis, %wt., dry basis					Yield	HHV (MJ/kg)	EY	Combustion analysis		
	Ash	VM	FC	C	H	N	S	O*				T _i	T _b	Rm
BTW	3.57	56.26	40.17	52.04	6.04	4.16	0.26	33.93	-	24.80	-	277	541	0.92
HC-220	4.24	41.89	53.87	61.39	6.11	3.19	0.32	24.75	58.92	28.24	67.08	284	513	1.42
HC-240	4.53	37.67	57.80	63.47	6.49	3.49	0.48	21.54	52.50	29.39	62.22	281	508	1.68
HC-260	4.99	30.63	64.38	67.52	6.32	3.81	0.19	17.17	46.33	30.54	57.04	283	507	0.85
HC-280	6.35	15.57	78.08	69.98	6.96	3.88	0.30	12.53	41.85	32.13	54.20	283	507	1.05
BC-260	4.86	54.82	40.32	62.96	5.72	5.51	0.06	20.89	73.58	28.05	83.22	286	544	0.95

*by difference. O% = 100-(C%+H%+N%+S%+Ash%)

Inorganic composition and estimated slagging and fouling indices of BTW and selected hydrochars are given in Table 2. As seen in Table 2 that main components of BTW ash are CaO and K₂O. The K₂O content decreased dramatically after HTC, while the CaO content increased. Alkali index values of hydrochars were observed to be lower than 0.17 implying that their combustion would be safe [4] as expected due to the removal of alkali oxides during HTC. Acid base ratios of hydrochars much higher than 1.0 and slagging index values much higher than 2.0 imply a high to severe risk of slagging during combustion. Fouling index values of hydrochars much lower than that of BTW implies a decrease in the fouling potential by HTC process from high to medium.

In conclusion, HTC eliminated some of the disadvantages of BTW as fuel by converting it to hydrochar with higher heating value and lower fouling potential, but it was insufficient in lowering the ash content and slagging potential of BTW.

Table 2. Inorganic content and fouling and slagging indices of BTW and its hydrochars

	Na ₂ O	MgO	Al ₂ O ₃	SiO ₂	K ₂ O	CaO	TiO ₂	Fe ₂ O ₃	Alkali index	Acid base ratio	Slagging index	Fouling index
BTW	<0,01	<0,003	<0,003	0,098	1,045	1,861	0,005	0,071	0,42	28,91	6,53	30,20
HC-220	<0,01	<0,003	<0,003	<0,01	0,127	2,358	0,02	0,125	0,03	17,39	3,38	1,37
HC-260	<0,01	<0,003	<0,003	<0,01	0,126	3,221	0,02	0,156	0,02	23,66	5,66	1,34

ACKNOWLEDGEMENT

The support of Gozde Duman Tag for Thermogravimetric Analysis of hydrochars and biochar is appreciated.

REFERENCES

- [1] Duman G. Balmuk G. Cay H. Kantarli IC. Yanik J. 2020. Comparative evaluation of torrefaction and hydrothermal carbonization: effect on fuel properties and combustion behavior of agricultural wastes. Energy Fuels. 34. 9. 11175-11185.
- [2] Toptas A. Yildirim Y. Duman G. Yanik J. 2015. Combustion behavior of different kinds of torrefied biomass and their blends with lignite. Bioresource Technol. 177. 328-336.
- [3] Kambo, H. S.; Dutta, A. Comparative evaluation of torrefaction and hydrothermal carbonization of lignocellulosic biomass for the production of solid biofuel, Energy Convers. Manage. 2015, 105, 746-755.
- [4] Smith A. M. Singh S. Ross A. B. 2016. Fate of inorganic material during hydrothermal carbonisation of biomass: Influence of feedstock on combustion behaviour of hydrochar. Fuel, 169, 135-145.

MODELING AND PERFORMANCE EVALUATION OF THE GEOTHERMAL ENERGY BASED COMBINED PLANT FOR DIFFERENT PRODUCTS

^{1*} Yunus Emre Yuksel ² Fatih Yilmaz, ² Murat Ozturk

¹ Electrical and Energy Department, Bolvadin Vocational School, Afyon Kocatepe University, Afyonkarahisar, Turkey

² Department of Mechatronics Engineering, Technology Faculty, Isparta University of Applied Sciences, Isparta Turkey

*e-mail: yeyuksel@aku.edu.tr

ABSTRACT

The fundamental purpose of this advised work is to study the geothermal energy-based integrated plant from the point of the thermodynamic analysis method. In this regard, a comprehensive energetic and exergetic efficiencies analysis is conducted to investigate the performance behavior of the modeled plant. The new configuration plant consists of a geothermal power system with the single flash, organic Rankine cycle (ORC), transcritical CO₂ Rankine cycle (tCO₂_RC), domestic hot water (DHW), a PEM electrolyzer, and magnetic refrigeration to produce hydrogen, power, heating, cooling and hot water. According to analyses results, the advised model's general energetic and exergetic performances are found as 44.81% and 46.32%, respectively.

Keywords: Combine plant, Geothermal energy, Thermodynamic, Hydrogen

INTRODUCTION

Since the industrial revolution, the increase in the usage of fossil fuels has given rise to significant harmful impacts on the atmosphere. Using these fuels to meet energy needs, especially electrical energy, causes an increase in the emission of toxic gases that cause serious health problems for human health and the environment [1,2]. For this reason, the use of sustainable energy derivations is one of the most noteworthy and prominent factors in the fight against environmentally harmful gas problems. Among renewable energy sources, geothermal energy stands out due to its advantages, such as being unaffected by environmental conditions (such as sun and wind) and uninterrupted. In addition, there are many studies on geothermal energy in the literature in terms of such advantages and suitability for different usage purposes [3-5]. In this light, this proposed work is designed to generate various beneficial productions by integrating different subsystems with geothermal energy and analyzed thermodynamically. The main difference of the proposed work is the analysis of increasing power and useful outputs using a single-flash system, an ORC, and a tCO₂_RC.

MATERIALS AND METHODS

The proposed integrated system consists of a single flash, steam turbine, ORC with R123 working fluid, a transcritical tCO₂-RC, a PEM electrolyzer, domestic water heater, and magnetic cooling cycle, as shown in Figure 1. In short, in its most general form, the new configuration system is thermally powered by geothermal energy and produces various useful products such as cooling-heating, energy, hot water, and hydrogen

The influence of changes in geothermal reservoir temperature and mass flow rate on the effectiveness of the total integrated model are examined and presented in Figures 2 and 3. In addition, the system analysis results are given in Table 1. Here, useful outputs from the system are presented.

Table 1. Thermodynamic analysis results

$W_{\text{steamturbine}}$	16689 kW
W_{ORC}	1850 kW
W_{tCO_2}	1681 kW
Q_{Heating}	8726 kW
m_{Hydrogen}	0.0124 kg/s
$m_{\text{cooling_water}}$	1.582 kg/s

A STRUCTURE PROPERTY ISSUE IN ORGANIC SOLID-SOLID PHASE CHANGE MATERIALS: 1,3-BISSTEAROYLUREA AND 1,1,3,3-TETRASTEAROYLUREA FOR POTENTIAL SOLAR APPLICATIONS

^{1*} Nazan Gökşen Tosun, ² Aylin Çetin, ³ Cemil Alkan

¹ Tokat Gaziosmanpaşa University, Faculty of Engineering and Architecture, Bioengineering, Tokat, TURKEY

² Tokat Gaziosmanpaşa University, Faculty of Science and Literature, Chemistry, Tokat, TURKEY

³ Tokat Gaziosmanpaşa University, Faculty of Science and Literature, Chemistry, Tokat, TURKEY

*Corresponding author e-mail: cemil.alkan@gop.edu.tr

ABSTRACT

1,3-bisstearylurea and 1,1,3,3-tetrastearylurea were produced as solid–solid phase change materials (SS-PCMs) for potential solar thermal energy storage (TES) applications via condensation of urea with the respective amount of carboxyl chloride (stearyl chloride). Both 1,3-bisstearylurea and 1,1,3,3-tetrastearylurea were characterized by FT-IR, NMR, DSC, and TG analysis techniques. 1,3-bisstearylurea and 1,1,3,3-tetrastearylurea had considerable melting/crystallization enthalpy. The reason of crystallization was structural symmetry and flexibility of long alkyl groups there. Di and tetra alkyl groups made it possible to discuss about the structure property relationship for organic PCMs. Besides, the compounds were characterized through DSC and FT-IR spectroscopy before and after thermal cycling to determine their thermal reliability. Solid-solid phase change enthalpies of them for melting and crystallization were found 95.86 and -87.60 Jg⁻¹ for 1,3-bisstearylurea respectively and 27.65 and -25.75 Jg⁻¹ for 1,1,3,3-tetrastearylurea, respectively. Thermal conductivity was studied to increase by simply expanded graphite addition. The thermal endurance limits of 1,3-bisstearylurea and 1,1,3,3-tetrastearylurea compounds were studied by TG analysis.

Keywords: Phase change materials, Thermal property, Fatty acid.

INTRODUCTION

Thermal energy storage (TES) materials are mostly organic and inorganic based phase change materials (PCMs) with considerable and reversible enthalpy uptake and release under controlled periods. PCMs have also some other typical properties like high thermal conductivity for suitable response time, a phase change temperature at the working intervals, congruent melting without overcooling, affordable cost, material consistency over the usage periods, and non-toxicity(1). Some of widely used or produced PCMs are paraffins, alcohols, fatty acids, esters, sulfonated paraffins, some eutectics, polymeric materials, salts, salt hydrates, alloys, etc. They were investigated for space explorations, solar energy storage systems, greenhouses and buildings, textiles thermal comfort, food and medical transportation, industrial waste heat recovery, high performance electronic equipment, etc. PCMs have been exploited in various applications like solar energy validation, industrial heat recovery, efficiency increase of air conditioning systems, building validations, greenhouses, cooling of electronic devices, sensors, and insulation clothing(2,3) and such applications bear some needs for further capability and functionality of the potential PCMs. Stearic acid is one of the easily available biosourced solid–liquid phase change heat storage material. Its storage density is considerable. Due to that it has poor thermal stability, corrosivity and considerable sublimation property during heating. It is generally preferred for improving its properties as a sample to all fatty acids(4). In this study, stearylurea compounds were produced for the first time by condensation of stearic acid acyl chloride and urea. The 2 compounds produced with di and tetra dentate stearyl amide functionality showed 2 distinct phase transitions for 2 different crystallite regions. In addition to materials novelty, it is also a sample to understand structure property relationship. The amide functionality is also expected to be used in miscellaneous potential applications. Stearic acid is an 18-carbon molecule named as octadecanoic acid according to IUPAC. Stearic acid is the second abundant biobased fatty acid after palmitic acid. Potential solar energy storage applications for manufactured materials could be heating and air conditioning in buildings and cooling of photovoltaic cells.

MATERIALS AND METHODS

Stearyl chloride was synthesized in a flask equipped with an agitator, a thermometer, and a condenser using a stoichiometric amount of stearic acid, thionyl chloride, pyridine, and toluene (with a stearic acid/thionyl chloride ratio of 1/1) at 50 °C for 2 hrs. 1,3-stearyl urea and 1,1,3,3-tetra stearyl urea compounds were obtained using stearic chloride/urea at molar ratios of 2/1 and 4/1, respectively at 80 C for 4 hrs thoroughly mixing. The reaction was ended with filtration and washings using water and drying in an oven. Synthetic scheme of the reaction was shown in Figure 1.

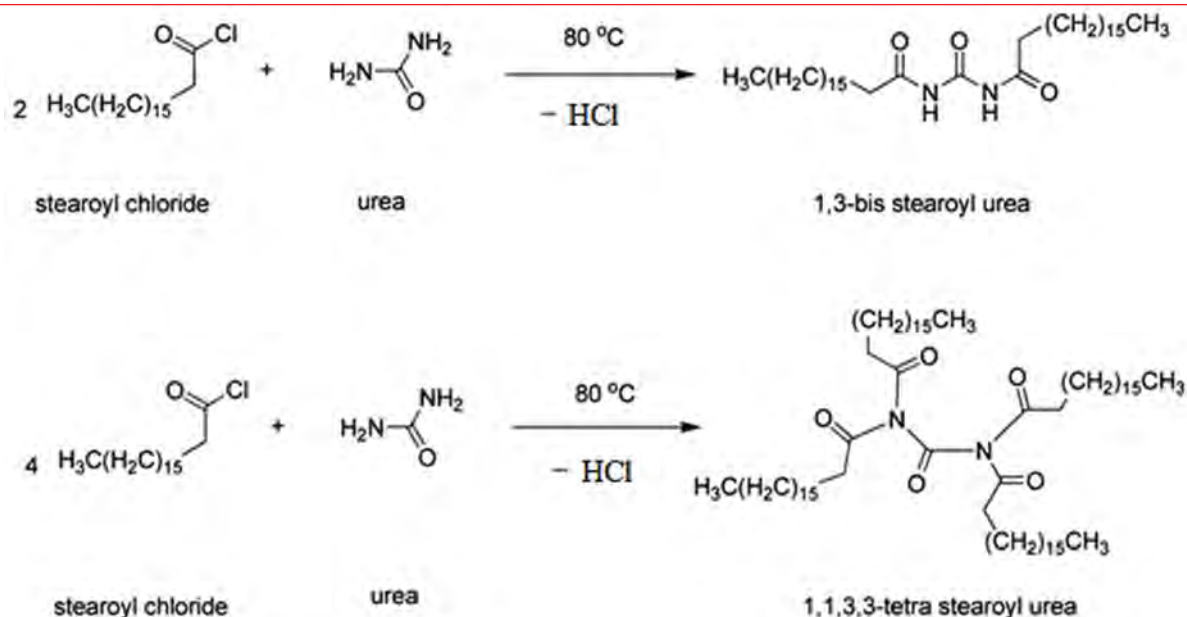


Figure 1. Synthetic scheme of 1,3-stearoyl urea and 1,1,3,3-tetra stearoyl urea compounds

CONCLUSIONS

1,3-bisstearylurea and 1,1,3,3-tetrastearylurea compounds were successfully prepared as novel organic SS-PCMs via the condensation of stoichiometric amount of stearyl chloride and urea at high purity and yield. Urea based center of the molecules were assigned to hold the structure in solid above the first phase transition due to the secondary crystallites of the urea structures. Secondary crystallites led to a secondary transition as melting. The compounds had considerable amount of TES density during phase change of both solid-solid and solid-liquid transitions. This would probably enable to use them as potential materials in some applications like solar heating and cooling. Tetra branch structure was expected to distort secondary crystallites and decrease phase transition temperature. The distorted structure was also assumed to affect the primary phase domains and decrease first (solid-solid) phase transition. And experimental findings were all consistent with the expectations. For structure of the produced compounds were studied by FT-IR and ¹H-NMR spectroscopy analysis. It was shown that di and tetra chain structure of the compounds were effective on the phase change characteristics tutorial to the energy storage property. It was due to that the crystallinity of di sided compounds was much easy to crystallize as tetra chain distorts the crystal structure and prevents crystallinity resulting in a decrease in phase change temperature and enthalpy.

REFERENCES

- [1] Sharma SD, Sagara K. Latent Heat Storage Materials and Systems: A Review. International Journal of Green Energy [Internet]. 2005;2(1):1–56. Available from: <https://www.tandfonline.com/doi/abs/10.1081/GE-200051299>
- [2] Chen C, Wang L, Huang Y. Electrospinning of thermo-regulating ultrafine fibers based on polyethylene glycol/cellulose acetate composite. Polymer [Internet]. 2007;48(18):5202–7. Available from: <https://www.sciencedirect.com/science/article/pii/S0032386107006829>
- [3] Gschwander S, Schossig P, Henning H-M. Micro-encapsulated paraffin in phase-change slurries. Solar Energy Materials and Solar Cells [Internet]. 2005;89(2):307–15. Available from: <https://www.sciencedirect.com/science/article/pii/S0927024805000802>
- [4] Canik G, Alkan C. Hexamethylene dilauroyl, dimyristoyl, and dipalmytoyl amides as phase change materials for thermal energy storage. Solar Energy [Internet]. 2010;84(4):666–72. Available from: <https://www.sciencedirect.com/science/article/pii/S0038092X10000290>

PRODUCTION OF PAN-PEG THERMAL ENERGY STORAGE NANOFIBERS BY ELECTROSPINNING METHOD

Timur Paçacı, Cemil Alkan,* Yağmur Dinç, Esra Kişioğlu
*Tokat Gaziosmanpaşa University, Chemistry Department, 60240, Tokat, Turkey

Corresponding author e-mail: cemil.alkan@gop.edu.tr

ABSTRACT

In this study, polyacrylonitrile (PAN)/polyethylene glycol (PEG) 2000 blend nanofibers were produced. In this way, the fiber forming properties of PAN and the heat storage properties of PEG are combined. PEG2000, PAN mixtures were electrospun by dissolving 10%, 20% and 35% by mass in dimethylformamide (DMF). Produced samples were characterized by SEM, T-history and DSC analysis. According to DSC results, 10% PEG2.000, 20% PEG2.000, 35% PEG2000 produce increasing melting enthalpy in the 0-70 °C range, respectively. While the best fiber formation is seen in PAN, according to SEM images, there is increasing agglomeration as the PEG 2000 ratio increases. With this study, it has been shown that by encapsulating PEG 2000 in nanofiber form, which turns into a liquid state by taking heat under normal conditions, structures that can be produced in composite form with high surface area can be developed.

Keywords Electrospinning, PEG, nanofiber, heat storage

INTRODUCTION

Thermal energy storage (TES) is considered as one of the important technologies for energy recovery in the future. There are 3 types of TES as sensible heat storage, latent heat storage and reversible chemical reaction heat storage. Among the TES methods, latent heat energy storage using a phase change material (PCM) is an effective technique due to its high energy storage capability and advantages of isothermal properties. Nanofibers are a kind of nanotechnology product. They have superior properties compared to traditional microfibers. Nanofibers provide important opportunities for the industry with their large surface area per unit, volume, ultraviolet resistance, chemical resistance, low density and large porous structures. In addition, nanofibers can be used in many different production areas such as drug delivery, fuel cells, tissue engineering, filtration systems and nanocomposites [1-3]. Nanofibers can be produced using polyacrylonitrile and its derivatives. Polyacrylonitrile (PAN) is a widely used material in nanofiber production with its wide range of uses with different properties. It is often used as a comonomer addition and vinyl acetate, methyl acrylate, methyl methacrylate or itaconic acid can be used as comonomers [2-3].

PEG is generally used as a solid-liquid phase change material and as a building block of solid-solid phase change materials [4]. There are polymeric mixtures such as PEG/polystyrene or composite structures such as PEG/sugar in the literature. In addition, solid-solid phase change polymers with thermal energy storage, produced using PEG and monomethyl ether-terminated PEG, are also available with various PEG molecular weight applications. The aim of this study is to produce the nanofibers of PEGs with high latent heat storage properties as impermeable and reusable by electrospin method. In this way, PEG, which turns into a liquid state by taking heat normally, will be stored in nanofibers with high surface area without showing flowing behavior and will gain reusability.

MATERIAL AND METHOD

Merck brand PEG 2000 and PEG20000, dimethyl formamide (DMF) and polyacrylonitrile (PAN) were used as materials and equipment. In addition, 5 mL ayset syringe and nano web electrospin 100 brand electrospin device operating between 0-25 kV were used in the experiments. A mixture of 10% PEG 2.000 and 90% PAN by mass is dissolved in 30 ml of DMF with stirring for 5 hours on a magnetic stirrer. It is filled into a 5 mL syringe without air bubbles and placed in the electrospin pump. The fiber formation on the collecting screen is adjusted by changing the distance between the syringe tip in the range of 7 cm-20 cm, the applied voltage in the range of 10-20 kV, and the pump flow rate in the range of 3.0-1.0 mL.

CONCLUSIONS

According to Table 1, while PAN did not give any enthalpy value, 35% PEG 2000 showed the highest enthalpy of melting and crystallization. In addition, the melting and crystallization enthalpy increased as the PEG2000 ratio in the nanofiber increased.

While Figure 2 shows that PAN forms the ideal nanofiber, the nanofibers containing PEG2000 give the appearance of agglomeration in places. The higher the PEG 2000 percentage, the greater the agglomerations. Studies have also shown that the fiber form disappears for higher molecular weight (PEG20000).

Table 1. DSC data for PAN and 10%PEG2000, 20%PEG2000 35%PEG2000 nanofibers

	Melting point (°C)	Melting enthalpy (j/g)	Crystalline point (°C)	Crystalline enthalpy (j/g)
%10PEG2.000	42.8	1.81	20.7	2.30
%20PEG2.000	44.9	39.39	34.3	39.03
%35PEG2.000	43.5	46.32	32.3	45.47
PAN	-	-	-	-

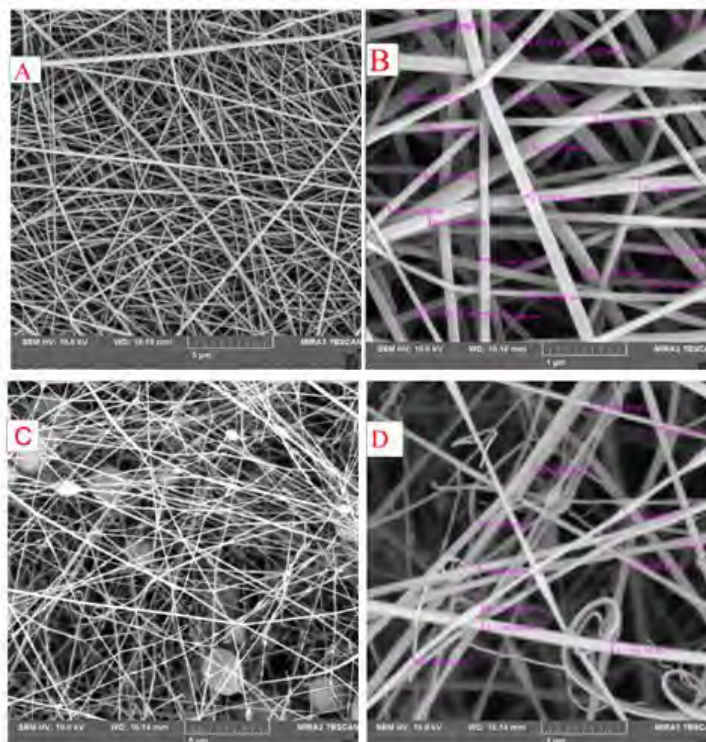


Figure 2. SEM images of A) PAN Nanofiber (10X) B) PAN Nanofiber (50X) C) 10% PEG2000 Nanofiber (10X) D) 10% PEG2000 Nanofiber (50X)

REFERENCES

- [1] Dharmaraj, N. Kadirvelu, K. Kim, H. Y. Thenmozhi, S. 2017. Electrospun Nanofibers: New Generation Materials for Advanced Applications. *Materials Science and Engineering B*. 217. 36-48.
- [2] Feng, C. Khulbe, K.C. Matsuura, T. 2009. Recent Progress in the Preparation, Characterization, and Applications of Nanofibers and Nanofiber Membranes via Electrospinning/Interfacial Polymerization. *Journal of Applied Polymer Science*. 115. 756-776.
- [3] Şen, S. 2012. Electrospun Nanofibers of Acrylonitrile And Itaconic Acid Copolymers (Doctoral dissertation). İstanbul Technical University. Institute of Science and Technology. İstanbul.
- [4] Pielichowski, K. Flejtuch, K. 2002. Differential scanning calorimetric studies on poly (ethylene glycol) with different molecular weights for thermal energy storage materials *Polymers for Advanced Technologies*. 13. pp. 690-696.

MICROENCAPSULATION OF THREE-COMPONENT THERMOCHROMIC SYSTEMS (FLUORAN DYE-PHENOLPHTHALEIN-N-TETRADECANOL) IN POLY(METHYL METHACRYLATE)

^{1*} Cemil Alkan, ² Simge Ozkayalar, ³ Sena Demirbağ Genç, ³ M.Selda Tözüm, ² Sennur Alay Aksoy

¹Tokat Gaziosmanpaşa University, Taslıçiftlik Kampusu, Tokat, Turkey

²Suleyman Demirel University, Bati Kampusu, Isparta, Turkey

³Usak University, 1 Eylül Kampusu, Usak, Turkey

*Corresponding author e-mail: cemil.alkan@gop.edu.tr

ABSTRACT

In this study, a thermochromic system (TS) consisting of a fluoran dye as a leuco dye, phenolphthalein as a color developer, and 1-tetradecanol (TD) as a solvent have been prepared and successfully microencapsulated in poly(methyl methacrylate) (PMMA). Microcapsules containing different type of fluoran dyes were synthesized to produce different color microcapsules and characterized. Also, phase transition temperatures and enthalpies, morphology, and particle size distributions of the microcapsules were analyzed deeply.

Keywords: thermochromic system, microcapsule, fluoran dye

INTRODUCTION

Smart materials response to external stimuli, such as temperature, pressure, light, pH, magnetic and electric fields via changing their properties. One of these materials is thermochromic dyes which change their color as a response to a change in temperature. Thermochromic materials change their color as a response to a change in temperature. They typically include materials made from liquid crystals, leuco dye systems, gold or silver nanoparticles, quantum dots, or dye-polymer blends [1]. The most commonly used types are liquid crystals and leuco dyes. Leuco dyes are electron donors and pH sensitive like spiro lactones, spiro pyrans, or fluorans. Leuco dyes which like spiro lactones, spiro pyrans, or fluorans are pH sensitive and electron donors [2]. Leuco dyes have been generally used as a component of the ternary thermochromic systems as color former. Ternary systems based on reversible color change of a color former by means of a color developer in a solvent medium are called as thermochromic systems or pigments. In the systems, the dye interacts with the developer to form one color when the solvent is in the solid form, while upon heating and melting of the solvent, this interaction is lost, forming an alternate color. Thus, the color change of the leuco dye system is controlled by the melting or crystallization of the long-chain solvent [1,3]. Evidently, such a reversible thermochromic behavior for thermochromic system involves the solid-liquid phase transitions, which can effectively absorb and release the thermal energy from environment as well as can monitor the state of solvent by color variation [4]. Recently, thermochromic systems (TSs) began to take place among the important materials in the production of materials exhibiting dual functional performances of temperature indication and thermal energy-storage. Thermochromic systems need to be microencapsulated prior to application to end products in many fields.

In this study, the thermochromic microcapsules containing ternary thermochromic system were prepared via emulsion polymerization method, and their thermal and thermochromic properties were explored. Thermochromic system was used as core and poly(methyl methacrylate) was synthesized as the polymeric shell material. Thermochromic systems were comprised of fluoran type leuco dyes, phenolphthalein as color developer, and 1-tetradecanol as solvent. Morphology, particle size distribution, and thermal properties of the microcapsules were determined by SEM, particle size analyzer, and DSC, respectively. Color-change behaviour of microcapsules depending on temperature was investigated digital camera photographs. To prove the presence of thermochromic systems in the microcapsules, FT-IR spectroscopy was used.

MATERIALS AND METHODS

2-Anilino-6-dibutylamino-3-methylfluoran (Colorant-1, from abcr GmbH), 6'-(Diethylamino)-1',2'-benzofluoran (Colorant-2, from abcr GmbH), 7-Anilino-3-diethylamino-6-methyl fluoran (Colorant-3, from abcr GmbH), phenolphthalein (PP, Carlo Erba), and 1-tetradecanol (TD, Alfa Aesar, 97%) were used as received without further purification. Methyl methacrylate (MMA, Sigma Aldrich, 99%) and ethylene glycol dimethacrylate (EGDM, Sigma Aldrich, 98%) were also used as received. PEG 1000 (Alfa Aesar) was the surfactant as 2,2'-Azobis(2-methylpropionamide) dihydrochloride (Aldrich, 97%) was initiator. The most effective ratio among components of TS was determined as 0.55/0.09/6.42 (Colorant:PP:TD) at 70-80 °C till homogeneous mixture. Core/shell ratio of microcapsules was selected as 1:0.5. At first, 6.5 g of TS as core material and 2 g of PEG1000 were mixed in 100 ml water at 50 °C at a speed of 2000 rpm. Secondly, a total of 3.25 g monomer, 1.35 g cross-linker, 1 g 2,2'-Azobis(2-methylpropionamide) dihydrochloride were added into the emulsion at 2000 rpm and heated to 80 °C under nitrogen atmosphere. At the end of the stirring time of 3 h, the emulsion was washed several times by using water at 70 °C

and filtered. The photographs, SEM images and particle size diagrams of the produced microcapsules were given in Fig. 1.

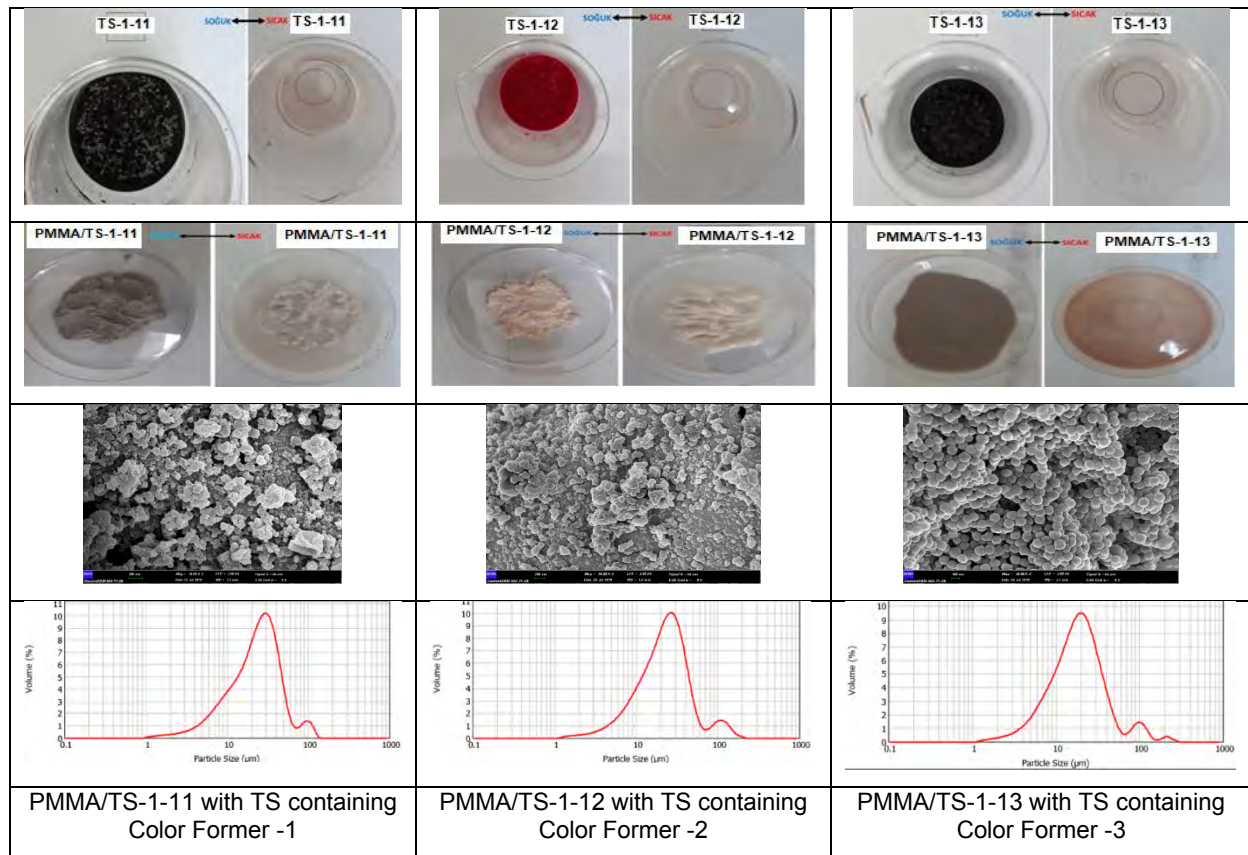


Fig. 1. The photographs, SEM images and particle size diagrams of the microcapsules

CONCLUSIONS

The reversible color changed PMMA microcapsules with a predetermined TS have successfully been prepared and microencapsulated in order to apply fabrics. The particles produced had considerable thermal energy storage capacity (178-198 J/g) at the phase change temperature slightly lower than TD precursor.

ACKNOWLEDGEMENT

The authors would like to express appreciation for the support to TUBITAK [Project Number 118M012].

REFERENCES

- [1] Liu B, Rasines Mazo A, Gurr PA, Qiao GG (2020) Reversible nontoxic thermochromic microcapsules. *ACS Applied Materials & Interfaces*, 12(8), p. 9782-9789.
- [2] Tözüm MS, Alay Aksoy S, Alkan C (2018). Microencapsulation of Three-Component Thermochromic System for Reversible Color Change and Thermal Energy Storage. *Fibers and Polymers*, 19(3), p. 660-669.
- [3] Tözüm MS, Alkan C, Alay Aksoy S (2020). Preparation of Poly (Methyl Methacrylate-Co-Ethylene Glycol Dimethacrylate-Co-Glycidyl Methacrylate) Walled Thermochromic Microcapsules and Their Application to Cotton Fabrics. *Journal of Applied Polymer Science*, 137(24), p. 48815.
- [4] Zhang Y, Liu H, Niu J, Wang X, Wu D. (2020). Development of Reversible and Durable Thermochromic Phase-Change Microcapsules for Real-Time Indication of Thermal Energy Storage and Management. *Applied Energy*, 264, p. 114729.

DEVELOPMENT OF SOLAR-DRIVEN AND HYDROGEN INTEGRATED CHARGING STATION FOR ELECTRIC VEHICLES

^{1,2*} Dogan Erdemir, ^{1,3} Ibrahim Dincer

¹ Ontario Tech University, Clean Energy Research Laboratory, Oshawa, ON, Canada

² Erciyes University, Department of Mechanical Engineering, Kayseri, Turkey

³ Yıldız Technical University, Department of Mechanical Engineering, Istanbul, Turkey

*Corresponding author e-mail: dogan.erdemir@ontariotechu.net; erdemir@erciyes.edu.tr

ABSTRACT

The present study develops a charging station for electric vehicles a solar energy-based integrated with hydrogen which is deployed as an energy storage option. It is primarily integrated into the system as an energy storage method in order to manage solar energy changes during the day. Thus, it is aimed to achieve the demand side load-levelling in the charging station with hydrogen. The present integrated system is further assessed through both energy and exergy efficiencies. At the end of the study, these energy and exergy efficiencies are observed to be 20% and 32%, respectively.

Keywords: Charging station; Electric vehicle; Energy Storage; Hydrogen; Solar energy

INTRODUCTION

It is crystal clear to everyone that electric vehicles are considered a major option to reduce carbon emissions, as long as electricity comes from renewables, in the transportation sector, which is responsible for almost a quarter of carbon emissions around the world. The influence of electric vehicles on grid loads is ever-increasing because of the increasing number of electric and plug-in hybrid vehicles. The power infrastructure required by the charging station is one of the biggest obstacles to broadcasting the use of electric vehicles for both individual and mass transportations. Therefore, meeting the energy demand of the charging station in a sustainable way is one of the most significant topics.

Renewable energy sources are promising options for the charging stations of electric vehicles like in every field. The main problem in including renewables in energy systems is their intermittent behaviours. Energy storage (ES) techniques are the key solution to solve challenges in renewables. ES methods can extend their availability period or balance the fluctuating behaviours. Today, many ES methods are practically used in engineering applications from various sectors. Hydrogen is a promising technology for a sustainable future, and today, it is included in almost all sectors. In near future, it is expecting that hydrogen-driven systems will be common with the extension of the hydrogen economy all around the world. Hydrogen is a significant energy storage medium due to its high energy storage density.

This study presents a solar-driven and hydrogen integrated charging station for electric vehicles where hydrogen is produced cleanly and used as a green energy storage solution for balancing the energy supply profile in order to minimize the need for grid supply. A case study from Kayseri, Turkey is presented for different capacity charging stations.

SYSTEM DEVELOPMENT AND DESCRIPTION

Figure 1 demonstrates the system layout of the proposed integrated system. Solar energy is converted to DC electricity in the PV panel. In a standard solar energy-driven charging station, the converted electricity in the PVs is directly sent to the charging station to meet the demand through boost and bidirectional converters. The difference between the demand and solar energy due to fluctuating behaviour of solar energy is met by grid energy. Here, hydrogen, as an energy storage solution, can play a significant role in minimizing the need for grid power. The excess solar energy can be used to produce hydrogen for later use when both the solar radiation is lower and none. For this purpose, an electrolyzer, hydrogen compressor, hydrogen storage tank and chiller are integrated into the system.

In this work, a charging station has 100 kW of power capacity has been modelled in Kayseri, Turkey conditions. The public transportation works between 6:00 - 23:59 during the day. The total PV area is 2000 m². Crystalline silicon-based PV panels that have about 0.20 of efficiency have been used. Figure 2 shows the hourly electricity capacity transformed from solar energy and the energy demand of the charging station. It is clear from Figure 2 that solar energy provides enough power to the charging station between 07:00 and 17:00. Also, between 08:00 and 16:00, there is excessive power generated by PV panels. This excess power capacity is used for generating hydrogen for later use in the early morning and after 17:00.

In the proposed integrated system, hydrogen is generated by an electrolyzer. 50-55 kWh of energy is needed for 1 kg of hydrogen production. The produced hydrogen is compressed up to 300 bars to store in a pressurized tank. For safety concerns, the hydrogen should be cool down below 80 °C with a chiller group. The hydrogen is used for power

generation in the fuel cell in order to meet the power demand of the charging station when solar radiation is not adequate and nighttime. In order to generate 1kWh energy 0.072 kg of hydrogen is needed. In order to assess the system, a thermodynamic analysis based on energy and exergy calculations is performed for a comparative evaluation.

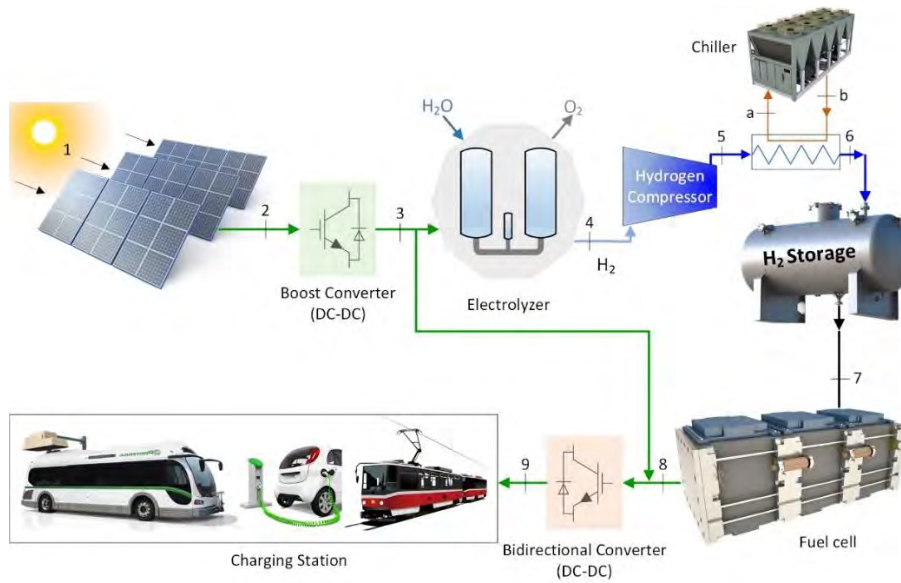


Figure 1. A schematic view of the solar energy driven and hydrogen integrated charging station for electric vehicles

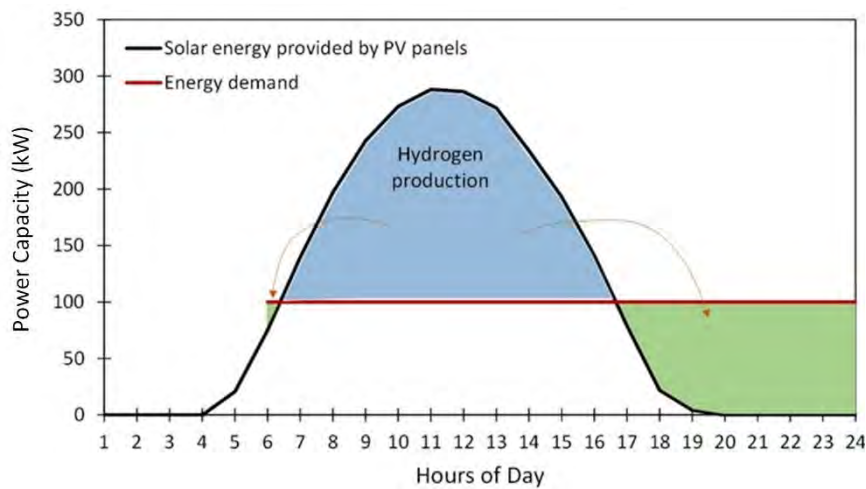


Figure 2. An illustration of the daily load distributions of the solar energy and charging station energy demand

CONCLUSIONS

In this study, the following key conclusions are obtained:

- The energy and exergy efficiencies of the proposed system are calculated to be 0.14 and 0.21, respectively. The exergy efficiency is higher than energy efficiency as the exergy content of the solar radiation is higher than the energy content at the source.
- The system would require 719 kWh of grid energy if the hydrogen energy storage systems had not been included in the system.
- The proposed charging station can work without requiring any grid power additionally.
- The system can be optimized for minimize the number of solar panels.
- A comprehensive power management and control systems are needed for future.

A PHOTOELECTROCHEMICAL REACTOR FOR ION SEPARATION AND HYDROGEN PRODUCTION

^{1,2*} Muhammed Iberia Aydin, ²Huseyin Selcuk, ^{1,3} Ibrahim Dincer

¹Clean Energy Research Laboratory, Faculty of Engineering and Applied Science, Ontario Tech University, Oshawa, Ontario, Canada

² Istanbul University-Cerrahpasa, Engineering Faculty, Environmental Engineering Department, Avcilar, Istanbul, Turkey

³ Faculty of Mechanical Engineering, Yildiz Technical University, Besiktas, Istanbul, Turkey

*Muhammed.Aydin@ontariotechu.ca

ABSTRACT

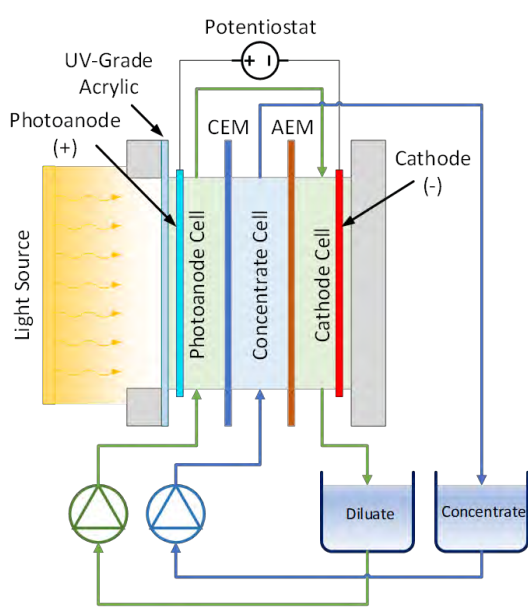
The need for water is increasing day by day due to human activities and necessities. Within the scope of sustainable environmental policies, certain restrictions are imposed on water use to shift the industry to adopting reuse methods. Therefore, in this study, a photoelectrocatalytic reactor is developed and utilized to treat and reuse the textile wastewaters. The treatment efficiencies and hydrogen production rates are compared under various applied potentials. The ion recovery efficiencies are 0.37, 0.39, 0.55, 0.66, 0.87, and the color removal efficiencies are 0.96, 0.95, 0.91, 0.75, 0.74 for 1.7, 1.9, 2.1, 2.3 and 2.5 V, respectively. The hydrogen production rates are measured as 0.024, 0.041, 0.061, 0.170, 0.302 mmol/h, respectively.

Keywords: Photoelectrochemical method, hydrogen production, ion removal, wastewater treatment, reuse

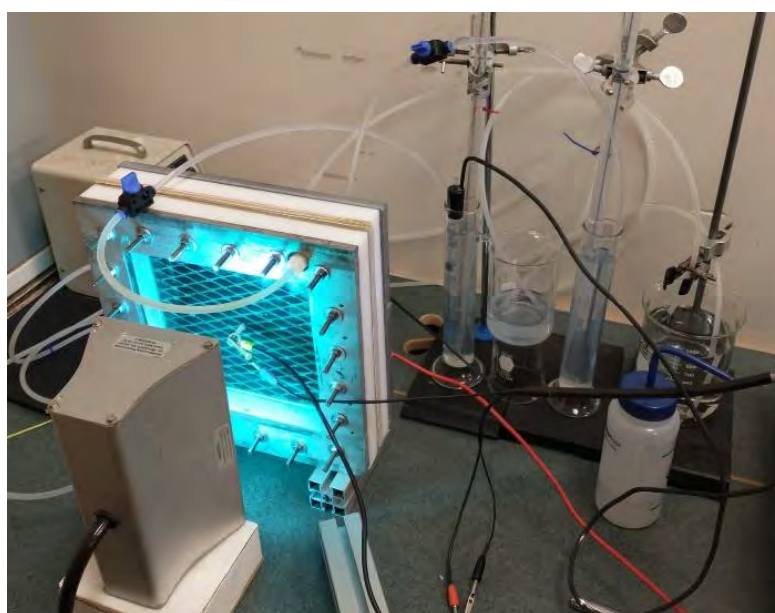
INTRODUCTION

Photocatalysis is the process of performing chemical reactions with a catalyst that becomes active under the light. An electron in the valence band of the photocatalyst activated under light moves to the conduction band. The resulting electron-hole pairs and the energy released due to returning electron movement form the basis of photocatalysis reactions. However, the electrons moved to the conduction band return to the valence band quickly, negatively affecting the photocatalysis efficiency [1]. Therefore, the photoelectrochemical (PEC) method has been developed. In the PEC method, the existence of electron-hole pairs is increased by applying an external electric current to the system. Although it is frequently used in organic matter removal and hydrogen production, it is not an efficient process for ion separation [2,3]. However, electrodialysis is used for ion separation and chemical purification by adopting anion and cation-selective membranes.

This study aims to combine electrodialysis and PEC methods. In the developed reactor, wastewater is cycled between anode and cathode cells for treatment. Positive and negative ions are collected in the concentrate cell located between the anion and cation exchange membranes with the applied electricity. While photoelectrocatalysis reactions occur in the anode cell, hydrogen production is carried out in the cathode cell, and ion recovery is carried out in the concentrate cell.



(a)



(b)

Figure 10. Graphical representation (a) and working prototype (b) of the developed PEC reactor

MATERIALS AND METHODS

A PEC reactor with cation and anion-selective membranes was used in this study. Figure 1 shows the PEC reactor used in the study. Both anode and cathode cells are separated with anion and cation exchange membranes that were purchased from PCCell GmbH. The stainless steel (Grade 316) coated with TiO₂ nanoparticles was used as the photoanode. Also, uncoated stainless steel (Grade 316) is used as a cathode. The ions are collected in the concentrate cell in the middle. The studies were carried out by illuminating the photoanode cell with UV light. The current produced by the system under different voltages was measured using a Gamry Reference 3000 potentiostat. The simulated textile wastewater cycled through the anode and cathode cells to conduct a treatment study. Table 1 gives the characteristics of used wastewater. A solution containing 0.025M NaOH cycled through the concentrate cell to decrease the resistance of the reactor. Conductivity, color, COD, the hydrogen production rate of the wastewater, and concentrate monitored under various applied electric potentials.

RESULTS AND DISCUSSION

Ion recovery efficiency increases when the applied potential is increased. The ion recovery efficiency was 0.37, 0.39, 0.55, 0.66, 0.87 for 1.7, 1.9, 2.1, 2.3 and 2.5 V after 10 hours, respectively. However, it was observed that the ion transfer slowed down after a while due to concentration polarization. The hydrogen production capacity increases with increasing applied potential. Hydrogen production rate under 2.5V with illumination was measured as 0.302 mmol/h. The conductivity change and hydrogen production rate data are given in Figure 2. Although ion mobility increased with increasing voltage, it had an adverse effect on color removal. The color removal efficiency was found to be 0.96, 0.95, 0.91, 0.75, 0.74 for 1.7, 1.9, 2.1, 2.3 and 2.5 V, respectively. Although the color removal efficiency in wastewater at higher voltages was decreased, no COD and color change occur in the sample obtained from the concentrate cell. In this case, it is possible to reuse the produced concentrate.

Table 5. Characteristics of the simulated textile wastewater

Parameter	Value
Conductivity, mS/cm	44.2
NaOH Concentration, M	0.25
COD, mg/L	2480
Color, PTU	1320
pH	>13

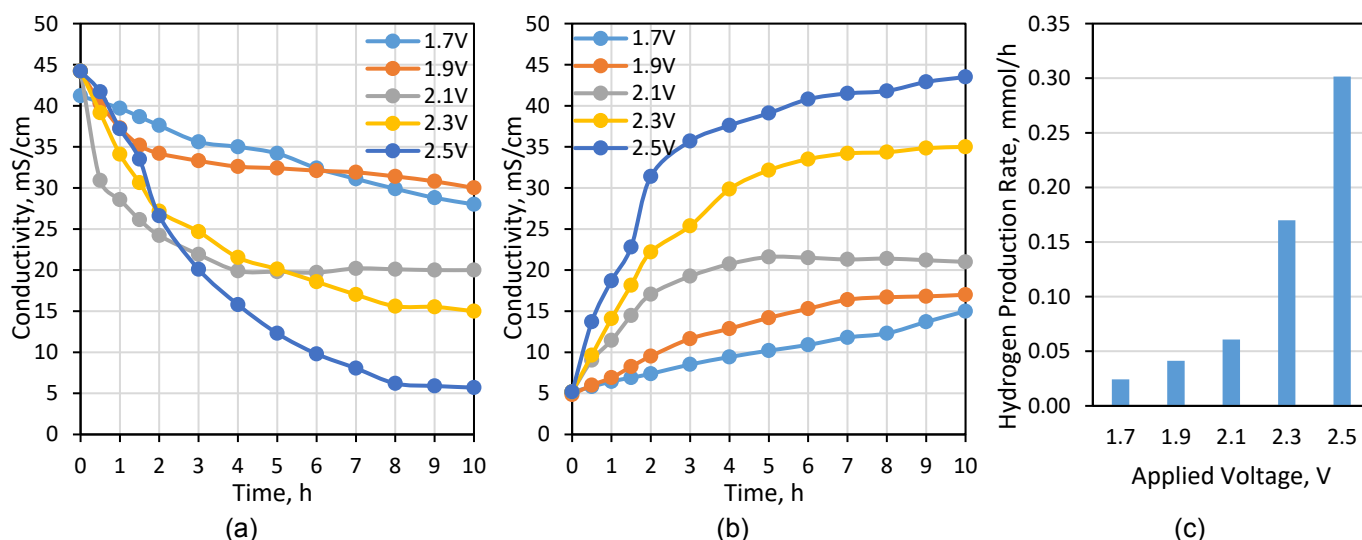


Figure 11. Conductivity measurements of wastewater (a), concentrate (b) over time, and hydrogen production rate of the reactor (c).

CONCLUSIONS

In this study, a PEC reactor capable of ion separation, decolorization, and hydrogen production was developed, built and tested. As a result of the study, the treatment and recovery efficiencies of the system are measured. Accordingly, the concentrate obtained was at a reusable state, and the system was also able to produce hydrogen satisfactorily.

REFERENCES

- [1] Gaya UI. Heterogeneous Photocatalysis Using Inorganic Semiconductor Solids. Springer Netherlands; 2013.
- [2] Rodrigues MAS, Amado FDR, Xavier JLN, Streit KF, Bernardes AM, Ferreira JZ. Application of photoelectrochemical-electrodialysis treatment for the recovery and reuse of water from tannery effluents. J Clean Prod. 2008;16(5):605–11.
- [3] Acar C, Dincer I, Naterer GF. Review of photocatalytic water-splitting methods for sustainable hydrogen production. Int J Energy Res. 2016 Sep 1;40(11):1449–73.

CLIMATE IMPACT OF BLOCKCHAIN IN THE VIEW OF CRYPTOCURRENCIES

^{1*} Nazenin Gure

¹Beykent University, Faculty of Engineering-Architecture, Mechanical Engineering Department, Ayazaga Campus, Istanbul, Turkey

*nazeningure@beykent.edu.tr

ABSTRACT

Cryptocurrency mining energy consumption resulted emissions stem from electric usage and electronic waste due to up-to-date mining hardware are at peak. Climate impact of bitcoin and Ethereum as well as cost comparison of cryptocurrencies, token economy with traditional finance are evaluated. It is seen that recorded peak levels of power consumption and consequent greenhouse gas emissions are not only limited to cryptocurrencies. Traditional finance global system also owns massive load for our demanding world economy, services, finance organs and data security. Important background prior to bitcoin mining future projection and potential energy demand estimations are presented by emphasizing the saturation of bitcoin supply curve. Up-to-date digital green solutions via proof-of-stake, novel suggestion to harvest mining waste heat and electronic waste awareness are presented.

Keywords: Cryptocurrency, Climate Impact, Green-Coin, Bitcoin (BTC), Ethereum (ETH)

INTRODUCTION

As peer-to-peer decentralized finance is popularized by Bitcoin, resulted climate impact and regarding researches become additional figure of merit. Digiconomist's energy consumption index highlights that Bitcoin (BTC) is responsible for the 0.15% of global energy consumption. According to CBECI's study in 2019, annual electric consumption of bitcoin is increased from 7.55 GW [1] (66 TWh for 24/7 mining [2]) to 87.1 TWh [3]. In line with CBECI, Digiconomist estimation for bitcoin is 77.78 TWh. Marketcap is dominated with bitcoin and Ethereum (ETH) by 80 and 10% [2]. Annual carbon footprint of bitcoin is 36.95 Mton CO₂ emission (CO₂). This emission value is equivalent of New Zealand. Annual electronic waste of bitcoin is 10.32 kton, equivalent e-waste of Luxemburg. Single bitcoin transaction results 332.69 kg CO₂; 700.41 kWh, equivalent of daily consumption of 24 US-houses; and 93 gr of electronic waste [4]–[6]. For Ethereum, annual power consumption is 12.29 TWh, equivalent power need of Georgia. For single Ethereum transaction, power consumption is 30.16 kWh, equivalent of single US-house need per day [7].

ANALYSIS AND DISCUSSION OF CLIMATE CHANGE IMPACT OF CRYPTOCURRENCIES

To begin with, cryptocurrency and traditional finance comparisons are performed upon visa transaction. Electricity consumption ratio of single bitcoin transaction to visa is nearly 700k. While sceptics state this ratio as 4k [8], Vries' up-to-date data analysis shows that the possible peak of this ratio can only be 2k (765.4 kWh/ 0.4 kWh) [6]. Moreover, green-coin defenders state that credit card costs have to be estimated systematically. Since crypto-currencies' systems and codes are transparent and public, all actions are clearly calculated [9]–[11]. Evaluation of credit card costs requires deeper investigation by compromising dependent organs of banking system. As a result, banking costs consist even from ministries of finances (c1); central banks (c2); all actors in stock markets, investors (c3) and all employees' income (c4); c1, c2, c3 and c4's power consumptions, costs of meetings and expenses (c5), up to their physical system and data security (c6), data centres (c7), analytics (c8) and fraud detection (c9). In order to compare objectively, both traditional and crypto-economy systems need to be transparent so that related costs and impacts can be estimated accurately. Supportively, it is stated that finance sector's impacts and energy consumption significantly greater than cryptocurrencies' since it has accumulated information and occupies massive volume around the globe [6]. Power consumption of data centres is reported that five-times of all crypto-currencies [12]. Vries presents that the global banking system processes 6k times (482.6B/ 81.4M) more annual transactions than bitcoin, and per transaction origin, banking consumes minimum 1.2k (491.4 kWh/ 0.4 kWh) and maximum 2k (765.4 kWh/ 0.4 kWh) less power than bitcoin. However, since total transaction is greater, resulted annual energy consumption of banking industry including c7 and ATMs increases up to 650 TWh [6], [13]. All in all, even crypto-finance and token economy's fundamental philosophy are based on decentralized, autonomous and trustless cash system; requirements of society always set ministries, banks and financial organs present. Therefore, cost of cryptocurrencies in real societies would consist common fundamentals and be greater than current estimations.

Another potential misleading statement is based on impossible assumptions of bitcoin mining. Mora et.al. states that the growth in bitcoin "at the rate of other popular technologies", is capable to produce enough emission that forces global warming even beyond 2 degree Celsius "in three decades" [9]. The one major reason for this estimation to be exaggerated is that renewable empowered mining is ignored. Most importantly, research is based on incorrect assumption because bitcoin mining duration is limited and will be saturated at 2025, which is far less than three decades used in the estimation. Therefore, both in terms of increased hash rate and the level of crypto-puzzle, the

only forecast is that mining to be reduced and finalized. In the best possible mining scenario, there will be *no bitcoin mining growth* after maximum of 5-10 years. Coded controlled supply curve of bitcoin indicates that peak value (21 M bitcoin) is reached in the year 2140. If 95% of saturation is taken, the upper limit is achieved in 2025. In other words, mining bitcoin is not a continuous action and future climate change impact estimations are not the case after 5 years [11]. Another supporting reason for the final statement is that the halving. In contrast to proposed mining growth claims in literature, as the halving occurs almost every four years, since block reward decreased by half, the realistic trend to mine is more likely to decrease in saturation zone unless Bitcoin value hyper-inflate.

CONCLUSIONS

As a novel suggestion in literature, thermal energy generators (TEGs) are perfect candidate to harvest waste heat [14]–[16] of ASICs to electricity. Generated energy can be redirected as a cascade cycle back to ASICS as well as other electronic devices or sensors monitoring mining facilities.

Alternative energy consumption solution is that setting the green blockchain consensus mechanism: Buterin, founder of Ethereum, together with Ethereum stake holders are about to fork Ethereum network with sustainable alternative, Ethereum 2.0 with a PoS (proof of stake) [4], [5], [8]. Once dominant network activity is on PoS, reduction of electronic wastes due to decreased mining procedure is also expected. Mining inactivity may first pose vast amount of ASIC waste. Planning measures to reuse, recycle and reduce the future e-wastes shall be reconsidered for green perspective.

REFERENCES

- [1] D. Hollerith, "Why Bitcoin Miners Don't Use More Renewable Energy," Decrypt, 2020. <https://decrypt.co/43848/why-bitcoin-miners-dont-use-more-renewable-energy> (accessed Nov. 20, 2020).
- [2] U. Gattersdo, L. Klaaßen, C. Stoll, and U. Gattersdo, "Energy Consumption of Cryptocurrencies Beyond Bitcoin Commentary," Joule Comment. CellPress, Elsevier, vol. 4, 2020, doi: 10.1016/j.joule.2020.07.013.
- [3] A. de Vries, "Bitcoin's energy consumption is underestimated: A market dynamics approach," Energy Res. Soc. Sci., vol. 70, p. 101721, 2020, doi: <https://doi.org/10.1016/j.erss.2020.101721>.
- [4] C. Stoll, L. Klaaßen, C. Stoll, L. Klaaßen, and U. Gattersdo, "The Carbon Footprint of Bitcoin The Carbon Footprint of Bitcoin," Joule, vol. 3, pp. 1647–1661, 2019, doi: 10.1016/j.joule.2019.05.012.
- [5] DIGICONOMIST, "Bitcoin Energy Consumption Index CO2," 2020. <https://digiconomist.net/bitcoin-energy-consumption> (accessed Nov. 20, 2020).
- [6] A. De Vries, "Renewable Energy Will Not Solve Bitcoin's Sustainability Problem," Joule, vol. 3, no. 4, pp. 893–898, 2019, doi: 10.1016/j.joule.2019.02.007.
- [7] DIGICONOMIST, "Ethereum Energy Consumption Index (beta) Energy," 2020. <https://digiconomist.net/ethereum-energy-consumption>.
- [8] B. C. Malmo, "A Single Bitcoin Transaction Takes Thousands of Times More Energy Than a Credit Card Swipe," VICE, 2017. <https://www.vice.com/en/article/ypkp3y/bitcoin-is-still-unsustainable>.
- [9] C. Mora et al., "Bitcoin emissions alone could push global warming above 2°C," Nat. Clim. Chang., vol. 8, no. 11, pp. 931–933, 2018, doi: 10.1038/s41558-018-0321-8.
- [10] T. Breunig, "Home Heating with Crypto Mining," Efficiency, Energy Harvesting, Green Building, Innovative Business Model-CLEANTECH CONCEPTS, 2018. <http://www.cleantechconcepts.com/2018/06/home-heating-with-crypto-mining/> (accessed Nov. 20, 2020).
- [11] A. Badev, M. Chen, A. Badev, and M. Chen, "Bitcoin: Technical Background and Data Analysis," in Finance and Economics Discussion Series, 2014.
- [12] Chicago Bitcoin & Open Blockchain community, "Bitcoin Q&A: Energy Consumption with Andreas M. Antonopoulos," mHUB innovation center, Chicago, Illinois, 2017.
- [13] N. Lei, "A robust modeling framework for energy analysis of data centers," pp. 2–5.
- [14] O. A. Saraereh, A. Alsaraira, I. Khan, and B. J. Choi, "A hybrid energy harvesting design for on-body internet-of-things (IoT) networks," Sensors (Switzerland), vol. 20, no. 2, pp. 1–16, 2020, doi: 10.3390/s20020407.
- [15] K. T. A. Elefsiniots and T. Becker, "Energy storage options for wireless sensors powered by aircraft specific thermoelectric energy harvester," pp. 701–707, 2014, doi: 10.1007/s00542-013-2009-3.
- [16] C. Bajrang, G. Vaira Suganthi, R. Tamilselvi, M. Parisabeham, and A. Nagaraj, "A systematic review of energy harvesting from biomechanical factors," Biomed. Pharmacol. J., vol. 12, no. 4, pp. 2063–2070, 2019, doi: 10.13005/bpj/1840.

ON ENERGY PERFORMANCE OF SOFC INTEGRATED S-CO₂ MICRO-GAS TURBINE

¹Uğur Akbulut, ²Adnan Midilli

¹Recep Tayyip Erdoğan Üniversitesi, Mühendislik ve Mimarlık Fakültesi, Makine Mühendisliği Bölümü, Rize, Türkiye

²Yıldız Teknik Üniversitesi, Makine Fakültesi, Makine Mühendisliği Bölümü, Beşiktaş, İstanbul, Türkiye

*Corresponding author e-mail: ugur.akbulut@erdogan.edu.tr

ABSTRACT

The main objective of this study is to investigate the effect of operating temperature on the energetic performance of SOFC integrated supercritical carbon-dioxide (s-CO₂) micro-gas turbine (m-GT) with intercooling system. Consequently, it is noticed that, based on the amount of heat production from SOFC, the energy performance of the system increases with the rise of SOFC operation temperature. Moreover, at the constant SOFC operating temperature, the energy performance of the system goes up with the increase of MGT inlet temperature.

Keywords: SOFC, hydrogen, exergetic efficiency, current density, rational overpotential.

INTRODUCTION

Power generation systems that use traditional steam Bryton and Rankine cycles can be upgraded to s-CO₂ to increase efficiency and power output [1]. A wide range of open and closed Brayton and Rankine cycle systems employing s-CO₂ as the working fluid have been proposed for power generation applications. The benefits of the s-CO₂ cycles are high efficiency in the mild turbine inlet temperature region and a small physical footprint with a simple layout, compact turbomachinery, and heat exchangers. Several heat sources including nuclear, fossil fuel, waste heat, and renewable heat sources such as solar thermal or fuel cells are potential application areas of the s-CO₂ [2]. In these systems, s-CO₂ is the main working fluid. The s-CO₂ effectively captures waste heat from sources such as turbine exhaust or other hot gases because of single-phase characteristics well above the critical which permits a higher fluid temperature extremely matching to the heat source temperature profile [3].

Micro-gas turbines (m-GT) are energy generators whose capacity ranges from 15 to 300 kW and they offer several typical features, such as: variable speed, high speed operation, compact size, simple operability, easy installation, low maintenance, air bearings and low NO_x emissions [4]. In energy integration systems, SOFCs have attracted considerable interest in domestic and industrial applications considering their competitive advantages such as higher energy efficiency, lower pollutant emissions, fuel extensibility, and highly operational temperature which allows a variety of cogeneration possibilities [5] Moreover, micro-gas turbine integrated fuel-cell power systems with multi-fuel capability and remarkable overall efficiency has come forward [6,7].

SYSTEM DESIGN AND OPERATION

It is planned to gain opportunity to increase electrical efficiency and power output of SOFC system by integrating a s-CO₂ intercooling layout cycle to the SOFC system while using the waste heat of SOFC. For this purpose a novel planar SOFC integrated s-CO₂ Micro-Gas Turbine power system which is given in the Fig.1 is designed.

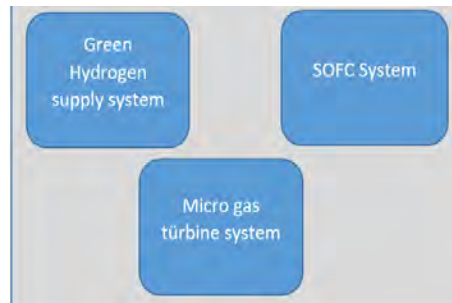


Fig.1. Schematic illustration of SOFC integrated s-CO₂ Micro-Gas Turbine power system

System performance can be calculated as

$$\eta_{\text{sys}} = \frac{\dot{W}_{\text{SOFC}} + \dot{W}_{\text{MGT}} - \dot{W}_{\text{C1}} - \dot{W}_{\text{C2}} + \dot{Q}_{\text{CL1}} + \dot{Q}_{\text{CL2}}}{\dot{E}_{\text{H}_2, \text{in}(\text{SOFC})} + \dot{E}_{\text{air, in}(\text{SOFC})}} \quad (1)$$

where, \dot{Q}_{SOFC} , $\dot{E}_{\text{H}_2, \text{in}(\text{SOFC})}$ and $\dot{E}_{\text{air, in}(\text{SOFC})}$ indicates amount of heat transferred to s-CO₂ Bryton cycle from the SOFC, energy input to the SOFC by H₂ fuel and energy input to the SOFC by air which is used as oxidant respectively.

RESULTS AND DISCUSSION

In this study a planar solid oxide fuel cell (SOFC) integrated supercritical carbon-dioxide (s-CO₂) micro-gas turbine with intercooling system for residential applications. SOFC system is accepted as the base system. That's why only SOFC operation temperature is changed which resulted change in power and heat generation. Fig.2 shows the variations of Bryton Cycle efficiency and total system efficiency as a function of SOFC efficiency.

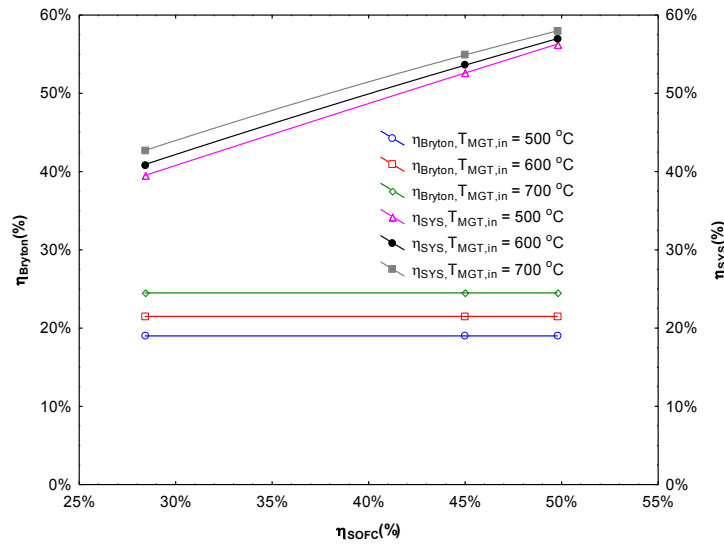


Fig. 2. The variations of Bryton Cycle efficiency and total system efficiency as a function of SOFC efficiency.

CONCLUSIONS

System efficiency increases (from 0.395 to 0.580) with the rise of SOFC efficiency (from 0.248 to 0.498) and at a constant SOFC efficiency system efficiency increases with the rise of Bryton Cycle efficiency.

REFERENCES

- [1] Persichilli M, Held T, Hostler S, Zdankiewicz E, Klapp D. Transforming waste heat to power through development of a CO₂-based power cycle. Paper presented at: Electric Power Expo; 2011 May 10-12; Rosemount, IL, U.S.A.
- [2] Ahn Y, Bae SJ, Kim M, Cho SK, Baik S, Lee JI, Cha JE. Review of supercritical CO₂ power cycle technology and current status of research and development. Nucl Eng Technol. 2015 October; 47(6): 647-661.
- [3] Persichilli M, Kacludis A, Zdankiewicz E, Held T. Supercritical CO₂ power cycle developments and commercialization: Why sCO₂ can displace steam. Paper presented at: Power-Gen India & Central Asia; 2012 April 19-21; Pragati Maidan, New Delhi, India.
- [4] Chambers A, Hamilton S, Schnoor B, editors. Distributed Generation: a nontechnical guide. chap. 3, pp. 33 – 72. Stephanie L. Hamilton.: PennWell Corporation, USA; 2001.
- [5] Akbulut U, Midilli A, Dincer I. Studying the effect of electrolyte thickness on exergetic performance for an electrolyte supported SOFC stack. In: Proceedings of the 8th International Exergy, Energy and Environment Symposium (IEEES-8). 2016 May 1-4; Antalya, Turkey; Antalya: 2016. p. 497-503.
- [6] Palsson J, Selimovic A, Sjunnesson L. Combined solid oxide fuel cell and gas turbine systems for efficient power and heat generation. Journal of Power Sources. 2000 March; 86 (1-2): 442–448.
- [7] Veyo SE, Shockling LA, Dederer JT, Gillett JE, Lundberg WL. Tubular solid oxide fuel cell/gas turbine hybrid cycle power systems: Status. Journal of Engineering for Gas Turbines and Power. 2002 October; 124(4):845.

EXPERIMENTAL INVESTIGATION OF A VAPOR COMPRESSION REFRIGERATION SYSTEM FOR THERMAL MANAGEMENT

^{1*} Fethiye Coskun, ² Mustafa Fazıl Serincan

¹Gebze Technical University, Faculty of Engineering, Mechanical Engineering Department, Gebze, Kocaeli 41400, Turkey

²Gebze Technical University, Faculty of Engineering, Mechanical Engineering Department, Gebze, Kocaeli 41400, Turkey

*Corresponding author e-mail: fethiyekucuk@gtu.edu.tr

ABSTRACT

This paper presents the performance assessment of vapor compression refrigeration system (VCRS) that is used for electronics cooling application experimentally. The system includes a compressor, two evaporators, a condenser, and an expansion valve. The working fluid in the system is R134a and the evaporator has a copper pipe with a length of 2800 mm and a diameter of 3 mm. The condenser is considered as a microchannel heat exchanger with 28 tubes, 6 passes. The system is tested at ambient temperatures of 24°C, 40°C and 55°C. The heaters are operated at 360 W and 180 W for half an hour. In tests at different ambient temperatures, compressor and fan speeds are also changed to improve cooling performance. The surface temperature of the compressor is taken into account in order not to cause any malfunctions during the test. While the cold plate temperature decreased at 24°C and 40°C, the compressor temperature remained in the operating range at the same time. However, in the test performed at 55 degrees, the compressor surface temperature reached the maximum operating temperature.

Keywords: Vapor compression refrigeration system, Electronic cooling, Thermal management.

INTRODUCTION

Thermal management of electronic components becomes a significant engineering task to use computer technologies more reliable and faster in the last decades. The cooling systems used in computers are usually passive cooling and forced convection. However, these systems are insufficient due to restricted application volumes and low performance at high temperatures. The main objective of this work is to conduct an experimental study on a compact vapor compression refrigeration cycle to be used for computer cooling systems under high cooling requirements. Through the presented cooling system, the cooling performance of the system is presented to keep the device temperature below the operating temperature, which ensures the reliable operation of electronics.

EXPERIMENTAL DESIGN AND TEST METHOD

The VCRS comprises four main components: two evaporators, a compressor, a condenser, and an expansion valve. Moreover, there are secondary elements such as fan, dryer, sight glass, temperature sensors, pressure manifolds, and heater plates (as shown in **Error! Not a valid bookmark self-reference.**). The refrigerant circulating through the system is R134a. The condenser is considered a micro-channel heat exchanger. Evaporator pipes are used on the two side walls of the case. The copper pipe used for each evaporator has a 3 mm inner diameter, 2800 mm length, and wall thickness of 1 mm. The compressor is operated at a temperature of 54°C, and speed control is done according to different heat loads. The expansion valve is an automatic expansion valve, while the fan is the DC axial compact fan with an air flow rate is 710 m³/h. Pressure manifolds and temperature sensors are put to use in order to measure pressure and temperature, respectively throughout the experimental study. The heaters that represent the case and can provide a total heat load of 360 W.

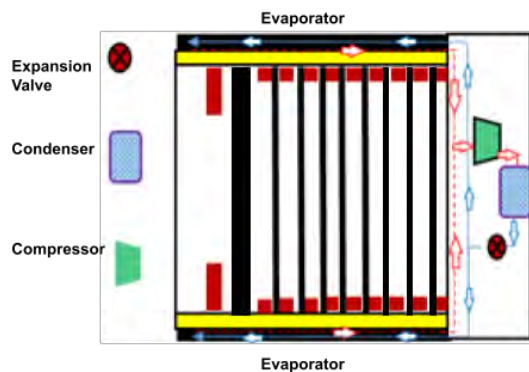


Fig. 1. Schematic diagram of VCRS.

CONCLUSIONS

The system is operated at full load for 30 minutes and at half load for 30 minutes. The test is continued until the temperature becomes stabilized. **Fig. 2a** shows that the system is started when the sidewall temperature reaches an average of 70°C. The fan and compressor speeds are found as 1050 rpm and 2300 rpm, respectively. The cold plate temperature varies between 27°C - 38°C in the condition of equilibrium period. The low-pressure value is in the range of 3.4- 3.7 mPa, the high-pressure value is in the range of 12 -13 mPa. The condenser side is at a minimum temperature of 24 °C and a maximum of 44 °C, and the temperature on the evaporator side is at 42 °C. **Fig. 2 (b)** shows the cold plate temperature at 40 °C ambient temperature. The fan speed is at 3500 rpm and the compressor at 3000 rpm. The operating pressure of the system is in the range of 3.5 -12 mPa. The condenser side is at a minimum temperature of 29 °C and a maximum of 42 °C, and the temperature on the evaporator side temperature is in the range of 25 -39 °C. **Fig. 2 (c)** also shows that the cold plate temperature of system at 55°C ambient temperature. The fan speed is at 7000 rpm and the compressor at 5000 rpm. The maximum dome temperature of the compressor is 115 °C, and during the test, the surface temperature almost reached these points. Although high fan and compressor speed were used, the cold plate temperature of the system was stable at values close to the initial temperature. The designed system is not suitable to be operated at high ambient temperature for a long time for electronic cooling. It is possible to damage the compressor and other system components. It is safer for the system to be used in places where the ambient temperature is 40°C and below.

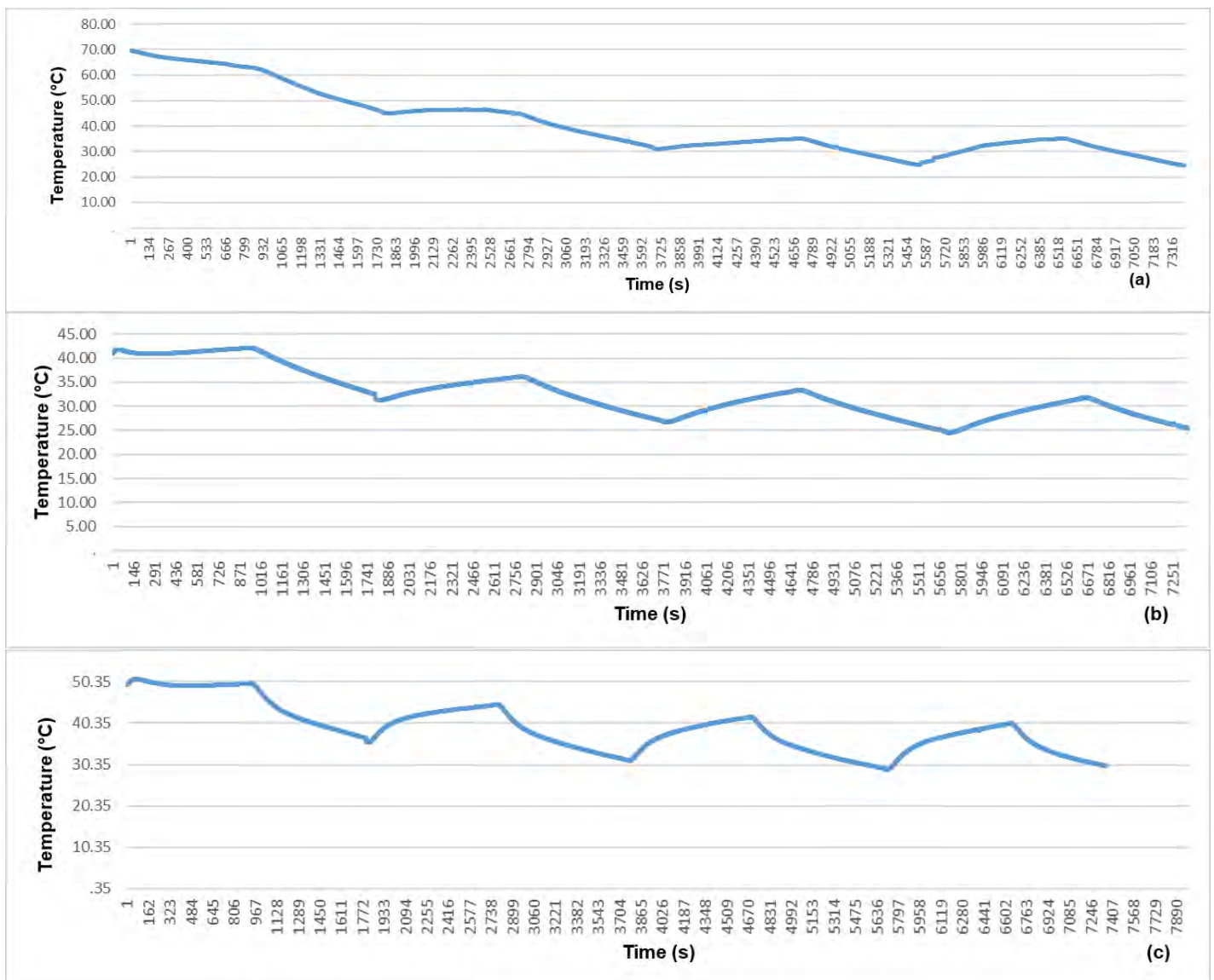


Fig. 2. Cold plate temperature under part-time load at ambient temperatures of 24 °C (a), 40°C (b) and 55°C (c).

INTERFACIAL THERMAL RESISTANCE BETWEEN WATER AND METALS USING MOLECULAR DYNAMICS SIMULATION

^{1*} Muhammed Murat Aksoy, ² Yıldız Bayazitoğlu

¹Osmaniye Korkut Ata University, Energy Systems Engineering Department, Osmaniye, Turkey

²Rice University, Mechanical Engineering Department, Houston, TX, USA

*Corresponding author e-mail: aksoy.cu@gmail.com

ABSTRACT

Energy systems in nanodevices constantly demand new developments. Interfacial Thermal Resistance (ITR) is one of those developments that is significant in understanding and tackling thermal transport technologies in nanoscales. The thermal transport at the interfaces of solids and liquids has been a measurement challenge for various nanoscale applications. Since materials would be considered as the bottlenecks to improve the energy performance of the systems, understanding the ITR of solids and liquids has an important role for nanodevices. Therefore, we have applied the non-equilibrium Molecular Dynamics (MD) method to investigate the ITR between liquid water and transient metals. We have comprehensively evaluated ITR of metal nanochannels filled with liquid water. We subsequently carried out MD simulation for gold (Au), silver (Ag), platinum (Pt), lead (Pb), palladium (Pd), and nickel (Ni) metals placed on each side of water creating a nanochannel system. The mean temperature of water was kept constant among the solid walls during the simulations and it was changed from 300 K to 600 K in increment of 50 K. We finally concluded a direct relation of ITR between temperature change and heat flux.

Keywords: Molecular Dynamics, Interfacial resistance, Water, Metals

INTRODUCTION

Interfacial Thermal Resistance (ITR), also known as Kapitza resistance (R_K), is the ratio of temperature difference (ΔT) between solid and liquid interface and the heat flux (\dot{q}) through the system ($R_K = \dot{q}/\Delta T$). To measure ITR, molecular dynamics (MD) simulation is chosen because of its deterministic approach to the systems, hence we can predict the atoms and molecules' final positions using the required interatomic force fields. In this study, reversed non-equilibrium MD simulations are conducted for a solid–liquid–solid system to determine the ITR values for solid metals and liquid water. Solid metals are constructed using Face Centered Cubic (FCC) lattice structures. Overall, understanding thermal interfaces between water and these metals enable us to design more energy efficient nanodevices especially in thermal design applications.

MATERIALS AND METHODS

Figure 1 schematically shows the nanochannel system for MD simulations. A FCC solid metal structure was built and then placed on each side of the water box creating sandwiched system. For this study, Polymer Consistent Force Field (PCFF) is used for the interatomic interactions for metals atoms and water molecules.

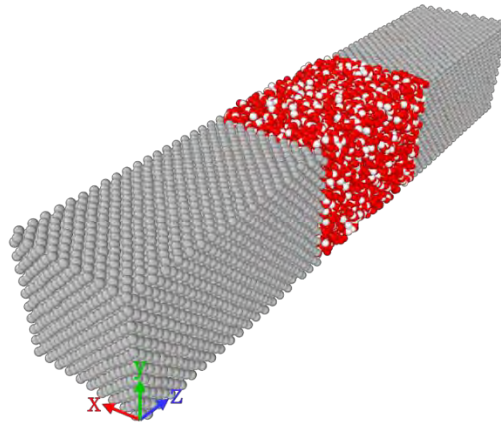


Fig. 1. Nano channel system for MD simulation set-up (Gray particles represent metal atoms. Red-White particles represent H₂O molecules.).

For required PCFF parameters for water and metals, we have used Fritz and Hofmann's work [1] and Heinz et al. paper [2], respectively. LAMMPS code is used for MD simulations.

NVT and NVE ensembles were applied to equilibrate the system and measure necessary parameters to find out the ITR. For reverse non-equilibrium MD (or Muller – Plathe Method), the temperature gradient is measured with respect to imposed heat flux.

RESULTS AND DISCUSSIONS

Figure 2 shows temperature jumps at the interface of Au and Ag nanochannels. Even though temperature change at the interface is small, we have to consider additional ITR in our nano devices. Table 1 shows the detailed version of temperature jumps with respect to ITR and the heat flux through the Au nanochannel. We can observe that ITR increases as temperature increases.

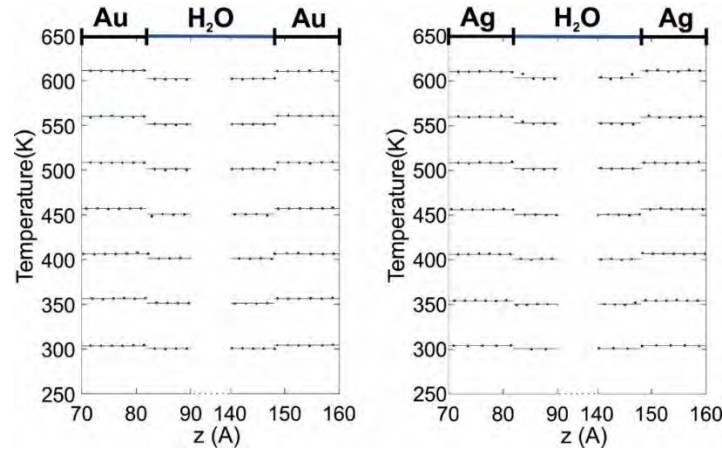


Fig. 2. Temperature dependence of Interfacial Thermal Resistance (ITR) including standard deviation as error bars

We also thoroughly compared Au and Ag results with a given literature [3, 4]. As can be inferred, we conclude that ITR increases with the temperature increase and the heat flux decrease. This relation would help us for the calculation of the one-dimensional heat conduction by including additional ITR between solid and liquid of any nano engineering problems.

Table 1. Detailed data for Au nanochannel

Temperature (K)	\dot{q} (W/m^2K) $\times 10^8$	ΔT (K)	R_k (m^2K/W) $\times 10^{-8}$
300	3.6532	3.3186	0.9084
350	4.3608	5.0245	1.1522
400	4.9092	4.4693	0.9104
450	5.6780	5.9937	1.0556
500	6.1082	7.2619	1.1889
550	6.8604	7.9214	1.1547
600	7.3608	9.5125	1.2923

REFERENCES

- [1] Fritz L, Hofmann D. Molecular dynamics simulations of the transport of water-ethanol mixtures through polydimethylsiloxane membranes. *Polymer*. 1997 Mar 1;38(5):1035–45.
- [2] Heinz H, Vaia RA, Farmer BL, Naik RR. Accurate Simulation of Surfaces and Interfaces of Face-Centered Cubic Metals Using 12–6 and 9–6 Lennard-Jones Potentials. *J Phys Chem C*. 2008 Nov 6;112(44):17281–90.
- [3] Vera J, Bayazitoglu Y. Temperature and heat flux dependence of thermal resistance of water/metal nanoparticle interfaces at sub-boiling temperatures. *International Journal of Heat and Mass Transfer*. 2015 Jul; 86:433–42.
- [4] Aksoy MM, AlHosani M, Bayazitoglu Y. Thermal Resistance for Au–Water and Ag–Water Interfaces: Molecular Dynamics Simulations. *Int J Thermophys*. 2021 Apr 9;42(6):87.

THERMAL CONDUCTIVITY OF COPPER-SINGLE WALLED CARBON NANOTUBE USING NON-EQUILIBRIUM MOLECULAR DYNAMICS

^{1*} Kasım Toprak, ² Yıldız Bayazıtöğlü

¹Izmir Institute of Technology, Mechanical Engineering Department, 35430 Urla, Turkey

²Rice University, Mechanical Engineering Houston, TX, USA

*Corresponding author e-mail: kasimtoprak@iyte.edu.tr

ABSTRACT

Core-shell nanostructured models are one of the ways of integrating Carbon NanoTubes (CNTs) into thermal applications. This study performed with Non-Equilibrium Molecular Dynamics (NEMD) simulations to analyze the thermal properties of coaxial nanostructure of Copper (Cu) core and Single-Walled Carbon Nanotube (SWCNT) shell. The thermal conductivity Cu-SWCNT as a function of length are examined. Since the pristine SWCNT has the highest thermal conductivity value, as SWCNT is filled with Cu, the thermal conductivity decreases.

Keywords: core-shell, molecular dynamics, copper-carbon nanotube, thermal conductivity

INTRODUCTION

There have been worthy innovations in microfabrication technology, micro-and nan-electromechanical systems, quantum structures, and computer technology. As these improvements evolve, newly design and manufactured devices must work under heavily loaded operations. In particular, the growing energy demand for advanced electrical energy systems such as high-efficient electronic components and supercomputers highlights the need to design advanced thermoelectric energy systems. These devices generate heat by the production of operation. When operated, these devices generate heat; therefore, overheating and heat transfer rates become critical problems. Thus, many studies have been done to solve these problems since overheating negatively affects material structures, mechanical and physical properties.

This continuing issue has become more important as the size of electronic devices reaches micro-and nano- sizes with the improvements in science and technology. At this scale, heat dissipation is a crucial problem for thermal systems because heat transfer impacts electrical and thermal performances, reliability, life, and physical properties. Design, optimization, and new materials are necessary to attain thermally conductive materials to keep the systems under the required working conditions and make cutting-edge nano-sized devices available for future applications [1].

Carbon-based low-dimensional materials have received great attention and exhibited promise in the field of nanotechnology owing to their exceptional mechanical, electric, optical, and thermal properties for integration in the next generation of energy-efficient nanoelectronic devices. Since CNT was discovered, it has been the focus of extensive research because of its unusual electrical, mechanical, and thermal properties. Among the carbon allotropes, differences in the scattering processes enable CNTs to have better thermal conductivity than graphite and diamond. CNT in a thermal application can play an important role in reducing oxidation, obtaining ultra-thin material, and enhancing thermal conductivity.

Apart from the fascinating properties of pristine CNT, the integration of CNT in thermoelectric applications is limited. Consequently, this issue has raised people's motivation. A remarkable amount of research efforts have been conducted on discovering, designing, and manufacturing other 1D structural analogs of CNT and their integration in electronic, thermal, and thermoelectric applications. In addition to its high thermal conductivity, the unique properties of CNT such as hollow space, high aspect ratio, and mechanical stiffness enable CNTs to integrate with various materials to enhance their application areas. Some researchers have chosen to manufacture CNT fill various including water, fullerene, and metals. Among these filling materials, copper is the most widely used thermoelectric material for electric and heat transfers. Copper has high electrical and thermal properties, low binding energy toward carbon, and is cost-effective. The core-shell metal-CNT nanowires have potential characteristics for thermal medical, power, and data storage applications [2].

Thermal properties are the main issue in our current work that we study with Cu-SWCNT core-shell hybrid nanowires. The thermal conductivity of the CNT filled with copper is obtained versus sample length and two edge directions using the nonequilibrium MD simulation.

SIMULATION DETAILS

We have modelled a core-shell structure that has SWCNT as a shell and Cu nanowire as a core with various lengths in order to predict the thermal conductivity of core-shell Cu-SWCNT. The heat transport is mostly by phonon in

semiconductors and semimetals, and the electron effect can be negligible. In contrast, the electron contribution dominates in metals. The current study calculates the phonon thermal conductivity of Cu-SWCNT in a longitudinal direction using MD simulations.

Two different approaches can be used to predict phonon thermal conductivity using molecular dynamics (MD) simulation: The Green-Kubo formula in equilibrium MD (EMD) or Fourier's law in nonequilibrium MD (NEMD) simulations. These two methods have been used for various materials with different dimensions in the literature. The Green-Kubo method is an equilibrium technique from the time decay of heat flux fluctuations based on the fluctuation-dissipation theorem. The NEMD instead calculates the thermal conductivity based on the resulting temperature gradients. Through this method, heat flux is created from two thermostatted reservoirs held at different temperatures and applied to a simulation cell along the direction of interest. From the imposed heat flux and steady-state temperature gradient from the result of the simulation, the thermal conductivity is calculated from Fourier's law. The NEMD method was used in this study to predict the thermal conductivity of a SWCNT filled with copper nanowire. The intra- and inter-atomic potentials influence the results. It pushes us to choose and apply them preciously. Tersoff and AIREBO potential are the two most common potentials that calculate the C-C interactions in the SWCNT. The embedded-atom method (EAM) is the one methods that has been used for metal and it successfully describes the Cu-Cu interaction in core copper. The Lennard-Jones interaction potential is used for core-shell. Two buffer parts are placed at the two edges of the hybrid nanowire. The heat flux is imposed using two thermostats to two edges after the buffer parts. During the simulations, the energy changes were monitored to calculate the heat flux. Using the heat flux and temperature gradient of the hybrid nanowire, the thermal conductivity is calculated from Fourier's law.

CONCLUSIONS

Through the NEMD simulation study, unfilled SWCNT and Cu-SWCNT structures are simulated. The pristine copper nanowire could not be simulated because it has an ultra-small diameter, and it did not keep its nanowire shape during the simulation. The thermal conductivity result for a pristine SWCNT closely agree with published literature. This is more so the case as structure length increases. The Cu-SWNCT results show similar behavior, however, the thermal conductivity results are exhibit lower than that pristine SWCNT. The length effect of the thermostatic region on the thermal conductivity has more effect than the buffer region, and thermal conductivity increases as structure length increases. When the copper fill ratio is examined, the thermal conductivity decreases as the fill ratio increases.

REFERENCES

- [1] Toprak K, Yilmaz A. Non-equilibrium Molecular Dynamics for Calculating the Thermal Conductivity of Graphene-Coated Aluminum. *Kocaeli J Sci Eng* 2020; 3:27–32. <https://doi.org/10.34088/kojose.663888>.
- [2] Toprak K, Bayazitoglu Y. Numerical modeling of a CNT-Cu coaxial nanowire in a vacuum to determine the thermal conductivity. *Int J Heat Mass Transf* 2013; 61:172–5. <https://doi.org/10.1016/j.ijheatmasstransfer.2013.01.082>.

DEVELOPMENT AND ANALYSIS OF A NOVEL GREENHOUSE ROOF FOR REDUCED COOLING LOAD IN HOT CLIMATES

^{1*} Yusuf Bicer, ¹ Muhammad Usman Sajid, ¹ Mohammed Al-Breiki

¹Division of Sustainable Development (DSD), College of Science and Engineering (CSE), Hamad Bin Khalifa University (HBKU), Qatar Foundation (QF), Education City, Doha, Qatar

*Corresponding author e-mail: ybicer@hbku.edu.qa

ABSTRACT

Excessive solar irradiance in hot and humid regions causes elevated temperature inside the agricultural greenhouses. The higher temperatures inside the greenhouses can damage plants, and effective cooling is required for optimal growth of the crop. A novel sun-tracking roof for the greenhouse is proposed in this study, which incorporates hot mirrors, semi-transparent crystalline silicon (c-Si) photovoltaics, and Indium Gallium Arsenide (InGaAs) solar photovoltaics for optimal spectra management and power production. The spectra management results in reducing cooling load inside the greenhouse, and power generated from solar panels can be used to operate the vapor compression cooling system. The visible spectrum (400nm – 750nm) of sunlight, which plants utilize during photosynthesis, transmits through the hot mirrors inside the greenhouse while solar radiations having a wavelength greater than 750 nm are reflected to InGaAs solar photovoltaics for power generation. The proposed greenhouse roof is capable of about 33% reduction in the cooling load compared to the conventional greenhouse during the summer season for a set greenhouse temperature of 28°C. The solar panels installed on the novel roof will provide about 51% of the total energy required for cooling the greenhouse.

Keywords: Agriculture, Hot mirrors, Spectrum selection, Solar Panels

INTRODUCTION

Food security and agriculture production is threatened by urbanization, salinization, desertification, and degradation of the environment by humans. Greenhouses are being proved to be an effective technique even in rough environmental conditions. The temperature has a significant impact on plant growth, and it is maximum at the optimum temperature, which may vary from plant to plant. The plants use some portion of the visible spectrum of sunlight during photosynthesis. The remaining portion of the solar spectrum leads to an increase in the temperature of the greenhouse. In hot arid areas, where solar irradiance is available in abundance, this phenomenon results in significantly higher temperatures inside the greenhouses and thus higher cooling loads.

Chavan et al. [1] applied smart glass film to a high-tech greenhouse. The smart glass film was able to block a significant portion of UV and infrared radiation. The application of film resulted in 19% reduction in photosynthetically active radiations. Mamouri et al. [2] theoretically investigated the reduction in the cooling load of a greenhouse by employing polymer hybrid metamaterials. The results revealed 25% reduction in cooling load with the usage of this material. Sajid and Bicer [3] proposed a novel integrated system for self-sustaining greenhouse. The spectrum selective nanofluid flows through the greenhouse roof, absorbing solar radiation in the infrared region. The nanofluid has higher transmittance in the visible spectrum and reduced the cooling load by about 26%. Alinejad et al. [4] integrated an adjustable photovoltaic blind system to a greenhouse. The system covered 19.2% of the roof and was able to generate 42.7 kWh/m² annually. Excessive shading or illumination is the drawback of that system. Ravishankar et al. [5] integrated semi-transparent organic cells on the greenhouse structure. The proposed greenhouse showed lower energy consumption than the conventional greenhouse. The main differences of the proposed design against the existing literature can be summarized as follows:

Existing systems provide partial shading using semi-transparent PV and do not utilize unwanted spectrum, which reduces system efficiency, while the proposed design uses unwanted spectrum for power generation. In existing systems, the semi-transparent PV may get overheated. In contrast, semi-transparent PV will not get overheated in the proposed method as PV will be near the greenhouse roof, which is at a lower temperature with active cooling. The existing systems do not use sun-tracking to reduce the greenhouse radiation input, while the proposed design uses sun-tracking to enhance power generation and optimal spectra management to reduce cooling load without compromising photosynthesis efficiency.

MATERIALS AND METHODS

This study proposes to permit only the needed portion of the solar spectrum into the greenhouse by a distinct technique of combining dielectric mirrors for spectrum splitting with semi-transparent c-Si and InGaAs photovoltaics, as illustrated in Figure 1. The cooling load of the greenhouse was computed using EQ (1)

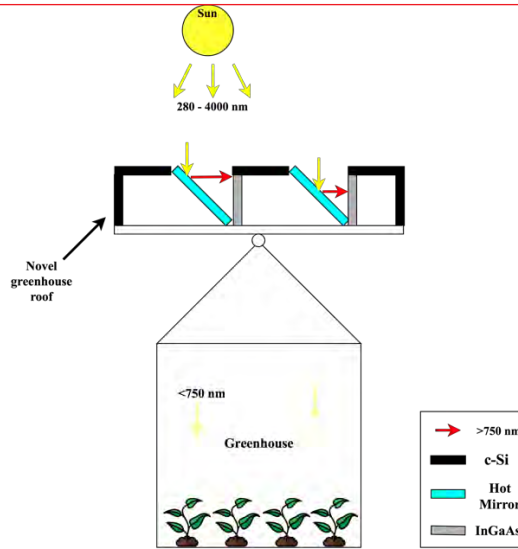


Figure 12: Schematic representation of greenhouse with novel roof design

$$\dot{Q}_{cooling} = \dot{Q}_{net,rad} + \dot{Q}_{cover} + \dot{Q}_{crop} + \dot{Q}_{reflected} + \dot{Q}_{ventilation} \quad (1)$$

The $\dot{Q}_{net,rad}$ can be calculated using Eq (2).

$$\dot{Q}_{net,rad} = \left(A_{floor} \left(\alpha_f I_T + \varepsilon_f \sigma (T_{sky}^4 - T_s^4) \right) \right) + \left(A_{plants} \left(\alpha_p I_T + \varepsilon_p \sigma (T_{sky}^4 - T_s^4) \right) \right) \quad (2)$$

where α_f is absorptivity of the floor, ε_f is the emissivity of floor, A_{floor} is the concrete floor area of greenhouse, α_p is absorptivity of plants, ε_p is the emissivity of plants, σ is Stefan Boltzmann constant ($\sigma = 5.67 \times 10^{-8} W/m^2 K^4$), T_s is surface temperature. The crop transpiration is given by Eq (3).

$$\dot{Q}_{crop} = A_{floor} \times L_H \times \left(\frac{a I_i}{L_H} + \frac{h_t (p_{sat,T_i} - p_{vp,T_i})}{L_H \psi_{psy}} \right) \quad (3)$$

where L_H is the latent heat of vaporization of water, ψ_{psy} is psychrometric constant, p_{sat,T_i} is saturation pressure at temperature T_i , p_{vp,T_i} is vapor pressure at temperature T_i . The output power from the solar panels is given by Eq (4).

$$\dot{W}_{out} = \dot{W}_{max} \frac{I_i}{I_{ref}} (1 - \xi (T_{cell} - 25)) \quad (4)$$

where \dot{W}_{max} is rated power of PV panel, I_{ref} is solar irradiance at which \dot{W}_{max} occurred, ξ is the power temperature coefficient. The SMARTS software developed by NREL was used to find the spectral irradiance being incident on wall and roof of the designed greenhouse. The Engineering Equation Solver (EES) software was used to solve equations during analysis.

CONCLUSIONS

In the present study, a novel roof design is proposed for greenhouses that incorporates hot mirrors, semi-transparent crystalline silicon cells, and InGaAs PV panels. The visible spectrum of sunlight was transmitted through the hot mirrors, while the infrared spectrum is reflected and incident on the InGaAs PV panels. The roof has a solar tracking system, which enables direct sunlight entrance to the greenhouse and maximizes the spectrum splitting and electricity production from PV panels. For similar conditions, the proposed greenhouse showed lower temperature than the conventional greenhouse. The proposed greenhouse roof is capable of about 33% reduction in the cooling load compared to the conventional greenhouse during the summer season for a set greenhouse temperature of 28°C. The proposed greenhouse can provide an average daily electrical energy of 2.11 kWh.

REFERENCES

- [1] Chavan SG, Maier C, Alagoz Y, et al. Light-limited photosynthesis under energy-saving film decreases eggplant yield. *Food Energy Secur*, 9. Epub ahead of print 2020. DOI: 10.1002/fes3.245.
- [2] Mamouri SJ, Tan X, Klausner JF, et al. Performance of an integrated greenhouse equipped with Light-Splitting material and an HDH desalination unit. *Energy Convers Manag X*; 7. Epub ahead of print 2020. DOI: 10.1016/j.ecmx.2020.100045.
- [3] Sajid MU, Bicer Y. Performance Assessment of Spectrum Selective Nanofluid-Based Cooling for a Self-Sustaining Greenhouse. *Energy Technol* 2021; 9: 2000875.
- [4] Alinejad T, Yaghoubi M, Vadiee A. Thermo-environmental assessment of an integrated greenhouse with an adjustable solar photovoltaic blind system. *Renew Energy* 2020; 156: 1–13.
- [5] Ravishankar E, Booth RE, Saravitz C, et al. Achieving Net Zero Energy Greenhouses by Integrating Semitransparent Organic Solar Cells. *Joule* 2020; 4: 490–506.

DEVELOPMENT AND VALIDATION OF A DYNAMIC THERMAL MODEL FOR A WATER WALL INTEGRATED INDOOR

^{1*} Nilay Altunacar, ¹ İbrahim Şener, ² Yonca Yaman, ³ Berkay Budakoğlu, ³ Erdem Topkara, ⁴ Ayça Esmer, ¹ Mehmet Akif Ezan, ² Ayça Tokuş, ³ Gülden Köktürk, ⁴ İrem Deniz

¹Dokuz Eylül University, Faculty of Engineering, Department of Mechanical Engineering, Tinaztepe Campus, 35190, Buca, Izmir, Turkey

²Dokuz Eylül University, Faculty of Architecture, Department of Architecture, Tinaztepe Campus, 35190, Buca, Izmir, Turkey

³Dokuz Eylül University, Faculty of Engineering, Department of Electrical-Electronics Engineering, Tinaztepe Campus, 35190, Buca, Izmir, Turkey

⁴Manisa Celal Bayar University, Faculty of Engineering, Department of Bioengineering, Şehit Prof. Dr. İlhan Varank Campus, 45040, Muradiye, Manisa, Turkey

*Corresponding author e-mail: nilay.altunacar@ogr.deu.edu.tr

ABSTRACT

Algae, which are photosynthetic creatures, are an important method of energy production, and recently there has been a growing interest in benefiting from the benefits of algae in an urban environment. The use of building facades as a microalgae growing area allows to form an insulating layer for energy conservation and act as a biomass reservoir that can be converted into active bio-energy for building use. A photobioreactor (PBR) resembles a double-layer window with water and algae mixture inside. In this study, a water wall model was validated as a preliminary study for the thermal analysis of an indoor environment with a PBR integrated on one of its façades. The results were compared with the numerical and experimental results of the reference study. Parametric analyzes were then carried out to understand the thermal effects of the implementation of opaque wall material (concrete) instead of water wall as facade element or using air instead of water on the thermal behavior of the indoor environment.

Keywords: Algae Window, Indoor Thermal Modelling, Photobioreactor, Water Wall

INTRODUCTION

Different types of mathematical modelling approaches are used to understand the dynamic variations inside the indoor, and considering the way in which the local temperature effect of indoor air is taken into account, modelling approaches are grouped into three as (i) lumped approach, (ii) two and three-dimensional thermal modelling, and (iii) computational fluid dynamics (CFD). The lumped approach (lumped model) considers a single temperature representative of the indoor air, completely ignoring local variations in the indoor air. Unlike the lumped approach, in 2D and 3D thermal modelling approaches, indoor air is discretized into a finite number of control volumes, and spatial temperature distributions can be obtained. Here, local velocity values are obtained through simplified relations in flow analysis. In the CFD method, in addition to the energy equation, the continuity and momentum equations are solved iteratively for the entire solution region, and the indoor temperature, velocity, and pressure distributions can be determined in detail.

MATERIALS AND METHODS

As briefly outlined in the previous section, different models exist for modelling transient indoor heat transfer behaviour in the literature. Still, studies on mathematical modelling of the water wall or PBR integration are limited. As a result of an extensive literature review, it was decided to create a mathematical model of the indoor with integrated water wall. The study of Wu and Lei [1] was reproduced to validate the developed model. The schematic representation of the reduced mathematical model discussed in the study by Wu and Lei [1] is given in Fig. 1. In the schematic representation, the heat transfer mechanisms on each surface are symbolically indicated. The red arrows indicate the radiative heat transfer on the surfaces. The blue arrows represent the convection heat transfer on the surfaces. Pink lines indicate heat conduction in solid materials. The progress of solar radiation acting on the perspex surface from the external environment through the layers is illustrated with a yellow line. The explicit method was used in the temporal discretization of the energy equation, and central differencing was used in the spatial discretization. The accuracy and reliability of the explicit method hardly depend on the mesh number and time step size; that is, preliminary analyzes were carried out to assess the effect of the mesh number and time step size.

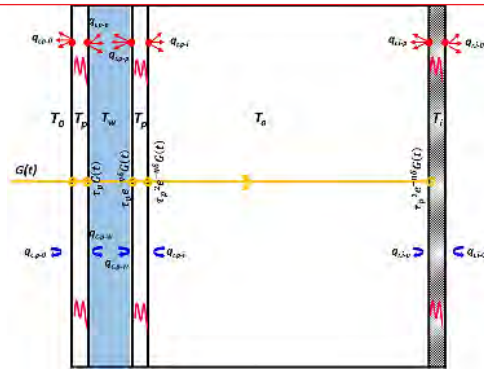


Fig. 1. Reduced mathematical model of indoor with water wall

In Figure 2, the comparisons of water and indoor air temperatures obtained from the current code and retrieved from the reference study [1] are provided. The current predictions show similar trends as in the numerical and experimental findings of the reference work. Further Parametric analyses were carried out to evaluate the thermal effects of using opaque wall material (concrete) instead of a water wall as a facade element or using air instead of water on the indoor. The results obtained with different facade structures are given in Fig. 3.

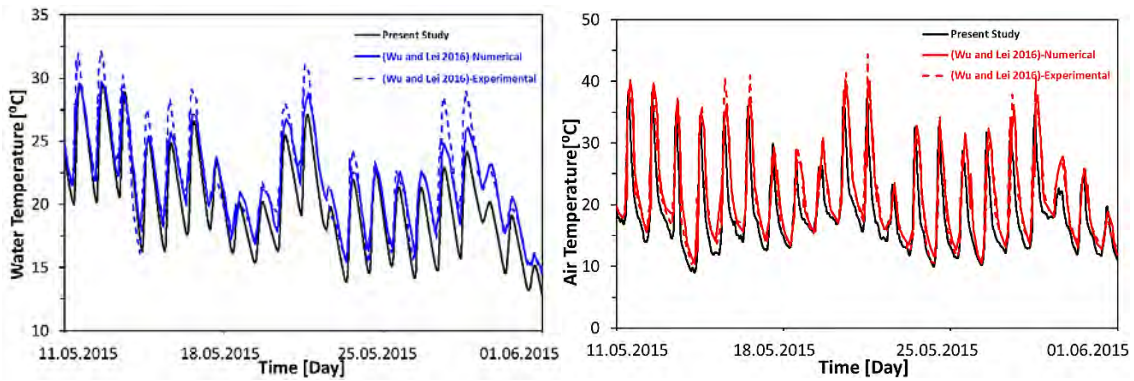


Fig. 2. Comparison of water and air temperatures between 11.05.2015-01.06.2015 [1]

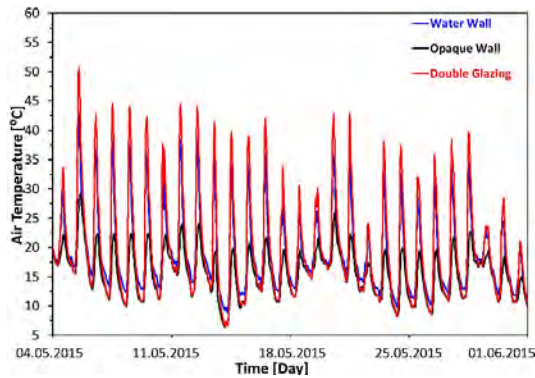


Fig. 3. Results obtained with different facade structures

CONCLUSIONS

It can be said that the numerical results obtained in the present study are generally compatible with the numerical and experimental results of the reference study. The highest indoor air temperatures were obtained with the facade structure using air instead of water (double glazing), while the lowest temperatures are obtained with the use of opaque wall material. The mean indoor air temperatures achieved with opaque wall, water wall and double glazing are 15.5934 °C, 19.0486 °C and 19.7861 °C, respectively.

REFERENCES

[1] Wu T, Lei C. Thermal modelling and experimental validation of a semi-transparent water wall system for Sydney climate. Solar Energy. 2016 ;136, 533-546

ANALYSIS OF OPTIMUM FLOW RATE OF A PHOTOVOLTAIC THERMAL SYSTEM (PVT) INTEGRATED WITH PHASE CHANGE MATERIALS (PCM)

^{1*} Canan Kandilli*, ² Burak Mertoglu

¹Usak University, Department of Mechanical Engineering, 1 Eylül Kampusu, Usak, TURKEY

² Usak University, Department of Mechanical Engineering, 1 Eylül Kampusu, Usak, TURKEY

*Corresponding author e-mail: canan.kandilli@usak.edu.tr

ABSTRACT

Photovoltaic thermal (PVT) systems could be defined as solar cogeneration systems, and it is noteworthy in energy supply in terms of both electrical and thermal energy with a single panel. Within the scope of Nearly Zero Energy Buildings (nZEB), there is a remarkable potential of PVT systems based on phase change materials (PCMs) in supplying both electrical and thermal energy demand for both facade and roofing applications in buildings. In the PVT system, the phase change materials (PCMs) could be used to provide thermal energy after the sun set and to manage the heat load on PV. In the present study, a PCM based PVT system was modeled, established and tested under real meteorological conditions. The experimental results of ambient, inlet and outlet temperatures and solar radiation were presented. Temperature distribution of the system tested was analyzed. The system was modeled by ANSYS FLUENT. The model was verified by the real data. Optimum flow rate was investigated for the system. Maximum outlet temperature was achieved at 19 l/h flow rate. It was concluded that flow rates of 15-21 l/h could be used in studies as the ideal flow rate for PVT-PCM system with paraffin.

Keywords: Photovoltaic thermal systems, Phase Change Materials, ANSYS Modelling, Optimization, Flow rate

INTRODUCTION

PVT systems are used to meet the thermal energy and to prevent the decrease in the electrical efficiency of PV systems. Within the scope of PVT-PCM systems, building integrated PV (BIPV) studies, there is a great potential in supplying energy demand for both facade and roofing applications in buildings. Although there are many numerical and experimental researches on PVT systems in the literature [1-10], there is no study on the modeling of these systems with ANSYS and the optimum flow rate, which is one of the most important operating parameters based on real experimental data for PCM based PVT system. Flow rate is one of the most important operation parameter at the stage of transferring the heat stored in PCM to the working fluid effectively. Power and efficiency obtained from PVT systems under real conditions are directly dependent on operating parameters such as flow rate, as well as many uncontrollable meteorological parameters. The main purpose of using these systems is to increase the power obtained from PVTs and to obtain higher outlet fluid temperatures. Under certain conditions, obtaining the highest output water temperature gives the thermal energy maximum to be obtained from the PVT system. The optimization of the flow rate based on this because the outlet water temperature is a measurable parameter, it will provide a great convenience in practice. In this study, for the first time in the literature, optimum flow rate for maximum outlet fluid temperatures for PVT systems with PCM is investigated.

SYSTEM DESCRIPTION

In the present study, it was aimed to model the PVT system integrated with paraffin as PCM and investigate the optimum flow rate. Paraffin is a petroleum product. It is an organic PCM that is frequently used in PVT systems. Paraffin stands out among other PCMs, with its average heat storage density, absence of phase separation, the amount of latent heat in the desired range, and its variable melting and solidification temperature.

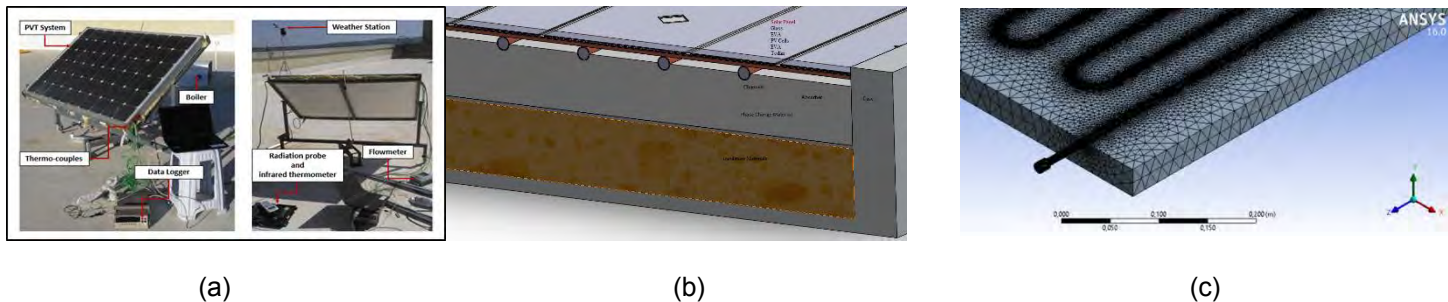


Fig.1. (a) PVT test system established, (b) Placement of thermocouples on the copper plate of PVT, (c) Meshing PVT system

In Fig. 1a, the PVT-PCM test system installed on the roof of Uşak University Engineering Faculty is shown. Kandilli has demonstrated the energy, exergy and economic performances of different PCM and heat storage materials in previous study [11]. In the system, water was chosen as the working fluid. The outlet water temperature values

obtained in different meteorological conditions were used in the verification phase of the designed model. The properties of the device employed in the experiments and the materials and components have been explained before [11,12]. In the PVT-PCM system discussed in the study, the layers from top to bottom are listed as follows: Glass, EVA, solar cell, EVA, copper coil pipe, copper plate, PCM, plastic backing, insulation material, and casing. In this study, paraffin wax commonly used as PCM in the literature has been chose for PVT system.

CONCLUSIONS

The experimentally tested PVT-PCM system was modeled with ANSYS Fluent 16 program in the present study. Design and operating parameters were considered during the analyses. The accuracy of the established model has been demonstrated by statistical comparison of the experimental and predicted results. After the validation of the model, the optimum value of the flow rate, one of the operating parameters that have a great impact on heat transfer, has been investigated.

In Fig.2, temperature distributions of the PVT-PCM at different flow rates during the day have been given. Figures a, b, c and d show the PCM temperature distribution obtained from the measurements taken during the day at flow rates of 12,13,14 and17 l/h. As can be seen from the distribution graphs, the PCM temperatures obtained increase with increasing flow rates.

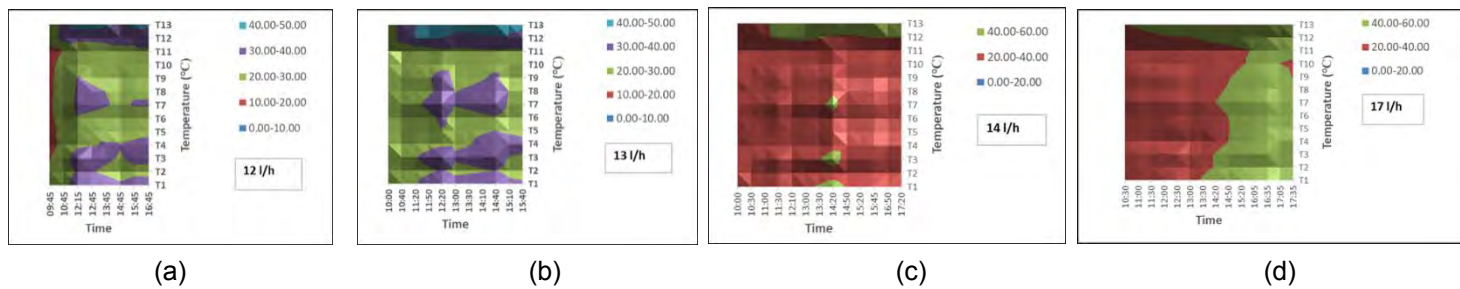


Fig.2. Temperature distributions of the PVT-PCM at different flow rates during the day

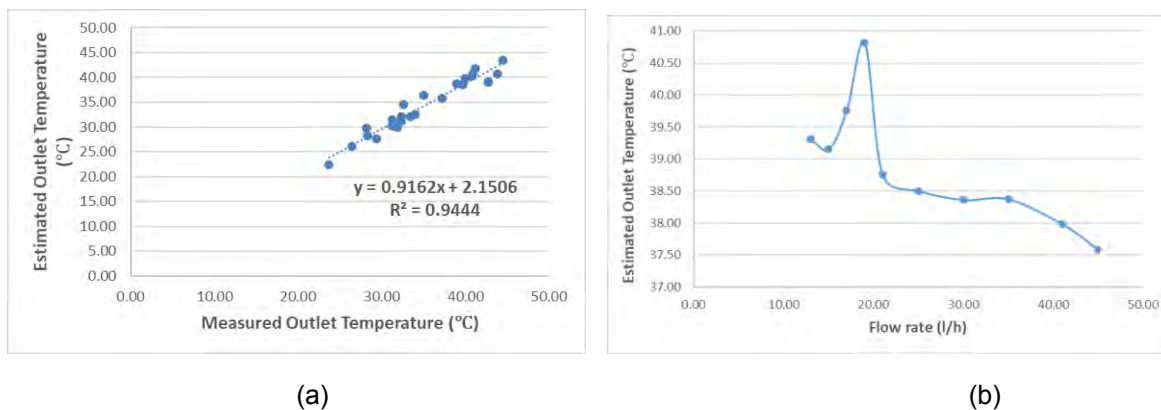


Fig.3. (a) Model validation based on outlet temperatures, (b) Variation of the estimated outlet temperature values at different flow rate values

In Fig.3, model validation based on outlet temperatures was presented and variation of the estimated outlet temperature values at different flow rate was plotted. Flow rate values were selected from 13 to 45 l/h, and the highest outlet water temperature was achieved for 19 l/h. After verifying the model, it was investigated the optimum flow rate for the PVT-PCM system. Ultimately, the aim in pvt systems is to obtain higher temperature outlet water. For this reason, in determining the optimum flow rate, the strategy of reaching maximum leaving water temperatures at constant inlet water temperature and constant solar radiation values was followed. For paraffin, the fact that the fluid is a little faster increases the heat transfer due to the increased molecular movement, while the heat transfer due to the shorter duration of the fluid in the system at higher speeds has decreased. Flow rates of 15-21 l/h can be used in studies as the ideal flow rate for paraffin.

REFERENCES

- [1] Kazemian A, Parcheforosh A, Salari A, Ma T. Optimization of a novel photovoltaic thermal module in series with a solar collector using Taguchi based grey relational analysis. *Sol Energy*, 2021; 215: 492-507.
- [2] Nižetić S, Jurčević M, Čoko D, Arıci M, HoangAT. Implementation of phase change materials for thermal regulation of photovoltaic thermal systems: Comprehensive analysis of design approaches. *Energy*, 2021; 228:120546.

- [3] Shahsavari A, Jha P, Arici M, Kefayati G. A comparative experimental investigation of energetic and exergetic performances of water/magnetite nanofluid-based photovoltaic/thermal system equipped with finned and unfinned collectors. *Energy*, 2021; 220:119714.
- [4] Babu C, Ponnambalam P. Economic analysis of hybrid Photovoltaic Thermal Configurations: A comparative study. *Sustain. Energy Technol*, 2021; 43: 100932.
- [5] Maghrabie HM, Elsaid K, Sayed ET, Abdelkareem MA, Wilberforce T, Olabi AG. Building-integrated photovoltaic/thermal (BIPVT) systems: Applications and challenges. *Sustain. Energy Technol*, 2021; 45:101151.
- [6] Antony A, Wang YD, Roskilly AP. A Detailed Optimisation of Solar Photovoltaic/Thermal Systems and its Application. *Energy Procedia*, 2019; 158: 1141-1148.
- [7] Ali AHH. Design optimization of staggered plates' channel heated by radiation heat flux based on the convective heat transfer and fluid flow for hybrid Photovoltaic/Thermal system. *Sustain. Energy Technol*, 2017;24: 55-70.
- [8] Belussi L, Barozzi B, Bellazzi A, et al. A review of performance of zero energy buildings and energy efficiency solutions. *J. Build. Eng.*, Volume 25, 2019, 100772.
- [9] Zhou Y, Zheng S, Zhang G. Multivariable optimisation of a new PCMs integrated hybrid renewable system with active cooling and hybrid ventilations. *J. Build. Eng.*, 2019; 26: 100845.
- [10] Misha S, Abdullah AL, Tamaldin N, Rosli M.A.M., Sachit FA. Simulation CFD and experimental investigation of PVT water system under natural Malaysian weather conditions. *Energy Rep.*, 2020; 6:28-44.
- [11] Kandilli C. Energy, exergy, and economical analyses of a photovoltaic thermal system integrated with the natural zeolites for heat management. *Int J Energy Res.* 2019; 43: 4670– 4685.
- [12] Kandilli C, Mertoğlu B, Optimisation design and operation parameters of a photovoltaic thermal system integrated with natural zeolite. *Int. J. Hydromechatronics*, 2020; 3: 128 – 139.

EFFECTS OF DESIGN VARIABLES ON EXERGY AND ENVIRONMENTAL PARAMETERS OF COMMERCIAL TURBOFAN ENGINE

¹ Hakan Aygun, ² Mohammad Rauf Sheikhi, ³ Hakan Caliskan*

¹Department of Air Frame and Power-Plant, Firat University, Elazig, Turkey

² Faculty of Aeronautics and Astronautics, Eskisehir Technical University, Eskisehir, Turkey

³ Department of Mechanical Engineering, Faculty of Engineering, Usak University, Usak, Turkey

*Corresponding author e-mail hakan.caliskan@usak.edu.tr

ABSTRACT

Exergetic and environmental metrics of aircraft engines are topics of paramount importance for studies examining the effects of fuel consumption & combustion on environment. Therefore, it is important to quantify these parameters so as to predict the extent of environmental impact originated from aircraft engines such as turbofans. In this study, effects of turbine inlet temperature (TIT) varying between 1450-1550 K and high pressure compressor pressure ratio (HPC PR) varying between 7.5-8.5 on several thermodynamics metrics of the turbofan engine producing thrust of 110 kN are parametrically analyzed for thirty-six cases. According to the exergetic evaluations, exergy efficiency of the turbofan engine varies between 33.46% and 36.78%, whereas the specific irreversibility production (*SIP*) of the engine varies between 0.1676 MW/kN and 0.1752 MW/kN due to variation of TIT and HPC PR.

Keywords: Improved exergy, irreversibility, sustainable efficiency factor, turbofan, energy research

INTRODUCTION

Aircraft emissions related to aviation activities have increased day by day. Compared with 2018, the number of passengers increased by 3.6% in 2019 [1]. In this regard, CO₂ emissions induced from flights were accounted for 915 million tonnes in 2019 [2]. Thermodynamic approaches should be properly employed in this sector to mitigate energy loss thereby causing environmental damage. Owing to the importance of energy-saving, many researchers have focused on increasing the efficiency of cycles. Therefore, assessments of aircraft propulsion system are necessary with exergetic and environmental metrics. In this study, effects of TIT and HPC PR on exergetic and environmental indicators are investigated. These results are compared with that of baseline operating point. For this aim, exergy approach involving many metrics is implemented to turbofan engine. The main motivations of this study are (i) to compute exergetic parameters for turbofan engine and its main components for thirty-six cases. (ii) to calculate several environmental parameters for whole turbofan engine for thirty-six cases and (iii) to apply new index (specific irreversibility production) to turbofan engine for thirty-six cases.

BACKGROUND OF EXERGY APPROACH

Exergy analysis provides the required information about system enhancement by considering the quality and quantity of energy. Therefore, this approach have been commonly adopted by many industries for three decades. Exergy method incorporates several parameters such as exergy efficiency, exergetic improvement potential, improved exergy efficiency, exergetic sustainability index, etc. These metrics are associated with environmental indicators such as environmental effect factor and sustainable efficiency factor. Exergy efficiency (η_{ex}) is the ratio between product exergy ($\dot{E}x_{Pr}$) and fuel exergy ($\dot{E}x_F$) as follows:

$$\eta_{ex} = \dot{E}x_{Pr} / \dot{E}x_F \quad (1)$$

Exergetic improvement potential rate ($ExIP_k$) shows how much exergy destruction ($\dot{E}x_{D,k}$) could be recovered.

$$ExIP_k = (1 - \eta_{ex}) \dot{E}x_{D,k} \quad (2)$$

Improved exergy efficiency (ψ) shows how much increase in efficiency occurs if the determined $ExIP$ is achieved [3]:

$$\psi = \dot{E}x_{Pr} / (\dot{E}x_F - ExIP_k) \quad (3)$$

As a new parameter, specific irreversibility production (*SIP*) is firstly proposed here. It measures how much exergy destruction occurs per unit thrust. It is presented as follows:

$$SIP_{engine} = (\sum \dot{E}x_D) / \tau_{engine} \quad (4)$$

CONCLUSIONS

In the present study, turbofan engine is investigated with exergetic approach with several important metrics. Exergy efficiency of components except Fan and LPT is affected from HPC PR and TIT. According to Fig.1a, the lowest exergy efficiency varying between 85.85% and 87.96% belongs to the combustor. Its baseline value is 87.11%. In Fig.1b, exergetic improvement potential of the combustor has the highest value changing between 1.12 MW and 1.72 MW. Its baseline value is 1.35 MW. On the other hand, improved exergy efficiency of the combustor is calculated between 87.6% and 89.25%. Its baseline value is 88.59%. Finally, as seen in Fig.2b, the highest exergy efficiency of turbofan is calculated as 36.94% at 8.3 HPC PR and 1550 K. However the lowest *SIP* index is computed as 0.1676 MW/kN at 8.5 HPC PR and 1550 K. Considering these findings, to detect optimum design values giving minimum

environmental impact, all of exergetic parameters should be considered together. As a next study, optimization of exergy and environmental parameters could be performed using different optimization methods.

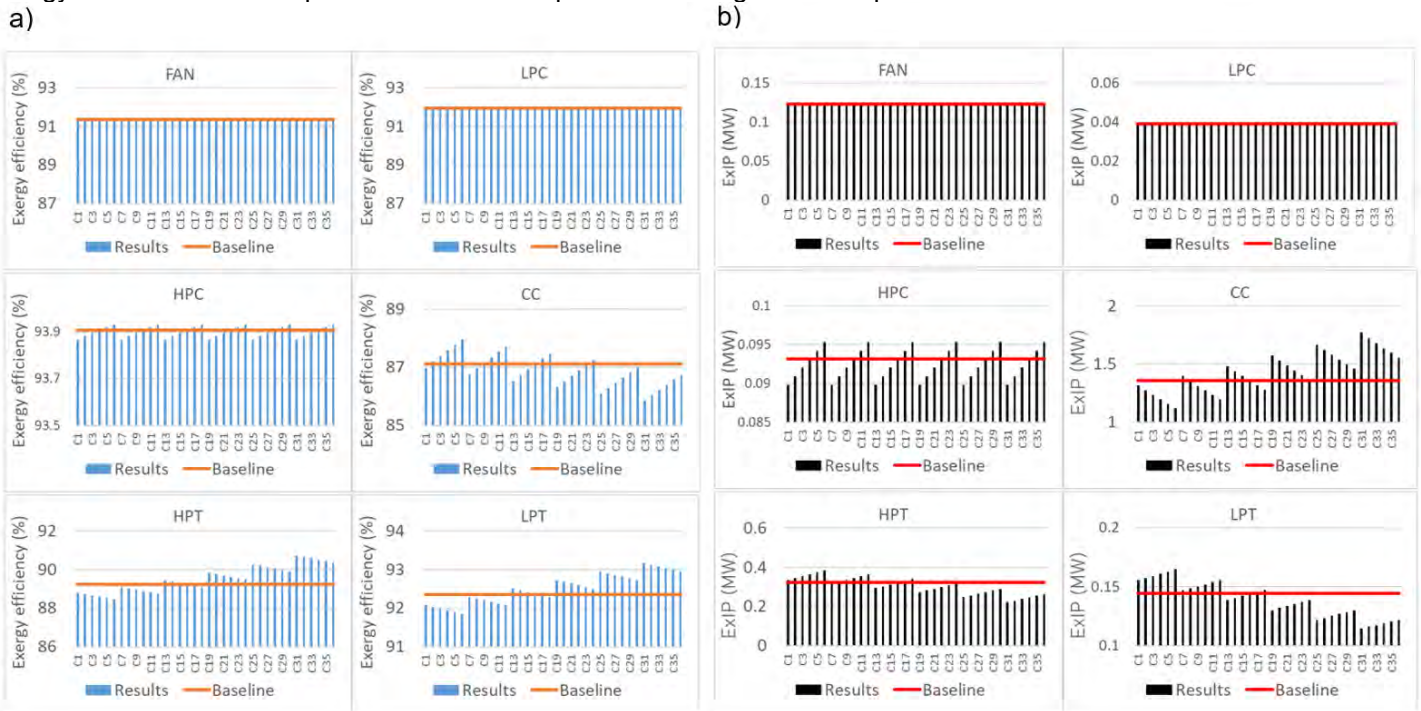


Fig. 1. Exergy efficiency and exergetic improvement potential rate of main components of turbofan engine.

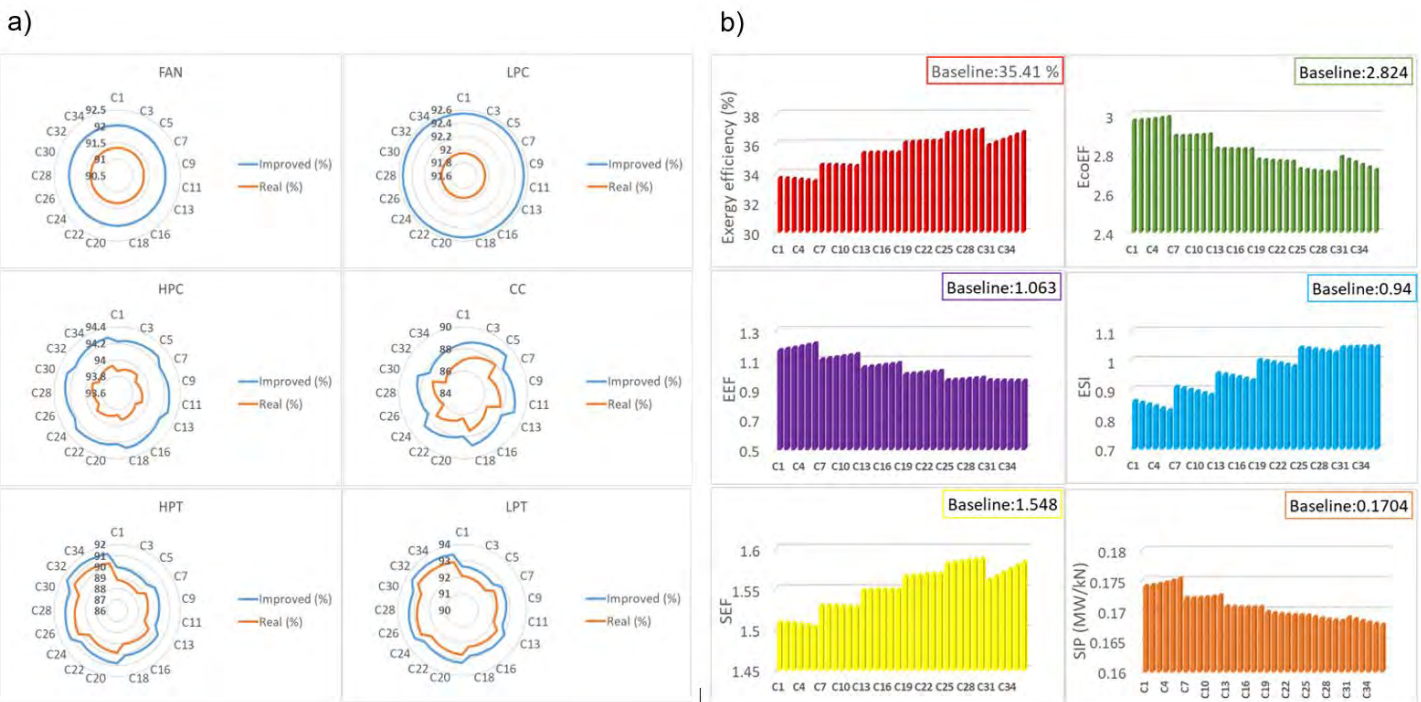


Fig. 2. Improved exergy efficiency of main components and environmental parameters of whole turbofan engine.

REFERENCES

[1] <https://www.icao.int/annual-report-2019/Pages/the-world-of-air-transport-in-2019.aspx> (Accessed 21 June 2021)
 [2] <https://www.ataq.org/facts-figures.html> (Accessed 12 June 2021)
 [3] Ballı, O., 2017. Exergy modeling for evaluating sustainability level of a high by-pass turbofan engine used on commercial aircrafts. Applied Thermal Engineering 123, 138-155

ASYMMETRIC AND SYMMETRIC COIN CELL SUPERCAPACITORS BY DEPOSITION OF GRAPHENE FOR ENERGY STORAGE APPLICATIONS

^{1*} Onder Yargi, ² Murat Ozmen, ² Sude Buyuk Pehlivan, ³ Ali Gelir

¹Department of Physics, Yildiz Technical University, Esenler, 34210, Istanbul, Turkey

² Department of Bioengineering, Yildiz Technical University, Esenler, 34210, Istanbul, Turkey

³ Department of Physics, Istanbul Technical University, Maslak, 34469, Istanbul, Turkey Affiliation

*Corresponding author e-mail: oyargi@yildiz.edu.tr

ABSTRACT

Graphene based supercapacitors (SC) with Polyacrylamide (PAAM) hydrogel separator is designed and assembled in CR2032 coin cell. Two different symmetrical and one assymetric SC cells are evaluated using graphene based electrodes, nickel foil current collector and ionic liquid bis (trifluoromethanesulfonyl) imide (Bisimide); TFMS electrolyte. While the first symmetric coincell is produced by deposition of graphene on porous nickel foam (NiF); (G-Ni/G-Ni), the second symmetric one is produced by deposition of graphene on copper foam (G-Cu/G-Cu). Then after, a third one is prepared in an asymmetrical structure as the combination of Cu and Ni foam electrodes (G-Ni/G-Cu), that are, graphene is deposited on nickel and copper electrodes by cyclic voltammetry (CV). The best electrochemical performance is found for the SC (G-Ni/G-Ni) in terms of higher energy, power, and current densities applied by galvanostatic charge-discharge (GCD) and CV. Specific capacitances of G-Ni/G-Ni, G-Ni/G-Cu coincells are found as 39 F/g, 59 F/g, at 1mA respectively and for the G-Cu/G-Cu is 27 F/g, at 0.1 mA. Capacitance retention of both two symmetric and assymetric SCs does not change and reveals excellent performance of 100 % up to 5000 cycles indicating long term durability in SCs applications.

Keywords: Coincell, Copper, Graphene, Supercapacitor, PAAM Hydrogel, Nickel

INTRODUCTION

Nickel foam (NiF) like NiO nanosheets have been of great interest for the current conductors because of their availability, cost-effectiveness, and corrosion resistance [1-5]. Approaches were presented to produce binder-free SC electrodes through depositing porous graphene networks into pores of NiF [1, 2]. Because graphene has improved conductivity due to the short diffusion distance of ions from porous graphene to NiF revealing improved stability and energy capacity, PG/NiF electrodes are used in SCs applications [6]. Herein, three different CR2032 coincell SCs were developed based on deposition of graphene on nickel and copper foam as two symmetric (G-Ni/G-Ni), (G-Cu/G-Cu) and one asymmetric (G-Ni/G-Cu) with TFMS as a redoxactive electrolyte. To achieve homogenous electrochemical deposition of graphene on porous NiF and CuF electrodes, LiClO₄ electrolyte was preferred. A nano porous Polyacrylamide (PAAM) hydrogel which allows high ion transfer between two electrodes was synthesized as a separator to prevent the contact of cathode and anode electrodes and allow ion passage. Finally, the electrodes, electrolytes, and separator obtained were successfully assembled to produce three coincell SCs. Cyclic voltammetry (CV), and galvanostatic charge–discharge cycling (GCD) measurements were used to investigate the redox couple, capacitive properties and cycling stability of the electroactive materials in an alkaline electrolyte. As will be seen below, capacitive retention revealed excellent cyclic stability for both symmetrical and asymmetrical SCs.

MATERIALS AND METHODS

Free radical crosslinking copolymerization was carried out to synthesize the PAAM hydrogel separator. 0.16 g APS and 0.50 mL TEMED were dissolved in 20 mL of distilled water to prepare APS and TEMED stock solutions. The initial monomer concentration was set to 30 % w/w. Certain amounts of AAm and BAAM were dissolved in 8 mL distilled water and 1 mL TEMED stock solution was added. After nitrogen gas exposure to the solution for 20 min, the APS stock solution (1 mL) was added. Finally, 1.5 mL parts of this solution were transferred to teflon molds, and kept at room temperature for 24h. Afterwards, the as prepared hydrogel samples were removed from the molds and used in further SC preparation steps. Two electrode system was used to deposit the graphene on to nickel and copper foams used as base has surface density of 350 g/m², thickness of 0.08 mm, purity of 99.9 %, and porosity of 70–80%. The working electrodes were chosen as nickel foam (NiF) and copper foam (CuF), and Pt was used as counter electrode, which has the same size with the NiF and CuF electrodes. NiF and CuF were subjected to ultrasonication and then washed in 37% HCl solution for 5 minutes to remove surface oxide films and then after dried in the vacuum oven at 100 °C. The deposition was performed in a suspension of the mixture of 1 M LiClO₄ and graphene. The suspension in deionized water was mixed by magnetic stirrer for 30 min and then cyclic voltammetry technique was applied for the deposition of graphene on the foams for 1000 cycle. The potential range and the scan rate of voltammetry was adjusted as (0.0-1.5 V) and 200 mV/s, respectively. Active graphane material was measured as 1.5 mg after 1000 cycle. All pieces required for SC were placed in the order of bottom cover, spacer, current collector (nickel foil), electrode, PAAM separator, electrode, current collector, spacer, and top cover. The ionic liquid bis (trifluoromethanesulfonyl) imide (TFMS) was

added to all pieces in SC. The SC prepared as CR2032 coin cell was clamped at stable force to provide adequate pressure for contact.

Table 1: Specific Capacitance, Energy and Power density values of G-Cu/G-Cu, G-Ni/G-Ni and G-Cu/G-Cu; SCs at different current densities of charge-discharge.

G-Cu/G-Cu				G-Ni/G-Ni				G-Ni/G-Cu											
Current Density	Specific Capacitance	Energy Density	Power Density	Specific Capacitance	Energy Density	Power Density	Specific Capacitance	Energy Density	Power Density										
I(mA/g)	C(F/g)	Wh/kg	kW/kg	C(F/g)	Wh/kg	kW/kg	C(F/g)	Wh/kg	kW/kg										
1	0.1	2	27.0	3	0.68	4	0.12	5	32.4	6	0.1	7	0.2	8	32.0	9	1.2	10	0.2
11	0.2	12	26.2	13	1.52	14	0.44	15	27.6	16	4.6	17	0.8	18	28.6	19	5.0	20	0.6
21	0.3	22	16.5	23	1.08	24	0.60	25	21.8	26	10.7	27	1.4	28	23.6	29	11	30	1.2
31	0.4	32	10.9	33	0.84	34	0.80	35	15.6	36	17.8	37	2.1	38	17.6	39	17.5	40	1.8
41	0.5	42	8.3	43	0.64	44	1.00	45	9.8	46	25.7	47	3.0	48	10.4	49	22.0	50	2.4
51	2.0	52	-	53	-	54	-	55	6.4	56	5.2	57	15.8	58	3.6	59	1.3	60	11.8
61	3.0	62	-	63	-	64	-	65	0.2	66	1.2	67	23.8	68	2.0	69	0.5	70	17.9
71	4.0	72	-	73	-	74	-	75	0.2	76	1.0	77	31.6	78	1.6	79	0.3	80	24.2
81	5.0	82	-	83	-	84	-	85	0.1	86	0.6	87	39.2	88	1.3	89	0.3	90	29.9

CONCLUSIONS

In this study, graphene in LiClO₄ on nickel and copper foams was deposited electrochemically. In addition, a flexible and nano structured PAAM hydrogel has been synthesized, which allows a significant ion transfer. The conclusions obtained from this study can be summarized as follows:

- I. From the electrodes prepared by electrochemical method, three different Cr2032 coin cells SCs were designed and evaluated.
- II. The capacitance, energy and power densities obtained have been found to be compatible with the literature.
- III. Capacitive retention has exhibited excellent results in two symmetrical and asymmetrical coin cells, and no loss has been observed up to 5000 charge-discharge cycles.
- IV. While it is not possible to reach high currents for copper-based SC, it is possible to operate up to 5 mA with a nickel-based SC.
- V. PAAM hydrogel separator and TFMS electrolyte have formed a very compatible structure. While nano porous PAAM hydrogel degrades in 6M KOH, it can be used for a long time without degradation in TFMS.

REFERENCES

- [1] M. Yu, W. Wang, C. Li, T. Zhai, X. Lu, Y. Tong, Scalable self-growth of Ni@NiO core-shell electrode with ultrahigh capacitance and super-long cyclic stability for supercapacitors, *NPG Asia Mater.* (2014). doi:10.1038/am.2014.78.
- [2] M. Huang, F. Li, J.Y. Ji, Y.X. Zhang, X.L. Zhao, X. Gao, Facile synthesis of single-crystalline NiO nanosheet arrays on Ni foam for high-performance supercapacitors, *CrystEngComm.* (2014). doi:10.1039/c3ce42335b.
- [3] M. Kundu, L. Liu, Binder-free electrodes consisting of porous NiO nanofibers directly electrospun on nickel foam for high-rate supercapacitors, *Mater. Lett.* 144 (2015) 114–118. doi:10.1016/j.matlet.2015.01.032.
- [4] H. Wang, Y. Liang, T. Mirfakhrai, Z. Chen, H.S. Casalongue, H. Dai, Advanced asymmetrical supercapacitors based on graphene hybrid materials, *Nano Res.* (2011). doi:10.1007/s12274-011-0129-6.
- [5] X. Xiong, D. Ding, D. Chen, G. Waller, Y. Bu, Z. Wang, M. Liu, Three-dimensional ultrathin Ni(OH)₂ nanosheets grown on nickel foam for high-performance supercapacitors, *Nano Energy.* (2015). doi:10.1016/j.nanoen.2014.10.029.
- [6] S. Yang, B. Deng, R. Ge, L. Zhang, H. Wang, Z. Zhang, W. Zhu, G. Wang, Electrodeposition of porous graphene networks on nickel foams as supercapacitor electrodes with high capacitance and remarkable cyclic stability, *Nanoscale Res. Lett.* 9 (2014) 1–11. doi:10.1186/1556-276X-9-672.

THERMO-ENVIRONMENTAL PERFORMANCE ASSESSMENTS OF A MEDIUM-SCALE AERO TURBOJET ENGINE

¹Halil Yalcin Akdeniz, ^{2,3}Ozgur Balli, ⁴Hakan Caliskan

¹Eskisehir Osmangazi University, Eskisehir Vocational School, Department of Mechanical, Industrial Zone Teknoloji Boulevard Antrepo Street No:1, Eskisehir, Turkey

²Aeronautical Engineer at 1st Air Maintenance Factory Directorate (1.HBFM), General Directorate of Military Factories (AFGM), Ministry of National Defence (MND), Eskisehir, Turkey

³Visiting Assoc.Prof.Dr. at Aviation Science and Technology, Graduate School of Natural and Applied Sciences, Eskisehir Osmangazi University, Batı Meselik Campus, Eskisehir, Turkey

⁴Usak University, Faculty of Engineering, Department of Mechanical Engineering, Usak, Turkey

*Corresponding author e-mail: halilyalcinakdeniz@gmail.com

ABSTRACT

In this study, the energetic and exergy-based thermo-environmental performance of a conventional (JP-8) fueled medium-scale turbojet engine is investigated. In the first stage, the specific power and specific thrust are found to be 147.810 kW/kg/s and 0.549 kN/kg/s while the specific fuel consumption is obtained to be 0.128 g/kN.s. After the combustion process, the percentage distributions of combustion emissions (CO₂, H₂O, O₂, and N₂) are found to be 5.89%, 3.47%, 16.28% and 74.36%, respectively. The emission index for NO_x is determined as 0.579 g NO_x/kg fuel. Also, while the thermal limit ratio of the overall system is found to be 3.76, the enthalpy ratio is found to be 4.53. In the second stage, the exergy efficiency of the engine is calculated as 17.01%, and the fuel exergy waste ratio is computed to be 82.99%. In the third stage, the environmental effect factor of the system is estimated to be 4.88, the exergetic sustainability of the system is found as 0.205, and the ecological effect factor of the system is obtained to be 5.88.

Keywords: Aero Engines, Turbojet Engine, Energetic Analysis, Thermo-environmental Aspect, Exergetic Analysis

INTRODUCTION

In this study, to evaluate the thermo-environmental performance which can be estimated by energy and exergy-based thermodynamic performance metrics of the medium scale turbojet engine, the energetic and exergetic analyses are performed, then the thermal and environmental performance metrics are used.

ANALYSES AND PERFORMANCE EVALUATIONS

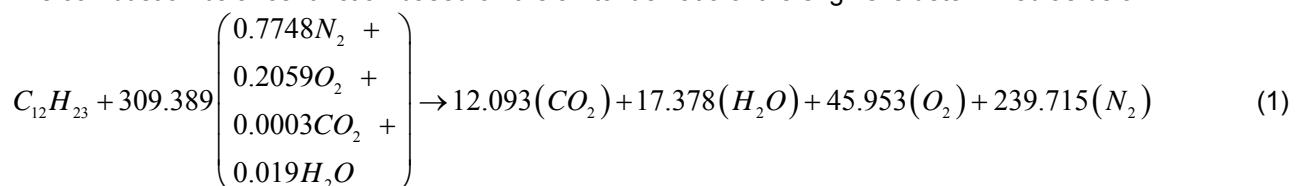
The major thermodynamic specifications of the engine are listed in Table 1.

Table 1. Major engine specifications

Parameter	Unit	Value
Inlet air mass flow	kg/s	4.45
Fuel mass flow	kg/s	0.084
Air to fuel ratio	-	52.976
Turbine inlet temperature (TIT)	K	1082.35
Turbine inlet pressure (TIP)	kPa	388.63
Compressor outlet temperature (COT)	K	450.75
Compressor outlet pressure (COP)	kPa	411.25
Exhaust outlet velocity	m/s	538.65

The assumptions which are used in the study are given as follows. The engine is under the steady state conditions, the temperature (T_0) and the pressure (P_0) of dead state are 288.15 K and 101.33 kPa, respectively [1]. The compressor and turbine components are adiabatic. It is assumed that the completed combustion reaction and the emissions have ideal behaviour [2]. The fuel used is JP-8 fuel (C₁₂H₂₃), and the LHV (Lower Heating Value) of this fuel is 43124 kJ/kg [1,2].

The combustion balance function based on the air to fuel ratio of the engine is determined as below.



After the combustion process, the c_p function of exhaust gases based on Equation (1) is determined as below.

$$c_{p,g}(T) = 0.98861 + \frac{0.01194}{10^2}(T) + \frac{0.01515}{10^5}(T^2) - \frac{0.06650}{10^9}(T^3) \quad (2)$$

The emission index for NOx can be determined via following equation [3,4].

$$EI_{NO_x} = 5.4728(10)^{-6}(T_4)(P_3)^{0.37} \left(e^{\frac{T_3}{191.67}} \right) \quad (3)$$

CONCLUSIONS

The specific power and specific thrust are found to be 147.810 kW/kg/s and 0.549 kN/kg/s while the specific fuel consumption is obtained to be 0.128 g/kNs. After the combustion process, the distributions of combustion emissions (CO₂, H₂O, O₂, and N₂) are found to be 5.89% (0.267 kg/s), 3.47% (0.157 kg/s), 16.28% (0.738) and 74.36% (3.372 kg/s), respectively.

Furthermore, the emission index for NOx is determined as 0.579 g NOx/kg fuel. Besides, while the thermal limit ratio of the overall system is found to be 3.76, the enthalpy ratio is found to be 4.53. Also, the exergy efficiency of the engine is calculated as 17.01%, and the fuel exergy waste ratio is computed to be 82.99%. Moreover, the environmental effect factor of the system is estimated to be 4.88, the exergetic sustainability of the system is found as 0.205, and the ecological effect factor of the system is obtained to be 5.88. The above-mentioned results are also illustrated in Figure 1.

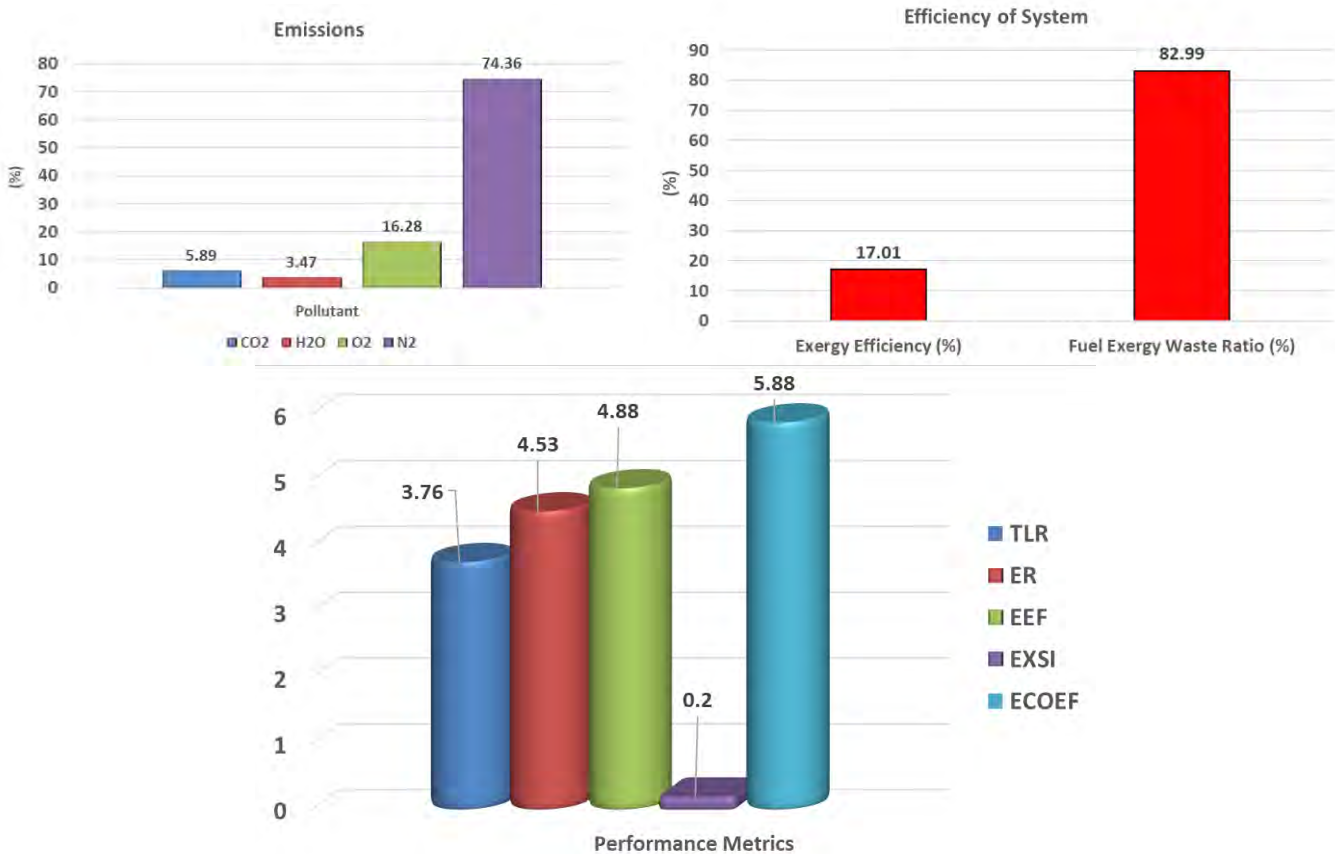


Figure 1. The overall results of the assessments

REFERENCES

- [1] Ballı O, Caliskan H. Turbofan engine performances from aviation, thermodynamic and environmental perspectives. Energy 2021; 232:121031. <https://doi.org/10.1016/j.energy.2021.121031>.
- [2] Ballı O, Caliskan H. On-design and off-design operation performance assessments of an aero turboprop engine used on unmanned aerial vehicles (UAVs) in terms of aviation, thermodynamic, environmental and sustainability perspectives. Energy Conversion and Management 2021; 243:114403. <https://doi.org/10.1016/j.enconman.2021.114403>.
- [3] Altuntas O. Designation of Environmental Impacts and Damages of Turbojet Engine: A Case Study with GE-J85. Atmosphere 2014; 5:307–23. <https://doi.org/10.3390/atmos5020307>.
- [4] Heywood JB. Internal combustion engine fundamentals. Second edition. New York: McGraw-Hill Education; 2018.

A NEW METHODOLOGY FOR DISTRIBUTOR SELECTION IN REFRIGERATION CYCLES

^{1*} Habip Akın Hacimusalar, ¹ Mehmet Harun Sökücü, ¹ Mehmed Rafet Özdemir, ² Ahmet Selim Dalkılıç
¹Marmara University, Faculty of Engineering, Mechanical Engineering Department, Goztepe Campus, Istanbul, TURKEY
²Yıldız Technical University, Mechanical Engineering Department, Besiktas Campus, Istanbul, TURKEY

*Corresponding author e-mail: akin.hacimusalar@gmail.com

ABSTRACT

Theoretical calculation of pressure drop plays a crucial role in refrigeration cycles in order to determine whether the system tends to homogenous refrigerant distribution in evaporator tubes or not. Because the efficiency of the cycle can be increased by avoiding flow maldistribution and hunting if the homogenous fluid flow can be satisfied through the evaporator tubes. Determining the suitable correlation for given conditions is important in two-phase flow to find accurate pressure drop and therefore selecting the right distributor. Although there exist commercial calculation modules in the industry for the purpose of pressure drop calculation, these products may not give accurate results and may not consider important features. This study aims at determining theoretical pressure drop in evaporator tubes and therefore help users to make suitable distributor selection in an accurate and convenient way. For this purpose, a new methodology considering two-phase flow patterns is developed and validated with experimental data for a refrigerant of R-404A. The experiments were carried out for five different cases, and it was found that the proposed methodology agreed better with the experimental data compared to commercial calculation module used in the market.

Keywords: Distributor selection, Pressure drop, Two-phase flow, Homogenous flow distribution

INTRODUCTION

The refrigeration cycle is a critical component of HVAC systems and is governed by the principles of thermodynamics. There are different components in the refrigeration cycles. The distributor is one of these components that aims to satisfy the distribution of refrigerant flow into the homogenous flow to each evaporator tube thus increasing the COP of the cycle and keeping the pressure drop at the appropriate values. By the light of experimental studies, it is stated that COP may change between 10-15% due to non-homogeneous flow distribution, [1]. Furthermore, having the knowledge of theoretical pressure drop prior to the experimental setup gives the designer chance to re-consider distributor selection so thus controlling the cycle in a more effective and convenient way. In the literature, many studies have been conducted to determine the pressure drop prediction in two-phase flow. Different methodologies occurred with various correlations and these studies aimed to analyze the two-phase pressure drop phenomenon and find accurate theoretical values. However, these traditional methodologies use relatively old correlations and do not consider some of the important features -such as flow regime, superheating & subcooling and consequently they may not yield accurate pressure drop values. Due to this issue, developing a new methodology that determines pressure drop with a theoretical approach -in a more accurate and convenient way- is aimed in this study. Determining tube pressure drop accurately prior to modelling and cycle construction, would help users to ensure suitable distributor selection and therefore optimizing the cycle by eliminating possible outcomes of non-homogenous distribution.

MATERIALS AND METHOD

In this study, Chisholm's two-phase pressure drop correlation [2] is chosen and new features are considered to develop accurate two-phase pressure drop calculation. These new features are considering flow regime map and considering sub-cooling and superheating conditions for the refrigeration cycle. To implement the flow regime map in the calculations, a recent study by Thome, J. R., & Cioncolini, A. (2016) [3] is considered. To utilize the sub-cooling & superheating effect during calculations, basics of thermodynamics are followed, and integration completed. An experimental study was conducted to validate the present proposed model. The experiments were performed for five different cases such as including the superheating effect, subcooling effect. The experiments were conducted three times for five different cases to ensure repeatability. During the experimentation process, R-404A was used. The experimental setup is given in Fig. 1.

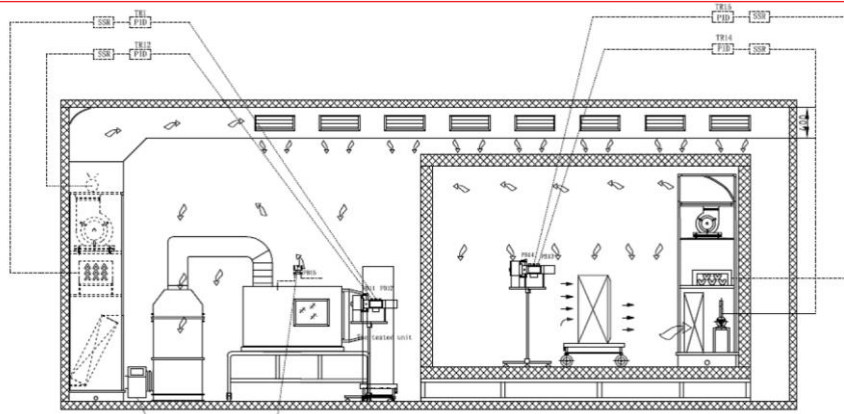


Figure 13. Schematic of Experiment Setup. LHS represent air-conditioning chamber, RHS Calorimetric Chamber

RESULTS AND DISCUSSIONS

The experimental two-phase pressure drop data were compared with the proposed methodology and pre-existing commercial software in Tables 1 and 2.

Table 6. Experimental Tube Pressure Drop Data vs Proposed Methodology Calculation

	Experimental Data (kPa)	Developed Methodology Output (kPa)	% Error
Case-1	72.14	68.07	5.642
Case-2	72.2	77.53	7.382
Case-3	96.8	81.19	16.126
Case-4	100	92.39	7.610
Case-5	197	191.4	2.843

Table 7. Experimental Tube Pressure Drop Data vs Pre-existing Methodology Calculation

	Experimental Data (kPa)	Existing Methodology Output (kPa)	% Error
Case-1	72.14	63	12.670
Case-2	72.2	73	1.108
Case-3	96.8	118	21.901
Case-4	100	134	34.000
Case-5	197	115	41.624

CONCLUSIONS

This study has identified new pressure drop methodology by combining existing solutions to develop theoretical pressure drop methodology in refrigeration cycle evaporator tubes. With this methodology, pressure drop in evaporator tubes can be evaluated with new features and more accurate way. Therefore, distributor selection can be done to minimize efficiency loss due to non-homogenous refrigerant distribution. Validation of the study is proceeded via R-404A refrigerant and experimental data proved that applying the presented method, would give more accurate result than the existing commercial methodology. The main differences between existing methodology and the developed one can be count as: Flow pattern integration, sub-cooling and superheating extension and accurate evaluation of these new features. Since, present study is validated with experimental data and comparison is held between existing and developed methodology, it can be stated that the new methodology gives more accurate result than the existing commercial methodology. Therefore, application of these study would provide better tube pressure drop and help user to determine distributor accordingly.

REFERENCES

- [1] "J. H. Kim, J. E. Braun, and E. A. Groll, "Evaluation of a hybrid method for refrigerant flow balancing in multi-circuit evaporators," *Int. J. Refrig.*, vol. 32, no. 6, pp. 1283–1292, 2009."
- [2] "D. Chisholm. Pressure gradients due to friction during the flow of evaporating two-phase mixtures in smooth tubes and channels. *Int. J. Heat Mass Transfer*, 16:347–358, 1973."
- [3] "Thome, J. R., & Cioncolini, A. (2016). Two-phase flow pattern maps for microchannels. In *ENCYCLOPEDIA OF TWO-PHASE HEAT TRANSFER AND FLOW I: FUNDAMENTALS AND METHODS* (pp. 47-84)."

Submission ID: 108

EXERGETIC OPTIMIZATION OF A COMBINED SOLAR POWER PLANT AND HYDROGEN PRODUCTION SYSTEM WITH NANO-FLUID AND ENERGY STORAGE SYSTEM

¹ Milad Shirazi, ^{1*} Ehsan Baniasadi, ¹Ebrahim Afshari, ²Nader Javani

¹ Department of Mechanical Engineering, Faculty of Engineering, University of Isfahan, Hezar Jerib Ave., Isfahan, Iran

² Yıldız Technical University, Department of Mechanical Engineering, Yıldız, Istanbul, 34349, Turkey

* Corresponding author e-mail: e.baniasadi@eng.ui.ac.ir

ABSTRACT

In this paper, the performance of a solar power generation combined cycle with thermal energy storage and three types of nano-fluid Al_2O_3 and TiO_2 and CuO is investigated. The effects of number of solar collectors, volume fraction of nano-particles, the mass flow rate of steam, material and the ratio of volume to surface area of thermal energy storage system are investigated. The genetic algorithm is used in order to optimize the performance of the system based on exergy destruction minimization. The use of nano-fluids increases the exergy efficiency of the cycle and hydrogen production by the electrolyzer. Among the selected nano-fluids, the CuO -oil working fluid yields the highest exergy efficiency. Also, the exergy analysis shows that more than 75% of the exergy destruction of the cycle take place in three components of solar collector, the thermal storage system and electrolyzer. Among the energy storage materials, the Silicone-oil has the highest exergy efficiency. The results show that by increasing the operating temperature of the electrolyzer the exergy efficiency of the cycle increases. Based on optimized working conditions, the exergy efficiency of the cycle using nano-fluids CuO , TiO_2 and Al_2O_3 , increases by 11%, 9% and 8%, respectively.

Keywords: Solid oxide electrolyzer, Parabolic solar collectors, Exergy optimization, Nano-fluid, Thermal energy storage

INTRODUCTION

Hydrogen is a clean and inexpensive fuel compared to fossil fuels and it is a promising solution to address the global warming changes [1]. Dincer et al. examined different methods of hydrogen production and they concluded that the low efficiency and high costs of hydrogen production is the main drawback [2]. The system studied in this paper is shown in Figure 1. The main components of the cycle are solar parabolic collector, energy storage system, Rankin power generation cycle, heat exchanger network and solid oxide electrolyzer (SOEC).

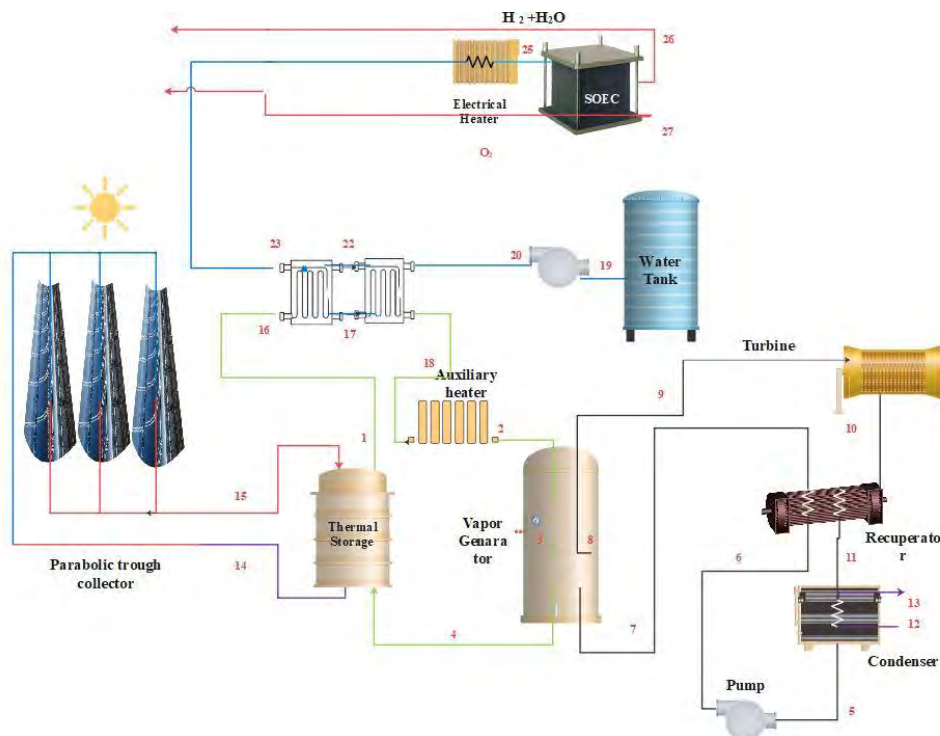


Figure 1. Flow diagram of the combined power and hydrogen production cycle

Since solar energy is the main source of energy supply for this cycle, for the continuous operation of the cycle during the day and night, an energy storage system should be considered. In order to supply the required energy of the electrolyzer, the output stream from the storage system is further heated by a heat recovery generator. The rest of thermal energy required for electrolysis is provided by energy recovery from the electrolysis output stream. Finally, an electric heater is used to increase the steam temperature to bring the electrolyzer to operating temperature. Three nano-fluids including mineral oil as the base fluid and CuO, TiO₂ and Al₂O₃ nano-particles are applied.

Exergy analysis

Exergy is the maximum amount of useful work that can be received from the system in a process of achieving thermodynamic equilibrium with an environment at dead state conditions [3]. The exergy balance for a control volume is defined as follows:

$$\dot{E}X^Q + \sum \dot{m}_{in} ex_{in} = \dot{E}X^W + \sum \dot{m}_{out} ex_{out} + \dot{E}X^D \quad (1)$$

where $\dot{E}X^Q$ and $\dot{E}X^W$ in the above equation are defined as follows:

$$\dot{E}X^Q = \left(1 - \frac{T_0}{T_r}\right) \dot{Q} \quad \text{and} \quad \dot{E}X^W = \dot{W}_{c.v.} \quad (2)$$

Figure 2 shows the effect of the number of solar collectors in the presence of nano-fluids on the exergy efficiency of the combined cycle. Increasing the number of solar collectors increases the exergy destruction of the solar collectors and consequently the overall exergy efficiency of the combined cycle decreases. Figure 3 shows that when the number of solar collectors increases from 800 and 1500, the outlet temperature of the solar collector increases by more than 30% using CuO-oil nano-fluid.

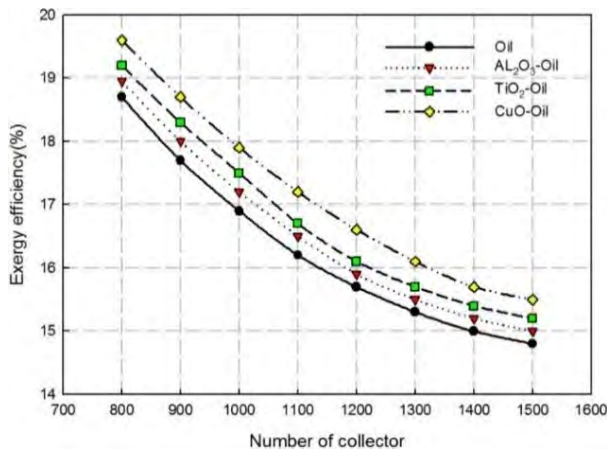


Figure 2. The effect number of collectors on exergy efficiency

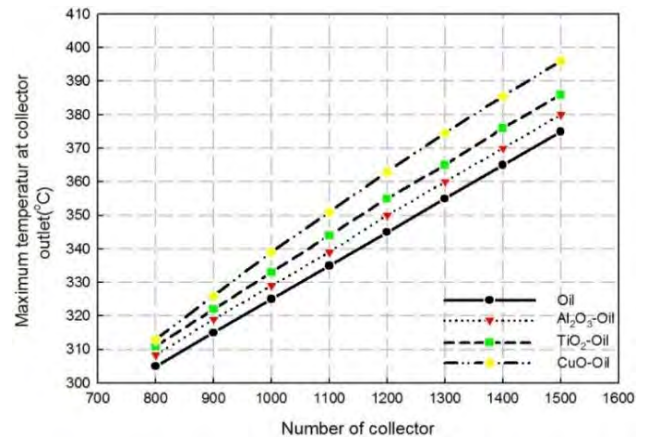


Figure 3. Effect of collector number on the maximum temperature

CONCLUSIONS

In this study, the exergy efficiency of the cycle and the rate of hydrogen production in a combined cycle is optimized in the presence of three nano-fluids CuO, TiO₂ and Al₂O₃. The main results of this research are as follows:

- 1- The analysis of the integrated cycle revealed that more than 75% of the cycle exergy degradation is related to the two components; namely solar collectors and the heat storage system. In order to improve the exergy efficiency and the rate of hydrogen production, special care must be taken in the design and selection of these two components of the cycle.
- 2- After optimization, the results show that the cycle exergy efficiency for nano-fluids CuO, TiO₂ and Al₂O₃ increases by 11%, 9% and 8%, respectively.
- 3- By increasing the volume fraction of nano-fluids and consequently reducing the energy required to increase the temperature of the fluid, the energy efficiency and exergy increase. Also, among the studied nano-fluids, CuO with the same volume fraction has a higher exergy efficiency than other two nano-fluids TiO₂ and Al₂O₃.

REFERENCES

- [1] Dincer, I., Acar, C., 2015. Review and evaluation of hydrogen production methods for better sustainability. International journal of hydrogen energy 40 (34),11094-11111
- [2] Acar, C., Dincer, I., 2014. Comparative assessment of hydrogen production methods from renewable and non-renewable sources. International journal of hydrogen energy 39 (1), 1-12.
- [3] Shayeghi, H., Pirayeshnegab, A., Jalili, A., Shayanfar, H.A., 2009. Application of PSO technique for GEP in restructured power systems. Energy Conversion and Management 50 (9), 2127-2135.

COUPLED THERMAL-ELECTROCHEMICAL ANALYSIS OF POLYMER ELECTROLYTE MEMBRANE ELECTROLYSER

Faezeh Moradi Nafchi, Ebrahim Afshari, Ehsan Baniasadi

Department of Mechanical Engineering, Faculty of Engineering, University of Isfahan, Hezar Jerib Ave., Isfahan, Iran, Postal Code 81746-73441

*Corresponding author e-mail: e.baniasadi@eng.ui.ac.ir

ABSTRACT

In this paper, a numerical model is developed for polymer electrolyte membrane electrolyser to investigate the thermal performance and temperature distribution in the electrolyser, as well as the effect of three important parameters including operating pressure, operating temperature and thickness of the membrane on thermal and overall performance of electrolyser. The results of numerical modeling are verified using experimental data. The results indicate when the operating temperature increases and the operating pressure decreases, the temperature distribution is more uniform, and the performance of the electrolyser improves. By increasing temperature from 333K to 353K, the mean temperature difference decreases 82%.

Keywords: PEM electrolyser, thermal performance, electrochemical performance, membrane, temperature distribution.

INTRODUCTION

Polymer electrolyte membrane (PEM) electrolysers have several benefits such as high current density, rapid response system, compact system design, high purity of gas, dynamic working conditions and high voltage efficiency that in last decade much attention has been paid to them[1]. Proper design and balanced operating conditions in PEM electrolyser is necessary to reduce the over-voltages in the electrolyser. In this regard, the most important parameters are working temperature and pressure, the structure of the cell and associated materials. The distribution of temperature in the electrolyser affects the open circuit voltage, anode and cathode activation overvoltage, ohmic and concentration overvoltage. The polymer membrane conductivity depends on humidity and temperature. When temperature increases, the hydrogen ion diffusion increases and decreases the mass transfer limits, but it causes membrane dehydration. Also, the rate of electrochemical reactions at active surface areas increases. Moreover, the temperature affects the hydrogen and oxygen concentrations at the interface between the electrode and membrane and the concentration overvoltage, subsequently. Therefore, the thermal management of electrolyser plays an important role in the operation. Unlike proton exchange membrane fuel cells, numerical modeling of PEM electrolyser has been recently developed [2-3]. There is a knowledge gap in the available literature about the temperature distribution and thermal performance of PEM electrolysers. In this regard, a one-dimensional CFD model is developed for thermal analysis of a PEM electrolyser. Moreover, the effects of operating temperature on the temperature distribution in the PEM electrolyser and its performance is investigated using an electrochemical model.

ELECTROCHEMICAL MODELING

The PEM electrolyser consists of anode and cathode catalysts, gas diffusion layers, membrane, flow channels and plates that conduct inlet and outlet streams. Water decomposition takes place at a higher DC input voltage than the reversible voltage. At anode, highly endothermic process of oxygen evolution occurs and electrons pass through an external circuit. Protons migrate from the anode to the cathode through the membrane to recombine with electrons and hydrogen gas is produced. Nafion is usually used as a membrane due to properties such as proton conduction and mechanical strength. Utilization of Nafion restricts the temperature of the electrolyser to 100°C. The PEM electrolyser operates at temperatures below 100 °C, therefore, the required thermal energy is low and it can be supplied by electrical energy. The minimum thermodynamic voltage required to initiate the water electrolysis is reversible voltage, but in actual systems, due to kinetic losses in polar plates and electrodes, the required voltage is more than reversible voltage.

$$V = V_{oc} + V_{act} + V_{con} + V_{ohm} \quad (1)$$

Where V_{oc} is open circuit voltage, V_{ohm} is ohmic overvoltage, V_{act} and V_{con} are activation and concentration overvoltage across the anode and cathode, respectively. The net molar flow rate of water in the membrane is transmitted ($\dot{N}_{H_2O}^{mem}$) through three processes that including the diffusion, the electro-osmotic drag and the effects of hydraulic pressure.

$$\dot{N}_{H_2O}^{mem} = \dot{N}_{H_2O}^{diff} + \dot{N}_{H_2O}^{eod} - \dot{N}_{H_2O}^{pe} \quad (2)$$

where, $\dot{N}_{H_2O}^{diff}$ is the water flow rate due to the diffusion from the anode to the cathode, $\dot{N}_{H_2O}^{eod}$ is the water flow rate from one side to the other side with the electro-osmotic drag and $\dot{N}_{H_2O}^{pe}$ is the flow rate of water due to pressure gradient effect.

THERMAL MODELING

The energy equation in the electrolyser for the anode and cathode electrodes and the membrane is written as follows.

$$\text{Cathode: } -k_{ele}^{eff} \frac{d^2T}{dx^2} + \left(\left(\frac{1}{2F} \right) W_{H_2} C_{p_{H_2}} + \dot{N}_{H_2O}^{cat} W_{H_2O} C_{p_{H_2O,l}} \right) \frac{dT}{dx} = \frac{I^2}{\sigma^{eff}} - \left| \frac{j(x)}{2F} \right| (T\Delta\bar{s}) + j(x) \times V_{act,c} \quad (3)$$

$$\text{Membrane: } -k_{mem}^{eff} \frac{d^2T}{dx^2} + \dot{N}_{H_2O}^{mem} W_{H_2O} C_{p_{H_2O,l}} \frac{dT}{dx} = \frac{i_m^2}{\sigma_{mem}} \quad (4)$$

$$\text{Anode: } -k_{ele}^{eff} \frac{d^2T}{dx^2} + \left(\left(\frac{1}{2F} \right) W_{O_2} C_{p_{O_2}} + \dot{N}_{H_2O}^{an} W_{H_2O} C_{p_{H_2O,l}} \right) \frac{dT}{dx} = \frac{I^2}{\sigma^{eff}} - \left| \frac{j(x)}{4F} \right| (T\Delta\bar{s}) + j(x) \times V_{act,a} \quad (5)$$

Where subscript l represents liquid water, W_i and C_p are the molecular weight and the specific heat under constant pressure of species i . k_{ele}^{eff} and k_{mem}^{eff} are the thermal conductivity coefficient of the electrode and membrane, σ^{eff} is the effective electrical conductivity coefficient of the electrode and σ_{mem} is the proton conductivity of the membrane.

RESULTS AND CONCLUSIONS

Fig. 1 shows the temperature distribution in the electrolyser along the thickness of the layers. Difference between the special temperature and the operating temperature of the electrolyser (T_c) is located on vertical axis and the dimensionless length, i.e., the ratio of x to the total thickness of the layers is located on horizontal axis. The hydrogen evolution reaction is endothermic, and the oxygen reduction reaction is exothermic, but the anodic reaction heat is relatively more than that the cathode reaction, which causes an endothermic overall reaction in the electrolyser. Therefore, the temperature decreases along the thickness of the electrolyser. The minimum temperature of electrolyser occurs at the anode catalyst surface. The reaction heat in high current densities is high and by decreasing the current density, this generated heat decreases. Consequently, the temperature distribution in the electrolyser becomes non-uniform. By increasing the current density from 0.1 A cm^{-2} to 1.1 A cm^{-2} , the average difference temperature of PEM electrolyser decreases from -0.1 K to -1.26 K .

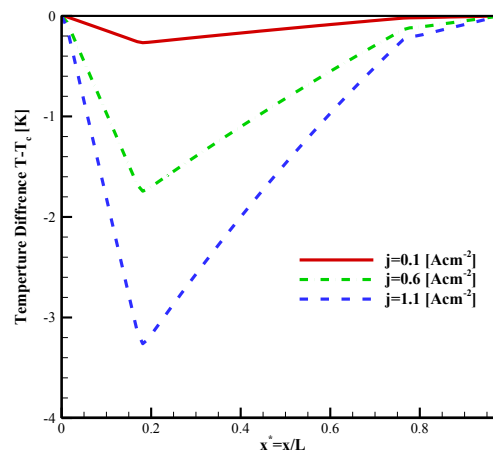


Fig. 1. Temperature distribution of electrolyser at operating temperature of 353 K

In this study, a one-dimensional numerical model is developed to evaluate temperature distribution of a PEM electrolyser. The main conclusion is that due to the endothermic process at anode, the minimum temperature of electrolyser occurs on the anode electrode half-cell. Moreover, increase of current density due to the increase in the over-voltage of the electrolyser and the irreversibility's leads to non-uniform temperature distribution of the electrolyser.

REFERENCES

- [1] K. Rajeshwar, R. McConnell, and S. Licht, "Solar hydrogen generation," Toward a renewable energy future. Springer: New York, 2008
- [2] K. Onda, T. Murakami, T. Hikosaka, M. Kobayashi, and K. Ito, "Performance analysis of polymer-electrolyte water electrolysis cell at a small-unit test cell and performance prediction of large stacked cell", Journal of the Electrochemical Society, vol. 149(8), pp. A1069-A1078, 2002.
- [3] M. E. Lebbal, M. E. and S. Lecœuche, "Identification and monitoring of a PEM electrolyser based on dynamical modelling. International journal of hydrogen energy, vol. 34(14), pp. 5992-5999, 2009.

A METHODOLOGY FOR THERMODYNAMIC PERFORMANCE COMPARISON OF THE CROP PRODUCTION

^{1*} Mustafa Tolga Balta

¹ Uşak University, Faculty of Engineering, Department of Mechanical Engineering, Uşak, Turkey

*Corresponding author e-mail: mustafa.balta@usak.edu.tr

ABSTRACT

Global energy demand increases day by day with the growth in population, urbanization and also industrialization. Consequently, it is resulted within the increase in greenhouse gas emissions. In this context, this global problem has to be solved immediately. Energy management in energy intensive processes is an important issue. In this context, energy-intensive processes should be taken into account for decreasing the accelerate in the global warming. Crop production in agriculture is one of the energy intensive processes that have to be focused for this issue. Energy utilization in an efficient way in agriculture is one of the main factors for ensuring the sustainable future. In this regard, sustainable energy applications in crop production are an important topic that can reduce the energy consumption. Performance of the crop production in agriculture is mainly analyzed through first law of the thermodynamics by the researchers and scientists. This paper presents a methodology for thermodynamic performance comparison of the crop production.

Keywords: CO₂ emission, Cumulative degree of perfection, Energy, Exergy, Agriculture.

INTRODUCTION

Global energy demand increases day by day with the growth in population, urbanization and also industrialization. Consequently, it is resulted within the increase in greenhouse gas emissions. The effect of crop productions on the released greenhouse gases to the atmosphere is about 10-12% [1,2]. 14% of total global CO₂ is caused by the crop production [2,3]. Energy management is one of the key issues for decreasing the energy demand and also greenhouse gas emissions in agriculture as well as various sectors to achieve sustainable future [2,4,5]. One of the main principles for sustainability is energy utilization in an efficient way. This principle is also valid in agriculture. In this context, increasing the efficiency in crop production is key challenges to ensure the sustainable agriculture. In agriculture, energy utilization is examined in two categories such as direct and indirect energy utilization. Utilization of fuel and electricity are called as direct energy usage. On the other hand, usage of fertilizers and chemicals are indirect energy usage (2,6-9). The need for crop increases with the increase in the population. In this regard, farmers have a great attention to how can grow more crop per area with low cost. One of the solutions to these problems is applying new technological and innovative applications. In literature, many scientists and researchers have conducted on optimize the inputs of agricultural crops, thermodynamically [2,10].

THERMODYNAMIC EVALUATION

In this section, mass, energy and exergy balance equations are defined for determining the thermodynamic performance analysis of crop production. In general, on the basis of the conservation of mass principle,

$$\sum \dot{m}_{in} = \sum \dot{m}_{out} \quad (1)$$

$$\sum \dot{E}_{in} - \sum \dot{E}_{out} = \sum \Delta \dot{E}_{system} \quad (2)$$

$$\sum \dot{Ex}_{in} - \sum \dot{Ex}_{out} - \dot{Ex}_d = \Delta \dot{Ex}_s \quad (3)$$

Also overall energy and exergy consumption, overall CO₂ emissions should be defined according to the related literature. The performance of any crop production is given by Szargut as the cumulative degree of perfection (CDP). The CDP of any crop production can be expressed as [11]

$$CDP = \frac{Ex_{crop}^{ch}}{\sum Ex_{in}} \quad (4)$$

The exergy efficiency of the crop production system can be calculated from [10]

$$\Psi_{crop} = \frac{\sum \dot{Ex}_{out}}{\sum \dot{Ex}_{in}} \quad (5)$$

CONCLUSIONS

Thermodynamic performance comparison of crop production can be calculated with given methodology using CDP and exergy efficiency. Cumulative consumption of the energy and exergy and CO₂ emission values to the production system should be determined and compared for the crop production.

Some concluding remarks from present study are as follows:

- This methodology can help reduce the energy and exergy utilization of the crop production.
- The utilization of energy and exergy in an efficient way in agriculture is one of the main factors for ensuring the sustainable agriculture.
- CDP and exergy efficiency of the crop production are increased with the reducing the exergy utilization.
- The utilization of renewable energy resources in agriculture sector are increased day by day.
- CO₂ emission values are also very important values for comparison purposes.

REFERENCES

- [1] Khoshnevisan, B., Rafiee, S., Omid, M., Mousazadeh, H. Reduction of CO₂ emission by improving energy use efficiency of greenhouse cucumber production using DEA approach. *Energy*, 2013; 55: 676-682.
- [2] Taki M, Yildizhan H. Evaluation the sustainable energy applications for fruit and vegetable productions processes; case study: Greenhouse cucumber production, *Journal of Cleaner Production*, 2018; 199: 164-172.
- [3] Pishgar KS., Keyhani, A. Energy use and economic analysis of corn silage production under three cultivated area levels in Tehran province of Iran. *Energy*, 2013; 36 (5): 3335-3341.
- [4] Nabavi PA, Abdi R, Rafiee S, Shamshirband S, Yousefinejad OM. Resource management in cropping systems using artificial intelligence techniques: a case study of orange orchards in north of Iran. *Stoch Environ Res Risk Assess* 2016; 30:413-427.
- [5] Khoshnevisan B, Bolandnazar E, Barak S, Shamshirband S, Maghsoudlou H, Altameem TA. A clustering model based on an evolutionary algorithm for better energy use in crop production, *Stochastic Environmental Research and Risk Assessment*, 2016;29 (8): 1921-1935.
- [6] Nabavi PA, Rafiee S, Homa HB, Shahaboddin S. Modeling energy consumption and greenhouse gas emissions for kiwifruit production using artificial neural networks. *J Clean Prod* 2016; 133:924-931.
- [7] Ozkan B, Akcaoz H, Fert C. Energy input-output analysis in Turkish agriculture. *Renew Energy* 2004; 29:39-51.
- [8] Eckebil J. *The Energy and Agriculture Nexus, Environment and Natural Resources*, Working Paper No. 4, Food and Agriculture Organization of the United Nations, Rome, 2000
- [9] Schnepf R. *Energy use in agriculture: background and issues*. 2004. CRS Report for Congress, November 19.
- [10] Yildizhan H., Taki M., Özilgen M., Gorjian S. Renewable energy utilization in apple production process: A thermodynamic approach, *Sustainable Energy Technologies and Assessments*, 2021; 43.
- [11] Szargut J, Morris DR, Steward FR. *Exergy analysis of thermal, chemical, and metallurgical processes*. New York: Hemisphere; 1988.

THERMODYNAMIC ASSESSMENT OF A POWER TO METHANE SYSTEM UNDER REAL-WORLD SCENARIO

^{1*} Alper Can Ince, ²Dilek Saygan Temel, ³ C. Ozgur Colpan, ⁴ Ali Keleş, ⁵ Mustafa Fazıl Serincan

^{1,5} Gebze Technical University, Faculty of Engineering, Mechanical Engineering Department, Gebze, Kocaeli, 41400, Turkey

^{2,4} GKE Energy R&D Center, Milas, Muğla, 48200, Turkey

³ Dokuz Eylül University, Faculty of Engineering, Mechanical Engineering Department, Buca, Izmir

*Corresponding author e-mail: a.ince@gtu.edu.tr

ABSTRACT

An increasing trend in the use of renewable power leads to an increase in energy storage needs. Converting renewable power into storable synthetic methane, which is also known as Power to methane (P-t-Methane), provides a potential solution to store excess electricity. This conversion generally consists of three essential sub-processes: hydrogen production (pure or H₂-rich syngas), CO₂ capture, and fuel upgrading (as displayed in Fig 1). Power is utilized to produce hydrogen through the water electrolyzers (e.g., alkaline, polymer electrolyte membrane electrolyzer, and solid oxide electrolyzer). CO₂ can be captured from air, biogas, or flue gas through different processes. The production of methane can be provided in a chemical reactor where hydrogen reacts with CO₂ and/or CO. In this pathway, hydrogen production is needed, and hydrogen is produced from water electrolyzers powered by renewable sources. This pathway has gained considerable attention in the last decades, and it is available in commercial markets.

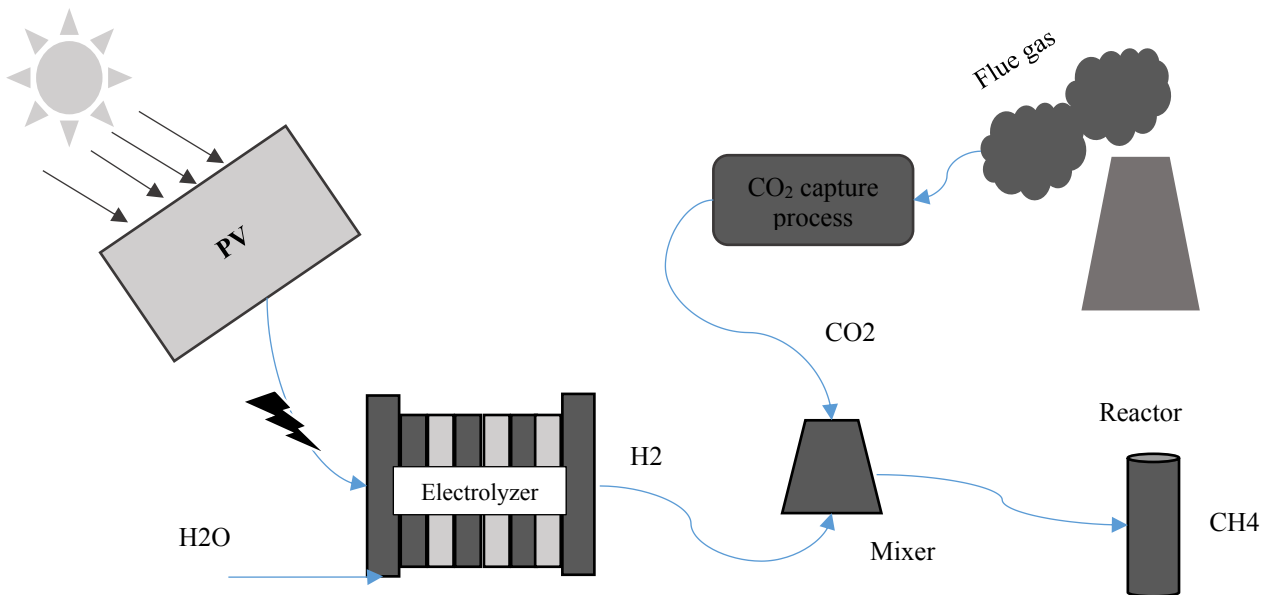


Figure 1/ A power-to-methane system considered

In this study, a thermodynamic assessment of the power-to-methane system is conducted under a real-world scenario through the mathematical model developed in the MATLAB environment. For this purpose, the average solar radiation data are used for Mugla, Turkey. The solar power required to drive the electrolyzer is calculated. The polymer electrolyte membrane (PEM) electrolyzer is used for hydrogen production. For the electrochemical performance of the PEM electrolyzer, the polarization data obtained from the literature are implemented into the mathematical model. The mass balance equations are applied around the control volume of the PEM electrolyzer to find the hydrogen production rate. The average CO₂ concentration that varies monthly in flue gas is taken from real data of the power plant. The time-dependent CO₂ concentration data are integrated into the model as a function. The CO₂ and hydrogen combine in a chemical methane reactor for methane production. Like other components, thermodynamic equations with mass balance are applied to control volume in the methane reactor. Here, the reaction kinetic mechanism is also used. Finally, the methane production rate [mol/s] is calculated. Moreover, the system's thermodynamic efficiency is calculated under variable operating conditions. Therefore, this study reveals the thermodynamic feasibility of a Power-to-Methane system under a real-world scenario.

Keywords: Power-to-Methane, synthetic methane, CO₂ utilization, mathematical model

ELECTROSPINNING IS A POWERFUL TOOL FOR THE DESIGN OF CARBON NANOFIBER TOWARDS HYDROGEN ENERGY SYSTEM

Aysel Kantürk Figen

Yıldız Technical University, Chemical Engineering Department, Davutpasa Campus, İstanbul, Turkey

*Corresponding author e-mail: akanturk@yildiz.edu.tr

ABSTRACT

Electrospinning is a powerful tool to design carbon nanofibers (CNF) through spinning polymer precursors into a nanofibrous structure. CNF has a one-dimensional nanostructure and has shown the similar multi-functional with carbon nanotubes with some advantages like easier production and lower cost. Therefore, CNF-based nanomaterials have been widely preferred for applications relating to energy conversion, storage, production. Nowadays, boron-based compounds such as sodium borohydride (NaBH_4) and ammonia borane (NH_3BH_3) own high hydrogen storage content, used as a fuel in fuel cells, especially in portable, automotive, and stationary power generation systems. The hydrogen storage system must be able to release hydrogen in sufficient quantities. Therefore, various effective catalysts in different types have been designed to accelerate and control the hydrogen rate. This study presented primary results of the fabrication and characterization of CNF and graphene doped CNF (gCNF) designed for the hydrogen energy system. Nanofibers were fabricated by electrospinning polyacrylonitrile (PAN) solution in N,N' dimethylformamide (DMF) solvent at optimized 17 kV, 2.2 ml/h, and 17 cm spinning conditions, subsequent post-treatments such as stabilization and carbonization. As a result, nanofibers are successfully fabricated and were confirmed by scanning electron microscopy (SEM) analysis.

Keywords: Electrospinning, Carbon Nanofiber, Catalyst Support, Hydrogen, Boron fuels

INTRODUCTION

The electrospinning method is frequently preferred in nanofiber fabrication based on controlling electric field strength into the polymer solution. The electrospinning process consists of the high voltage source, nozzle, dosing pump, and fiber collection. Synthesized fibers are porous and have a surface-area-to-volume ratio. Therefore, they find wide use in polymer composites, biomedical and medical applications, electrical and optical material synthesis, filtration processes, agriculture, and energy fields. Today, catalysts and catalyst support are produced by traditional methods, mainly sol-gel, impregnation, and precipitation. However, the surface properties of the catalysts need to be improved or modified to show a highly catalytic efficiency. It is possible to produce high surface area, porous, nano-sized, and catalytically superior catalysts by applying the suitable fabrication method as electrospinning. The optimization of spinning parameters is critical that affects the structural properties of nanofibers [1]. Boron fuels provide advantages in the storage of hydrogen and the release of stored hydrogen [2, 3]. Ammonium borane (NH_3BH_3 , 19.6% H_2 wt.) and sodium borohydride (NaBH_4 , 10.8% wt.) show the unique capacity to store and transport large amounts of molecular hydrogen. The first study on NaBH_4 ability to store and transport molecular hydrogen and NaBH_4 usability in hydrogen production was published in 1973 by Schlesinger. Since the late 1990s, NaBH_4 has been presented directly as a promising fuel for fuel cells. In the following years, studies on synthesizing new boron-based compounds were continued. In 2007, the US Department of Energy underlined that NaBH_4 is an indispensable hydrogen storage medium for vehicle applications and also needs to work directly on NH_3BH_3 , another promising hydrogen storage material for the fuel cell. Due to its advantages, such as high hydrogen storage capacity, high stability in air and aqueous environments, and controllable reaction conditions, the studies are focused on adapting the NH_3BH_3 to vehicle applications [4]. However, catalysts are needed to realize efficient and rapid hydrogen release through the hydrolysis reaction of boron fuel. Therefore, it is crucial to develop the cheapest and most active catalyst to reduce the cost of hydrogen production. In the present study, the electrospinning method following the thermal stabilization and carbonization was applied to prepare graphene doped carbon nanofiber to be utilization in a hydrogen energy system.

MATERIALS AND METHODS

Within the scope of this study, CNF is selected as catalyst support to carry the catalytically active phase again to the boron fuels NaBH_4 or NH_3BH_3 hydrolysis for hydrogen production. The following studies were carried out to synthesize composite nanofiber using the electrospinning technique: (i) Preparation of electrospinning solutions containing polyacrylonitrile (PAN): Within the scope of experimental studies, two different electrospinning solutions were prepared to obtain composite nanofibers: PAN-containing and graphene-doped PAN-containing. PAN ($\text{C}_3\text{H}_3\text{N}$)_n, 99.995%, Sigma-Aldrich, MW = 150000 g/mol) was dissolved in DMF ($\text{HCON}(\text{CH}_3)_2$, Merck) at a concentration of 9% by weight. It was stirred continuously for 2 hours at 50 °C followed by 24 hours at room temperature to obtain a homogeneous solution. Electrospinning solution containing graphene doped PAN was prepared by following a similar procedure, containing 1% by weight graphene (99.9% nanoplatelet, Nanography).(ii)

Synthesis of nanofibers using electrospinning technique: The synthesis of nanofibers was carried out using the electrospinning device (Basic System-Nanospinner). First of all, electrospinning parameters such as voltage, solution flow rate, and needle-collector distance were optimized and carefully adjusted to obtain homogeneous and continuous fibers. Then, using the prepared PAN and graphene-doped PAN solutions, it was exposed to the electric field in the electrospinning device, and the formed fibers were collected. In fiber production, optimum electrospinning conditions were applied at 17 kV, 2.2 ml/h, and 17 cm. PAN and graphene-doped PAN fibers were pre-dried under atmospheric conditions. They then were oxidized (at 2 °C/min heating rate, 260°C, 2 hours) following carbonization (5 °C/min heating rate, 1000 °C, 1 hour) in a tubular high-temperature furnace (iii) SEM analysis of nanofibers: SEM analysis (Zeiss EVO® LS 10) was carried out to determine the nanofiber synthesis. SEM analysis was performed to determine the fiber formation in the samples and to examine the morphologies. The samples were prepared for analysis by coating with gold-palladium under a high vacuum. In addition, digital images were also made.

CONCLUSIONS

Figure 1 and 2 shows the SEM (a,b,c,) and digital images (d) of fabricated CNF and gCNF, respectively. When the PAN solution is spun, white PAN fibers are formed. Nanofibers were obtained by spinning the PAN solution after graphene doping; it retained white color and homogeneous color distribution. It figures out that the nanolayer graphene is homogeneously dispersed in the PAN solution. After the heat treatment under oxidative atmosphere, it was determined that both samples turned brown, and after carbonization, black colored fibers were obtained, which is unique to carbon fiber.

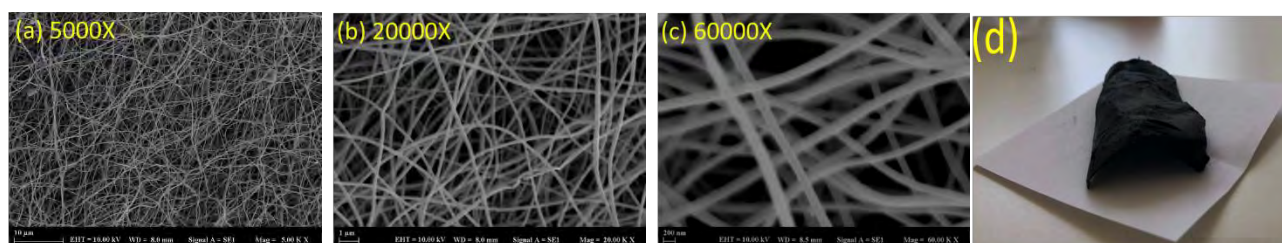


Figure 1. Images of carbon nanofiber: SEM (a) at 5000X, (b) at 20000X, (c) at 60000X, (d) digital

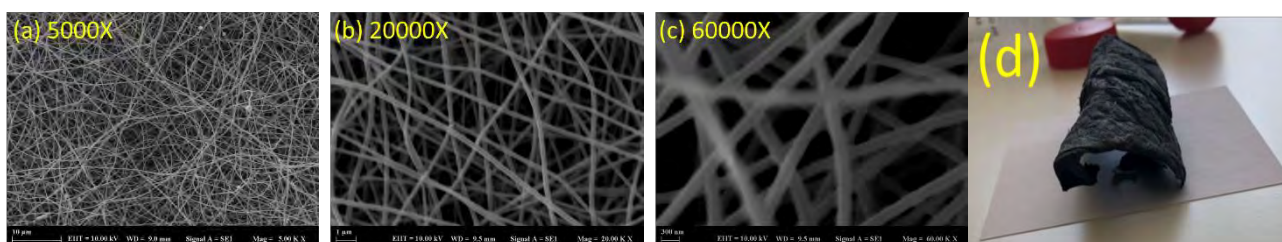


Figure 2. Images of graphene doped carbon nanofiber: SEM (a) at 5000X, (b) at 20000X, (c) at 60000X, (d) digital

It is noteworthy that the network structure is not deteriorated and preserved after the oxidation and carbonization processes applied for stabilization and activation. However, the dimensions of the fiber diameters were measured from the SEM images. Under the applied electrospinning parameters, PAN fibers below 400 nm were synthesized. After stabilization and activation, the average diameter of the carbon nanofibers obtained was measured as 177 nm. The reduction in diameters is due to non-burning during oxidation. It has been determined that the graphene addition causes the formation of thicker diameter carbon nanofiber. It can be explained by the fact that the graphene additive increases the viscosity of the electrospinning solution. The study provides CNF and gCNF with homogeneous, spun, continuous, and random non-woven morphology that would benefit future applications in the hydrogen energy system.

ACKNOWLEDGMENTS

The authors acknowledge the Turkish Academy of Sciences (TUBA) in the Outstanding Young Scientists Awards (GEBIP/2021).

REFERENCES

- [1] Figen, Aysel Kantürk. "Improved catalytic performance of metal oxide catalysts fabricated with electrospinning in ammonia borane methanolysis for hydrogen production." *International Journal of Hydrogen Energy* 44.53 (2019): 28451-28462.
- [2] H.I. Schlesinger, H.C. Brown, A.E. Finholt, J.R. Gilbreath, H.R. Hoekstra, E.K. Hyde, Sodium Borohydride, Its Hydrolysis and its Use as a Reducing Agent and in the Generation of Hydrogen *J Am Chem Soc*, 75 (1) (1953), pp. 215-219.
- [3] E. Fakiolu, Y. Yürüm, T.N. Veziroğlu, A review of hydrogen storage systems originated on boron and its compounds, *Int J Hydrog Energy*, 29 (13) (2004), pp. 1371-1376
- [4] Demirci, Umit B., and Philippe Miele. "Sodium borohydride versus ammonia borane, in hydrogen storage and direct fuel cell applications." *Energy & Environmental Science* 2.6 (2009): 627-637.

ASSESSMENT OF OPERATIONAL CONTROL STRATEGIES ON ENERGY EFFICIENCY AND MANAGEMENT OF PRODUCTION PROCESSES

^{1*} M.Ziya Sogut, ² T.Hikmet Karakoç

¹Maritime Faculty, Pirireis University, Tuzla, İstanbul, Turkey

² Eskisehir Technical University, Faculty of Aeronautics and Astronautics, 26470, Eskisehir, Turkey

*Corresponding author e-mail: mzsogut@gmail.com

ABSTRACT

The manageability of energy in corporate strategies does not only depend on technology and resource management. Developing business culture and developing operational control strategies also have significant energy savings opportunities. This study deals with the improvements in energy consumption that will be provided in the system by optimizing the operating parameters by directly considering different production processes, together with a cement production process example. In studies conducted on different processes in different enterprises, the effects of direct operating parameters on energy consumption and their CO₂ saving potentials depending on fuel type were evaluated separately. At the end of the study, improvements related to operating parameters were evaluated and their contributions to a sustainable energy management were examined.

Keywords: Operational control, energy management, efficiency, Cost, Sustainability

INTRODUCTION

Today, where the fight against global climate change gains value, the critical role in reducing greenhouse gas emissions, which has become a social pressure, is to reduce fossil fuel consumption. With a share of 40%, the industrial sector has a leading role in this direction. However, this directional control approach for corporate structures and especially for production processes should not be handled only with technology and resource management tools. In the industrial sector, for situations where unit energy costs in production processes reach 50%, effective use and management of energy emerges as a necessity in sustainable competitive conditions. In this respect, effective management models of the industry are needed to reach the targets defined in the national strategies. In this context, significant gains in energy efficiency are achieved by optimizing consumption with operational controls within effective energy management in processes [1].

First of all, operational control in corporate strategies should be seen as a guide for effective system management. In this context, in this study, the improvements in energy consumption that will be provided in the system by optimizing the operating parameters by directly considering different production processes, are examined on the basis of a cement production process. In studies conducted on different processes, the effects of direct operating parameters on energy consumption and their CO₂ saving potential depending on fuel type were evaluated separately. At the end of the study, the improvements depending on the operating parameters and their effects on the sustainability of energy in the institutional direction were also evaluated.

METHOD FOR OPERATIONAL CONTROL

The effectiveness of energy management systems directly depends on the effectiveness of the developed planning process. Energy management, which has become widespread in industrial sectors and has different application processes, basically takes into account important energy usage points with a consumption share of 80% in total consumption potentials. The planning process, especially target definition, developed depending on energy management strategies, is an important step in achieving policy targets for important energy users. These targets and the effective energy management of the system are defined by energy efficient actions during the implementation process. These actions are, respectively, energy efficient training based on important energy users, operational control, energy efficient design, energy efficient purchasing and action processes based on improving performance. One of the most important points in these processes is the operational control process, which directly affects the performance of the energy user. As a matter of fact, in a study based on energy efficiency, it was evaluated that the improvements made in operational businesses could save about 20% [2].

Operational processes based on energy efficiency directly cover the key areas required for efficient operation, operation and maintenance, service providers and training. In this respect, operational controls in a business define a methodological approach that should be handled within the energy management system. In this study, the methodology given in Fig.1 was developed.

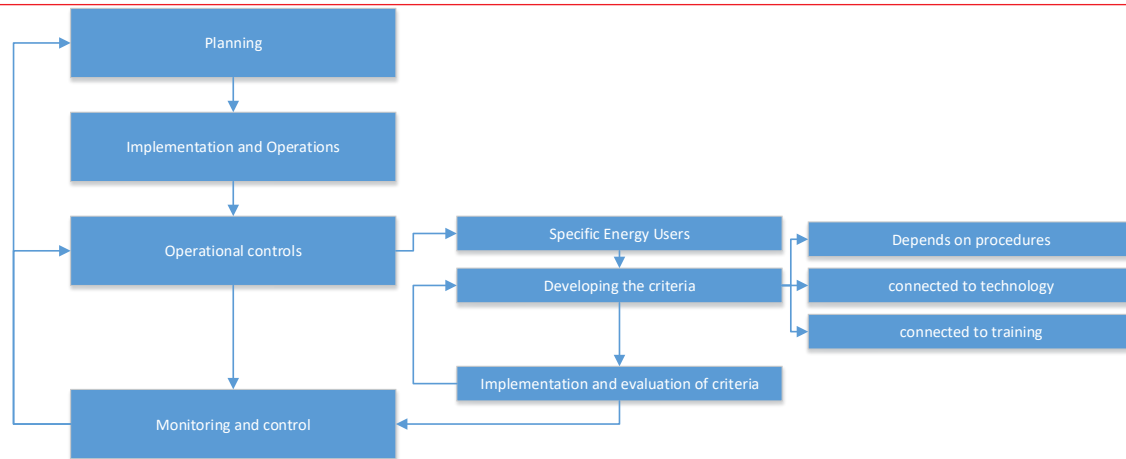


Fig.1. Operational control methodology

RESULTS AND DISCUSSION

Clinker and cement, which are obtained as products in cement production, are the two basic criteria taken into account in the enterprise, as in the whole sector. In this context, the energy density of the enterprise was evaluated with these two criteria. Accordingly, the three-year average of the enterprise based on total energy was found to be 0.099 tep/ton.clinker in clinker, while this value was found as 0.081 toe/ton.cement in cement. If it is evaluated that this ratio is 0.07-0.75 toe/ton.cement in weight for developed countries in world cement consumption, it can be seen that energy efficiency needs to be improved in sectoral terms. The most important player in the distribution of energy consumption in the cement sector is the rotary kiln process. In this respect, the rotary kiln process can be seen as the most important user. However, it would be a more accurate approach to identify important consumers based on energy sources. In this respect, 6 important users in electricity and 2 important users in rotary kiln 1 and 2 processes for heat energy were examined for operational evaluations. Especially in heat processes, these two processes consume 99% of the total heat energy. According to these distributions, the operating parameters examined for a cement production and their limit values are defined. Intense operational parameters are remarkable for each important energy user in cement production. Cement production has many measurement parameters that every user takes as a reference due to its heavy consumption. In the study developed with the energy management system, 26 operational procedures and 119 operating parameters that concern all users were determined. For the application to the action plans, 5 actions related to the operational operating parameters were defined and the savings targets were examined. In the analyzes made, a saving of 16500 mwh in thermal loads and an average of 550000 kwh in electricity was determined. With the optimization of the operational operating parameters of the enterprise, a saving potential of approximately 3% for electricity and 3.5% for heat energy has been determined in the annual total energy efficiency potential.

CONCLUSIONS

This study includes a field study to demonstrate the effectiveness of operational parameters in the energy management system. According to the analyzes made, it was seen that the efficiency of the operating parameters is about 3.5% in cement production. Keeping the operating parameters under control is valuable not only in terms of energy efficiency, but also in terms of life processes, maintenance costs and maintenance procedures of the production processes in the enterprise. In this respect, questioning based on the proposed methodology can be seen as an important management element instead of the traditional approach. Although this is revised depending on the processes, the control of operational parameters as a general approach is an important energy efficiency tool. It should be seen as a process that must be examined for processes with high consumption intensity in the enterprise.

REFERENCES

- [1] Sermin Onaygil, Efficiency in Industry, Energy Management and Savings, 5th National Efficiency Congress, Ankara, 6-7 October 2015
- [2] Heck, Stefan and Humayun Tai. "Sizing the Potential of Behavioral Energy-Efficiency Initiatives in the US Residential Market." McKinsey & Company. May 2013

DEVELOPMENT OF ENVIRONMENTAL SUSTAINABILITY INDICATORS BASED ON THE EFFICIENCY OF INTEGRATED BUILDINGS

^{1*} M.Ziya Sogut

¹Maritime Faculty, Pirireis University, Tuzla, İstanbul, Turkey

*Corresponding author e-mail: mzsogut@gmail.com

ABSTRACT

It is known that the building sector has a significant potential in global climate change with the energy demand based on fossil fuel consumption and the emission release it causes. The low efficiency of traditional heating preferences, especially in different climate zones, can be seen as the main reason for this potential. Potentials based on such system inefficiencies are basically a measure of the entropy potential of the system. This system-induced exergy destruction can also be expressed with exergy destruction due to the management problem of operational processes. For all these parametric evaluations, environmental indicators on an environmental scale will provide important conveniences for decision processes. In this study, exergy efficiency and entropy performances of an institutional building block related to heating demand management are comparatively examined. In this context, environmental sustainability indicators developed for the evaluation of systems have been defined. In addition, the improvements that can be made in the system with the effective parametric controls of the demand control are evaluated in terms of both efficiency and entropy in the system. At the end of the study, especially environmental effects were evaluated, and performance results related to process analyzes were defined.

Keywords: Integrated Buildings, Energy, Environmental, Indicators, Sustainability

INTRODUCTION

Fossil fuel consumption, which is the main problem caused by global climate change and the main input of sustainable economy, is an indicator that should be managed within institutional structures and the share of these structures in total consumption is important. Especially within the scope of combating climate change, considering the emission potential of approximately 30%, energy and environmental management should be considered as a managerial process in corporate strategies. The first step in the fight against climate change was the United Nations Rio conference held in 1992. In this conference, the goal defined as "to realize sound, harmonious and consistent production policies at national and international level, taking into account environmental concerns in order to improve the functioning of goods and production markets and to optimize the contribution of this sector to sustainable development" is accepted as a start in the development of international awareness [1]. In fact, the international struggle process continued with the Kyoto protocol signed in 1997 and continues today with the Paris Agreement [2,3]. All these processes define a struggle process and responsibility in social structures. Considering the consumption share and responsibilities of the public authority, it is a fact that it has an active role in the development of energy efficient solutions for corporate strategies. The public authority has implemented some holistic projects that will improve energy efficiency and management, especially in recent years. The implementation targets in these projects show that they can provide significant gains depending on their current consumption in buildings. However, it should not be forgotten that application structures are a multidisciplinary choice in this structural transformation, target definition and system preferences for energy managements. For the basic target transformations, an effective model study according to the building sample of the public authority and the climate zone it is in is the basic need. First of all, the entropy potential was defined by considering the school sample referenced in this study. Then, the indicators developed for environmental sustainability were defined and their potential effects were examined.

ENVIRONMENTAL SUSTAINABILITY INDICATORS

The main criterion of inefficiency in energy systems is the losses caused by the systems. They are also the main source for the disorder of the environment. In thermodynamic terms, the criterion of this disorder is entropy production. Entropy in its most general form is a direct quantitative measure of disorder in a system. Therefore, the management of entropy has a key role in environmental sustainability. The main factors affecting the administrative processes of entropy are;

- 1) System structure and factors affecting processes; The greater the functional complexity in system tools, the harder the entropy management and the greater the entropy generation.
- 2) Structure and structural relationships of system components; System management and control is directly related to the structure of system components. Structural complexity affects the production of entropy.
- 3) The efficiency and management of the system; Effective management of the system is a factor that directly reduces entropy production.
- 4) Management continuity of the system; corporate governance continuity allows entropy to be controlled

Entropy management is an important parameter for environmental protection, primarily in environmental management strategies. For all processes that will improve energy efficiency in corporate structures, entropy management should be seen as an approach based on performance optimization [4-6]. In this study, two basic criteria were taken into account to define environmental sustainability. These have been developed based on the Environmental Performance Index (EPI), the functional relationship between entropy energy and the environment under ambient temperature. Sustainability in energy systems depends on effective efficiency management. The Sustainability index defined in the study expresses the boundary condition of possible improvements in systems and is a function of the entropy, energy and environment relationship directly related to improvement.

RESULTS AND DISCUSSION

This study evaluated the environmental performance of energy use behaviors in institutional structures. In this context, while the heat energy use behaviors of the reference building were evaluated cumulatively, the environmental criterion of system inefficiency was handled with two developed indices. In institutional structures, energy management infrastructure is a process that is often neglected, although it requires an institutional infrastructure. In this context, a study was carried out on a very productive example. The reference corporate structure is an integrated structure consisting of approximately 280,000 m² of indoor space and six different building types and two boiler rooms. The usage area of the building has been planned as a service building and the construction feature of the building has been handled by evaluating the LEED certificate. The energy system infrastructure is a structure that is monitored and effectively controlled. The climate characteristics of the campus, especially in Istanbul, the consumptions are handled over the monthly average temperature values. The heat demand of the building group has been calculated based on these climate data, taking into account the holistic needs of the building. The indoor comfort temperature of the building was taken as 22 °C and the operating demand was defined through the management processes of the building.

The epis for both boiler systems are discussed separately. According to this performance distribution, the performance for p1 was found to be 0.42. However, the reference criterion was calculated as 0.0.28. The total exergy destruction at this potential was calculated as 41.07%. Within this potential, the improvement potential effect was calculated as 5.87%. This performance is important in terms of overall sustainability index. The improvement potential of the institutional structure according to the business characteristics, while a potential of 5.87% for P1, this value indicates a potential of 9.41% for P2. In this context, while the sustainability index was 0.36 for P1, this value was 0.38 for P2. The institutional target represents a savings of 14.33% for p1, and this target of 20.31% for P2. This is seen as an achievable target in the energy management strategies of the enterprise. As a matter of fact, about 38% improvement opportunities were found in the cumulative total.

CONCLUSIONS

This study includes an evaluation based on two impact indicators based on the improvement of energy management and environmental sustainability in the strategies of corporate structures. While the main objectives of energy managements provide continuous improvement in energy efficiency in corporate strategies, they should also improve economic and environmental sustainability. In this context, the energy efficiency potential of the reference enterprise was calculated and the environmental impact indicators depending on the effect of this inefficiency were defined. In this context, the energy and exergy efficiency of the enterprise were found to be 57.23% and 55.02%, respectively. In this performance, the improvement potential due to environmental sustainability was found to be 14.33 for P1 and 20.31% for P2, respectively. This value can be seen directly as target productivity values for the organization.

REFERENCES

- [1] Cao, X.; Dai, X.; Liu, J. Building energy-consumption status worldwide and the state-of-the-art Technologies for zero-energy buildings during the past decade. *Energy Build.* 2016, 128, 198–213.
- [2] Alam Shawkat, Sustainable development and free trade institutional approaches, Routledge Taylor&Francis Group, London, 2008, ISBN0-203-93606-X e book, Page 38
- [3] H.Soner Aplak, M. Z. Söğüt, Game Theory Approach In Decisional Process Of Energy Management For Industrial Sector, *Energy Conversion and Management (ISI)* ,74 (2013) 70–80
- [4] Thakkar V. (2015) Entropy Management Along with Energy Management for Sustainability, *International Journal of Scientific & Engineering Research*, Volume 6, Issue 6, June-2015, ISSN 2229-5518
- [5] Jing D. (2012) The Study on Business Growth Process Management Entropy Model, *Physics Procedia* 24 (2012) 2105 – 2110
- [6] Markina I.and Dyachkov D. (2014) Entropy Model Management of Organization, *World Applied Sciences Journal* 30 (Management, Economics, Technology & Tourism): 159-164, 2014, ISSN 1818-4952, DOI: 10.5829/idosi.wasj.2014.30.mett.66

EXPERIMENTAL AIR-COOLED BATTERY THERMAL MANAGEMENT APPROACH

¹Burak Tarhan, ²Ozge Yetik, ¹T. Hikmet Karakoc

¹Eskisehir Technical University, Country Faculty of Aeronautics and Astronautics, 2 Eylul campus, Eskisehir, Turkey

²Eskisehir Osmangazi University, Department of Mechanical Engineering, Faculty of Engineering and Architecture, 26480, Bati Meselik, Eskisehir, Turkey

*Corresponding author e-mail: buraktarhan@eskisehir.edu.tr

ABSTRACT

Sustainable life requires the use of renewable energy. For this reason, the use of batteries stands out as a solution that takes environmental sensitivities into account. The importance and necessity of thermal management of batteries has been demonstrated through practice. Thermal management is necessary in order to ensure the balance between the cells, to prevent thermal escape and to improve the economic life of the batteries. In line with this goal, a new approach has been made with air-cooled cylindrical contact around the Li-Ion battery. It was studied on 20 Li-Ion battery cells connected in 4 series, 5 parallel and charged and discharged at 2C, 3C and 4C values. As a battery thermal method, a new approach has been made that is cylindrically wrapped around the Li-Ion battery cells. Battery tests were conducted under room conditions (25 °C). As a result, its temperature was measured as 29.8 °C without thermal management at 2C charge rate, and 27.4 °C in the air-cooled method at 2C charge rate.

Keywords: Li-Ion battery, Air-cooled method, Thermal management

INTRODUCTION

The fact that emissions from the activities of modern life threaten human health and its future on a world scale gradually increases concerns about climate change and environmental health. Concerns about the environment trigger efforts to reduce pollution and costs in every field and guide the search for solutions. Transportation stands out as an area where these efforts are concentrated due to its share in environmental pollution. With the increase in pressure in terms of environmental effects in transportation, the need for fuel savings and increasing costs have made the use of battery technology mandatory [1]. According to the "Greenhouse gas emission statistics" published by TUIK in 2019, especially for the evaluation of greenhouse gas emissions and values in Turkey, it has been observed that the transportation sector accounts for 10% of the total CO₂ gas emissions [2].

It is not ideal to use batteries only in transportation vehicles. For this reason, batteries are generally used together with a thermal method. In this way, it is ensured that the battery works at the ideal temperature and the battery life is increased. There are 2 methods for the thermal management of the battery; Liquid-cooled method [3,4] and air-cooled [5,6] method. Since the design and applicability of air-cooled battery thermal systems is easier, this method was preferred in the study. But for the thermal design of air cooling, different flow paths such as symmetrical air flow, Z-type, U-type and J-type are designed.

In an attempt to improve upon Z and U-type air flow channel configuration optimization for battery thermal management system, Li et al. (2019) introduced a novel J-Type air flow configuration. Simulation study was and optimization was carried out for a battery module cooled in a Z, U and J-Type air flow configuration battery thermal management system for comparisons. Based on their parametric optimization, their result showed a 35.3%, 46.6% and 31.1% reduction in temperature rise of cells under U, Z and J-Type air flow configuration respectively [7].

Chen et al. (2020), numerically studied five battery pack configuration and verified simulation results by conducting physical experiments. They developed a simple method to achieve symmetrical air flow inside each of the five battery pack by repositioning inlet and outlet vents on each original battery pack designs to get newly optimized battery packs; Further parametric optimization of cells spacing revealed that uneven cell spacing in the improved battery packs resulted in better battery thermal management system cooling performance just as battery packs with symmetrical air flow path did over their original counterparts [8].

Peng et al. (2020) carried out a study on the arrangement of the battery cells of the air-cooling system in their work. CFD analysis was carried out with horizontal and vertical air cooling by arranging the batteries as 1*20, 2*10 and 4*5. It has been observed that air cooling is more effective when the battery cells are closer to each other [9].

In our study, 20 Li-Ion battery cells were used and designed as 4*5. It is made on a battery air cooling thermal management that wraps the lower and upper parts of the battery cells in a cylindrical manner.

MATERIALS AND METHODS

In the study, he worked on the 18650 cylindrical Li-Ion battery cell. The battery cells are connected in 4 series and 5 parallel, and the connection type is given in figure 1. The battery pack has a voltage of 14.8 volts and a capacity of 10.4 Ah.

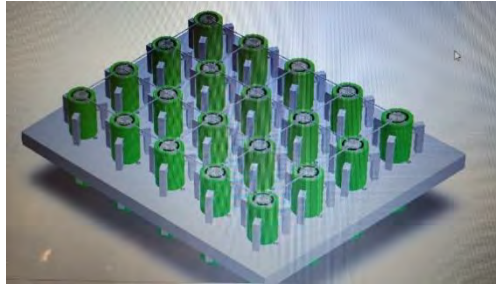


Fig. 1: Battery cell Connection

The battery cells are air cooled under 10 psi pressure. Battery cells charge-discharge cycle tests were tested at room temperature. Battery cells were tested at 2C, 3C and 4C charge-discharge rates.

The devices used for battery thermal management and their functions are given in Table 1.

Table 1.

Device	Function
1 kW Source metre	It provides battery charge and discharge settings and measurements.
Thermal Camera	It allows to examine the temperature change and air-cooling effect of the charge-discharge cycle of the battery.
Climatic Test Cabinet	It ensures that the initial temperature of the charge-discharge cycle of the battery remains constant.
BMS kart	By controlling the voltage and current values of the battery cells during charging and discharging of the battery, damage to the cells is prevented.
Battery cell load	It discharges the battery.
Compressor	Provides air cooling required for thermal management of the battery.

CONCLUSIONS

When the battery cells are charged at 2C, 3C and 4C;

-Reaching 29.8°C, 31.2°C and 34.7°C temperatures respectively in the absence of any thermal management

-In the thermal management of the air-cooled coil, temperatures of 27.4°C, 30.2°C and 32.1°C were reached, respectively.

According to this result, it was observed that air cooling thermal management was more successful at high C value.

REFERENCES

- [1] Miller, J.M., Ehsani, M., & Emadi, A. Vehicular Electric Power Systems: Land, Sea, Air, and Space Vehicles (1st ed.). CRC Press. 2003. <https://doi.org/10.1201/9780203913468>
- [2] Sel A, Göktoğa Z . Projection of Sectoral CO2 Emission Values with Input-Output Models in the Framework of 11th Development Plan. Akdeniz İİBF Dergisi. 2020; 20(2): 158-168.
- [3] Celen A, Kaba M . Parametric Investigation of Cooling of Cylindrical Lithium-Ion Batteries Used in Electric Vehicles. Firat Üniversitesi Mühendislik Bilimleri Dergisi. 2021; 33(1): 49-61
- [4] Lai Y. A compact and lightweight liquid-cooled thermal management solution for cylindrical lithium-ion power battery pack. International Journal of Heat and Mass Transfer, 2019, 144: 118581.
- [5] Akinlabi A. Solyali D. Configuration, design, and optimization of air-cooled battery thermal management system for electric vehicles: A review. Renewable and Sustainable Energy Reviews, 2020, 125: 109815.
- [6] Jaewan K. Jinwoo O. Hoseong L. Review on battery thermal management system for electric vehicles. Applied thermal engineering, 2019, 149: 192-212.
- [7] Yuanzhi L. Jie Z. Design a J-type air-based battery thermal management system through surrogate-based optimization. Applied Energy, 2019, 252: 113426.
- [8] Chen K. Chen Y. She Y. Song M. Wang S. Chen L. Construction of effective symmetrical air-cooled system for battery thermal management. Applied Thermal Engineering, 2020, 166: 114679.
- [9] Peng X, Cui X, Liao X, Garg A. A Thermal Investigation and Optimization of an Air-Cooled Lithium-Ion Battery Pack. Energies. 2020; 13(11):2956. <https://doi.org/10.3390/en13112956>

INVESTIGATING THE ENVIRONMENTAL EFFECTS OF A HYBRID UAV WITH FUEL CELL, ACCORDING TO TWO DIFFERENT SCENARIOS

Duran Çalişir^{1*}, Selçuk Ekici², Adnan Midilli³, Tahir Hikmet Karakoç¹

¹ Eskişehir Technical University, Faculty of Aeronautics and Astronautics Science, Eskişehir, Turkey

² Iğdır University, Department of Aviation, Iğdır, Turkey

³ Yıldız Technical University, Faculty of Engineering, Mechanical Engineering Department, Istanbul, Turkey

* E-mail: dcalisir@eskisehir.edu.tr

ABSTRACT

In recent years, abnormal environmental events have been observed frequently in our country and in the world. Against increasing environmental problems, more environmentally friendly and energy efficient products are preferred. With the developing technology, unmanned aerial vehicles (UAV) are used in many areas. In this study, the environmental effects of a fixed-wing UAV with a proton exchange membrane (PEM) fuel cell and a hybrid power group on agricultural lands and the sea were investigated. The life cycle assessment (LCA) method was used to reveal environmental impacts. Within the scope of the study, scientific researches on the use of PEM fuel cells in UAVs were examined. The PEM Hydrogen fuel cell UAV used in the study is introduced. Two different scenarios have been defined for this UAV. The PEM Hydrogen fuel cell UAV used in the study is introduced. According to the calculated environmental effects as a result of the study, the environmental effects on agricultural lands were higher than the effects on the sea.

Keywords: Hydrogen fuel cell, Unmanned aerial vehicle (UAV), Life cycle assessment (LCA), Environmental impact

INTRODUCTION

Scientific researches are carried out on the use of fuel cells for the purpose of increase the flight times of UAVs. In this direction, optimum power consumption in fuel cells is modeled [1]. PEM hydrogen fuel cells were used to create the hybrid power pack [2], [3]. The energy production functions of fuel cells (DMFC) that use methanol fuel directly, which is another type of fuel cell, were investigated [4]. In recent years, research has been done on new types of fuel cells that use ammonia (NH₃) as a fuel [5]. Research has been done on fuel cells that produce energy from H₂ provided by the hydrolysis of NaBrH₄ [6]. Especially in mini-UAVs, there are studies indicating that aerostack-shaped H₂ fueled PEM-FCs outperform Lithium-ion, Ni-MH batteries [7], [8]. LCA studies have been carried out on H₂ and alternative fuels used in fuel cells [9].

MATERIALS AND METHODS

In this study, a fixed-wing mini-UAV was used, and its name is Hydra. Hydra was designed by Eskişehir Technical University Anatolia Aero Design Team. Hydra can take off by hand launch and has no landing gear. Therefore, it can land on the fuselage. The body, wings and part of the tail set are made of EPS foam. The wingspan is 2.8 meters. Its length is 1.6 meters. Maximum take-off weight is 6.5 kg.

The main power unit consists of a 1300-Watt electric motor, 7-cell Lithium Polymer (LiPo) battery and propeller. Aerostack shaped 250-watt hydrogen PEM fuel cell was added to this power unit and a hybrid power unit was formed. It consists of PEM fuel cell, hydrogen tank and regulator. This power group is shown in Figure 1.

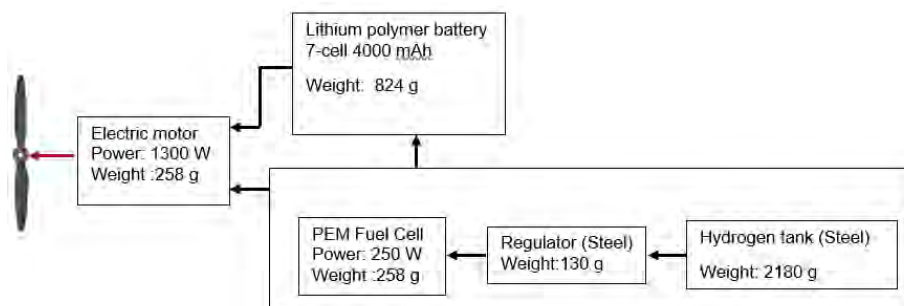


Fig. 1. Power Unit of Hydra

Two different scenarios were defined within the scope of the study. The first is a 1-hour flight over the agricultural lands in the Eskişehir Sarıcakaya Valley. The second is a 1-hour flight on a seacoast at an altitude of 0 – 300 meters, at a distance of 100 meters from the seashore to the sea. In both scenarios, there is no wind, and the average temperature is 15 °C. the LCA method was applied in the cradle-to-door process for calculate the environmental effects. In LCA

application, SimaPro 9.1 software was used. The analysis is based on the Ecoinvent 3.6 database. Calculated using CML-IA Baseline and ReCiPe method in software. In the calculations, impact categories such as abiotic depletion, abiotic depletion (fossil fuels), global warming (GWP100a), ozone layer depletion (ODP), human toxicity, freshwater aquatic ecotoxicity, terrestrial ecotoxicity, photochemical oxidation, acidification and eutrophication were selected.

CONCLUSIONS

A contribution to the literature will be made by revealing the environmental effects of a UAV with a hybrid power unit equipped with a hydrogen-fueled PEM fuel cell using the LCA method. Thus, with the developing UAV technology, it will set light to the production of more environmentally friendly and energy efficient UAVs.

ACKNOWLEDGEMENTS

We would like to thank the Eskişehir Technical University for supporting this research with the 20DRP054 project.

REFERENCES

- [1] Bradley, T. H., Moffitt, B. A., Mavris, D. N., Fuller, T. F., & Parekh, D. E. (2009). Hardware-in-the-loop testing of a fuel cell aircraft powerplant. *Journal of Propulsion and Power*, 25(6), 1336-1344.
- [2] Dudek, M., Tomczyk, P., Wygonik, P., Korkosz, M., Bogusz, P., & Lis, B. (2013). Hybrid fuel cell–battery system as a main power unit for small unmanned aerial vehicles (UAV). *Int. J. Electrochem. Sci.*, 8(6), 8442-8463.
- [3] Ozbek, E., Yalin, G., Karaoglan, M. U., Ekici, S., Colpan, C. O., & Karakoc, T. H. (2021). Architecture design and performance analysis of a hybrid hydrogen fuel cell system for unmanned aerial vehicle. *International Journal of Hydrogen Energy*.
- [4] Gonzalez-Espasandín, Ó., Leo, T. J., Raso, M. A., & Navarro, E. (2019). Direct methanol fuel cell (DMFC) and H₂ proton exchange membrane fuel (PEMFC/H₂) cell performance under atmospheric flight conditions of Unmanned Aerial Vehicles. *Renewable Energy*, 130, 762-773.
- [5] Siddiqui, O., & Dincer, I. (2018). A review and comparative assessment of direct ammonia fuel cells. *Thermal Science and Engineering Progress*, 5, 568-578.
- [6] Lapena-Rey, N., Blanco, J. A., Ferreyra, E., Lemus, J. L., Pereira, S., & Serrot, E. (2017). A fuel cell powered unmanned aerial vehicle for low altitude surveillance missions. *International Journal of Hydrogen Energy*, 42(10), 6926-6940.
- [7] Verstraete, D., Lehmkuehler, K., Gong, A., Harvey, J. R., Brian, G., & Palmer, J. L. (2014). Characterisation of a hybrid, fuel-cell-based propulsion system for small unmanned aircraft. *Journal of power sources*, 250, 204-211.
- [8] Bayrak, Z. U., Kaya, U., & Oksuztepe, E. (2020). Investigation of PEMFC performance for cruising hybrid powered fixed-wing electric UAV in different temperatures. *International Journal of Hydrogen Energy*, 45(11), 7036-7045.
- [9] Bicer, Y., & Dincer, I. (2017). Life cycle evaluation of hydrogen and other potential fuels for aircrafts. *International Journal of Hydrogen Energy*, 42(16), 10722-10738.

DESIGN AND MODELING OF A MULTIGENERATION SYSTEM DRIVEN BY WASTE HEAT OF A MARINE DIESEL ENGINE

^{1*} Murat Emre Demir, ¹ Furkan Çıtakoğlu

¹Faculty of Naval Architecture and Ocean Engineering, Istanbul Technical University, Maslak-Sariyer, Istanbul, 34469, Turkey

*E-mail: medemir@itu.edu.tr

ABSTRACT

In this study, a novel marine diesel engine waste heat recovery layout is designed and thermodynamically analyzed for hydrogen production, electricity generation, water desalination, space heating, and cooling purposes. The integrated system proposed in this study utilizes waste heat from a marine diesel engine to charge an organic Rankine and an absorption refrigeration cycle. The condenser of the ORC provides the heat for the multi-stage flash distillation (MSF) process, which uses seawater as the feedwater. A portion of the produced freshwater is used to supply the PEM electrolyzer array. This study aims to store the excess desalinated water in ballast tanks after a UV treatment. Therefore, it is expected to preclude the damage of ballast water discharge on marine fauna. The integrated system's thermodynamic analysis is performed using the Engineering Equation Solver software package. All system components are subjected to performance assessments based on their energy and exergy efficiencies. Additionally, the capacities for power generation, freshwater production, hydrogen production, and cooling are determined. The system's overall energy and exergy efficiencies are calculated as 25.3% and 13.4%, respectively, where the hydrogen production, power generation, and freshwater production capacities are 300.9 kg/day, 659 kW, and 0.535 kg/s, respectively. COP of the absorption refrigeration cycle is calculated as 0.4463.

Keywords: Waste heat recovery, hydrogen production, desalination, power production, efficiency

INTRODUCTION

CO₂ emissions caused by ships will significantly increase in the future, as the number of marine vessels is expected to grow continuously. According to a review conducted by D.Toscana and F.Murena [1], sea transportation now accounts for a more significant proportion of global trade in both quantitative and monetary terms. The number of commercial products is expected to grow at a 3.2 percent of annual rate till 2022. According to M.Yang [2], SO₂, CO₂, and NO₂ gases emitted from exhausts are potential pollutants for rivers and the atmosphere. Furthermore, 30% of total NO_x ejection is caused by ships, and CO₂ poses a global warming risk. Two-stroke diesel engines are more prevalent in marine propulsion and continue to be used to power ships in the near future. According to the literature [3], a standard two-stroke diesel engine only transmits 49.3% of the thermal energy to the shaft while rejects 25.5% of the potential directly via the exhaust. The purpose of this study is to provide an in-depth examination of waste heat recovery (WHR) concepts for marine vessels. From this perspective, integration with WHR enables the system to produce more with the same input, allowing ships to consume less fuel, resulting in economic and environmental benefits. After turbocharging, exhaust gas temperatures range between 250 and 300 °C for two-stroke engines and 300–350 °C for four-stroke engines, depending on engine load and surrounding conditions [4]. Therefore, even generating implements and electricity in a ship's main and side operations may be possible with a WHR system without increasing CO₂ emissions or fuel consumption[5].

SYSTEM DESCRIPTION

The proposed system is presented in Fig. 1. The exhaust gas with a potential heat capacity released out from the exhaust manifold with a temperature of 300-celsius degrees and a mass flow ratio of 111.1 kilograms per second. Specific amounts of heat will be transferred to isobutane and so that the energy need for ORC is supplied. After this point, the exhaust stream continues to the generator, which is a part of the absorption refrigeration system. Here, it brings the heat required to the system, which is worked with water and ammonia. The assumptions, such as the effectiveness and pressure losses pertaining to the heat exchanger and rectifier, are taken from the ref [6]. Then, the isobutene, which is in superheated vapor form since it is charged with the waste heat, and that gained pressure by the pumps, enters the expander. The produced work feeds the generator and so that electricity is generated as the alternative current. A certain amount of AC can be used for different purposes in the ship. Excess electricity can be converted into direct current to be sent to the PEM electrolyzer stack. The thermal efficiency of the PEM electrolyzer is chosen as 75%, according to the literature survey. The dead steam that comes out of the expander enters the heat-exchanger for condensation. Here, it rejects its heat to the seawater and changes phase. After that, the seawater, which is heated up, continues into multi-stage flash chambers, losing its pressure and the temperature gradually through cascade flash chambers from 100 kPa to 7.4 kPa. This study aims to store the excess desalinated water in ballast tanks after a UV treatment. Therefore, it is expected to preclude the damage of ballast water discharge on marine fauna. The rest of the water can be sent to the ballast and other water tanks. Water that is required for the PEM system is also supplied from this point. In this way, PEM delivers the electricity need from the ORC while providing the water from desalination chambers. Finally, it produces hydrogen and conveys it to the hydrogen storage unit. The brine at moderate temperature is also utilized for space heating with a radiator/heat exchanger mechanism.

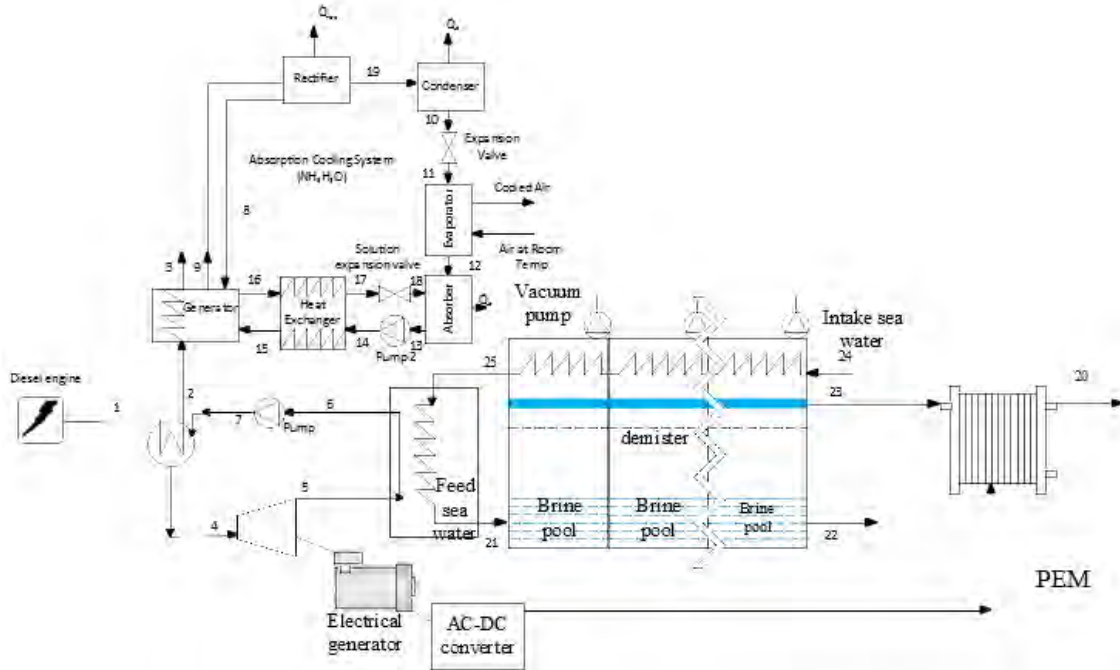


Fig.1. Waste heat driven multigeneration system layout

The system is modeled in EES. Calculations are performed under the assumption of steady-state flow, negligible changes in potential and kinetic energies. Considering the system's inputs and outputs, the overall energy, exergy efficiencies, and COP of the absorption refrigeration cycle are defined as follows:

$$\eta = \frac{\dot{W}_{net} + \dot{m}_{H_2} HHV_{H_2} + \dot{m}_{brine} \Delta h_{brine}}{\dot{m}_{exhaust} \Delta h_{exhaust}}, \quad \psi = \frac{\dot{W}_{net} + \dot{m}_{H_2} ex_{H_2} + \dot{m}_{brine} ex_{brine}}{\dot{E}x_{exhaust}}, \quad COP = \frac{\dot{Q}_{evap}}{\dot{Q}_{gen} + \dot{W}_p}$$

CONCLUSIONS

In this study, a marine vessel waste heat recovery system for hydrogen production, electricity generation, freshwater production, cooling, and heating is designed and analyzed thermodynamically. The main findings of this study can be listed as follows:

- The energy and exergy efficiency of the WHR system is determined as 25.3% and 13.4%, respectively
- COP of the absorption refrigeration cycle is calculated as 0.4463
- The energy of the organic Rankine cycle is determined as 12.7%
- The net power production capacity of the WHR system is determined as 659 kW
- The hydrogen production capacity of the PEM stack is calculated as 300.9 kilograms per day.
- The freshwater production capacity of the WHR system is calculated as 0.535 kg per second

REFERENCES

- [1] D. Toscano and F. Murena, "Atmospheric ship emissions in ports: A review. Correlation with data of ship traffic," *Atmos. Environ. X*, vol. 4, p. 100050, Oct. 2019.
- [2] M. Yang, "Shipping and Maritime Transport," in *Encyclopedia of Environmental Health*, Elsevier, 2011, pp. 33–40.
- [3] MAN B&W Diesel LTD., "Thermo Efficiency System (TES) for reduction of fuel consumption and CO2 emission. : MAN B&W Diesel A/S," Copenhagen, Denmark, 2005.
- [4] S. Zhu, K. Zhang, and K. Deng, "A review of waste heat recovery from the marine engine with highly efficient bottoming power cycles," *Renew. Sustain. Energy Rev.*, vol. 120, p. 109611, Mar. 2020.
- [5] D. V. Singh and E. Pedersen, "A review of waste heat recovery technologies for maritime applications," *Energy Convers. Manag.*, vol. 111, pp. 315–328, Mar. 2016.
- [6] K. E. Herold, R. Radermacher, and S. A. Klein, *Absorption chillers and heat pumps*. New York: CRC press, 1996.

AN URBAN GREEN ENERGY STRATEGY PROPOSALS FOR LOCAL GOVERNMENTS

^{1*} Munevver Ozge Balta

¹Uşak University, Department of Urban and Regional Planning, Uşak Turkey

*Corresponding author e-mail: ozgearas@gmail.com

ABSTRACT

Green energy strategies that offer an opportunity to reduce negative impacts on global warming has become more attention in recent years. This study presents a perspective on various green energy strategies for local governments through technical and environmental framework. The utilization of green energy is known as one of the rational solutions to urban environmental problems. The combination of energy efficient building design, energy efficient urban planning and energy efficient of transportation increases the capacity to cope with climate change of local governments. Furthermore, in today's green development, cities need to adopt environmentally friendly practices to maintain their competitiveness. In recent years, green energy strategies of local governments have been successful in reducing environmental problems caused by global warming.

Keywords: Green energy, Global warming, Local governments, Urban planning,

INTRODUCTION

Urban energy use increases dramatically with the rapid population growth. Today, this energy demand is mostly met with non-renewable energy resources. The excessive use of non-renewable energy sources causes various major environmental problems in cities. Cities are major responsible of the global climate change with releasing the greenhouse gases, extensively. Decision makers are interested in green energy strategies for many reasons such as environmental and economic. In this regard, many scientists and research groups have proposed various energy strategies to ensure the sustainable future [1-5]. Midilli et al. presented the main steps of the use of green energy technologies and implementation of the green energy strategies [5].

By the way, we have to solve these environmental problems urgently by implementing the green energy strategies, effectively. Planning the green energy strategies are more powerful if the national and local governments have a cooperation [6-8]. These strategies are mainly based on Ref. [5];

- Understanding the concept of the green energy utilization,
- Understanding the concept of sustainability,
- Increasing the utilization of the green energy sources,
- Providing the energy security,
- Meeting the growing energy demand from renewable energy sources,
- Reducing the environmental problems with the green energy strategies,
- Determining the green energy strategic proposals for local governments with relevant actors, in detail.

This study presents some green energy strategy proposals for local governments with a specific focus on urban planning.

GREEN ENERGY STRATEGY PROPOSALS

In the literature, there has been several projects applied to achieve the sustainable urban environment. These projects can be categorized as; net zero building, installation of street LED lights, biogas plants, smart transportation systems and renewable energy source farms such as wind, solar, hydrogen etc.

In this regard, some green energy strategy proposals are offered in the below with considering the open literature.

- Transition to new sustainable energy system
- Production from different renewable energy sources
- Ensure the energy self-sufficiency
- The green growth vision for urban planning process
- Low carbon cities by reducing greenhouse gas emissions

CONCLUSIONS

"Urban green energy strategies" should be promoted that can make the cities sustainable with an comprehensive approach for environmental and energy problems. While the cities can become more sustainable by the new urban green energy strategies and also, urban environmental problems can be minimized. Cities should define a green energy concept for ensure the low carbon city according to the given criteria in the above. As a result, the defined green energy strategies are more useful if it cooperates at local and national level.

REFERENCES

- [1] Matraeva, L., Solodukha, P., Erokhin, S., & Babenko, M. (2019). Improvement of Russian energy efficiency strategy within the framework of "green economy" concept (based on the analysis of experience of foreign countries). *Energy Policy*, 125, 478-486.
- [2] Chilundo, R. J., Neves, D., & Mahanjane, U. S. (2019). Photovoltaic water pumping systems for horticultural crops irrigation: Advancements and opportunities towards a green energy strategy for Mozambique. *Sustainable Energy Technologies and Assessments*, 33, 61-68.
- [3] Dell'Anna, F. (2021). Green jobs and energy efficiency as strategies for economic growth and the reduction of environmental impacts. *Energy Policy*, 149, 112031.
- [4] Liu, Q., & Ren, J. (2020). Research on the building energy efficiency design strategy of Chinese universities based on green performance analysis. *Energy and Buildings*, 224, 110242.
- [5] Midilli, A., Dincer, I., & Ay, M. (2006). Green energy strategies for sustainable development. *Energy policy*, 34(18), 3623-3633.
- [6] Krog L. (2019). How municipalities act under the new paradigm for energy planning. *Sustain Cities Soc.*, 47.
- [7] Krog L, Sperling K. (2019). A comprehensive framework for strategic energy planning based on Danish and international insights. *Energy Strateg Rev*, 24:83–93.
- [8] Sperling K, Hvelplund F, Mathiesen BV. (2011). Centralisation and decentralisation in strategic municipal energy planning in Denmark. *Energy Pol.*, 39:1338–51.

TEACHING FUEL CELL AND HYDROGEN SCIENCE AND ENGINEERING ACROSS EUROPE

* Ioan Iordache

¹ The National R&D Institute for Cryogenic and Isotopic Technologies – ICSI, no. 4 Uzinei Str., Rm. Valcea, Romania
² University POLITEHNICA of Bucharest, Faculty of Power Engineering, no.313 Independenței Str., Bucharest, Romania

*Corresponding author e-mail: iordache.ioan@icsi.ro

ABSTRACT

TeachHy is a project funded by the Horizon 2020 program through FCH JU. The offers its network partners access to its educational material and the use of the MSc course modules available on the TeachHy web site. There are 12 partners from 11 European countries. Until this moment the partners contributed together to the realization of 20 didactical modules.

Keywords: TeachHy, hydrogen, modules, master

INTRODUCTION

The project, entitled: *Teaching Fuel Cell and Hydrogen Science and Engineering Across Europe within Horizon 2020*, acronym *TeachHy*, is addressed to universities that have master's courses covering elements related to hydrogen economics and the benefits that will be obtained by implementing it. Also, the deliverables generated by the project are intended to be useful tools for teachers in various European universities, which deal with the implementation of hydrogen in the renewable energy and alternative fuels, so that the number of students, PhD students and specialists with up-to-date knowledge in this field, to be bigger and bigger.

METHODS

As hydrogen and its industry develop, gradually creating a specific market, the need for trained personnel becomes more pressing. TeachHy specifically addresses university and postgraduate education in hydrogen technologies across Europe. Through this project, the members of the consortium aim to train the student / master student in a scientific and technical-economic field of great interest and very current, with the obvious purpose of clarifying certain aspects that will be part and will contribute to the development of hydrogen economy.

TeachHy made progresses in building a repository of educational material, and design and run a master course in the area of hydrogen and fuel cells technologies, accessible to students from all universities of Europe. The project has created a core group of highly experienced institutions collaborating with a network of associate partners (universities, vocational training bodies, industry, and networks). The consortia offers these partners access to its educational material and the use of the master course modules available on the TeachHy webpage. Any institution being able to offer 20% of the course content locally, can draw on the other 80% to be supplied by TeachHy project. This will allow any institution to participate in this European initiative with a minimised local investment. The project consortia provides solutions for accreditation and quality control of modules, and support student and industry staff mobility by giving access to placements. The continuous professional development (CPD) is integrated into the project activities. There is a portfolio of the educational material for the general public (e.g., MOOC's. The project partnership covers the prevalent languages and educational systems in Europe. The associated network has over 20 partners, including two IPHE countries, and a strong link to IPHE activities in education.

The didactic deliverables of the project deal with various problems posed by the beginning of the use of hydrogen in the energy sector, insisting on all aspects, in the immediate, medium and long term. The materials were produced as a result of extensive documentation of the 12 partners from 11 countries, scrutinizing the European and international portfolio of research, development and innovation of technologies involving hydrogen.

The partners have prepared 7 compulsory (mandatory) modules, 11 optional modules and 2 additional modules.

Compulsory modules:

1. Thermodynamics (KIT), electrochemistry (KIT, BAS-IEES, INP), chemistry (KIT),
2. Introduction to fuel cells,
3. Hydrogen (production, storage, handling), fuels (P2G, P2X), electrolyzers,
4. Fuel cell modelling tools (POLITO, Grenoble INP) and control,
5. Characterisation methods,
6. Lab experience,

7. Hydrogen safety,

Optional modules:

1. Environmental analysis, life cycle analysis,
2. Low temperature fuel cells (materials, stacks, thermodynamics, electrochemistry, chemistry),
3. High temperature fuel cells (materials, stacks, thermodynamics, electrochemistry, chemistry),
4. Low temperature systems,
5. High temperature systems,
6. Advanced characterisation,
7. High temperature chemistry for SOFCs/SOEs,
8. Fuel cell electric vehicles,
9. Politics, markets, regulation, codes and standards,
10. Energy systems and storage,
11. Advanced modelling,

Additional modules:

1. Electrocatalysis,
2. Power to X.

Participants:

1. University of Birmingham – UBHAM; UK
2. Technical University of Delft – TUD; The Netherland
3. Politecnico di Torino – POLITO; Italy
4. National Technical University of Ukraine 'Kyiv Polytechnic Institute' – KPI; Ukraine
5. Denmark Technical University – DTU; Denmark
6. University of Chemistry and Technology, Prague – UCPT; Czech Republic
7. École Polytechnique Fédérale de Lausanne – EPFL; Switzerland
8. Université libre de Bruxelles - ULB Belgium
9. University "Politehnica" of Bucharest (and ICSI Rm. Vâlcea); Romania
10. Grenoble Institute of Technology - Grenoble INP; France
11. Ulster University – UU; UK
12. Karlsruhe Institute of Technology – KIT; Germany

CONCLUSIONS

The innovative contribution is that TeachHy enable institutions to offer educational courses that would otherwise not be available locally and allow students access to a mix of both face-to-face and e-learning content across borders. Any educational institution across Europe that fulfils minimum requirements and adheres to the project quality standards of delivery can participate in these activities.

IMPACT OF USING ETHANOL-GASOLINE COMPOUND FUEL ON PERFORMANCE OF A DUAL-FUEL VEHICLE

¹Parnida Kamarei, ^{1,2}Pouria Ahmadi, ³Nader Javani ⁴Mehrdad Raeesi

¹School of Mechanical Engineering, Faculty of Engineering, University of Tehran, Tehran, Iran

²Faculty of Engineering, Istinye University, Istanbul, Turkey

³Department of Mechanical Engineering, Yıldız Technical University, Istanbul, 34349, Istanbul, Turkey

⁴School of Automotive Engineering, Faculty of Automotive Engineering, Iran University of Science and Technology, Tehran, Iran

*Corresponding author e-mail: njavani@yildiz.edu.tr

ABSTRACT

Ethanol and ethanol-gasoline blends have lower well-to-wheel emissions and are easily applicable for existing engine technologies. In the current study, a real engine has been modelled in which an ethanol-gasoline blend fuel is used. In addition, the effect of a real driving cycle on the performance of the engine is investigated. Considering the effect of the blend on the emissions, Life Cycle Assessment (LCA) for the vehicle is studied. The pollution effects of adding ethanol to gasoline fuel in well-to-wheels (WTW) in ICE engines are evaluated. Results show that these blends are viable alternatives for gasoline spark-ignition (SI) engines, regardless of their lower energy density.

Keywords: Ethanol-gasoline vehicle, Electric car, Fuel consumption, Global warming.

INTRODUCTION

Bioethanol is increasingly promoted as an alternative transport fuel worldwide and its global production increased from 17 to 86 billion litres between 2000 and 2011, accelerated with government supports such as mandates, subsidies and tax benefits [1]. Ethanol and ethanol-gasoline blends are being considered as alternatives to the gasoline in spark-ignition (SI) engines. Ethanol is commonly used as a blend with gasoline and the most typical blends are low blends such as E10 (E represents ethanol and the number represents the volume percentage of ethanol) for regular gasoline vehicles. High blends such as E85 are used in flexible fuel vehicles (FFVs) that can run on any mixture between pure gasoline and E85. These blends have some disadvantages compared to gasoline. The lower energy density of the fuel mixture results in higher volumetric fuel consumption, which decreases the vehicle driving range for each charging of the fuel tank. The higher latent heat of vaporization results in cold-start issues [2]. The issues are more pronounced when higher-level ethanol blends are used. On the other hand, higher knock resistance results in better engine efficiency at higher loads [3]. The flex-fuel vehicles that are currently available in the market have demonstrated improvements in terms of material compatibility, calibration changes to meet fueling requirements, and injection timing. The higher octane number of ethanol blends can be further exploited by using higher compression ratios and making additional calibration changes [4, 5]. In this study, a real engine has been modeled and ethanol-gasoline blend fuel is used which is a new fuel that is used all around the world. In addition, the effect of a real driving cycle on the performance and LCA of the vehicle is investigated.

MATERIALS AND METHODS

Life Cycle Assessment (LCA) method is based on a comprehensive assessment of the economic and environmental impacts of a technology, product, or service. This internationally recognized evaluation tool helps decision-makers to determine the impact of new products on the environment. The pollution effects of adding ethanol to gasoline fuel in well-to-wheels (WTW) in ICE engines are evaluated in this regard. For the current research, GREET software is used. It is obtained through the analysis of greenhouse gas emissions so that the vehicle travels through the worldwide harmonized Light vehicles Test (WLTC) driving cycle over a distance of 100 km.

It is also worth noting that ethanol and gasoline production results from the US are considered as a basis. The engine has been simulated to calculate the fuel consumption. For this purpose, the naturally aspirated PFI engine EF7 has been simulated in AMESIM software. Then with the help of EF& typical vehicle modelling in AMESIM software, fuel consumption has been simulated. It is calculated in the desired driving cycle, which is shown in Figure 1.

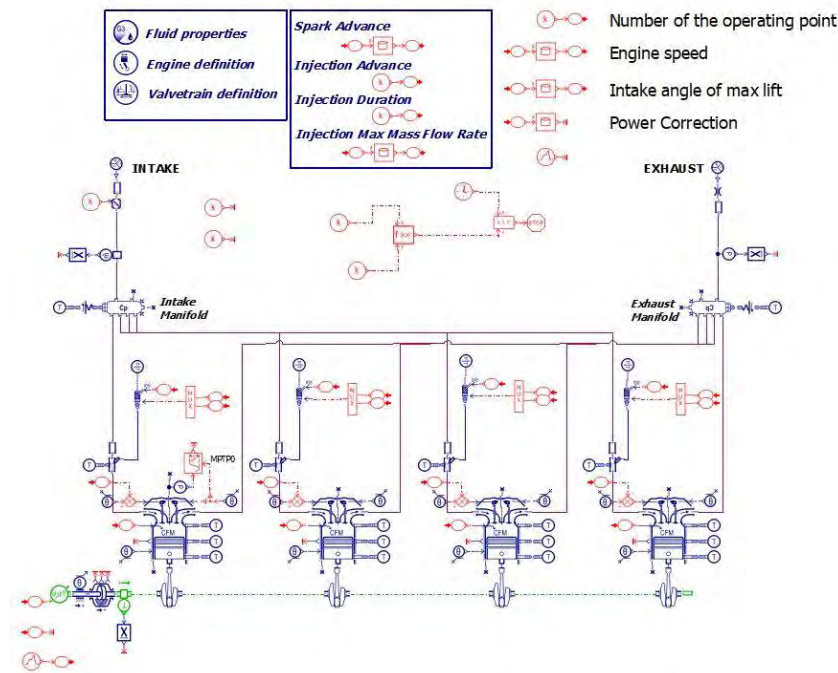


Figure 1. AMESIM model of ICE engine

RESULTS AND DISCUSSION

The use of ethanol in gasoline as a potential option to reduce net CO₂ emissions in the atmosphere, increase the octane rating of gasoline and reduce dependence on petroleum products has become a global trend.

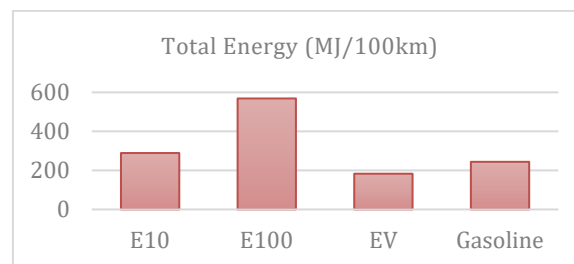


Figure 2. Total energy used for different fuels

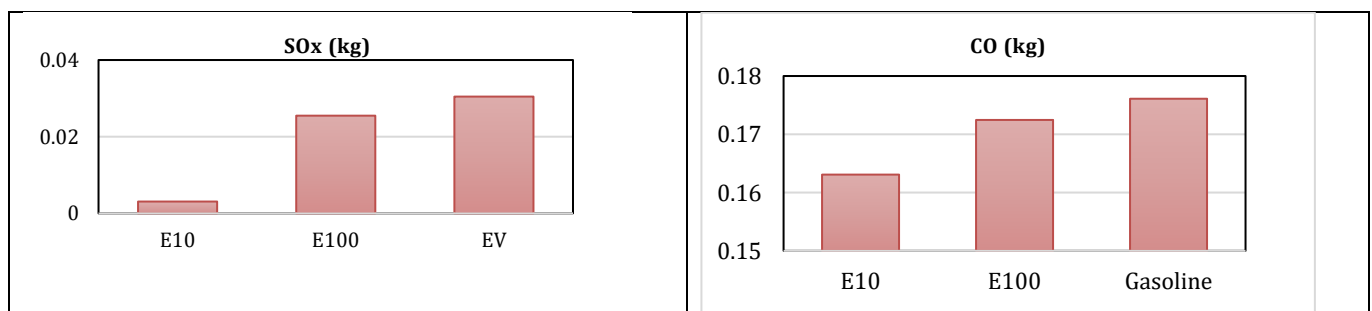


Figure 3. Comparison of the amount of Sox and Co as an example pollutants produced by each of the simulated vehicles for 100 Km with the help of GREET software.

Adding ethanol to gasoline increases energy consumption (Figure 2) but shows a factor in reducing CO₂ emissions in LCA analysis. This increase in energy compared to conventional and electric vehicles is the amount of fuel consumption. The simulation shows that when 10% of ethanol is added to gasoline (E10), fuel consumption increases by almost 12%. When 100% ethanol is used, it causes a 58% increase in consumption (Figure 2). Gasoline has 15 times less SO_x emission than EVs, where electricity comes from the natural gas power plants, and adding ethanol increases the amount of SO_x, mainly due to ethanol production (Figure 3). The current study results also show that CO is one of the most dangerous pollutants, and the results show that the E10 mode reduces CO by about 7% compared to gasoline, but the use of E100 fuel reduces CO production by 2%.

CONCLUSIONS

In general, the addition of ethanol increases the fuel consumption of the vehicle. It reduces CO₂, which can be mentioned as a factor to reduce the consumption of other pollutants in the fossil fuel power plant. EVs. We also found that as the percentage of ethanol increases, the amount of energy consumption per km of vehicle drive increases but does not reduce pollution. In some cases, according to the ethanol production cycle, it also increases the SO_x.

REFERENCES

- [1] Xiaoyu Yan, Oliver R. Inderwildi David A. King and Adam M. Boies, "Effects of Ethanol on Vehicle Energy Efficiency and Implications on Ethanol Life-Cycle Greenhouse Gas Analysis", dx.doi.org/10.1021/es305209a /Environ. Sci. Technol. 2013, 47, 5535–5544.
- [2] Wallner, T., Shidore, N., and Ickes, A., "Impact of Ethanol and Butanol as Oxygenates on SIDI Engine Efficiency and Emissions Using Steady State and Transient Test Procedures," presented at 16th Directions in Engine Efficiency and Emissions Research (DEER) Conference, September 2010, Detroit, MI.
- [3] Wallner, T., Miers, S.A., and McConnell, S., "A Comparison of Ethanol and Butanol as Oxygenates Using Direct-Injection Spark-Ignition Engine," ASME Journal of Engineering for Gas Turbines and Power, Volume 131, May 2009.
- [4] Piques, J-D., "Engine Management Systems for Alternative Fuels," Proceedings of the 2006 AEA Conference, Poitiers, France.
- [5] Christie, M., Fortino, N., and Yilmaz, H., "Parameter Optimization of a Turbo Charged Direct Injection Flex Fuel SI Engine," SAE Int. J. Engines 2(1):123-133, 2009, doi: 10.4271/2009-01-0238.

DESIGN AND TESTING OF AN IOT BASED CARBON MONOXIDE MONITORING UAV: METHODOLOGY, CHALLENGES, OPPORTUNITIES

¹ Emre Ozbek, ² Orhan Aras, ² Ozge Kucukkor, ³ Selcuk Ekici, ⁴ T.Hikmet Karakoc

¹ UAV Technology and Operations Program, Eskisehir Technical University, TR-26000, Eskisehir, Turkey

² Department of Avionics, Eskisehir Technical University, TR-26000, Eskisehir, Turkey

³ Department of Aviation, Igdır University, TR-76000, Igdır, Turkey

⁴ Department of Aircraft Airframe Powerplant Maintenance, Eskisehir Technical University, TR-26000, Eskisehir, Turkey

*Corresponding author e-mail: ozgekucukkor123@gmail.com

ABSTRACT

Air quality has been an important topic due to its effects on both environment and human health. The local air quality measurements at emission sources hold importance in optimizing the overall air quality in a region. Hazardous particle emission locations as industrial chimneys, landfill crematoriums, thermal reactors must be filtered for better air quality. Even after filtering, problematic locations must be inspected within periods to understand if the filter is faulty. In this point, unmanned aerial vehicles (UAVs) are efficient platforms in terms of costs that have been used in inspection works. In this study, a custom-designed multirotor UAV with carbon monoxide sensor and a data collection module was designed. Collected data transmitted to a cloud server using Internet of Things (IoT) technology. A novel sensor extension design was used to keep the sensor away from propellers. Flight tests have been conducted and the air quality measurements were performed. A heatmap was created using live flight data. Challenges in this operation were explained to provide guidance for future researchers and entrepreneurs. Opportunities in such UAV platform appliances were detailed.

Keywords: UAV, Drone, Air Quality, Pollution, Remote Sensing

INTRODUCTION

Unmanned aerial vehicle applications are considered as multi-disciplinary studies. Thus, the introduction was prepared as two sections to provide readers a well-rounded background. The motivation of this study is explained within the first section. The requirement for air quality measurements and control was explained in detail. The second section includes conventional methods for air quality measurements and previous UAV appliances in inspection tasks.

MATERIALS AND METHODS

Performing air quality measurement operations using a UAV as remote sensing platform requires a number of special design requirements. The vertical flow problem is an important characteristic issue must be considered when designing an air quality measurement drone. The vertical flow occurs around the propellers and mixes the air around the multirotor UAV. There are studies in the literature including airframe upgrades such as booms to extend the sensor for sampling from the undisturbed air [1,2].

Rotary wing UAV frames carry a high percentage of the structural and electronic equipment of UAVs and are generally the largest volumetric components of UAVs. Vacuum infusion technique provides a better fiber-resin ratio and spread closer to the optimum level compared to the other production techniques such as hand lay-up [3].

The rotor arms and landing gear of the UAV were made of shelf purchased carbon fiber tubes. Carbon fiber tubes have been widely used in UAV design applications to connect motors and the frame [4,5]. Polylactide (PLA) thermoplastic material was heated and then layered up using a 3D printer.

Mission subsystem design of the AQM UAV were held carefully since its the most important subsystem that defines the performance of the overall system. The mission of the AQM UAV could be defined as autonomously detect and measure carbon monoxide particles in air as stated in previous chapters. The subsystem consists of a sensor that detects carbon monoxide, a sensor extension and a mission computer/board that gather the sensor data and perform the transmission. the AQM UAV were flown autonomously over the area on six meters altitude from the ground. Pre-determined waypoints were created using the ground station and the flight control card created a flight path for the mission. A heatmap of the flight area that based on carbon monoxide particle per million value was generated using the sensor data. Sensor carbon monoxide PPM readings were uploaded as live data to the IoT cloud server through Wi-Fi communication during the flight as labeled with timestamps. The sensor data that uploaded to IoT server with live connection is also presented as Figure1.

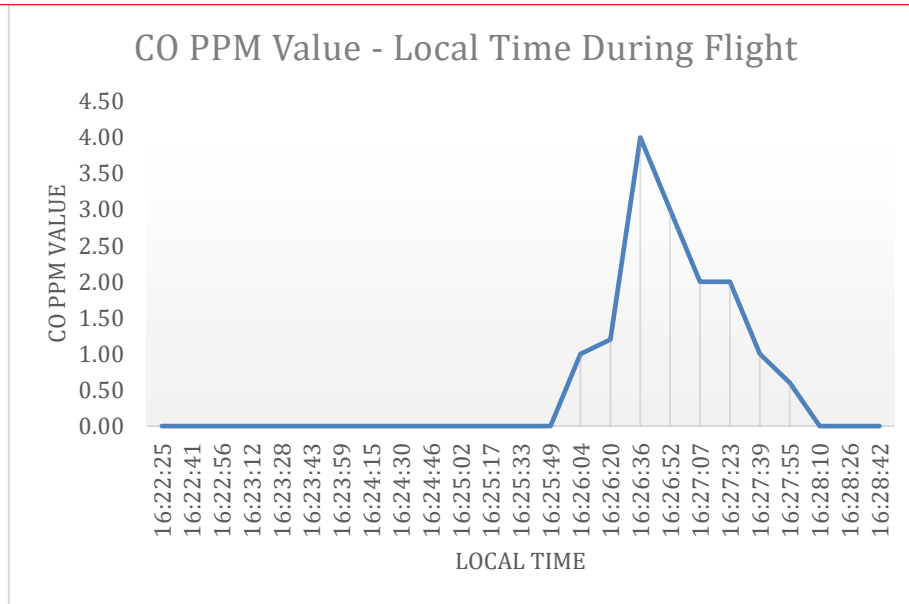


Figure 1. CO PPM Value - Local Time Chart

CONCLUSIONS

The conclusions of the study were detailed in the bases of methodology, challenges, and opportunities. Distancing the sensor and the airflow generated by the UAV components requires attention in these studies. There are applications in the open literature with no precaution and the rest of the applications use a solid boom type extension from the airframe as a conventional method. Thus, the hanging sensor extension used in the study provides a novel method for air quality monitoring UAV concept. Furthermore, the flight altitude of the UAV is not limited by the emission source. If the air pollution source is in ground level, UAV can maintain its flight in a safe altitude and avoid collision risks in the operation environment.

IoT technology utilization in the study provided opportunity to gather and assess data on live transmission. Instead of saving the data on removable drives like an SD card would require human interaction for data assessment. Using IoT, entirely autonomous monitoring could be performed around potential problem sources.

The main drawback of the autonomous monitoring using an AQM UAV is the uncertainties may arise during the operation. Windy air both affects data measurement quality and the UAV flight negatively. Thus, operation under this condition should be avoided for a healthy data acquisition.

REFERENCES

- [1] Falabella, A. D., Wallin, D. O., & Lund, J. A. (2018, June). Application of a customizable sensor platform to detection of atmospheric gases by UAS. In 2018 International Conference on Unmanned Aircraft Systems (ICUAS) (pp. 883-890). IEEE.
- [2] Smith, B. J., John, G., Christensen, L. E., & Chen, Y. (2017, June). Fugitive methane leak detection using sUAS and miniature laser spectrometer payload: System, application and groundtruthing tests. In 2017 International Conference on Unmanned Aircraft Systems (ICUAS) (pp. 369-374). IEEE....
- [3] Abdurouhman, K., Satrio, T., & Muzayadah, N. L. (2018, November). A comparison process between hand lay-up, vacuum infusion and vacuum bagging method toward e-glass EW 185/lycal composites. In Journal of Physics: Conference Series (Vol. 1130, No. 1, p. 012018). IOP Publishing.
- [4] Imdoukh, A., Shaker, A., Al-Toukhy, A., Kablaoui, D., & El-Abd, M. (2017, July). Semi-autonomous indoor firefighting UAV. In 2017 18th International Conference on Advanced Robotics (ICAR) (pp. 310-315). IEEE.
- [5] Goh, C. S., Kuan, J. R., Yeo, J. H., Teo, B. S., & Danner, A. (2019, June). A 100% solar-powered quadcopter with monocrystalline silicon cells. In 2019 IEEE 46th Photovoltaic Specialists Conference (PVSC) (pp. 2829-2834). IEEE.

GREEN HYDROGEN PRODUCTION POTENTIAL IN TURKEY WITH WIND POWER

^{1,2}Ibrahim Dincer, ²Nader Javani, ³Gorkem Kubilay Karayel

¹Faculty of Engineering and Applied Science, University of Ontario Institute of Technology, Oshawa, Ontario, Canada

²Faculty of Mechanical Engineering, Yildiz Technical University, Besiktas, Istanbul, Turkey

³Faculty of Engineering, Istinye University, Istanbul, Turkey

*Corresponding author e-mail: njavani@yildiz.edu.tr

ABSTRACT

The current study is undertaken to investigate the renewable-based hydrogen production potential using wind power in Turkey with the statistical data. The wind energy options in different locations and cities are in this regard considered for both on-shore and off-shore applications. Also, the undersea turbines are considered as a renewable energy potential. The output of generated hydrogen is described in detail for each city and for Turkey as whole, showing a big picture of wind-driven hydrogen generation. It shows a great potential for Turkey to be one of the leaders in green hydrogen production.

Keywords: Green hydrogen, Wind energy, PEM electrolyser, Renewable Energy

INTRODUCTION

Intermittency is recognized as one of the main obstacles for renewable energy resources, particularly for solar and wind sources. One of the solutions is considered through Power to Gas or P2G to overcome this. The output of the main renewable resources, namely wind and solar are electricity, therefore, transforming the produced surplus electricity into a suitable energy carrier is expected to play a big role in improving the renewable energy systems. Hydrogen is treated as a promising energy solution, and there is a synergy among hydrogen, electricity and renewable energies. In terms of hydrogen production methods, two main groups are renewable and non-renewable resources. One can choose among different methods including steam reforming of methane, oil/naphtha reforming, coal gasification, biomass, biological sources and water splitting methods [1-2].

The main idea of developing new infrastructures for hydrogen production is to utilize renewable resources out of the above-mentioned options which will lead to the production of green hydrogen. The concept of hydrogen farm is developed for this purpose in which the available resources are exploited to provide green hydrogen as a sustainable path to feed the economic sectors and their activities [3]. Wind energy and hence wind farms are recognized as very feasible for energy production to be used in the electrolyzers to generate hydrogen. How much potential do we have in different regions of Turkey and more specifically in every city to produce green hydrogen is the main idea behind this study? The energy input to water splitters and the amount of produced hydrogen depends on the type of the electrolyzer. The proton exchange membrane (PEM) type electrolyzers are deployed widely. This type of electrolyzer is considered in this particular study to convert the excess power available from three sources, namely on-shore wind, off-shore wind and undersea current into hydrogen. In this regard, every city in Turkey is studied very carefully for its wind and current sources available and excess power availability after deducting the electricity needs. The hydrogen production potential for every city is then calculated based on the excess power availability.

SYSTEM DESCRIPTION, ANALYSIS AND ASSESSMENT

Electrolysis is known as an easily applicable approach for producing pure hydrogen where water electrolysis is based on the movement of electrons through an external circuit [4]. Table 1 lists the specifications for the polymer membrane (PEM) type electrolyser in the study.

Table 1. Typical specifications of (PEM) type electrolyser.

Specification	PEM
Cell temperature, °C	50-80
Cell pressure, bar	<30
Current density, A/cm ²	0.6-2.0
Cell voltage, V	1.8-2.2
Power Density, W/cm ²	Up to 4.4
Specific energy consumption, kWh/Nm ³	4.5-7.5
Hydrogen production, Nm ³ /h	<300
System lifetime, yr	10-20
Hydrogen purity, %	>99.999

In the current study, a PEM electrolyser with an efficiency of 80% is considered for hydrogen production. Turkey's average wind speed both in onshore and offshore areas, changes between 3.5 and 13.26 m/s as published by the General Directory of Meteorology [5]. This value increases in offshore areas. In this study, wind turbine with an 80 m height and 90 m wing length taken into account with a coefficient of 40% for both onshore and offshore calculations. For undersea commercial type turbine with a cut in speed 0.14 m/s is chosen because the undersea current potential is not very strong in Turkey.

RESULTS AND DISCUSSION

In this study, Turkey's wind power sources are divided into two potential areas, namely onshore and offshore applications. For the coastal cities, the potential undersea current is also considered. There are many cities in Turkey where mountains

are available. Some specific location factors are considered for identifying the availability for every location, including mountainous areas. Table 2 lists total hydrogen production potentials in Million tons (Mt) using wind power for onshore and offshore regions along with the undersea current power.

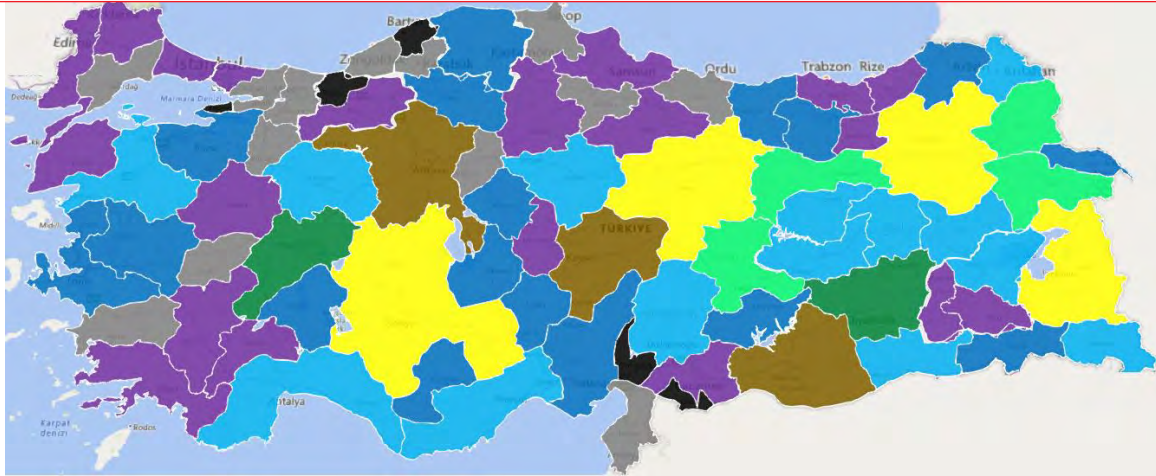
Table 2. Total hydrogen production potential for every city.

No.	City	Average Speed (m/s)	Hydrogen Production (Mt)	No.	City	Average Speed (m/s)	Hydrogen Production (Mt)
1	Adana	5.14	2.75	42	Konya	5.65	11.57
2	Adıyaman	4.11	2.33	43	Kütahya	5.54	1.39
3	Afyon	5.65	4.43	44	Malatya	4.5	5.27
4	Ağrı	6.2	5.02	45	Manisa	5.65	2.04
5	Amasya	5	0.78	46	Maraş	6.68	3.98
6	Ankara	6.6	6.66	47	Mardin	4.7	3.05
7	Antalya	4.16	6.79	48	Muğla	5.65	3.24
8	Artvin	4.11	2.15	49	Muş	4.5	3.68
9	Aydın	5.14	1.15	50	Nevşehir	5.11	1.43
10	Balıkesir	6.17	3.58	51	Niğde	5.09	2.68
11	Bilecik	5.1	0.69	52	Ordu	5.9	1.01
12	Bingöl	5.6	3.46	53	Rize	3.90	1.13
13	Bitlis	5.1	3.47	54	Sakarya	5.65	0.81
14	Bolu	5.09	1.27	55	Samsun	6.17	1.57
15	Burdur	5.7	1.64	56	Siirt	4.16	1.76
16	Bursa	5.14	2.3	57	Sinop	5.65	1.76
17	Çanakkale	8.23	2.84	58	Sivas	7.20	11.09
18	Çankırı	4.1	2.53	59	Tekirdağ	6.68	1.14
19	Çorum	5.11	1.82	60	Tokat	6.17	1.47
20	Denizli	4.6	1.82	61	Trabzon	4.01	1.41
21	Diyarbakır	4.5	4.7	62	Tunceli	4.0	3.1
22	Edirne	6.68	1.75	63	Urfa	7.0	6.4
23	Elazığ	4.16	3.97	64	Uşak	5.65	0.81
24	Erzincan	5.8	5.64	65	Van	5.10	11.75
25	Erzurum	5.65	11.06	66	Yozgat	6.17	3.24
26	Eskişehir	4.16	2.97	67	Zonguldak	5.2	1.11
27	Gaziantep	6.17	1.53	68	Aksaray	4.8	2.71
28	Giresun	4.5	2.03	69	Bayburt	5.16	1.65
29	Gümüşhane	5.3	2.29	70	Karaman	4.5	2.02
30	Hakkari	5.1	3.25	71	Kırkkale	4.9	0.78
31	Hatay	6.6	1.31	72	Batman	4.1	1.81
32	Isparta	5	2.19	73	Şırnak	4.0	2.39
33	Mersin	5.1	3.25	74	Bartın	4.0	0.99
34	Istanbul	6.68	2.25	75	Ardahan	6.6	2.81
35	Izmir	5.65	4.18	76	Iğdır	3.5	2.01
36	Kars	5.5	5.11	77	Yalova	6.17	0.28
37	Kastamonu	5.4	2.72	78	Karabük	4.7	0.67
38	Kayseri	6.17	6.38	79	Kilis	5.9	0.09
39	Kırklareli	6.8	1.28	80	Osmaniye	4.5	0.38
40	Kırşehir	5.1	2.01	81	Düzce	4.1	0.37
41	Kocaeli	4.8	0.96		Total		235.15

Figure 1 shows hydrogen energy map for Turkey in terms of hydrogen production potential using the excess power coming out of the onshore wind power in every city. The color codes are provided depending on the average wind speeds. The locations with highest hydrogen production potential are shown in yellow while the black areas have insufficient potentials to generate hydrogen. The offshore wind energy potential is also considered in this study. The offshore wind increases the hydrogen production potential for cities, particularly for the ones on coastal areas. Figure 2 shows both offshore wind potential and undersea current potential cumulatively for every city.

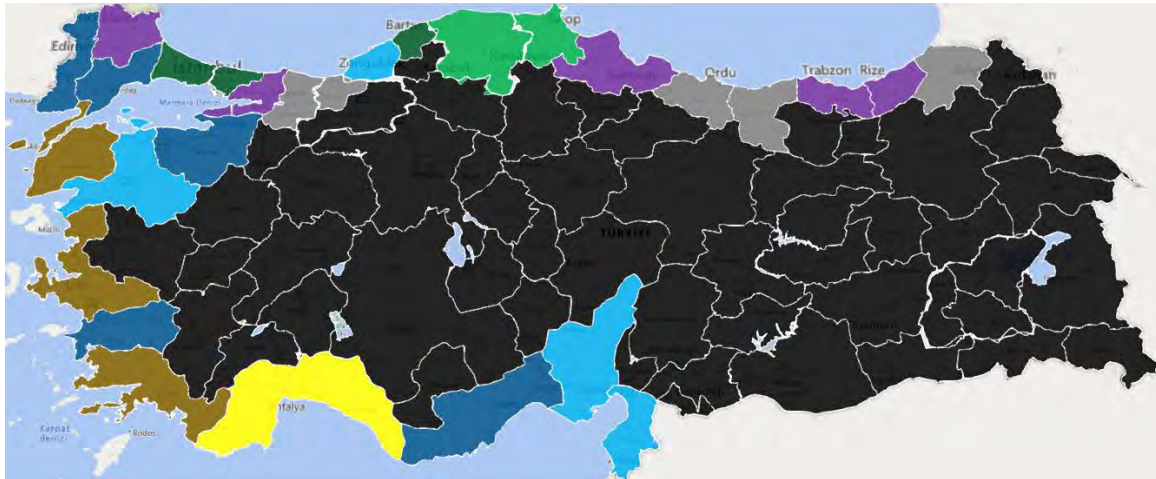
CONCLUSIONS

This paper has aimed to study the hydrogen production potential of Turkey by utilizing the excess electricity potentially available from wind and undersea current sources. This study has considered 81 cities together for cumulative potential of Turkey to play a critical role with its wind power. The results of the current study have shown that wind energy potential is a promising alternative resource for hydrogen production in different zones of Turkey using the actual data available.



Color	Total Production Potential (Mt)	Color	Total Production Potential (Mt)
Black	From 0 to 0.39	Green	From 3.98 to 4.7
Grey	From 0.39 to 0.95	Light Green	From 4.7 to 5.64
Purple	From 0.95 to 1.82	Brown	From 5.64 to 6.66
Blue	From 1.82 to 2.72	Yellow	From 6.66 to 11.75
Light Blue	From 2.72 to 3.98		

Figure 1. Hydrogen production potential based on the excess power coming out of onshore wind power.



Color	Total Production Potential (Mt)	Color	Total Production Potential (Mt)
Black	0	Green	From 0.48 to 0.61
Grey	From 0 to 0.08	Light Green	From 0.61 to 0.89
Purple	From 0.08 to 0.15	Brown	From 0.89 to 1.73
Blue	From 0.15 to 0.26	Yellow	From 1.73 to 3.17
Light Blue	From 0.26 to 0.48		

Figure 2. Hydrogen production potential based on the excess power coming out offshore wind and undersea current.

REFERENCES

- [1] Seyitoglu SS, Dincer I, Kilicarslan A. Energy and exergy analyses of hydrogen production by coal gasification. *International Journal of Hydrogen Energy*. 2017 Jan 26;42(4):2592-600.
- [2] Abuadala A, Dincer I. A review on biomass-based hydrogen production and potential applications. *International Journal of Energy Research*. 2012 Mar 25;36(4):415-55.
- [3] Dincer I, Javani, N., Karayel K.G. Hydrogen Farm Concept: An Application for Turkey. *International Journal of Energy Research*, 2021, Article DOI: 10.1002/er.7086
- [4] Godula-Jopek A. *Hydrogen Production by Electrolysis*. Germany: Wiley-VCH, (2015)
- [5] General Directorate of Meteorology, website, visited 01.07, 2021, <https://www.mgm.gov.tr/>

BLUE H₂ GENERATION BY STEAM REFORMING OF SYNTHETIC BIOGAS IN A MEMBRANE REACTOR PACKED WITH A NOVEL RUTHENIUM-NICKEL CATALYST

^{1*} A. Iulianelli, ² C. Italiano, ¹ M. Manisco, ¹ A. Brunetti, ¹ A. Figoli, ² G. Drago Ferrante, ² L. Pino, ² A. Vita
¹ Institute on Membrane Technology - Italian National Research Council – Rende, Italy
² The Advanced Energy Technology Institute - Italian National Research Council - Messina, Italy

*Corresponding author e-mail: a.iulianelli@itm.cnr.it

ABSTRACT

This work focuses on the generation of blue hydrogen by steam reforming of a synthetic biogas mixture (CH₄:CO₂ = 60:40) in a Pd-Ag membrane reactor, packed with a novel Ru-Ni catalyst, prepared via solution combustion method. The experimental campaign was carried out at 400 °C, weight hourly space velocity (WHSV) of 0.2 h⁻¹, H₂O/CH₄ feed molar ratio between 1.5 and 2 and reaction pressure between 150 kPa and 250 kPa. As best result, the membrane reactor converted 99% of the inlet CH₄, recovering a CO_x-free hydrogen stream in the permeate side and reducing the CO₂ content present in the inlet biogas stream of around 90%.

Keywords: hydrogen, membrane reactor, biogas reforming, CO₂ reduction

INTRODUCTION

Nowadays, the necessity of pursuing a sustainable development is passing through the utilization of new and more eco-friendly energy carriers. Among them, hydrogen is receiving particular attention as it is seen as the fuel of the future to drive the society towards a green and decarbonized World [1]. Industrially, most of the hydrogen produced today comes from the steam reforming of natural gas [2]. According to the requests to limit the utilization of fossil fuels and favor the exploitation of bio-derived sources, biogas and biomethane have been recently proposed as an alternative to the natural gas to generate hydrogen through reforming reactions, with the objective of reducing the greenhouse gases pollution, under the perspective of the net-zero carbon emission [3]. In the meanwhile, membrane reactors (MRs) are receiving considerable interest as alternative devices able to generate and purify hydrogen simultaneously in only one stage process [4]. Combining biogas and MRs to generate blue hydrogen may represent a valid option to the conventional multi stages process. The aim of this experimental work is to generate blue hydrogen by steam reforming of a synthetic biogas over a novel bimetallic (Ru-Ni) catalyst, recovering a CO_x-free hydrogen stream in the permeate side and reducing the CO₂ amount present in the inlet stream.

DISCUSSION

Figure 1 shows that, during the biogas steam reforming tests at 400 °C, H₂O:CH₄ = 2:1 and WHSV = 0.2 h⁻¹, CH₄ conversion in the MR increased with the pressure up to 99%, meanwhile favoring a larger recovery of CO_x-free H₂ in the permeate side (> 30% at 250 kPa) due to the enhanced H₂ permeation driving force through the membrane (higher transmembrane pressure). Furthermore, the removal of H₂ from the reaction towards the permeate side promoted the shift of the steam reforming reaction, which was emphasized at higher pressure, globally favoring the inlet CO₂ reduction up to achieving almost 90% at 250 kPa.

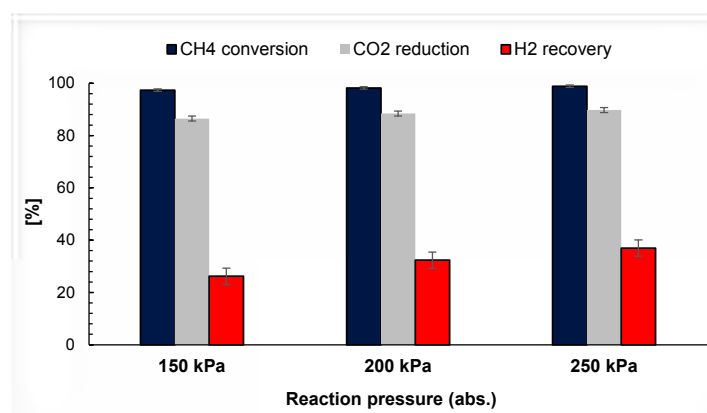


Figure 1. CH₄ conversion, CO₂ reduction and H₂ recovery vs reaction pressure during the steam reforming of biogas in a MR exercised at 400 °C, H₂O:CH₄ = 2:1, WHSV = 0.2 h⁻¹.

Comparing the performance of the MR with an equivalent conventional reformer exercised at the same conditions, a general decrease of CH₄ conversion and CO₂ reduction were observed by increasing the pressure, caused by the adverse thermodynamic, reaching at 250 kPa the values of around 40 and 26%, respectively.

CONCLUSIONS

A Pd-Ag MR packed with a novel Ru-Ni catalyst was used to carry out the steam reforming of a synthetic biogas mixture reaching almost complete CH₄ conversion at 400 °C, well below the normal industrial temperature used to perform the steam reforming of CH₄ (700-900 °C) and recovering more than 30% of CO_x-free H₂ in the permeate stream at 250 kPa and stoichiometric feed ratio. Furthermore, comparing the results between the MR and an equivalent conventional reformer operated at the same conditions, the MR showed superior performance in terms of either CH₄ conversion either inlet CO₂ reduction, demonstrating to be a valid and advantageous alternative to generate blue H₂ with respect to the conventional reactors.

ACKNOWLEDGEMENTS

The project “Mission Innovation” – Scientific Agreement (21A03302) (GU Serie Generale n.133 del 05-06-2021) between the Italian Ministry of the Economic Development and the Italian National Agency for New Technologies Energy and Sustainable Economic Development - , and the Italian Ministry of Economic Development in the framework of the “Fondo per la Ricerca di Sistema Elettrico - Piano Triennale 2019-2021 - Progetto Sistemi di accumulo, compresi elettrochimico e power to gas, e relative interface con le reti - are particularly acknowledged for co-funding this work.

REFERENCES

- [1] IEA report (G20, Japan – 2019): The Future of Hydrogen, Seizing today’s opportunities. https://iea.blob.core.windows.net/assets/9e3a3493-b9a6-4b7d-b499-7ca48e357561/The_Future_of_Hydrogen.pdf
- [2] A. Iulianelli, S. Liguori, J. Wilcox, A. Basile, Advances on methane steam reforming to produce hydrogen through membrane reactors technology: a review, *Catalysis Reviews Science and Engineering*, 58 (2016) 1-35.
- [3] C. Antonini, K. Treyer, A. Streb, M. van der Spek, C. Bauer, M. Mazzotti, Hydrogen production from natural gas and biomethane with carbon capture and storage – A techno-environmental analysis, *Sustainable Energy & Fuels*, 4 (2020) 2967.
- [4] T.Y. Amiri, K. Ghasemzadeh, A. Iulianelli, Membrane reactors for sustainable hydrogen production through steam reforming of hydrocarbons, *Chemical Engineering and Processing: Process Intensification*, 157 (2020) 108148.

EXPERIMENTAL STUDIES TO IMPROVE THE PERFORMANCE, EMISSION AND COMBUSTION CHARACTERISTICS OF SWEET ALMOND OIL FUELED CI ENGINE USING HYDROGEN INJECTION IN PCCI MODE

¹V. Edwin Geo, ²S.Thiyagarajan ³Ankit Sonthalia

¹ Green Vehicle Technology Research Centre, Department of Automobile Engineering, SRM Institute of Science and Technology, Kattankulathur, Tamil Nadu, India

² Department of Automobile Engineering, SRM Institute of Science and Technology, NCR Campus, Modi Nagar 201204, India

*Corresponding author e-mail: vedwingeo@gmail.com

ABSTRACT

Diesel engine is the prime mover of any economy. However, it emits harmful emissions which are a serious health issue for the humans, and it is also a cause of global warming. The consumption of diesel is also very high and the fossil fuel is depleting at an alarming rate. Therefore, it is imperative to look for alternates to diesel. One such alternate is the use of biomass-based fuel. In the present study 20% sweet almond oil was mixed with diesel on volume basis and engine tests were carried out. To further improve the engine performance and reduce emissions, hydrogen was inducted in the inlet manifold at different flow rates. The highest improvement in engine characteristics were observed at 30 LPM (litre per minute) flow rate of hydrogen. The thermal efficiency improved by 8.38% at full load for 30LPM flow rate of hydrogen as compared to blend fuel operation. Moreover, HC, CO and smoke emission for the same flow rate showed a maximum reduction of 70%, 56% and 27%, respectively, whereas NO_x emission increased by 14% as compared to engine operation with only blend.

Keywords: Sweet almond oil, Hydrogen, Emission reduction

INTRODUCTION

The growth of economy of any country is dependent upon energy. A report by International Energy Agency says that by the year 2040, the energy requirement of the world will increase by 40% of its present energy requirement and India's energy requirement will be doubled [1]. To cater to its requirement for fuel, India imports oil from Saudi Arabia, Iran, Iraq and the USA. The issue with using petroleum oil is its rapid depletion and its negative effects on the environment [2,3]. Therefore countries are moving towards biomass based fuels which are renewable in nature, non-toxic and biodegradable [4]. For compression ignition (CI) engines, biofuels as a fuel is being emphasized upon in last two decades. Since the CI engines are the preferred prime movers in the transportation and off-road sectors.

In the present work, the feasibility of using 20% blend of sweet almond oil in diesel as a fuel for a single cylinder diesel engine is studied. Then hydrogen was inducted in the intake manifold and the engine's performance and emission characteristics at various flow rates of hydrogen were studied. Since India has a huge population of single cylinder diesel engines therefore the characteristics of a dual fuel engine is worth studying.

RESULTS AND DISCUSSION

The engine used in the present study is a four-stroke, water-cooled, direct injection single cylinder diesel engine. The engine was manufactured by Kirloskar. The engine was loaded with the help of a water-cooled eddy current dynamometer. The fuel flow rate was measured using a burette and a stop watch. The engine exhaust emissions namely HC, CO and NO_x were measured using an AVL gas analyzer. While the smoke opacity was measured using an AVL smoke meter. 20% blend of sweet almond oil with diesel and varying hydrogen flow rates (0 LPM – 30 LPM) were used for operating the engine. The engine was loaded from no load to full load in steps of 25%. The data was taken when the engine reached stable conditions.

The variation in brake thermal efficiency with load for 20% blend of sweet almond and diesel, with and without hydrogen induction is shown in Fig. 1. It is seen that the efficiency increases with increase in load for all the test fuels as more fuel is injected with increase in load thereby releasing more heat energy. Also, as the hydrogen flow rate is increased the thermal efficiency increases and the maximum efficiency was observed with the highest flow rate of hydrogen. Since hydrogen is homogeneously mixed with air, the start of combustion causes the hydrogen to burn almost instantly and as hydrogen has a very high flame velocity, the entire combustion chamber is engulfed within no time.

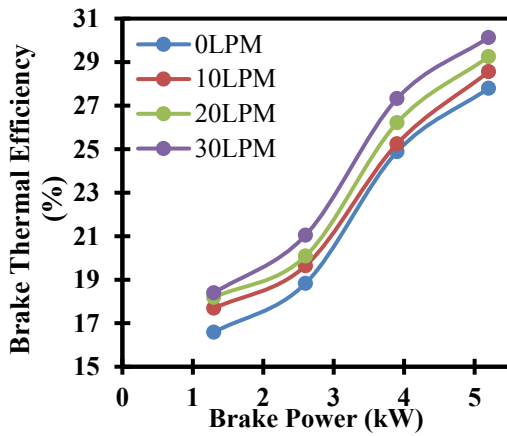


Fig. 1 Brake thermal efficiency versus brake power

The variation in unburned hydrocarbon emission is given in Fig. 2. The emission increases with increase in load for all the test fuels. The HC emission with hydrogen induction was lower than neat blend operation at all the loads. Increase in hydrogen flow rate resulted in decrease in emission and the lowest emission was observed with the maximum flow rate of hydrogen. The decrease in emission with hydrogen induction can be attributed to the substitution of carbon containing fuel with zero carbon fuel. Another reason for decrease in emission is the improvement in combustion with hydrogen as the flame reaches the crevices where the fuel is generally left unburnt. The variation in CO emission with load for the test fuels is shown in Fig. 3. It is seen that the CO emission increases with increase in load for all the test fuels.

The CO emissions are formed when the oxygen availability is less and there are local fuel rich zones. As hydrogen replaces the liquid fuel, the emission is reduced and with increase in substitution the emission further reduces. As discussed previously, hydrogen is a carbon free gas hence on its combustion no carbon products are formed. However, the emission is formed due to the carbon containing blend. As the flame speed increases the turbulence in the cylinder increases which in turn allows the fuel molecules to find oxygen resulting in the near complete combustion of fuel thereby lowering the CO emission.

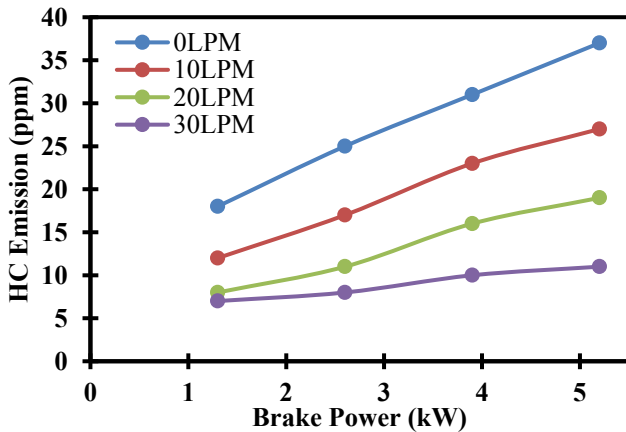


Fig. 2 Unburned hydrocarbon emission versus brake power

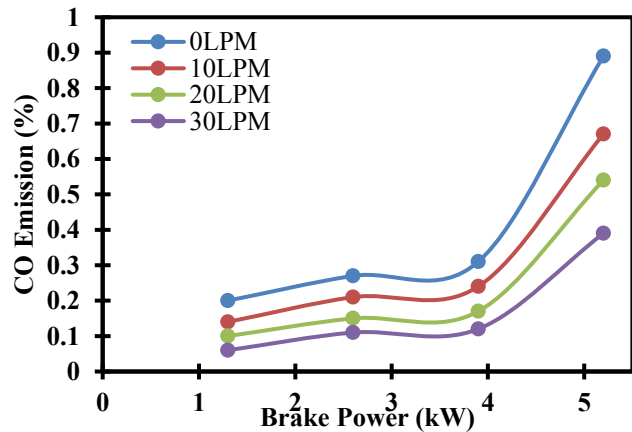


Fig. 3 Carbon Monoxide emission versus brake power

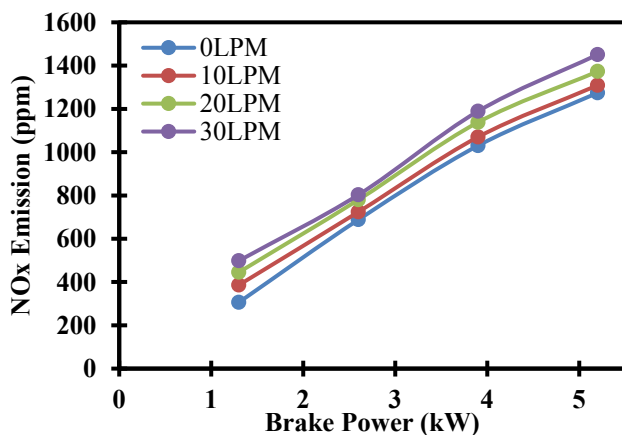


Fig. 4 Oxides of nitrogen emission versus brake power

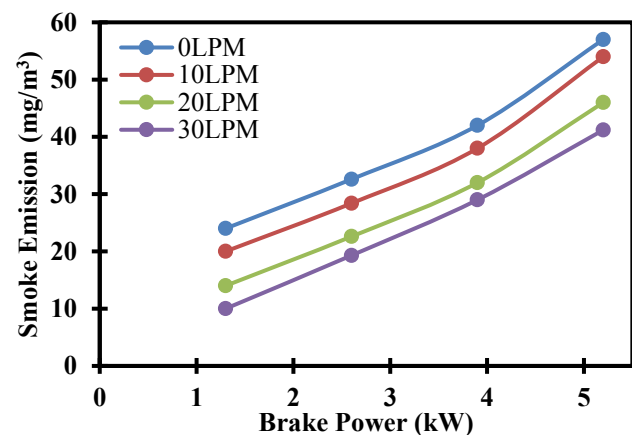


Fig. 5 Smoke emission versus brake power

The variation in NO_x emission with engine load is shown in Fig. 4. It is seen that the NO_x emission increases with increase in load. The 20% blend of sweet almond oil and diesel resulted in lowest NO_x emission since the combustion temperature and pressure was lowest with the fuel. As the high combustion temperature and pressure are the main reasons for NO_x formation. Another reason for NO_x formation is the presence of excess oxygen which is generally present in a diesel engine as the engine operates on lean mixtures. With the induction of hydrogen, the emission increases and as the flow rate increases the emission further increases. As hydrogen burns almost instantly, the heat

is released at a very high rate and the rate of pressure rise is also very high resulting in an environment conducive enough for oxidation of nitrogen.

Fig. 5 shows the variation of the smoke opacity with load. The opacity increases with increase in load for all the test fuels. The highest emission was observed with the blend in single fuel mode. Induction of hydrogen in the intake manifold resulted in decrease in emission and with the increase in hydrogen flow rate the emission further decreases. Soot particles are formed due to thermal pyrolysis of the fuel molecules in absence of oxygen. As hydrogen replaces the carbon containing liquid fuel the probability of fuel getting pyrolyzed reduces thereby reducing the smoke emission. Also, the increase in turbulence due to burning of hydrogen allows the liquid fuel to burn in presence of oxygen thereby further reducing the emission.

CONCLUSIONS

In the present study, the performance and emission characteristics of a compression ignition engine were studied. 20% blend of sweet almond oil and diesel was selected for reduction in engine out emission and improvement in performance. To further improve the engine characteristics, hydrogen was inducted in the intake manifold at different flow rates (10LPM – 30LPM). At maximum flow rate of hydrogen, the maximum improvement in thermal efficiency was observed. At full load the thermal efficiency improved by 8.38% as compared to the engine operation with the sweet almond oil blend in single fuel mode. Similarly, a reduction in HC, CO and smoke emission was observed with hydrogen induction for all the loads. As the percentage substitution of hydrogen increases the emissions reduces. The maximum reduction in emission was observed at 30LPM flow rate of hydrogen. The HC, CO and smoke emission emissions reduced by 70%, 56% and 27% as compared to single fuel mode engine operation. Moreover, NO_x emission increased by 14%. The study shows that the combination of hydrogen and sweet almond oil can give the dual benefit of improvement in engine performance and reduction in engine emission.

REFERENCES

- [1] I. International Energy Agency, "World Energy Outlook 2018," 2018.
- [2] Y. Huang, L. Wei, J. Julson, Y. Gao, and X. Zhao, "Converting pine sawdust to advanced biofuel over HZSM-5 using a two-stage catalytic pyrolysis reactor," *J. Anal. Appl. Pyrolysis*, vol. 111, pp. 148–155, Jan. 2015.
- [3] Y. Huang, L. Wei, Z. Crandall, J. Julson, and Z. Gu, "Combining Mo–Cu/HZSM-5 with a two-stage catalytic pyrolysis system for pine sawdust thermal conversion," *Fuel*, vol. 150, pp. 656–663, Jun. 2015.
- [4] Y. Huang *et al.*, "Upgrading pine sawdust pyrolysis oil to green biofuels by HDO over zinc-assisted Pd/C catalyst," *Energy Convers. Manag.*, vol. 115, pp. 8–16, 2016.

IMPROVEMENT OF TERMINAL BUILDINGS' ENVIRONMENTAL PERFORMANCE BY RENEWABLE ENERGY

^{1*} Alper Dalkıran, ² O. Ballı, ³ M. Ziya Söğüt, ⁴ T. Hikmet Karakoç

¹ Suleyman Demirel University, School of Aviation, Isparta, Turkey

² First Air Maintenance Factory Directorate (1.HBFM), Ministry of National Defence (MND), Eskişehir, Turkey

³ Piri Reis University, The Department of Marine Engineering, İstanbul, Turkey

⁴ Eskişehir Technical University, Faculty of Aeronautics and Astronautics, Eskişehir, Turkey

*Corresponding author e-mail: alperdalkiran@sdu.edu.tr

ABSTRACT

Energy consumption of the airport terminals is intensive due to the passenger circulation and the enormous amount of closed volume. On the other hand, terminal buildings compromises service layers, food and beverage area, offices and shopping areas consumes high energy too. The energy consumption in these areas creates a severe environmental effect in the neighbourhood area. This paper is focused on highlighting the differences in environmental effects when using renewable energy.

Keywords: Airport terminal buildings, Environmental effects, Energy consumption, Renewable energy, Environmental performance

INTRODUCTION

Airport terminals consume energy in three main sections: heating, ventilating and chilling (HVAC) of the building spaces, lighting of the areas, and the automation conveyors for the people and luggage items [1]. There have been many technological developments made for the current lighting technologies. These technological attempts ended with numerous transition projects to the light effect diode (LED) lighting in the airport terminal buildings [2]. LED technology can be developed into some intelligent technologies for the lighting of airport terminals [3]. Lighting comfort is an essential subject like the thermal and other amenities like automation systems in airports. Although information technology consumes power in the airport terminal buildings, computers and the system rooms consume high power as neither the automation devices nor the lighting implementation.

On the other hand, heating, ventilating, and chilling systems consume much higher energy in airports, considering the environmental effects of the used energy type. The change in the energy supply can reduce the environmental effects caused by the consumption of energy. However, more efficient approaches to control environmental heat comfort control the zones in the large space buildings like airport terminal buildings [4]. Zonal modelling will help to improve the building's thermal comfort and efficient energy consumption by the terminal management.

The automation devices in the terminal buildings can be divided into two parts as passenger used devices and baggage systems. Baggage belts can assume 5 kW for each 10-meter part, carry 600 kilograms, and workload differs on the operating conditions of the slope [5]. The total baggage capacity for the airport will change by the length of the baggage system and the load on the belt system. Passenger travelators, escalators, and lifts are other automation parameters for the airport terminal energy consumption. This part of the problem can be solved by counting the number of items in the airport terminal [6].

MATERIALS AND METHODS

The HVAC systems cause the biggest input variable for the airport energy consumption because of the intense nature of heating energy compared to the mechanical needs of the terminal's baggage conveyors or lighting needs.

Table 1: Water cooled chiller capacity and COP ranges for the airports related part-load values [7]

Chiller Type	Capacity Range (tons)	COP Range	IPLV Range (COP)
Reciprocating/Scroll	50 - 230 (400)	4.2 - 5.5	4.6 - 5.8
Screw	70 - 400 (1250)	4.9 - 5.8	5.4 - 6.1
Centrifugal	200 - 2000 (10,000)	5.8 - 7.1	6.5 - 7.9
Single-Effect Absorption	100 - 1700	0.60 - 0.70	0.63 - 0.77
Double-Effect Absorption	100 - 1700	0.92 - 1.20	1.04 - 1.30
Engine Driven	100 - 3000 (10,000)	1.5 - 1.9	1.8 - 2.3

Table 1 summarizes the installation capacity for the chillers of airport terminals. Although the coefficient of performance (COP) can be higher in some small-sized chiller units in HVAC, many other components consume energy or affect the environment by evaporating water in cooling towers. On the other hand, integrated part-load value (IPLV) defines the similar performance of the equipment and can be used for the total load of the chiller unit. There are similar energy-

based assumptions and calculations for the heating part of the HVAC systems. In each type of energy consumption, there will be the cost of environmental performance can be calculated by the below exergy and exergo-economic equations [8].

$$\dot{E}x_Q + \sum_i \dot{m}_i ex_i = \sum_e \dot{m}_e ex_e + \dot{E}x_W + \dot{E}x_D \quad (1)$$

$$\dot{C}_{Q,gen} + \dot{C}_P + \dot{Z}_{chiller} = \dot{C}_{Q,eva} \quad (2)$$

Where \dot{E} is the exergy rate and \dot{C} represents the cost of the system. \dot{m} describe the mass flow rates of the appropriate system components. \dot{Z} represents the function of the cooling capacity of the chiller. The indices of Q shows the heat rejection rate of each chiller unit. As W indicates the work and D indicates the destruction rate of the relevant chiller system.

The Chiller system's main parts have been described in the Fig. 1. Absorber, Solution Heat Exchanger, Generator, Condenser, and Evaporator are the system's main components. These components have their thermodynamic analyses, and each of them can be calculated by their inputs and outputs. The environmental performance of the terminal building can be calculated after the total energy and work are calculated.

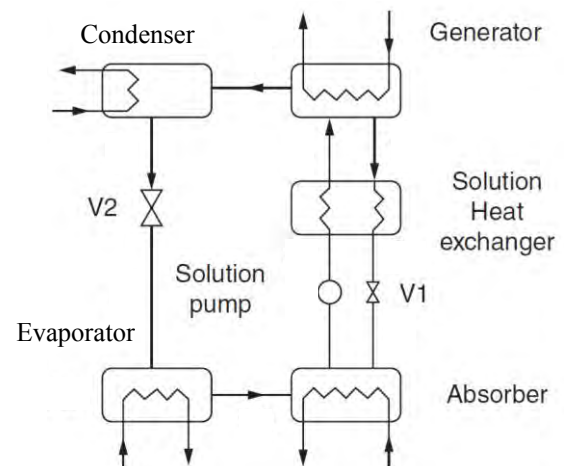


Fig. 1: A diagram for an absorption chiller [8]

The heating system's thermodynamic, exergetic and exergo-economic analyses can be done by each of the systems. These analyses will show the performance of the terminal building. Terminal building's design and HVAC efficiency will guide the points to improve environmental performance. These points can be exploited on the lighting strategy and automation smart-start approaches [9]. The energy consumption and energy used in the working areas will highlight the energetic environmental impact.

CONCLUSIONS

The complex energetic environmental effects and the guide points have been given for the large airport terminal buildings in this study. The major impact for environmental performance has been defined as HVAC systems. The lighting and electrical automation systems have been considered as a secondary effect in these buildings.

REFERENCES

- [1] DALKIRAN A, SOGUT MZ, ACIKKALP E, KARAKOÇ TH. INVESTIGATION OF AIRPORT TERMINAL BUILDINGS' ENVIRONMENTAL ENERGY SUSTAINABILITY WITH ECO-INDICATORS. In: Javani N, Sorgulu F, editors. World Energy Strateg Congr Exhib [Internet]. Istanbul: Yıldız Technical University; 2019. p. 236–41. Available from: https://wesce.com/wp-content/uploads/2019/11/Wesce_Proceedings_Final-Version.pdf
- [3] Alba SO, Manana M. Energy research in airports: A review. Energies [Internet]. 2016;9:1–19. Available from: <https://www.mdpi.com/1996-1073/9/5/349>
- [3] Tzempelikos A. Development and Implementation of Lighting and Shading Control Algorithms in an Airport Building. J Archit Eng. 2012;18:242–50.
- [4] Lu Y, Dong J, Liu J. Zonal modelling for thermal and energy performance of large space buildings: A review. Renew Sustain Energy Rev. Pergamon; 2020;133:110241.
- [5] Axles W. TECHNICAL SPECIFICATION OF BAGGAGE CONVEYOR-8MTR [Internet]. [cited 2021 Jul 20]. p. 1–6. Available from: <https://www.airport-suppliers.com/wp-content/uploads/2017/08/TRANSTEC-8MTR-CONVEYOR.pdf>
- [6] Dalkiran A. Investigation of Energy Consumption Based Environmental Sustainability in Airports: A Suggestion for Environmental Effects Per Passenger [Internet]. Anadolu Univeristy - Graduate School of Science; 2017 [cited 2020 Aug 15]. Available from: <https://earsiv.anadolu.edu.tr/xmlui/handle/11421/6489>
- [7] Taylor ST. Chilled Water Plant Design Guide. Energy Des Resour [Internet]. 2009;281. Available from: https://www.taylor-engineering.com/wp-content/uploads/2020/04/EDR_DesignGuidelines_CoolToolsChilledWater.pdf
- [8] Dincer I, Rosen MA, Ahmadi P. Optimization of Energy Systems [Internet]. JohnWiley & Sons Ltd; 2017. Available from: <https://www.wiley.com/en-us/Optimization+of+Energy+Systems-p-9781118894491>
- [9] Trianni A, Cagno E, Accordini D. Energy efficiency measures in electric motors systems: A novel classification highlighting specific implications in their adoption. Appl Energy. Elsevier; 2019;252:113481.

SUGARCANE LEAVES AND TOPS FOR BIOGAS PRODUCTION BY BATCH EXPERIMENTS

^{1*} Nusara Sinbuathong, ² Boonsong Sillapacharoenkul, ³ Roj Khun-anake, ¹Yupadee Paopun

¹ Kasetsart University, Kasetsart University Research and Development Institute (KURDI), Scientific Equipment and Research Division, Bangkok 10900, Thailand.

² King Mongkut's University of Technology North Bangkok, Faculty of Applied Science, Department of Agro-Industrial, Food and Environmental Technology, Bangkok 10800, Thailand

³ Thammasat University, Faculty of Science and Technology, Department of Environmental Science, Pathumtani 12121, Thailand

*Corresponding author E-mail: rdinrs@ku.ac.th

ABSTRACT

The digestion of a slurry of sugarcane leaves and tops was compared with the co-digestion of a mixture of sugarcane leaves and tops and cow manure. The substrate slurry of sugarcane leaves and tops:cow manure:water at the ratio of 20:0:80 and that of the ratio 10:10:80 were prepared as the substrate for digestion and co-digestion, respectively. Fifty-milliliter syringes were used as anaerobic batch reactors in a trial to compare biogas production. Experiments were performed at 30 °C. The methane (CH₄) yield from the system was used as an indicator of the reactor performance. The results showed that the CH₄ yield obtained from the co-digestion of a slurry of sugarcane leaves and tops with cow manure was 145 L at standard temperature and pressure (STP)/kg chemical oxygen demand (COD) degraded while that of the digestion of sugarcane leaves and tops was 61 L at STP/COD degraded. The pH of the reactor for digestion was acidic and showed at 6.48 while that for co-digestion was just over neutral and showed at 7.33.

Keywords: Agricultural waste, Anaerobic digestion, Biogas, Renewable energy, Sugarcane

INTRODUCTION

Nowadays, there is an increasing awareness that renewable energy is crucial for creating economic opportunities and protecting the environment. Anaerobic digestion is the bioreaction process for biogas production which can change agricultural wastes into renewable sources of energy. Leaves and tops of sugarcane can be sources of renewable energy because they have the ability to generate electricity [1] that increases energy costs to protect the industry from economic decline. The harvesting of sugarcane is mostly done by labour or by mechanical harvesters. Sugarcane leaves and tops are often burnt prior to harvesting. This causes the increase of particular matter in the environmental perspective. A farmer of the sugarcane crop intends to earn extra income from the leaves and tops available from the sugarcane crop. In this paper, the leaves and tops were studied to be a source of biogas because their nutritional value is superior. The anaerobic co-digestion process is a reliable way to solve the disadvantages of a single substrate digestion system concerning substrate characteristics. In this study, the digestion of a slurry of sugarcane leaves and tops was compared with the co-digestion of a mixture of sugarcane leaves and tops and cow manure at 20% solid content. The methane (CH₄) yield from the system was used as an indicator of the reactor performance.

MATERIALS AND METHODS

Ten 50 mL syringes were used as anaerobic batch reactors. The plain tip of syringes was sealed with silicone glue. The mixed substrate slurry of sugarcane leaves and tops:cow manure:water at the ratio of 20:0:80 (a slurry of sugarcane leaves and tops) was prepared as the substrate for digestion and that of 10:10:80 (a slurry of mixed sugarcane leaves and tops with cow manure) was prepared as the substrate for co-digestion. The ratio prepared was recommended by the previous studies [2,3,4]. The initial substrate slurry was analyzed for chemical oxygen demand (COD), total solids (TS), total volatile solids (TVS) and pH. Mixed ruminal microorganisms from cow rumen were used as the inoculum. The inoculum of 4 mL was added in all ten syringes. The bacterial biomass was measured in terms of mixed liquor volatile suspended solids (MLVSS). The prepared substrate slurry of sugarcane leaves and tops was added to four syringes for digestion and the prepared mixed substrate slurry of sugarcane leaves and tops and cow manure was added to another four syringes for co-digestion to make up 20 mL (Fig.1). Blank was prepared by adding inoculum and water (substitute for substrate) in the last two syringes. All ten syringes were placed upstanding in a rack. The bioreaction started at room conditions (30°C). The produced biogas in syringes was recorded every day and was sampled for CH₄ analysis. A Shimadzu GC-2014 gas chromatograph equipped with a thermal conductivity detector was used to quantify the CH₄ content in total biogas. The pH of the digested slurry was recorded every five days. The bioreaction stopped by 57 days when the biogas ceased. At the end of the batch process, the digested slurry was analyzed for COD, TVS, and pH. The experiment was repeated three times under the same conditions. Analysis was performed according to the procedure of the Standard Methods [5] and was conducted in duplicate. The results were calculated and expressed as the mean of the experimental values.

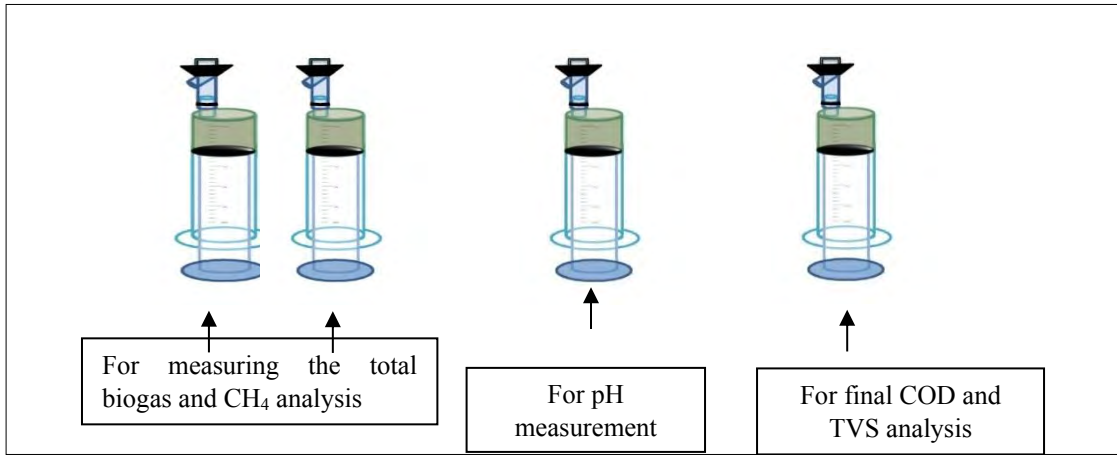


Fig.1. Syringes as anaerobic batch reactors for digestion and co-digestion.

CONCLUSIONS

Sugarcane leaves and tops could be a source of energy to produce biogas by using co-digestion process. The bacterial biomass was recorded approximately 5 g MLVSS/L. The results showed that the pH of the digested slurry in the reactor for digestion was acidic and showed at 6.48 while that for co-digestion was just over neutral and showed at 7.33 which is appropriate for microbial reaction. Co-digestion of the mixture of sugarcane leaves and tops and cow manure gave a higher yield than that of digestion of sugarcane leaves and tops. The methane yield obtained from the co-digestion of a slurry of sugarcane leaves and tops with cow manure was 145 L at STP/kg COD degraded while that of the digestion of sugarcane leaves and tops was 61 L at STP/COD degraded. The addition of different environmentally friendly co-substrate can improve the performance of the anaerobic process. However, the methane yield obtained from this study was still far from the theoretical methane yield (350 L at STP/kg COD degraded) [6]. The process improvement of biogas production from sugarcane leaves and tops still seeks further investigation.

REFERENCES

- [1] Pierossi MA, Bernhardt HW, Funke T. Sugarcane leaves and tops: Their current use for energy and hurdles to be overcome, particularly in South Africa, for greater utilization. *Proceedings of the South African Sugar Technologists' Association*; 2016,89:350–360.
- [2] Sawanon S, Sangsri P, Leungprasert S, Sinbuathong N. Methane Production from Napier Grass by Co-digestion with Cow Dung. Chapter 7 in *Energy Solutions to Combat Global Warming. Lecture Notes in Energy*; 2017. 33:169–180. Edited by Xin-Rong Zhang and Ibrahim Dincer. Springer Nature
- [3] Sinbuathong N, Khun-Anake R, Sawanon S. Biogas production from sunn hemp: *International Journal of Global Warming*; 2019,19(1/2):24–36.
- [4] Sinbuathong N, Sillapacharoenkul B. Enhancement of biogas production from sunnhemp using alkaline pretreatment. *Int J Hydrogen Energy*; 2021,46(6): 4870–4878.
- [5] APHA, AWWA, and WEF. *Standard Methods for the Examination of Water and Wastewater*, 21 st ed. Washington, DC: American Public Health Administration; 2005.
- [6] Tchobanoglous G, Burton FL. *Wastewater Engineering Treatment, Disposal, and Reuse*, Revised from Metcalf & Eddy Inc. 3rd ed. Singapore: McGraw Hill Inc.;1991.

COMPARATIVE SUSTAINABILITY INVESTIGATION OF HYDROGEN PRODUCTION METHODS

^{1, 2*} Canan Acar

¹ Bahcesehir University, Faculty of Engineering and Natural Sciences, Energy Systems Engineering
Ciragan Cad No: 4 – 6 34353 Beşiktaş, Istanbul, Turkey

² University of Twente, Faculty of Engineering Technology, Thermal Engineering, 7500 AE Enschede, The Netherlands

*Corresponding author e-mail: Canan.Acar@eng.bau.edu.tr; C.A.Acar@utwente.nl

ABSTRACT

Hydrogen has a crucial importance in combating global energy challenges. As a carbon-free energy carrier, hydrogen not only can be used to bridge the gap between intermittent renewable energy supply and ever-growing continuous energy demand. Hydrogen can also replace the use of fossil fuels in many applications as a sustainable fuel. Globally, the majority of the hydrogen supply comes from fossil fuels. However, in order to curb emissions causing climate change and address the limited nature of fossil fuels, hydrogen needs to be produced from renewable sources in a sustainable manner. With this motivation in mind, the aim of this study is to comparatively assess the sustainability of hydrogen production methods. Sustainability investigation is conducted by taking various criteria into account to ensure a comprehensive approach. The selected sustainability criteria are energy and exergy efficiencies, production cost, social cost of carbon, global warming and acidification potentials, and technology maturity level. 16 methods are assessed in this study, which are namely electrolysis, plasma reforming, thermolysis, thermochemical water splitting, biomass gasification, PV electrolysis, photocatalysis, photoelectrochemical cell, high temperature electrolysis, hybrid thermochemical cycles, coal gasification, coal gasification with carbon capture, steam methane reforming, steam methane reforming with carbon capture, photofermentation, and artificial photosynthesis.

Keywords: Energy efficiency, Exergy efficiency, Global warming, Hydrogen production, Sustainability

INTRODUCTION

Our heavy fossil fuel-dependent energy systems are the primary driver of climate change. We see the results of climate change in its impacts on the environment, economy, health, biodiversity, and more. Extreme weather events, biodiversity loss, droughts, wildfires, disappearing of Arctic and Antarctic ice, sea-level rise, and loss of agricultural productivity are some of the effects of climate change that are expected to be worsened in the future if no actions are taken. In order to tackle all of the issues related to climate change, stopping the problem at its source, transitioning from fossil fuels to renewables is a must. Hydrogen is the key to enable this transition.

In this study, a comprehensive classification of hydrogen production methods from renewable and non-renewable sources is presented, and these methods are discussed, assessed and compared. 16 hydrogen production technologies are compared based on technology maturity level, energy and exergy efficiencies, production cost, global warming potential (GWP), acidification potential (AP), and social cost of carbon.

MATERIALS AND METHODS

The hydrogen production methods evaluated in this study are given in Table 1. The performance data are taken from the sources [1-3]. The sustainability ranking performance of the selected methods are conducted based on the procedure described in [4].

CONCLUSIONS

The primary sustainability investigation results show the following:

- High temperature electrolysis has the highest and photofermentation has the lowest energy efficiency.
- Hybrid thermochemical cycles have the highest and photofermentation has the lowest exergy efficiency.
- Photoelectrochemical cells have the highest and steam methane reforming has the lowest hydrogen production cost.
- Coal gasification has the highest and photonic based hydrogen production methods have the lowest global warming potential.
- Biomass based hydrogen production options have the highest and photonic based hydrogen production methods have the lowest acidification potential.
- Overall performance investigation shows that in the short term, steam methane reforming with carbon capture has the highest potential.

Table 1. Selected hydrogen production methods.

Method		Source		Brief Description
		Primary Energy	Material	
M1	Electrolysis	Electrical	Water	Direct current is used to split water into O ₂ and H ₂ (electrochemical reaction)
M2	Plasma reforming		Fossil fuels	Cleaned natural gas is passed through plasma arc to generate H ₂ and carbon soot
M3	Thermolysis	Thermal	Water	Thermal decomposition of steam at temperatures over 2500 K
M4	Thermochemical processes		Water splitting	Cyclical chemical reactions (net reaction: water splitting into H ₂)
M5			Gasification	Biomass
M6	PV electrolysis	Photonic	Water	PV panels are used to generate electricity
M7	Photocatalysis			Water is split into H ₂ by using the electron-hole pair generated by the photocatalyst
M8	Photoelectrochemical method			A hybrid cell simultaneously produces current and voltage upon absorption of light
M9	High temperature electrolysis	Electrical + Thermal	Water	Electrical and thermal energy are used together to drive water splitting at high temperatures
M10	Hybrid thermochemical cycles			Electrical and thermal energy are used together to drive cyclical chemical reactions
M11	Coal gasification		Coal	Conversion of coal into syngas
M12	Coal gasification with CC			Conversion of coal into syngas
M13	Natural gas reforming		Natural gas	Fossil fuels are converted to H ₂ and CO ₂
M14	Natural gas reforming with CC			Fossil fuels are converted to H ₂ and CO ₂
M15	Photofermentation	Photonic + Biochemical	Biomass + Water	Fermentation process activated by exposure to light
M16	Artificial photosynthesis			Chemically engineered systems mimic photosynthesis to generate H ₂

REFERENCES

- [1] Parra D, Valverde L, Pino FJ, Patel MK. A review on the role, cost and value of hydrogen energy systems for deep decarbonisation. *Renewable and Sustainable Energy Reviews*. 2019 Mar 1; 101:279-94.
- [2] Wang YJ, Fang B, Wang X, Ignaszak A, Liu Y, Li A, Zhang L, Zhang J. Recent advancements in the development of bifunctional electrocatalysts for oxygen electrodes in unitized regenerative fuel cells (URFCs). *Progress in Materials Science*. 2018 Oct 1; 98:108-67.
- [3] Nikolaidis P, Poullikkas A. A comparative overview of hydrogen production processes. *Renewable and sustainable energy reviews*. 2017 Jan 1; 67:597-611.
- [4] Dincer I, Acar C. Review and evaluation of hydrogen production methods for better sustainability. *International journal of hydrogen energy*. 2015 Sep 14;40(34):11094-111.

HYDROGEN REFUELLING STATIONS: STATE OF THE ART AND PERSPECTIVES

*Doria Marciuš, *Ankica Kovač, Matej Paranos*
University of Zagreb, Faculty of Mechanical Engineering and Naval Architecture, Department of Energy, Power and Environmental Engineering, Ivana Lučića 5, Zagreb, Croatia

*Corresponding author e-mail: ankica.kovac@fsb.hr

ABSTRACT

The rapid development of hydrogen technology over the last decade is the result of the public comprehending the gravity of environmental pollution and global warming necessitating a drastic reduction of greenhouse gas emissions. Hydrogen technology that has the biggest impact in media is a fuel cell electric vehicle (FCEV), no matter its small segment in the overall hydrogen application. For this reason, amongst the other considerable benefits, FCEVs are ideal promoters of a hydrogen society. For hydrogen to progress further into the vehicles industry and for users to comfortably drive FCEVs, it is imperative to build an adequate infrastructure of hydrogen refuelling stations (HRSs). Ergo, the rapidly growing number of HRSs and worldwide interest in forming hydrogen infrastructure, evident through hydrogen strategies incorporated in the newest national policies, are the key indicators of hydrogen technology development overall. This review brings HRSs infrastructure progress over the last decade, the period of the emerging hydrogen market, as well as estimated trends and future perspectives on the global level.

Keywords: Hydrogen, Hydrogen refuelling station, Fuel cell electric vehicles, National hydrogen strategies

INTRODUCTION

Hydrogen in conjunction with renewable energy sources (RES) is established as an accelerant of the ongoing energy transition. The change in people's awareness regarding the severity of climate change as well as the need for implementation of green energy solutions is being reflected through the newest national strategies. On July 14th, 2021, as a part of the European New Green Deal, the European Commission announced a set of proposals 'Fit for 55' with the most enthusiastic target yet, to reduce the greenhouse gas emissions by 55% (relative to 1990) by 2030 [1]. With the newest legislation, European Union (EU) is promoting green hydrogen as a renewable fuel in the transport sector, where the decarbonization progress is slow [2]. The recognized vast potential of hydrogen resulted in a growing number of research and development (R&D) projects in the last decade, presently reaching its peak, with predictions of an even bigger increase [3]. According to Hydrogen Council's report from July 15th, 2021 [4], 359 large-scale projects worldwide with a total investment of circ. USD 500 billion through 2030, have been announced since the last report from February 2021. Moreover, their estimations show that low-carbon hydrogen production capacity will exceed 10 million tons by 2030 (an increase of 60% since February 2021). This positive upward trend is also evident through the fast-rising number of HRSs. The global investments through 2030 in hydrogen-linked transportation projects, which include HRSs, amount to USD 16 billion, which makes transport the second most invested sector, just behind industry [5].

HRS RECENT PROGRESS

By the end of 2020, the number of 100 newly installed HRSs was exceeded for the first time, with an estimation of currently 553 active HRSs in the world [6]. When comparing these data with 2011, the number of installed HRSs increased by 157%. Moreover, in just 6 years, the number of HRSs in the world has more than tripled. Given the number of announced projects, it is realistic to expect the continuation of the positive trend in the years to come. Another contributing factor to the increasing numbers is the implementation of hydrogen strategies in national policies worldwide, as well as directives towards clean solutions to overcome climate change. The latest report of the IEA Technology Collaboration Programme [7] in 2021 shows that South Korea has opened the most HRSs, currently having 52 of them (with 1,200 HRSs planed by 2040), thus joining Japan (137), Germany (90), China (85), and USA (63). South Korea has the majority of the total of 34,804 FCEVs on the global level, which is the result of the country's significant increase in the number of FCVEs during a single year (2020) due to their national roadmap development plan published in 2019. This accomplishment serves as a great motivator and proves that fulfilling the ambitious hydrogen strategy targets is achievable. One of the examples of such targets is Japan's vision for 2025 and 2030, which includes the rise in the number of HRSs to 320 and 900, respectively [8]. Although according to the 2011 – 2021 statistics, USA trend of HRSs number is stagnant, their government declared a goal to have zero-emission by 2050. Therefore, California announced a yearly investment of USD 20 million until 100 HRSs are available for the public, with a plan to have 200 HRSs in operation by 2025 [9]. Other commendable examples of turning national policy towards decarbonization are the EU and China with the common goal to become carbon neutral by 2050. China's government announced 53 hydrogen projects of which 50% are related to transport applications, with the most prominent one being Sinopec's target to build 1,000 HRSs with 500,000 t of green hydrogen capacity by 2025 [10]. Their further ahead plan is to build 5,000 HRSs by 2035 [11]. EU expects to have a minimum of 747 HRSs by 2025, of which Germany plans to contribute the most with 400

installed HRSs. According to Hydrogen Roadmap Europe [12], there should be 3,700 HRSs across the EU by 2030, and 15,000 HRSs by 2040. As a part of the 'Fit for 55' legislative, the EU directed that one HRS will be installed every 150 km along an urban area and the Trans-European Networks for Transport core network [13]. This hydrogen framework is expected to be finished in December 2021 and will explain in detail how green hydrogen will play a key role in fulfilling 2030 energy targets. One of Hydrogen Europe's [14] recommendations for hydrogen strategy, is to implement multipurpose HRSs, usable for different transport applications (e.g., at airports and ports) at appropriate locations. Another notable proposal is for the Member States to include in their national policies, binding requirements on the HRSs number increase. Also, they suggest the regulatory framework for HRSs network alongside EU's ports for supplying small ships on the same location where they are being constructed, to eliminate the 'chicken-and-egg dilemma'. Fuel Cells and Hydrogen Joint Undertaking (FCH JU) [15] also stated 2030 targets for their projects regarding HRSs. Among them, the most notable ones being a reduction in energy consumption and green hydrogen cost to 3 kWh / kg_{H2} and 6 EUR / kg_{H2}, expanded lifetime and durability to 20 and 15, respectively, and making 99% of HRSs available for the public. Listed association's future perspectives alongside inspiring regulations emerging across the whole world, the forming of a commendable hydrogen framework is imminent.

CONCLUSIONS

To achieve climate neutrality by 2050, hydrogen technology development and worldwide implementation in the next decade is crucial for the present greenhouse gas emission (GHG) levels to drop substantially. Therefore, the governments are instituting scaling-up projects for clean energy solutions with the incorporation of national hydrogen strategies. An example of it being the EUs 'Fit for 55' proposal with extensive investments into green hydrogen projects. The development of hydrogen society is the most evident through the rapid expansion of HRSs infrastructure as well as multiple nation's ambitious plans, which if accomplished, will increase the global number of HRSs to at least 22,351. Present leading countries in the number of installed HRSs are Japan, Germany, China, and the USA. Given the worldwide incline trend of the number of active HRSs, it is eminent that the huge potential of hydrogen in the transport sector is recognized, contributing to the stabilization and social acceptance of hydrogen technology. Presently, GHGs in the transport sector are still increasing, which is why the expansion of the HRSs network is essential for accelerating the ongoing energy transition.

REFERENCES

- [1] "Fit for 55." Green Transition Plan 2021. <https://www.consilium.europa.eu/en/policies> (accessed July 21, 2021).
- [2] Energy. Commission presents Renewable Energy Directive revision 2021.
- [3] Kovač A, Paranos M, Marciuš D. Hydrogen in energy transition: A review. *Int J Hydrogen Energy* 2021;46:10016–35. <https://doi.org/10.1016/j.ijhydene.2020.11.256>.
- [4] Hydrogen Council, McKinsey & Company. *Hydrogen Insights*. 2021.
- [5] Hydrogen Council. *A Perspective on Hydrogen Investment, Deployment and Cost Competitiveness* n.d. <https://hydrogencouncil.com/en/hydrogen-insights-2021/> (accessed July 21, 2021).
- [6] Ludwig-Bölkow-Systemtechnik GmbH. *H2 Stations Map* n.d. <https://www.h2stations.org/> (accessed July 21, 2021).
- [7] Can Samsun R, Antoni L, Rex M, Stolten D. Deployment Status of Fuel Cells in Road Transport: 2021 Update. *Energy & Environment* 2021;542.
- [8] Ministry of Economy, Trade and Industry, Japan https://www.meti.go.jp/eng-lish/press/2017/pdf/1226_003a.pdf n.d.
- [9] California Assembly Bill No. 8 https://leginfo.legislature.ca.gov/faces/billNavClient.xhtml?bill_id=201320140AB8 n.d.
- [10] REUTERS. China's Sinopec targets 500,000 T of "green" hydrogen capacity by 2025. *Sustainable Business* 2021. <https://www.reuters.com/business/sustainable-business> (accessed July 21, 2021).
- [11] Hydrogen Fuel Cell Vehicle Technology Roadmap 2.0, SAE China. n.d.
- [12] https://www.fch.europa.eu/sites/default/files/20190206_Hydro-gen%20Roadmap%20Europe_Keynote_Final.pdf n.d.
- [13] European Commission. *THE ROLE OF HYDROGEN IN MEETING OUR 2030 CLIMATE AND ENERGY TARGETS 2021*.
- [14] Hydrogen Europe. *Hydrogen Europe Position Paper on the Fit for 55 Package 2021*.
- [15] Fuel Cells and Hydrogen Joint Undertaking. *Multi-Annual Work Plan* n.d. <https://www.fch.europa.eu/> (accessed July 22, 2021).

HYDROGEN FUEL CELL BUS PERFORMANCE ASSESSMENT WITH MACHINE LEARNING DEGRADATION PREDICTION

¹ P. Ahmadi

¹Faculty of Engineering, IstinYE University, Istanbul, Turkey

ABSTRACT

The main intention of this study is to look at hydrogen as a clean and promising alternative to diesel fuel for buses. As fuel cells are the heart of the hydrogen buses, their degradation is one of the main challenges for their widespread deployment. In this study, a dynamic simulation for an actual city bus driving cycle and an existing fuel cell bus in Vancouver, BC, Canada is carried out. To have a realistic simulation and proper results, fuel cell degradation is predicted using various machine learning (ML) techniques. The results showed that PEM FC degradation can increase the bus fuel consumption for 21% which is equivalent to 12% of the total lifecycle GHG emission. The economic assessment prediction showed that if hydrogen FC bus wants to be cost competitive, 600 hydrogen FC bus should be produced each year.

Keywords: Hydrogen fuel cell, degradation, machine learning, efficiency, fuel economy. LCA

INTRODUCTION

We are living in an era that both energy and the environment are the two major concerns. Energy is linked with almost all activities human beings are involved in. Environment, on the other hand, is strongly connected to energy, and the higher the energy consumption, the higher the emission will be released to the environment [1]. The importance of energy is significant when we know that during the last 30 years the world population has increased by about 45% and reached 7.9 Billion people. It is worth noting that during the same period, world primary energy consumption has increased by almost 63% between 1990 to 2020. It is also interesting to know that more than 85% of the world's primary energy consumption still comes from fossil fuels and the rest is provided by renewable energies, hydropower, and nuclear energy [2]. Looking at the global CO₂ emission during this time shows an increase in approximately 50% of the total global CO₂ emission. Transportation accounts for about 25% of the global CO₂ emission where 74% of this emission contributed to road transportation. In road transportation, HDV and buses are responsible for almost 47% of the road transportation. Therefore, reducing the emission from HDV and buses is of great significant importance to mitigate global warming. There are several methods to reduce the emission from the transportation sector such as increasing public transportation, driving less, driving wise, improving the vehicle engine performance, reducing the vehicle weight, do not idle the vehicle, using low carbon fuels, using alternative fuels, etc. Among these options, alternative fuels such as CNG, LNG, biofuels, hydrogen, and electricity have gained growing interest during the last decades. Although CNG, LNG, and biofuels are good options to reduce emissions, they still come from fossil fuels which results in releasing emissions to the environment. Since most of the power plants still consume fossil-based fuels such as natural gas, oil, and coal, electric vehicles (EVs) face several limitations for widespread deployment. Hydrogen on the other hand is a good and viable option that can be considered as an alternative to gasoline and diesel as it does not have any Carbon which eventually eliminates the CO and CO₂ emissions [3]. In addition, its heating value is higher than all the conventional fuels. Hydrogen fuel cell vehicles can offer a promising way to reduce emissions however they still face some challenges such as the high cost of fuel cells, fuel cells longevity and degradation mitigation, how to produce and store hydrogen. Load cycling, freezing/thaw, humidity changes, mechanical stress, and radical attacks are the major causes of PEM fuel cell degradation [4]. In addition to this, the high cost of fuel cell buses is one of the challenges of using them. Whenever fuel cell costs are significantly decreased to the DOE objective of \$40 kW⁻¹, fuel cells can be cost-competitive for almost any form of power generation. Most of the research has not considered a fuel cell degradation when they want to see technical, economical, and environmental aspects of hydrogen fuel cell buses. Thus, their results are not reliable. The main contribution of this study is to predict fuel cell degradation using some experimental data and with the help of various machine learning techniques. Once we predict the fuel cell degradation (i.e., voltage drop versus time), we can employ that in the vehicle simulation tool for the dynamic simulation. Since the driving cycle is one of the main parameters affecting any EVs, we consider a real driving cycle of a bus route in British Columbia, Canada. Simcenter Amesim software is used with the ability of dynamic simulation to calculate real-time fuel consumption, fuel cell degradation, and engine performance.

MATERIALS AND METHODS

For the dynamic simulation of a hydrogen fuel cell bus, a real driving cycle of a bus route in the city of Victoria, the capital of British Columbia, Canada is selected where velocity and road angle as a function of time is given. In Figure 1, the bus route and the velocity and road angle are shown.

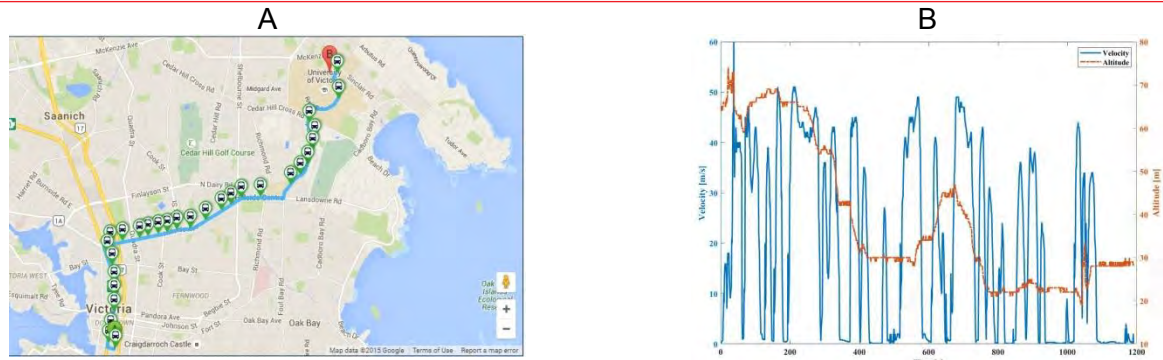


Figure 1. The bus route in the city of Victoria, BC, Canada (A), the velocity and road angle profile (B)

For the PEM fuel cell degradation, four different machine learning (ML) prediction methods including, Deep Neural Network (DNN), Simple Recurrent Neural Network (SRNN), Long Short Term Memory network (LSTM), and Bidirectional Long Short Term Memory (BLSTM) are implemented to predict the fuel cell output voltage. Figure 2a shows the fuel cell voltage drop training and prediction and Figure 2b shows the screenshot of the simulation of a hydrogen fuel cell bus.

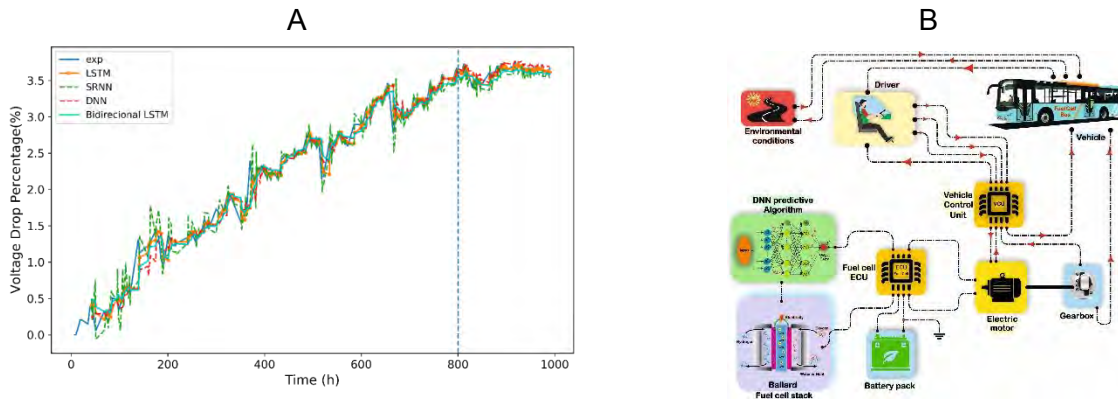


Figure 2. PEM fuel cell voltage drop prediction using machine learning methods (A), a screenshot of the simulation from Amsiem software

To see the effect of fuel cell degradation on the total energy consumption and the fuel consumption, the dynamic simulation is used with the driving cycle, hydrogen bus specifications such as weight, drag coefficient, front area, etc and they have been implemented in the software. The results are shown in Figure 3. It indicates that after 2000 h of FC bus operation, the total energy consumption and the fuel consumption increase for about 23% and 21%, respectively.

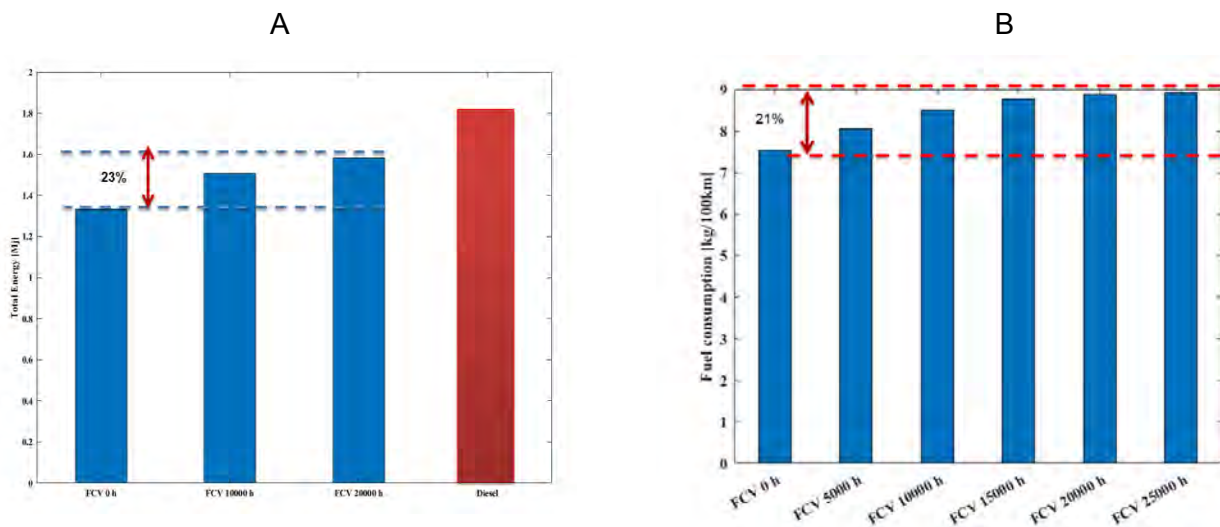


Figure 3. The effect of fuel cell degradation on the total energy consumption (A), fuel economy (B)

In addition, the LCA showed that fuel cell degradation can increase the total lifecycle GHG emission for about 12%. It means that if the fuel cell degradation for FC buses were not considered, the results would not have been reliable and that can misguide the policy maker when they try to mitigate the global warming. A comprehensive economic

assessment is carried out between 2009 to 2020 to see how fuel cell cost has varied. The results showed that in 2009 the total lifecycle cost of hydrogen FC bus was almost five times more than diesel-power bus. In 2016, both FC bus purchase cost and FC maintenance dropped which eventually resulted in 50% reduction in the total lifecycle cost of hydrogen FC bus. However, this cost was almost double that the one for diesel. FC bus purchase cost and hydrogen cost prediction revealed that if more than 600 bus are produced per year and hydrogen comes from SMR and the cost of this hydrogen production methods could drop for 15%, the hydrogen FC bus would be cost competitive, and the total lifecycle cost of FC bus would be 15% cheaper than diesel-powered bus.

CONCLUSIONS

In this research study, a hydrogen fuel cell bus with PEM fuel cell degradation prediction via ML is considered and dynamic simulation for a real driving cycle for the city of Victoria, BC, Canada was investigated. The results showed that fuel cell degradation plays a key role when FC bus deployment needs to be considered as a part of sustainable ground transportation. The results showed that PEM FC degradation can increase the bus fuel consumption for 21% which is equivalent to 12% of the total lifecycle GHG emission. The economic assessment prediction showed that if hydrogen FC bus wants to be cost competitive, 600 hydrogen FC bus should be produced each year. It should be noted that all these numbers are based on the prediction and the hydrogen production method was from fossil fuel sources (i.e., SMR).

REFERENCES

- [1] Raymond F, Ahmadi P, Mashayekhi S. Evaluating a light duty vehicle fleet against climate change mitigation targets under different scenarios up to 2050 on a national level. *Energy Policy*. 2021; 149:111942.
- [2] Ahmadi P. Environmental impacts and behavioral drivers of deep decarbonization for transportation through electric vehicles. *Journal of cleaner production*. 2019; 225:1209-19.
- [3] Dincer I. Green methods for hydrogen production. *International journal of hydrogen energy*. 2012;37(2):1954-71.
- [4] Ahmadi P, Kjeang E. Realistic simulation of fuel economy and life cycle metrics for hydrogen fuel cell vehicles. *International Journal of Energy Research*. 2017;41(5):714-27.

TECHNOLOGICAL ASSESSMENT OF A SOLAR PV COLLECTOR FOR FRESHWATER, COOLING, AND ELECTRICITY

^{1*} Farrukh Khalid

¹Department of Mechanical Engineering, Istinye University, Topkapi Kampüsü, Teyyareci Sami, Sk. No.3, 34010, Zeytinburnu, Istanbul, Turkey

*Corresponding author e-mail: farrukh.khalid@istinye.edu.tr

ABSTRACT

In this paper, a technological assessment of a solar PV collector system for freshwater, cooling and electricity is evaluated. Technological assessment is made via use of energy and exergy analyses and system performance is carried out in terms of exergetic and energetic efficiencies. Desalination of water is carried out by employing freezing defreezing technique run by the evaporator of a vapor compression cycle. The heat from the PV is utilized for defreezing the water. A parametric study is carried out to see the effect of key parameters such as ambient temperature, evaporator temperature, and mass flow rate of freshwater. Analysis shows that system attains an energetic efficiency of 19.2% whilst exergetic efficiency as 7.5%. The system produces a net electric power of 4.7 kW and freshwater of 54 liter per hour.

Keywords: PV collector, Freshwater, Cooling, Electricity, Energy

INTRODUCTION

In today's era availability of fresh water to masses is one of the main challenges and numerous efforts have been carried out by the researchers worldwide to solve this problem in a cost and energy effective way. One of the most popular method is the purification of seawater. Various methods like freezing defreezing, multistage flashing, reverse osmosis, forward osmosis, humidification dehumidification etc. are being employed to purify the seawater to obtain freshwater [1-3]. According to Youssef et al. [4] freezing defreezing technique may be an efficient way to produce freshwater for drinking purpose. With the use of solar energy one can make this method more sustainable and renewable. This can be achieved by employing a vapor compression cycle to run freezing defreezing process operated by photovoltaic collectors. Atia [5] concluded that if the freezing defreezing process run by vapor compression method it can be a cost effective compare to other available methods.

The key goals of the present study are as follows:

- To design a system for cooling, electric power, and freshwater run by photovoltaic collectors
- To use freezing defreezing process employing R-134a based vapor compression cycle
- To do the technological assessment of the designed system via thermodynamic analysis

ANALYSIS

Photovoltaic collectors

Cell temperature has an essential role in the performance of the photovoltaic collector. Duffey and Beckman [6] used the following equation is employed to find the temperature of the cell

$$T_{cell} = \frac{T_{ambient} + (T_{cell,NOCT} - T_{ambient,NOCT}) \left(\frac{G_T}{G_{T,NOCT}} \right) \left[1 - \frac{\eta_{mp,STC}(1 - \alpha_p T_{c,STC})}{\tau\alpha} \right]}{1 + (T_{cell,NOCT} - T_{ambient,NOCT}) \left(\frac{G_T}{G_{T,NOCT}} \right) \left[\frac{(\alpha_p \eta_{mp,STC})}{\tau\alpha} \right]} \quad (1)$$

The energetic and exergetic performance of the overall system are computed as follows:

$$\eta_{en,ov} = \frac{(\dot{Q}_{cool} + \dot{W}_{net} + \dot{E}n_{out,water} - \dot{E}n_{in,sw})}{(\dot{Q}_{sol})} \quad (2)$$

$$\eta_{ex,ov} = \frac{(\dot{Q}_{cool} \left(\frac{T_0}{T_{evap}} - 1 \right) + \dot{W}_{net} + \dot{E}x_{out,water} - \dot{E}x_{in,sw})}{(\dot{E}x_{sol})} \quad (3)$$

RESULTS AND DISCUSSION

Technological assessment of the proposed system gives rise to various values of some key parameters which have been tabulated in Table 1. The COP of the vapor compression system found to be as 2.6 while the rate of work done by its compressor is 5.8 kW The net cooling produced by the proposed system is 6.0 kW.

Table 8 Value of key parameter obtain via technological assessment

Key Parameter	Value
Isentropic efficiency of compressor (%)	74.1
Evaporator temperature (°C)	-5
COP of the vapor compression cycle	2.6
Cooling effect (kW)	6.0
Work rate of compressor (kW)	5.8

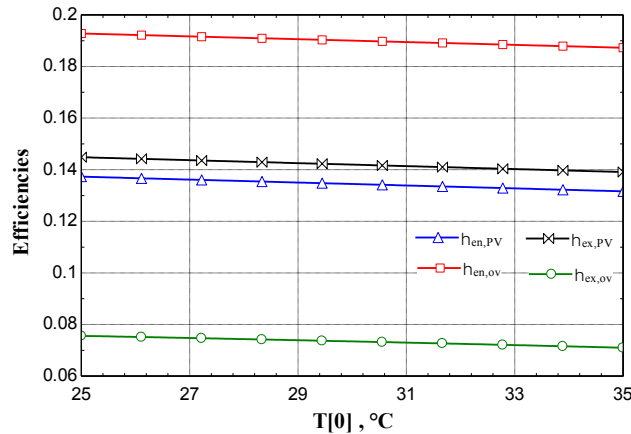


Fig. 1. Effect of ambient temperature on various efficiencies

The effect of ambient temperature on the performance of photovoltaic collectors, and overall system is presented in Fig. 1. With the rise in ambient temperature, photovoltaic collectors and overall system performances declines. This trend can be a bit described by the point as the temperature of the ambient environment rises, work rate produced by the photovoltaic collector declines.

CONCLUSIONS

A solar operated trigeneration system that can be produced three useful outputs namely cooling, electricity, and freshwater is presented and evaluated for technological assessment by a thermodynamic analysis. Simulation results shows that presented system can produced a cooling effect of 6.0 kW with a freshwater production rate as 54 kg/h. The findings reported in the current research may assist the investigators to design more efficient system for remote areas where solar energy is abundant in nature and access to freshwater is limited.

REFERENCES

- [1] Khalid F, Dincer I, Rosen MA. Analysis and Assessment of a Gas Turbine-Modular Helium Reactor for Nuclear Desalination. ASME Journal of Nuclear Engineering and Radiation Science. 2016;2(3):031014.
- [2] Sahin S, Sahin HM, Kusayer TA, Sefidvash F. An innovative nuclear reactor for electricity and desalination. International Journal of Energy Research. 2011; 35:96-102.
- [3] Kim HS, No HC. Thermal coupling of HTGRs and MED desalination plants, and its performance and cost analysis for nuclear desalination. Desalination. 2014; 303:17-22.
- [4] Youssef P, Al-Dadah R, Mahmoud S. Comparative analysis of desalination technologies. Energy Procedia. 2014; 61:2604-2607.
- [5] Attia AAA. New proposed system for freeze water desalination using auto reversed R-22 vapor compression heat pump. Desalination. 2010; 254:179-184.
- [6] Duffey JA, Beckman WA. Solar engineering of thermal processes. 1991. 2nd ed. New York, NY: Wiley.

EXERGETIC ANALYSIS OF A NEW HYBRID VEHICLE OPERATING WITH CARBON-FREE FUELS

^{1,2,3*} Muhammad Ezzat*, ¹ Ibrahim Dincer

¹ Faculty of Engineering and Applied Science, Ontario Tech University, 2000 Simcoe Street North, Oshawa, Ontario, L1H 7K4, Canada.

² Faculty of Engineering and Natural Science, Istinye University, Istanbul, Turkey

³ Faculty of Engineering, Minia University, Minya, Egypt.

*Corresponding author e-mail: muhammad.ezzat@ontariotechu.net

ABSTRACT

In this study, a carbon-free ammonia-hydrogen internal combustion engine is integrated with ammonia dissociation separation unit (DSU) and proposed for green vehicles. This integrated system aims to produce hydrogen onboard to enhance the combustion characteristics of the ammonia fuel and enhance internal combustion engine (ICE) performance to achieve an adequate performance comparable to conventional gasoline ICE. The proposed system is analyzed both energetically and exergetically. Also, the variation of ICE power and torque and available ammonia decomposition heat are studied during the different phases of the driving cycle.

Keywords: Ammonia, Hydrogen, Fuel Cells, Hybrid Vehicle, Energy, Exergy, Efficiency

INTRODUCTION

The utilization of fossil fuels has a significant effect on releasing the greenhouse gas (GHG) emissions, particularly the release of carbon dioxide, which is believed to cause global warming (1). Transportation sector contributes with a significant share of around 61.2% of the world oil reserves, and it also emits around 23% of the global carbon dioxide emissions due to fuel combustion (2). Thus, utilizing alternative clean fuels in the transportation sector should be promoted and applied (3). Implementation of ammonia as a fuel in internal combustion engines (ICE) took place in Belgium during World War II because of the scarcity of fossil fuels supplies (4). Since then, there has been increasing interest in using ammonia as a potential fuel in vehicle applications has been flourished. Grannell et al. (5) concluded that utilizing ammonia as a sole fuel in spark ignition (SI) ICE will result in a deterioration in engine performance. However, blending ammonia with combustion promoter such as gasoline with specific percentages leads to a substantial enhancement in the SI engine performance. Reiter and Kong (6) blended ammonia and diesel in compression ignition (CI) engine to study the combustion mechanism and emissions. The results demonstrated that, for the same engine power output, the engine with blended ammonia and diesel recorded higher carbon monoxide and hydrocarbon emissions compared to the engine operating with diesel fuel. Moreover, they observed that increasing the ammonia ratio in the fuel blend resulted in a higher ignition delay and causes a deterioration in the peak pressure of combustion. Hydrogen can efficiently function as a combustion promoter in ammonia ICEs, even a small amount of hydrogen (around 1% hydrogen to ammonia ratio by mass and nearly 10% by volume) blended with ammonia can achieve satisfactory combustion speed and better engine performance (7,8). Frigo and Gentili (8) utilized hydrogen as combustion promoter in an ammonia ICE. They found that adding hydrogen to the ammonia combustion process enhances combustion speed. However, the performance of the hydrogen-ammonia ICE was relatively low compared to a gasoline engine. Furthermore, no significant mechanical inconvenience existed in the ammonia-hydrogen ICE during the experiment. Ezzat and Dincer (9) proposed two energy systems for vehicle applications, the first one comprises liquefied ammonia tank, dissociation and separation unit (DSU) for thermal decomposition of ammonia and an internal combustion engine (ICE) to power the vehicle, hydrogen was produced on board and blended with ammonia for better engine performance. The present system is a hybrid system consisting of liquefied ammonia tank, DSC unit, a small ICE and a fuel cell system. In the present system, the hydrogen is ultimately produced on board and supplied to operate both the ICE and fuel cell system.

SYSTEM DESCRIPTION

The system displayed in Fig.1 consists of ICE, which is the primary powering source and can generate up to a maximum traction power of 118 kW. The power generated from the ICE will be delivered to the front axle drive via a manual transmission system. The starting of the ICE will be initiated by the battery as shown in the figure. The ICE will be fueled with a blend of ammonia and hydrogen fuels with a mass ratio of 1% hydrogen to ammonia. Ammonia is supplied to the ICE from the liquid NH₃ tank placed at the rear of the vehicle. Liquefied ammonia leaves the tank and enters the pressure regulator at state point 1 so that the ammonia fuel is supplied to the ICE at the designated pressure of 2.5 bar. Ammonia leaves pressure regulator at state point 2, and the main stream will be divided into two streams. The first one enters the ICE at state point 4 providing the ICE with the required ammonia fuel, while the second stream will be used in the ammonia thermal cracking process via the dissociation and separation unit (DSU). The heat required for the ammonia decomposition process will be provided by the high temperature exhaust gasses which leave the ICE. The exhaust gases enter the DSU at state point 8 and leave the DSU at state point 9. Ammonia inside the DSU will be decomposed and separated into hydrogen and nitrogen. Nitrogen is released into the air

through state point 11. Hydrogen enters a heat exchanger at state point 6 so that its temperature can be reduced before it is supplied to the ICE and to provide a pre-heating process for the ammonia which enters the DSU unit. Hydrogen exits from the heat exchanger at state point 7 and enters the ICE to enhance the combustion process of ammonia.

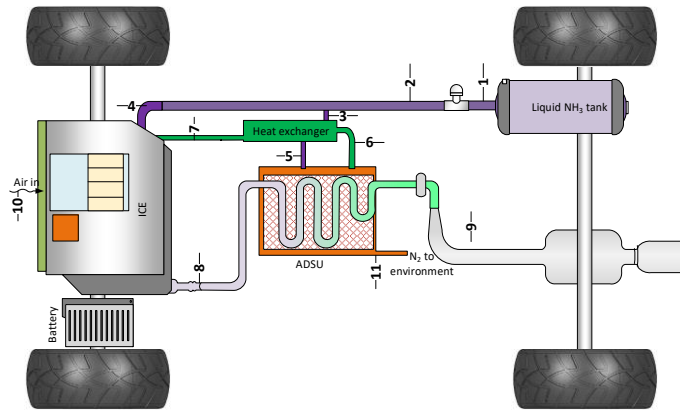


Fig. 1. Schematic of the integrated system with an ICE fueled with ammonia and hydrogen, and ammonia DSU for onboard hydrogen production.

ANALYSIS

The thermodynamics analyses of the suggested systems will be based on energetic and exergetic approaches. In this section, basic equations of energy and exergy for the different system components will be introduced. The analysis of the main powering option will be described. In addition, equations that are used for the dynamic analysis will be provided.

The general conservation of mass in a control volume for any system can be expressed as follows:

$$\sum \dot{m}_{in} - \sum \dot{m}_{out} = \frac{dm}{dt} \quad (1)$$

Here, \dot{m} denotes mass flow rate, and the terms “in” and “out” refer to the inlet and outlet of the control volume.

The conservation of energy equation can be obtained from the first law of thermodynamics as follow:

$$E_2 - E_1 = \delta Q - \delta W \quad (2)$$

Here, E , Q , and W are the energy of the system, the heat, and work that the system exchange with the environment. The general energy balance equation can be presented as follows:

$$\dot{Q}_{cv} + \sum \dot{m}_{in} \left(h + \frac{u^2}{2} + gz \right)_{in} = \dot{W}_{cv} + \sum \dot{m}_{out} \left(h + \frac{u^2}{2} + gz \right)_{out} \quad (3)$$

where z is the elevation, V is the velocity and h is the specific enthalpy.

The exergy balance equation describing any system is presented as follows:

$$\sum \dot{E}x_Q + \sum_{in} \dot{E}x_{flow} = \sum \dot{E}x_w + \sum_{out} \dot{E}x_{flow} + \dot{E}x_d \quad (4)$$

where $\dot{E}x_Q$ represents the exergy transfer rate. $\dot{E}x_{flow}$ denotes the exergy flow which transfer in or out of the system $\dot{E}x_w$ refers to shaft work applied to or done by the system. And finally, $\dot{E}x_d$ is the exergy destruction.

RESULTS AND DISCUSSION

For this system, a dynamic analysis is carried out using the world harmonized light vehicle test procedure (WLTP). This system is chosen to be modeled dynamically because it have the potential to replace the current conventional vehicle systems with minor manufacturing modifications to the current ICE design. Moreover, the parts that need to be added to the introduced system are not expensive. In overall, this system can be easily commercialized in the near future. The WLTP driving cycle consists of 4 phases with a total duration of 1800 seconds, and the vehicle in these phases experiences transition modes such as; accelerations, decelerations and idling, this is mainly to evaluate vehicle performance in every possible driving condition. The first phase is called the low phase, and its duration is 589 second, the vehicle in this phase attains a maximum speed of 56.5 km/h. The second phase is called the medium phase, and its duration is 433 seconds, and the vehicle attains a maximum speed of 76.6 km/h.

Fig.2 shows the ICE output power, torque, and DSU decomposition heat variation during the WLTP driving cycle. The

four phases of the driving cycles are separated for better presentation. In the first phase, the ICE output power and torque attains a maximum value of 43.79 kW and 210.3 N.m respectively at 228 seconds. The maximum decomposition heat available for ammonia decomposition is found to be 14.21 kW at 228 seconds as shown in Fig. 4a. In addition, in the second phase, the ICE output power, torque, and decomposition heat attain maximum values of 43.88 kW, 210.3 N.m, and 14.24 kW respectively at 646 seconds as shown in Fig.2b. In the third phase, the ICE output power, torque and the heat available for ammonia thermal cracking reach maximum values of 43.79 kW, 210.3 N.m, and 14.21 kW respectively at 1126 seconds as shown in Fig 2c. Finally, in the fourth phase, the ICE output power, torque, and decomposition heat reach maximum values of 52.74 kW, 213.6 N.m, and 17.12 kW respectively at 1724 seconds as shown in Fig.2d.

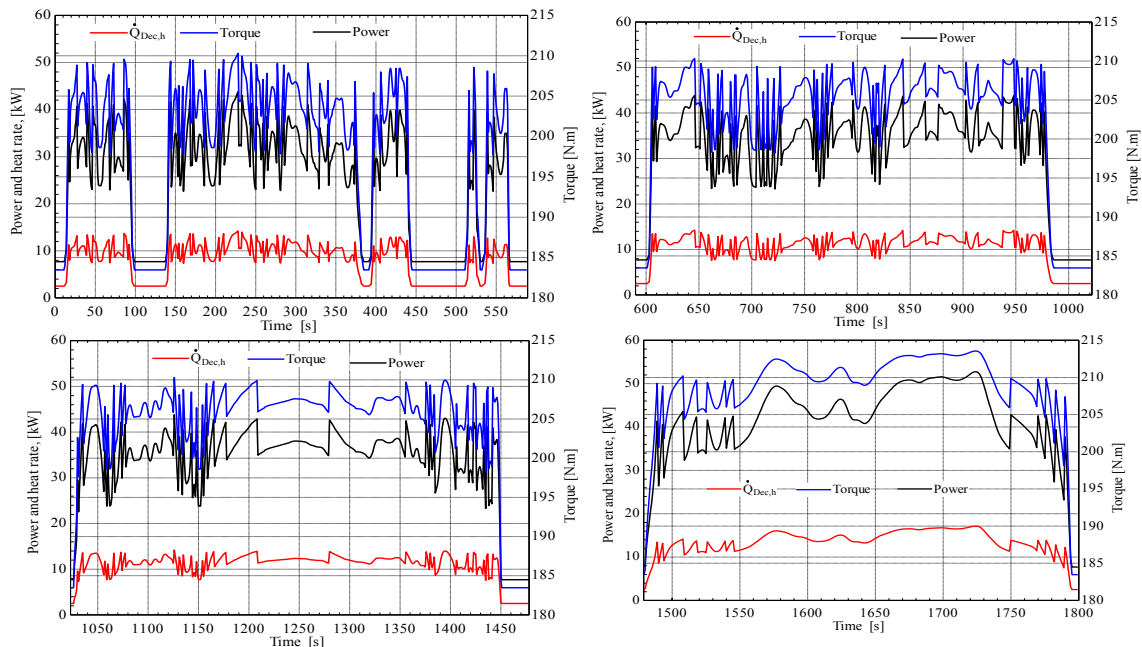


Fig. 2. Torque and power and heat rates during the during the WLTP driving cycle for four cases.

CONCLUSIONS

An integrated energy system for vehicle applications comprising ICE, DSU unit is introduced and analyzed using energy and exergy approaches. The purpose of the introduced integrated energy system is to provide an alternative environmental clean transportation option for vehicle applications. The performance of the system is analyzed dynamically using WLTP cycle. The ICE output power, torque, and decomposition heat reach maximum values of 52.74 kW, 213.6 N.m, and 17.12 kW respectively at 1724 seconds during phase four of the WLTP driving cycle.

REFERENCES

- [1] Dincer I, Zamfirescu C. Sustainable Hydrogen Production. Sustainable Hydrogen Production. Elsevier; 2016. 1–479 p.
- [2] International Energy Agency I. Key world energy statistics [Internet]. 2016 [cited 2017 Jun 10]. Available from: <https://www.iea.org/publications/freepublications/publication/KeyWorld2016.pdf>
- [3] Zamfirescu C, Dincer I. Ammonia as a green fuel and hydrogen source for vehicular applications. Fuel Process Technol. 2009;90(5):729–37.
- [4] Brohi EA. Ammonia as fuel for internal combustion engines ? An evaluation of the feasibility of using nitrogen-based fuels in ICE [Internet]. Chalmers University of Technology, Gothenburg, Sweden; 2014 [cited 2017 Mar 19]. Available from: <http://energy.gov/eere/sunshot/sunshot-initiative>
- [5] Grannell SM, Assanis DN, Bohac S V., Gillespie DE. The Fuel Mix Limits and Efficiency of a Stoichiometric, Ammonia, and Gasoline Dual Fueled Spark Ignition Engine. J Eng Gas Turbines Power [Internet]. 2008 [cited 2017 Mar 19];130(4):042802. Available from: <http://gasturbinespower.asmedigitalcollection.asme.org/article.aspx?articleid=1474412>
- [6] Reiter AJ, Kong S-C. Combustion and emissions characteristics of compression-ignition engine using dual ammonia-diesel fuel. Fuel [Internet]. 2011 Jan [cited 2017 Mar 19];90(1):87–97. Available from: <http://linkinghub.elsevier.com/retrieve/pii/S001623611000414X>
- [7] Mørch CS, Bjerre A, Gøttrup MP, Sorenson SC, Schramm J. Ammonia/hydrogen mixtures in an SI-engine: Engine performance and analysis of a proposed fuel system. Fuel [Internet]. 2011 Feb [cited 2017 Mar 19];90(2):854–64. Available from: <http://linkinghub.elsevier.com/retrieve/pii/S0016236110005132>
- [8] Frigo S, Gentili R, Ricci G, Pozzana G, Comotti M. Experimental Results Using Ammonia Plus Hydrogen in a S.I. Engine. In: SAE-China F, editor. Proceedings of the FISITA 2012 World Automotive Congress [Internet]. Springer, Berlin, Heidelberg; 2013 [cited 2017 Mar 19]. p. 65–76. Available from: http://link.springer.com/10.1007/978-3-642-33777-2_6
- [9] Ezzat, M. F., and I. Dincer. 2018. "Comparative Assessments of Two Integrated Systems with/without Fuel Cells Utilizing Liquefied Ammonia as a Fuel for. Int J Hydrogen Energy. 2018;

MODELLING AND SIMULATION OF MOLTEN CARBONATE FUEL CELL AND COPPER-CHLORINE CYCLE BASED POWER GENERATION SYSTEM WITH THE INCORPORATION OF PID CONTROLLER

¹ Haseeb Kamran, ¹ Uzair Mudassir, ¹ Abdul Moiz Ali, ¹ M. Abbas Raza, ¹ Karam Khan, ¹ Khurram Kamal, ¹ Tahir Abdul Hussain Ratlamwala

¹ National University of Sciences and Technology, Islamabad, Pakistan

*Corresponding Author e-mail: tahir.ratlamwala@pnec.nust.edu.pk

ABSTRACT

Regenerative cycle, copper-chlorine cycle, and electric heater with PID controller are studied in this paper to integrate them with MCFC to increase the efficiency of the overall system. Copper-Chlorine cycle is integrated to provide a stable stream of hydrogen and oxygen for the fuel cell. The Molten Carbonate fuel cell generates 1.203MW of power at 1.2V per cell. Waste Heat recovery system is installed, namely regenerative Steam cycle which produces 2.94MW of power. The total efficiency of system was found to be 57% with the total power generation of 4.143MW.

Keywords: Molten Carbonate Fuel Cell, Copper-Chlorine Cycle, Regenerative Steam Cycle, Electric Heater, PID Controller

INTRODUCTION

The proposed system is different from the regular or typical multigeneration system with two or three components. The system incorporates Copper-Chlorine Cycle, Molten Carbonate Fuel Cell, Regenerative Rankine Cycle, and Electric Heater with PID Controller to maximize efficiency of this multigeneration system. Heated water exactly at 450°C coming from Electric Heater with PID Controller is fed into Copper-Chlorine Cycle, which splits water into H₂ and O₂ at 450°C and 500°C respectively. H₂ and O₂ are fed into Molten Carbonate fuel Cell for the generation of power with Heat and water as by-products. Water is then fed to regenerative cycle which recovers the waste heat and converts it into power. Exhaust heat from regenerative cycle heats water to 311°C which is fed into Electric Heater with PID Controller. PID Controller ensures that water is heated to precisely 450°C. The overview of the system is portrayed in the Figure 1. below.

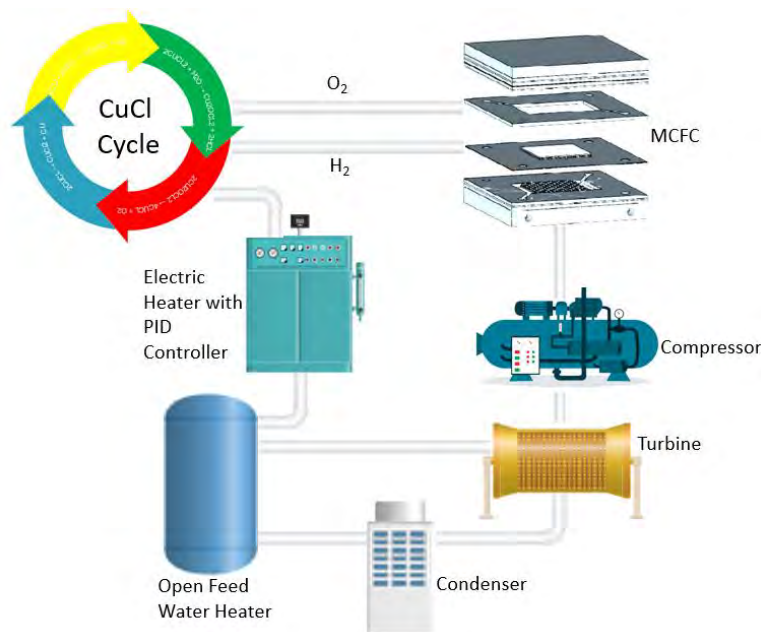


Figure 1. Project Overview

System Description

Nowadays the need for clean and cost-effective source of energy is evolving a lot. A cogeneration system is the one in which the production of usable heat and electricity merges into a single system which can substantially reduce carbon emissions and energy costs due to higher efficiency. Our cogeneration system starts with the Copper-Chlorine cycle. Copper-Chlorine cycle splits water to hydrogen at 450°C and oxygen at 500°C with specific flowrates which is fed into Molten carbonate fuel cells (MCFCs). Heat lost from MCFC is recovered by incorporating a regenerative steam cycle which receives the waste heat as input. Regenerative steam cycle involves extracting turbine's

steam(bleeding) at various places for feed water heating, called feed water heater. Steam leaves the Regenerative cycle at 311°C and is directed to an electric heater, whose output is regulated by a PID controller at 450°C. This steam at controlled temperature is fed back into the CUCL cycle where the process repeats. Due to regeneration, efficiency of the Rankine cycle improves considerably.

Dynamic model represents how the output parameters of whole system changes with time along with input parameters to achieve stability. The governing input parameter is the temperature of steam at the input of Cu-Cl cycle that is controlled with PID controller operating an electric heater. Stability of this temperature holds immense importance in attaining maximum efficiency of whole system.

The heat which enters the copper chlorine cycle is governed by this thermodynamic model, which results in dynamic mass flow rates of hydrogen and oxygen as usable outputs from the Cu-Cl cycle. These flow rates generate dynamic voltage and output power response of the stack of fuel cell. By-product of the fuel cell is water which is produced dynamically. This water flowrate is then fed into regenerative cycle that produces dynamically stable output power of turbine. This water then enters the Cu-Cl cycle after passing through electric heater. This is how cycle is completed with a dynamically behavioral response. It is very important to have stable response of every sub system as stable system are robust, efficient, and effective. For this reason, tuning of PID controller is essential to achieve desired stable response. Tuning of PID controller needs optimized proportional (Kp), integral (Ki) and derivative (Kd) gain parameters to achieve maximum stability. $K_p = -28807.622$, $K_i = -5510.389$, $K_d = 6070.815$.

RESULTS AND DISCUSSION

The proposed system presents the integration of Copper-Chlorine Cycle with Molten Carbonate Fuel Cell along with waste Heat Recovery cycle. Molten Carbonate Fuel Cell's steady state and dynamic models are modelled using MATLAB/SIMULINK R2020a. Implementation of Copper-Chlorine Cycle results in the generation of steady state flow of hydrogen and oxygen with mass flow rates of 3.23kg/s and 8.47kg/s respectively. Hydrogen and Oxygen with these flow rates are fed into Molten Carbonate Fuel Cell to generate a steady state Power of 1.2039750 MW as shown in Fig. 2. The voltage generated for each cell is 1.2V and a Cell stack of 100 cells is used. Simulation is carried out to evaluate these stated values which gives us an insight; before fabrication as to how the real system will operate and reduces the chances of defects as well as failures.

A Regenerative Steam Cycle is used with open feed water heater to recover the heat lost from fuel cell. The overall output power achieved from the regenerative cycle is 2.944MW. Wastewater from Regenerative Cycle at 311°C is taken to an Electric heater with PID controller which heats water precisely to 450°C. PID controller is tuned as to optimize the heat supplied by electric heater. Every component of the system has an individual efficiency of less than 50%, but once integrated together in such a way that losses are reduced by utilizing waste heat and optimizations by the use of PID controller, the overall system's efficiency came out to be 57% by using these approaches as shown in Fig. 3.

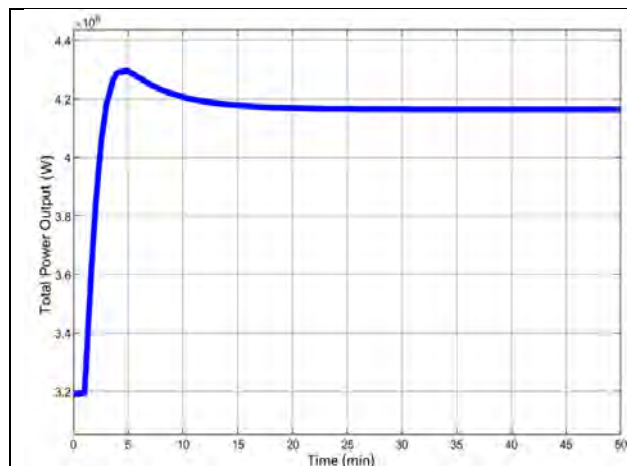


Figure 2. Net Power Output of the system

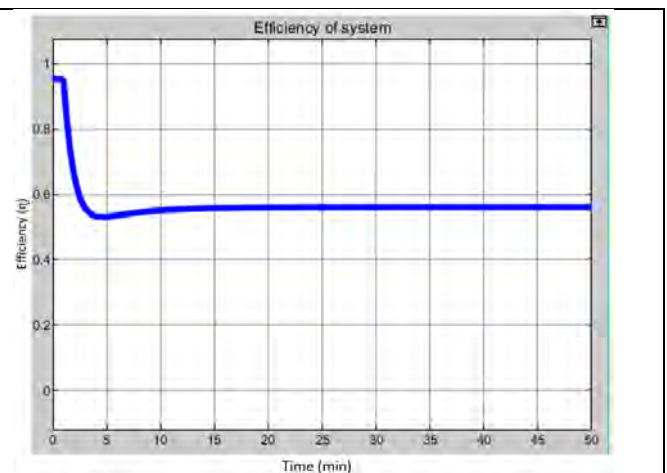


Figure 3. Overall Efficiency of the system

CONCLUSION

This cogeneration system turned out to produce acceptable results with considerably high efficiency. In this work a detailed model was developed in the MATLAB/SIMULINK R2020a. However, a typical efficiency of 70-80 % which is common for cogeneration systems can be achieved by carefully studying and minimizing some limitations. There are several limitations in the various components of the system used. Noticeably in MCFC ohmic losses, concentration losses and activation losses occur which significantly affects the efficiency of fuel cell. Taking measures to minimize them can considerably improve the efficiency of fuel cell. Other issues include combustibility of fuel, high installation costs, transportation of hydrogen etc. The efficiency of the regenerative steam cycle can be improved by increasing the number of feedwater heaters. Solution to these issues will be proposed in further studies.

ARTIFICIAL INTELLIGENCE BASED PREDICTION OF OUTPUTS OF GEOTHERMAL ENERGY BASED MULTIGENERATION SYSTEM

¹ Qasim Nawab Haider, ¹ Syed Muhammad Ali, ¹ Khurram Kamal, ^{1,*} Tahir Abdul Hussain Ratlamwala
¹ National University of Sciences and Technology, Islamabad, Pakistan

*Corresponding Author e-mail: tahir.ratlamwala@pnec.nust.edu.pk

ABSTRACT

The present study focuses on the use of Back Propagation Neural Network for prediction of outputs from geothermal energy based multigeneration system. Accuracy of the system is studied with variable number of neurons. Errors have been calculated for all instances and compared with Neural networks consisting of different number of neurons. Results show that higher number of neurons will provide better accuracies for prediction but will take more time for learning of the algorithm.

Keywords: Geothermal Energy, Multigeneration, Neural Networks, Machine Learning, Back Propagation

INTRODUCTION

Geothermal Energy across the world is used in Power Generation as well as other heating purposes [1,2]. These systems are used in countries where Geothermal Energy is available abundantly. Some of these countries are Iceland [3, 4], Philippines, El Salvador, Costa Rica, Kenya, New Zealand and United States of America. Multigeneration systems are designed to extract the most out of a Geothermal Energy system [5]. These systems can provide multiple outputs simultaneously without any change in form of energy as geothermal fluid is already in the form where consumption is easy [6]. Such systems can provide outputs which can easily be quantified by using thermodynamic equations. But another approach may be using Machine Learning and Neural Networks [7]. With the advancement in technology all around the world, Machine Learning is increasingly being used in different kinds of prediction systems with very high accuracies [8].

SYSTEM MODELING

The complete multigeneration system as shown in fig. 1 was modelled on EES and the following variables were selected as inputs; the mass flow rate of water extracted from the well, the quality of the mixture extracted from the well, and the operating temperature of the Generator in VAC [9].

The following four outputs were predicted using the artificial neural network; the work output of the turbine, the heat released by the condenser, the heat absorbed by the generator, and the heat available for water heating.

Following assumptions were made for the analysis; no pressure losses in the pipe, steady state conditions, isenthalpic flashing and throttling, pressure at exit of the flash chamber is 1500kPa, turbine efficiency is 0.6, no heat losses in the pipes, turbine exit temperature at 170°C, dead state 25°C and 101.3 kPa, and negligible kinetic and potential energy changes.

NETWORK DESIGN AND ANALYSIS

Using a Matlab script, an input data comprising of 18000 different sets of inputs was generated. The mass flowrate of the water extracted from the geothermal mixture was varied between 10 kg/s to 300 kg/s with an increment of 5kg/s. The quality of geothermal mixture was varied between 0.4 to 0.9 for each value of mass flowrate and the operating temperature of generator was varied between 323K to 399K for each value of quality and mass flowrate.

Back Propagation Neural Network [10] was selected for the prediction of outputs. The input layer consisted of three neurons for the three inputs and the output layer consisted of four neurons for the four outputs. A single hidden layer was used and the number of neurons in the hidden layer was varied with 5, 10, 15, 20, and 25 neurons. Parameters used for training of neural networks are presented in Table 1.

Table 1. Training parameters fixed for the training of all five neural networks.

Training Function	TRAINLM
Adaption Learning Function	LEARNGDM
Performance Function	MSE
Transfer Function	TANSIG
Total Epochs	1000

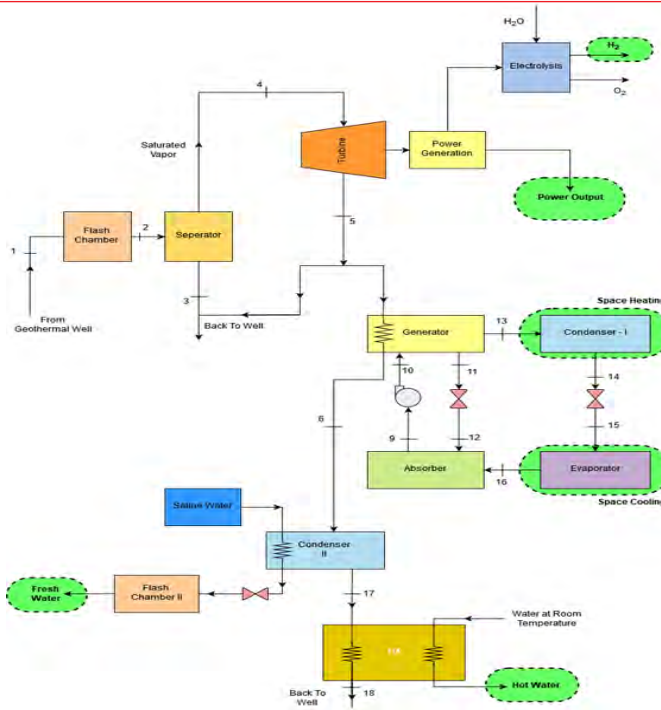


Fig. 1. Schematic of the multigeneration system

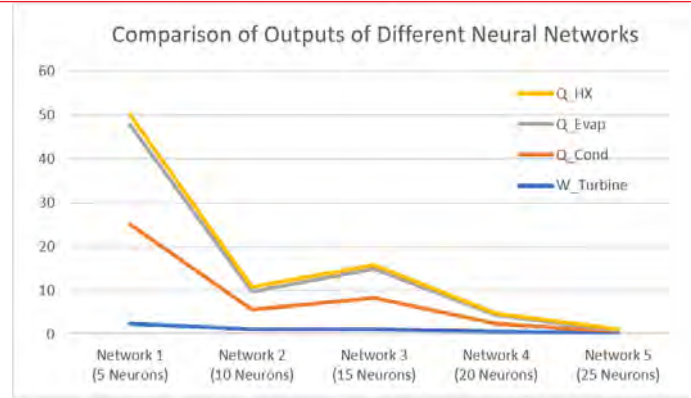


Fig. 2. Comparison of outputs of five neural networks

RESULTS AND CONCLUSION

The analysis of outputs of each of the five neural networks concluded that the network with 25 neurons in the hidden layer provided the most accurate prediction of outputs of the neural network. The comparison of output of this network with the target data is shown in table 2 while a comparison of outputs of the five networks is shown in fig. 2.

Table 2. Comparison of output of neural network data with target output.

	W_turbine	Q_Cond	Q_Evap	Q_Hx
Minimum Errors	0.0000%	0.0000%	0.0000%	0.0000%
Maximum Errors	48.7720%	2.2140%	1.9872%	48.7205%
Average Errors	0.3410%	0.1692%	0.1540%	0.3413%

REFERENCES

- [1] Azhar, M. and M.A. Siddiqui, *Exergy analysis of single to triple effect lithium bromide-water vapour absorption cycles and optimization of the operating parameters*. Energy conversion and management, 2019. 180: p. 1225-1246.
- [2] Arslan, O., *Power generation from medium temperature geothermal resources: ANN-based optimization of Kalina cycle system*. Energy, 2011. 36(5): p. 2528-2534.
- [3] Dalla Longa, F., et al., *Scenarios for geothermal energy deployment in Europe*. Energy, 2020. 206: p. 118060.
- [4] Mikhaylov, A., *Geothermal energy development in Iceland*. International Journal of Energy Economics and Policy, 2020. 10(4): p. 31.
- [5] Tester, J.W., et al., *The future of geothermal energy*. Massachusetts Institute of Technology, 2006. 358.
- [6] Lund, J.W. and A.N. Toth, *Direct utilization of geothermal energy 2020 worldwide review*. Geothermics, 2020: p. 101915.
- [7] Keçebaş, A., İ. Yabanova, and M. Yumurtacı, *Artificial neural network modeling of geothermal district heating system thought exergy analysis*. Energy Conversion and Management, 2012. 64: p. 206-212.
- [8] Jordan, M.I. and T.M. Mitchell, *Machine learning: Trends, perspectives, and prospects*. Science, 2015. 349(6245): p. 255-260.
- [9] Singh, D.V. and T.N. Verma, *Energy and exergy analysis of LiBr-H₂O-operated vapour absorption refrigeration system using the ANN approach*. International Journal of Ambient Energy, 2019: p. 1-13.
- [10] Yadav, A., et al., *Application of Artificial Neural Networks in Geothermal system*.

THE ROLE OF MACHINE LEARNING ON METAL HYDRIDE FOR HYDROGEN STORAGE

¹Melike Sultan Karasu Asnaz, ²Adnan Midilli

¹Balikesir University, Faculty of Engineering, Dept. of Industrial Engineering, Balikesir, Turkey

²Yildiz Technical University, Faculty of Mechanical Engineering, Dept. of Mechanical Engineering, Istanbul, Turkey

*Corresponding author e-mail: karasu@balikesir.edu.tr

ABSTRACT

The main objective of this study is to investigate the role of machine learning on metal hydride based hydrogen storage which is one of the most important hydrogen storage technologies. In this regard, metal hydrides that are important technological materials used for hydrogen storage were discussed, including lithium hydride, sodium borohydride, lithium aluminium hydride, and ammonia hydride. Considering the features of these hydrides, it is investigated how machine learning can contribute to design and development of novel metal hydrides that offer high hydrogen absorption capacity, thermodynamically stable and fast kinetics in the transition to hydrogen economy.

Keywords: Hydrogen storage, Metal hydrides, Machine learning, Artificial intelligence

INTRODUCTION

Solid-state hydrogen storage studies are focused on understanding the behavior of both composition and structure as hydrogen interacts with a variety of materials [1]. A desired metal hydride used for hydrogen storage should meet the all requirements of high gravimetric and volumetric density, reversibility, fast dehydrogenation/rehydrogenation kinetics, resistance to O₂ for long cycle life, high stability, and high safety [2]. In order to find a suitable material and go beyond the current materials, several researchers conducted their studies by applying Machine Learning (ML) techniques. Prediction of material behaviours is the most common area of study in the literature (e.g. Rahmada et al. [3] attempted (i) to predict hydrogen storage capacity of MHs by comparing four ML models, and (ii) rank the importance of variables that effects the storage capacity. Ding et al. [4] adopted an ensemble ML to find out the most significant factor for the hydrogen release ability from LiBH₄, and dehydrogenation temperature was found to be the most important one among fourteen variables. Under these considerations, this study focuses on the importance of utilizing ML methods for discovering new MHs that offers improved kinetics and thermal requirements for hydrogen storage systems.

MATERIALS AND METHODS

Machine learning is a subbranch of artificial intelligence that extracts patterns from a set of data, and then uses these patterns through algorithms to improve themselves with experience [1]. Its techniques can be classified into three categories viz. supervised, unsupervised and reinforcement learning, each has its own objectives and uses depending on the data. In the context of hydrogen storage materials the most employed ML models are mainly supervised approaches. The type of algorithm to be chosen based on the amount of data and data type (numerical, categorical, image etc.) can also greatly change the predictive capabilities of the ML model [5]. Fig. 1 shows the process of a supervised ML in metal hydrides for hydrogen storage.

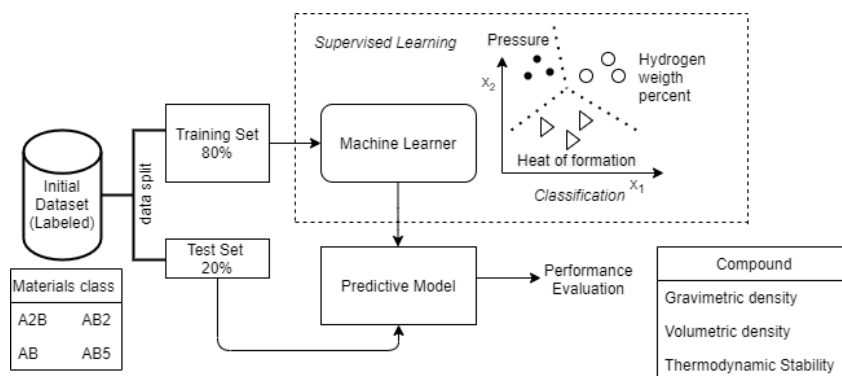


Figure 14. Flowchart of a supervised machine learning example

Generally, in the design of MHs, besides high gravimetric and volumetric density, appropriate hydrogen binding energy, thermodynamic stability, fast charge and discharge kinetics, and mild operating conditions are desirable [6]. Any of these variables and/or the hydrogen storage targets can be specified as the output parameters (objective

function) to be optimized in the algorithm. However, determination of the parameters is a challenging process that needs to be carefully tuned. Common input parameters used in the literature are stoichiometries, elemental property statistics, heat rate, temperature ranges from PCT curves, pressure kinetic curves, dehydrogenation temperature, rehydrogenation temperature, rehydrogenation time, the cycle, enthalpy, thermal conductivity, molar ratio in case of using catalyst and other additives [1,3,7,8]

CONCLUSIONS

Strategically, the role of ML on metal hydride hydrogen storage can be listed as follows;

1. Conducting studies of metal hydride for hydrogen storage by ML can take an important place in the transition to hydrogen economy globally. Because the discovery of new thermodynamically stable and fast kinetic compounds that can be used in both mobile and stationary applications is crucial to make this transition faster.
2. ML is a low-cost and safe way to explore new MHs with high hydrogen storage capacity before conducting real experiments.
3. With the ability to design MHs by learning from existing material behaviors, ML can offer various optimal compounds that are suitable for any hydrogen storage applications by testing numerous combinations of metals and predicting their thermodynamic properties in a short time.

REFERENCES

- [1] Huang SJ, Mose MP, Kannaiyan S. Artificial intelligence application in solid state mg-based hydrogen energy storage. *J Compos Sci.* 2021;5(6).
- [2] Zhang YH, Jia ZC, Yuan ZM, Yang T, Qi Y, Zhao DL. Development and Application of Hydrogen Storage. *J Iron Steel Res Int.* 2015;22(9):757–70.
- [3] Rahnema A, Zepon G, Sridhar S. Machine learning based prediction of metal hydrides for hydrogen storage, part I: Prediction of hydrogen weight percent. *Int J Hydrogen Energy.* 2019;44(14):7337–44.
- [4] Ding Z, Chen Z, Ma T, Lu CT, Ma W, Shaw L. Predicting the hydrogen release ability of LiBH₄-based mixtures by ensemble machine learning. Vol. 27, *Energy Storage Materials.* 2020. p. 466–77.
- [5] Belle CE, Aksakalli V, Russo SP. A machine learning platform for the discovery of materials. Vol. 13, *Journal of Cheminformatics.* 2021.
- [6] Lai Q, Sun Y, Wang T, Modi P, Cazorla C, Demirci UB, et al. How to Design Hydrogen Storage Materials? Fundamentals, Synthesis, and Storage Tanks. *Adv Sustain Syst.* 2019;3(9).
- [7] Rahnema A, Zepon G, Sridhar S. Machine learning based prediction of metal hydrides for hydrogen storage, part II: Prediction of material class. *Int J Hydrogen Energy.* 2019;44(14):7345–53.
- [8] Hattrick-Simpers JR, Choudhary K, Corgnale C. A simple constrained machine learning model for predicting high-pressure-hydrogen-compressor materials. *Mol Syst Des Eng.* 2018;3(3):509–17.

MULTI-OBJECTIVE OPTIMIZATION OF A MULTISTAGE VAPOR COMPRESSION REFRIGERATION CYCLE

¹Abid Ustaoglu, ¹Bilal Kursuncu, ²Alaattin Metin Kaya, ³Hakan Caliskan
¹Bartın University, Department of Mechanical Engineering, Bartın, 74110, Turkey
²Bursa Uludağ University, Department of Mechanical Engineering, Bursa, 16120, Turkey
³Usak University, Department of Mechanical Engineering, Usak, 64200, Turkey

*Corresponding author e-mail: austaoglu@bartin.edu.tr

ABSTRACT

In this study, a detail optimization study of the multistage refrigeration vapor compression cycle is carried out with the statistical and thermodynamical approaches. The energy and exergy efficiencies are calculated for various experimental designs. R152a shows the best thermal performance according to Taguchi approach. In the specified optimum conditions, the COP of 5.072 and the exergy efficiency of 18.46% are achieved. The evaporator temperature has the largest effect on the performance with about 51% in the case of COP and exergy performance.

Keywords: Energy and Exergy analyses, Multiobjective optimization, Multistage cycle, Vapor compression refrigeration cycle

INTRODUCTION

The air-conditioning, heat pumps, and refrigeration systems are some of the largest energy consuming components in the global share. Vapor compression refrigeration systems are extensively employed for the domestic, commercial, and industrial applications due to their high coefficient of the performances (COP). Industrial refrigeration systems operate in low temperatures thereby requiring high grade energy and components with larger capacity. One of the most logical approach to achieve low temperatures is operating more than one stage refrigeration cycles in series. A mixing chamber can be used between the cycles instead of the heat exchanger when the same fluid is used in the cycles since it has a better heat transfer performance. There are a couple of studies to evaluate the multistage refrigeration-system as a function of the energy and exergy efficiency.

The analysis for the refrigeration system is mostly about the fluid selection or deciding the optimum operation conditions regarding to the results of the general energy and exergy performances. There are many studies in the literature dealing with the optimization of the operational parameter with energetic or exergetic performance evaluations and deciding the appropriate refrigerant selection. Exergy is a useful tool for deciding location, magnitudes, and causes of irreversibility. However, the optimization approach may be misleading without considering a more detailed investigation. Parametric design through the Taguchi method was successfully applied in many engineering disciplines. There are a few researches about optimization of the thermodynamic cycles involving refrigeration cycles, organic Rankine cycle (ORC), heat exchangers and heat-pumps. Shajaeefard and Zare [1] optimized the performance of the condenser without changing dimensions of the system by utilizing modified NSGA-II and TOPSIS. The results indicated that the optimized condenser effectiveness improved about 3.3% compared to the fundamental condenser. Bekiloglu et al. [2] made a multiobjective optimization study of an organic Rankine cycle. The thermal conductance regarding to net power and performance-factor were selected as objective function. Isobutane, R1234ze(e), and R1234yf were the optimum fluids at the source temperature of 90°C, 120°C, and 150°C, respectively.

The refrigerants selected by using TOPSIS solutions is considered as a group of ideal refrigerants for the optimization of the operating conditions of the multistage refrigeration. ANOVA and Taguchi analysis were employed to decide the significance of the operating parameters, the best possible working conditions, and their contribution ratio on the performance. The study aims to reveal the parameters' impact weights, to find out the optimal working conditions and to decide the ideal refrigerants by considering with many aspects.

MATERIALS AND METHODS

A two-stage vapor compression refrigeration cycle was considered for the evaluation. Flash-chamber are used instead of heat exchanger because they have a better heat transfer characteristic. The system works in steady-state conditions. The heat loss in connection-pipe among the components and pressure drops connection of the components throughout the cycle were ignored. The expansion valves process was isenthalpic. The compression processes were assumed irreversible adiabatic. The balance equation regarding to the first and second law of the thermodynamic are used in the energy and exergy analysis. Taguchi method is frequently used in all engineering fields in experiment design, obtaining optimum test parameters and deciding the effects of the system parameters on the performance. Taguchi enables to determine of the effect of parameters on the efficiency of the system by doing less experiments. The larger the better method was used due to the evaluation of performance in this study. S/N ratio is obtained as follows:

$$S/N = -10 \log \left(\frac{1}{n} \sum_{i=1}^n \frac{1}{y_i^2} \right) \quad (1)$$

where i represents the test number, y_i represents the result obtained in test number i [3].

CONCLUSIONS

The contribution ratio of the parameters is illustrated for the case of COP and exergy efficiency in Figure 1. The parameters have quite similar effect on the COP and exergy efficiency of the system. The results indicate that the evaporator temperature has the largest effect on the performance with about 51% for the case of COP and exergy efficiency. It is followed by the condenser pressure effect of 40.9%. The contribution ratios of the other parameters have very low effect compared to the others. These are followed by the isentropic efficiency of the low- and high-pressure compressor with about 3.4% and 2.5%, respectively. The contribution ratio of the refrigerants is about 1.3%. The cooling capacity and interstage pressure have very insignificant effect on the performance. The parameters' importance-levels were comparably found in Taguchi and ANOVA methods. The parameters having impact on the COP were found as $B > C > E > F > A > D > G$ in descending order. Namely, the order is $T_{EVA} > T_{CON} > \eta_{C,L} > \eta_{C,H} > \text{Refrigerant} > Q_L > P_{int}$. R152a show the best thermal performance according to Taguchi approach. In the specified optimum conditions, the COP of 5.072 and the exergy efficiency of 18.46% were achieved.

Table 1. System parameters and their levels

Parameters	Levels		
	1	2	3
A Working fluid	R134a	R152a	R600a
B Evaporator temperature (T_{EVA} , °C)	-20	-15	-10
C Condenser temperature (T_{CON} , °C)	30	35	40
D Cooling capacity (kW)	1	10	20
E Isentropic efficiency of low pressure compressors ($\eta_{C,L}$)	0.75	0.8	0.85
F Isentropic efficiency of high pressure compressors ($\eta_{C,H}$)	0.75	0.8	0.85
G Interstage pressure (P_{int} , kPa)	$(T_{EVA} + T_{CON})/2$	$\sqrt{P_{EVA} P_{CON}}$	$(\sqrt{P_{EVA} P_{CON}}) + 5$ °C

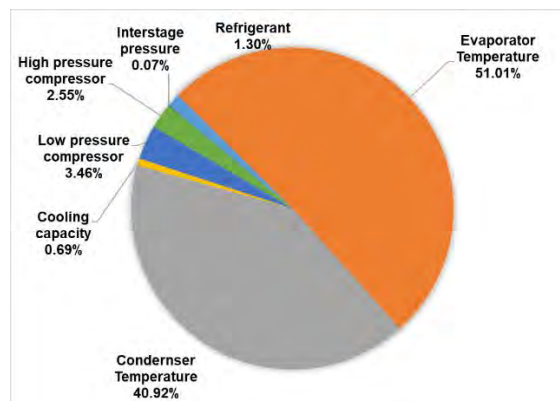


Figure 1. Parameters' contribution ratio of the exergy performance of Multistage Compression Refrigeration-system

REFERENCES

- [1] Shojaeefard M H, Zare J. Modeling and combined application of the modified NSGA-II and TOPSIS to optimize a refrigerant-to-air multi-pass louvered fin-and-flat tube condenser. Applied Thermal Engineering, 2016;103:212-225
- [2] Bekiloğlu H E, Bedir H, Anlaş G. Multi-objective optimization of ORC parameters and selection of working fluid using preliminary radial inflow turbine design. Energy Convers. Manag., 2019,183:833-847
- [3] Ustaoglu A, Kursuncu B, Alptekin M, Gok M S. Performance optimization and parametric evaluation of the cascade vapor compression refrigeration cycle using Taguchi and ANOVA methods. Appl Therm Eng, 2020; 180:115816

A POLICY ON RENEWABLE HYDROGEN ECOSYSTEM IN TURKEY

Adnan Midilli

Yildiz Technical University, Faculty of Mechanical Engineering, Dept. of Mechanical Engineering, Istanbul, Turkey

*Corresponding author e-mail: midilli@yildiz.edu.tr

ABSTRACT

Renewable hydrogen for a deeply decarbonized future is considered to be an attractive energy carrier, which can be produced from many sources such as water, biomass, organic wastes, etc. by using different production techniques such as electrolysis, gasification, etc. In order to produce, store, distribute and use the renewable hydrogen, the renewable energy integrated hydrogen supply chain is required, which is one of the most important part of the renewable hydrogen ecosystem. Under these considerations, the main objective of this study is to investigate the basic criteria and determine the strategic framework for a renewable hydrogen ecosystem by developing the required hydrogen energy policies and strategies in terms of renewable hydrogen roadmap. In this regard, the following important issues are investigated and discussed in detail: i) why Turkey needs a renewable hydrogen ecosystem, ii) the key components, dimensions, structure, functions and stakeholders of the renewable hydrogen ecosystem, iii) the required key strategies and policies for renewable hydrogen roadmap, and iv) renewable hydrogen ecosystem readiness level (RHERL). Accordingly, the basic conceptual framework of renewable hydrogen ecosystem should be taken into consideration, including smart management of hydrogen ecosystem, applicable hydrogen policies and strategies, artificial intelligence integrated hydrogen ecosystem security and hydrogen ecosystem sustainability.

Keywords: Hydrogen, Renewable Energy, Hydrogen supply chain, Hydrogen ecosystem

INTRODUCTION

Recently, world energy demand has increased because of the population growth, rapid technological developments and the high living standards. This has accelerated the consumption of economically available energy sources and caused some important world energy problems such as i) waste of resources, ii) decrease of economically usable fossil fuel reserves, iii) difficulties in alternative energy production, iv) Increased energy wastage, v) the emergence of inefficient energy sectors, vi) intermittent energy supply and supply-demand imbalance, vii) inequality and injustice in energy sharing, viii) energy security problem, ix) increasing energy demand, x) increasing energy cost, xi) increasing energy and environmental pollution, etc. All these problems are disrupting the global energy stability day by day [1-4]. Accordingly, they cause a negative impact on the social, environmental, cultural, industrial, technological and economic developments of a society in a country. In order to struggle these problems and overcome many difficulties, it is required to establish the cost-efficient renewable and clean energy ecosystem which can be renewable hydrogen ecosystem. A renewable hydrogen ecosystem includes renewable hydrogen energy demand and supply chain (containing of raw materials, renewable energy sources, renewable energy production technologies, renewable hydrogen production processes, renewable energy conversion technologies, integrated power generation systems, hydrogen storage systems, hydrogen distribution systems, hydrogen dispensing technologies), renewable hydrogen management sectors, hydrogen energy demand chain, hydrogen energy services, hydrogen energy utilization sectors, manufacturing sectors, artificial intelligence sectors, R&I and Commercialization sectors, hydrogen energy markets, hydrogen energy producers, hydrogen energy consumers, hydrogen policy makers, governments, media, private sectors, hydrogen import and export sectors, environment, livings, animals, flora, etc. Such an ecosystem is extremely important for the geostrategic, geoeconomic, geoenergetic, geopolitical, geocological stability of the countries, as well as the security of the countries, as well as the economic and industrial stabilities.

STRATEGY FRAMEWORK

Renewable hydrogen ecosystem is a stable, renewable and sustainable techno-ecological system that creates a clean, balanced, efficient, economical and sustainable interaction among all components and stakeholders related to renewable energy supported hydrogen energy, the livings and the non-living environment surrounding those components and stakeholders.

In order to develop a renewable hydrogen ecosystem, some strategies and policies are required. The most important of the such policies and strategies is to conduct a strategic sustainable useful interaction among the renewable hydrogen ecosystem, the livings and the non-living environment hydrogen in the region. Moreover, constitution of a strategic hydrogen terminal and bridge is another important strategy for a deeply decarbonized future of such an ecosystem. Although being a hydrogen energy terminal and a bridge brings many risks, it means managing and controlling the regional and even continental distribution of hydrogen energy and being a hydrogen playmaker. Being a hydrogen energy terminal and a bridge does not only mean managing hydrogen energy. It also requires the establishment of a

hydrogen energy knowledge pool, the establishment of highly specific hydrogen energy education institutions, hydrogen energy research centers, hydrogen energy technology zones. It also requires realizing the production and export of hydrogen raw materials, materials and products, the development and export of hydrogen technologies, as well as the diversification of hydrogen energy. In addition to these, renewable hydrogen ecosystem requires to manage a hydrogen demand and supply chain that includes hydrogen energy production, hydrogen energy conservation, hydrogen energy processing, hydrogen energy storage, hydrogen energy transportation, hydrogen energy consumers after hydrogen energy use in the process from the source to the end user. A schematic illustration of a renewable hydrogen energy ecosystem and the main sources of the instabilities in a renewable hydrogen ecosystem are illustrated in Fig. 1.

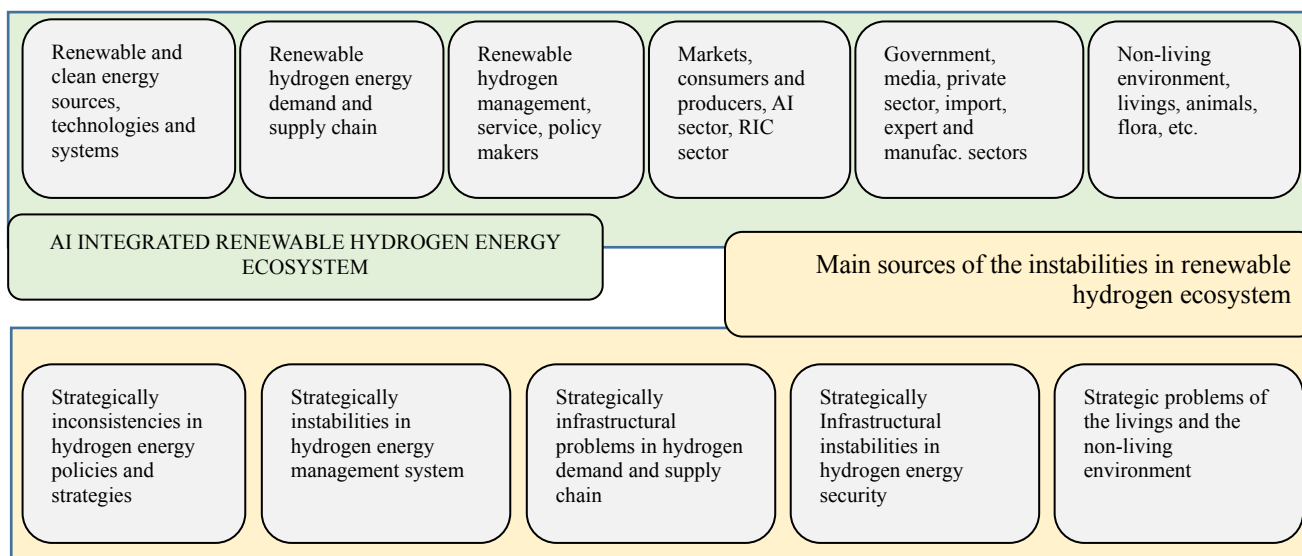


Figure 1. Main sources of the instabilities in a renewable hydrogen ecosystem

CONCLUSIONS

In order to establish a renewable hydrogen energy ecosystem, the basic conceptual framework should include smart management of hydrogen ecosystem, applicable hydrogen policies and strategies, hydrogen ecosystem security and hydrogen ecosystem sustainability. In this regard, the following strategies can contribute to establish a smart renewable hydrogen energy ecosystem:

- Establishment of resource, data, information, knowledge, technology and marketing system related to hydrogen energy.
- Empowering the stakeholders and sharing the knowledge for a sustainable hydrogen ecosystem in a deeply decarbonized future.
- Establishing a hydrogen market economy based on the massification, internationalization, industrialization of renewable hydrogen ecosystem with country priorities.

REFERENCES

- [1] A. Midilli, I. Dincer, M. Ay, Green energy strategies for sustainable development, *Energy Policy*, 34(18) (2006) 3623-3633.
- [2] A. Midilli, I. Dincer, M.A. Rosen, The role and future benefits of green energy, *International Journal of Green Energy*, 4 (2007) 1-23.
- [3] A. Midilli, Green hydrogen energy system: a policy on reducing petroleum-based global unrest, *International Journal of Global Warming*, 10 (2016) 354-370.
- [4] A. Midilli, I. Dincer, Key strategies of hydrogen energy systems for sustainability, *International Journal of Hydrogen Energy*, 32(5) (2007) 511-524.
- [5] A. Midilli, I. Dincer, Hydrogen as a renewable and sustainable solution in reducing global fossil fuel consumption, *International Journal of Hydrogen Energy*, 33 (2008) 4209-4222.

0-D PARALLEL CIRCUIT MODELING OF SOLID OXIDE FUEL CELL

^{1*} Anil Erdogan, ² Alper Can İnce, ³ C. Ozgur Colpan

¹The Graduate School of Natural and Applied Sciences, Dokuz Eylul University, Buca, Izmir, Turkey

²Gebze Technical University, Faculty of Engineering, Mechanical Engineering Department, Gebze, Kocaeli, 41400, Turkey

³Faculty of Engineering, Department of Mechanical Engineering, Dokuz Eylul University, Buca, Izmir, Turkey

*Corresponding author e-mail: anilerdogan1992@hotmail.com

ABSTRACT

A solid oxide fuel cell (SOFC) is an electrochemical conversion device that generate electricity directly from oxidizing a fuel. SOFCs are made up of ceramic based material with operating temperatures ranging from 600°C to 1000°C that are mainly used in electricity and heat generations (especially combi-boiler applications). Single-cell SOFCs are combined with bipolar layers and transformed into stacks with obtaining high power densities. SOFCs have many advantages over other types of fuel cells [1,2]. These advantages can be explained as follows. (1) Since these type of fuel cells operate at high temperatures, there is no fluid in the liquid phase; thus there is no water management problem in this type of fuel cells; (2) cheaper materials and methods are used to produce electro-catalysts; (3) can be thermally integrated with other systems (e.g. Rankine cycle, Brayton cycle, and gas turbine) and can be easily used in compound power cycles; (4) It has a wide range of fuel usage due to its availability with fuels such as hydrocarbon, methanol and biomass; (5) carbon-containing gases transform into useful fuel by undergoing chemical conversion inside of fuel cell. This type of fuel cell has advantages as well as disadvantages: (1) Due to its high-temperature operation, it has difficulties with its manufacture and durability, and (2) carbon deposition and sulfur poisoning problems occur when carbon-based gases such as methane and biogas are used. The main application of these fuel cell types is stationary power and heat generations. In addition, it has limited uses in transportation, military and portable applications.

The aim of this study is to conduct mathematical model for SOFC with a novel approach to assess the electrochemical performance. Moreover, this model is suitable for the SOFC based integrated systems. In this study, the parallel circuit approach model is explained, as shown in Fig 1. In this approach, the oxidation of hydrogen and carbon monoxide is handled separately. Considering the parallel circuit approach, the cell voltages due to the hydrogen oxidation and carbon-monoxide oxidations is identical. The equations used in this model are also taken into account. It should be noted that the calculations of molar flow rates of each species entering and exiting the SOFC, equilibrium constant equations for reactions inside of the SOFC, steam to carbon ratio and fuel utilization calculations are considered in the model. The synthetic gas fed solid oxide fuel cell with anode recirculation is also considered.

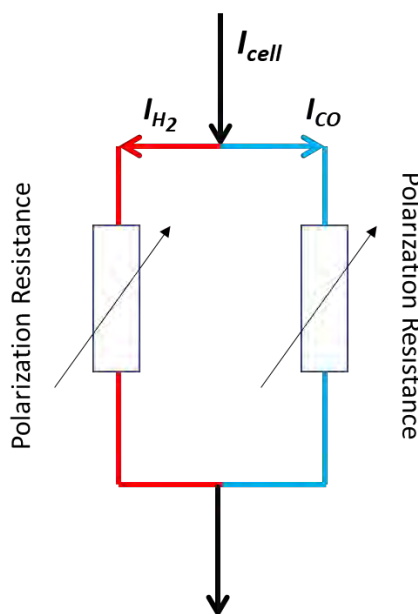


Figure 1. The equivalent circuit model for SOFC (adapted from Ref [3])

The results derived from the SOFC model are presented. In order to validate the model, a validation study is conducted to compare cell voltage and power density values taken from the literature data. Figs. (2a) and (2b) show the polarization and power density curves compared with the study published by Tao et al. (2005) [4]. The figures

show that the cell voltage and power density values are very agreeable to those of the Tao's study. The detailed comparison with the errors is also presented in Table 1.

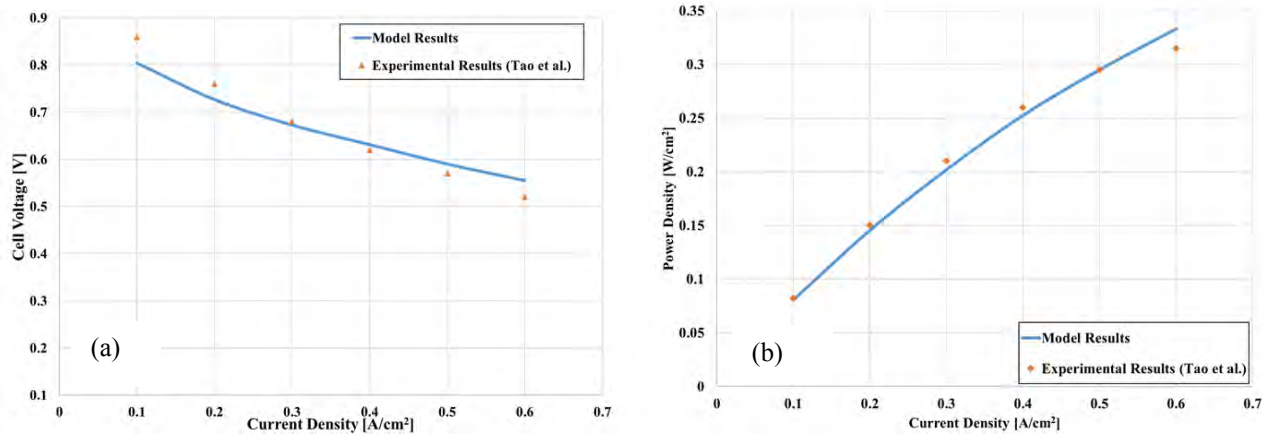


Figure 2 The electrochemical performance curves (a) polarization curve (b) power density curve compared with literature data

Table 1. The compared performance values between model and literature data

Cell Current Density (A/cm ²)	Cell voltage from the experimental (V)	Cell voltage found from the model (V)	Error for cell voltage (%)	Power density from the experimental study (W/cm ²)	Power density found from the model (W/cm ²)	Error for power density (%)
0.1	0.86	0.8044	6.91	0.082	0.080438	1.94
0.2	0.76	0.7267	4.58	0.15	0.14534	3.21
0.3	0.68	0.6728	1.07	0.21	0.201836	4.04
0.4	0.62	0.6313	1.79	0.26	0.252512	2.97
0.5	0.57	0.5901	3.41	0.295	0.295048	0.02
0.6	0.52	0.5552	6.34	0.315	0.333134	5.44

REFERENCES

- [1] Colpan CO, Dincer I, Hamdullahpur F. A review on macro-level modeling of planar solid oxide fuel cells. *Int J Energy Res* 2008; 32:336–55. <https://doi.org/10.1002/er.1363>.
- [2] Ferrari ML, Damo UM, Turan A, Sánchez D. *Hybrid Systems Based on Solid Oxide Fuel Cells*. Chichester, UK: John Wiley & Sons, Ltd; 2017. <https://doi.org/10.1002/9781119039044>
- [3] Aicart, J., Laurencin, J., Petitjean, M., & Dessemond, L. (2014). Experimental Validation of Two-Dimensional H₂O and CO₂ Co-Electrolysis Modeling. *Fuel Cells*, 14(3), 430-447.
- [4] Tao, G., Armstrong, T., & Virkar A. Intermediate temperature solid oxide fuel cell (IT-SOFC) research and development activities at MSRI. *Ninet. Annu. ACERC&ICES Conf.*, 2005.

PERFORMANCE OF SOLAR ASSISTED DUAL SOURCE HEAT PUMP

Kamil Kaygusuz^{1,*}; Ömer Kaygusuz² and Teoman Ayhan²

¹Department of Chemistry, Karadeniz Technical University, Trabzon, Turkey

²Department of Mechanical Engineering, Avrasya University, Trabzon, Turkey

*Corresponding author e-mail: kamilk@ktu.edu.tr

ABSTRACT

Dual source heat pump systems comprise of a main cold source heat pump that is supported by an additional heat source. Two arrangements have been studied in detail: air source heat pumps combined with solar collectors; and ground source heat pumps coupled with solar collectors. In addition to a situation where solar collectors are devoted solely to direct heating, the solar system can be used with the heat pump in either a series or a dual source scheme. When set up in series, a higher COP can be achieved, but there is often a lower free energy fraction. This is due to the lack of direct solar heating, meaning that auxiliary energy is required more frequently. A careful analysis of all the plant elements, including location, heating and cooling demand, solar collector area, thermal ground probe length, etc. is fundamental for achieving the best outcome in terms of both good primary energy savings and profitable economic performance.

Keywords: Solar energy; Heat pumps; Energy storage; Residential heating

INTRODUCTION

Heat pumps have a tremendous potential to bring renewable heating into houses. Because heat pumps are electricity-driven, there is a direct interaction with other energy demands within the built environment, such as PV panels and electric vehicles. By using heat pumps in a flexible way, it is possible to better integrate these different electricity-producing and electricity-consuming devices. Solar energy systems and heat pumps are two promising means of reducing the consumption of fossil energy sources and, potentially, the cost of delivered energy for domestic space heating and cooling with water heating. A logical extension of each is to try to combine the two to further reduce the cost of delivered energy. It is widely believed that solar heat pump combined systems will save energy, but what is not often known is the magnitude of the possible energy savings and the value of such savings relative to the additional expense. The principal advantage of employing solar radiation as a heat pump heat source is that, when available, it provides heat at a higher temperature level than do other sources, resulting in an increase in the coefficient of performance (COP). Compared with a solar heating system without a heat pump, the collector efficiency and capacity are materially increased due to the lower collector temperature required.

The combination of a heat pump and solar energy system would appear to alleviate many of the disadvantages that each has when operating separately. During winter, the energy that could be collected by the solar system, but that would be too low in temperature to be useful for direct heating, may be used as a source for the heat pump. Because the solar collector storage system can supply energy at temperatures higher than the ambient outdoor air, the capacity and COP of the heat pump would increase over those for the heat pump alone, the peak auxiliary load requirement would be reduced, and the combined heating system would seem to operate more economically. The operation of the solar system at temperatures near or below room temperature would decrease the collector losses and allow more energy to be collected. The lower collection temperature might allow the use of collectors with one or no covers, and this would reduce the first cost from a conventional two-cover solar system. Finally, for those areas where warm temperatures occur during cloudy periods, the combined system might compensate for the reduced performance of the conventional solar system under cloudy conditions and the low capacity of the heat pump in cold weather.

MATERIALS AND METHODS

The dual-source SAHP system, illustrated in Fig. 1, combines the advantages of the parallel and series systems and overcomes their disadvantages. The solar collector, heat storage, and building heat exchanger all continue to work as a simple solar system so long as the tank temperature remains above 40°C. At temperatures below that, the heat pump system is called on by a microprocessor controller, and a decision is made as to whether it is better to draw the heat pump's heat from the tank or from the outside air. The control strategy options are numerous for this system; it can be operated to optimize savings of electricity or to reduce peak loads. It would be the most efficient of all the systems described here. It has the disadvantage that the required heat pump is complex and will be costly to manufacture. Considerable development work will be required to ensure that the unit can be operated in all sequences of its modes with full reliability. With this system, air conditioning is accomplished by operating the unit as a simple air-to-air heat pump in the cooling mode, using only the outside heat exchanger as a condenser. So, it is obvious that the dual-source heat pump system takes advantage of the best features of the series and parallel heat pump systems. The system is not capable of using the storage tank to reduce air-conditioning peak loads during the summer because the heat pump cannot be used to cool the tank to the outside air.

Integrating solar thermal collectors with heat pump systems shows also positive nonenergetic advantages. For example, adopting solar thermal collectors as an additional heat source reduces the yearly operation time of the device resulting in an increased lifespan once again. Moreover, the noise of air source heat pumps is reduced or eliminated in summer, when customers are more likely to open buildings' windows.

Among all these advantages of SHP systems, energetic and environmental aspects have a leading position. The combination of solar thermal and heat pump technologies contributes to increasing the system SPF and consequently in reducing the final energy (FE) consumption of the system and consequently the CO₂ emissions. The additional SPF induced by solar collectors is variable and dependent upon the SHP system configuration (series and parallel), the heat source typology, the surface area of the solar field, and the building loads. A value of SPF per m² of solar field has been given according to parallel and series SHP system layouts. The benefit in terms of FE savings is dependent on the SPF_{ref} of a reference system and on the consequent SPF [2].

$$SPF_{ref} = \frac{\int (Q_{SH} + Q_{DHW}) dt}{\int (\sum P_{el}) dt} \quad (1)$$

$$FE (\%) = \frac{FE_{ref} - FE_{SHP}}{FE_{ref}} = \left(\frac{1}{SPF_{ref}} - \frac{1}{SPF_{SHP}} \right) / \left(\frac{1}{SPF_{ref}} \right) \quad (2)$$

CONCLUSIONS

When the sun is shining, the collectors will be the primary source of energy for the domestic hot water preparation and for the space heating. Furthermore, the daily solar production can be stored for future use during a few days. When the sun is less abundant or when the solar storage is empty, the heat pump will take over the duty. The source of the primary low-energy "heat" for the heat pump to operate can be air, ground, or water from a river or an aquifer. A nice feature of the hybrid combination is that the solar collectors can also be used as the provider of the primary heat for the heat pump. The two components will then operate in the so-called serial mode. Combining solar and heat pump technologies is relevant in several aspects: a high renewable fraction can be achieved (solar + the heat pump heat source) and the safety of the solution makes it a good choice for many homeowners. The solar heat can help enhance the performance of the heat pump by raising the evaporation temperature. And the solar heat can be stored at low temperatures (0-80 °C) thus making good use of the collectors even during the cold season, cloudy days or at night. A good use of the latent heat of 1.0 m³ of water changed into ice around 0° C can also be achieved. Or a good use of the latent heat of 2.0 m³ of CaCl₂.6H₂O melted/solidified around 30 °C for heating and cooling applications (see Figs. 2-12).

REFERENCES

- [1] Hadorn, J.C. Solar and heat pump systems for residential buildings. Berlin: Ernst & Sohn, 2015.
 [2] Duffie, J.A., Beckman, W.A. Solar engineering of thermal processes, Fourth Edition, New Jersey: John Wiley & Sons, 2013.
 [3] Freeman, T.L., Mitchell, J.W. Audit, T.E. Performance of combined solar-heat pump systems, Solar Energy 1979; 22: 125-135.
 [4] Kaygusuz, K. Performance of solar-assisted heat-pump systems, Applied Energy 1995; 51: 93-109.
 [6] Kaygusuz, K. Investigation of a Combined Solar-Heat Pump System for Residential Heating. Part 2: Simulation Results. Int. J. Energy Research 1999; 23: 1213-1223.
 [7] Kaygusuz, K., Ayhan, T. Experimental and theoretical Investigation of Combined solar heat pump system for residential heating. Energy Convers Mgmt 1999; 40: 1377-1396.

Table 1. Theoretical performance of the solar-assisted dual-source heat pump system for heating season

Months	Working days for SADSHPS	Heat Pump COP	Outdoor Air temp. (°C)	Solar Radiation (MJ/m ² .day)	Collector Efficiency (%)	Storage Efficiency (%)	Heating load supplied by the SADSPS (%)
November	30	2.94	14.2	6.24	53	58	82
December	30	2.92	10.1	4.74	55	60	78
January	30	2.82	6.7	5.12	56	64	52
February	28	2.72	5.4	8.06	52	62	42
March	30	2.86	7.3	6.94	56	66	78
April	30	3.00	11.7	11.84	58	68	88
May	20	3.21	15.7	16.62	64	70	94

SADSHPS: Solar Assisted Dual Source Heat Pump System

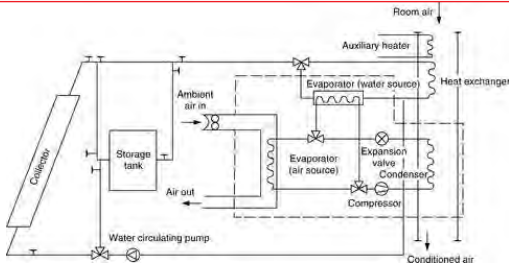


Fig. 1. Dual-source system.

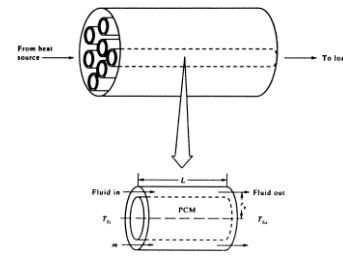


Fig. 2. The PCM energy storage tank.

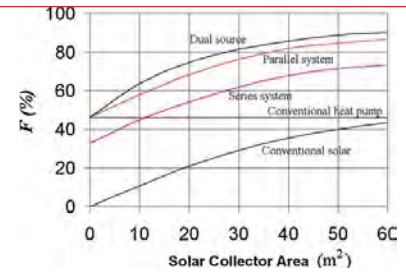


Fig. 3. Fraction of the annual load met by free energy.

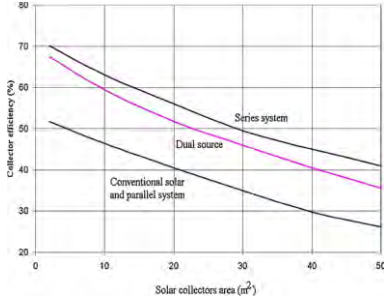


Fig. 4. Collector efficiency as a function of area.

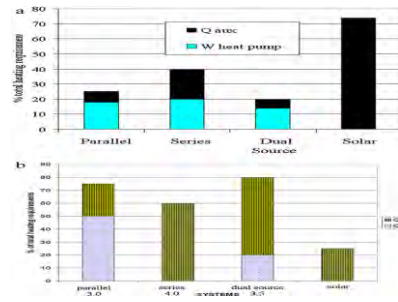


Fig. 5. (a,b) Fraction of the heating requirement to purchased and free energy.

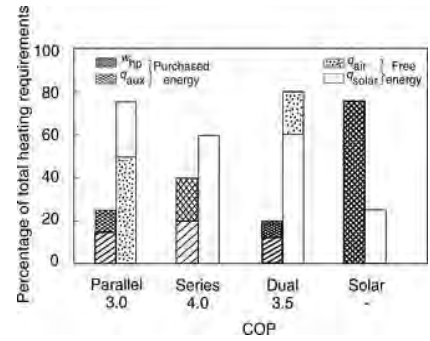


Fig. 6. Heating contributions from all possible sources.

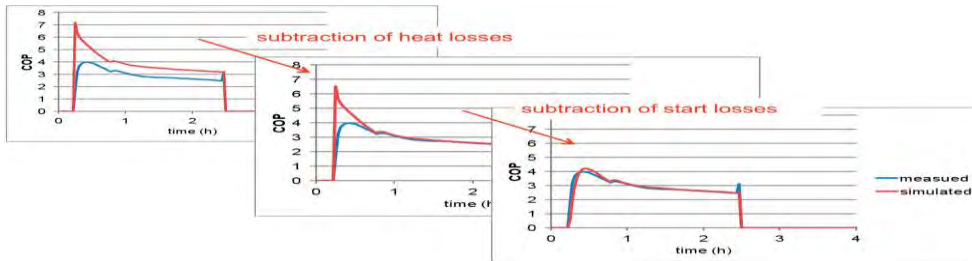


Fig. 7. A dynamic model of a heat pump can be improved by taking into account transient heat losses.

CAPRIC AND MYRISTIC ACID MIXTURE WITH GYPSUM WALLBOARD FOR LATENT HEAT ENERGY STORAGE

Kamil Kaygusuz¹ and Ahmet Sari^{2,*}

Karadeniz Technical University, Department of Chemistry and Metallurgy, 61080 Trabzon, Turkey

*Corresponding author. e-mail: asari@ktu.edu.tr

ABSTRACT

The present study was focused on three aims: (1) preparation of the phase change gypsum wallboard as novel phase change wallboard incorporating with the eutectic mixture of capric acid (CA) and myristic acid (MA) for latent heat energy storage (LHES) (2) determination of thermal properties and thermal reliability of prepared phase change wallboard using differential scanning calorimetry (DSC) technique; (3) estimation of thermal performance of the phase change wallboard in a simple building envelope. The maximum proportion of CA/MA eutectic mixture as phase change material (PCM) absorbed in gypsum wallboard was about 25 wt % of total weight. The melting and freezing temperatures and latent heats of phase change wallboard were measured as 21.12 and 21.46°C, 36.23 and 38.28 J/g, respectively by DSC analysis. These properties make it functional as LHES medium can be applied to peak load shifting, improved use of waste heat and solar energy as well as more efficient operation of heating and cooling equipment. In addition, the phase change wallboard has good thermal reliability in terms of the changes in its thermal properties after 500 and 1000 thermal cycling.

Keywords: Capric acid, myristic acid, phase change material, latent heat thermal energy storage.

INTRODUCTION

Thermal energy storage (TES) techniques are receiving more and more attention because of their main importance in energy economy, utilization of renewable energy resources and their ability to assist to match supply and demand patterns. Latent heat thermal energy storage (LHTES) is more attractive than sensible heat due to the advantages of its high storage density and isothermal characteristics of charging/discharging processes. The magnitude of the energy recovered from a LHTES system basically depends on the heat storage capacity of a phase change material (PCM) during the phase change at an almost constant temperature. PCMs can be incorporated in the building envelope to achieve latent heat with respect to the thermal comfort criteria. Within the human comfort temperature range (approximately 16-25 °C), PCMs are very effective. Research has been primarily concerned with salt hydrate type-PCMs require support and containment and cannot therefore be directly incorporated into a building material. In the last decade, the use of organic type-PCMs such as butyl stearate, capric acid/lauric acid mixture, paraffin, 1-dodecanol, 1-tetradecanol and propyl palmitate has been investigated due to the advantage of their suitability for impregnation into porous building materials and thus creating a direct gain storage element. Literature survey revealed that PCM-impregnated building materials show great promise as functional and effective building elements which can affect significant energy savings. It will be seen that besides a direct reduction in energy consumption, these energy-storing building materials can reduce peaks in demand by creating a more even load-time characteristic.

MATERIALS AND METHODS

Capric acid (CA, 98% pure) and myristic acid (MA, 97% pure) were used in preparation of the eutectic mixture. Gypsum material with Turkish origin was used as wallboard material. The pore size distribution of the gypsum was determined using a mercury porosimeter. It consists of mesopores and macropores since the pore size is mostly in the range of 20 and 1000 nm (Fig. 1). The organic PCMs can be easily held into its porous matrix. The eutectic combination ratio was found as 75.0 wt % CA and 25.0 wt % MA. Phase change wallboard samples in amount of about 100 g were formed by soaking the gypsum material in melted CA/MA eutectic mixture for about 1 h. The mixture absorbed in the gypsum was 25% in maximum ratio of total weight and no PCM seepage from the phase change wallboard was observed after 1000 melting/freezing cycles.

Thermal properties of CA, PA, CA/MA eutectic mixture and phase change wallboard such as melting temperature (T_m), freezing temperature (T_f), latent heat of melting (ΔH_m), and latent heat of freezing (ΔH_f) were measured by a DSC instrument (SETARAM DSC 131 model). A 5°C/min heating rate was considered optimal for all the experiments taking into account broad peaks in melting characteristics of the fatty acids as well as the broader peaks of their mixtures. Stearic acid with reagent grade (m.p.: 70.47°C) was used as a reference for temperature calibration. Samples were measured in sealed aluminum pan with a mass of 4.5-8.5 mg. The DSC thermal analyses of CA/MA mixtures were carried out in the temperature range of 0–50°C under a constant stream of nitrogen at atmospheric pressure. T_m and T_f values was taken as onset temperatures by drawing lines at the points of maximum slope of the

leading edges of the melting and freezing peak and extrapolating base lines on the same side as the leading edge of the peaks. ΔH_m and ΔH_f values were determined by numerical integration of the area under the melting and freezing peak, respectively. All DSC measurements were repeated three times and the mean standard deviation was calculated as $\pm 0.14^\circ\text{C}$ for phase change temperature and $\pm 0.65 \text{ J/g}$ for latent heat of phase change.

Thermal cycling test was conducted to determine the thermal reliability of phase change wallboard in terms of the changes in its thermal properties after repeated thermal cycling. The test was conducted up to 1000 thermal cycling using the procedure given in literature. To determine the variation of thermal reliability with respect to the thermal cycling number, T_m , T_f , ΔH_m and ΔH_f values of the phase change wallboard were measured after 500 and 1000 thermal cycling. To study thermal performance of the phase change wallboard, six identical phase change wallboards were fabricated as mold in dimensions of 100 mm x 100 mm x 10 mm by pouring the prepared slurry (gypsum powder, water, and CA/MA eutectic mixture) into a stainless-steel mold. After vibrated for about 10 min, the molds were first kept at the room temperature for 24 h, and then dried in a vacuum drier at 50°C before use. In addition, six identical ordinary gypsum wallboards with control purpose were fabricated using the same method. After then, two simple test rooms were separately constructed by these molds. A photograph of the experimental apparatus designed for testing the thermal performance of the wallboards is shown in Fig. 2. A halogen tungsten lamp (150 W) was used as heat source. Temperature variations at inner surface of front wall, outer surface of front wall, indoor center of the both test rooms and environment were recorded by thermocouples linked to a data logger unit. When the lamp was switch on, the temperature variations at specified locals of the test room above were monitored (see Figs. 3-6).

CONCLUSIONS

The phase transition temperatures and latent heat values of eutectic mixtures which consist of 75 wt %CA and 25 wt % MA was suitable PCM for LHTES applications in building envelopes. The CA/MA eutectic mixture can be loaded in gypsum wallboard in maximum proportion of 25 % of total weight and no eutectic PCM leakage from the phase change wallboard was observed at the temperature range $20\text{-}50^\circ\text{C}$ after 1000 thermal cycling. The prepared wallboard impregnated with the CA/MA eutectic mixture melted and frozen at a narrow temperature range of $21.12\text{-}21.46^\circ\text{C}$ which was proper for storing and releasing heat in the human comfort zone. The phase change wallboard absorbed a heat of 36.123 J/g during the heat charging period and revealed a latent heat of 38.28 J/g during heat discharging period. The prepared phase change wallboard had good thermal reliability in terms of the changes in its thermal properties with respect to thermal cycling. Thermal performance test indicated that the phase change wallboard can significantly decreased the indoor temperature of a building envelope as about 4°C due to absorption of heat in conjunction with melting of the CA/MA eutectic mixture. Furthermore, the phase change wallboards can be used considered as an effective building element for storage of solar gains and improvement of thermal comfort. However, a further study is needed to investigate large scale thermal performance of a building envelope in practical dimensions and to test the fire resistance, mechanical properties and compatibility with the paints and wallpapers.

REFERENCES

- [1] Feldman, D., M.M. Shapiro, D. Banu, and C.J. Fuks. 1989. Fatty acids and their mixtures as phase change materials for thermal energy storage. *Solar Energy Materials* 18:201-216.
- [2] Feldman, D., D. Banu, D.W. Hawes. 1995. Development and application of organic phase change mixtures in thermal storage gypsum wallboard, *Solar Energy Materials Solar Cells* 36:47-157.
- [3] Kaygusuz, K. 1999. The viability of thermal energy storage. *Energy Sources* 21:745-56.
- [4] Sari, A. 2003. Thermal reliability test of some fatty acids as PCMs used for solar thermal latent heat storage applications. *Energy Conversion and Management* 44:2277-87.
- [5] Sari, A., and K. Kaygusuz. 2001. Thermal energy storage system using some fatty acids as latent heat energy storage materials. *Energy Sources* 23: 275-285.
- [6] Sari, A., K. Kaygusuz. 2002. Thermal performance of a eutectic mixture of lauric and stearic acids as PCM encapsulated in the annulus of two concentric pipes, *Solar Energy* 72: 493-504.
- [7] Sharma, A., S.D. Sharma, D. Budhi, and R.L. Sawhney. 2001. Thermal cycle test of urea for latent heat storage applications. *International Journal of Energy Research* 25:465-8.
- [8] Sharma, S.D and K. Sagara. 2005. Latent heat storage materials and systems. A review. *International Journal of Green Energy* 2: 1-56.

Table 1. Changes In Thermal Properties of Wallboard with Respect to Thermal Cycling Number

Number of thermal cycling	Phase change wallboard			
	T_m , ($^\circ\text{C}$)	ΔH_m , (J/g)	T_f , ($^\circ\text{C}$)	ΔH_f , (J/g)
0	21.12	36.23	21.46	38.28
500	19.72	35.18	19.21	36.21
1000	20.86	34.06	19.61	35.32

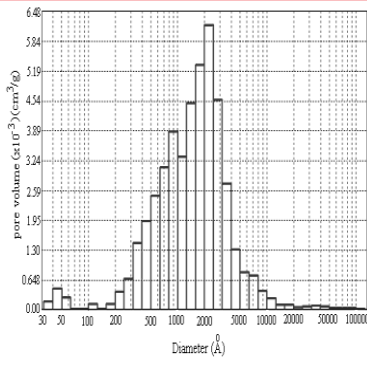


Figure 1.



Figure 2.

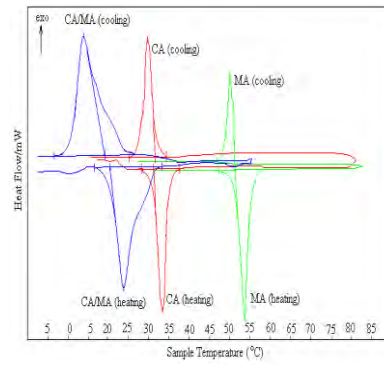


Figure 3.

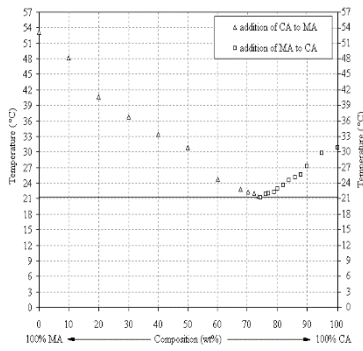


Figure 4.

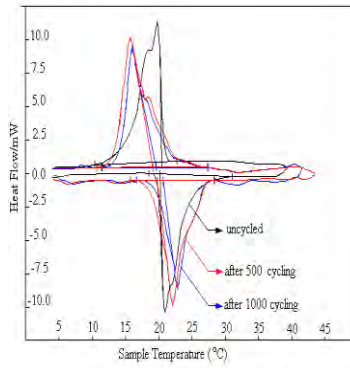


Figure 5.

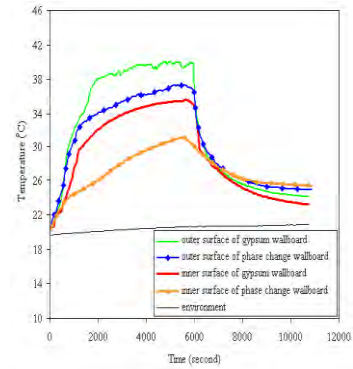


Figure 6.



Some Publications from Turkish Academy of Sciences





TÜRKİYE BİLİMLER AKADEMİSİ
TURKISH ACADEMY OF SCIENCES

www.tuba.gov.tr

Vedat Dalokay Caddesi: 112
06670 GOP/Çankaya - Ankara
Tel: 0312 442 29 03 (pbx) (#168)
Faks: 0312 442 72 36 / 2358 / 6491



TÜRKİYE BİLİMLER AKADEMİSİ
TURKISH ACADEMY OF SCIENCES

TUBA World Conference on
Energy Science and Technology

(TUBA WCEST-2021) August 8-12, 2021 / Online

CERTIFICATE OF PRESENTATION

This is to certify that

Derya Betül UNSAL

has presented the paper entitled

INVESTIGATION OF LSTM FOR ENERGY DEMAND RESPONSE
APPLICATIONS

at the TUBA World Conference on Energy Science and Technology (TUBA WCEST - 2021) between August 8-12, 2021

Prof. Dr. Ibrahim DINCER

Conference Chair

Prof. Dr. Muzaffer SEKER

General Chair & President of TÜBA



TÜRKİYE BİLİMLER AKADEMİSİ

TURKISH ACADEMY OF SCIENCES

TUBA World Conference on Energy Science and Technology (TUBA WCEST-2021), which will be held virtually between August 8-12, 2021.

The conference program posted on the conference website (<https://wcest.tuba.gov.tr/>) and presented below, participants who attempted to the conference from 22 different countries and it can be confirmed with the conference program that more than half of the papers are presented by participants from outside of Turkey.

Thank you for continuing your interest in TUBA WCEST-2021.

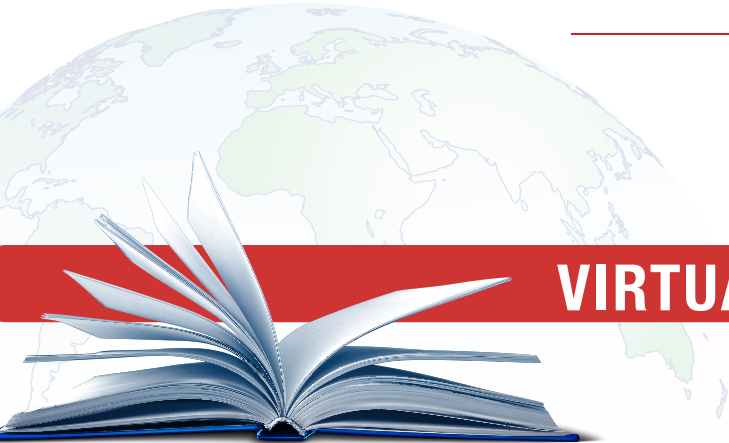
Sincerely,
Conference Chair



TÜRKİYE BİLİMLER AKADEMİSİ
TURKISH ACADEMY OF SCIENCES

TUBA World Conference on Energy Science and Technology (TUBA WCEST-2021)

8-12 August 2021



VIRTUAL CONFERENCE PROGRAM

 <https://wcest.tuba.gov.tr>

 wcest@tuba.gov.tr

Sunday - August 8, 2021 - [Zoom Link](#)

Panel Discussion Session 1: Energy, Environment & Economy

Moderator: Ilgi Karapinar, Turkey

Panel Speakers

Azize Ayol, Dokuz Eylül University, Turkey

Chris Cook, ISRS at University College London, UK

Mihri Ozkan, University of California, Riverside, USA

Seeram Ramakrishna, National University of Singapore, Singapore

Olcay Unver, Arizona State University, USA

Zafer Ure, PCM Products, UK

14:00
16:00
(GMT+3)

16:00 - 16:15 (GMT+3)

Break

Panel Discussion Session 2: Energy & Education

Moderator: Hatice Eser Okten, Turkey

Panel Speakers

Feridun Hamdullahpur, University of Waterloo, Canada

Onur Mutlu, ETH Zurich, Switzerland

Celile Eren Okten, Yildiz Technical University, Turkey

Bestami Ozkaya, Yildiz Technical University, Turkey

Marc A. Rosen, Ontario Tech University, Canada

Mehmet Yildiz, Sabanci University, Turkey

16:15
18:15
(GMT+3)

Monday - August 9, 2021 - [Zoom Link](#)

Opening Speeches

09:00

(GMT+3)

Prof. Dr. Muzaffer Seker, *President of Turkish Academy of Sciences (TUBA) & General Chair of Conference*

H.E. Fatih Dönmez, *Minister of Energy and Natural Resources, Turkey*

H.E. Mustafa Varank, *Minister of Industry and Technology, Turkey*

10:30 - 10:45 (GMT+3)

Break

Plenary Session

Session Chair: Ibrahim Dincer, Canada/Turkey

10:45

12:15

(GMT+3)

Christian Rakos

President of World Bioenergy Association (WBA), Austria

Transforming Bioenergy Use in the Developing World – A Key Target for Sustainable Development and Net Zero Carbon Emissions

Feridun Hamdullahpur

Past President, University of Waterloo, Canada

An Overview of the Role of Universities on Energy and Sustainability

12:15 - 13:15 (GMT+3)

Break

Monday - August 9, 2021

Zoom Link 1

Keynote Session 1

Session Chair: Adolfo Iulianelli, Italy

Keynote Talk 1

13:15 – 14:00 (GMT+3)

Benjamin K. Sovacool

University of Sussex, UK

**Decarbonisation and Its Discontents: A
Critical Justice Perspective on Four Low-
Carbon Transitions**

Keynote Talk 2

14:00 – 14:45 (GMT+3)

Richard S.J. Tol

University of Sussex, UK

**The Economic Impact of Climate and
Weather**

13:15
14:45
(GMT+3)

Zoom Link 2

Invited Session 1

Session Chair: Ali Kosar, Turkey

Invited Talk 1

13:15 – 13:45 (GMT+3)

Umberto Desideri

University of Pisa, Italy

**Power to Fuel Technologies: Is a Necessary
Option for the Future?**

Invited Talk 2

13:45 – 14:15 (GMT+3)

Chris Cook

The ISRS at University College London, UK

**Introducing the Energy Treasury: from \$
Economics to Energy Economics**

Invited Talk 3

14:15 – 14:45 (GMT+3)

James Carton

Dublin City University & Hydrogen Ireland
Association, Ireland

**Hydrogen; Building a Hydrogen Economy on
the Island of Ireland**

Zoom Link 3

General Session 1

Biofuels and Bioenergy

Session Chair: M. Hakkı Alma, Turkey

#7 “Hydrothermal Carbonization of Wet Olive Mill
Waste” G. Balmuk, H. Cay, G. Duman Tac, I. C.
Kantarlı & J. Yanik

#65 “Biochar: Physical Properties and Effects on
the Soil” M.H. Alma, A. Altıkat & S. Altıkat

#66 “Bio-Oil Separation and Upgrading
Techniques” M.H. Alma, A. Altıkat & S. Altıkat

#89 “Utilization of Soft Drink Industry Waste as
Energy Feedstock” I.C. Kantarlı

#120 “Impact of Using Ethanol-Gasoline
Compound Fuel on Performance of a Dual-Fuel
Vehicle” P. Kamarei, P. Ahmadi, N. Javani & M.
Raeesi

#126 “Sugarcane Leaves and Tops for
Biogas Production by Batch Experiments” N.
Sinbuathong, B. Sillapacharoenkul, R. Khun-
anake & Y. Paopun

14:45 - 15:00 (GMT+3)

Break

Monday - August 9, 2021

Zoom Link 1

Keynote Session 2

Session Chair: **Ilgi Karapinar**, Turkey

Keynote Talk 3

15:00 – 15:45 (GMT+3)

Neven Duić

University of Zagreb, Croatia

Decarbonisation of Energy Systems with Variable Renewables

Keynote Talk 4

15:45 – 16:30 (GMT+3)

Erol Gelenbe

Polish Academy of Sciences, Poland

Energy Consumption by ICT: Facts, Measurements, and Trends

15:00

16:30

(GMT+3)

Zoom Link 2

Invited Session 2

Session Chair: **Umberto Desideri**, Italy

Invited Talk 4

15:00 – 15:30 (GMT+3)

Muhammad Ali Imran

University of Glasgow, UK

5G Communication Systems and Energy Efficient Future

Invited Talk 5

15:30 – 16:00 (GMT+3)

Mehmet Sarikaya

University of Washington, USA

Energy Materials - Current & Future

Invited Talk 6

16:00 – 16:30 (GMT+3)

Alejandro H. Buschmann

Universidad de Los Lagos, Chile

Macroalgal Sea-farming and Biofuels: Desires and Facts

Zoom Link 3

General Session 2

Fuel Cell & Batteries

Session Chair: **Bora Timurkutluk**, Turkey

#45 "Pd-Modified Polyrhodanine for Methanol Electrooxidation Reaction" **R. Solmaz** & D. Öztürk

#52 "Selection and Synthesis of Ceramic Electrolytes for Intermediate Temperature Solid Oxide Fuel Cells" **H. Ozlu Torun**

#97 "On Energy Performance of SOFC Integrated S-CO₂ Micro-Gas Turbine" **U. Akbulut** & A. Midilli

#30 "Highly Stable Pouch Cell Scale Quasi-Solid-State Lithium-Air Batteries" **M. Çelik**, A. Kizilaslan, T. Çetinkaya & H. Akbulut

#129 "Hydrogen Fuel Cell Bus Performance Assessment with Machine Learning Degradation Prediction" **P. Ahmadi**

#116 "Investigating the Environmental Effects of a Hybrid UAV with Fuel Cell, According to Two Different Scenarios" **D. Çalişir**, S. Ekici, A. Midilli & T.H. Karakoç

16:30 - 16:45 (GMT+3)

Break

Monday - August 9, 2021

Zoom Link 1

Keynote Session 3

Session Chair: Neven Duić, Croatia

Keynote Talk 5

16:45 – 17:30 (GMT+3)

S. Ravi P. Silva CBE

University of Surrey, UK

A Net Zero Carbon World through Innovation in Energy Materials

Keynote Talk 6

17:30 – 18:15 (GMT+3)

Marc A. Rosen

Ontario Tech University, Canada

Energy Sustainability for Sustainable Development

16:45

18:15

(GMT+3)

Zoom Link 2

Invited Session 3

Session Chair: Murat Koksal, Turkey

Invited Talk 7

16:45 – 17:15 (GMT+3)

Steven Brown

Director, New Strain Development, LanzaTech, USA

Stepping on the Gas to a Circular Economy: Accelerating the Development of Carbon-Negative Chemical Production from Gas Fermentation

Invited Talk 8

17:15 – 17:45 (GMT+3)

Cengiz Sinan Ozkan

Materials of California, Riverside, USA

Materials Design for Sustainability and Energy Storage

Invited Talk 9

17:45 – 18:15 (GMT+3)

Tianzhen Hong

Lawrence Berkeley National Laboratory, USA

Applications of Machine Learning Techniques in Buildings: An Overview and Examples

Zoom Link 3

General Session 3

Sustainable Development - I

Session Chair: Barbaros Cetin, Turkey

#9 “Emissions and Its Driver Analysis for the United Kingdom Higher Education Institute” **A. Nayak, N. Turner & E. Gobina**

#32 “Evolution of Microclimate Effect of an Urban Park over Their Built Environment” **M.A. Ruiz, M.F. Colli, C.F. Martinez & E.N.C. Cantaloube**

#42 “Analysis of Urban Scale Energy Certification Systems for Efficient Communities” **M.B. Sosa, E.N. Correa & M.A. Cantón**

#71 “Bioclimate of Urban Areas at the Russian far North in the Context of Climate Change: Energy and Human Health” **E.A. Grigorjeva**

#92 “Production of Pan-Peg Thermal Energy Storage Nanofibers by Electrospinning Method” **T. Paçacı, C. Alkan, Y. Dinç & E. Kişioğlu**

#107 “A New Methodology for Distributor Selection in Refrigeration Cycles” **H.A. Hacimusalar, M.H. Sökücü, M.R. Özdemir & A.S. Dalkılıç**

Tuesday - August 10, 2021

Zoom Link 1

Keynote Session 4

Session Chair: Ilker Tari, Turkey

Keynote Talk 7

09:00 – 09:45 (GMT+3)

Kevin Trenberth

National Center for Atmospheric Research
(UCAR), USA

**The Changing Flow of Energy Through the
Climate System**

Keynote Talk 8

09:45 – 10:30 (GMT+3)

Jianlei Niu

The Hong Kong Polytechnic University, Hong
Kong

**Progresses in Thermal Energy Storage
Research to Reduce the Energy Use in
Buildings**

09:00
10:30
(GMT+3)

Zoom Link 2

General Session 4

Renewable Energy – I

Session Chair: Arif Hepbasli, Turkey

#29 "Geothermal Energy Production from Oil and
Gas Wells: A Technical Review" A. Mukhtarov, G.
Gokcen Akkurt & N. Yildirim

#69 "Working Fluid Selection and Performance
Analysis of a Geothermal Binary Power Plant" Z.
Ozcan & G. Gokcen Akkurt

#90 "Modeling and Performance Evaluation of the
Geothermal Energy Based Combined Plant for
Different Products" Y.E. Yuksel, F. Yilmaz & M.
Ozturk

#34 "Determining Compensation Rate for Wind-
Solar Hybrid Energy System in Istanbul Based on
ANFIS Modeling" E. Gün & A.D. Şahin

#23 "Outdoor Performance of an Improved
Thermoelectric Heat Pumping Solar Air Heater" J.
R. Segnon & H.O. Njoku

#24 "Development of Hybrid Power Systems for
North India Rural Areas" G. Muthukumaran & B.
Kosoy

10:30 - 10:45 (GMT+3)

Break

Tuesday - August 10, 2021

[Zoom Link 1](#)

Specialized Session 1

New Dimensions in Fossil Fuels

Session Chair: Ismail Boz, Turkey

Specialized Talk 1

10:45 – 11:05 (GMT+3)

Emre Artun

Istanbul Technical University, Turkey

Machine-Learning Based Modeling of Hydrocarbon Reservoirs

Specialized Talk 2

11:05 – 11:25 (GMT+3)

Ozge Bozkurt

TUPRAS R&D Center, Turkey

The Clean Fuel Technology Approach of TUPRAS R&D

Specialized Talk 3

11:25 – 11:45 (GMT+3)

Salomé Larmier

Le Mans Université, France

Beef Veins: a Multi-marker for Mature Source Rock

Specialized Talk 4

11:45 – 12:05 (GMT+3)

Samil Sen

Istanbul University – Cerrahpasa, Turkey

Determination of a Deep Learning-Based Model for Shale Porosity Prediction Using World Scale Data Set

[Zoom Link 2](#)

General Session 5

Hydrogen Energy Technologies – I

Session Chair: Yilser Devrim, Turkey

#53 “Environmental Impact Assessment of a Novel Photoelectrochemical Reactor for Hydrogen Production” [A.E. Karaca](#) & I. Dincer

#135 “The Role of Machine Learning on Metal Hydride for Hydrogen Storage” [M.S. Karasu Asnaz](#) & A. Midilli

#64 “Activated Carbon-Decorated Spherical Titanium Oxide Nanoparticles for Enhanced Hydrogen Production” S. Sekar, D.Y. Kim & [Sejoon Lee](#)

#67 “Influence of Biohydrogen Production on the Ratio of Generated Acids and Regulation of Δ pH in *E. Coli* During Fermentation of Mixed Carbon Sources at pH 7.5” [H. Gevorgyan](#) & K. Trchounian

#80 “Design of a Future Hydrogen Supply Chain: A Multi-Objective Model for Turkey” [E. Geçici](#), A. Erdoğan & M.G. Güler

#112 “Electrospinning is a Powerful Tool for the Design of Carbon Nanofiber Towards Hydrogen Energy System” [A.K. Figen](#)

10:45
12:15
(GMT+3)

12:15 - 13:15

Break

Tuesday - August 10, 2021

[Zoom Link 1](#)

Keynote Session 5

Session Chair: Meng Ni, China

Keynote Talk 9

13:15 – 14:00 (GMT+3)

Olcay Unver

Arizona State University, USA

Pathways to Sustainability in an Increasingly Water-Scarce World

Keynote Talk 10

14:00 – 14:45 (GMT+3)

Henrik Lund

Aalborg University, Denmark

Smart Renewable Energy Systems and Decarbonisation.

The Danish Target of a 70% Decrease in CO₂ Emission by 2030

13:15

14:45
(GMT+3)

[Zoom Link 2](#)

Invited Session 4

Session Chair: Can Ozgur Colpan, Turkey

Invited Talk 10

13:15 – 13:45 (GMT+3)

Umit B. Demirci

University of Montpellier, France

Boron for Carrying/Storing Hydrogen

Invited Talk 11

13:45 – 14:15 (GMT+3)

Zafer Ure

Managing Director, Phase Change Material Products Ltd., UK

Thermal Energy Storage Technologies and their Global Application Examples

Invited Talk 12

14:15 – 14:45 (GMT+3)

Erkan Oterkus

University of Strathclyde, UK

Fracture Modeling Based on Peridynamic Theory

14:45 - 15:00 (GMT+3)

Break

Tuesday - August 10, 2021

[Zoom Link 1](#)

Keynote Session 6

Session Chair: Selda Oterkus, UK

Keynote Talk 11

15:00 – 15:45 (GMT+3)

Igor Pioro

Ontario Tech University, Canada

**Current Status and Future Developments
in the Nuclear-power Industry of the World**

Keynote Talk 12

15:45 – 16:30 (GMT+3)

Zhu Han

University of Houston, USA

**Distributed Deep Reinforcement Learning
for Renewable Energy**

[Zoom Link 2](#)

Invited Session 5

Session Chair: Olcay Unver, USA

Invited Talk 13

15:30 – 16:00 (GMT+3)

Meng Ni

The Hong Kong Polytechnic University,
China

**New Developments in Zn-Air Batteries for
Energy Storage**

Invited Talk 14

16:00 – 16:30 (GMT+3)

Bahareh Seyedi

United Nations Department of Economic and
Social Affairs (UNDESA), USA

**Achieving Universal Energy Access and
Net Zero Emissions – A Policy Perspective**

[Zoom Link 3](#)

General Session 6

Renewable Energy – II

Session Chair: Ramazan Solmaz, Turkey

#18 “Potential Use of Renewable Energy for
Rural Electrification in Pakistan by Incorporating
Blockchain Technology” [A. Rana](#) & G. Gróf

#36 “Effect of Auxiliary Acceptors on Quinoline-
Based Dye-Sensitized Solar Cells” [B. S. Arslan](#),
N. Öztürk, M. Gezgin, Y. Derin, A. Tutar, M.
Nebioğlu & İ. Şişman

#37 “A New Methodological Approach for the
Techno-Economic Analysis of Hydroelectric
Power Plants in Turkey” [S. Çelikdemir](#) & M.T.
Özdemir

#40 “Extreme Winds and Risk Analysis in Turkey
for Wind Energy Applications” [T. Kara](#), S.E.
Yakut, O. Tek, M. Peköz, M. Aksakal & A.D.
Şahin

#77 “Techno-Economic Analysis of Onshore and
Offshore Wind Power Plants” [S. Çelikdemir](#) &
[M.T. Özdemir](#)

#57 “Performance Evaluation of Solar Dryer with
and without Solar Photovoltaic Heat Extraction
(PVHE) Duct” S. Monesh, A. Shankar, S.
Ezhilarasan & [S. Tiwari](#)

15:00
16:30
(GMT+3)

16:30 - 16:45 (GMT+3)

Break

Tuesday - August 10, 2021

[Zoom Link 1](#)

Keynote Session 7

Session Chair: Alper Baba, Turkey

Keynote Talk 13

16:45 – 17:30 (GMT+3)

Mohammad Shahidehpour

Illinois Institute of Technology, USA

Optimal Expansion and Operation Planning of Microgrids using a Two-Stage Data Clustering Strategy

Keynote Talk 14

17:30 – 18:15 (GMT+3)

Roland N. Horne

Stanford University, USA

Global Geothermal Outlook and Sustainable Development 2021

Keynote Talk 15

18:15 – 19:00 (GMT+3)

Arumugam Manthiram

The University of Texas at Austin, USA

Sustainable Battery Chemistries for E-Mobility and Renewable Energy Storage

[Zoom Link 2](#)

Invited Session 6

Session Chair: Samil Sen, Turkey

Invited Talk 15

16:45 – 17:15 (GMT+3)

Salih Saner

Near East University, TRNC

Geological and Geopolitical Controls on the Hydrocarbon Search in the Eastern Mediterranean Basin

Invited Talk 16

17:15 – 17:45 (GMT+3)

Ibrahim Çemen

University of Alabama, USA

Quantitative Natural Fracture Analysis in unconventional gas-shale reservoirs: An example from Woodford Shale in Oklahoma, USA

Invited Talk 17

17:45 – 18:15 (GMT+3)

Biröl Dindoruk

University of Houston, USA

Data Mining/Machine Learning in the Oil and Gas Sector: Applications in the Area of Petroleum Engineering

[Zoom Link 3](#)

General Session 7

Microgrids & Smart Grids

Session Chair: Sertac Bayhan, Qatar

#81 "The Lightweight Deep Learning Model for Smart Grid Stability Prediction" [F. Ucar](#)

#48 "A Smart Monitoring and Protection System Design Using Visible Light Communication for Grid Integration of Microgrids" M. Das, M. Sonmez & G. Bayrak

#27 "A Supervised Learning-Based Method Using a Modified Voting Algorithm for Classification of Complex Power Quality Disturbances in a Hydrogen Energy-Based Microgrid" A. Küçükler, A. Yılmaz & [G. Bayrak](#)

#6 "Nature-Inspired Two-Layer Optimizations for Interconnected Heat and Power Multi-Microgrids" [P. Fracas](#), E. Zondervan, M. Franke & K.V. Camarda

#78 "Adaptive Control Technique for Grid Integrated SPV Generating System for Power Quality Enrichment" [D. Prasad](#), N. Kumar & R. Sharma

#84 "Bid Optimization in Electricity Markets" [E. Polat](#), M.G. Güler & M.Y. Ulukuş

16:45
19:00
(GMT+3)

Wednesday - August 11, 2021

Zoom Link 1

Keynote Session 8

Session Chair: Hatice Eser Okten, Turkey

Keynote Talk 16

09:00 – 09:45 (GMT+3)

Seeram Ramakrishna

National University of Singapore, Singapore

Build Back Better Materials World to Deal with the Existential Threats to Humanity – Reimagine Materials

Keynote Talk 17

09:45 – 10:30 (GMT+3)

Andrea “Andy” Blair

President of International Geothermal Association (IGA), New Zealand

Global Geothermal Movements: What’s Happening in the World of Geothermal, Current Focus, Latest Thinking, and Global Trends

Zoom Link 2

General Session 8

Green Energy

Session Chair: Azize Ayol, Turkey

#79 “State-of-Art Green Cryptocurrency Mining Models” N. Güre

#44 “Capital-Energy Substitution in Turkish Manufacturing Firms: Role of Firm Size” P. Sezer

#121 “Design and Testing of an IoT Based Carbon Monoxide Monitoring UAV: Methodology, Challenges, Opportunities” E. Ozbek, O. Aras, O. Kucukkor, S. Ekici & T.H. Karakoc

#98 “Experimental Investigation of a Vapor Compression Refrigeration System for Thermal Management” F. Coskun & M.F. Serincan

#28 “Biocomposite and Polymeric Materials in Radiation Shielding Applications: A Review” E. Demir, Z. Candan & M.N. Mirzayev

#15 “Comparative Evaluation of Oil-In-Water Emulsion Separation with Aluminum Oxide & Zinc Oxide Nanoparticles Ceramic Membrane” F. Aisueni, I. Hashim, E. Ogoun & E. Gobina

Zoom Link 3

General Session 9

Energy Conversion & Management – I

Session Chair: Pouria Ahmadi, USA

#16 “Investigation of Buildings with Optimum Insulation Thickness Depending on Different External Wall Types and Insulation Materials in Terms of Mold and Moisture Risk” O Kon & L. Caner

#59 “Energy Consumption for Silage Maize Production in Kocaeli Province of Turkey” H.H. Öztürk & H. Goker

#58 “Estimation of Crude Oil Production in Turkey Via Holt-Winters Method” E. Güler & S. Yerele Kandemir

#47 “Investigation of LSTM for Energy Demand Response Applications” M Güler & D.B. Unsal

#76 “An On-Board Energy and Environmental Analysis within the Covid-19 Effects” A. Sari, E. Sulukan, D. Özkan & T.S. Uyar

#70 “Precasted Timber-Concrete Composite as a Component of Sustainable Construction” P. Mika, S. Kuc & Ł. Wesolowski

09:00
10:30
(GMT+3)

10:30 - 10:45 (GMT+3)

Break

Wednesday - August 11, 2021

Zoom Link 1

Keynote Session 9

Session Chair: Orhan Cakir, Turkey

Keynote Talk 18

10:45 – 11:30 (GMT+3)

Qingyan (Yan) Chen

Purdue University, USA

Energy Use in Buildings: Past, Present, and Future

Keynote Talk 19

11:30 – 12:15 (GMT+3)

Onur Mutlu

ETH Zurich, Switzerland

Intelligent Architectures for Intelligent Machines

10:45
12:15
(GMT+3)

Zoom Link 2

General Session 10

Solar Energy

Session Chair: Ankica Kovać, Croatia

#72 "Performance Analysis of Double Slope Passive and Active Solar Still for Indian Climatic Condition" T.A.S.S. Krishna, S. Tiwari, R. Sharma & D.B. Singh

#75 "Comparative Analysis of Solar Energy-Based Water Purification Systems Based on Various Designs" N. Kumar, V.K. Dwivedi & D.B. Singh

#60 "Solar Energy use for Drip Irrigation of Maize Production in Harran Plain of Turkey" H.H. Ozturk & H.K. Kucukerdem

#86 "Experimental Investigation and Theoretical Model of R718/LiBr Bubble Pump Operated Absorption Refrigeration Machine" N. Ben Ezzine, R. Garma, M. Chatti & A. Bellagi

#43 "Assessment of the Floating Photovoltaic (FPV) Systems Build in Extreme Weather Locations and Comparison with Terrestrial System" M.K. Kaymak & A.D. Şahin

#74 "Effect of Water Depth on Efficiencies and Productivity of N-Alike Evacuated Tubular Solar Collectors Coupled to Solar Still of Single Slope Type by Incorporating Exergy" D. B. Singh, R.K. Yadav, Y. Chaturvedi, G.K. Sharma, S.K. Sharma & N. Kumar

Zoom Link 3

General Session 11

Hydrogen Energy Technologies – II

Session Chair: Ehsan Baniasadi, Iran

#83 "Hydrogen Energy Utilization – A Review" E. Akiskalioglu

#88 "New Enhanced Design of Hydrogen-Based Thermally Driven R717 Absorption Refrigeration System" N. Ben Ezzine, M. Chatti, R. Garma & A. Bellagi

#94 "Development of Solar-Driven and Hydrogen Integrated Charging Station for Electric Vehicles" D. Erdemir & I. Dincer

#56 "Location Selection of the Hydrogen Refueling Stations: An Istanbul Case" E. Geçici, M.G. Güler & T. Bilgiç

#119 "Teaching Fuel Cell and Hydrogen Science and Engineering Across Europe" I. Lordache

#124 "Experimental Studies to Improve the Performance, Emission and Combustion Characteristics of Sweet Almond Oil Fuelled CI Engine Using Hydrogen Injection in PCCI Mode" V.E. Geo, S. Thiyagarajan & A. Sonthalia

12:15 - 13:15 (GMT+3)

Break

Wednesday - August 11, 2021

Zoom Link 1

Keynote Session 10

Session Chair: Erkan Oterkus, UK

Keynote Talk 20

13:15 – 14:00 (GMT+3)

Bruce Rittmann

Arizona State University, USA

Moving from Treatment to Resource

Keynote Talk 21

14:00 – 14:45 (GMT+3)

Mohamed-Slim Alouini

King Abdullah University of Sciences and
Technology (KAUST), Saudi Arabia

**Towards Sustainable and Environment-Aware
Wireless Networks**

13:15
14:45
(GMT+3)

Zoom Link 2

Invited Session 7

Session Chair: Safa'a Riad, Egypt

Invited Talk 18

13:15 – 13:45 (GMT+3)

Ali Kindap

Zorlu Energy & Geothermal Energy Association, Turkey

Geothermal Energy in Turkey

Invited Talk 19

13:45 – 14:15 (GMT+3)

Alper Baba

Izmir Institute of Technology, Turkey

**Importance of the Geothermal Resources and Its
Innovative Properties: A Case Study: Turkey**

Invited Talk 20

14:15 – 14:45 (GMT+3)

Arthur Weeber

TNO and Delft University of Technology, Netherlands

**Trends and Future Aspects of PV Technology and
its Applications**

Zoom Link 3

General Session 12

Modeling & Simulation – I

Session Chair: Adnan Midilli, Turkey

#73 "A Sensitivity Study of N-Alike Partly Enclosed
with Photovoltaic Thermal Compound Parabolic
Concentrators Having Series Connection" R.V.
Patel, R.K. Sharma, S. Tiwari, A. Raturi, D.B. Singh
& N. Kumar

#22 "Analysis of Roof Thermal Performance with
Innovative Technology" N. Alchapar & E. Correa

#26 "Causal Investigation of Energy Storage
Technology Criteria by Applying a Novel Integrated
Decision-Making Methodology" A. Karasan & L.
Kaya

#35 "Hot Air Drying of Spherical Moist Objects in
a 3D Rectangular Channel" S. Özcan Çoban, F.
Selimefendil & H.F. Öztop

#117 "Design and Modeling of a Multigeneration
System Driven by Waste Heat of a Marine Diesel
Engine" M.E. Demir & F. Çıtakoğlu

#131 "Exergetic Analysis of a New Hybrid Vehicle
Operating with Carbon-Free Fuels" M. Ezzat & I.
Dincer

14:45 - 15:00 (GMT+3)

Break

Wednesday - August 11, 2021

Zoom Link 1

Keynote Session 11

Session Chair: Arthur Weeber, Netherlands

Keynote Talk 22

15:00 – 15:45 (GMT+3)

Amar K. Mohanty

University of Guelph, Canada

Improved Utilization of Co-Products from Biofuel Industries in New Industrial Uses for a Sustainable Biorefinery

Keynote Talk 23

15:45 – 16:30 (GMT+3)

Victor C.M. Leung

The University of British Columbia, Canada

AIoT as a Service – Framework, Opportunities, and Challenges

15:00
16:30
(GMT+3)

Zoom Link 2

General Session 13

Sustainable Development - II

Session Chair: Tahir A.H. Ratlamwala, Pakistan

#127 “Comparative Sustainability Investigation of Hydrogen Production Methods” C. Acar

#10 “Testing Membranes for Separation of CO₂ From Small Molecules in Landfill Gas” P. Ogunlode, O. Abunumah, F. Muhammad-Sukki & E. Gobina

#128 “Hydrogen Refuelling Stations: State of the Art and Perspectives” D. Marcius, A. Kovač & M. Paranos

#111 “Thermodynamic Assessment of a Power to Methane System Under Real-World Scenario” A.C. Ince, D. Saygan Temel, C.O. Colpan, A. Keleş, & M.F. Serincan

#87 “Suitability of Siderite as Oxygen Carrier in Chemical Looping Combustion” M. Durmaz, N. Dilmaç & Ö.F. Dilmaç

#125 “Improvement of Terminal Buildings’ Environmental Performance by Renewable Energy” A. Dalkıran, O. Ballı, M.Z. Söğüt & T.H. Karakoç

Zoom Link 3

General Session 14

Energy Materials,

Session Chair: Nader Javani, Turkey

#41 “Nanocellulose in Energy Applications: Current Status and Future Prospect” M. Yıldırım & Z. Candan

#46 “Detection of Temperature Elevations in Encased Smartphones Due to Multitask Processes” C. Ndujisi & H. Njoku

#55 “Iron Oxide-Based Photocatalysts for Hydrogen Production and Dye Degradation Under Natural Sunlight” V. Preethi, S. Ananth, P.S. Chandana, M.G. Krishna & S.L. Subramanyam

#91 “A Structure Property Issue in Organic Solid-Solid Phase Change Materials: 1,3-Bisstearyolurea and 1,1,3,3-Tetrastearyolurea for Potential Solar Applications” N. Gökşen Tosun, A. Çetin & C. Alkan

#99 “Interfacial Thermal Resistance Between Water and Metals Using Molecular Dynamics Simulation” M.M. Aksoy & Y. Bayazitöglü

#100 “Thermal Conductivity of Copper-Single Walled Carbon Nanotube Using Non-Equilibrium Molecular Dynamics” K. Toprak & Y. Bayazitöglü

16:30 - 16:45 (GMT+3)

Break

Wednesday - August 11, 2021

Zoom Link 1

Keynote Session 12

Session Chair: Can Ozgur Colpan, Turkey

Keynote Talk 24

16:45 – 17:30 (GMT+3)

Li Shi

The University of Texas at Austin, USA

Atomic-Scale Phonon Band Engineering of Semiconductors

Keynote Talk 25

17:30 – 18:15 (GMT+3)

Mochammad Hadid Subki

International Atomic Energy Agency (IAEA), Austria

Advances on Small Modular Nuclear Reactor Technology Developments

16:45
18:15
(GMT+3)

Zoom Link 2

Invited Session 8

Session Chair: Nuri Azbar, Turkey

Invited Talk 21

17:15 – 17:45 (GMT+3)

Sandro Nizetić

University of Split, Croatia

Photovoltaic Thermal Collectors with Incorporated Phase Change Materials: Analysis of Design Approaches

Invited Talk 22

17:45 – 18:15 (GMT+3)

David G. Whitten

The University of New Mexico, USA

Novel, Light-Activated Antimicrobials for Elimination of Viral Pathogens

Zoom Link 3

General Session 15

Energy & Environment – II,

Session Chair: Farrukh Khalid, Turkey

#17 "Experimental Study of Red Pine Biocoal and Soma Lignite Blends in a Circulating Fluidised Bed Under Oxy-Fuel Combustion" B. Keivani, H. Olgun & A.T. Atimtay

#114 "Development of Environmental Sustainability Indicators Based on the Efficiency of Integrated Buildings" M.Z. Sogut

#106 "Thermo-Environmental Performance Assessments of a Medium-Scale Aero Turbojet Engine" H.Y. Akdeniz, O. Balli & H. Caliskan

#104 "Effects of Design Variables on Exergy and Environmental Parameters of Commercial Turbofan Engine" H. Aygun, M.R. Sheikhi & H. Caliskan

#110 "A Methodology for Thermodynamic Performance Comparison of the Crop Production" M.T. Balta

#14 "Cost Description and Characterisation of Gas Enhanced Oil Recovery Processes" O. Abunumah, P. Ogunlode & E. Gobin

Thursday - August 12, 2021

[Zoom Link 1](#)

Keynote Session 13

Session Chair: Sandro Nižetić, Croatia

Keynote Talk 26

09:00 – 09:45 (GMT+3)

Lidia Morawska

Queensland University of Technology (QUT),
Australia

Air Pollution and Energy: “this discussion is closed”!

Keynote Talk 27

09:45 – 10:30 (GMT+3)

Keith Bell

UK Energy Research Centre & University of
Strathclyde, UK

**Powering Past Fossil Fuels: Electricity and
Net-Zero Greenhouse Gas Emissions**

09:00
10:30
(GMT+3)

[Zoom Link 2](#)

General Session 16

Energy Management & Strategies

Session Chair: Emrah Biyik, Turkey

#113 “Assessment of Operational Control
Strategies on Energy Efficiency and Management
of Production Processes” M.Z. Sogut & T.H.
Karakoc

#118 “An Urban Green Energy Strategy
Proposals for Local Governments” M.O. Balta

#33 “Methylene Blue Adsorption on Biochar
Prepared from Pumpkin Shell” D. Bala, Ç. Özer &
M. İmamoğlu

#85 “Production Scheduling of a Natural Gas
Power Plant” M.G. Güler, E. Geçici & S.B.
Gündüz

#115 “Experimental Air-Cooled Battery Thermal
Management Approach” B. Tarhan, O. Yetik &
T.H. Karakoc

#13 “The Effect of Pressure and Porous Media
Structural Parameters Coupling on Gas Apparent
Viscosity” O. Abunumah, P. Ogunlode & E.
Gobina

[Zoom Link 3](#)

General Session 17

Modeling & Simulation – II

Session Chair: Hasan Ozcan, UK

#101 “Development and Analysis of a Novel
Greenhouse Roof for Reduced Cooling Load in Hot
Climates” Y. Bicer, M.U. Sajid & M. Al-Breiki

#102 “Development and Validation of a Dynamic
Thermal Model for a Water Wall Integrated Indoor”
N. Altunacar, I. Şener, Y. Yaman, B. Budakoğlu, E.
Topkara, A. Esmer, M.A. Ezan, A. Tokuç, G. Köktürk
& I. Deniz

#103 “Analysis of Optimum Flow Rate of a
Photovoltaic Thermal System (PVT) Integrated with
Phase Change Materials (PCM)” C. Kandilli & B.
Mertoglu

#61 “Exergy Analysis of a Steam Power Plant at Full
and Partial Load Conditions” U.G. Azubiike, H.O.
Njoku & O.V. Ekechukwu

#130 “Technological Assessment of a Solar PV
Collector for Freshwater, Cooling, and Electricity” E.
Khalid

#68 “Mathematical Modelling of Adsorption Isotherms
for Porous Bed with Axial Dispersion Model” M.
Sidhareddy & S. Tiwari

10:30 - 10:45 (GMT+3)

Break

Thursday - August 12, 2021

Zoom Link 1

General Session 18

Energy Conversion & Management – II,

Session Chair: Yusuf Bicer, Qatar

#31 "Development and Characterization of UV-Curing Coatings Containing Active Carbon" M. Zor, F. Şen, B. Oran & Z. Candan

Invited Talk 23

11:00 – 11:30 (GMT+3)

Arif Günyar

Managing Director ENERCON, Turkey

The Future of Wind Energy Sector

#133 "Modelling and Simulation of Molten Carbonate Fuel Cell and Copper-Chlorine Cycle Based Power Generation System with The Incorporation of PID Controller" H. Kamran, U. Mudassar, A.M. Ali, M.A. Raza, K. Khan, K. Kamal & T.A.H. Ratlamwala

#54 "Techno-Economic and Environmental Impact Assessments of Trigereneration Systems with Various Fuels" E. Sorgulu & I. Dincer

#134 "Artificial Intelligence Based Prediction of Outputs of Geothermal Energy Based Multigeneration System" Q.N. Haider, S.M. Ali, K. Kamal & T.A.H. Ratlamwala

Zoom Link 2

General Session 19

Hydrogen Energy Technologies - III

Session Chair: Canan Acar, Netherlands

#122 "Green Hydrogen Production Potential in Turkey with Wind Power" I. Dincer, N. Javani & G.K. Karayel

#123 "Blue H₂ Generation by Steam Reforming of Synthetic Biogas in a Membrane Reactor Packed with a Novel Ruthenium-Nickel Catalyst" A. Lulianelli, C. Italiano, M. Manisco, A. Brunetti, A. Figoli, G. Drago Ferrante, L. Pino & A. Vita

#95 "A Photoelectrochemical Reactor for Ion Separation and Hydrogen Production" M.I. Aydin, H. Selcuk & I. Dincer

#50 "Solar and Sonolysis Assisted Hydrogen Recovery from Industrial Sulphide Wastewater using CNT-ZnS/Fe₂O₃" P. Vijayarangan, S. Maurya & S. Manoharan

#109 "Coupled Thermal-Electrochemical Analysis of Polymer Electrolyte Membrane Electrolyser" F.M. Nafchi, E. Afshari & E. Baniasadi

#108 "Energetic Optimization of a Combined Solar Power Plant and Hydrogen Production System with Nano-Fluid and Energy Storage System" M. Shirazi, E. Baniasadi, E. Afshari & N. Javani

#136 "Multi-Objective Optimization of a Multistage Vapor Compression Refrigeration Cycle" A. Ustaoglu, B. Kursuncu, A.M. Kaya & H. Caliskan

Zoom Link 3

General Session 20

Energy & Environment – II

Session Chair: Ayca Tokuc, Turkey

#138 "0-D Parallel Circuit Modeling of Solid Oxide Fuel Cell" A. Erdogan, A.C. Ince & C.O. Colpan

#139 "Performance of Solar Assisted Dual Source Heat Pump" K. Kaygusuz, Ö. Kaygusuz & T. Ayhan

#140 "Capric and Myristic Acid Mixture with Gypsum Wallboard for Latent Heat Energy Storage" K. Kaygusuz & A. Sari

#105 "Asymmetric and Symmetric Coin Cell Supercapacitors by Deposition of Graphene for Energy Storage Applications" O. Yargi, M. Ozmen, S. Buyuk Pehlivan & A. Gelir

#93 "Microencapsulation of Three-Component Thermochromic Systems (Fluoran Dye-Phenolphthalein-N-Tetradecanol) in Poly (Methyl Methacrylate)" C. Alkan, S. Ozkayalar, S. Demirbağ Genç, M.S. Tözüm & S. Alay Aksoy

#96 "Climate Impact of Blockchain in the View of Cryptocurrencies" N. Gure

#137 "A Policy on Renewable Hydrogen Ecosystem in Turkey" A. Midilli

10:45
12:15

(GMT+3)

12:15 - 13:15 (GMT+3)

Break



Thursday - August 12, 2021 - [Zoom Link](#)

Panel Discussion Session 3: Status and Perspectives of Photovoltaic Technologies: Global and Local Approaches

Moderator: Rasit Turan, Turkey

Panel Speakers

13:15

15:15

(GMT+3)

Shravan Kumar Chunduri, Head of Technology at TaiyangNews UG

Dr. Firat Es, Head of the R&D Department, Kalyon PV, Turkey

Dr. Paul Ni, Vice President and CTO of Talesun Solar.

Dr. Hariharsudan Sivaramakrishnan, IMEC, Belgium

15:15 - 15:30 (GMT+3)

Closing Ceremony



TÜBA – Energy Working Group Members

- Prof. Dr. İbrahim Dinçer / Chairman
- Prof. Dr. Mehmet Hakkı Alma
- Prof. Dr. Erol Arcaklıođlu
- Prof. Dr. Yıldız Bayazitođlu
- Prof. Dr. Arif Hepbaşı
- Prof. Dr. Sadık Kakaç
- Prof. Dr. Kamil Kaygusuz
- Prof. Dr. Adnan Midilli
- Prof. Dr. Murat Öztürk
- Prof. Dr. Niyazi Serdar Sarıçiftçi
- Prof. Dr. Bahri Şahin
- Prof. Dr. Raşıit Turan



TÜRKİYE BİLİMLER AKADEMİSİ
TURKISH ACADEMY OF SCIENCES

www.tuba.gov.tr

Vedat Dalokay Caddesi: 112 06670 GOP/Çankaya - Ankara
Tel: 0312 442 29 03 (pbx) (#168) Faks: 0312 442 72 36 / 2358 / 6491